
[All ETDs from UAB](#)

[UAB Theses & Dissertations](#)

2001

Design of conformationally defined retinoids: Synthesis, nuclear receptor binding, and transcriptional activity of derivatives of (9Z)-UAB30.

Kimberly Kay Vines
University of Alabama at Birmingham

Follow this and additional works at: <https://digitalcommons.library.uab.edu/etd-collection>

Recommended Citation

Vines, Kimberly Kay, "Design of conformationally defined retinoids: Synthesis, nuclear receptor binding, and transcriptional activity of derivatives of (9Z)-UAB30." (2001). *All ETDs from UAB*. 4882.
<https://digitalcommons.library.uab.edu/etd-collection/4882>

This content has been accepted for inclusion by an authorized administrator of the UAB Digital Commons, and is provided as a free open access item. All inquiries regarding this item or the UAB Digital Commons should be directed to the [UAB Libraries Office of Scholarly Communication](#).

INFORMATION TO USERS

This manuscript has been reproduced from the microfilm master. UMI films the text directly from the original or copy submitted. Thus, some thesis and dissertation copies are in typewriter face, while others may be from any type of computer printer.

The quality of this reproduction is dependent upon the quality of the copy submitted. Broken or indistinct print, colored or poor quality illustrations and photographs, print bleedthrough, substandard margins, and improper alignment can adversely affect reproduction.

In the unlikely event that the author did not send UMI a complete manuscript and there are missing pages, these will be noted. Also, if unauthorized copyright material had to be removed, a note will indicate the deletion.

Oversize materials (e.g., maps, drawings, charts) are reproduced by sectioning the original, beginning at the upper left-hand corner and continuing from left to right in equal sections with small overlaps.

Photographs included in the original manuscript have been reproduced xerographically in this copy. Higher quality 6" x 9" black and white photographic prints are available for any photographs or illustrations appearing in this copy for an additional charge. Contact UMI directly to order.

**ProQuest Information and Learning
300 North Zeeb Road, Ann Arbor, MI 48106-1346 USA
800-521-0600**

UMI[®]

**DESIGN OF CONFORMATIONALLY DEFINED RETINOIDS: SYNTHESIS,
NUCLEAR RECEPTOR BINDING, AND TRANSCRIPTIONAL ACTIVITY OF
DERIVATIVES OF (9Z)-UAB30**

by

KIMBERLY KAY VINES

A DISSERTATION

**Submitted to the graduate faculty of the University of Alabama at Birmingham,
in partial fulfillment for the requirements for the degree of
Doctor of Philosophy**

BIRMINGHAM, ALABAMA

2001

UMI Number: 3023973

UMI[®]

UMI Microform 3023973

Copyright 2001 by Bell & Howell Information and Learning Company.

**All rights reserved. This microform edition is protected against
unauthorized copying under Title 17, United States Code.**

**Bell & Howell Information and Learning Company
300 North Zeeb Road
P.O. Box 1346
Ann Arbor, MI 48106-1346**

ABSTRACT OF DISSERTATION
GRADUATE SCHOOL, UNIVERSITY OF ALABAMA AT BIRMINGHAM

Degree Ph.D. Program Chemistry

Name of Candidate Kimberly Kay Vines

Committee Chairs Wayne J. Brouillette and Donald D. Muccio

Title Design of Conformationally Defined Retinoids. Synthesis, Nuclear

Receptor Binding, and Transcriptional Activity of Derivatives of (9Z)-UAB30

Retinoic Acid (RA) and synthetic retinoids interact with hormone nuclear receptors (RARs and RXRs), and regulate transcription of genes that control cell processes such as differentiation, proliferation and apoptosis. Due to these effects, retinoids have also been shown to prevent and treat different types of cancer. The N-methyl nitrosourea (MNU) carcinogen initiates mammary cancer in rats and retinoids have been shown to prevent those tumors. The capacity of (9Z)-UAB30, an RXR-selective retinoid, to prevent mammary cancer in rats was studied using the MNU-initiated model for mammary chemoprevention. It was shown that at a 200 mg/kg diet dose, this retinoid was very effective in tumors and was also nontoxic at this dose. In order to further assess the chemopreventive activity of (9Z)-UAB30 in rats, large quantities of this retinoid (10-75 g) were required. The previously reported synthesis of (9Z)-UAB30 was altered to make it amenable to large-scale preparations. The results from the chemoprevention assay indicate that (9Z)-UAB30 may have clinical potential in the treatment of breast cancer.

Further, we explored the requirements for RXR potency and selectivity of (9Z)-UAB30 by creating a series of tetraene analogs whereby the hydrophobic dihydronaphthalene ring was substituted with methyl and methoxy groups. Of the five (9Z)-UAB30

analogs prepared, (2*E*,4*E*,6*Z*,8*E*)-8-(4'-Methyl-3',4'-dihydro-1'(2'H)-naphthalen-1'-ylidene)-3,7-dimethyl-2,4,6-octatrienoic Acid exhibited greater RXR transactivation activity than 9-*cis* RA accompanied by an enhancement in RAR (α , β , γ) transactivation activity. In an effort to enhance the selectivity of (9*Z*)-UAB30, we changed the size of the cyclohexenyl portion of the dihydronaphthalene ring. The ring-expanded analog, (2*E*,4*E*,6*Z*,8*E*)-8-(6',7',8',9'-Tetrahydro-benzocyclohepten-5'-ylidene)-3,7-dimethyl-2,4,6-octatrienoic Acid, showed improved RXR transactivation activity in comparison to (9*Z*)-UAB30. Finally, we investigated the effect on receptor potency and selectivity of replacing the dienolic terminus of (9*Z*)-UAB30 with a 4-amino benzoic acid group, which is a strategy that resulted in three RAR γ -selective compounds.

DEDICATION

I dedicate my life to Jesus Christ, devoting all that He given me to advance His message of salvation. I lovingly dedicate this dissertation in honor of my parents, Mr. and Mrs. James D. Vines, and my best friend and fiancé, Benjamin H. Sanders.

ACKNOWLEDGEMENTS

I publicly acknowledge the saving grace of Jesus Christ and I am compelled to credit past, present, and future success to Him.

To my parents, thank you for your support and prayers. Without your support and guidance, I would never have made it this far. I love and thank you.

To my best friend and fiancé, Benjamin H. Sanders, thank you for the love and encouragement that you have given me over the past 12 years.

To Drs. Wayne J. Brouillette and Donald D. Muccio, I thank you for your instructions in chemistry, leadership in my research project, and role in my development as a scientist. Thanks to my committee members, Drs. Peter D. Emanuel, Jimmie Mays, and Brahma P. Sani for your contributions to my research project. Special thanks to all my friends in the UAB Chemistry Department, especially Dr. Charles Zha, Dr. Reddy Atigadda, Dr. Shoukath Ali, Eric Johnson, Stephanie Weiss, Brandon Pybus, and Ben Davis-thanks for your friendship and encouragement.

I would also like to thank my friends, the members of the SKGG-you know who you are. Your support and encouragement during both my undergraduate and graduate school days are deeply appreciated.

I gratefully acknowledge the UAB Department of Chemistry and Graduate School for their financial support.

TABLE OF CONTENTS

	<u>Page</u>
ABSTRACT	ii
DEDICATION	iv
ACKNOWLEDGEMENT	v
LIST OF TABLES	ix
LIST OF FIGURES	xii
LIST OF SCHEMES	xvii
INTRODUCTION.....	1
Early Synthetic Strategies	4
Retinoid Nuclear Receptors	18
Biological Assays	30
Early Synthetic Retinoids.....	32
Receptor Subtype-Selective Agonists.....	44
RAR β/γ Receptor-Selective Retinoids.....	50
Crystal Structures of Agonists Bound to Retinoid Receptor RAR γ	56
Retinoid Antagonists.....	62
AP-1 Transrepression by Retinoids	64
Heteroaromatic RAR Pan-Antagonists.....	66
RAR α -Selective Antagonists.....	70
Evolution of RXR-Selective Agonists	72
Structure of 9-cis RA Bound RXR	82
Physiological Role of Retinoid Receptor Subtypes.....	87
Retinoid Synergists.....	90
GOALS AND RATIONALE.....	94
THE LARGE SCALE SYNTHESIS OF (9Z)-UAB30AND THE EFFECT ON PREVENTION OFCHEMICALLY INDUCED MAMMARY TUMORS	98

TABLE OF CONTENTS (Continued)

	<u>Page</u>
CONFORMATIONALLY DEFINED RETINOIC ACID ANALOGUES: SYNTHESIS, NUCLEAR RECEPTOR BINDING, AND TRANSCRIPTIONAL ACTIVATION ACTIVITY OF DERIVATIVES OF RXR-SELECTIVE (9Z)-UAB30.....	122
CONFORMATIONALLY DEFINED ANALOGUES OF RETINOIC ACID. SYNTHESIS, NUCLEAR RECEPTOR BINDING AND TRANSCRIPTIONAL ACTIVATION ACTIVITY OF A RING-EXPANDED DERIVATIVE OF (9Z)-UAB30.....	161
CONFORMATIONALLY DEFINED RETINOIC ACID ANALOGUES. SYNTHESIS AND NUCLEAR RECEPTOR TRANSCRIPTIONAL ACTIVATION ACTIVITY FOR AMIDE DERIVATIVES OF (9Z)-UAB30, RAR γ SELECTIVE LIGANDS.....	180
UNPUBLISHED DATA	204
Synthesis of Derivatives of (<i>all-E</i>)-UAB30.....	204
A Ring-Contracted Analog of (9Z)-UAB30	211
A Ring-Contracted Amide Analog of (9Z)-UAB30.....	217
CONCLUSIONS.....	221
LIST OF REFERENCES.....	225
APPENDIX	
A SPECTROSCOPIC DATA FOR COMPOUNDS IN “THE LARGE SCALE SYNTHESIS OF (9Z)-UAB30AND THE EFFECT ON PREVENTION OF CHEMICALLY INDUCED MAMMARY TUMORS”	241
B SPECTROSCOPIC DATA FOR COMPOUNDS IN “CONFORMATIONALLY DEFINED RETINOIC ACID ANALOGUES: SYNTHESIS, NUCLEAR RECEPTOR BINDING, AND TRANSCRIPTIONAL ACTIVATION ACTIVITY OF DERIVATIVES OF RXR-SELECTIVE (9Z)-UAB30”	266
C SPECTROSCOPIC DATA FOR COMPOUNDS IN “CONFORMATIONALLY DEFINED ANALOGUES OF RETINOIC ACID: SYNTHESIS, NUCLEAR RECEPTOR BINDING, AND TRANSCRIPTIONAL ACTIVATION ACTIVITY OF A RING-EXPANDED DERIVATIVE OF (9Z)-UAB30”	387

TABLE OF CONTENTS (Continued)

	<u>Page</u>
D SPECTROSCOPIC DATA FOR COMPOUNDS IN “CONFORMATIONALLY DEFINED RETINOIC ACID ANALOGUES. SYNTHESIS AND NUCLEAR RECEPTOR TRANSCRIPTIONAL ACTIVATION ACTIVITY FOR AMIDE DERIVATIVES OF (9Z)-UAB30, RAR γ -SELECTIVE LIGANDS”	410
E SPECTROSCOPIC DATA FOR COMPOUNDS IN “UNPUBLISHED DATA”	466

LIST OF TABLES

<u>Table</u>		<u>Page</u>
INTRODUCTION		
1	Starting Materials for the Various Approaches to Retinoid Synthesis ²	8
2	<i>In Vivo</i> Activities of ATRA, Etretnate, and TTNPB.....	34
3	Summary of Dawson's Retinoids with Modified Rings on TPA-Induced Mouse Epidermal ODC Activity.....	37
4	ODC Assay Results for Dawson's Benzoic Acid and Naphthalene Carboxylic Acid Terminated Retinoids.....	38
5	Differentiation-Inducing Ability of Shudo's Retinoids in HL-60 Cells.....	41
6	Nuclear Receptor Binding Affinities for the UAB Retinoids.....	43
7	Comparison of Binding Affinities [K_d (nM)] to RAR Subtypes for Retinoids that are RAR Pan-Agonists (ATRA and TTNPB) and RAR α -Selective Retinoids (Am580 and AGN193836)	46
8	Comparison of Receptor Binding Affinities (IC_{50}), Transcriptional Potency (EC_{30}), and HL-60 Differentiating Ability (ED_{30}) of the New RAR α Agonists	49
9	Novel Retinoids With RAR α Selectivity.....	50
10	Binding Affinities and Transactivation Abilities of Thienyl-Retinoids ¹¹⁰	52
11	Binding Constants of Naphthalene Carboxylic Acids for the RARs	55
12	Divergent Residues in the Ligand-Binding Pocket of the RARs.....	57
13	Racemic BMS961 and the Enantiomers of BMS961 With Differing EC_{30} (nM) Values for RARs	60
14	Binding Affinity and Antagonism of Retinoid Receptor Antagonists	67

LIST OF TABLES (Continued)

<u>Table</u>	<u>Page</u>
15 Relative Potency and K_d Values of RAR Antagonists in the Inhibition of Transcriptional Activity by the RAR Agonist TTNPB	68
16 RAR Pan-Antagonists That Inhibit TTNPB-Induced Mucocutaneous Toxicity	69
17 The Effect of Varying θ_2 or the Linker of 3-Methyl TTNPB Derivatives on the RXR Activity and Selectivity	75
18 Competitive Receptor Binding Assay Results for the 3-Alkyl Derivatives of TTNPB.....	76
19 Retinoid Receptor Transactivation Activities (EC_{50}) for Some of Dawson's RXR-Selective Retinoids	78
20 Receptor Binding of 9- <i>cis</i> RA Analogs With an Isosterically Replaced 9,10 Double Bond	80
21 Retinoids Designed by Farmer et al. ^{146,147}	81
22 Transactivation Data for Tetrahydroquinoline Retinoids ¹⁴⁸	83
23 The Effects of Retinoids on Proliferation, Differentiation, and Apoptosis in HL-60 Cells	88
24 The Binding Affinities and Synergistic Activities of Diazepinylbenzoic Acids	92
THE LARGE SCALE SYNTHESIS OF (9Z)-UAB30 AND THE EFFECT ON PREVENTION OF CHEMICALLY INDUCED MAMMARY TUMORS	
1 Effects of (9Z)-UAB30 on Plasma Levels of Estradiol and Progesterone and on the Liver Concentration of Retinyl Palmitate in Rats	110
2 Effect of (9Z)-UAB30 on Body Weight and on the Weights of Liver, Uterus, and Ovaries of Rats	111

LIST OF TABLES (Continued)

<u>Table</u>	<u>Page</u>
CONFORMATIONALLY DEFINED RETINOIC ACID ANALOGUES: SYNTHESIS, NUCLEAR RECEPTOR BINDING, AND TRANSCRIPTIONAL ACTIVATION ACTIVITY OF DERIVATIVES OF RXR-SELECTIVE (9Z)-UAB30	
1	Summary of the IC₅₀ and EC₅₀ Values (nM) for (9Z)-UAB8 and (9Z)-UAB30 Retinoids in Nuclear Receptor Binding and Transcriptional Activation Assays.....
	129
2	Inhibition Concentrations at 50% (nM) for the Binding of Retinoids 1-6 and (9Z)-Retinoic Acid (RA) to Mouse Retinoic Acid Receptors (mRARs) and Retinoid X Receptors (mRXRs).....
	135
CONFORMATIONALLY DEFINED RETINOIC ACIDANALOGUES: SYNTHESIS, NUCLEAR RECEPTOR BINDING, AND TRANSCRIPTIONAL ACTIVATION ACTIVITY OF A RING-EXPANDED DERIVATIVE OF (9Z)-UAB30	
1	Inhibition Concentrations at 50% (nM) for the Binding of Retinoids (9Z)-UAB30, (9Z)-Retinoic Acid (RA), and 2 to Mouse Retinoic Acid Receptors (mRARs) and Retinoid X Receptors (mRXRa)
	168
UNPUBLISHED DATA	
1	Nuclear Receptor Binding Profile for Retinoid 5
	208

LIST OF FIGURES

<u>Figure</u>		<u>Page</u>
INTRODUCTION		
1	Major naturally occurring isomers of Retinoic Acid.....	2
2	The <i>in vivo</i> conversion of β -carotene (3) to retinol (8). ²	3
3	Classification system for approaches to synthesis of retinoids. ²	7
4	Comparison of sequence homology between the LBDs and DBDs of the retinoid receptors.....	23
5	Structure of ATRA bound to RAR γ	28
6	Comparison of the position of H12 in the apo- and holo-conformations. ⁴⁸	28
7	Metabolites of ATRA.	35
8	Amide derivatives of TTNPB.	40
9	Conformational restriction of single bonds s_1 and s_2 in Ch80 lead to the design of Fv80 and Re80.....	42
10	Superposition of Fv80 (blue) with Re80 (red).....	42
11	Design of quinoxaline derivatives by Kikuchi et al. ¹⁰⁴	47
12	RAR β,γ -selective acetylenic retinoids.....	51
13	Stereoisomers of the acetylenic THP ethers designed by Vuligonda. ¹¹¹	53
14	Pan-agonist 9- <i>cis</i> RA bound to RAR γ	59
15	RAR γ -selective ligand BMS961 bound to RAR γ	59
16	Superposition of BMS394 and BMS395 in the LBP of RAR γ . ¹¹⁸	61

LIST OF FIGURES (Continued)

<u>Figure</u>	<u>Page</u>
17 Strategy for the design of retinoid antagonists. ¹²¹	63
18 Structure of the retinoid antagonist MX781 with anti-AP-1 activity.....	65
19 RAR α antagonists AGN194574 and BMS614 ¹³²	71
20 Key interactions of RAR α agonist BMS614 with RAR γ . ¹³²	71
21 Retinoids selective for RXR response pathways	73
22 The steric interaction between the 3-methyl and C10 hydrogen induced a change in θ_1	74
23 The RXR-selective retinoid Targretin or LGD1069	77
24 RXR-selective conformationally defined 6- <i>s-trans</i> retinoids ^{142,143}	79
25 Illustration of interactions of 9- <i>cis</i> RA with the RXR α LBP ¹⁴⁹	84
26 Comparison of structure of 9- <i>cis</i> RA bound to RXR α and the apo-RXR α Structure ¹⁴⁹	86
27 Comparison of the conformations of 9- <i>cis</i> RA when bound to RAR γ and RXR α ¹⁴⁹	86

GOALS AND RATIONALE

1 Structures of 9- <i>cis</i> RA, Targretin and (9Z)-UAB30	94
2 Ring-substituted analogs of (9Z)-UAB30	95
3 Ring-expanded analog of (9Z)-UAB30.....	96
4 Structures of TTNPB, Am80 and the amide derivatives of (9Z)-UAB30.....	110

THE LARGE SCALE SYNTHESIS OF (9Z)-UAB30 AND THE EFFECT ON PREVENTION OF CHEMICALLY INDUCED MAMMARY TUMORS

1 Comparison of body weights of the control vs. rats treated with (9Z)-UAB30	108
---	-----

LIST OF FIGURES (Continued)

<u>Figure</u>	<u>Page</u>
2 Comparison of average number of tumors per rat in the control animals vs. rats treated with (9Z)-UAB30.....	109
CONFORMATIONALLY DEFINED RETINOIC ACID ANALOGUES: SYNTHESIS, NUCLEAR RECEPTOR BINDING, AND TRANSCRIPTIONAL ACTIVATION ACTIVITY OF DERIVATIVES OF RXR-SELECTIVE (9Z)-UAB30	
1 Structures of two natural retinoids	124
2 Design strategy for the conformationally constrained 6- <i>s-trans</i> analogs of (9Z)-RA	128
3 RAR α -receptor transcriptional activation.....	136
4 RAR β -receptor transcriptional activation.....	136
5 RAR γ -receptor transcriptional activation	137
6 RXR α -receptor transcriptional activation.....	137
7 Results from the dose-response assay for RXR α transactivation	138
CONFORMATIONALLY DEFINED RETINOIC ACID ANALOGUES: SYNTHESIS, NUCLEAR RECEPTOR BINDING, AND TRANSCRIPTIONAL ACTIVATION ACTIVITY OF A RING-EXPANDED DERIVATIVE OF (9Z)-UAB30	
1 (9Z)-UAB30 (1) and ring-expanded analog 2	166
2 RAR α -receptor transcriptional activation.....	169
3 RAR β -receptor transcriptional activation.....	169
4 RAR γ -receptor transcriptional activation.....	169
5 RXR α -receptor transcriptional activation.....	170

LIST OF FIGURES (Continued)

<u>Figure</u>	<u>Page</u>
CONFORMATIONALLY DEFINED RETINOIC ACID ANALOGUES: SYNTHESIS AND TRANSCRIPTIONAL ACTIVATION ACTIVITY OF AMIDE DERIVATIVES OF (9Z)-UAB30, RARγ-SELECTIVE LIGANDS	
1 Pan-agonist TTNPB, RAR α -selective retinoid Am80, and RXR-selective retinoid Targretin	182
2 Structures of (9Z)-UAB30 1 and the amide derivative 2	183
2 Key interactions in the trans and cis amides	186
3 RAR α -receptor transcriptional activation (10^{-6} M)	187
4 RAR β -receptor transcriptional activation (10^{-6} M)	188
5 RAR γ -receptor transcriptional activation (10^{-6} M)	188
6 RXR α -receptor transcriptional activation (10^{-6} M)	188
7 Previously synthesized (9Z)-UAB30 analogs	189
8 Receptor subtype selective retinoids used to treat proliferative skin disease	189
UNPUBLISHED DATA	
1 Receptor-selective retinoids	205
2 Transcriptional activation for retinoid 7	209
3 RXR-selective (9Z)-UAB30 1 and the ring-altered analogs 19 and 20	212
4 Structures of TTNPB, Am80, and Targretin	217
5 Structures of the (9Z)-UAB30 amide (32) and the ring-contracted amide (33).	218
CONCLUSIONS	
1 Structures of 9- <i>cis</i> RA, Targretin, and (9Z)-UAB30	221
2 Ring-substituted analogs of (9Z)-UAB30.	222
3 Ring-expanded analog of (9Z)-UAB30	223

LIST OF FIGURES (Continued)

<u>Figure</u>	<u>Page</u>
4 Structures of TTNPB, Am80, (9Z)-UAB30 and the amide derivatives of (9Z)-UAB30	224

LIST OF SCHEMES

<u>Scheme</u>	<u>Page</u>
---------------	-------------

INTRODUCTION

1	The First Reported Synthesis of a Retinoid ^{8,a}	5
2	β -ionone was Obtained from Natural Sources ^{9,a}	5
3	Synthesis of β -ionone ^a	6
4	First Industrial Synthesis of Vitamin A ^{12,a}	9
5	The Synthesis of Vitamin A Acetate ^{15,a}	10
6	Preparation of the 9- <i>cis</i> and All- <i>trans</i> Isomers of β -ionylideneacetaldehyde ^{17,a}	12
7	Preparation of the 9- <i>cis</i> and 13- <i>cis</i> Isomers of Vitamin A ^{2,a}	13
8	Merck's Synthesis of Vitamin A ^{18,a}	14
9	The C ₉ + C ₁₁ Convergent Synthesis ^{19,20,a}	15
10	The C ₁₀ + C ₁₀ Approach ^{21-24,a}	17

THE LARGE SCALE SYNTHESIS OF (9Z)-UAB30 AND THE EFFECT ON PREVENTION OF CHEMICALLY INDUCED MAMMARY TUMORS

1	Synthesis of 1 ^a	105
---	-----------------------------------	-----

CONFORMATIONALLY DEFINED RETINOIC ACID ANALOGUES. SYNTHESIS, NUCLEAR RECEPTOR BINDING, AND TRANSCRIPTIONAL ACTIVATION ACTIVITY OF DERIVATIVES OF RXR-SELECTIVE (9Z)-UAB30

1	Synthesis of Analogs of (9Z)-UAB30 ^a	131
---	---	-----

LIST OF SCHEMES (Continued)

<u>Scheme</u>	<u>Page</u>
CONFORMATIONALLY DEFINED ANALOGUES OF RETINOIC ACID: SYNTHESIS, NUCLEAR RECEPTOR BINDING, AND TRANSCRIPTIONAL ACTIVATION ACTIVITY OF A RING-EXPANDED DERIVATIVE OF (9Z)-UAB30	
1	Synthesis of Ring-Expanded Analog (2) of (9Z)-UAB30^a..... 167
CONFORMATIONALLY DEFINED RETINOIC ACID ANALOGUES: SYNTHESIS AND TRANSCRIPTIONAL ACTIVATION ACTIVITY OF AMIDE DERIVATIVES OF (9Z)-UAB30, RARγ-SELECTIVE LIGANDS	
1	Synthesis of Amides 2-8^a 183
UNPUBLISHED DATA	
1	Synthetic Strategy for (9Z)- and (<i>all-E</i>)-UAB30^a 206
2	Attempted Synthesis of 19^a 214
3	Attempted Horner-Emmons Reaction^a. 215
4	Synthetic Strategy for the Preparation of 19 Using the Wittig Reaction^a 216
5	Synthetic Scheme for the Preparation of the Amide 33^a 219

INTRODUCTION

Retinoic acid (RA) is a hormone that regulates cellular processes such as proliferation, differentiation, and apoptosis. Since tumors occur due to uncontrolled cell proliferation and defective signaling pathways involved in differentiation, RA has found utility in the treatment and prevention of different cancers. Shown in Figure 1, the two most important isomers biologically are (*all-trans*)-RA (1) and 9-*cis* RA (2), which are responsible for the pleiotropic effects of retinoids through binding of retinoid nuclear receptors and other retinoid binding proteins. The term “retinoid” first referred to a class of compounds that were structurally related to RA (structure in Figure 1). This class of compounds is defined by four isoprenoid units joined in a head to tail manner. Many retinoids may be formally derived from this monocyclic parent compound containing five carbon-carbon double bonds and a functional terminal group at the terminus of the acyclic portion.¹ However, the term retinoid has been broadened considerably in the past 20 years, and it now defines compounds that do not share these structural features, but which share common biological properties of RA.

Vitamin A or retinol is derived from the chemical breakdown of β -carotene, which has received much attention in the past decade due to its antioxidant and possible capacity to prevent some cancers. Figure 2 shows the two possible pathways for the *in vivo* conversion of β -carotene to vitamin A.² First, retinol 8 is esterified using long-chain fatty acids. The retinyl ester is stored in the liver until it is needed by peripheral tissue,

and then the retinyl esters are converted to retinol by an esterase. Retinol can be oxidized via retinal to RA 1 by nicotinamide adenine dinucleotide phosphate (NADPH)-dependent dehydration. The alternative pathway involves the cleavage of β -carotene to yield two aldehyde molecules 7, which then undergo oxidation to RA 1 or reduction to retinol 8.

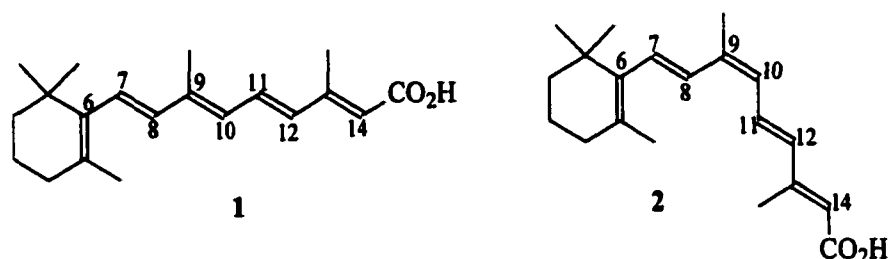


Figure 1. Major naturally occurring isomers of Retinoic Acid.

Retinol was first observed by Stepp in 1909³ and described by McCollum and Davis in 1915 as “fat soluble A.”⁴ It was isolated from animal fats and fish oils and shown to be associated with growth-promoting activity. Drummond later suggested that the “fat soluble A” should be named vitamin A.⁵ Vitamin A deficiency was associated with xerophthalmia and night blindness. Wald supported these observations with a series of experiments that identified retinal as the pigment obtained from bleached retinas.⁶ The structure of vitamin A was solved by Karrer et al. using a highly purified extract from shark liver.⁷ Prior to World War II, vitamin A was obtained from fish oils, but, due to a decreased supply, there was a need to synthesize large quantities of vitamin A on an industrial scale.

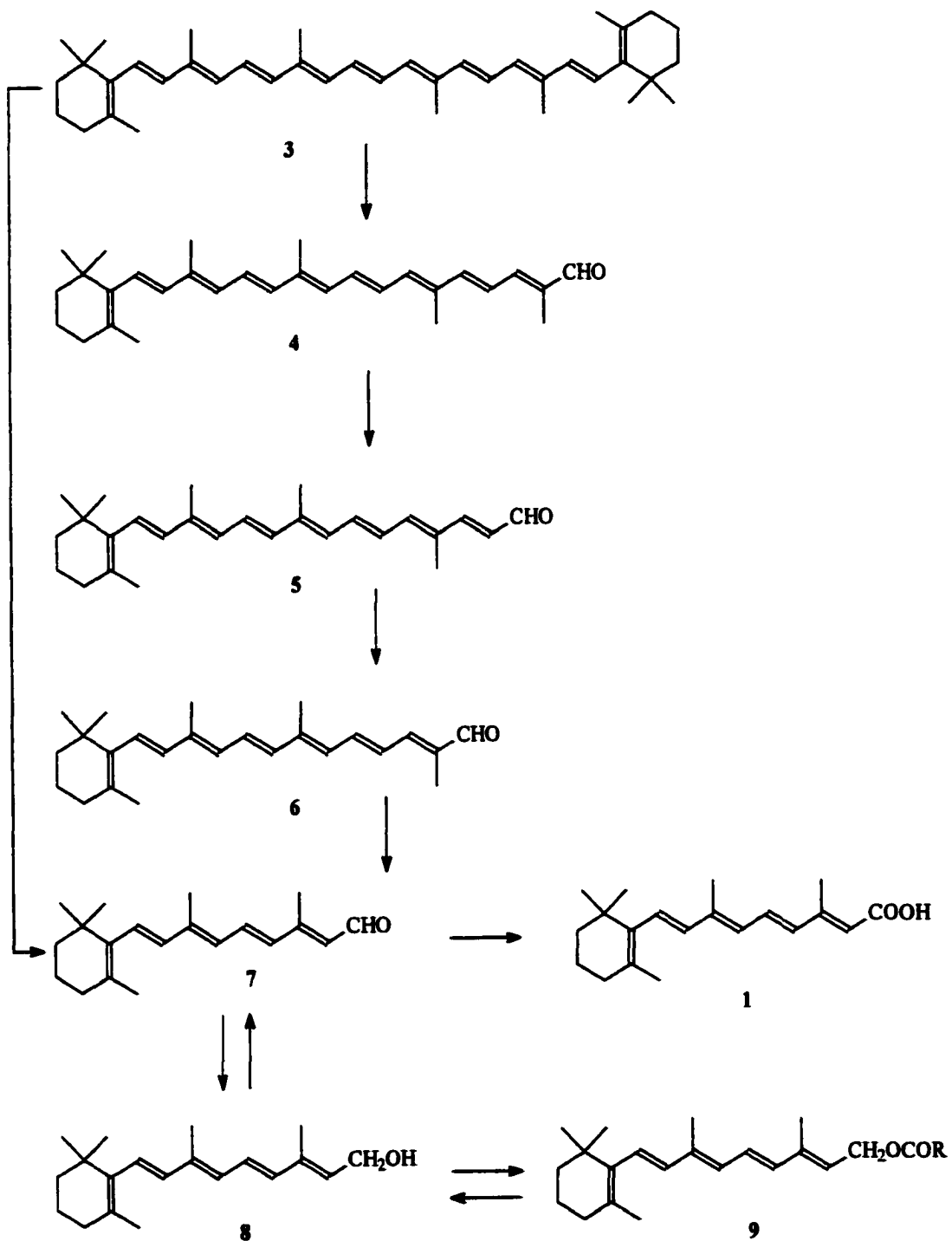


Figure 2. The *in vivo* conversion of β -carotene (3) to retinol (8).²

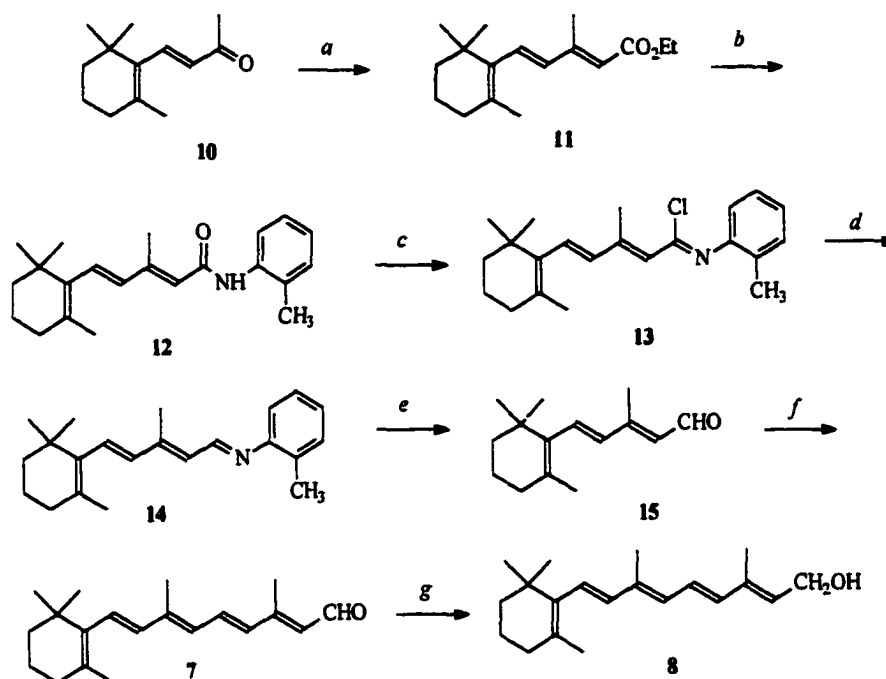
Early Synthetic Strategies

As early as 1937, Kuhn and Morris reported the first total synthesis of retinol.⁸ As shown in Scheme 1, the starting material, β -ionone **10**, was converted to the ethyl ester **11** via a Reformatsky reaction followed by a Grignard reaction to produce the amide **12**. Conversion to the chloro-imine **13** with PCl_5 followed by dehydrohalogenation produced the Schiff base **14**. Treatment with oxalic acid yielded the β -C₁₅ aldehyde **15**. Knoevenagel condensation of **15** with 3-methyl-2-butenal and piperidine acetate yielded the C-20 aldehyde, retinal, that was then reduced with aluminum isopropoxide to afford a dark viscous oil with approximately 7.5% vitamin A content.

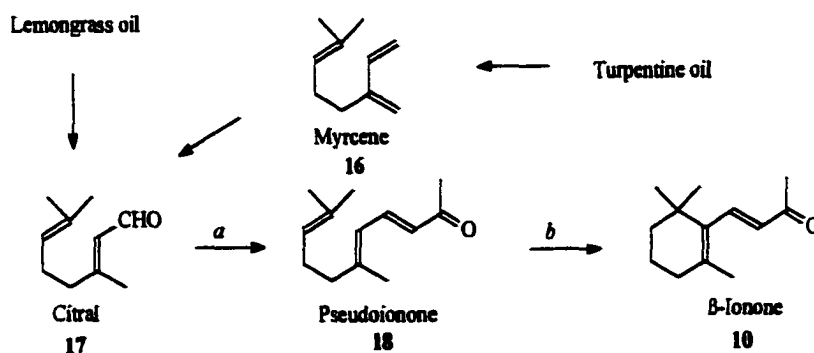
Prior to 1940, β -ionone could be obtained only from natural sources.⁹ As shown in Scheme 2, citral **17** could be obtained via distillation of lemongrass oil. Distillation of turpentine oil yielded myrcene **16**, which could be converted to citral **17**. Base-catalyzed condensation of citral with acetone yielded pseudoionone **18**, which afforded β -ionone **10** when treated with anhydrous sulfuric acid.

Fortunately, after 1940, researchers at Roche laboratories disclosed the higher yielding synthesis of β -ionone from acetone.¹⁰ As shown in Scheme 3, reaction of acetone with acetylene and partial hydrogenation of the triple bond yielded **20**, which was then reacted with methyl acetate in the method described by Saucy and Marbet to yield **21**.¹¹ Alcohol **22** was obtained upon reaction of **21** with acetylene, and treatment of **22** with methyl acetate gave pseudoionone (**18**). Ring-closure of **18** was accomplished under anhydrous acidic conditions affording β -ionone **10**.

Between 1946 and 1956, a large number of manuscripts were published on the successful syntheses of retinol, retinal, and RA. In addition, nine industrial processes

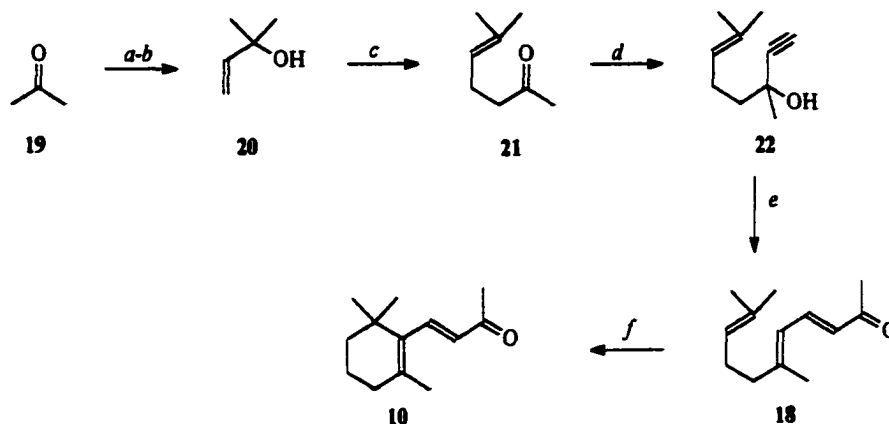
Scheme 1. The First Reported Synthesis of a Retinoid^{8,a}


^a (a) Zn, ethyl bromoacetate; (b) (i) CH₃I, Mg, ether; (ii) 2-methyl aniline; (iii) 0.1 N HCl; (c) PCl₅, anhydrous benzene, 0 °C; (d) Cr(OAc)₂·H₂O, HCl, ether; (e) CrCl₃; (f) 3-methyl-2-butenal, piperidine, acetic acid; (g) (i) Al(OiPr)₃, isopropanol; (ii) 2N H₃PO₄.

Scheme 2. β-Ionone was Obtained from Natural Sources^{9,a}


^a (a) acetone, base; (b) anhydrous H₂SO₄.

Scheme 3. Synthesis of β -ionone^a



^a (a) acetylene, NH_3 ; (b) H_2 /Lindlar's catalyst; (c) methyl acetate, Saucy/Marbet; (d) acetylene; (e) methyl acetate, Saucy/Marbet; (f) H_2SO_4 , acetic acid.

for the synthesis of vitamin A were developed.² The various approaches were convergent syntheses classified according to the synthons used and are summarized in Figure 3 and Table 1.

The first reported industrial synthesis of vitamin A was developed by Isler et al. at Roche (Scheme 4).¹² This particular approach was referred to as a $\text{C}_{14} + \text{C}_6$ approach because β - C_{14} aldehyde and 3-methyl-1-penten-4-yn-1-ol were the synthons used. These synthons were not commercially available and had to be synthesized. Using Darzen's glycidic ester synthesis, β -ionone 10 was converted to the epoxide 23, and treatment with base afforded the β - C_{14} aldehyde, 24. Reaction of the readily available methyl vinyl ketone 25 with sodium acetylide produced 26, which was dehydrated with H_2SO_4 to yield a mixture of *cis*- and *trans*-3-methyl-1-penten-4-yn-1-ol (27a and 27b). A Grignard reaction of β - C_{14} aldehyde 24 with the *trans* isomer (27a) afforded the alkyne 28, which upon

hydrogenation gave the dihydroxy-alkene **29**. The primary alcohol of **29** was selectively protected with an acetyl group followed by rearrangement and dehydration. Finally, the acetate was hydrolyzed to yield **8**, vitamin A. Eiter and Truscheit reported a similar synthesis ($C_{14} + C_6$) but obtained the 9-*cis* isomer of **8**, which at the time was believed to be biologically unimportant.¹³

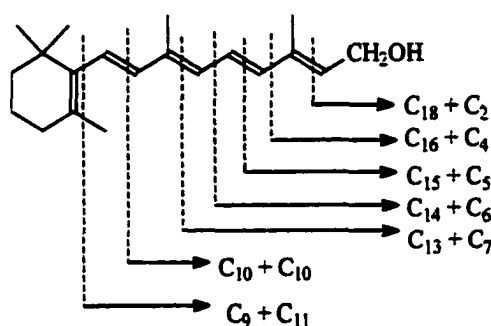
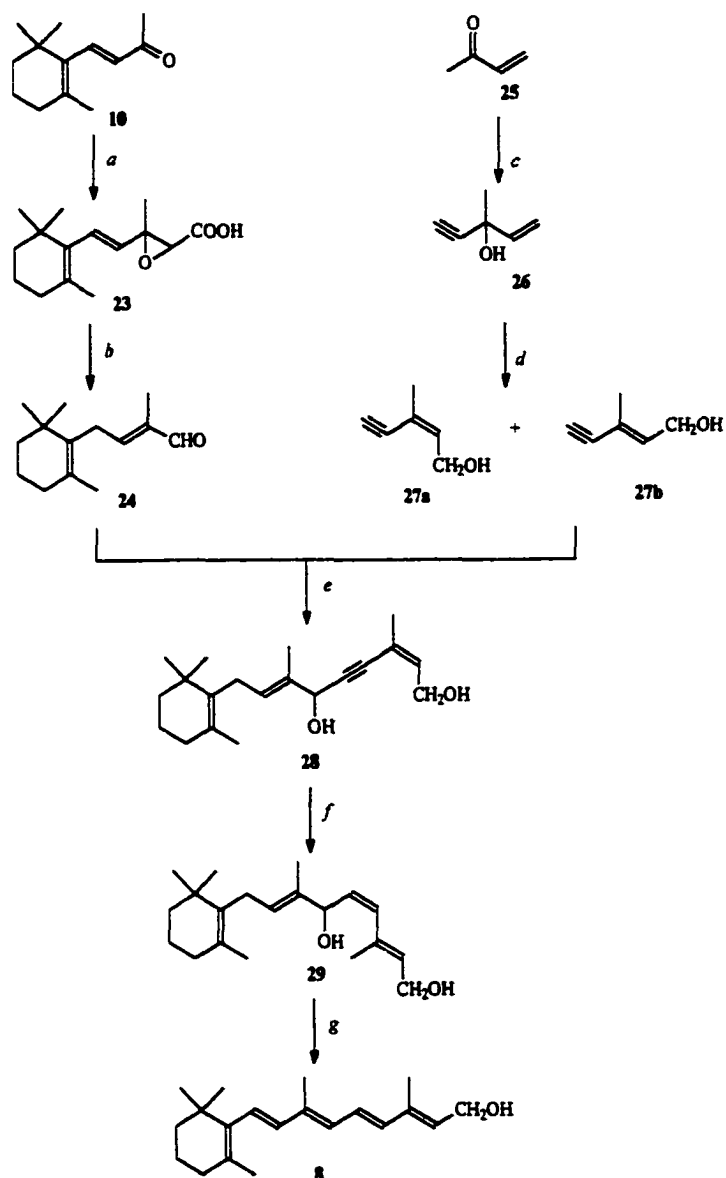


Figure 3. Classification system for approaches to synthesis of retinoids.²

After Wittig and Geisler reported the principles of the Wittig reaction,¹⁴ Pommer and co-workers revolutionized polyene chemistry with a new industrial synthesis of vitamin A employing the Wittig reaction.¹⁵ Pommer's $C_{15} + C_5$ approach, shown in Scheme 5, started with vinyl- β -ionol **31**, which was synthesized from the Nef reaction of β -ionone **10** with lithium acetylide followed by partial hydrogenation of the triple bond.¹⁶ The Wittig reagent **32** was prepared by reaction of **31** with triphenylphosphonium chloride. The oxo-crotonate **36** was obtained in three steps, and the first step was the conversion of the ether **33** to the bromoacetal **34**. Treatment of **34** with potassium acetate yielded the acetal-protected ester **35**, which upon hydrolysis gave the oxocrotonate **36**. Reaction of **36** with the Wittig reagent **32** afforded the vitamin A acetate **37**. In the two

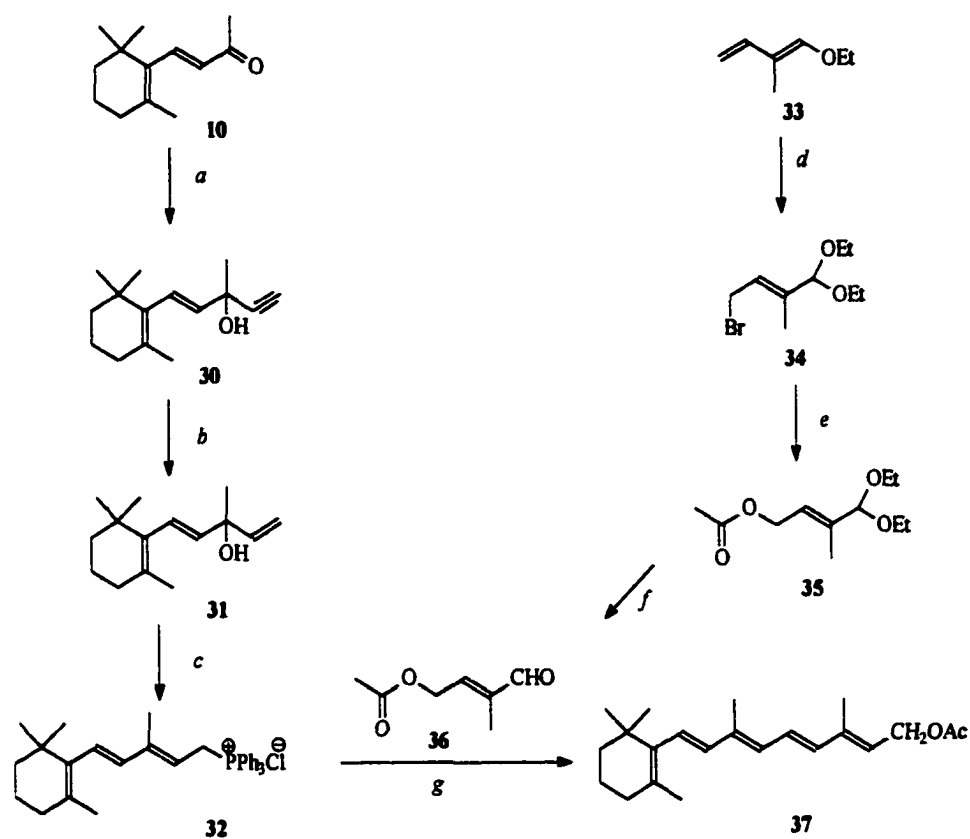
Table 1. Starting Materials for the Various Approaches to Retinoid Synthesis²

name	structure	classification
2,2,6-Trimethylcyclohexanone		C ₉ + C ₁₁
β-Cyclocitral		C ₁₀ + C ₁₀
β-Cyclogeraniol		C ₁₀ + C ₁₀
β-Ionone		C ₁₃ + C ₇
β-C ₁₄ aldehyde		C ₁₄ + C ₆
β-Ionylidene-acetaldehyde		C ₁₅ + C ₅
Vinyl-β-ionol		C ₁₅ + C ₅
β-C ₁₆ acetylenic carbinol		C ₁₆ + C ₄
β-C ₁₆ hydrocarbon		C ₁₆ + C ₄
β-C ₁₈ ketone		C ₁₈ + C ₂

Scheme 4. First Industrial Synthesis of Vitamin A^{12,a}


^a (a) (i) $\text{ClCH}_2\text{CO}_2\text{Et}$, NaOMe , benzene; (ii) OH^- , heat; (b) 15% NaOH ; (c) NaNH_2 , NH_3 , acetylene; (d) 25% H_2SO_4 ; (e) Mg , ether; (f) H_2 , Lindlars catalyst; (g) (i) Acetic anhydride; (ii) I_2 , ether.

Scheme 5. The Synthesis of Vitamin A Acetate^{15,a}



^a (a) lithium acetylide; (b) H_2 , Lindlar's catalyst; (c) PPh_3HCl ; (d) *N*-bromo-succinimide, anhydrous ethanol; (e) potassium acetate; (f) H_2O , HCl ; (g) NaH .

methods discussed previously, the goal was the synthesis of the *all-trans* isomer of vitamin A.

Matsui et al. reported a $\text{C}_{15} + \text{C}_5$ synthetic route whereby four isomers could be obtained.¹⁷ Starting with β -ionone 10, the 9-*cis* and *all-trans* isomers of β -ionylidene-acetaldehyde were prepared (Scheme 6). The Reformatsky reaction of β -ionone and ethyl bromoacetate yielded the hydroxy-ester 38, which was then hydrolyzed and dehydrated to give the retro-acid 39. Rearrangement of 39 to the desired acid was accom-

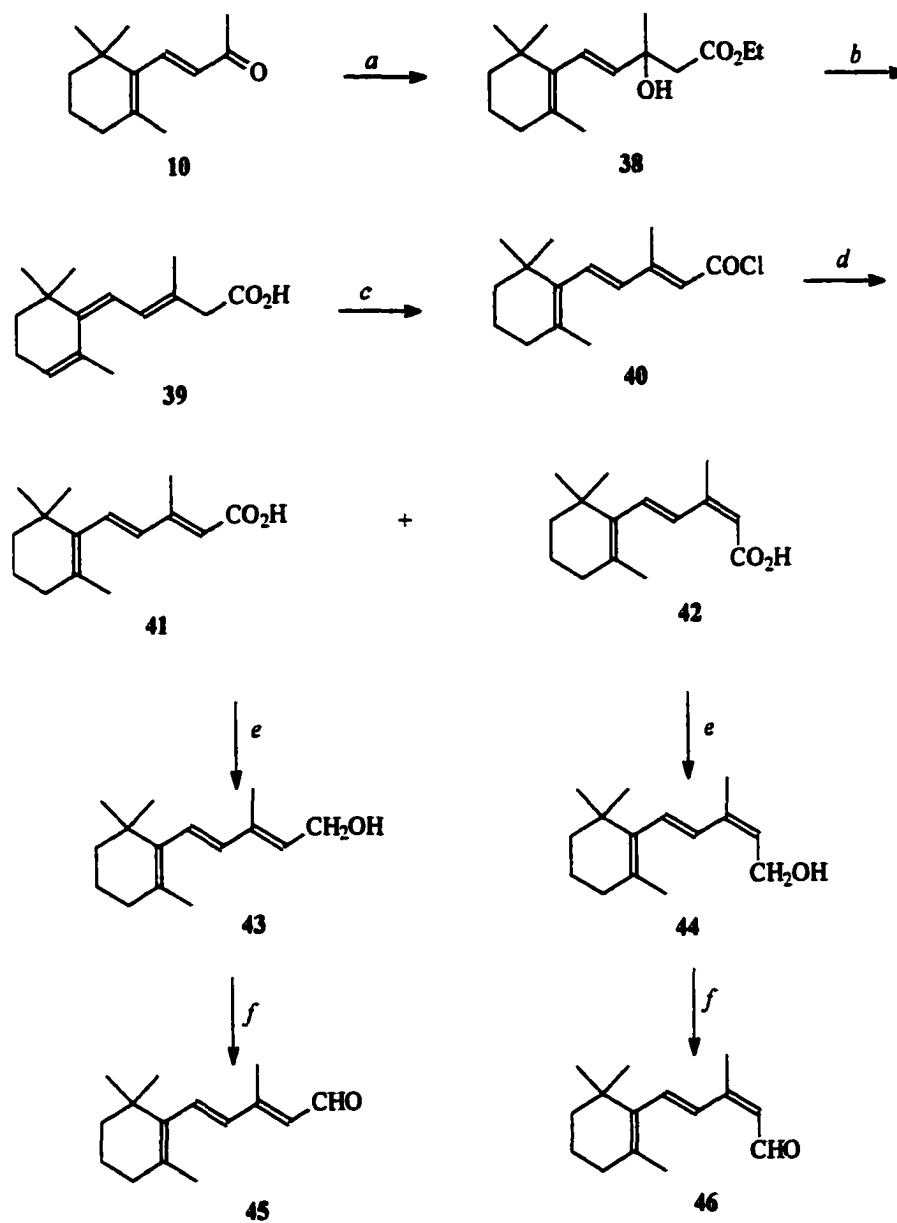
plished by first forming the acid chloride **40** and conversion to the C-15 acid via exposure to water. The C15 intermediate acid was obtained as a mixture of trans and cis geometric isomers **41** and **42**, which were separable by fractional crystallization. Each acid was reduced with LiAlH_4 followed by manganese dioxide oxidation to yield the aldehydes **45** and **46**.

Scheme 7 shows the preparation of the 9-*cis* and 13-*cis* isomers from the 9-*cis*-aldehyde **46**. Elongation of the aldehyde polyene chain of **46** was accomplished via condensation of ethyl 3,3-dimethylacrylate with base. When the base employed was sodamide, the 9-*cis* isomer **47** was favored, but, when potassium amide was utilized, the 13-*cis* configuration was favored, yielding the 9-*cis* and di-*cis* isomer of vitamin A acetate, **48**. Subsequent reduction of the respective esters afforded the alcohols **49** and **50**.

The method reported by Wendler et al. (Merck) is very similar to the approach used in our lab (Scheme 8).¹⁸ Starting with β -ionone **10**, the ethyl ester **51** was obtained via Reformatsky reaction with ethyl bromoacetate. Reduction with LiAlH_4 followed by oxidation with MnO_2 yielded the aldehyde as a 1:1 mixture of 9-*cis* and *all-trans* isomers. Elongation of the polyene chain of the 9-*cis*-aldehyde via a condensation reaction with acetone gave the ketone **55**, which was then converted to hydroxyl ester **56** via the Reformatsky reaction. Ester hydrolysis followed by dehydration yielded ATRA **1**, which could then be reduced with LiAlH_4 to afford retinol **8**.

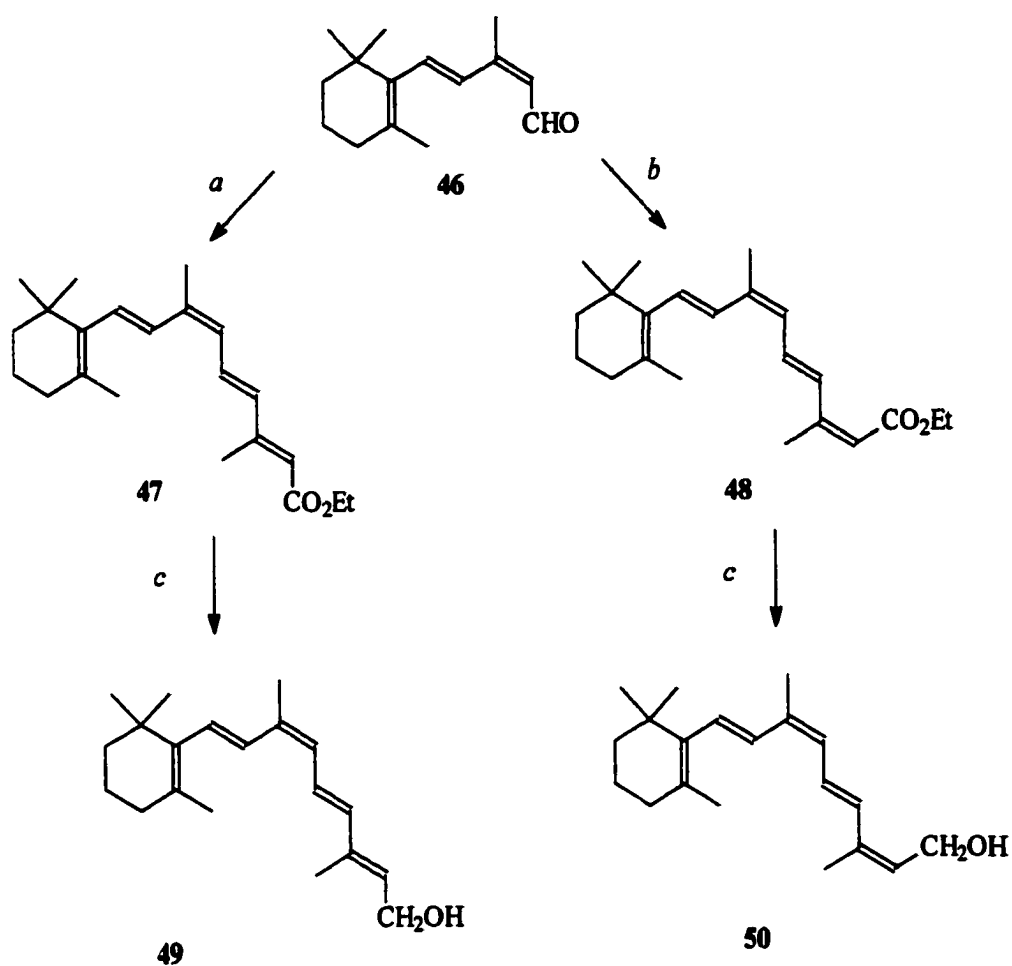
A less often utilized approach is the $\text{C}_9 + \text{C}_{11}$ approach (Scheme 9). Cheeseman and co-workers proposed the $\text{C}_9 + \text{C}_{11}$ synthesis starting with 2,2,6-trimethylcyclohexanone,¹⁹ and Attenburrow et al. successfully synthesized vitamin A using this approach.²⁰

Scheme 6. Preparation of the 9-*cis* and *All-trans* Isomers of β -ionylideneacetaldehyde^{17,a}

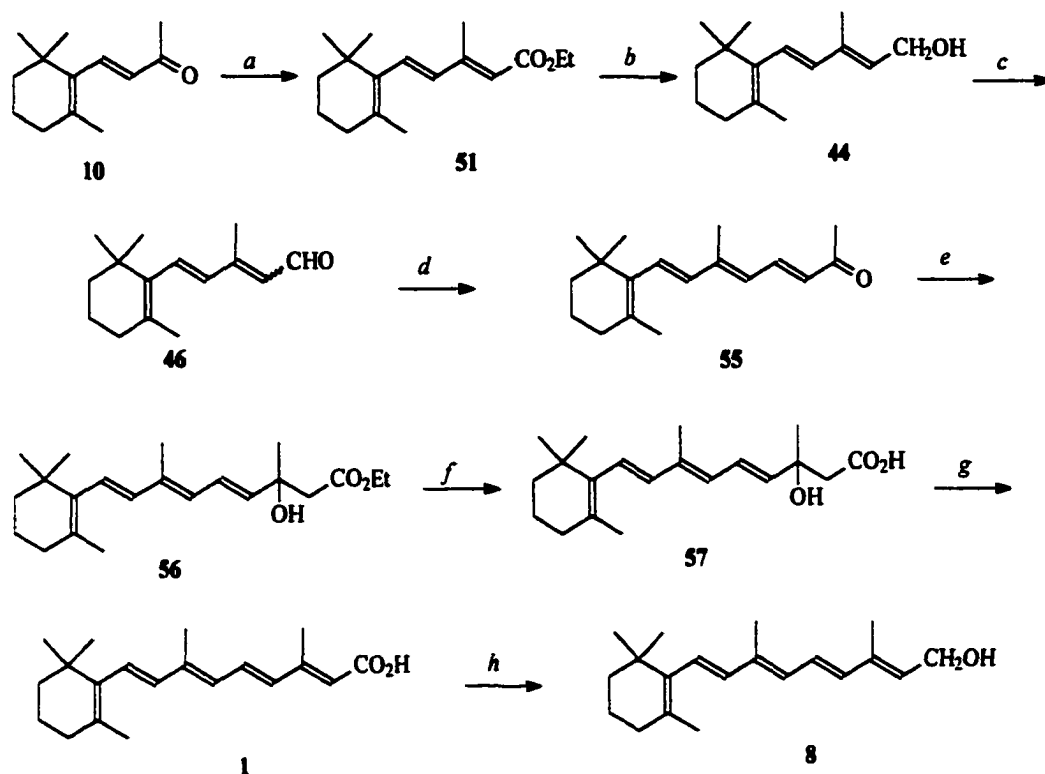


^a (a) Zn, BrCH₂CO₂Et, benzene; (b) (i) HCl, EtOH; (ii) 0.1 N KOH; (d) PCl₃, benzene; (e) LiAlH₄, ether; (f) MnO₂, ether.

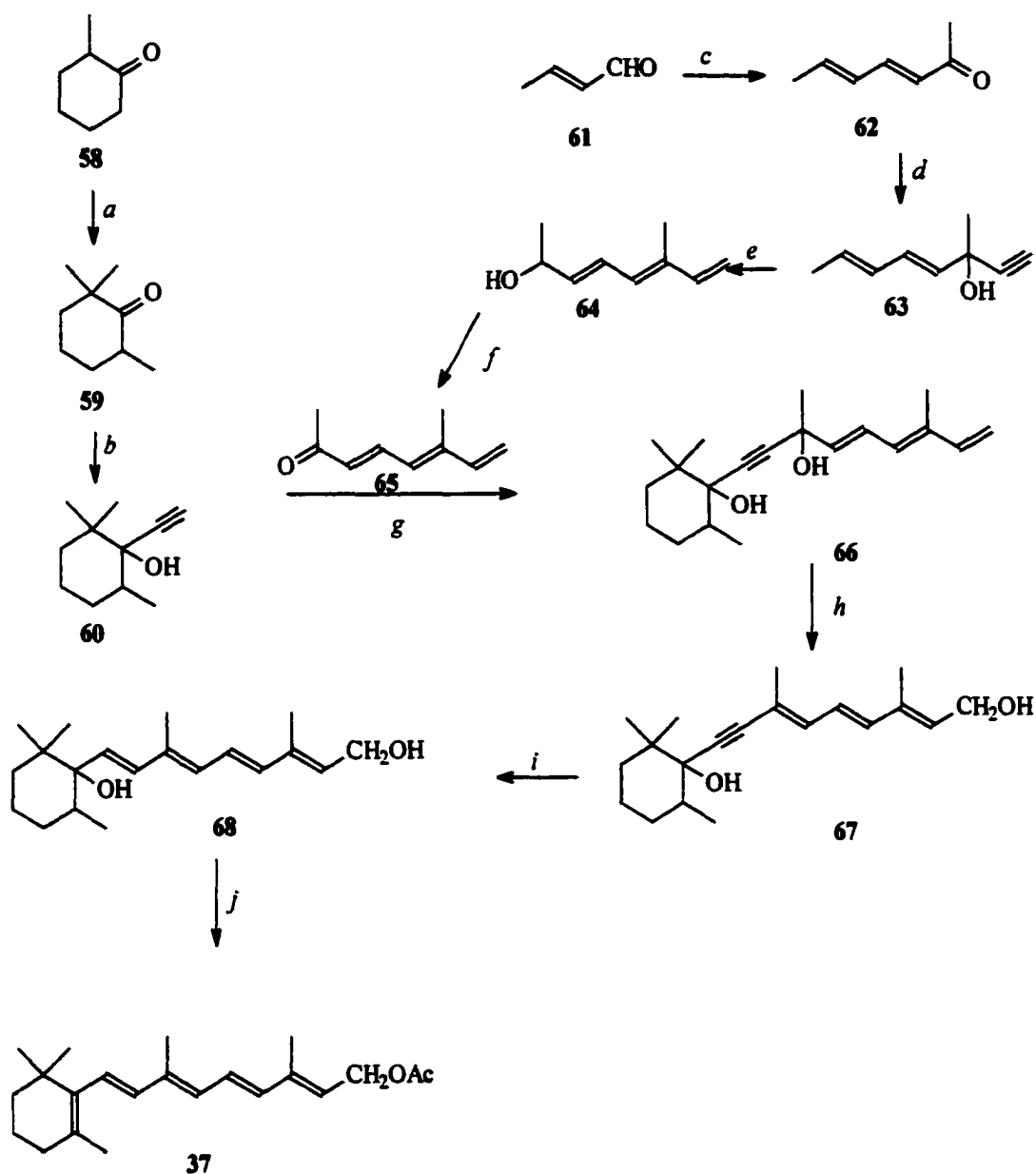
Scheme 7. Preparation of the 9-*cis* and 13-*cis* Isomers of Vitamin A^{2,a}



^a (a) ethyl 3,3-dimethylacrylate, KNH_2 , NH_3 , ether; (b) ethyl 3,3-dimethylacrylate, NaNH_2 , NH_3 , ether; (c) LiAlH_4 , ether.

Scheme 8. Merck's Synthesis of Vitamin A^{18,a}


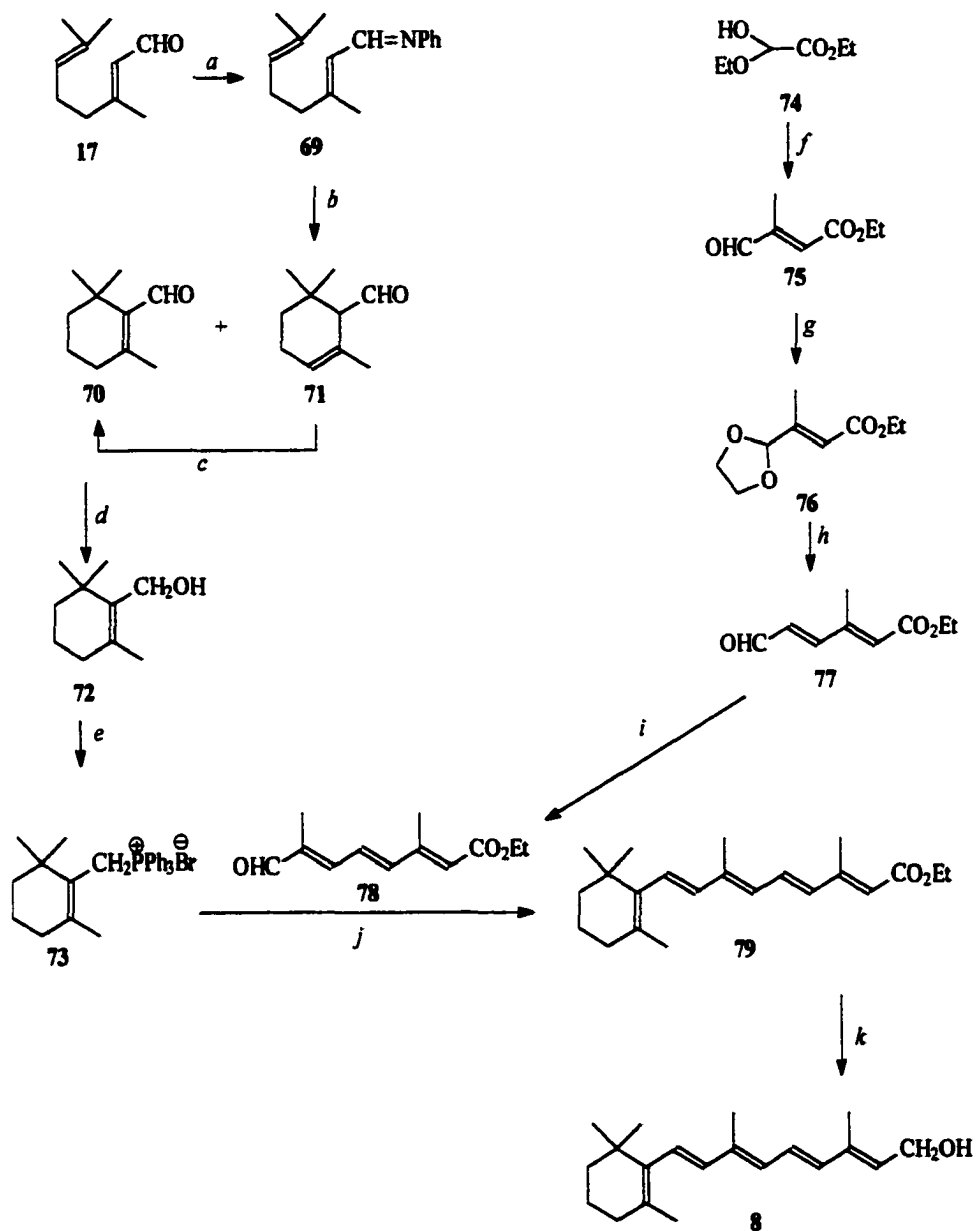
^a (a) Zn, ethyl 2-bromoacetate; (b) LiAlH₄; (c) MnO₂; (d) acetone, aluminum t-butylate; (e) Zn, ethyl bromoacetate, benzene; (f) 0.1 N KOH, ethanol; (g) I₂, petroleum ether, reflux; (h) LiAlH₄, ether, 0 °C.

Scheme 9. The C₉ + C₁₁ Convergent Synthesis^{19,20,a}

^a (a) NaNH₂, CH₃I; (b) NaNH₂, NH₃, acetylene; (c) acetone, Ba(OH)₂·8H₂O; (d) NaNH₂, NH₃, acetylene; (e) (i) H₂, Lindlar's catalyst; (ii) 0.05% H₂SO₄; (f) MnO₂; (g) EtMgBr, ether, benzene; (h) acetone, 0.1% H₂SO₄; (i) LiAlH₄, ether, reflux; (j) (i) acetic anhydride; (ii) p-toluenesulfonic acid, toluene, 80 °C.

This approach was developed due to the lack of a direct route from β -ionone. Starting with 2-methyl cyclohexanone **58**, the cyclohexanone ring was methylated twice when treated with two equivalents of methyl iodide and sodamide to yield 2,2,6-trimethylcyclohexanone **59**. Nucleophilic attack by acetylene on **59** afforded **60**. The polyene intermediates were prepared by first condensing 2-butenal (**61**) with acetone to give the ketone **62**. Reaction with sodium acetylide gave the ethynyl carbinol **64** that underwent partial hydrogenation and acid-catalyzed rearrangement to afford the trienone **65**. Grignard reaction of **65** with **60** gave the acetylenic diol **66**, which rearranged to yield the diol **67**. Reduction with LiAlH_4 followed by acid-catalyzed dehydration yielded vitamin A acetate **37**.

Another lesser-used approach ($\text{C}_{10} + \text{C}_{10}$) started with the readily available citral (Scheme 10).²¹ The conversion of citral (**17**) to the Wittig reagent first proceeded through the Schiff base **69** followed by ring-closure and hydrolysis of the imine, which resulted in a mixture of regioisomers **70** and **71**.²² The isomeric mixture could then be treated with KOH in ethanol to convert the β,γ -unsaturated aldehyde **71** to the α,β -unsaturated aldehyde **70**.²³ Reduction of **70** to the β -cyclogeraniol (**72**) and formation of the Wittig reagent resulted in **73**.²⁴ The polyene synthon was obtained in four steps. First, propionaldehyde was condensed with the hemiacetal of ethyl glyoxylate (**74**) to yield β -formylcrotonate (**75**).²⁵ Second, the aldehyde functionality was protected as a cyclic acetal **76**, and the alkene was extended via reaction with ethylvinyl ether in the presence of boron trifluoride etherate. The acetal of the diene **77** was hydrolyzed during work-up, thus necessitating the re-protection of the aldehyde **77**. Third, condensation of

Scheme 10. The C₁₀ + C₁₀ Approach^{21-24,a}


^a (a) aniline; (b) H₂SO₄; (c) KOH, ethanol; (d) LiAlH₄, ether; (e) PPh₃HBr, DMF; (f) (C₄H₉)₂NH, propanal; (g) ethylene glycol; (h) ethylvinyl ether, BF₃; (i) ethylpropenyl ether, BF₃; (j) NaH; (k) LiAlH₄, ether.

the diene acetal with ethylpropenyl ether yielded the triene acetal that was hydrolyzed to give the polyene synthon **78** used in the Wittig reaction with the Wittig reagent **73**.

Fourth, following the olefination of **73**, the ethyl ester was reduced with lithium aluminum hydride to give retinol **8**.

Retinoid Nuclear Receptors

Natural and synthetic retinoids exert control over cell processes by binding receptors that can then dimerize with other hormone nuclear receptors and bind DNA. This tertiary complex (retinoid/receptor/DNA) then interacts with co-regulators of the transcriptional machinery, which includes co-repressors and co-activators. There are two classes of retinoid nuclear receptors: retinoic acid receptors (RARs) and retinoid X receptors (RXRs). *All-trans* retinoic acid (ATRA) binds and activates only the RARs, while 9-*cis* RA binds and activates both the RARs and RXRs. The two subclasses of retinoid nuclear receptors (RARs and RXRs) are each comprised of three isoforms (α , β , γ).

The discovery of RAR α can be attributed to two groups who published their findings in December 1987. The Evans laboratory was searching for ligand-induced transcription factors related to the steroid and thyroid hormone receptors.²⁵ The steroid and thyroid receptors are members of the hormone superfamily of nuclear receptors. Among these nuclear receptors, the DNA-binding domains (DBD) are highly conserved. Using the DBD of the thyroid receptor as a probe, a cDNA library representing the human genome was scanned for related ligand-inducible receptors. A full-length cDNA was isolated with a similar DBD and ligand-binding domain (LBD) to the steroid and thyroid hormone receptors. In an attempt to identify the ligand that induced this new receptor, a

chimaeric receptor was formed by replacing the DBD of the new receptor with the DBD of the glucocortic receptor (GR). When this chimaeric sequence was expressed in cells, a hybrid receptor was obtained, which had a GR-independent promoter that was dependent on the new ligand, ATRA.

Chambon's group, the co-discoverers of RAR α , proposed that RA mediated its effects not through the cytosolic retinoic acid binding proteins (CRABPs) but via nuclear receptor binding. This group proposed that the RA nuclear receptors were members of the nuclear hormone superfamily.²⁶ A cDNA library derived from the poly-(A⁺) RNA from MCF-7 and T-47D cells (breast cancer cell lines) was screened with three different probes. These probes possessed the sequence of the DBDs of the human estrogen receptor (hER), human prostaglandin receptor (hPR), and the human glucocortic receptor (hGR). In order to identify the ligand that induced the new receptor, a fragment from the clone was inserted into an expression vector and introduced into HeLa cells. Prospective radiolabeled ligands were added, and ATRA had high binding affinity for the receptor.

Two groups were credited with the discovery of RAR β .^{27,28} Prior to that discovery, Dejean et al. were studying the hepatitis B virus (HBV) integration site due to the involvement of HBV in liver oncogenesis.²⁹ Sequencing of DNA from human hepatocellular carcinoma (HCC) cells revealed that adjacent to the HBV sequence was a sequence similar to the DBD for a hormone nuclear receptor such as hGR or hER. This gene encodes for a protein that they termed *hap*. In order to test whether or not the *hap* protein was a retinoid receptor, a chimaeric receptor was created by replacing the DBD of the new receptor with the DBD of hER. The *hap*-ER chimaera was then tested for its ability to transactivate the estrogen-responsive reporter gene (*vit-tk-chloramphenicol acetyl-*

transferase [CAT]) in the presence of various ligands including retinol, retinal, retinyl acetate, and ATRA. CAT activity was induced by ATRA, which does not come as a surprise considering the LBD of the new receptor shares 90% homology with RAR α . Since this was the second retinoid receptor discovered, it was named RAR β .

The third retinoid receptor, discovered by Chambon and co-workers in 1989, was first found in mice by screening a cDNA library with mRAR α and mRAR β probes.³⁰ Upon sequencing of the clones, they found that the new receptor (RAR γ) had six distinct domains (A-F), and the DBD (domain C) and the LBD (domain E) were very similar to those regions in both RAR α and RAR β . This suggested that RAR γ was induced by the same ligand as the other RARs as well as binding the same response elements. This same group later reported the isolation and characterization of hRAR γ , which is mainly expressed in the skin.

Evans and co-workers were also searching for additional hormone nuclear receptors by performing low-stringency screening of a cDNA library obtained from human liver and kidney.³¹ The probe was a cDNA fragment encoding the RAR γ DBD. After sequencing the clones, it was found that one of the clones encoded for a new receptor. The sequence of the DBD shared 61% homology with the RARs, but, surprisingly, the LBD only shared 27% homology with RARs, indicating that ATRA may not be the ligand for this new receptor. The new receptor was tested to see if it would induce transcription by transfecting cells with the TRE β promoter (thyroid response element) and a CAT reporter gene. Schneider (S2) cells were used because they did not contain endogenous retinoid receptors. The cells were treated with a variety of ligands including ATRA, which elicited a 100-fold induction of CAT activity. This level of induction was not as

substantial as found for the RARs, and ATRA was not considered to be the physiological ligand for the nuclear receptor. This receptor was named RXR since it had no associated ligand as of yet.

The high-affinity ligand for RXR was subsequently identified by Heymann et al. at Ligand Pharmaceuticals³² and Levin et al. at Hoffman LaRoche.³³ S2 cells were treated with radiolabeled ATRA, and, following incubation for 24 h, the cells were harvested and extracted with organic solvent. The extract was fractionated by high pressure liquid chromatography (HPLC), and the different fractions were then assayed for their ability to activate RXR. This assay involved transfection of cells with an expression plasmid for RXR α and a luciferase reporter plasmid under the control of a promoter containing an RXRE (RXR response element). The fraction that induced the luciferase activity was then characterized.

First, the compound was treated with diazomethane and injected on HPLC. Diazomethane methylates carboxylic acids to form methyl esters. Reverse-phase HPLC was used to measure any change in the retention time (R_t) between the original compound and the diazomethane reaction product. No change in R_t would indicate that the compound did not possess any carboxylic acid functionality, but an increase in R_t would indicate that the original compound did have a carboxylic acid group that was methylated when treated with diazomethane. The methylated compound was then analyzed by gas chromatography/mass spectrometry (GC/MS) and the spectrum revealed a molecular ion at 314 corresponding to the methyl ester of RA. When the retention times for the various stereoisomers of RA were compared, it was revealed that the RXR ligand was 9-*cis* RA, which is a stereoisomer of ATRA.

The manner by which the nuclear receptors interacted with DNA was still not well understood until Evans' group and Pfahl's group discovered that RXR interacts with other nuclear hormone receptors as a heterodimer to induce transcription. Evans and co-workers observed that the C-terminal sequences of RAR and RXR contained regions necessary for homo- and heterodimerization.³⁴ Gel mobility shift experiments were utilized with *in vitro* synthesized RAR and RXR and a radiolabeled oligonucleotide encoding the CRBP-II-RXRE. RAR in the absence of RXR failed to bind the RXR response element CRBP-II-RXRE. Similarly, RXR failed to bind the response element when RAR was absent. Therefore, both RAR and RXR were required for DNA-protein interaction. They also observed that RXR was necessary for both the vitamin D receptor (VDR) and thyroid hormone receptor (TR) to bind to their DNA response elements. Therefore, RXR heterodimerizes with other nuclear receptors, including RAR, VDR, and TR, to induce transcription.

Pfahl et al. also were attributed with this discovery, since they observed via a gel shift mobility assay that TR α DNA binding was greatly enhanced in the presence of RXR α .³⁵ Other nuclear hormone receptors, including RAR α and ER, did not enhance DNA binding. They also observed that RXR α enhanced the binding of RAR α , β , and γ , which lead them to postulate that RXR α heterodimerizes with other nuclear hormone receptors in order to bind to various response elements and thus induce transcription. Pfahl and co-workers were also credited with the discovery that RXRs homodimerize.³⁶ As mentioned previously, RXR did not bind effectively to TREp and required either TR or RAR. However, DNA binding of RXR in the absence of either RAR or TR was increased dramatically when treated with 9-*cis* RA. Thus, 9-*cis* RA induced RXR

homodimer binding to TREp. Other response elements were tested for RXR homodimer binding, and it became apparent that the RXR homodimer did not bind to the same response elements as the heterodimer.

Each nuclear retinoid receptor can be divided into six domains labeled A through F.^{37,38} Domain C contains the DBD and is highly conserved among the receptor subtypes (Figure 4). The specific sequence that is recognized by the activated receptor complex is referred to as a retinoic acid response element (RARE) or the RXRE.

The DBD contains eight conserved cysteine residues, which interact with two zinc ions to form two helix-loop-helix zinc finger domains. These domains interact with the bases in the DNA response element. The structures of the DBDs have been determined for both RAR and RXR α .^{39,40} In the case of RXR α , one Zn²⁺ complexes to Cys 135, 138, 152, and 155; the second zinc ion is complexed to Cys 171, 177, 187, and 190 to form the second zinc finger.⁴¹

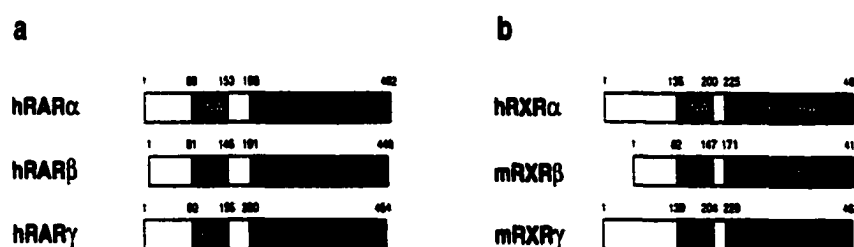


Figure 4. Comparison of sequence homology between the LBDs and DBDs of the retinoid receptors.

These zinc fingers of the DBD interact with the hormone response elements (HREs) of DNA. There are three types of HREs, which include the direct repeat,

palindrome, and complex response elements. The direct repeat elicits the strongest transcriptional response and is the most common response element. Selective recognition of HREs is accomplished through variable spacing between the half site repeats.⁴² Those HREs composed of direct repeats have a core sequence AGGTCA with variable spacing between the repeats. Direct repeats (DR) with spacers of 3, 4, or 5 nucleotides, commonly known as DR-3, DR-4, and DR-5, serve as the preferred response elements for the VDR, TR, and RAR, respectively, and this pattern is referred to as the “3-4-5 rule.”

Further, by screening the GenBank database for DRs separated by variable numbers of nucleotides, both the DR-1 and DR-2 response elements were discovered. Those repeats separated by only one nucleotide (DR-1) are recognized by hormone nuclear receptors RXR and the peroxisome proliferator activating receptor (PPAR), while, in addition to DR-5, RAR also recognizes those repeats separated by two nucleotides (DR-2) and the DR-5 response element. Another type of response element, the palindromic HRE, is less responsive to RA than the direct repeat HRE, which requires an overexpression of RAR to be active. An example of a palindromic HRE is TRE-pal, a synthetic HRE commonly used in the *in vitro* assay to screen compounds for transcriptional activation activity.⁴³

Highly conserved Region E possesses the LBD as well as activation function AF-2, a ligand-dependent transcription activation factor. The A and B regions of the receptors contain AF-1, which is a ligand-independent transcription activation factor. The B region is conserved, but the A regions among receptor subtype isoforms are unrelated. Region D is highly conserved, but its function is not well understood. Region F is also not well understood and is not present in the RXRs.

In the case of the RARs, either ATRA or 9-*cis* RA bind the LBD of the receptor, which can then interact with an RXR receptor to form a heterodimer (RAR/RXR). In the case of the RXRs, 9-*cis* RA binds and activates the receptor to form either a heterodimer (RAR/RXR) or a homodimer (RXR/RXR). In solution, the RXR receptor does not exist as a monomer prior to dimerization but as a tetramer. Binding of 9-*cis* RA to RXR causes a conformational change to take place, which causes the tetramer to dissociate into dimers and monomers.⁴⁴ *In vitro* studies have shown that RXR LBD self-associates into tetramers with high-affinity ($K_d = 4\text{--}5\text{ nM}$ for dimer-dimer association). At endogenous levels of 9-*cis* RA, tetrameric RXR was the most prevalent oligomeric form. Because the tetramer is transcriptionally inactive, it was suggested that the first step in the activation of RXR is the ligand-induced dissociation of the tetramer.⁴⁵ Only after binding with 9-*cis* RA does the tetramer dissociate to form heterodimers.⁴⁶ This theory was consistent with the transcriptional activities of RXR mutants with altered properties.⁴⁷ The first example had an R321A mutation with a tetramer that failed to dissociate upon ligand binding and was thus transcriptionally inactive. The second example was the F318A mutation that failed to form a tetramer and was transcriptionally active even in the absence of ligand. Therefore, the formation of the tetramer was vital for transcriptionally active RXRs.

The importance of the tetramerization domain was studied by mutation of three phenylalanine residues located in helix 11(H11).⁴⁵ Mutation of these residues was capable of disrupting the tetramer but did not affect the formation of dimers, binding of ligand, or DNA binding by the receptor. Therefore, because these mutations abolished transcriptional activity, tetramer dissociation was implicated in transcriptional regulation of the RXRs and serves as the first step in signaling by RXR.⁴⁷

The question remained as to exactly how ligand binding induced tetramer dissociation. Bourget et al. suggested an auto-repression mechanism whereby the AF-2 helix of the tetramer blocked co-activator binding by occupying the co-activator site of the adjacent dimer.⁴⁸ Gampe et al. obtained the crystal structure of the RXR tetramer in both the apo and holo forms.⁴⁹ The tetramerization interface was composed of three interactions: the H3/ H3 interface, the H11/ H11 interface, and the AF-2/co-activator binding site interface. In the unbound structure, the AF-2 helix protruded outward from the LBD to occupy the co-activator binding site of the corresponding monomer in the adjacent dimer. The amino acid sequence between 451 and 455 of LMEML is homologous to the LXXLL motif (L = leucine, X = any amino acid) required for co-activator recognition. Knowing the interactions necessary for tetramer formation helps explain why binding of 9-*cis* RA would disrupt these interactions. In the first step, upon binding of 9-*cis* RA, the β -ionone ring of RA in the ligand-binding site interacts with H11 and causes it to rejoin with H10 to form an uninterrupted helix. In the second step, the amino end of H3 collapses into the void left by H11 and H10, still allowing a substantial binding site for 9-*cis* RA between H3, H4/5, and H10/H11. In the third step, the AF-2 helix rotates back against the main body of the LBD. The tetramer interface, which consists of interactions between H3, H11, and the AF-2 helix, would be disrupted by these conformational changes.

RARs interact with both co-activators and co-repressors. Prior to ligand binding, RAR interacts with co-repressors to suppress basal level transcription. Interestingly, ligand binding is not necessary for co-repressor binding, while ligand association is required for co-activator recruitment. It has been suggested that the co-repressor α -helix

extends three residues longer in the amino-terminal direction than the co-activator helix. Thus, the co-repressor helix fills some of the space usually occupied by the AF-2 helix of RAR.⁵⁰ When a co-repressor is associated with a nuclear receptor such as RAR, histones are deacetylated, which leads to a suppression of transcription. Dissociation of the co-repressor allows for acetylation of the histones, and transcription can proceed.⁵¹ In contrast, agonist binding of RXR does not affect the release of a co-repressor; in fact, there is no evidence that co-repressors bind RXR at all.⁵²

There are several types of co-repressors, and two of the most common are SMRT (silencing mediator for retinoid and thyroid hormone receptors) and N-CoR (nuclear receptor co-repressor), which exert their repressive effects through the recruitment of histone deacetylase complexes.^{53,54} SMRT and N-CoR contain two interaction domains (ID1 and ID2) with the consensus sequence (I/L)XX(I/V)I that interacts with the LBD of nuclear receptors.^{55,56} Agonist binding of RAR releases the co-repressor, and the co-activator is recruited. In contrast, antagonist binding of RAR does not disrupt co-repressor binding, thus explaining why an antagonist does not induce transcription.⁵⁷

The holo-structure of ATRA bound to RAR γ -LBD (Figure 5) was published in 1995 illustrating that a significant conformational change occurs upon ligand binding.⁵⁸ Although the structure of apo-RAR γ -LBD was not known, the structure of apo-RXR α -LBD was available (Figure 6).⁴⁸ The LBD of RAR γ , like RXR α and most members of the nuclear receptor (NR) superfamily, was composed of 12 helices (H1-12) and a β -turn, which together formed a sort of α -helical “sandwich,” a fold described previously for apo-RXR α -LBD. The carboxylate of ATRA served to guide the ligand into the hydrophobic cavity of the LBD via hydrogen-bonding interactions. The first carboxyl oxygen

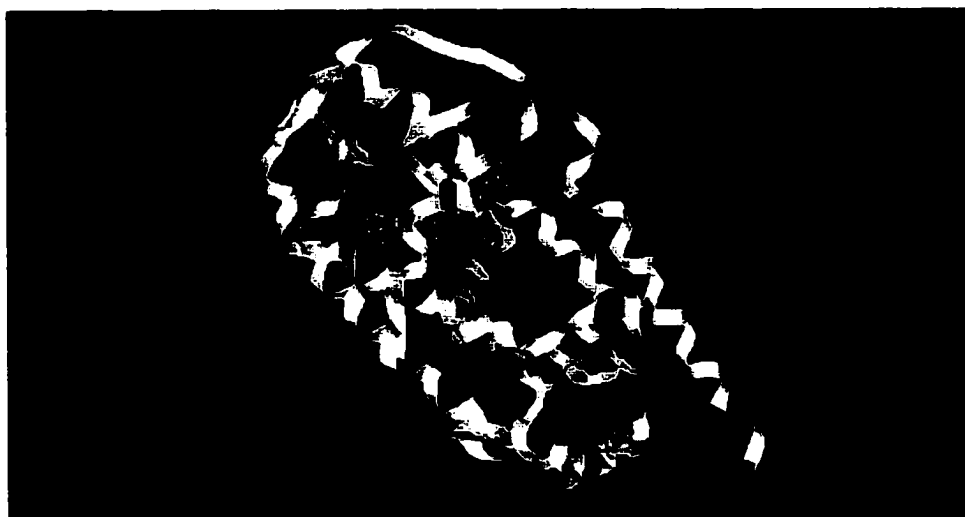


Figure 5. Structure of ATRA bound to RAR γ .

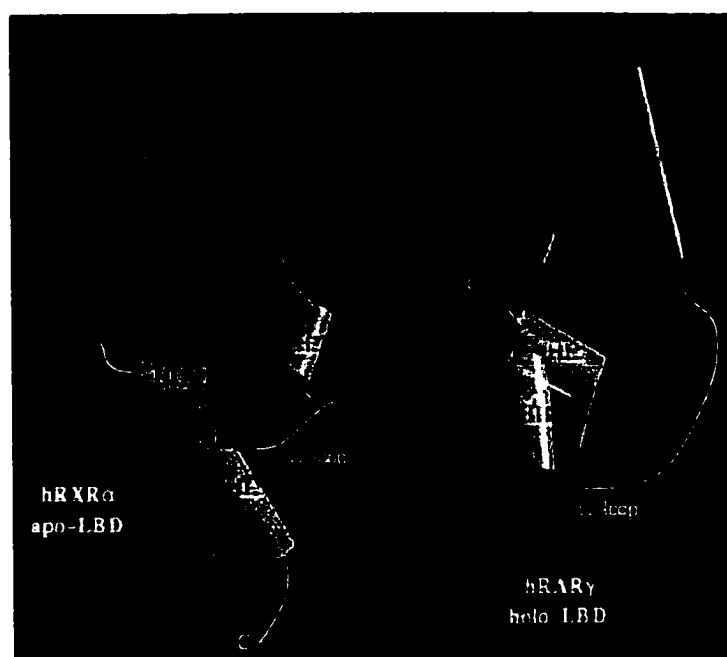


Figure 6. Comparison of the position of H12 in the apo- and holo-conformations.⁴⁸

hydrogen-bonds to both the guanidine of Arg278 and the hydroxyl of Ser289. The second carboxyl oxygen hydrogen-bonds to the amino groups of both Ser289 and Lys236. After these hydrogen-bonding interactions had secured the ligand in the hydrophobic pocket, Lys264 formed salt bridges with Glu414 and Glu417 of H12 in order to seal the cavity. This conformational change of H12 was referred to as the “mouse-trap” mechanism that was commonplace among hormone nuclear receptors. In fact, it has been proposed that H12 of the various NRs are interchangeable. For example, replacement of H12 of RAR with the H12 of RXR does not alter transcriptional activation via ligand binding to the individual receptor.⁵⁹ This conformational change of H12 was significant because the AF-2 core (the ligand-dependent transcription factor) was located on H12. The carboxyl terminal AF-2 core served to interact with certain co-activators and co-repressors.

Upon binding of an RAR agonist to the RAR receptor, the co-repressor is released, and a co-activator is recruited that interacts with the transcriptional machinery. The co-activators interact with NRs via an LXXLL signature motif (X signifies any amino acid). Each co-activator has three of these sequences or interaction domains (LXD1, 2, 3), with varying sequences intervening.^{60,61} As stated before, the AF-2 core is located on H12 in domain E where the binding sites for the co-repressor and co-activator overlap.⁶²

When agonists bind NR and H12 is properly oriented for activation, the AF-2 helix is able to interact with the helical motifs of the putative LXXLL domains for the co-activators. This is possible through the interaction of the LXXLL motif(s) with the “charge clamp” formed by the AF-2 core. This charge clamp refers to the conserved glu-

tamic acid residue in AF-2 at position 471 and the lysine residue in H3 at position 301, which hydrogen-bond to the leucines of the LXXLL motif of the co-activator. The glutamic acid (E471) hydrogen bonds to both the backbone amide of leucine in position 1 of LXXLL and the amino-terminal adjacent residue. The leucine of H3 (K301) is hydrogen-bonded to the backbone carbonyl of leucines in positions 4 and 5 of the LXXLL motif.⁶³ A critical determinant of co-activator binding is the length of the LXXLL helix, which fits precisely between the conserved glutamic acid and lysine residues upon the closure of the H12 in presence of ligand. Ligand and receptor-dependent specificity for co-activator binding are determined by residues flanking the LXXLL core motif.^{61,64} In addition, different receptors interact with varying numbers of LXDs. The sheer number of co-activators is overwhelming and beyond the scope of this introduction, but the topic has been reviewed.⁶⁵

Biological Assays

The discovery that retinoids can prevent the transformation of normal cells to the malignant state has enhanced interest in retinoids as potential pharmaceutical agents for cancer therapy and prevention.⁶⁶ However, ATRA at pharmacological doses exhibits toxic side effects such as retinoid dermatitis, hypertriglyceridemia, bone spurs, liver toxicity (cirrhosis), teratogenicity, and neutropenia.⁶⁷ Because the natural retinoids cannot be administered in sufficient doses to have chemopreventive effects without exhibiting toxic systemic side effects, efforts were directed to the synthesis of structurally altered analogs of the natural retinoids.^{68,69} In order to test the biological activity of these analogs, a rapid screening procedure was needed.

Retinoids have been screened using various *in vitro* and *in vivo* methods to assess their efficacy in preventing and reversing neoplastic transformation. The hamster tracheal organ culture (TOC) assay was an early *in vitro* assay that was sensitive and quantitative, and it was applicable to screening large numbers of retinoids.⁷⁰ One advantage of the TOC assay was that the medium was serum-free and hence did not contain endogenous retinoids. The TOC assay was a measure of the physiological induction of differentiation, and the results are sensitive and reproducible due to the simple scoring procedure used. The effects of retinoid deficiency on tracheobronchial epithelium in experimental animals and its reversal by administration of diets containing active retinoids have been described.^{71,72} Keratinizing squamous metaplasia of the normal mucociliary epithelium was the most distinctive lesion of retinoid deficiency in the trachea. The normal epithelium becomes undermined by the new stratified squamous keratinizing epithelium, and the distinctive keratohyaline granules can be seen before the development of sheets of keratin. The histological endpoint of the TOC assay was the presence or absence of dark purple keratohyaline granules and bright pink keratin.

Another of the *in vivo* assays utilized for screening retinoids was the ornithine decarboxylase (ODC) assay, which has been studied extensively by Verma and Boutwell.⁷³ Retinoids inhibit the induction of ODC in mouse epidermis that has been treated with a tumor promoter such as a phorbol ester. Therefore, the ODC assay was considered rapid assay for developing structure-activity relationships, thus leading to structural modifications of the retinoid skeleton that could enhance chemopreventive activity.

Increased polyamine synthesis is an essential requirement for normal cell growth as well as malignant transformation.^{74,75,76} ODC catalyzes the transformation of ornithine

to putrescine, which is the rate-limiting step in the biosynthesis of polyamines. ODC activity is higher in those cells and tissues induced to proliferate, thus ODC activity is considered a marker for tumor promotion. A tumor promoter such as 12-*O*-tetradecanoylphorbol-13-acetate (TPA) was administered topically to the shaved skin of mice. The retinoid was also applied topically to the skin of mice in the treated group just prior to TPA application. After 4.5 h, the mouse was sacrificed, and the skin was removed, homogenized, and centrifuged briefly to obtain a clear extract. The ODC activity was determined from the extract by measuring the release of labeled CO₂ from [¹⁴C]-ornithine.⁷⁷ Another useful *in vivo* assay is antipapilloma assay, which is based on the two-step model of skin carcinogenesis. In this assay, the shaved mouse skin is first treated with a chemical carcinogen such as 7,12-dimethylbenz[*a*]anthracene (DMBA) to initiate cancer followed by repeated application of a tumor promoter such as TPA. Once the tumor promoter has been administered repetitively, promotion occurs and tumors appear in the epidermis of the mouse skin.^{78,79} Continued retinoid treatment during the promotion phase prevented tumor appearance in a dose-dependent manner. However, many of the papillomas were benign, and only a few proved malignant. Therefore, the results obtained from the papilloma regression assay were variable unless extreme care was taken in this assay.

Early Synthetic Retinoids

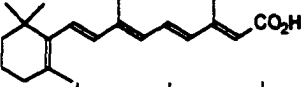
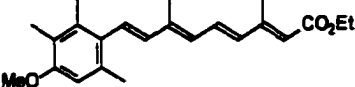
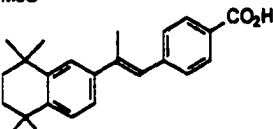
Structural modifications were made to the retinoid skeleton in the ring, polyolefinic chain, and the polar terminus of RA. These modifications were made to prevent metabolism to a less active species, to restrict conformational mobility in order to obtain

a structure with the optimum conformation for putative protein or receptor binding, to reduce toxicity by changing lipophilicity, and to provide prodrugs that could be metabolized to the active species.

A retinoid of appreciable significance, ethyl (E)-4-methoxy-2,3,6-trimethylphenyl-3,7-dimethylnonatetraenoate (Etretinate), was introduced by Hoffman-LaRoche for the treatment of psoriasis and other skin diseases.⁸⁰ Shown in Table 2, this retinoid decreased the conformational freedom of the cyclohexenyl ring by replacing it with a substituted phenyl ring. Etretinate inhibited the growth and caused marked regression of chemically induced papillomas and carcinomas in mice. Although Etretinate was less toxic than ATRA, hypervitaminosis A was a side effect associated with Etretinate therapy, and the poor therapeutic ratio limited treatment only to those patients with severe psoriasis.^{80,81} Therefore, further structural modifications were required to reduce toxicity.

Because there was free rotation about the single bonds in the polyene chain, the natural retinoids could exist in several different conformations. Coupled with the fact that the crystal structures of the receptors were unavailable, the active conformer of RA was a matter of conjecture. Hence, the active conformation could only be elucidated by conformationally constraining some of the rotatable bonds. The retinoid research group at Hoffman-LaRoche investigated the conformational restrictions of the polyene portion of the retinoid skeleton, which led to 4-[2-(5,6,7,8-tetrahydro-5,5,8,8-tetramethyl-2-naphthalenyl)-1E-propenyl]benzoic acid (TTNPB) (Table 2).⁸² TTNPB is a 4-substituted benzoic acid in which the 5,7E- and 11,13E-double bond systems of RA were restricted to *s-cis* conformations by including those bonds in an aromatic ring system. In addition,

Table 2. *In Vivo* Activities of ATRA, Etretinate, and TTNPB

retinoid	structure	ED ₅₀ (M)	ID ₅₀ (nmol)	papilloma regression ID ₅₀ (μmol/kg/day)
ATRA		1×10^{-11}	0.04	1330
Etretinate		NR ^a	12.8	40
TTNPB		2×10^{-12}	0.03	2.3

^a NR: not reported.

oxidative metabolism leading to compounds of reduced biological activity was blocked at the 5-position of the tetrahydronaphthalene ring.⁸³ TTNPB had greater activity than ATRA in the TOC assay ($ED_{50} = 1 \times 10^{-12}$ M) and inhibited the formation of papillomas by 91%, which is 500 times more active than ATRA at an equivalent dose. However, TTNPB was very toxic and produced hypervitaminosis A at doses of 0.1 mg/kg body weight/day, which was several orders of magnitude lower than ATRA. In a separate study, doses of 0.04 mg/kg/day caused weight loss in a dose-dependent manner and resulted in signs of hypervitaminosis A, such as hair loss, redness and scaling of the skin, and excessive mucous secretion in the nasal and oral passages.⁸⁴ Although extremely toxic, TTNPB proved useful as a template for the design of other retinoid analogs by replacing the tetraene chain with an aromatic ring system.

Dawson et al. sought to block metabolic deactivation of the synthetic derivatives.⁸⁵ By blocking metabolic deactivation of the synthetic retinoids, the therapeutic

dose would be expected to decrease, and toxicity would also decrease. Some metabolites of RA are shown in Figure 7. A major pathway for metabolic deactivation was allylic oxidation at the 4_R position of the β-cyclogeranylidene ring (91) of ATRA as well as oxidation of the 5_R-methyl group (92).

Therefore, modifications were made in the region of the 5,6_R double bond to reduce the allylic nature of the 4_R protons, which resulted in the 2-norbornenyl retinoid 94, as shown in Table 3. However, this analog was very unstable, and the 5,6_R double bond

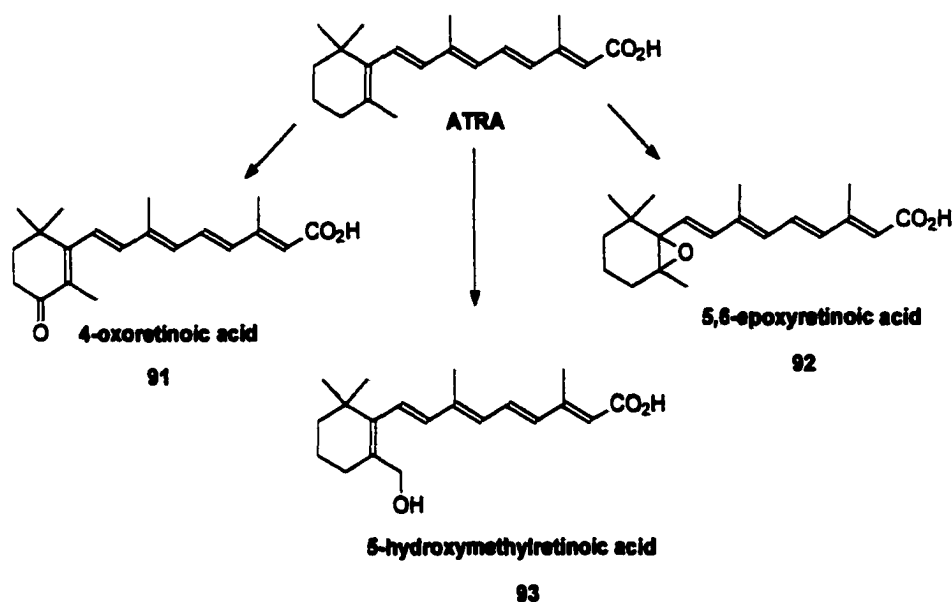


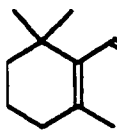


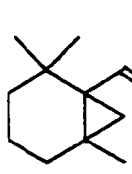
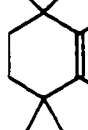
Figure 7. Metabolites of ATRA.

was changed to a saturated bond (95). Another analog designed to prevent the formation of metabolites such as 4-oxoretinoic acid (91) was 97 in which a cyclopropyl ring was substituted at the 4-position to yield a spiro system. Dawson et al. also designed analogs of the 5,6-epoxy retinoic acid (92) where the 5,6_R double bond was replaced by a cyclo-

propyl ring to yield a carbocyclic analog (**96**). The carbocyclic analog **96** had activity comparable to that of ATRA in the ODC assay (90 ± 2 % inhibition).

The discovery that a benzoic acid terminated retinoid had high activity in cell differentiation assays was a salient point in the development of synthetic retinoids.^{86,87} Dawson's group was the first to report benzoic and naphthalene-carboxylic acid terminated retinoids where the 9,10 and 11,12 bonds were included in an aromatic ring system. As shown in Table 4, the first conformationally restricted retinoid, 4-[2-methyl-4-(2,6,6-trimethyl-1-cyclohexenyl)-1*E*,3*E*-butadienyl]benzoic acid (**98**), had significant biological activity in the TOC ($ED_{50} = 3 \times 10^{-10}$ M).⁸⁸ The purpose of synthesizing retinoid **98** was to investigate the effect of varying the distance between the β -cyclogeranylidene ring and the polar terminus. The benzoic acid terminus of **98** replaced the 11*E*, 13*E*-double bond system of RA, affording a 12-*cis*-locked retinoid that possessed comparable activity to ATRA. Additional conformational restriction was achieved by incorporating the 9,10 bond in a naphthalene ring system (**99**), which decreased activity compared to **98** in the ODC assay. This suggested that conformational flexibility about the 9,10 bond was necessary for retinoidal activity. However, when 5_R- and 7_R-conformational restrictions were incorporated into **99** to yield **100**, TOC activity was improved by 100-fold.⁸⁹ Therefore, conformational restriction about the 7,8_R double bond locking it into a 7-*s-trans* conformation enhanced retinoidal activity. Even though these synthetic retinoids showed retinoidal activity, none were as active as TTNPB (Table 4). Upon *in vivo* testing in mice, it was discovered that TTNPB was more toxic than ATRA or any other synthetic retinoid. In an effort to retain retinoidal activity while minimizing toxicity, heterocyclic analogs were designed and synthesized (**101** and **102**).⁹⁰

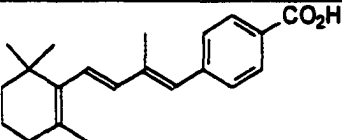
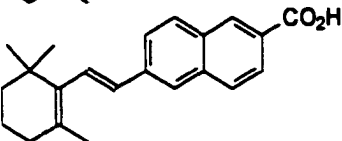
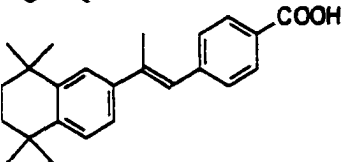
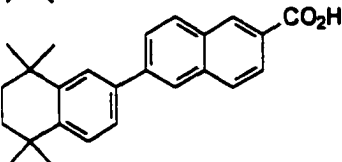
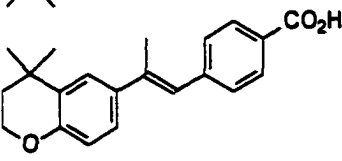
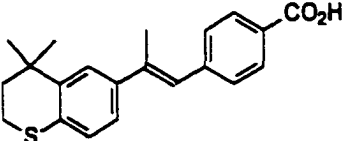
Table 3. Summary of Dawson's Retinoids with Modified Rings on TPA-Induced Mouse Epidermal ODC Activity

compound	structure	TPA (nmol)	% inhibition
ATRA		1.7	92 ± 2
94		17	64 ± 1
95		17	54 ± 10
96		1.7 17	90 ± 2 90 ± 0
97		17	72 ± 2

Replacement of the carbon at the 1-position with either an S or an O was based on an observation made by Huisman et al., who reported that, although (*E*)-4-thiaretinyl acetate had 5% of the growth potency of (*E*)-retinyl acetate in chickens, it had 18% of the liver storage capacity and was less toxic.⁹¹ Therefore, similarly substituted analogs of TTNPB may retain activity but have reduced toxicity.

These analogs (98-102) were tested for *in vivo* activity. Even though the 1.7 nmol dose of TTNPB decreased the number of tumors by 92% in the antipapilloma assay, the animals displayed signs of hypervitaminosis A toxicity, including skin redness and scaling and hair loss. The 17 and 170 nmol doses of TTNPB caused death during the experi-

Table 4. ODC Assay Results for Dawson's Benzoic Acid and Naphthalene Carboxylic Acid Terminated Retinoids

retinoid	structure	TOC ED ₅₀ (M)	ODC % inhibition
98		3×10^{-10}	77 ± 6
99		1×10^{-10}	48 ± 1
TTNPB		1×10^{-12}	91 ± 1
100		3×10^{-12}	80 ± 3
101		2×10^{-10}	81 ± 2
102		5×10^{-11}	85 ± 2

ment. The naphthalene carboxylic acid **100** almost completely inhibited papilloma formation at the 170 nmol dose accompanied by some signs of hypervitaminosis A toxicity; however, ATRA decreased the number of papillomas by 90% at the same dose without the appearance of side effects. Therefore, this particular retinoid was more toxic than ATRA, which defeated the purpose of synthesizing analogs of ATRA. The heterocyclic analogs of **101** and **102** prevented tumor formation by 94% and 93%, respectively, at the

170 nmol dose, and no toxic symptoms were observed in the animals. Therefore, 101 and 102 were less toxic than ATRA and had potential in the treatment of proliferative skin diseases.

Breitman et al. showed that HL-60 cells are induced to terminally differentiate when exposed to ATRA. HL-60 cells, obtained from the blood of a patient who was re-diagnosed with acute promyelocytic leukemia (APL), proliferate continuously and consist mainly of promyelocytes.⁹² Stimulation with TPA followed by treatment with the retinoid causes HL-60 cells to differentiate and to produce superoxide anions (O_2^-). Following incubation of the resulting culture with nitro blue triformazan (NBT), an aliquot of the culture was applied to a microscope slide and stained with Wright-Giesma stain. Superoxide reduces NBT to produce cell-associated nitro blue diformazan (NBD) deposits. By counting the number of cells with blue deposits (%NBD⁺), the percent of differentiated cells was determined. In general, the more potent the retinoid in inducing differentiation, the higher the percent NBD⁺.

Shudo's group was among the first to introduce retinoids that induced differentiation of leukemia cells using the NBT assay. Using TTNPB as a lead compound, Shudo's group designed analogs where the dihydronaphthalene ring of TTNPB was replaced by substituted phenyl rings.^{93,94,95} In addition, the linker region between the two aromatic rings was varied using amide, ketone, and azo functionality. Shudo reported an amide analog of TTNPB, Am80 (Figure 8 and Table 5), that induced differentiation of promyelocytes to granulocytes in the HL-60 *in vitro* assay (87% NBD⁺). This value was comparable to that of ATRA (85%). Methyl substitution of the nitrogen of the amide bond (Am90, Figure 8) obliterated activity. This could be explained by the conformation about

the amide bond in each of these analogs. Spectroscopic analysis of Am80 and Am90 revealed that the amide bond of the unsubstituted analog Am80 was *trans*, while the amide bond of the N-methyl analog Am90 was *cis*.⁹⁶

In a 1986 report, Shudo and co-workers synthesized analogs in which the amide bond was reversed. The differentiation inducing ability of this analog (Am580, Table 5) was similar to Am80. Because the electronic nature of the two benzene rings was very different in the two amides, a difference in the biological activity was expected. Shudo

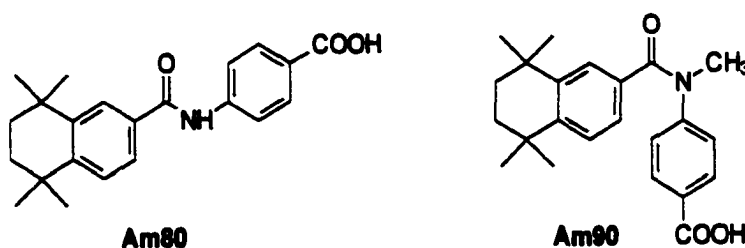
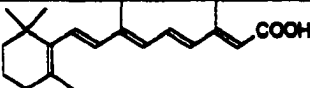
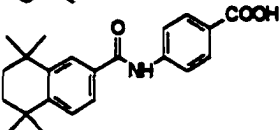
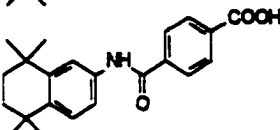
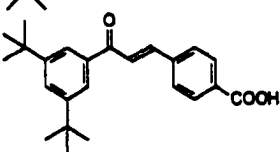
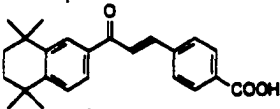
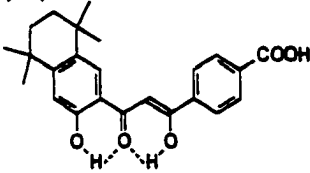
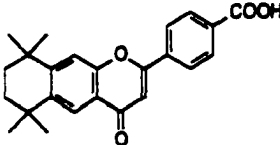


Figure 8. Amide derivatives of TTNPB.

postulated that the amide linker might play a role in determining the steric conformation between the polar carboxylic acid group and the hydrophobic alkyl substituent on the phenyl ring in order to position the groups to interact with the binding site.⁹⁵

Expanding on this hypothesis, Shudo's group synthesized analogs with an α,β -unsaturated ketone linker. This class of compounds, referred to as chalcones, could adopt several conformations as shown in Figure 9. As shown in Figure 9, Shudo sought to find the active conformer, which led to the design and synthesis of a new class of compounds by restricting rotation about the two single bonds.⁹⁶ The flavone class of retinoids locked

Table 5. Differentiation-Inducing Ability of Shudo's Retinoids in HL-60 Cells

name	structure	ED ₅₀ (M)
ATRA		2.4×10^{-9}
Am80		7.9×10^{-10}
Am580		3.4×10^{-10}
Ch55		2.1×10^{-10}
Ch80		6.4×10^{-10}
Re80		6.3×10^{-11}
Fv80		6.4×10^{-10}

the rotatable single bonds of the linker in the *s*₁-*cis*, *s*₂-*trans* conformation, yielding Fv80 with improved *in vitro* biological activity to differentiate HL-60 cells (Table 5, ED₅₀ = 4.6×10^{-11} M). However, the *s*₁-*trans*, *s*₂-*cis* analog Re80 also showed a 10-fold improvement in differentiation-inducing activity of HL-60 cells over Ch80 (ED₅₀ = 6.3×10^{-11} M). These biological results indicated that there might be two biologically active conformations. This can be explained by overlaying the structures of Fv80 and Re80

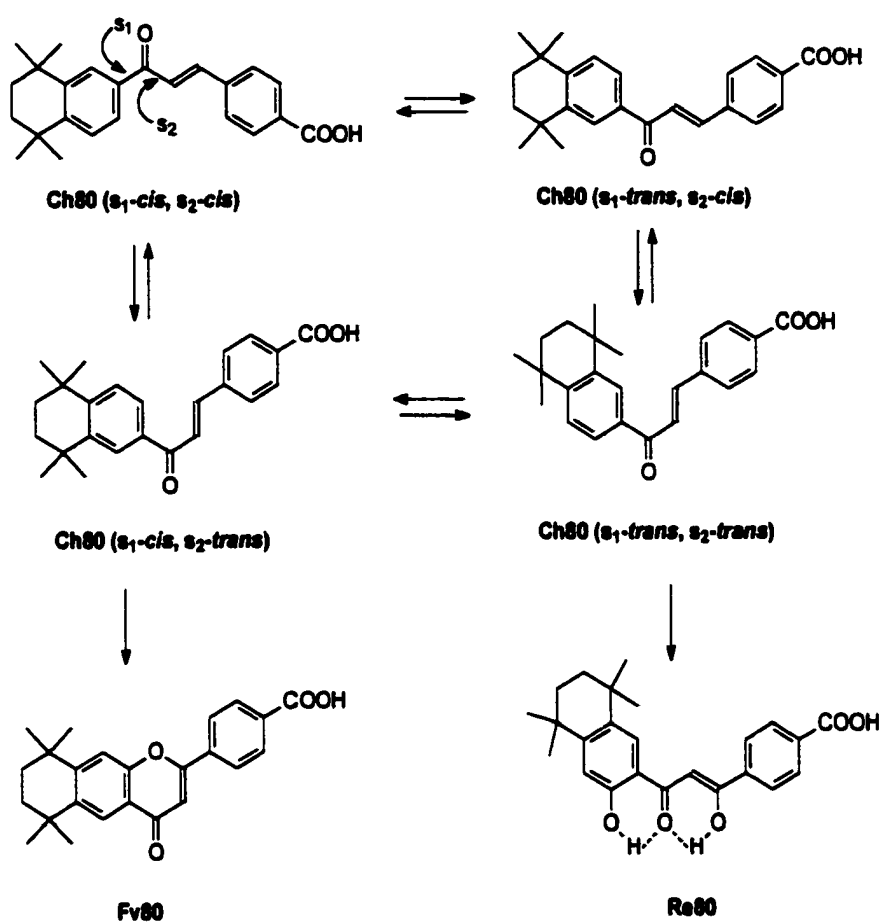


Figure 9. Conformational restriction of single bonds s_1 and s_2 in Ch80 lead to the design of Fv80 and Re80.

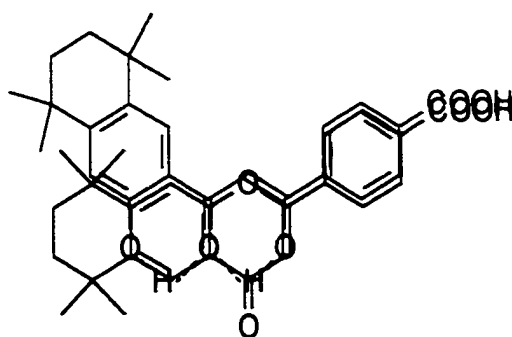
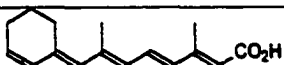
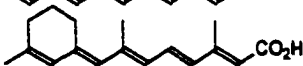
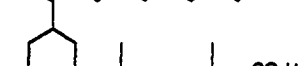
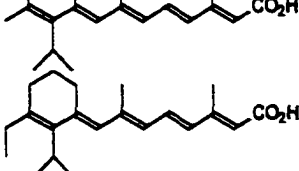


Figure 10. Superposition of Fv80 (blue) with Re80 (red).

(Figure 10), using the benzoic acid portion of the retinoids to align the structures. The slight improvement in biological activity of Re80 over Fv80 was likely due to more favorable hydrophobic interactions of the tetrahydronaphthalene ring of the former with the binding-site.

Brouillette and Muccio, at the University of Alabama at Birmingham, developed a series of conformationally defined 6-*s-trans* retinoids (UAB1-8, Table 6).^{97,98} For RA in solution, the cyclohexenyl ring of RA adopts two rapidly interconverting low-energy conformational states relative to the polyene chain; a 6-*s-cis* isomer is dominant, and a 6-*s-trans* is slightly higher in energy.⁹⁹ A dimethylene bridge was employed to rigidly create either a 6-*s-cis* or 6-*s-trans* conformation. The 6-*s-trans* analog (*all-E*)-UAB7 exhibited similar biological activities *in vitro* as RA but had a slightly lower toxicity than the natural vitamin.⁹⁷ These observations led to the development of a homologous series of compounds based on the structure of (*all-E*)-UAB7 (Table 6). The RAR α and RXR α nuclear

Table 6. Nuclear Receptor Binding Affinities for the UAB Retinoids

retinoid isomer	structure	RAR α IC ₅₀ (nM)	RXR α IC ₅₀ (nM)	ED ₅₀ ^a (nM) (papilloma)
(<i>all-E</i>)-UAB1		600	>2000	>1000
(<i>all-E</i>)-UAB4		55	>2000	490
(<i>all-E</i>)-UAB7		8	>2000	5.0
(<i>all-E</i>)-UAB8		11	>2000	2.5

^a ED₅₀ values were determined by a probit analysis of a dose-response curve. Estimated standard error is 20% of the mean.

receptor binding affinities are summarized in Table 6. The UAB retinoids were also evaluated for activity in the chemical induction of papillomas on mouse skin.⁷³ At a 45.9 nM dose, ATRA prevented 95% of tumor formation. (*all-E*)-UAB7 and (*all-E*)-UAB8 were as effective as ATRA in this assay, but (*all-E*)-UAB4 was much less active and (*all-E*)-UAB1 was essentially inactive. This SAR shows the importance of the bulk of the alkyl substituents on the cyclohexenyl ring not only in receptor binding and activation but also in cancer chemoprevention of the skin. In fact, (*all-E*)-UAB8 ($ED_{50}=2.5$ nm) was more potent than ATRA ($ED_{50}=3.0$ nM) in the skin papilloma assay.

Receptor-Subtype Selective Agonists (RARs)

ATRA and other synthetic retinoids have been used therapeutically in the treatment of proliferative skin diseases such as psoriasis and acne. In addition, ATRA has been used to treat APL. However, the clinical use of retinoids has been hampered by toxicity of the epidermis (skin redness, itching, scaling) as well as other symptoms of hypervitaminosis A. A major concern regarding retinoid therapy has been teratogenicity, thus limiting the therapeutic applications of classical retinoids in women of childbearing age.

It was believed that the toxicity associated with retinoid treatment could be reduced by selectively activating a receptor-subtype. The distribution of each RAR isotype was not uniform in the tissues of both embryos and the adult. Thus, selective compounds could possess a higher therapeutic index by targeting a restricted number of tissues and sparing other tissues. Furthermore, for receptor subtype-selective retinoids, some may exhibit a lower teratogenic risk and produce fewer side effects. In addition, the develop-

ment of receptor-subtype selective agonists could elucidate the precise physiological significance of each receptor subtype.

Following the discovery of the retinoid nuclear receptors RAR (α, β, γ), Delecleuse et al. screened many synthetic retinoids for binding to the receptor subtypes.¹⁰⁰ In this report, Delecleuse et al. tested both natural retinoids and synthetic retinoids for their ability to bind and activate each receptor subtype (RAR α , β , γ). Among those retinoids listed in Table 5, Delecleuse et al. found that ATRA was not selective, but two of Shudo's retinamides, Am80 and Am580, were RAR α -selective. Since this initial discovery, Am80 has been developed extensively and recently used in a clinical trial to treat leukemia patients who had relapsed from ATRA-induced complete remission.¹⁰¹

According to Chandraratna and co-workers, because both Am80 and Am580 have measurable binding affinity for RAR β and RAR γ , each of these receptors will be activated at pharmacological doses (1 μ M) in addition to RAR α .¹⁰² Therefore, there was a need for new and more selective RAR α retinoids. Chandraratna attributed the RAR α -selectivity of Am80 and Am580 to the hydrogen-bonding ability of the internal amide linkage. By including additional hydrogen-bonding groups in the linker region, Chandraratna designed and synthesized a potent RAR α agonist, AGN193836 (Table 7). This Allergan retinoid had greatly improved selectivity for the RAR α receptor with >2000-fold higher binding affinity for RAR α relative to RAR β and no measurable binding affinity for RAR γ (Table 7). AGN193836 had an antiproliferative effect in *in vitro* assays in ER⁺ breast cancer cells (mammary tumors that express the estrogen receptor) and exhibited no cytotoxicity at high doses.¹⁰³ However, the antiproliferative effect required 12 days of treatment compared to 4 days using 9-*cis* RA.

Table 7. Comparison of Binding Affinities [K_d (nM)] to RAR Subtypes for Retinoids that are RAR Pan-Agonists (ATRA and TTNPB) and RAR α -Selective Retinoids (Am580 and AGN193836)

name	structure	K_d (nM)		
		RAR α	RAR β	RAR γ
ATRA		15 ± 1.7	13 ± 2.5	18 ± 1.7
TTNPB		72 ± 37	5 ± 2	26 ± 2
Am580		36 ± 1.5	1361 ± 321	15 ± 1.7
AGN193836		8.4 ± 1.3	17374 ± 6347	$>30,000$

Recently, new nonamide RAR α agonists were reported by Shudo's group. Using Am80 as a lead compound, Kikuchi et al.¹⁰⁴ designed and synthesized analogs by introducing heteroatoms into the hydrophobic tetrahydronaphthalene ring and replacing the amide linkage with a pyrrole ring (Figure 11). For example, in the case of ER-33635, heteroatoms were introduced into the hydrophobic tetrahydronaphthalene ring to increase the polarity of the retinoids and hopefully improve the pharmacokinetic characteristics. Comparison of the TTNPB RAR pan-agonist with the RAR α agonist Am580 emphasized the importance of the amide bond in order to confer RAR α -selectivity. Believing that an acidic proton in the linker region was required for RAR α selectivity, workers at Badische Anilin Soda Fabrik (BASF) used a heterocycle as the linker moiety to produce **103** (Fig

ure 11).¹⁰⁵ This approach was successful in improving the selectivity for RAR α and enhancing potency. A combination of the two structural alterations resulted in an RAR α agonist (ER34617, Figure 11, Table 8) that had improved capability to induce differentiation of HL-60 cells over ATRA. These new retinoids have not undergone evaluation for toxicity.

It was reported that a RAR α agonist was a potent inhibitor of murine B-lymphocyte proliferation.¹⁰⁶ Am80 was also shown to inhibit the inflammatory cytokine interleukin-6 (IL-6) *in vitro*.⁹⁵ These results suggested that there is a strong correlation between RAR α agonistic activity and immunosuppressive effects, especially in the inhibition of antibody production.

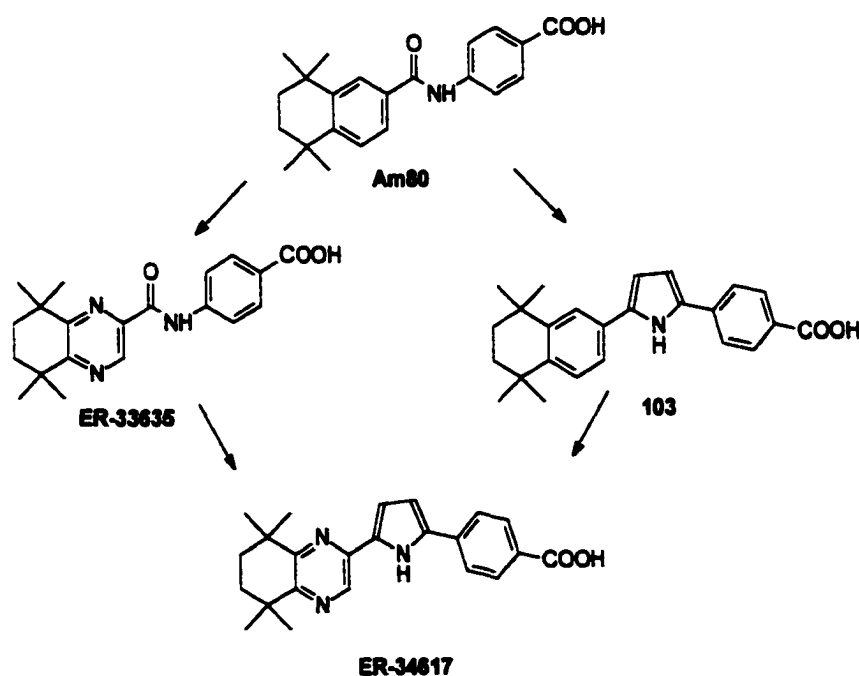


Figure 11. Design of quinoxaline derivatives by Kikuchi et al.¹⁰⁴

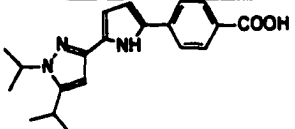
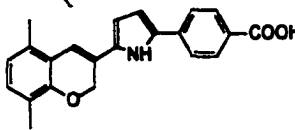
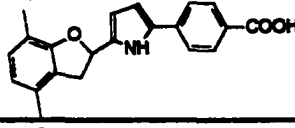
Table 8. Comparison of Receptor Binding Affinities (IC₅₀), Transcriptional Potency (EC₃₀), and HL-60 Differentiating Ability (ED₃₀) of the New RAR α Agonists

retinoid	structure	IC ₅₀ (nM) ^a			EC ₃₀ (nM) ^c			HL-60 cells ED ₃₀ (nM)
		RAR α	RAR β	RAR γ	RAR α	RAR β	RAR γ	
ATRA		1.0	1.0	1.0	1.0	1.0	1.0	0.94 ± 0.20
Am80		78±20	nd ^b	nd ^b	1.3 ± 0	48 ± 13	150 ± 90	0.67 ± 0.32
Am580		41±9	nd ^b	nd ^b	0.30±0.01	12±3	33±5	0.34±0.08
ER-33635		40±2	140±20	nd ^b	0.15±0.04	0.40±0	1.6±0.8	0.87±0.41
103		0.45±0.15	100±8	21±5	0.34±0.10	3.9±1.4	3.5±0.5	0.54±0.27
ER-34617		2.2±1.5	230±120	310±140	0.32±0.03	2.5±0.3	20±6	0.11±0.04

^aRelative IC₅₀ = Mean of IC₅₀/ATRA IC₅₀ ± SEM. ^b nd: not detectable (relative IC₅₀ > 1000). ^cRelative EC₃₀ = Mean IC₃₀/ATRA IC₃₀ ± SEM.

As shown in Table 9, novel RAR α agonists were recently reported by Shudo's group. Using the RAR α selective agonist ER-34617 as a lead, Kikuchi et al.¹⁰⁴ sought to obtain more potent RAR α -selective and less toxic retinoids by replacing the tetrahydronaphthalene moiety with an alkyl substituted pyrrole group. Monocyclic retinoids have been described in which the hydrophobic ring of ATRA was replaced with a pyrrole or an imidazole, resulting in retinoid agonists.¹⁰⁷ Kikuchi et al. incorporated a similar monocyclic group to successfully yield an RAR agonist ER-38930 that was not extremely selective. Kikuchi et al. later reported additional RAR α agonists such as ER-41666 with enhanced RAR α selectivity using a naphthalene or benzopyran moiety to replace the substituted pyrrole ring of ER-38930.¹⁰⁷ This ring system is more planar than the corresponding tetrahydronaphthalenyl ring of many of the known RAR α agonists. The purpose of synthesizing the benzopyran derivatives (ER-41666) was to improve the pharmacokinetic characteristics. In the next generation of compounds, the most potent and selective RAR α agonists of this new structural class were obtained by reducing the size

Table 9. Novel Retinoids with RAR α Selectivity

retinoid	structure	RAR α	relative EC ₃₀ ^a	
			RAR β	RAR γ
ER-38930		0.19	1.8	14
ER-41666		1.8	240	3600
ER-38925		0.80	92	1000

^aEC₃₀/ATRA EC₃₀.

of the six-membered ring containing the heteroatom to a five-membered ring, as in ER-38925, again increasing the planarity of the molecule at the terminal end. This retinoid ER-38925 and similar derivatives are currently being evaluated for immunosuppressive activity, pharmacokinetics, and safety to select a clinical candidate suitable for use as an immunosuppressive agent.

RAR β / γ Receptor-Selective Retinoids

The RAR β / γ selective agonists all possess an aromatic carboxyl terminus. Chandraratna et al.¹⁰⁸ reported the synthesis of acetylenic RAR β / γ selective agonists with no affinity for the RAR α or the RXR α receptors. It was suggested that the reason that the natural retinoids lack receptor subtype selectivity is its conformational flexibility, allowing adjustment to ligand binding pockets of the different receptors. Identification of active conformations at each receptor would facilitate the future design of more selective and effective retinoids.

Conformational flexibility was restricted by incorporating the bond corresponding to the 9,10_R bond of ATRA in a triple bond to yield **104**.¹⁰⁸ As shown in Figure 12, in order to improve pharmacological properties, a 2-pyridyl ester of **104** was synthesized, resulting in a RAR β , γ agonist (EC_{50} (RAR β) = 2 nM; EC_{50} (RAR γ) = 10 nM). Information regarding toxicity was not included in this report, but this ethyl ester is currently used therapeutically in the treatment of plaque psoriasis (Tazarotene).¹⁰⁹

Using the RAR α -selective agonist Am80 as a lead compound, Johnson et al.¹¹⁰ at Allergan developed an RAR β agonist by introducing a 2-thienyl group onto the sp²-hybridized C-1 position of the tetrahydronaphthalene ring (AGN193639 in Table 10). As

mentioned previously, most of the known RAR α agonists had an amide linking the hydrophobic region with the carboxylate moiety because the acidic proton of the amide nitrogen selectively enhanced RAR α binding affinity. As shown in Table 10, Johnson et al.¹¹⁰ synthesized two other 2-thienyl retinoids with a different linker than the amide (AGN193676 and AGN193174). The retinoid AGN193639 with an amide linker bound tightly only to RAR α but did not promote transactivation mediated by any RAR nuclear receptors. Retinoid AGN193639 proved to be an RAR α antagonist and RAR β agonist. Retinoid AGN193174 with an ester linker bound to the RAR β nuclear receptor and activated transcription using this receptor, and it had weaker RAR α and RAR γ antagonist effects. Retinoid AGN193676 had an alkyne linkage and displayed similar binding and activation profiles as AGN193174. The decrease in RAR α binding affinity with AGN193676 and AGN193174 was not surprising due to the lack of an acidic proton in the linker. Thus, these RAR β -selective agonists, which were also antagonists for the RAR α and RAR γ receptors, were formed by using a thienyl group. These retinoids could be helpful in elucidating the roles of the receptor subtypes in specific cellular processes.

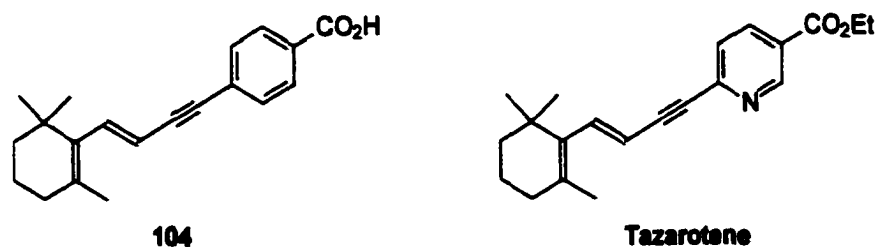
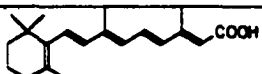
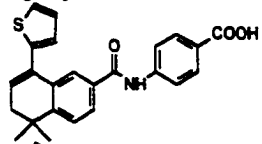
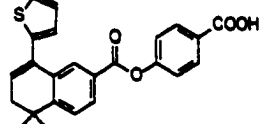
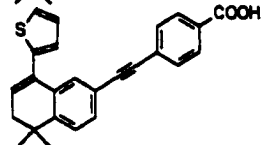


Figure 12. RAR β , γ -selective acetylenic retinoids.

Table 10. Binding Affinities and Transactivation Abilities of Thienyl-Retinoids¹¹⁰

retinoid	structure		RAR		
			α	β	γ
ATRA		EC_{50}^a K_d^b	459 15	87 13	20 18
AGN193639		EC_{50}^a K_d^b	NA ^c 94	115 996	NA ^c >10 ⁴
AGN193676		EC_{50}^a K_d^b	NA ^c 303	26 189	NA ^c 1490
AGN193174		EC_{50}^a K_d^b	NA ^c 129	25 189	NA ^c 1490

^a EC_{50} values are the mean of at least three experiments performed in triplicate using CV-1 cells cotransfected with the luciferase reporter plasmid MTV-4(R5G)-Luc and an expression vector of the indicated retinoic acid receptor. ^b K_d values are reported as the mean value of three determinants by competition of [³H]-(*all-E*)-retinoic acid (5nM) binding with unlabeled test retinoid using baculovirus expressed RARs. ^c NA: not active.

Vuligonda et al.¹¹¹ at Allergan Pharmaceuticals recently reported an acetylenic RAR β agonist substituted with tetrahydropyran (THP) on the sp^3 -hybridized C-1 position of the dihydronaphthalene ring (Figure 13). Incorporation of the THP ether substituent created a chiral center in addition to the inherent chirality of the THP ether itself, thus creating diastereomers. Vuligonda et al.¹¹¹ demonstrated that RAR receptor selectivity was dependent on the stereochemistry at the C-1 position of the THP. The diastereomers with S stereochemistry at C-1 bound selectively to the RAR β nuclear receptor. However, both **107** and **108** activated gene expression mediated by the RAR β and the RAR γ receptors. In contrast, the THP ethers with R stereochemistry (**105** and **106**) at C-1 were only

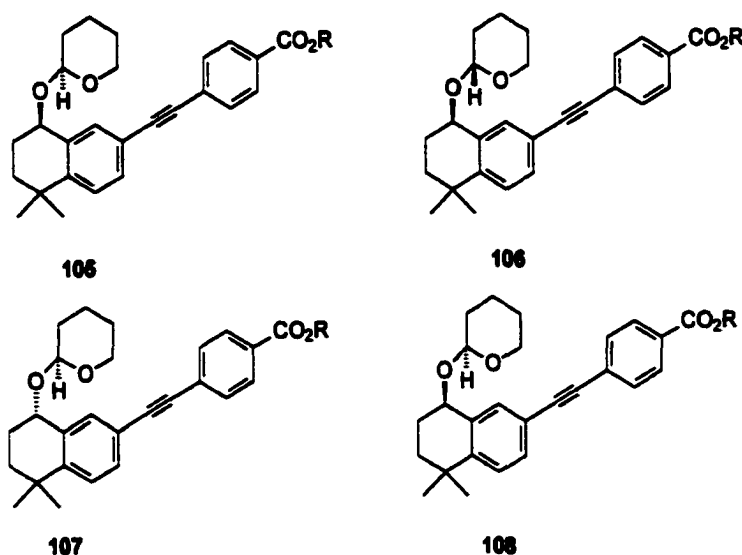


Figure 13. Stereoisomers of the acetylenic THP ethers designed by Vuligonda.¹¹¹

RAR β -selective agonists. Stereochemistry of the THP anomeric carbon induced more subtle changes in receptor selectivity. The (S)-THP anomeric carbon conferred RAR γ transactivation ability. By obtaining receptor-selective retinoids, the physiological role of the receptor subtypes could be studied in the ODC assay. The ethyl esters of retinoids **105-108** were tested in the ODC assay, and a positive correlation was observed between the ability to activate the RAR γ nuclear receptor and the ability to inhibit the production of ODC. In addition, retinoids **105-108** were evaluated for mucocutaneous toxicity. Retinoids **107** and **108** were the most toxic, receiving scores of 11 out of the maximum score of 17. Interestingly, retinoids **105** and **106**, which were the least toxic, were also the least effective in ODC inhibition. Thus, retinoids that activate RAR γ also induce mucocutaneous toxicity.

The teratogenic potential of **105-108** was tested via the chondrogenesis assay. Inhibition of chondrogenesis (cartilage development) by retinoids in limb bud cells correlates well with teratogenicity *in vivo*.¹¹² In addition to mucocutaneous toxicity, retinoids **107** and **108** were potent inhibitors of chondrogenesis *in vitro* and were deemed teratogenic. The RAR β retinoid **105** lacking RAR γ activity was not active in the chondrogenesis assay. These studies showed that RAR γ activation was associated with mucocutaneous toxicity and teratogenicity. Therefore, this RAR β agonist **105** might find usefulness in the treatment of proliferative skin diseases such as psoriasis without exhibiting side effects such as mucocutaneous toxicity or teratogenicity.

Charpentier et al.¹¹³ synthesized a variety of retinoids with substituted naphthalene carboxylic acids at the polar end (Table 11). One class of agonists possessed a propenyl linker between the phenyl and naphthalene rings, while the other class did not have a linker at all. One of the naphthalene carboxylic acid retinoids of the latter class had an adamantyl substituent in addition to a hydroxyl substituent on the phenyl ring, producing an agonist **109** with optimal RAR γ selectivity (Table 11). The methyl ether of retinoid **109**, commercially known as Adapalene or Differin, was approved by the Food and Drug Administration (FDA) for the treatment of *acne vulgaris*.

Graupner et al.¹¹⁴ reported the design and synthesis of a RAR β,γ agonist containing a naphthalene-2-carboxylic acid terminus. Using 13-*cis* RA and TTNPB as the lead compounds, 6'-substituted-naphthalene-2-carboxylic acid retinoids were synthesized and assessed for binding affinity for the RARs. The linker between the dihydronaphthalene ring and the naphthalene carboxylic acid terminus was shortened to one carbon. A hy

Table 11. Binding Constants of Naphthalene Carboxylic Acids for the RARs

retinoid	structure	RAR α	apparent K _d (nM) RAR β	RAR γ
ATRA		2.3	0.4	0.3
109		6500	2480	77
110		7500	679	64
111		16500	531	75
112		7500	4095	816
113		700	50	3.3

droxyl substituent (**110**, Table 11) at this linker position yielded a RAR γ , while a carboxyl group resulted in a RAR β , γ agonist.

Yu et al.¹¹⁵ explored the requirements for RAR β and RAR γ selectivity by altering the linker in the substituted naphthalene carboxylic acid derivatives. All of the naphthalene carboxylic acids synthesized in this report activated either the RAR β or the RAR γ receptors with minimal RAR α activity. The sp³-hybridized linkers containing polar functionality such as a hydroxyl group resulted in retinoids that were RAR γ selective.

As previously mentioned, Graupner et al.¹¹⁴ were the first to synthesize this retinoid; however, the racemic mixture was evaluated for receptor binding and activation. Yu et al.¹¹⁵ were able to separate the R (**111**) and S (**112**) enantiomers and evaluate them separately. Interestingly, the two isomers had different binding affinities for the RARs

(Table 11) with 112 displaying the most potent RAR γ -selectivity of the two. Among the sp^2 -hybridized linkers, the oxime linker resulted in a potent RAR γ agonist 113 (apparent $K_d = 3.3$ nM). Therefore, a polar substituent in the linker region enhanced RAR γ selectivity in both the sp^2 - and sp^3 -hybridized linkers.

Crystal Structures of Agonists Bound to Retinoid Receptor RAR γ

The Moras group in Strausborg has been primarily responsible for determining the structure of retinoids bound to the LBDs of RARs. Bourget et al.⁴⁸ solved the structure of the LBD of apo-RXR α , and Renaud et al.¹¹⁶ refined the structure of the LBD of holo-RAR γ containing ATRA. These structures are shown in Figures 6 and 7. Using sequence alignment, it was shown that only three residues are divergent in the ligand-binding pocket of the RARs (Table 12). These divergent residues are obvious candidates to account for the RAR selectivity of certain synthetic retinoids. In holo-RAR γ , A234 and M272 interact with the isoprene tail and A397 with the C-4 carbon of the β -ionone ring of RA. The RAR α selectivity achieved by the amides Am80 and Am580 was most likely due to hydrogen bonding between the nitrogen of the amide bond and the OH group of Ser 232. In other RARs, Am80 or Am580 would not be able to hydrogen-bond to the R-groups of Ala225 and Ala232.

A common structural feature of the RAR γ agonists was the presence of a polar functionality (hydroxyl) of the linker. Following the crystal structure report of (*all-trans*)-RA bound to RAR γ , Klaholz et al. sought to explain the structural reasons for RAR γ selectivity by crystallizing 9-*cis* RA with RAR γ at a resolution of 2.4 Å (Figure 14).¹¹⁷ Comparison of the ATRA crystal structure (Figure 5) with the 9-*cis* RA structure

Table 12. Divergent Residues in the Ligand-Binding Pocket of the RARs

Receptor	Divergent Residues		
RAR α	Serine 232	Isoleucine 270	Valine 395
RAR β	Alanine 225	Isoleucine 263	Valine 388
RAR γ	Alanine 232	Methionine 272	Alanine 397

(Figure 14) highlighted certain similarities as well as differences. Both the *9-cis* and *all-trans* isomers were anchored by a salt bridge between Arg 278 of helix 5 and their carboxylate group. The RARs bind *9-cis* RA with only 10-fold less efficiency. The structures of ATRA and *9-cis* RA are very similar, both possessing *6-s-cis* geometry between the ring and the chain. The C6-C7 dihedral angles between the β -ionone ring and the tetraene chain were 43° and 24° for ATRA and *9-cis* RA, respectively. The only significant difference was the position of the sulfur atom of Met 272, which was pushed away by 0.9 Å by the 19-methyl group of *9-cis* RA. Therefore, the lower binding affinity of *9-cis* RA for RAR γ was most likely due to a steric clash between the 19-methyl group with Met 272. The more compact side chains of the corresponding isoleucine residues in both RAR α and RAR β probably left room for the 19-methyl group, which explained why *9-cis* RA had better binding affinity for these two receptors. The 20-methyl group of the two RA ligands point in opposite directions, with both orientations being sterically allowed by the protein-binding pocket.

Klaholz et al. recently reported the crystal structure of racemic BMS961 complexed with RAR γ . This structure revealed the interactions that were responsible for the selective binding of BMS961 and other ligands possessing a hydroxyl group on the linker

to RAR γ (Figure 15).¹¹⁷ Bristol Myers Squibb researchers reported the crystal structure of the RAR γ agonist BMS961 bound to RAR γ at 2.5 Å resolution (Figure 15, Table 12). The fluorine atom pointed towards Ala 234 (helix 3), mimicking the 20-methyl group of 9-*cis* RA, and the hydroxyl group was repositioned near the 19-methyl group of RA, with geometry and distances for hydrogen-bonding to the sulfur of Met 272 (2.9 Å). The orientation of the hydroxyl group seemed to be crucial because only the S-enantiomer was observed to bind to RAR γ when a racemic mixture was used in the crystallization. The R-enantiomer would place the hydroxyl group approximately 3.4 Å from the sulfur of Met 272, which was too far away for hydrogen bonding.

Klaholz et al.¹¹⁸ later reported on the crystal structures of each of the enantiomers of BMS961 (BMS394 and 395) with differential binding affinities for the RARs (resolution = 1.59 Å) (Table 13). These experiments were performed at a higher resolution, and it was found that the earlier report¹¹⁷ was incorrect in stating that the S-enantiomer was the favored conformation for RAR γ binding. The crystal structure of the R-enantiomer BMS394 showed that the orientation of the hydroxyl group was favorable for interaction with RAR γ with a distance of 3.20 Å between the oxygen atom of the hydroxyl moiety and the sulfur atom of Met-272. In addition, the fluorine made van der Waals contacts with Ala-234, the oxygen of the amide group exhibited a short distance to Phe-230, and the amide nitrogen hydrogen bonded to Leu-271. The S-enantiomer (BMS395)-RAR γ complex exhibited some unexpected characteristics. It was expected that the hydroxyl group would be unable to hydrogen-bond to Met 272, but this was shown to be a false assumption. Clearly, the hydroxyl was able to hydrogen-bond to Met 272 with a bond



Figure 14. Pan-agonist 9-*cis* RA bound to RARγ.

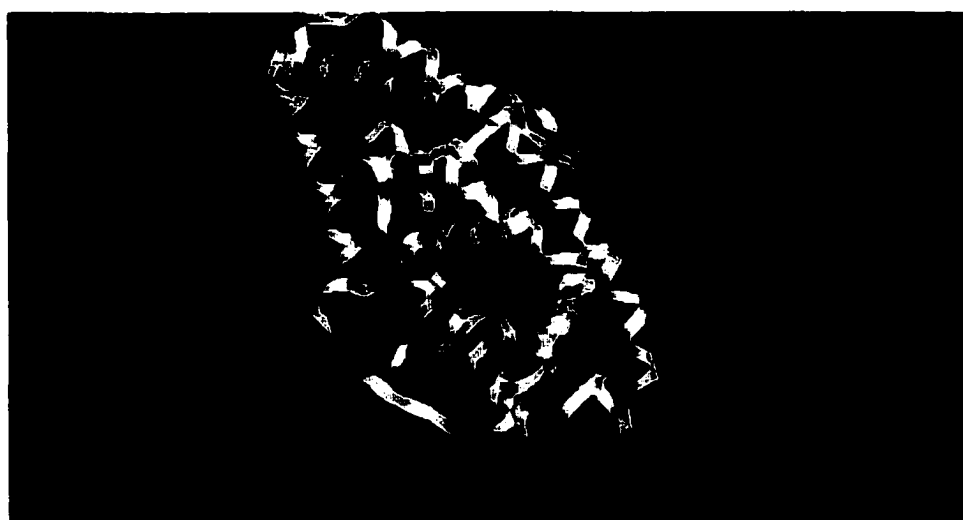
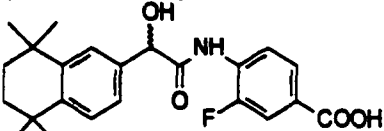
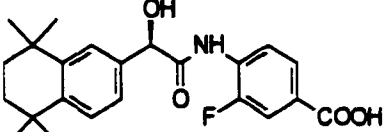
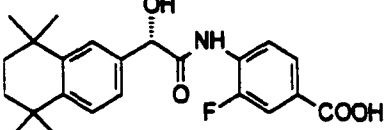


Figure 15. RARγ-selective ligand BMS961 bound to RARγ.

Table 13. Racemic BMS961 and the Enantiomers of BMS961 with Differing EC₅₀ (nM) Values for RARs

retinoid	structure	RAR α	RAR β	RAR γ
BMS961		NA ^a	1000	30
BMS394		NA ^a	400	30
BMS395		NA ^a	NA ^a	NA ^a

^a NA: not active.

distance of 3.19 Å. However, superposition of both complexes (Figure 16) showed that the hydrophobic ring moiety (tetrahydronaphthalene, TTN) of BMS395 was rotated by 98° around the bond linking the TTN and methylenehydroxyl moieties, leading to a completely different ligand conformation compared to BMS394. This conformational difference was unfavorable for interactions with residues in the ligand-binding pocket, which Klaholz et al. explained more fully in his report.¹¹⁸

Moras and co-workers¹¹⁹ explained the structural basis for isotype selectivity for the RARs by studying the crystal structures of three complexes of the RAR γ LBD bound to agonists. The retinoid agonists were selective either for RAR γ (BMS184394) or for RAR β , γ (CD564) or were potent for all RAR-isotypes (pan-agonist BMS181156). As mentioned previously, RAR γ selectivity was achieved due to the hydrogen bond between the hydroxyl of BMS184394 with Met272 (3.29 Å). In the case of the RAR γ complex with RAR β , γ agonist (CD564), the sulfur atom of Met272 was oriented away from the

ligand (4.95 Å), and the shortest distance to Met272 corresponded to van der Waals contacts (3.64 Å between the keto group of CD564 and C γ Met272). The corresponding residue in RAR β was an isoleucine. The keto moiety of CD564 exhibited a distance of 3.37 Å to Phe304, which suggested the existence of a weak hydrogen bond. Such C-H \cdots O=C hydrogen bonds involving aromatic residues were known for other structures.¹²⁰ This contact was also probably present in the RAR β complex, since Phe304 was

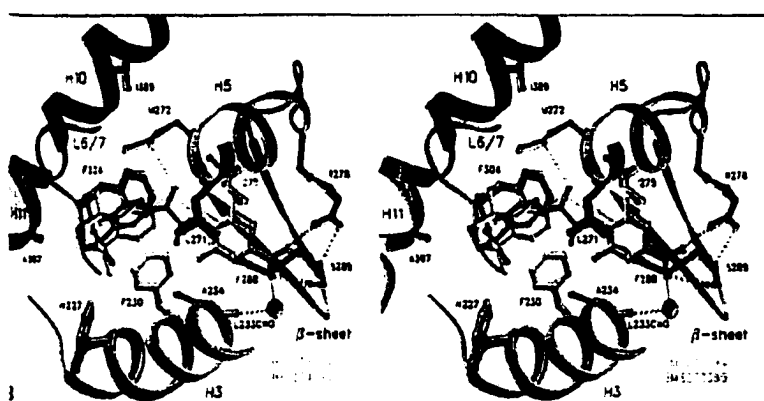


Figure 16. Superposition of BMS394 and BMS395 in the LBP of RAR γ .¹¹⁸

conserved among the RAR α , β , and γ sequences. The different interactions of BMS181156 and BMS270394 with RAR γ revealed why some retinoids are pan-agonists. Pan-agonist BMS181156 interacted with Phe304 and the C γ of Met272, while RAR γ agonist BMS270394 interacted with the sulfur atom of Met272 and provided additional hydrogen bonds to the backbone carbonyl group of Leu271 and the side-chain of Phe230. The flexible sp³-hybridized bridge of BMS280394 linking the TTN and benzoic acid moieties adopted a conformation different from that of BMS181156 to avoid close contacts between the oxygen atom of the amide group and residues Leu271 and Ile275.

When the structures of the pan-agonist BMS181156 and RAR β,γ agonist CD564 were compared, the requirements for RAR α binding were delineated. Sequence alignment of RAR isotypes showed that the LBPs differed only by one residue, which was a serine that corresponded to an alanine in both RAR β and γ . Therefore, steric hindrance between the serine side-chain and the 2-napthoic group of CD564 was responsible for RAR α discrimination, whereas the smaller 4-ethenylbenzoic acid moiety of BMS181156 could be accommodated readily. This was supported by the observation that most napthoic acids or propenylbenzoic acids did not bind RAR α . The RAR α agonists Am80 and Am580 contained the small benzoic acid group, which could be accommodated by the receptor.

Retinoid Antagonists

In order to further elucidate the physiological role of each receptor subtype, retinoid antagonists were designed and synthesized by Eryolles et al.¹²¹ These RAR antagonists were designed using both the structures of RAR α agonist Am80 and the estrogen antagonist Tamoxifen as leads (Figure 17). Eryolles et al. hypothesized that, because RARs belong to the steroid/thyroid nuclear receptor superfamily, it might be expected that a ligand superfamily also exists. From that standpoint, ligands for nuclear receptors should be structurally superimposable. Such superimposition indicates that the carbon skeletons of the ligands play a role in locating the functional groups at suitable positions for binding to the cognate nuclear receptors. This implies the existence of antagonistic functional groups, which are common to all nuclear receptors. In the case of the estrogen receptor, substitution of a bulky aromatic substituent at the “top” of the structure of di

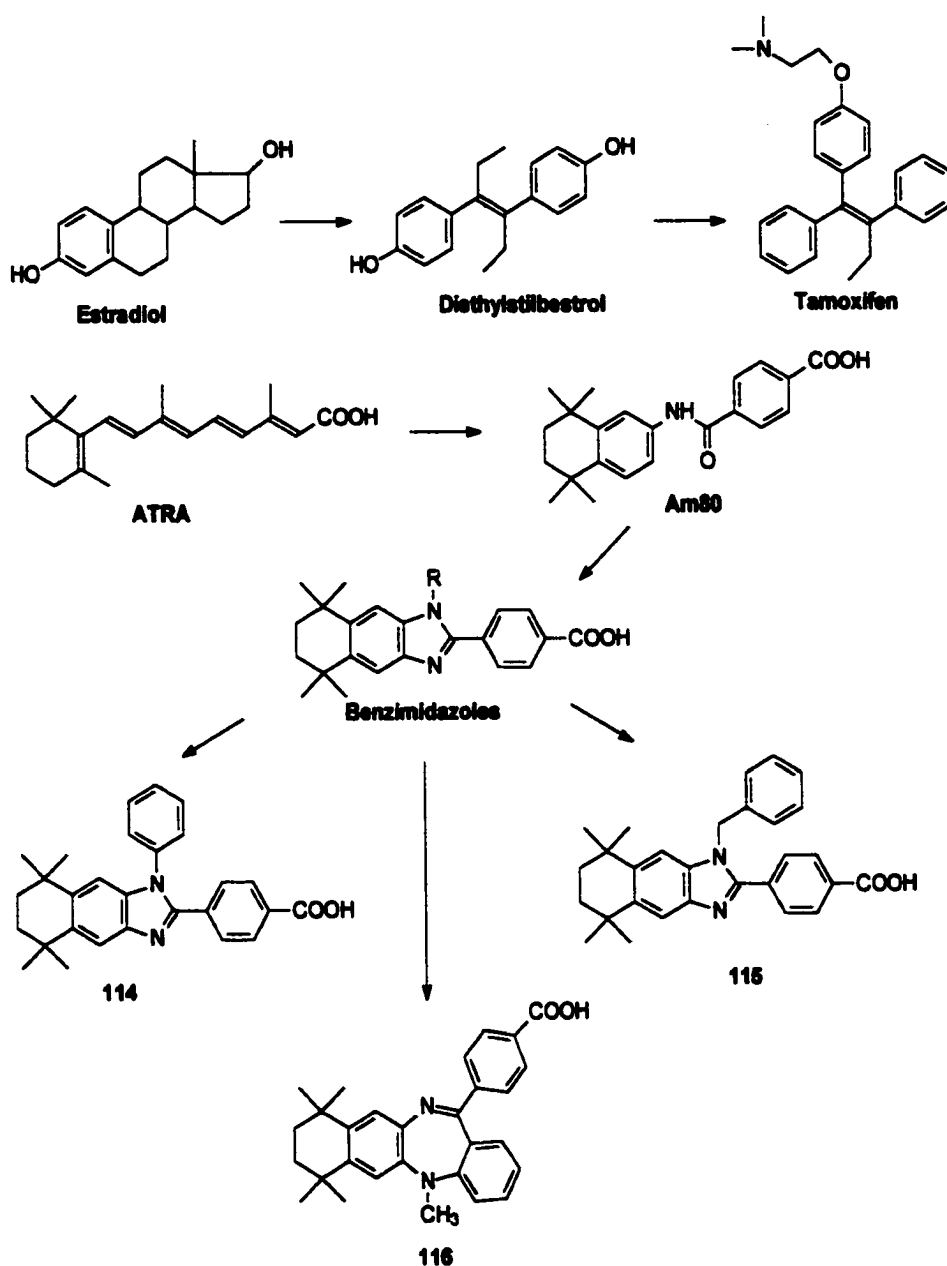


Figure 17. Strategy for the design of retinoid antagonists.¹²¹

ethylstilbestrol (DES) resulted in the potent estrogen antagonist Tamoxifen (Figure 17). Using the RAR α agonist Am80 as a template, the site for aromatic substitution that would confer antagonistic activity corresponded to the amide nitrogen. Kagechika et al.⁹⁶ had proven previously that substitution of the amide nitrogen induced a *cis* conformation about the amide bond, which abolished retinoidal activity. Therefore, to prevent a conformational change of the linking group by the introduction of a bulky group, the linker was conformationally constrained by including it in a benzimidazole ring system. One of the nitrogens was substituted with a variety of aliphatic and aromatic substituents yielding antagonists 114 and 115.

Another class of retinoid antagonists was synthesized by accident in an attempt to prepare the N-phenyl analog of the benzimidazoles 114-115. This new class included the linker in a seven-membered ring (116). This dibenzodiazepine retinoid as well as the other two benzimidazole retinoids (114 and 115) was completely inactive in inducing HL-60 cells to differentiate in the NBT assay. Furthermore, they exhibited antagonistic activity by inhibiting Am80-induced differentiation in HL-60 cells in a dose-dependent manner.

AP-1 Transrepression by Retinoids

Fanjul et al.¹²² reported the *in vivo* apoptosis induction and antiproliferative activity of the retinoid antagonist MX781, which is a retinobenzoic acid analog (Figure 18). *In vitro* testing of MX781 also showed activity in both estrogen receptor positive ER⁺ and ER⁻ tumor cell lines. ER⁺ tumors express the estrogen receptor and are treatable with ER

antagonists such as Tamoxifen, and ER⁺ tumors do not respond to Tamoxifen treatment. Thus agents like MX781 could be useful for combination therapy with Tamoxifen (TAM). It was demonstrated that the induction of apoptosis by MX781 occurred through AP-1 transrepression rather than activation of RXRs (see below). This was expected because MX781 was an RAR analog and did not bind RXRs.

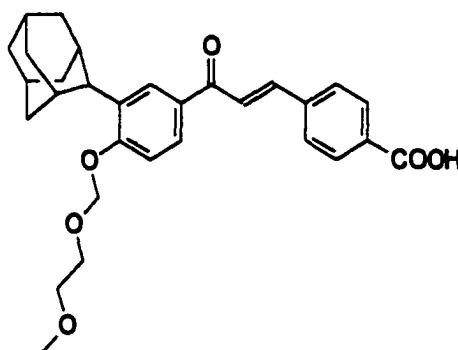


Figure 18. Structure of the retinoid antagonist MX781 with anti-AP-1 activity.

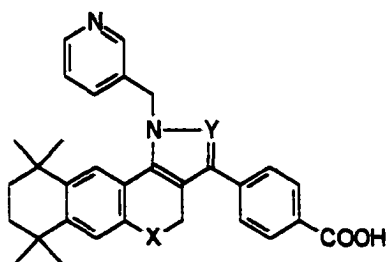
The activation of HREs by the RAR heterodimers and the RXR homodimers has been previously established, and this interaction provides the signaling pathway by which gene activation. In analogy to the positive elements for transcriptional activation, negative response elements that mediate hormone-induced repression have been reported.¹²³ Receptor binding to such negative response elements in the presence of ligand prevents the receptor from functioning as a transcriptional activator but allows negative interference with adjacent or overlapping sites that bind other transcription factors. Thus, it is apparent that an additional regulatory mechanism for nuclear receptors that does not require receptor-DNA interaction exists. This mechanism involves the protein-protein interaction that allows hormone-dependent repression or activation of gene transcription

through the interaction of the nuclear receptors and the transcription factor AP-1. AP-1 is a protein complex composed of a *c-Jun* and *c-Fos* heterodimer whose activity is modulated by growth factors, cytokines, oncogenes, and tumor promoters that activate protein kinase C. AP-1 induces transcriptional activation through interaction with a specific DNA recognition sequence, the TPA response element. Thus, a regulatory switch exists between the two pathways that allows for cross-talk. The mechanism for this cross-talk is still not well understood, but certain retinoids induce a conformational change in the retinoid receptor so that it is able to repress AP-1 by inhibiting the ability of AP-1 to bind its response element.

Heteroaromatic RAR Pan-Antagonists

Yoshimura et al.¹²⁴ reported antagonists containing a heteroaryl group. The heteroatoms were included in order to decrease the lipophilicity of the molecules and improve the pharmacokinetic profile. The effects of varying the orientation between the aryl groups upon activity had not been explored previously. Yoshimura et al. conformationally constrained the rotation between the aryl groups by including the linker in either a pyrrole or a pyrazole ring (Table 14). Because acidic protons in the linker region confer RAR α agonistic activity, the heteroatom was substituted with various aromatic groups. Substitution of both the pyrrole and the pyrazole nitrogens with a pyridylmethyl group resulted in potent antagonists that inhibited the binding of ATRA to RAR and prevented ATRA from differentiating HL-60 cells.¹²⁵

Recently, researchers at Allergan have increased efforts to design and synthesize potent RAR antagonists as antidotes to retinoid induced toxicity. Johnson et al.¹²⁶

Table 14. Binding Affinity and Antagonism of Retinoid Receptor Antagonists

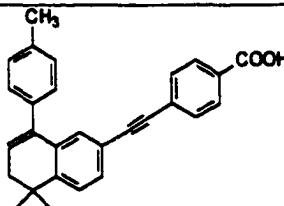
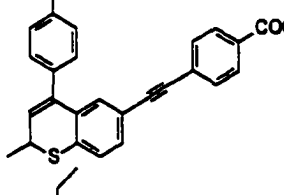
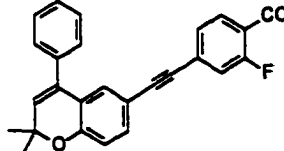
HL-60 IC ₅₀ (M)				
retinoid	X	Y	binding ^a	antagonism ^b
117	CH ₂	CH ₂	3.4 x 10 ⁻¹⁰	4.9 x 10 ⁻⁹
118	S	CH ₂	1.6 x 10 ⁻¹⁰	5.6 x 10 ⁻⁹
119	CH ₂	N	9.1 x 10 ⁻¹⁰	1.3 x 10 ⁻⁹

^a Concentration of the test compound inhibiting the binding of [³H] ATRA. IC₅₀ values were obtained from plots of the binding affinity at 5.0 x 10⁻¹⁰ M [³H] ATRA versus the logarithmic concentration of the test compound. Values are the mean of two experiments. ^b Concentration of the test compound inhibiting the differentiation-inducing activity of ATRA (1.0 x 10⁻⁸ M). IC₅₀ values were obtained from plots of activity at 1.0 x 10⁻⁸ M ATRA versus the logarithmic concentration of the test compound. Values are the mean of two experiments.

reported the synthesis of a potent RAR pan-antagonist AGN193109. This aryl substituted diarylacetylene retinoid inhibited activation of the RARs by ATRA. In a more recent report, the synthesis of several substituted chromenes and thiochromenes with antagonistic activity was described.¹²⁷ The rationale for the inclusion of the heteroatom was not stated, but it can be assumed that the intention was to improve pharmacokinetic properties. The binding affinities as well as the capacities to inhibit the binding of TTNPB for

the most promising antagonists are shown in Table 15. The potential use of these compounds as inhibitors of retinoid-induced toxicity *in vivo* was clearly demonstrated by their ability to block the activity of the potent and toxic RAR agonist TTNPB. As a result, AGN194310 is currently in preclinical development as a topical agent for the treatment and prevention of the mucocutaneous toxicity produced by systemic retinoids such as Accutane.

Table 15. Relative Potency^a and K_d^b Values of RAR Antagonists in the Inhibition of Transcriptional Activity by the RAR Agonist TTNPB

retinoid	structure		RAR		
			α	β	γ
AGN193109		Rel. Potency K _d	1.0 17 ± 5	1.0 7 ± 3	1.0 7 ± 1
AGN194310		Rel. Potency K _d	7.5 3 ± 2	6.5 2 ± 1	4.0 5 ± 1
120		Rel. Potency K _d	2.4 5 ± 1	12.2 2 ± 0	2.2 16 ± 4

^aRelative Potency = IC₅₀ (test compound)/IC₅₀ (AGN193109).; ^bK_d + SEM (nM).

Also reported was a similar class of RAR pan-antagonists, which might have improved pharmacokinetic properties due to the presence of heteroatoms in the structure.¹²⁸ These antagonists, such as 121-123 (Table 16), were tested in hairless mice that had been treated with the highly toxic pan-agonist TTNPB and resulted in a reduction in mucocutaneous toxicity. This cutaneous toxicity score is an aggregate of the flaking and abrasion caused by the test compounds. Therefore, these antagonists may also be useful in the prevention of mucocutaneous toxicity.

Table 16. RAR Pan-Antagonists That Inhibit TTNPB-Induced Mucocutaneous Toxicity

retinoid	structure	cutaneous tox. score ^a
TTNPB		11 ± 2
121		2.0 ± 0.6
122		1.9 ± 0.7
123		1.4 ± 0

^aThe ratio of TTNPB to test compound was 1:2. (Dose = 3.6 nmol TTNPB + 7.2 nmol test compound per 25 g body weight).

RAR α -Selective Antagonists

Apfel et al.¹²⁹ reported one of the first RAR α -selective antagonists that counteracted the differentiation-inducing ability of RA in the HL-60 assay. Not only was this useful for elucidating the physiological role of the retinoid receptor subtypes, but also this RAR α antagonist inhibited proliferation and induced apoptosis in ER⁺ breast cancer cell lines.¹³⁰

Scientists at Allergan combined the structural features of the antagonist AGN193109 with the framework of the RAR α agonist AGN193836 to produce a true RAR α -selective antagonist AGN194574 with binding affinity for the RAR subtypes as follows: K_d (RAR α) = 1.5 nM, K_d (RAR β) = 898 nM, K_d (RAR γ) = 10618 nM.¹³¹ AGN194574 inhibited the activation of RARs by RA in a dose-dependent manner and will serve as a valuable physiological tool in determining the mechanism of action associated with RAR α .

Recently, the crystal structure of the RAR/RXR heterodimer bound to the antagonist BMS614 was reported.¹³² BMS614 (Figures 19 and 20) is a bipartite molecule comprised of an agonistic core with an antagonistic quinolyl group. It was expected that the RAR α selectivity was due to hydrogen-bonding between Ser-232 of RAR α and the amide nitrogen of BMS614. Therefore, it was surprising to learn that the hydroxyl group of Ser-232 formed a hydrogen bond with an aromatic hydrogen of the quinoline moiety rather than the amide nitrogen. The RAR α residues located in the dimerization interface in the heterodimer were in the same positions as in the monomer. Important differences associated with the ligand-induced *trans*-conformation involved the C-terminal end of the LBD.

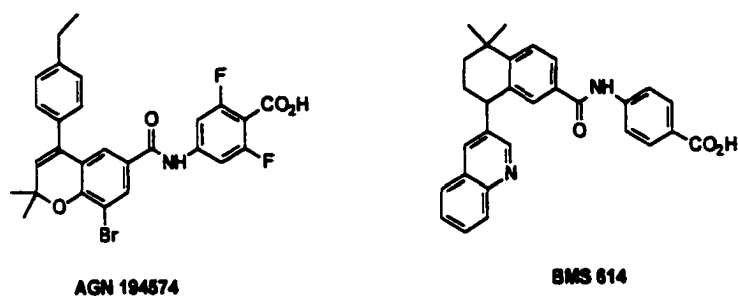


Figure 19. RAR α antagonists AGN194574 and BMS614.¹³²

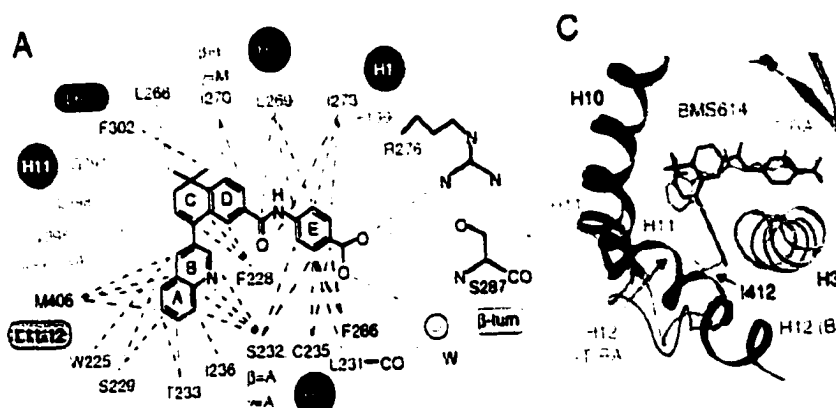


Figure 20. Key interactions of RAR α agonist BMS614 with RAR γ .¹³²

This conformation was similar to that observed for two ER antagonists, raloxifene and tamoxifen, bound to the LBDs of ER.

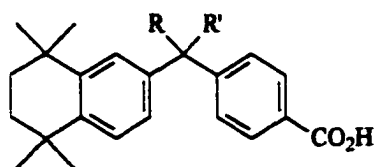
Two features of the antagonist BMS614 might explain the structural differences between the agonist and antagonist-bound LBDs. First, when compared to ATRA, BMS614 was shorter, which shifted the steric constraints, leading to a tilt in H11, and drawing it into the binding cavity. Second, the quinoline group extended between H3 and H11, preventing positioning of H12 in the active conformation. Instead, H12 adopted an

alternative position by binding to a groove known to contribute within the LBDs of PPAR δ , TR β , and ER α to the binding surface of the consensus LXXLL motif of co-activator NR boxes. Thus, in the RAR α / BMS614 complex, the cognate surface for binding of co-activator LXXLL NR boxes, which involved residues of both the groove and holo-H12, was not generated.

Evolution of RXR-Selective Agonists

Johnson et al.¹³³ reported synthetic retinoids that had binding affinity for both RARs and RXRs. Using TTNPB and 9-*cis* RA as models, they shortened the linker from a propenyl group to a one-carbon spacer in order to decrease the distance between the tetrahydronaphthalene ring and the carboxylate. In some cases, they included the linker carbon in a ring. A ring size of five carbons or fewer was necessary for optimal activity and receptor selectivity. Conformational analysis indicated that the spatial orientations of the lipophilic head and the carboxyl terminus of these retinoids were similar to those of 9-*cis* RA, and the activity could be related to the length and volume of the group linking the tetrahydronaphthalene ring and the benzoic acid terminus. Optimal RXR homodimer activation was achieved with either an isopropyl substituent or a ketal ring, as shown in Figure 21. These retinoids were also screened for binding to RXR of the RAR/RXR heterodimer, and they were shown to be very selective for RXR.

The Dawson group¹³⁴ explored the geometry about the 9-10 double bond that was required for RXR binding. This was accomplished by making derivatives of TTNPB (a known RAR agonist). In TTNPB, there is free rotation about the single bonds adjacent to the 9-10 double bond. Therefore, the active conformer was undetermined. Using



SR 11217 R, R' = $(\text{CH}_3)_2\text{C}$

SR11237 R, R' = $\text{OCH}_2\text{CH}_2\text{O}$

Figure 21. Retinoids selective for RXR response pathways.

molecular modeling on the X-ray crystal structures of the two molecules, Jong et al.¹³⁴ determined the two lowest-energy conformations for each molecule. Based on comparisons of the ^1H NMR of the two molecules, the Dawson group was able to identify the low energy conformation of each molecule. Superimposition of these two retinoids with both 9-*cis* RA and the RXR ligand SR11237 revealed the RXR pharmacophoric requirements. The most apparent requirement for RXR activity was a distance of 9.6-10 Å from the C5' of the tetrahydronaphthalene ring to the carboxyl terminus.

The active conformation about the two single bonds of TTNPB analogs was explored next. Beard et al.¹³⁵ synthesized derivatives of TTNPB in order to vary the rotation about the single bond (C2-C9), linking the tetrahydronaphthalene ring with the double bond of the linker (Figure 22). It was shown in binding assays that the 3-methyl derivative of TTNPB bound RXRs with slightly more affinity than the RARs. This observation led the Chandraratna group to postulate that replacement of the C-3 hydrogen with a methyl group caused a conformational change in the molecule that allowed it to interact more favorably with RXR and less favorably with the RARs. An unfavorable steric interaction between the C-3 methyl substituent and the C-10 hydrogen was present in the 3-methyl TTNPB, but not TTNPB (Figure 22). Using molecular modeling, they examined

the differences in the dihedral angles and found that the dihedral angles are $\theta_1 = -38.7^\circ$ and $\theta_2 = 48.7^\circ$ for TTNPB and are $\theta_1 = 71.7^\circ$ and $\theta_2 = 52.6^\circ$ for 3-methyl TTNPB. This confirmed that relative to TTNPB, the 3-methyl substituent of 3-methyl TTNPB caused a pronounced twist of θ_1 but had only a minor effect on θ_2 . Therefore, the differences in receptor selectivity was attributed to the differences in the dihedral angles θ_1 and θ_2 about the C2-C9 and C10-C4' single bonds, respectively.

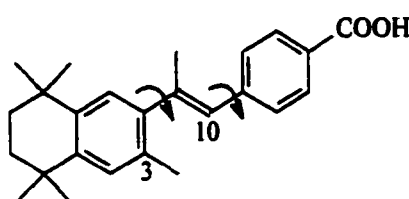
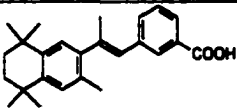
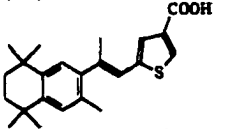
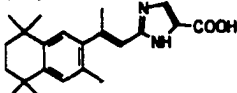


Figure 22. The steric interaction between the 3-methyl and C10 hydrogen induced a change in θ_1 .

Beard et al.¹³⁶ also investigated the effect of varying the dihedral angle θ_2 of TTNPB by altering the benzoic acid terminus. These used a five membered heterocyclic ring to reduce the size of the benzoic acid ring (Table 17) thereby altering θ_2 . The purpose of the heteroatom was to induce a twist in the C10-C2' bond (Figure 22) through the steric repulsion between the C10 hydrogen and the heteroatom at C1'. Small heteroatoms such as oxygen and nitrogen did not induce a twist in the C10-C2' bond, and the heterocycle was essentially planar with the C9-C10 double bond. When sulfur was introduced, the larger third-row atom caused a change in θ_2 , resulting in the RXR selective retinoid **124**. Additionally, when a substituted imidazole ring for the benzoic acid terminus also yielded a potent RXR selective agonist, **125** was generated.

Table 17. The Effect of Varying θ_2 or the Linker of 3-Methyl TTNPB Derivatives on the RXR Activity and Selectivity

retinoid	structure	RAR α	EC ₅₀ (nM)		RXR α
			RAR β	RAR γ	
3-methyl TTNPB		340	230	180	1200
124		NA ^a	NA ^a	NA ^a	201
125		NA ^a	NA ^a	NA ^a	89

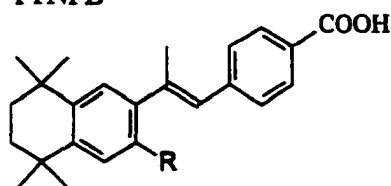
^a NA: not active.

However, conformational analysis showed that the imidazole and the 9,10 double bond were planar. These studies suggested that the θ_2 dihedral angle was not of primary importance in determining RXR selectivity. The most valuable findings in this report concerned the *in vitro* assay results for the RXR-selective retinoids. In the ODC assay, the RXR-selective retinoids were inactive, leading Beard et al. to conclude that the anti-proliferative activity of retinoids was associated with RAR-mediated events. In addition, these retinoids were evaluated in the chondrogenesis assay for teratogenicity. Comparison of the RAR and RXR retinoids in this assay showed a correlation between the RAR binding affinity and inhibition of chondrogenesis. Therefore, the teratogenic effects of retinoids were more mediated through the binding or transcriptional activation of RAR rather than RXR.

At Ligand Pharmaceuticals, Boehm et al.¹³⁷ explored the effects of the size of the 3-alkyl substituent of TTNPB on RXR selectivity. By increasing the size of the 3-alkyl substituent, the dihedral angle θ_1 should increase due to the steric interaction between the

C3 group and the C10 hydrogen. Surprisingly, the methyl substituent was the optimal size for RXR activity. As the size of the alkyl group was increased, the RXR activity was decreased, but selectivity was increased (Table 18). Later, Boehm et al. replaced the propenyl linker of 3-methyl TTNPB with an sp^2 -hybridized one-carbon linker.¹³⁷ In general, the methylene linker was superior to the carbonyl linker for binding and activation of RXR-mediated transcription. The most potent and selective of these retinoids was LGD1069 (Figure 23), which is the first RXR-selective retinoid reported. Because it was one of the first truly RXR-selective retinoids reported, LGD1069 was used to determine the physiological role of the RXR receptor. Additionally, LGD1069, now known as Targretin, has shown promise as a breast chemopreventive agent.^{138,139} Targretin (also called Bexarotene), has been proven effective in the treatment of cutaneous T-cell lymphoma (CTCL) and is approved by the FDA for this clinical use.¹⁴⁰

Table 18. Competitive Receptor Binding Assay Results for the 3-Alkyl Derivatives of TTNPB



retinoid	RAR α	RAR β	EC ₅₀ (nM)	
			RAR γ	RXR α
9-cis RA	7 \pm 1.7	7 \pm 1.3	17 \pm 1.1	32 \pm 3.5
TTNPB	36 \pm 5.1	5 \pm 2.3	26 \pm 4.3	>1000
3-methyl TTNPB	638 \pm 75	1169 \pm 274	645 \pm 120	32 \pm 8.0
3-ethyl TTNPB	100 \pm 49	75 \pm 20	250 \pm 38	320 \pm 40
3-isopropyl TTNPB	>1000	150 \pm 42	>1000	320 \pm 40

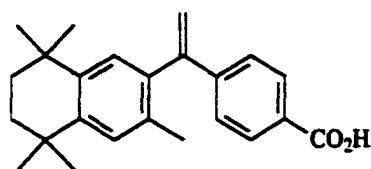


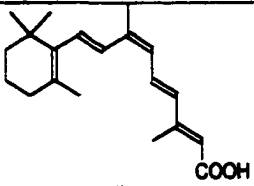
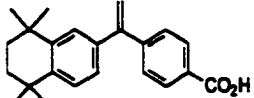
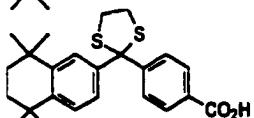
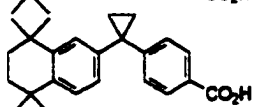
Figure 23. The RXR-selective retinoid Targretin or LGD1069.

Dawson et al.¹⁴¹ used TTNPB and LGD1069 as leads to design RXR-selective molecules. By varying the hybridization and substitution pattern of the bridge carbon, the Dawson group explored the requirements for RXR binding and selectivity. Variations of the linker included substitution with polar or alkyl functionality, changes from sp^2 or sp^3 -hybridization, and heterocyclic modifications of the linker carbon. Some examples of potent RXR-selective ligands discovered by this group are shown in Table 19.

Results of the binding assays revealed the parameters necessary for RXR activity: (1) reduced polarity and increased lipophilic bulk on the one-carbon linker, (2) addition of a 3-methyl group on the tetrahydronaphthalene ring, and (3) a benzoic acid or dienoic acid terminus. RXR selectivity was enhanced by lipophilic bulk on the spacer as well as a benzoic acid terminus.

Dawson et al.¹⁴¹ also explored the low-energy conformation responsible for binding RXRs. The flexibility of the tetraene side chain allowed 9-*cis* RA to assume both the *s-cis* and *s-trans* geometries about the 11*E*, 13*E*-double bond system. Overlapping the two conformers of 9-*cis* RA with RXR-selective retinoids, they were able to predict the low-energy conformation responsible for binding RXRs, which was the *s-transoid* conformer of 9-*cis* RA with a C1-C15 distance of 10.7 Å and a C4-C15 distance 9.6 Å.

Table 19. Retinoid Receptor Transactivation Activities (EC₅₀) for Some of Dawson's RXR-Selective Retinoids

retinoid	structure	RXR α	EC ₅₀ (nM)		
			RAR α	RAR β	RAR γ
9- <i>cis</i> RA		6	23	2.6	4.3
SR11201		270	2300	320	3000
SR11234		170	NA ^a	NA ^a	NA ^a
SR11246		55	NA ^a	NA ^a	NA ^a

^a NA: not active.

Dawson and co-workers¹⁴¹ used computational studies to show that the distance between the tetrahydronaphthalene ring and the carboxyl terminus (C4-C15) of the various retinoids correlated with both RXR activity and selectivity. The optimal distance required for RXR activity ranged from 9.5 to 10.5 Å. High activity was also dependent on the geometry of the retinoid skeleton between C4 and C15. Retinoids that assumed a bent conformation were RXR-selective, whereas those that were more linear favored RAR binding.

Muccio et al.^{142,143} reported 6-*s-trans* conformationally defined tetraene retinoids that exhibited RXR α selectivity. By incorporating the C6-C7 bond in a cyclohexenyl ring, selectivity was achieved. The C5 and C6 positions were substituted with various alkyl groups to mimic the cyclohexenyl ring of RA, resulting in an RXR-selective agonist (9Z)-UAB8 (Figure 24). The structure was further conformationally constrained by in-

cluding the C5 and C6 substituents in an aromatic ring to yield a more potent and selective RXR agonist (9Z)-UAB30 (Figure 24).

Several groups designed and synthesized retinoids of the tetranene class where the 9,10-double bond was replaced with a double bond isostere. As shown in Table 20, Vuligonda et al.¹⁴⁴ at Allergan combined structural characteristics of both the natural retinoid 9-*cis* RA (polyene chain) with 3-methyl TTNPB (tetrahydronaphthalene ring) that resulted in one of the most potent RXR agonists reported to date (126). Vuligonda et al.¹⁴⁵ recently reported the design and synthesis of derivatives of 126. By replacing the tetrahydronaphthalene ring of 126 with the trimethyl cyclohexenyl ring of 9-*cis* RA and using a furan linker to fix the 9-*cis* configuration, they designed retinoid 127. Unlike previously synthesized analogs, the 6,7 single bond was not conformationally constrained in 127 and could exist in either the *s-cis* or *s-trans* conformation. Because the cyclopropyl analog was unstable, the furyl and phenyl rings were used as isosteric replacements for the 9,10 double bond (127 and 128). Although the RXR selectivity was retained, RXR binding affinity was slightly diminished when compared to 126. This could be attributed to decreased steric bulk of the hydrophobic ring.

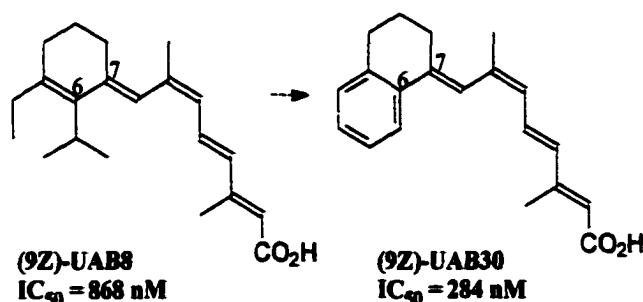


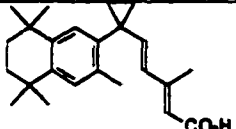
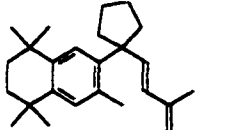
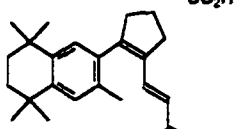
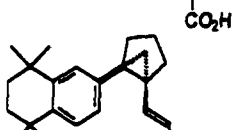
Figure 24. RXR-selective conformationally defined 6-*s-trans* retinoids.^{142,143}

Table 20. Receptor Binding of 9-*cis* RA Analogs With an Isosterically Replaced 9,10 Double Bond

retinoid	structure	RAR α	K _d (nM) RAR β	RAR γ	RXR α
9- <i>cis</i> RA		11	7	22	9
126		>10 ⁴	>10 ⁴	>10 ⁴	1.5
127		>10 ³	>10 ³	>10 ³	7±2
128		>10 ³	>10 ³	>10 ³	26±7

Farmer et al.¹⁴⁶ at Ligand Pharmaceuticals reported conformationally restricted RXR selective retinoids where the 9-methyl group was replaced with cyclic groups to yield spiro molecules. The hydrophobic moiety was modeled after TTNPB and 3-methyl TTNPB. The goal in synthesizing these retinoids was to develop truly RXR selective retinoids with no residual RAR affinity. As shown in Table 21, the binding affinity of the retinoids 129-130 for the RARs was greater than 1000 nM (K_i). Replacement of the 9-methyl with a cyclopropyl group served to enhance RXR binding affinity. In contrast, replacement of the 9-methyl group with a cyclopentyl group resulted in abrogation of RXR activity. The differences in RXR activity for 129 and 130 can be explained by the

Table 21. Retinoids Designed by Farmer et al.^{146,147}

retinoids	structure	EC ₅₀ (nM)			
		RAR α	RAR β	RAR γ	RXR α
129		NA ^a	NA ^a	144	5
130		NA ^a	809	1779	2520
131		>10 ³	>10 ³	>10 ³	5
132		>10 ³	>10 ³	209	4

^a NA: not active.

conformation of the tetraene side chain relative to the tetrahydronaphthalene ring. Conformational analysis of **129** showed that the cyclopropyl group oriented the triene side chain in a bent conformation relative to the tetrahydronaphthalene ring, which favored RXR binding. With the cyclopentyl retinoid **130**, the molecule adopted a linear conformation instead of the bent conformation, thus reducing the RXR binding affinity.

Farmer et al.^{146,147} also reported retinoids similar to those described by Vuligonda et al.¹⁴⁵ by isosterically replacing the 9,10 double bond with cyclopropyl, cyclopentyl, and cyclopentenyl groups to produce retinoids **129-132** (Table 21). The cyclopropyl retinoid **130** exhibited greater RXR activity than the retinoid possessing a cyclopentyl ring (**129**). This can be attributed to the increased sp² character ($\Phi = 118.8^\circ$) of the carbon of the cyclopropyl ring relative to the sp³ carbon ($\Phi = 110.1^\circ$) of the cyclopentyl retinoid.

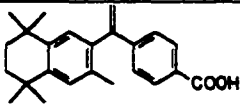
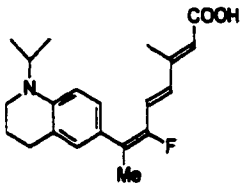
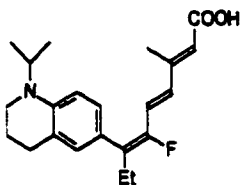
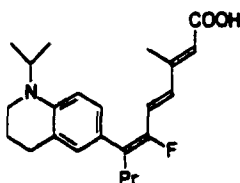
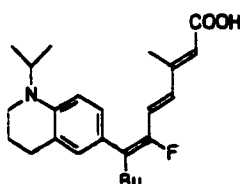
The sp^2 character of the cyclopropyl carbon plays a crucial role in orienting the dienoic acid terminus in a more bent conformation for optimal RXR potency and selectivity. The retinoid with a cyclopentenyl isostere (131) was more potent for RXR than the cyclopropyl retinoid 129. Interestingly, substitution of a bicyclic moiety for the 9,10-double bond resulted in one of the most potent RXR agonists (132) to date.

Hibi et al.¹⁴⁸ reported analogs of 9-*cis* RA by substituting the oxidizable 4-position of the tetrahydronaphthalene ring with an amino functionality (tetrahydroquinoline) in order to reduce retinoidal activities (RAR binding affinity). In addition, fluorine was introduced at the 10-position of the tetraene chain in order to stabilize the 9-*cis* isomer (Table 22). The isopropyl-substituted nitrogen of tetrahydroquinoline 132 had increased RXR activity; however, RXR selectivity was diminished as evidenced by the RAR activity, which was comparable to that of ATRA. Replacement of the 9-methyl group with the larger ethyl substituent in addition to the 10-fluoro group increased RXR activity as well as selectivity. Further increases in size at C-9 (propyl or butyl) resulted in a decrease in RXR transcription by these retinoids.

Structure of 9-*cis* RA Bound RXR

The holo-RXR α structure with 9-*cis* RA bound was reported very recently by Egea et al.¹⁴⁹ This structure revealed how RXR discriminated between binding the 9-*cis* stereoisomer of RA over its all-*trans* isomer (Figure 25). This structure (2.5 Å resolution) further validated the mechanism of ligand-induced activation of the RXR receptor corresponding to the “mouse-trap” model. In the holo structure, H12 is repositioned by

Table 22. Transactivation Data for Tetrahydroquinoline Retinoids¹⁴⁸

retinoid	structure	RAR α	RAR β	EC ₃₀ ^a RAR γ	RXR α	RXR β	RXR γ
Targretin		3900	450	3400	1.2	0.86	0.61
132		6100	40	230	0.16	0.12	0.081
132		NA ^b	1600	NA ^b	0.067	0.068	0.033
133		NA ^b	660	NA ^b	0.68	0.45	0.30
134		NA ^b	NA ^b	NA ^b	110	59	32

^a Retinoid activity is expressed in terms of relative EC₃₀, which is the concentration of retinoid required to produce 30% of the maximal response, normalized relative to 9-*cis* RA (for the RXRs) and ATRA (for the RARs). ^b NA: not active.

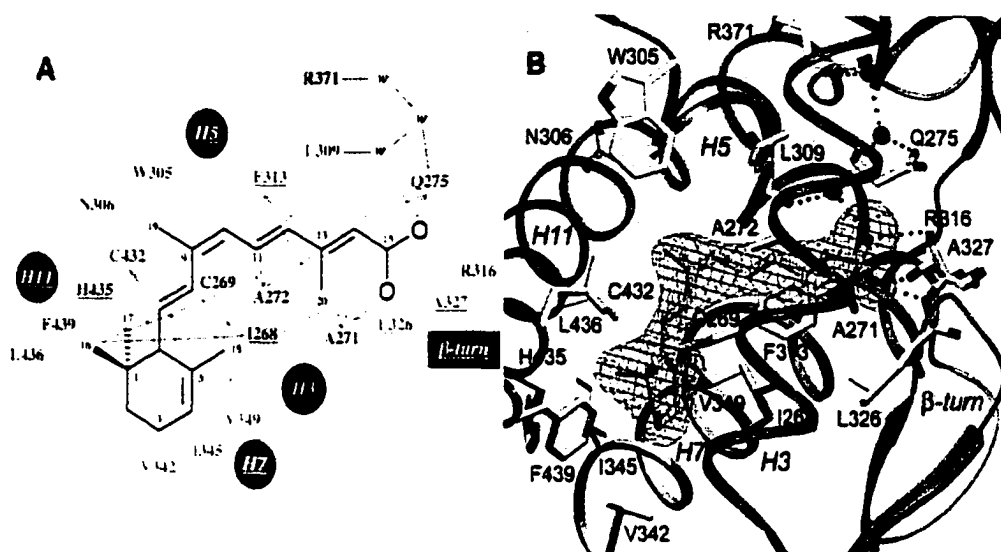


Figure 25. Illustration of interactions of 9-*cis* RA with the RXR α LBP.¹⁴⁹

the ligand in a similar manner by which this retinoid induced a conformational change in the RAR γ -LBD. residues on helices 3,7, and 11. 9-*cis* RA was buried in a hydrophobic pocket formed by residues located on helices H3, H5, and H11 and the β -turn. These residues were conserved in all three RXR (α , β , and γ) isotypes, thus reducing the chances of finding α , β , or γ isotype-specific ligands. The pocket was sealed by Arg316 of helix H5 on one side and H12 on the other side. However, in contrast to RAR γ , 9-*cis* RA does not interact directly with H12 as it does in the RAR γ LBD. Instead, the trimethyl cyclohexenyl ring interacts with The accessible volume of the cavity in the ligand-binding pocket of RXR α is 489 Å³, which is much larger than the volume occupied by 9-*cis* RA in RARs (291 Å³). Unoccupied volume was visible near the C19 methyl group close to Trp305 and Asn306 and the vicinity of the C18 methyl group close to Val349, thus offering interesting possibilities of new, more specific ligands. The size

of such substituents is critical because some RXR antagonists display bulky groups in the area of the C19 methyl group. The antagonistic effect of some retinoids may be due to the displacement of residue Trp305 and the subsequent disruption of the hydrophobic interactions that stabilize the agonist position of H12. The comparison of 9-*cis* RA bound to each RAR γ and RXR α revealed two major differences (Figures 26 and 27). First, 9-*cis* RA bound to RXR α had a more pronounced bending angle (70° versus 60° in RAR γ). Second, the relative orientation of the β -ionone ring of 9-*cis* RA was rotated by 90° around the C9-C10 bond in RXR α . This was a consequence of the different orientation and location of the β -ionone binding sites, which were separated by 9 Å. In the RAR γ *holo*-LBD, the β -ionone ring of 9-*cis* RA pointed toward helix H12 and made hydrophobic contacts with it, whereas, in RXR α , it pointed away from H12. Superimposition of the two complexes revealed that, in RXR α , 9-*cis* RA was shifted 2.7 Å toward the center of the cavity.

Egea et al.¹⁴⁹ also performed modeling studies with an RXR agonist (HX600) and an antagonist (HX531). Both retinoids were anchored in the LBP by interaction of their carboxylates with the arginine of helix H5. Agonist HX600 occupied the LBP at the level of residues Leu433, Trp305, and Gln306. In contrast, the antagonist HX531 possessed a nitro group that caused steric hindrance with the side chains of residues Leu433, Trp305, and Gln306. The latter two residues are involved in the stabilization of H12 in the agonist conformation.

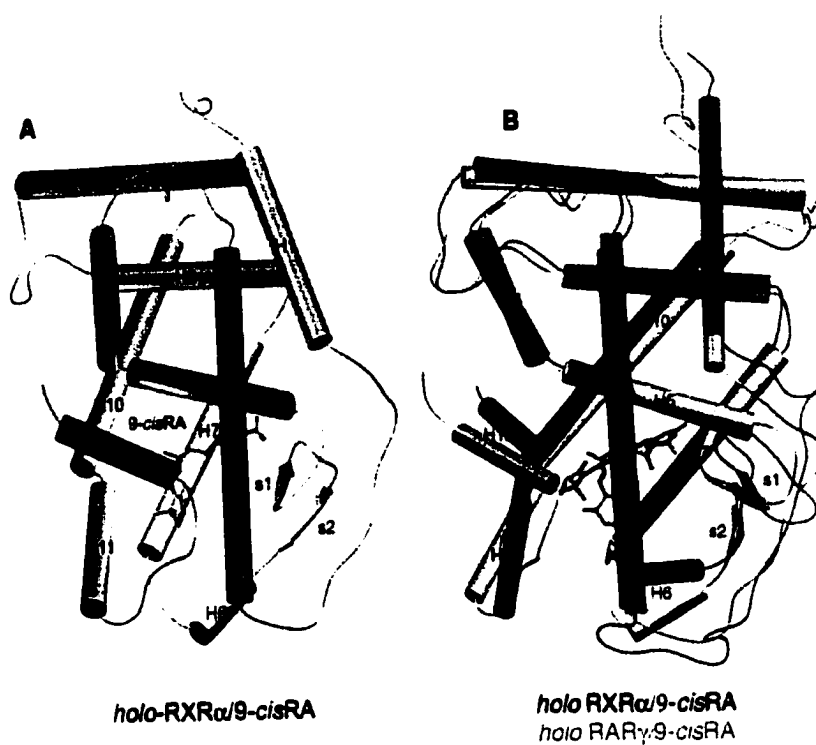


Figure 26. Comparison of structure of 9-*cis* RA bound to RXRα and the apo-RXRα structure.¹⁴⁹

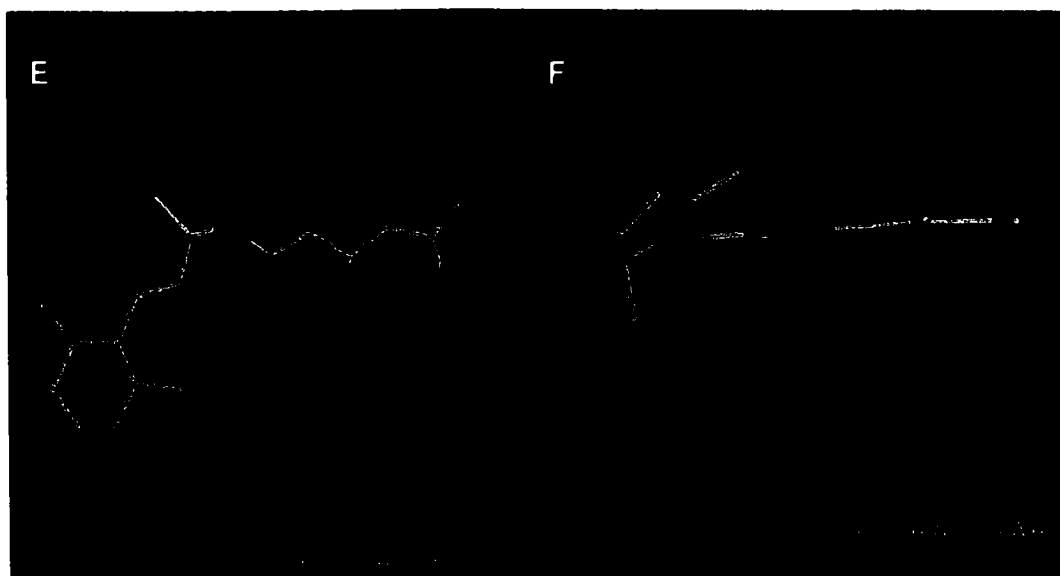


Figure 27. Comparison of the conformations of 9-*cis* RA when bound to RARγ and RXRα.¹⁴⁹

Physiological Role of Retinoid Receptor Subtypes

With the introduction of receptor-selective agonists and antagonists, the molecular signaling pathways involved in the effect of ATRA and 9-*cis* RA on HL-60 cells could be dissected. Nagy et al.¹⁵⁰ used HL-60 sublines with differing patterns of retinoid responsiveness to delineate the role of the two classes of retinoid receptors (RARs and RXRs). In general, these HL-60 cell lines expressed RAR α , RXR α , and RXR β . Both ATRA and 9-*cis* RA have been shown to induce differentiation and apoptosis, but the two isomers of RA can be interconverted by enzymatic or nonenzymatic isomerization. In order to delineate the role of each receptor in the processes of cell proliferation, differentiation, and apoptosis, Nagy et al.¹⁵⁰ used synthetic retinoids, including TTNPB (RAR agonist), Am80 (RAR α agonist), 3-methyl TTNPB (RAR and RXR pan-agonist), and AGN191701 (RXR agonist), and compared the effects of these retinoids to the natural retinoids ATRA and 9-*cis* RA (Table 23). The effect of the retinoids on proliferation in HL-60 cells was monitored over a 6-day period. The agonists can be ranked according to their ability to inhibit cell proliferation (TTNPB = Am80 > 9-*cis* RA = ATRA = 3-methyl TTNPB >> AGN191701). Those agonists capable of activating RAR transcription inhibited HL-60 cell proliferation. Cultures treated with AGN191701, an RXR-selective agonist, had no antiproliferative effect.

The ability of these retinoids to induce HL-60 cell differentiation was also studied. Those retinoids that were capable of binding and transactivating both RAR and RXR nuclear receptors had the most potent effect on differentiation, with the pan-agonists having the greatest effect (3-methyl TTNPB > 9-*cis* RA > TTNPB = ATRA >> AGN191701).

Table 23. The Effects of Retinoids on Proliferation, Differentiation and Apoptosis in HL-60 Cells

retinoid	type agonist	inhibited proliferation	induced differentiation	induced apoptosis
ATRA	RAR	No	Yes	Yes
9-cis RA	RAR, RXR	Yes	Yes	Yes
TTNPB	RAR	Yes	Yes	No
3-methyl TTNPB	RAR, RXR	Yes	Yes	Yes
Am80	RAR α	Yes	Yes	No
AGN191710	RXR	No	No	No

The ability to induce apoptosis was evaluated in the same *in vitro* system. Neither RXR-selective agonist AGN191701 nor RAR agonists (TTNPB, Am80) were able to induce apoptosis. The apoptotic effect was greatest for the pan-agonist 3-methyl TTNPB (3-methyl TTNPB >> 9-cis RA = ATRA >> TTNPB = AGN191701 = Am80). Taken together, these results indicated that the mediator of differentiation-inducing activity of RA in HL-60 cells was the RAR-RXR heterodimer and that ligand activation of RAR was sufficient to induce differentiation. Ligand activation of RXR only through homodimers was not sufficient to induce differentiation in HL-60 cells, and RAR-selective retinoids were only weakly effective in inducing differentiation presumably through RAR/RXR heterodimers. However, pan-agonists were the most effective since they could bind and activate both parts of the RAR/RXR heterodimer. Thus, RXR-selective ligands may potentiate the differentiation-inducing activity of RAR-binding ligands when used in combination with an RAR agonist. The most important role of

RXR-selective retinoids was in the induction of apoptosis. Apoptosis was observed only in those cultures treated with agents capable of activating both RARs and RXRs.

Roy et al.¹⁵¹ explored the ability of an RXR-selective ligand to potentiate the effects of the RAR retinoids. By treating embryonic carcinoma cells (P19 and F9) with RAR-selective agonists Am80 (RAR α), CD666 (RAR β), or SR189453 (RAR γ), in combination with the RXR agonist SR11237, the Chambon laboratory was able to determine the optimal combination for the best synergistic response. At low concentrations, these receptor subtype selective retinoids were unable to induce differentiation alone. In contrast, at these same concentrations, various combinations of RAR (RAR α , RAR β , or RAR γ) and RXR selective retinoids resulted in synergistic induction of all RA target genes examined (STRa4, Hoxa-1, RAR β), as well as in induction of cell differentiation. These results are in agreement with those reported by Nagy et al.¹⁵⁰

Apfel et al.¹⁵² also found that a combination of an RAR agonist with an RXR agonist resulted in synergistic effects on HL-60 cell differentiation. Apfel et al. had previously reported that the differentiation of HL-60 cells into granulocytes was mediated by RAR α . In this report, it was shown that RXR selective retinoids, at doses that are inactive alone, potentiated the effects of ATRA and a RAR α selective retinoid (Am80). They also suggested that HL-60 cell differentiation was mediated by RAR/RXR heterodimers due to the finding that the RXR-selective retinoids could bind the RAR ligand-activated heterodimer complex.

Furthermore, Chen et al.¹⁵³ studied the combination effects of RAR and RXR selective agonists and antagonists on an acute promyelocytic leukemia cell line, NB4. The retinoids employed in this study included RAR-selective agonists BMS753 (RAR α),

BMS453 (RAR β), BMS411 (RAR β,γ), BMS961 (RAR β,γ), and BMS681 (RAR α,β), as well as the RXR-selective agonist SR11237 (RXR α) and the RAR α antagonist BMS614. At concentrations below 0.5-1.0 nM, these agonists were unable to induce differentiation alone, but, when used in combination with the RXR agonist SR11237 (100 nM), differentiation was induced. This was especially true in the case of the RAR α agonist Am80, which suggested that combination of an RAR α and an RXR agonist could be beneficial in the treatment of APL. Furthermore, Minucci et al.¹⁵⁴ proposed that the reason for the ability of an RXR agonist to potentiate the effect of an RAR agonist was due to the fact that binding of an RXR ligand to the heterodimer stabilized the interaction of the heterodimer with its reporter.

Retinoid Synergists

Umemiya et al.¹⁵⁵ reported the design and synthesis of dibenzodiazepinyl retinoids (Table 24), which bound weakly to the RXRs but synergized with the RAR α agonist Am80 in inducing differentiation of HL-60 cells. These synergists evolved from the design and synthesis of some retinoid antagonists. LE135, a conformationally restricted analog of the RAR α agonist Am80, was designed on the basis of the ligand superfamily concept and resulted in an antagonist. In an effort to improve the antagonistic potency of LE135, the hydrophobic aromatic ring was substituted with various bulky aromatic groups.¹⁵⁵ Substitution with a tetramethyl-tetrahydronaphthalene ring resulted in LE590, which showed antagonistic activity in HL-60 cells. However, LE590 was only able to decrease the potency of the RAR α agonist Am80 by half, regardless of the concentration of Am80, which indicated that LE590 was a noncompetitive antagonist.

This observation led Umemiya et al.¹⁵⁵ to design derivatives of LE590 in which one of the cyclic alkyl moieties was removed. This structural class, named the HX series, had no retinoidal activity in the HL-60 assay alone but potentiated the effects of Am80. Alone, HX600 (Table 24) was unable to affect the proliferation or the differentiation of HL-60 cells (maximal concentration 1×10^{-6} M). However, HX600 strongly enhanced the differentiation-inducing ability of Am80, since the percentages of cells differentiated by 3×10^{-10} M Am80 (approximately 15%) were increased to 41% and 72% in the presence of 1×10^{-8} and 1×10^{-7} M HX600, respectively. When compared with the potent RXR agonist LGD1069, the synergistic potency was similar. This was of interest because LGD1069 was a more potent activator of the RXRs. Perhaps, the HX synergists could better bind the heterodimer within the transcriptionally active complex formed with co-activators, while they may not, or very weakly, interact with the RXR monomers or the homodimers in the *in vitro* binding assays. Therefore, at low concentrations, these RXR synergists may be useful in the treatment of leukemia. By reducing the dose of ATRA required for biological effect, they could also be helpful in reducing retinoid-associated toxicity.

Table 24. The Binding Affinities and Synergistic Activities of Diazepinybenzoic Acids

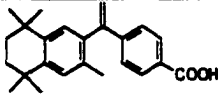
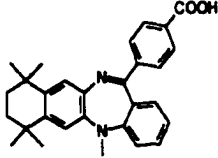
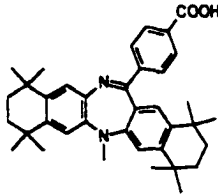
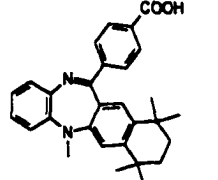
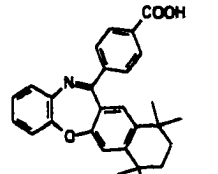
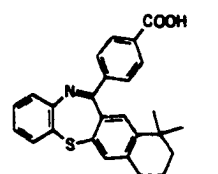
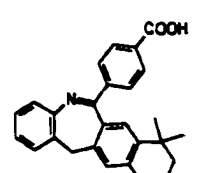
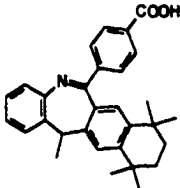
retinoid	structure	K _i (nM)				SEC ₅₀ (M) ^a
		RAR α	RAR β	RAR γ	RXR α	
LGD1069		180	50	130	16	3.1 x 10 ⁻¹⁰
LE135		1400	220	NA ^b	NA ^b	NR
LE590		NR ^c	NR ^c	NR ^c	NR ^c	NR
HX600		NA ^b	680	NA ^b	1900	3.2 x 10 ⁻⁹
HX620		980	320	NA ^b	900	5.8 x 10 ⁻⁹
HX630		900	320	NA ^b	900	6.2 x 10 ⁻¹⁰
HX640		1600	810	NA ^b	1800	5.5 x 10 ⁻¹⁰

Table 24 (Continued)

retinoid	structure	K _i (nM)				SEC ₅₀ (M) ^a
		RAR α	RAR β	RAR γ	RXR α	
HX641		2000	-----	NA ^b	900	2.8 x 10 ⁻⁹

^aSEC₅₀ was determined as the concentration of a test compound that induces HL-60 cell differentiation to the extent of 50% in the presence of 3.0 x 10⁻¹⁰ M Am80.

^bNA: not active. One-hundred-fold excess of the test compound did not affect the binding of the labeled compound to the receptors. ^cNR: not reported.

GOALS AND RATIONALE

By developing receptor subtype selective retinoids, retinoid-associated toxicity may be greatly reduced. In addition, receptor-subtype selective retinoids have found new therapeutic applications. Recently, both the pan-agonist 9-*cis* RA¹⁵⁶ and the RXR agonist LGD1069^{138,139} exhibited chemopreventive activity when used as a single agent or in combination with the estrogen antagonist Tamoxifen in rats.

This laboratory recently reported that (9Z)-UAB30 is an RXR-selective retinoid. In order to assess the chemopreventive ability of (9Z)-UAB30 (Figure 1) in the *N*-methylnitrosourea (MNU) rat mammary chemoprevention assay, multigram quantities were required (10-75 g). The first goal of this dissertation was to scale up the synthesis of (9Z)-UAB30 in order to provide the necessary quantities for evaluating its capacity to prevent mammary tumors *in vivo*. This required optimization of the published synthetic methods for (9Z)-UAB30.⁹⁸

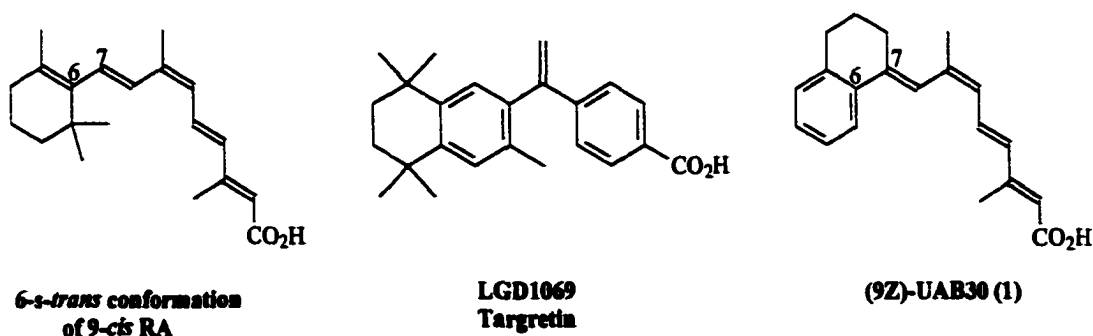


Figure 1. Structures of 9-*cis* RA, Targretin, and (9Z)-UAB30.

A sound major goal of this proposal was to prepare analogs of (9Z)-UAB30 to determine if RXR selectivity and potency could be improved. Three classes of analogs were proposed. First, we proposed synthesizing a homologous series of ring-substituted analogs (2-6, Figure 2). We believed that RXR selectivity might be enhanced by hydrophobic interactions between these substituents and the residues of the LBP or by effects on electron density of the aromatic ring.

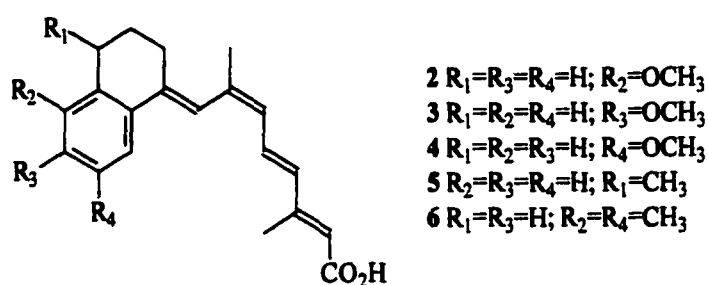


Figure 2. Ring-substituted analogs of (9Z)-UAB30.

Examples of potent RXR-selective ligands from the literature, such as LGD1069, are twisted about the central linker in the molecule.¹³⁷ Further, it was believed that, when bound to the RXR receptor, 9-*cis* RA adopted a bent conformation.^{137,141} This was later confirmed by Egea et al.¹⁴⁹ when the crystal structure of 9-*cis* RA bound to RXR α was published. Therefore, we proposed that by altering the torsion angle of the C6-C7 bond of (9Z)-UAB30, RXR-selectivity and potency might be enhanced (Figure 3). Thus the synthesis of compound 7 was proposed, in which the torsion angle about the C6-C7 bond would be increased via a more conformationally flexible seven-membered ring.

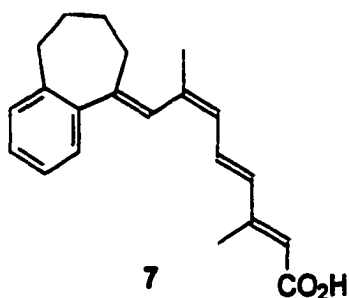


Figure 3. Ring-expanded analog of (9Z)-UAB30.

Examples of potent RXR-selective ligands from the literature, such as LGD1069, contain a terminal benzoic acid.¹³⁷ Also, it had been shown that inclusion of an internal amide group changed the selectivity of the potent pan-agonist TTNPB and resulted in a RAR α -selective retinoid Am80.^{93,96} Using a similar strategy, we proposed to alter the structure of (9Z)-UAB30 by replacing the carboxyl terminus of (9Z)-UAB30 with an amide linked p-amino benzoic acid (Figures 1 and 4). Even if this does not enhance potency and/or selectivity, these structural changes would simplify and shorten the synthesis, and these retinoids (8-14) would be more resistant to oxidation as compared to (9Z)-UAB30.

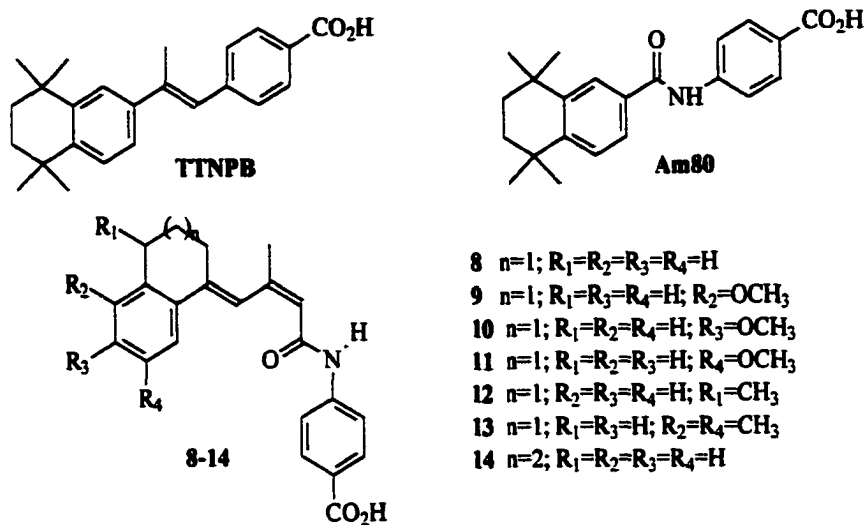


Figure 4. Structures of TTNPB, Am80, and the amide derivatives of (9Z)-UAB30.

**THE LARGE SCALE SYNTHESIS OF (9Z)-UAB30 AND THE EFFECT
ON PREVENTION OF CHEMICALLY INDUCED MAMMARY TUMORS**

by

**KIMBERLY K. VINES, WAYNE J. BROUILLETTE, DONALD D. MUCCIO,
CLINTON L. GRUBBS**

In preparation for Journal of Medicinal Chemistry

Format adapted for dissertation

Abstract

We previously reported the synthesis and *in vitro* activity of the conformationally constrained 9-*cis* retinoic acid (RA) analog, (2*E*,4*E*,6*Z*,8*E*)-8-(3',4'-dihydro-1'(2'H)-naphthalen-1'-ylidene)-3,7-dimethyl-2,4,6-octatrienoic acid ((9*Z*)-UAB30) (Muccio et al. *J. Med. Chem.* **1998**, *41*, 1679). (9*Z*)-UAB30 is a conformationally constrained analog of 9-*cis* RA that locks the tetraene chain in a 6-*s-trans* conformation (Vaezi et al. *J. Med. Chem.* **1994**, *37*, 4499-4507). (9*Z*)-UAB30 was evaluated for nuclear receptor binding and transactivation, and the results were compared to previously synthesized analogs. We previously reported that, in a nuclear receptor binding assay, (9*Z*)-UAB30 exhibited retinoid X receptor (RXR α) selectivity (IC₅₀ = 284 nM), which was a four-fold improvement in binding efficiency over (9*Z*)-UAB8 (IC₅ = 868 nM), which is an earlier synthesized RXR α agonist. Improvement in the RXR α transcriptional activation activity of (9*Z*)-UAB30 (ED₅₀ = 118 nM) was approximately two-fold relative to (9*Z*)-UAB8 (ED₅₀ = 220 nM). Here we report an improved synthesis of (9*Z*)-UAB30 and its evaluation as an effective chemopreventive agent in the rat mammary *N*-methyl nitrosourea (MNU) model.

Introduction

Retinoic acid (RA) is required for diverse biological events such as growth, development, and reproduction.^{1,2} On a cellular level, RA regulates processes such as cell differentiation, proliferation, and cell death. Because RA participates in the regulation of gene expression, its utility as a cancer chemopreventive or a chemotherapeutic agent has been studied using animal models.³ Even though studies have shown that RA may be ef-

fective in the prevention of cancer, its clinical use has been restricted due to toxicity⁴ and teratogenicity.⁵

Retinoids exert these pleiotropic effects through activation of retinoid receptors, which are members of the hormone nuclear receptor superfamily that includes steroid, vitamin D, and thyroid receptors. These retinoid receptors, which cooperatively act as ligand-dependent transcription factors, can be divided into two classes retinoic acid receptors (RARs⁶) and retinoid X receptors (RXRs⁷) and also include several subtypes (α, β, γ).⁸ The RARs and RXRs differ substantially in their respective ligand binding domains (LBD). RARs are activated by (*all-E*)-RA (ATRA), while both RARs and RXRs are activated by (9Z)-RA.⁹ After this discovery, (9Z)-RA was shown to activate both the RXR homodimers¹⁰ and RAR/RXR heterodimers.¹¹

Recent advances in chemoprevention have led to increased attention to retinoids, which are currently used in the treatments of various cancers. Tretinoin (ATRA) is used in the treatment of acute promyelocytic leukemia (APL) and leads to a 90% remission rate.¹² Alitretinoin ((9Z)-RA) is effective and well tolerated in the treatment of Kaposi sarcoma (KS), which is an AIDS-related syndrome.¹³ Myeloproliferation can be controlled by Isotretinoin ((13Z)-RA) in 50% of children with juvenile myelomonocytic leukemia (JMML).¹⁴ Targretin (also called Bexarotene), which is an RXR-selective ligand, has been proven effective in the treatment of cutaneous T-cell lymphoma (CTCL).¹⁵

In humans, the current chemoprevention of breast cancer includes the estrogen receptor antagonist Tamoxifen (TAM)¹⁶ for high-risk patients. Tamoxifen has been used to treat existing breast tumors for 20 years and is currently the only Food and Drug Administration (FDA) approved mammary cancer chemopreventive agent. However, long-term

administration of TAM increases the risk of endometrial cancers,¹⁷ since it acts as an agonist rather than an antagonist in the endometrium. As an estrogen antagonist in mammary epithelial tissue, TAM inhibits estrogen-dependent cell growth, but in endometrial tissue, TAM acts as an agonist triggering increased estrogen-dependent cell growth. Therefore, there is a need for alternative chemopreventive agents for breast cancer. One approach is to develop new estrogen antagonists for all tissues. Raloxifen is currently being studied in a Phase III clinical trial for breast cancer prevention. A second approach to limit side effects associated with Tamoxifen therapy is by using combination therapy of Tamoxifen with other chemoprevention agents. The lower dose of TAM in combination with another chemopreventive agent may provide the same protective effect without disadvantages.

Anzano et al.¹⁸ showed that (9Z)-RA when used as a single agent decreased the number of tumors in rats by 50% in the *N*-methyl nitrosourea (MNU) chemoprevention model. They also explored using (9Z)-RA in combination with TAM and found that a synergistic effect was obtained. RXR-selective drugs have shown chemopreventive activity in animal models. Gottardis et al.¹⁹ at Ligand Pharmaceuticals established that the RXR-selective compound, Targretin, exhibited chemopreventive activity when used alone and in combination with TAM. This establishes the use of retinoids, especially those that are RXR-selective, as potential chemopreventive agents. However, Targretin has side effects and has caused hypothyroidism in humans.²⁰ There is clearly a need for other RXR-selective agents that have no toxicity at their effective dose.

As previously reported, this laboratory developed a new RXR-selective retinoid, (9Z)-UAB30 and evaluated its capacity to prevent tumors.²¹ In this study we developed a

large-scale synthesis of (9Z)-UAB30 for evaluation in the MNU animal model for breast cancer. Here we demonstrate that (9Z)-UAB30 at a single dose of 200 mg/kg diet reduced tumor incidence by at least 50% with no observed toxicity. Additional studies are underway to determine efficacy at the maximum tolerated dose.

Biology

In the whole animal chemoprevention assay, portions of each diet mixture were analyzed using high-pressure liquid chromatography (HPLC) methods for retinyl acetate and (9Z)-UAB30 to assure that the proper concentrations were present and the preparations were stable and homogeneous. All procedures were performed under yellow light, and the samples were protected from light. For samples collected at the end of the study, the concentrations of (9Z)-UAB30, retinyl acetate, and retinyl palmitate in liver, mammary, and abdominal fat were determined. Samples (0.5 g) were homogenized in 2 mL of an aqueous solution containing 0.5 mg/mL each of ethylenediaminetetraacetic acid (EDTA) and ascorbic acid. These preparations were extracted with methanol/ butanol (1:1 v/v). HPLC analyses of methanol-butanol extracts of retinoid diet samples and of the plasma and tissue samples (for both the dosed retinoid and retinyl palmitate) were performed with Spherisorb ODS 5- γ columns (4.6 x 250 mm, Phase Separations, Norwalk, CT). The flow rate was 1 mL/min, detection was by UV absorbance at 340 nm, and quantification was by peak area integration and external standardization. The eluents for extracts of diet samples were 100% methanol for (9Z)-UAB30 (retention time, 3.40 min), 100% acetonitrile for retinyl acetate (retention time, 6.5 min), and 100% methanol for retinyl palmitate (retention time, 19.7 min). To determine its activity in rats, (9Z)-

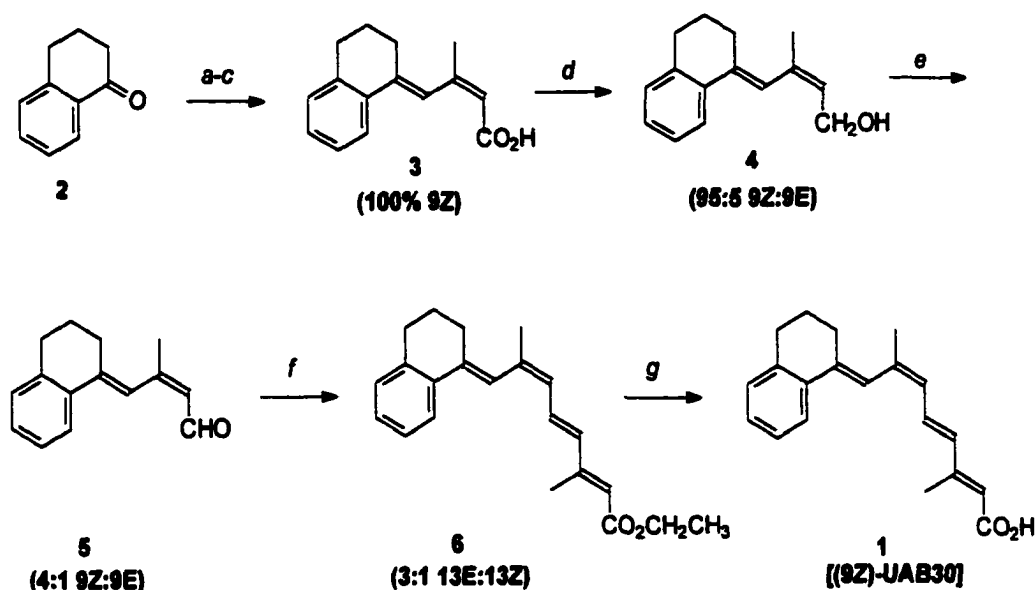
UAB30 was evaluated in an experiment involving two groups of 20 female Sprague-Dawley rats/group. At 50 days of age, the rats received one intravenous injection via the jugular vein of MNU (50 mg/kg bodyweight) that had been adjusted to pH 5.0 with acetic acid. These animals were administered (9Z)-UAB30 in the diet beginning at 53 days of age (or 3 days after the carcinogen). The methods employed in the preparation of diets, analyses of retinoid-containing diets, and exposure of MNU-dosed Sprague-Dawley rats to diets containing (9Z)-UAB30 were previously described.²² Briefly, diets were prepared by mixing the appropriate amount of (9Z)-UAB30 with Teklad (4%) mash diet. For each kilogram of diet, the appropriate amount of (9Z)-UAB30 was dissolved in 12 g ethanol, 19 g trioctanoin, 0.05 ml of Tenox 20 and 0.05 ml of *d,l*- α -tocopherol. The retinoid vehicle was added to the control diet. Diets were mixed in a blender (Patterson Kelley Co., East Stroudsburg, PA) and stored at 4 °C. The rats were given fresh diet three times per week. Because of the limited amount of compound (12 g), only one dose level of (9Z)-UAB30 was tested in the mammary cancer model. The rats in Group I (N = 20) received the carcinogen plus (9Z)-UAB30 (200 mg/kg diet), while the control group (Group II) (N = 20) was fed the Teklad (4%) mash diet without (9Z)-UAB30. (9Z)-UAB30 was given to Group I until the end of the study.

The rats were weighed once per week, palpated for mammary tumors twice per week, and checked daily for signs of toxicity. Following termination of the study 140 days after the carcinogen treatment, mammary tumors were excised and processed for histological classification. Greater than 99% were classified as adenocarcinomas. Statistical analyses of cancer incidence and latency were determined using log-rank analysis,²³ and differences in cancer multiplicity were determined by the Armitage test.²⁴ At the

time of sacrifice, serum was collected for analysis of estradiol and progesterone levels and for analysis of the concentration of (9Z)-UAB30. In addition, the liver, uterus, and ovaries were weighed, and the liver was analyzed for levels of (9Z)-UAB30 and retinyl palmitate.

Chemistry

As shown in Scheme 1, the first step in the synthesis of (9Z)-UAB30 was the Reformatsky reaction using commercially available 1-tetralone (**2**). Due to the large scale, the first three reactions were each performed twice. The Reformatsky reaction was performed using 2 x 100 g of **2** to yield approximately 150 g of purified acid (combined, 60%). This reaction proceeded through a γ -lactone intermediate to stereospecifically yield the acid (9Z)-**3**.²⁵ (9Z)-**3** (2 x 75 g) was then reduced with LiAlH_4 to produce the solid alcohol (**4**) in a 95% yield, which contained 95% 9Z and 5% 9E (by NMR). The published synthesis²⁶ differed in that the yield was 67%, and the isomer ratio was 1:1. In addition, the alcohol (**4**) was obtained as an oil rather than a solid. The alcohol (**4**), unlike many intermediate alcohols in retinoid synthesis, tended to be very stable, even when exposed to both light and heat. In fact, recrystallization was used to purify the crude alcohol for elemental analysis. Following storage at -78 °C overnight, alcohol **4** (84.6 g) was oxidized with MnO_2 . After the reaction was complete, the reaction mixture was stored in a cold room at 5 °C overnight and then filtered through a pad of silica gel (50% $\text{Et}_2\text{O}/\text{CH}_2\text{Cl}_2$). Approximately 10 L of solvent were required to thoroughly wash the aldehyde product from the surface of the MnO_2 . After concentrating the combined

Scheme 1. Synthesis of 1^a

^a (a) Zn/HCl; (b) ethyl 4-bromo-3-methyl-2-butenate, 1,4 dioxane, reflux; (c) HCl work-up; (d) LiAlH₄, ether, 0 °C; (e) MnO₂, molecular sieves, CH₂Cl₂, 0 °C; (f) NaH, TEPS, DMPU, THF, 0 °C; (g) (aq) KOH, MeOH, 60 °C.

filtrates *in vacuo*, the crude aldehyde **5** (4:1 ratio of (9Z)-**5** to (*all-E*)-**5**) was purified on two flash columns where excellent resolution was achieved with only 200 mg of the two aldehydes co-eluting. The higher R_f (9Z)-**5** was a solid and could also be further purified by recrystallization for elemental analysis. The published synthesis²⁶ reported the same combined yield for the E/Z isomers, but the isomers were produced as an oil in a 1:1 ratio of 9Z/ 9E. Triethylphosphonoseneioate (TEPS) was then used to olefinate (9Z)-**5** to produce the ester **6**. This step was performed at 0 °C to prevent further isomerization. The ester was obtained as a 3:1 mixture of (9Z, 13E)-**6** to (9Z, 13Z)-**6**. In the published synthesis, the ester was a 2:1 mixture of (9Z, 13E)-**6** and (9Z, 13Z)-**6**, which were sepa-

rated by HPLC to yield oils in both cases. Using normal phase HPLC, the mobile phase was 97% [3:1 ether/tetrahydrofuran (THF)] in hexanes. While satisfactory for a small scale, this procedure was not attractive for scale-up.

In order to avoid using HPLC as a large-scale separation method, other approaches were attempted. Fractional distillation of the bromoester mixture was not an advantageous approach, as discussed by Robinson et al.²⁵ Even though it was possible to separate the two isomers of the bromoester by fractional distillation²⁷ and convert the desired E isomer to the Horner-Emmons reagent, generation of the anion at 0 °C when treated with base caused the double bond to equilibrate to a 3:1 mixture of E:Z.

An alternative to HPLC purification of the ester was developed, which involved hydrolyzing the isomeric mixture of esters ((9Z,13E)-6 and (9Z,13Z)-6) to yield the acid. This isomer mixture was fractionally recrystallized to obtain (9Z)-UAB30 (1). However, this approach was inefficient because the crude acid typically contained only 66-75% (9Z,13E). Therefore, only one preparation of pure (9Z)-UAB30 was obtained. Concentration of the mother liquor (1:1 of 13E/13Z) resulted in an oil, which could not be recrystallized. For example, the recrystallization of 25 g of crude acid yielded only 5 g of pure (9Z)-UAB30. Thus, a more efficient method of separating the isomers was explored.

While the separation of the esters (9Z,13E)-6 and (9Z,13Z)-6 on TLC using a number of solvent systems was unsuccessful early in the study, a good separation was eventually achieved by using 30% hexanes in toluene with 1 mL glacial acetic acid/500 mL solvent. In 100% hexanes, the ester was a single spot near the baseline of the TLC

plate, but, surprisingly, in 100% toluene the spot was near the solvent front. The optimal combination of the two solvents was found to be 30% hexanes in toluene. After isolation of (9Z,13E)-6 by column chromatography, the ethyl ester solid was hydrolyzed under basic conditions to yield the crude acid. NMR analysis of the crude acid showed retention of stereochemistry without isomerization. Recrystallization of the crude acid afforded the yellow needles (9Z)-UAB30, **1**, which was neither light- nor heat-sensitive and thus stable at room temperature for up to 3 days.

Results and Discussion

The results from the MNU assay showed that 200 mg/kg doses of (9Z)-UAB30 did not induce loss of body weight (Figure 1) or clinical signs of toxicity and inhibited the development of mammary tumors (Figure 2). Rats treated with (9Z)-UAB30 prior to the administration of MNU experienced a 54% decrease in the number of tumors when compared to the control group after 140 days. Because of the limited amount of (9Z)-UAB30 available, neither the maximum tolerated dose nor the optimal dose was determined. (9Z)-UAB30, at the dose used in this assay (200 mg/kg), was highly effective in delaying the time of appearance of mammary tumors and decreased the total number of tumors at the end of the study (Figure 1). The carcinogen-treated-only group (Group 1) had 7.5 mammary tumors/rat, while the (9Z)-UAB30-treated animals had 3.5 tumors/rat (a 53% reduction).

Other retinoids have also been tested in the MNU assay for mammary cancer chemoprevention. Anzano et al.¹⁸ first reported the potential of 9-*cis* RA both as a single

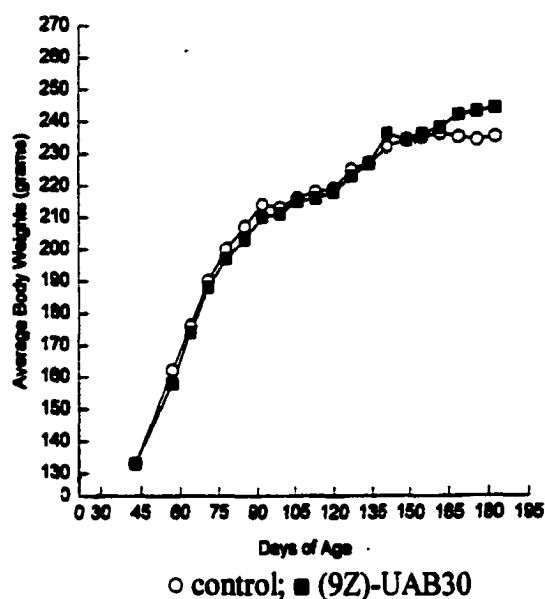


Figure 1. Comparison of body weights of the control vs. rats treated with (9Z)-UAB30.

agent and in combination with Tamoxifen. After treating the rats with 9-*cis* RA for 4.5 months, the number of tumors was decreased from 2.6 tumors/rat (control group) to 0.6 tumors/rat at a dose of 120 mg/kg diet. However, doses exceeding 50 mg have been associated with teratogenicity.

Gottardis et al.¹⁹ also reported the results from the MNU assay for the RXR-selective retinoid Targretin, which is currently approved in the treatment of cutaneous T-cell lymphoma. LGD1069 (Targretin) was also tested at two doses for 12 weeks. In this model, final tumor incidence for the 30 and 100 mg/kg-treated animals was 22% (N = 18) and 12% (N = 16) of controls, respectively, after 21 days. Retinoids may have systemic toxic effects. For example, it is well known that dosing of rats with retinyl acetate leads to increased hepatic concentrations of retinyl palmitate.²⁸ Administration of natural

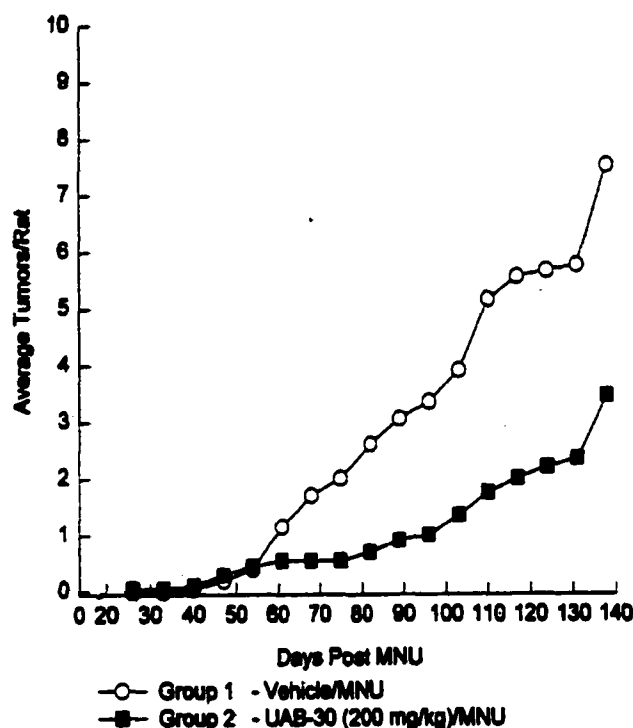


Figure 2. Comparison of average number of tumors per rat in the control animals vs. rats treated with (9Z)-UAB30.

retinoids can result in retinyl palmitate levels as high as 500 mg/g of liver, which can lead to cirrhosis. Synthetic retinoids may also affect liver storage of retinyl palmitate.

We evaluated indicators of retinoid-associated toxicity in the present MNU assay. As shown in Table 1, for rats receiving Teklad diet only, the retinyl palmitate level in the liver was 1.29 mg/kg, while, in the rats receiving (9Z)-UAB30, the level was 0.54 mg/kg. Thus, as opposed to other retinoids such as retinyl acetate or retinyl methyl ether, this retinoid did not increase retinyl palmitate levels. A slight increase in liver weight from 3.2 to 3.7 was observed in the (9Z)-UAB30-treated animals, but this increase may not be significant due to the small number of rats involved in this study.

Treatment with (9Z)-UAB30 resulted in moderately decreased retinyl palmitate levels (0.54 mg/g) in comparison to untreated rats (1.29 mg/g). The lower concentrations of retinyl palmitate in the livers of the rats treated with (9Z)-UAB30 revealed that the drug does not enhance the storage of retinyl esters. Another indication of the lack of toxicity was the absence of detectable levels of (9Z)-UAB30 in the liver. This is in contrast to other retinoids, like retinyl acetate, which accumulate in the liver.

Overt signs of toxicity were also absent in whole animals as shown by the effect of (9Z)-UAB30 on the body weights of rats during the course of the study (Figure 1). As indicated in Figure 1, at a 200 mg/kg dose (9Z)-UAB30 did not alter body weight gain. Furthermore, there were no other signs of clinical toxicity (alopecia, bone fractures, limping). Overt signs of toxicity were not observed with LGD1069 at the 100 mg/kg dose, with only one rat showing signs of alopecia.

Table 1. Effects of (9Z)-UAB30 on Plasma Levels of Estradiol and Progesterone and on the Liver Concentration of Retinyl Palmitate in Rats

diet	Estradiol (pg/ml of serum)	Progesterone (ng/ml of serum)	Retinyl palmitate (mg/g of liver)
Teklad Diet only	6.48 ± 2.37	5.96 ± 1.02	1.29 ± 0.02
(9Z)-UAB30^a	3.45 ± 1.12	3.16 ± 0.77	0.54 ± 0.03

^a Dose: 200 mg/kg diet.

The development of mammary tumors is dependent on levels of the sex steroid hormones estrogen and progesterone. These levels were not reported in the MNU assay involving 9-*cis* RA.¹⁸ However, these hormone levels were monitored for both LGD1069¹⁹ and (9Z)-UAB30. It is of interest that serum estradiol and progesterone

levels were decreased in rats receiving (9Z)-UAB30 (Table 2). It is possible that this is the mechanism by which the agent prevents mammary carcinogenesis since many of the tumors are hormone dependent.

Table 2. Effect of (9Z)-UAB30 on Body Weight and on the Weights of Liver, Uterus, and Ovaries of Rats

diet	body	liver	uterus	ovaries
Teklad Diet	261 ± 7	3.2 ± 0.1	0.17 ± 0.02	0.044 ± 0.001
(9Z)-UAB30	247 ± 11	3.7 ± 0.1	0.22 ± 0.03	0.062 ± 0.002

The same phenomenon was previously reported for LGD1069 as well.¹⁹ Estradiol was decreased from 23.6 ± 4.2 to 16.3 ± 2.7 pg/mL (a 31% decrease), while progesterone levels remained similar (from 32.0 ± 5.8 to 35.3 ± 5.8 pg/mL). In contrast to Targretin, (9Z)-UAB30 dosing resulted in decreases in both estradiol and progesterone levels each by 47%. Unexpectedly, both uterine and ovarian weights were increased. This is a surprising result since estradiol and progesterone levels were both lowered. Due to the small number of animals (N = 20) used in this preliminary screen, the 15% increase in uterine weight may not be statistically or biologically significant. The 41% increase in ovarian weight could be due to a negative feedback mechanism. Depressed estradiol levels tend to increase follicle-stimulating hormone (FSH) levels, which in turn sense a lack of steroids and stimulates ovarian cell proliferation, thus accounting for the increase in ovarian weight. Of course, this is matter of conjecture, and further studies must be performed in order to monitor serum levels of FSH and lutenizing hormone (LH) in order to support this conjecture.

Clinical trials of the RXR-selective drug Bexarotene (Targretin) have shown that hypothyroidism (caused by thyrotropin inhibition) and leukopenia are side effects in patients treated for cutaneous T-cell lymphoma at a dose of 650 mg/m².²⁰ Therefore, the serum levels of thyroid stimulating hormone (TSH), produced in the anterior pituitary gland and responsible for the secretion of thyroid hormones such as thyrotropin, need to be evaluated.

In summary, (9Z)-UAB30 is active in the prevention of mammary tumorigenesis in rats at a nontoxic dose level. Additional studies at higher dose levels are warranted, as well as the evaluation of the compound in other cancer models.

Experimental Section

Biology. Chemicals and other materials and their sources are as follows: [11,12-³H] retinol and [11,12-³H] retinoic acid (NEN Life Science Products, Boston, MA); retinol, retinyl acetate, retinoic acid, trioctanoin, and d,l- α -tocopherol (Sigma Chemical Co., St. Louis, MO); *N*-methyl nitrosourea (MNU) (Ash Stevens, Inc., Detroit, MI); Tenox 20 (Eastman Chemical Co., Kingsport, TN); and Teklad mash diet and Sprague-Dawley rats (Harlan Sprague-Dawley, Indianapolis, IN).

Chemistry. ¹H NMR spectra were obtained at 300.1 MHz on a Bruker spectrometer in CDCl₃. UV-Vis spectra were recorded on both an AVIV 14DS spectrophotometer and a Hewlett-Packard spectrophotometer in methanol or acetonitrile solutions (Fisher, spectrograde). IR spectra were recorded using a Bomem FTIR spectrometer. TLC was performed on a precoated 250 μ m silica gel plates (Analtech, Inc.; 5 x 10 cm).

Solvents and liquid starting materials were distilled prior to use. Reactions and purifications were conducted with deoxygenated solvents, under inert gas (N₂) and subdued lighting. Melting points were recorded on a Melt-Temp melting point apparatus and are uncorrected.

(2Z, 4E)-4-(3', 4'-Dihydro-1'(2'H)-naphthalen-1'-ylidene)-3-methyl-2-butenic Acid (3). Zn dust (312 g, 4.80 mol) was stirred with 20% HCl (740 mL) for 20 min at room temperature. The mixture was allowed to settle, and the liquid was carefully removed with a pipet. The Zn was then washed with water (3 x 1 L), anhydrous acetone (3 x 1 L), and anhydrous ether (3 x 1 L). After residual ether was removed under a stream of N₂, the flask was gently heated with a heating mantle for 30 min, followed by strong heating with a bunsen burner flame for 1 min. The cooled Zn dust was suspended in anhydrous 1,4 dioxane (750 mL) and a solution of 1-tetralone (2, 100 g, 0.680 mol), ethyl 4-bromo-3-methyl-2-butenate 8 (283 g, 1.37 mol), and anhydrous 1,4 dioxane (750 mL) was added over 10 min, which produced an exothermic reaction. The resulting reaction mixture was stirred at reflux for 3 h and then cooled to room temperature. The reaction mixture was diluted with ether (1 L), acidified with 5% HCl (1 L), and filtered through a pad of Celite. The filter was washed well with ether (250 mL), and the ether layer from the filtrate was split into two fractions due to the limited capacity of the separatory funnel. The ether layer (1 L) was extracted with 1 N NaOH (3 x 1L). The pH of the basic aqueous layer was adjusted to pH 1-2 with 5% HCl and extracted with ether (3 x 1L). The organic layer was washed with saturated NaCl solution, dried (Na₂SO₄), and concentrated under vacuum to provide the (9Z)-acid 3 (100 g, 70% yield) as a crude oily

solid. Purification of this solid was accomplished by trituration with cold 10% EtOAc/Hexanes (200 mL) to yield **3** (75 g, 49%) as a yellow crystalline solid: mp 148-149° (ether/hexanes) (lit.²⁶ mp 153-154°); FTIR (KBr) 1677 (C=O), 1618 (C=C) cm⁻¹; MS m/e 229.1 (MH⁺); UV-Vis (MeOH) λ_{max} 311 nm (ϵ =11928); ¹H NMR (CDCl₃): δ 7.67-7.64 (m, 1H), 7.18-7.07 (m, 4H), 5.78 (s, 1H), 2.80 (t, 2H, J=6.23), 2.57 (dt, 2H, J=1.40 & 6.20), 2.13 (s, 3H), 1.83 (p, 2H, J=6.27); ¹³C NMR (CDCl₃): δ 171.88, 156.41, 140.22, 138.62, 136.15, 129.43, 128.17, 126.63, 125.28, 122.50, 118.41, 30.60, 29.05, 26.13, 23.68.

Anal. (C₁₅H₁₆O₂) calcd.: C 78.92% H 7.06%. Found: C 78.93% H 7.15%.

(2Z,4E)-4-(3',4'-dihydro-1'(2'H)-naphthalen-1'-ylidene)-3-methyl-2-buten-1-ol (4). A solution of the acid **3** (92.0 g, 0.400 mol) in anhydrous ether (4 L) was cooled to -78 °C, and a 1 M solution of LiAlH₄ in ether (400 mL, 0.400 mol) was added with stirring under nitrogen. After the dry ice-isopropanol bath was removed, the reaction temperature was brought to 0 °C with an ice water bath and allowed to stir for 3h. The reaction was quenched with methanol (100 mL) followed by the addition of 5% HCl (1 L). The mixture was extracted with ether (2 x 500 mL), washed with saturated NaCl solution (1 L), dried (Na₂SO₄), and concentrated *in vacuo* to give a solid residue **4** (84.6 g, 98%) as a white solid: mp 50-51 °C (ether/hexanes); FTIR (KBr) 3334 (OH), 1612 (C=C); MS m/e 215 (MH⁺); UV-Vis (MeOH): λ_{max} 265 nm (ϵ =13300); ¹H NMR (CDCl₃): δ 7.60-7.57 (m, 1H), 7.18-7.07 (m, 4H), 6.36 (s, 1H), 5.55 (t, 1H, J=6.63), 4.05 (d, 2H, J=6.63), 2.82 (t, 2H, J=6.30), 2.35 (tt, 2H, J=1.44 & 4.69), 1.86-1.73 (m, 5H); ¹³C

NMR (CDCl₃): δ 137.90, 137.77, 136.57, 135.93, 129.63, 129.42, 127.78, 126.73, 126.41, 124.59, 122.45, 32.04, 30.64, 28.40, 24.42, 24.07, 23.11, 14.58.

4-(3', 4'-dihydro-1'(2'H)-naphthalen-1'-ylidene)-3-methyl-2-buten-1-al [(9Z)-5 and *all-E* 5]. A slurry containing activated MnO₂ (688 g, 8.00 mol), powdered molecular sieves (250 g), and anhydrous CH₂Cl₂ (2 L) was prepared and cooled to 0 °C. A solution of the alcohol 4 (84.6 g, 0.400 mol) in anhydrous CH₂Cl₂ (2 L) was added, and the reaction mixture was vigorously stirred (overhead stirrer) at 0 °C for 3 h. The reaction mixture was filtered through a pad of flash silica gel, and the filter was washed with a cold 50% ether/CH₂Cl₂ solution (10 L). The filtrate was concentrated under vacuum to give an oily residue (60 g). This was placed on a flash silica gel column (50 x 6 cm) and eluted with 10% EtOAc/hexanes to yield both (9Z)- and (*all-E*)- 5.

(9Z-5): 35.6 g (42%) yellow solid; mp 66-68 °C; FTIR (KBr) 1661 (C=O), 1603 (C=C) cm⁻¹; MS m/e 213 (MH⁺); UV-Vis (MeOH) λ_{max} 237 nm (ϵ =13950); ¹H NMR (CDCl₃): δ 9.77 (d, 1H, J=8.25), 7.65-7.59 (m, 1H), 7.24-7.11 (m, 3H), 6.56 (s, 1H), 5.82 (td, 1H, J=1.28 & 8.36), 2.86 (t, 2H, J=6.31), 2.49 (td, 2H, J=6.20 & 1.58), 2.09 (s, 3H), 1.83 (p, 2H, J=6.27); ¹³C NMR (CDCl₃): δ 193.58, 159.78, 142.15, 138.55, 135.02, 129.86, 129.44, 128.80, 126.61, 124.83, 120.60, 30.45, 28.84, 25.68, 24.09.

Anal. (C₁₅H₁₆O) calcd.: C 84.87% H 7.60%. Found: C 84.57% H 7.61%.

(*all-E*)-5: 2.0 g (2.4%) yellow oil; FTIR (neat) 1664 (C=O), 1604 (C=C) cm⁻¹; MS m/e 213 (MH⁺); UV-Vis (MeOH): λ_{max} 277 nm (ϵ =10780); ¹H NMR (CDCl₃): δ 10.10 (d, 1H, J=8.16), 7.60 (d, 1H, J=8.10), 7.26-7.11 (m, 3H), 6.50 (s, 1H), 6.04 (d, 1H, J=8.15), 2.83 (t, 2H, J=6.25), 2.76 (t, 2H, J=6.29), 2.35 (s, 3H), 1.84 (p, 2H, J=6.24); ¹³C

NMR (CDCl₃): δ 156.38, 142.94, 138.86, 135.39, 129.19, 128.47, 127.73, 126.41, 125.53, 124.65, 30.03, 29.00, 23.51, 18.77.

(2E,4E,6Z,8E)-Ethyl 8-(3',4'-dihydro-1'(2'H)-naphthalen-1'-ylidene)-3, 7-dimethyl-2,4,6-octatrienoate ((9Z)-6). In a dry round-bottom flask flushed with N₂ (g), NaH (60% dispersion in mineral oil) (2.06 g, 61.3 mmol) was washed with hexanes three times to eliminate the mineral oil. At 0 °C, the NaH was suspended in anhydrous THF (25 mL), and freshly distilled triethyl phosphonosencioate (15.0 g, 56.6 mmol) was added followed by distilled 1,3-Dimethyl-3,4,5,6-tetrahydro-2(1H)-pyrimidinone (DMPU) (catalytic amount) and allowed to stir for 20 min. To this mixture was added (9Z)-5 (10.0 g, 47.2 mmol), and the reaction proceeded for 30 min. The reaction was quenched with methanol (20 mL), and the reaction mixture was diluted with ether (300 mL). The ether layer was washed with saturated NaHCO₃ (300 mL) followed by brine (300 mL). The product was dried (Na₂SO₄) and concentrated *in vacuo* to give the ester as a mixture of geometrical isomers. The product was purified by flash chromatography and eluted with 30% hexanes in toluene to yield (9Z)-6 (19.3 g, 84%) yellow solid. FTIR (neat) 1709 (C=O), 1604 (C=C) cm⁻¹; MS m/e 277 (MH⁺); UV-Vis (MeOH) λ_{max} 334 nm (ϵ =28297); ¹H NMR (CDCl₃): δ 7.67-7.62 (m, 1H), 7.21-7.11 (m, 3H), 6.69-6.59 (m, 1H), 6.47 (s, 1H), 6.23 (d, 1H, J=15.6), 6.12 (d, 1H, J=11.0), 5.75 (s, 1H), 4.19-4.14 (m, 2H), 2.85 (t, 2H, J=6.25), 2.40 (m, 2H), 2.22 (d, 3H, J=0.75), 1.98 (s, 3H), 1.83 (p, 2H, J=6.26), 1.33-1.23 (m, 3H); ¹³C NMR (CDCl₃): δ 232.47, 153.33, 151.84, 140.87, 138.18, 134.45, 133.29, 129.66, 128.67, 128.54, 127.85, 126.44, 124.81, 122.91, 118.82, 116.81, 30.66, 28.96, 25.11, 24.16, 21.50, 14.78, 14.29.

(2E,4E,6Z,8E)-8-(3',4'-Dihydro-1'(2'H)-naphthalen-1'-ylidene)-3,7-dimethyl-2,4,6-octatrienoic Acid [(9Z)-1 or (9Z)-UAB30]. The ester (9Z,13E)-6 (10.0 g, 31.0 mmol) was dissolved in HPLC grade methanol (517 mL, final concentration 0.06 M) and a solution of 2 M aqueous KOH (186 mL) was added. The reaction mixture was heated to 60 °C and the reaction proceeded for 2 h, after which the hot solution was allowed to cool to room temperature. The flask was then cooled to 10 °C in an ice bath and acidified with 5% HCl (pH 1-2). The mixture was then filtered, and the filtered solid was dissolved in ether, dried (Na₂SO₄), and concentrated *in vacuo*. The acid was recrystallized from ether/ CH₂Cl₂ to yield (9Z)-1 (6.9 g, 76%) as yellow needles: mp 183-184 °C (ether/CH₂Cl₂) (lit.²⁶ mp: 180-185°C); FTIR (KBr) 3563 (OH), 1670 (C=O), 1592 (C=C) cm⁻¹; MS m/e 295 (MH⁺); UV-Vis (MeOH) λ_{max} 332 nm (ε=29470); ¹H NMR (CDCl₃): δ 7.68-7.59 (m, 1H), 7.23-7.11 (m, 3H), 6.68 (dd, 1H, J=11.02 & 4.25), 6.47 (s, 1H), 6.26 (d, 1H, J=15.3), 6.12 (d, 1H, J=11.0), 5.77 (s, 1H), 2.85 (t, 2H, J=6.27), 2.40 (dt, 2H, J=6.12 & 1.29), 2.23 (s, 3H), 1.98 (s, 3H), 1.82 (p, 2H, J=6.24); ¹³C NMR (CDCl₃): δ 172.92, 155.96, 141.71, 138.56, 138.22, 136.08, 134.25, 134.20, 129.69, 128.00, 127.79, 126.48, 124.84, 122.87, 117.99, 30.65, 28.97, 25.17, 24.16, 14.49.

Anal. (C₂₀H₂₂O₂) calcd.: C 81.60% H 7.53%. Found: C 81.78% H 7.53%.

References

- (1) For recent reviews, see: (a) *Chemistry and Biology of Synthetic Retinoids*; Dawson, M. A.; Okamura, W. H., Eds.; CRC Press: Boca Raton, FL, 1990. (b) *THE RETINOIDS: Biology, Chemistry and Medicine*, 2nd ed., Sporn, M. B.; Roberts, A. B.; Goodman, D. S., Eds. Raven Press: New York, 1994.
- (2) Thaller, C.; Eichele, G. Identification and Spatial Distribution of Retinoids in the Developing Chick Limb Bud. *Nature (London)* **1987**, *327*, 624-628.

- (3) Moon, R. C.; Mehta, R. G.; Rao, K. V. N. Retinoids and Cancer in Experimental Animals. In *THE RETINOIDS Biology, Chemistry and Medicine*, 2nd ed.; Sporn, M. B., Roberts, A. B., Goodman, D. S., Eds.; Raven Press: New York, 1994; pp 573-630.
- (4) (a) Hixson, E. J.; Denine, E. P. Comparative Subacute Toxicity of *All-trans*- and 13-*cis*-Retinoic Acid in Swiss Mice. *Toxicol. Appl. Pharmacol.* **1978**, *44*, 29-40. (b) Kamm, J. J. Toxicology, Carcinogenicity, and Teratogenicity of Some Orally Administered Retinoids. *J. Am. Acad. Dermatol.* **1982**, *6*, 652-659. (c) Cohen, M. Tretinoin: A Review of Preclinical Toxicological Studies. *Drug Dev. Res.* **1993**, *30*, 244-51.
- (5) Kochhar, D. M. Teratogenic Activity of Retinoic Acid. *Acta Pathol. Microbiol. Immunol.* **1967**, *967*, *70*, 398-404. (b) Willhite, C. C. In *Chemistry and Biology of Synthetic Retinoids*; Dawson, M. I., Okamura, W. H., Eds.; CRC Press: Boca Raton, FL, 1990, pp 539-573. (c) Adams, J. Structure-Activity and Dose-Response Relationships in the Neural and Behavioral Teratogenesis of Retinoids, *Neurotoxicol. Teratol.* **1993**, *15*, 193-202.
- (6) (a) Petkovich, M.; Brand, N. J.; Krust, A.; Chambon, P. A Human Retinoic Acid Receptor Which Belongs to the Family of Nuclear Receptors. *Nature (London)* **1987**, *330*, 444-450. (b) Giguere, V.; Ong, E.; Segui, P.; Evans, R. Identification of a Receptor for the Morphogen Retinoic Acid. *Nature (London)* **1987**, *330*, 624-629. (c) Brand, N.; Petkovich, M.; Krust, A.; Chambon, P.; de The, H.; Marchio, A.; Tiollais, P.; Dejean, A. Identification of a Second Human Retinoic Acid Receptor. *Nature (London)* **1988**, *332*, 850-53. (d) Dejean, A.; Bougueleret, L.; Grzeschik, K.-H.; Tiollais, P. Hepatitis B Virus DNA Integration in a Sequence Homologous to *v-erb-A* and Steroid Receptor Genes in a Hepatocellular Carcinoma. *Nature (London)* **1986**, *322*, 70-72. (e) Krust, A.; Kastner, Ph.; Petkovich, M.; Zelent, A.; Chambon, P.; A Third Human Retinoic Acid Receptor, hRAR- γ . *Proc. Natl. Acad. Sci. U.S.A.* **1989**, *86*, 5310-5314. (f) Klaholz, B. P.; Renaud, J.-P.; Mitschler, A.; Zusi, C.; Chambon, P.; Gronemeyer, H.; Moras, D. Conformational Adaptation of Agonists to the Human Nuclear Receptor RAR γ . *Nature Structural Biology* **1998**, *5*, 3, 199-202.
- (7) (a) Mangelsdorf, D.; Ong, E.; Dyck, J.; Evans, R. Nuclear Receptor That Identifies a Novel Retinoic Acid Response Pathway. *Nature* **1990**, *345*, 224-229. (b) Bourget, W.; Ruff, M.; Chambon, P.; Gronemeyer, H.; Moras, D. Crystal Structure of the Ligand-Binding Domain of the Human Nuclear Receptor RXR α . *Nature (London)* **1995**, *375*, 377-382.
- (8) For recent reviews, see: (a) Mangelsdorf, D.J., Umesons, K., Evans, R.M. The Retinoid Receptors. In *THE RETINOIDS Biology, Chemistry and Medicine*, 2nd ed.; Sporn, M.B., Roberts, A.B., Goodman, D.S., Eds.; Raven Press: New York, 1994; pp 319-349. (b) Chambon, P. A Decade of Molecular Biology Receptors. *FASEB* **1996**, *10*, 940-54. (c) Mangelsdorf, D.; Thummel, C.; Beato, M.; Herrlich,

- P.; Schütz, G.; Umesono, K.; Blumberg, B.; Kastner, P.; Mark, M.; Chambon, P.; Evans, R.; The Nuclear Receptor Superfamily: The Second Decade. *Cell* **1995**, *83*, 835-39.
- (9) Levin, A. A.; Sturzenbecker, L. J.; Kazmer, S.; Bosakowski, T.; Huselton, C.; Allenby, G.; Speck, J.; Kratzeisen, C.; Rosenberger, M.; Lovey, A.; Grippo, J. F. 9-*Cis* Retinoic Acid Stereoisomer Binds and Activates the Nuclear Receptor RXR α . *Nature (London)*, **1992**, *355*, 359-361. (b) Heyman, R.; Mangelsdorf, D.; Dyck, J.; Stein, R.; Eichele, G.; Evans, R.; Thaller, C. 9-*Cis* Retinoic Acid is a High Affinity Ligand for the Retinoid X Receptor. *Cell* **1992**, *68*, 397-406.
 - (10) Zhang, X.-K.; Lehmann, J. M.; Hoffman, B.; Dawson, M. I.; Cameron, J.; Graupner, G.; Hermann, T.; Tran, P.; Pfahl, M. Homodimer Formation of the Retinoid X Receptor Induced by 9-*cis* Retinoic Acid. *Nature (London)* **1992**, *358*, 587-591.
 - (11) Allenby, G.; Janocha, R.; Kazmer, S.; Speck, J.; Grippo, J.; Levin, A. Binding of 9-*cis* Retinoic Acid and All-*trans*-Retinoic Acid to Retinoic Acid Receptors α , β , and γ . *J. Biol. Chem.* **1994**, 16689-16695.
 - (12) For a review, see: (a) Norum, K. R. Retinoids and Acute Myeloid Leukemia. In *Vitamin A in Health and Disease*. Blomhoff, R., Ed.; Dekker Press: New York, 1994; pp 485-501. (b) Chomienne, C.; Fenaux, P.; Degos, L. Retinoid Differentiation Therapy in Acute Promyelocytic Leukemia. *FASEB*, **1996**, *10*, 1025-1030. (c) Coco, F. L.; Nerci, C.; Mandelli, F. Acute Promyelocytic Leukemia: A Curable Disease. *Leukemia* **1998**, *12*, 1866-1880. (d) Clinical Pharmacology of Oral All-*trans* Retinoic Acid in Patients With Acute Promyelocytic Leukemia. *Cancer Res.* **1992**, *52*, 2138-2142.
 - (13) (a) Walmsley, S.; Northfelt, D. W.; Melosky, B.; Conant, M.; Friedman, Kien A. E.; Wagner B. Treatment of AIDS-Related Cutaneous Kaposi's Sarcoma With Topical Alitretinoin (9-*cis*-Retinoic Acid) Gel. *J. Acquir. Immune Defic. Syndr.* **1999**, *22*, 235-246.
 - (14) Castleberry, R. P.; Emanuel, P. D.; Zuckerman, K. S.; Cohn, S.; Strauss, L.; Byrd, R. L.; Homans, A.; Chaffee, S.; Nitschke, R.; Gualtieri, R. J. A Pilot Study of Isotretinoin in the Treatment of Juvenile Chronic Myelogenous Leukemia. *N. Engl. J. Med.* **1994**, *331*, 1680-1684.
 - (15) Carolin, K. A.; Pass, H. A. Bexarotene (Targretin) for Cutaneous T-Cell Lymphoma. *Med. Lett. Drugs Ther.* **2000**, *42*, 31-32.
 - (16) (a) Chang, C. N. A Review of Breast Cancer Chemoprevention. *Biomed. and Pharmacother.* **1998**, *52*, 133-136. (b) O'Shaughnessy, J. Chemoprevention and Breast Cancer. *JAMA* **1996**, *275*, 1349-1353. (c) Swan, D. K.; Ford, B. Chemoprevention and Cancer: Review of the Literature. *ONF* **1997**, *24*, 719-727.

- (17) Stearns, V.; Gelmann, E. P. Does Tamoxifen Cause Cancer in Humans? *J. Clin. Oncol.* **1998**, *16*, 779-92.
- (18) Anzano, M. A.; Byers, S. W.; Smith, J. M.; Peer, C. W.; Mullen, L. T.; Brown, C. C.; Roberts, A. B.; Sporn, M. B. Prevention of Breast Cancer in the Rat With 9-*cis*-Retinoic Acid as a Single Agent and in Combination With Tamoxifen. *Cancer Res.* **1994**, *54*, 4614-4617.
- (19) (a) Gottardis, M. M.; Bischoff, E. D.; Shirley, M. A.; Wagoner, M. A.; Lamph, W. W.; Heyman, R. A. Chemoprevention of Mammary Carcinoma by LGD1069 (Targretin): An RXR-Selective Ligand. *Cancer Res.* **1996**, *56*, 5566-5570. (b) Bischoff, E. D.; Gottardis, M. M.; Moon, T. E.; Heyman, R. A.; Lamph, W. W. Beyond Tamoxifen: The Retinoid X Receptor-Selective Ligand LGD1069 (Targretin) Causes Complete Regression of Mammary Carcinoma. *Anticancer Res.* **1998**, *58*, 479-484.
- (20) Sherman, S. I.; Gopal, J.; Haugen, B. R.; Chiu, A. C.; Whaley, K.; Nowlakha, P.; Duvic, M. Central Hypothyroidism Associated With Retinoid X Receptor-Selective Ligands. *N. Engl. J. Med.* **1999**, *340*, 1075-1079.
- (21) Muccio, D. D.; Brouillette, W. J.; Alam, M.; Vaezi, M. F.; Sani, B. P.; Venepally, P.; Reddy, L.; Li, E.; Norris, A. W.; Simpson-Herren, L.; Hill, D. Conformationally Defined 6-*s-trans* Retinoic Acid Analogs. 3. Structure-Activity Relationships for Nuclear Receptor Binding, Transcriptional Activity, and Cancer Chemopreventive Activity. *J. Med. Chem.* **1996**, *39*, 3625-3635.
- (22) (a) Grubbs, C.J.; Steele, V.E.; Casebolt, T.; Juliana, M.M.; Eto, I.; Whitaker, L.M.; Dragnev, K.H.; Kelloff, G.J.; Lubet, R.L. Chemoprevention of Chemically-Induced Mammary Carcinogenesis by Indole-3-Carbinol. *Anticancer Res.* **1995**, *15*, 709-716. (b) Shealy, Y.F.; Frye, J.L.; Riordan, J.M.; Hill, D.L.; McPhillips, M.; Willie, J.J.; Sani, B.P.; Kalin, J.R.; Eto, I.; Grubbs, C.J. Retinyl Ethers as Cancer Chemopreventive Agents. Suppression of Mammary Cancer. *Anticancer Drug Des.* **1997**, *12*, 15-33.
- (23) Peto, J. The Calculation and Interpretation of Survival Curves. In *Cancer Clinical Trials: Methods and Practice*; Buyse, M. E.; Staquet, M. J.; Sylvester, R. J., Eds.; Oxford University Press: Oxford, 1994; pp 361-380.
- (24) Armitage, P. The Chi-Square Test for Heterogeneity of Proportion After Adjustment for Stratification. *J.R. Statist. Soc. B* **1966**, *28*, 150-163.
- (25) Robinson, C. Y.; Brouillette, W. J.; Muccio, D. M. Reactions of Vinylogous Phosphonate Carbanions and Reformatsky Reagents With a Sterically Hindered Ketone and Enone. *J. Org. Chem.* **1989**, *54*, 1992-1997.

- (26) Muccio, D. D.; Brouillette, W. J.; Breitman, T. R.; Taimi, M.; Emanuel, P. D.; Zhang, X.-K.; Chen, G.-Q.; Sani, B. P.; Venepally, P.; Reddy, L.; Alam, M.; Simpson-Herren, L.; Hill, D. L. Conformationally Defined Retinoic Acid Analogues. 4. Potential New Agents for Acute Promyelocytic and Juvenile Myelomonocytic Leukemias. *J. Med. Chem.* **1998**, *41*, 1679-1687.
- (27) Gedye, R.N.; Adora, P.; Khalil, A.H. The Stereochemistry of the Reformatsky Reaction of Methyl 4-Bromo-3-Methyl-But-2-Enoate With β -Cyclocitral and Related Compounds. *Can. J. Chem.* **1975**, *53*, 1943-1948.
- (28) Grubbs, C.J.; Eto, I.; Juliana, M.M.; Hardin, J.M.; Whitaker, L.M. Effect of Retinyl Acetate and 4-Hydroxyphenylretinamide on Initiation of Chemically-Induced Mammary Tumors. *Anticancer Res.* **1990**, *10*, 661-666.

**CONFORMATIONALLY DEFINED RETINOIC ACID ANALOGUES:
SYNTHESIS, NUCLEAR RECEPTOR BINDING, AND TRANSCRIPTIONAL
ACTIVATION ACTIVITY OF DERIVATIVES OF RXR-SELECTIVE (9Z)-
UAB30**

by

**KIMBERLY K. VINES, WAYNE J. BROUILLETTE, DONALD D. MUCCIO,
BRAHMA .P. SANI, AND XIAO-KUN ZHANG**

In preparation for Journal of Medicinal Chemistry

Format adapted for dissertation

Abstract

We recently reported the synthesis and biological activity of the conformationally defined 6-*s-trans* retinoic acid (RA) analogue, (9*Z*)-UAB30 [(2*E*,4*E*,6*Z*,8*E*)-8-(3',4'-dihydro-1'(2'H)-naphthalen-1'-ylidene)-3,7-dimethyl-2,4,6-octatrienoic acid], which is retinoid X receptor (RXR α) selective (IC₅₀= 284 nM; EC₅₀ = 118 nM) (Muccio et al. *J. Med. Chem.* 1998, 41, 1679). In order to explore which structural characteristics affect RXR α binding and selectivity, analogues were synthesized with substituents on both the phenyl and cyclohexenyl rings of the fused ring system of UAB30. Both the binding affinity and the transcriptional activation ability of these retinoids were measured for the retinoid nuclear receptors retinoic acid receptor (RAR) (α , β , γ) and RXR α . Substitution at the 5', 6', and 7' positions on the phenyl ring abrogated RXR α binding affinity, but substitution at the 4' position on the cyclohexenyl ring resulted in a dual RAR α /RXR α -selective agonist with enhanced binding affinity and activation for both receptors.

Introduction

Retinoic acid (RA) is requisite for diverse biological events such as growth, development, and reproduction.^{1,2} On a cellular level, RA regulates processes such as cell differentiation, proliferation, and cell death. Because RA participates in the regulation of gene expression, its utility as a cancer chemopreventive or as a chemotherapeutic agent has been studied using animal models.³ Even though studies have shown that RA may be effective in the prevention and treatment of cancer, its clinical use has been restricted due to toxicity⁴ and teratogenicity.⁵

Retinoids presumably exert these pleiotropic effects through activation of retinoid nuclear receptors, which are members of the hormone nuclear receptor superfamily that

includes steroid, vitamin D, and thyroid receptors. These retinoid receptors, acting cooperatively as ligand-dependent transcription factors, can be divided into two classes (RARs⁶ and RXRs⁷) and also include several subtypes (α, β, γ).⁸ The RARs and RXRs differ substantially in their respective ligand binding domains (LBD) and are thus activated by different ligands (Figure 1). RARs are activated by (*all-trans*)-RA (ATRA),⁶ while both RARs and RXRs are activated by (9Z)-RA.⁹ After this discovery, (9Z)-RA was shown to activate both the RXR homodimers¹⁰ and RAR/RXR heterodimers.¹¹

Recent advances in chemoprevention have led to increased attention to retinoids, which are currently used in the treatments of various cancers. Tretoinin (ATRA) is used in the treatment of acute promyelocytic leukemia (APL) and leads to a 90% remission rate.¹² Alitretinoin ((9Z)-RA) is effective and well tolerated in the treatment of Kaposi Sarcoma (KS), which is an AIDS-related syndrome.¹³

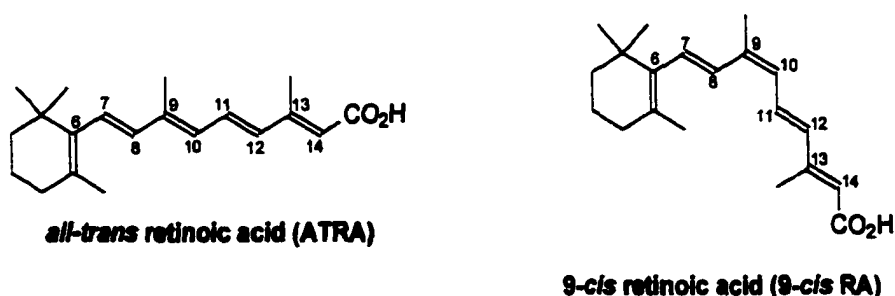


Figure 1. Structures of two natural retinoids.

Myeloproliferation can be controlled by Isotretinoin ((13Z)-RA) in 50% of children with juvenile myelomonocytic leukemia (JMML).¹⁴ Targretin (also called Bexarotene), which is an RXR-selective ligand, has been proven effective in the treatment of cutaneous T-cell lymphoma (CTCL).¹⁵ Targretin is also currently undergoing clinical

taneous T-cell lymphoma (CTCL).¹⁵ Targretin is also currently undergoing clinical trials for breast cancer chemoprevention after showing promising activity in rats in the *N*-methyl nitrosourea (MNU) model for mammary cancer chemoprevention. RAR and RXR selective ligands have shown promise as therapeutic agents for breast cancer in animal models.¹⁶

Another possible use for retinoids is chemoprevention, either alone or in combination with other hormone agonists or antagonists.¹⁶ In animal models, the RAR/RXR pan-agonist (9Z)-RA and other RXR-selective retinoids are effective in animal models for the chemoprevention of breast cancer.¹⁷ In humans, the only currently Food and Drug Administration (FDA) approved chemopreventive drug is the estrogen antagonist Tamoxifen (TAM).¹⁸ Preliminary results have shown that long-term administration of TAM increases the risk for endometrial cancers¹⁹ as well as formation of blood clots. The increased risk for endometrial cancer is due to the ability of TAM to act as either an agonist or an antagonist, depending on tissue type. As an estrogen antagonist in mammary tissue, TAM inhibits estrogen-dependent cell growth, but, in endometrial tissue, TAM acts as an agonist triggering increased estrogen-dependent cell growth. Another major complication with long-term TAM therapy is the development of resistance to the drug. Possible explanations for TAM resistance include absence or loss of estrogen receptors, agonist activity, altered expression of receptor-interacting proteins and cross talk among the growth signaling pathways.²⁰ In many cases of TAM resistance, estrogen receptor positive (ER⁺) tumor cells become ER⁻, which are refractory to TAM treatment. The main course of action in the case of the very aggressive ER⁻ tumor involves chemotherapy. Therefore, there is a need for alternative chemopreventive agents for breast cancer. An

approach to limit the aforementioned side effects associated with TAM therapy would be to decrease the dose by use in combination with other drugs such as retinoids.

It is well known that classic retinoids such as ATRA inhibit proliferation as well as induce apoptosis in ER⁺ cells. ER⁺ cells are generally more sensitive to the effects of RAR-selective retinoids rather than RXR-selective retinoids because ER⁺ cells express RAR receptors. In ER⁺ cells, RAR-selective retinoids are much more effective in growth inhibition with RAR α specific agonists eliciting the greatest effect.²¹ However, ER⁻ cell lines are resistant to the effects of ATRA. Raffo and co-workers demonstrated that RXR-selective ligands were able to inhibit proliferation and induce apoptosis in the ER⁻ ATRA-resistant cell line MDA-MB-231.²² Interestingly, retinoid analogs were able to induce apoptosis in ZR-75.1 cells, which is a result unlike that of ATRA in the same cell line, which was only able to inhibit proliferation.²³ Thus, retinoid analogs with RXR specificity may be used as chemotherapeutic agents for ER⁻ tumors.

As mentioned previously, RXR-selective drugs have shown chemopreventive activity in animal models. In addition, RXR-selective drugs are associated with fewer side effects than RAR-selective drugs. Anzano and coworkers showed that (9Z)-RA, when used as a single agent in the MNU assay, decreased the number of tumors in rats by 50%.¹⁷ They also explored using (9Z)-RA in combination with TAM and found that a synergistic effect was obtained. Ligand Pharmaceuticals found that the RXR-selective compound, Targretin, exhibited chemopreventive activity when used alone or in combination with TAM,²⁴ however, Targretin has caused hypothyroidism as well as leukopenia in humans.²⁵ Therefore, there is a need for other RXR α ligands with reduced side effects.

RXR ligands have also been used in combination with RAR agonists. In fact, RXR α ligands potentiate the transcriptional effects of RAR ligands²⁶ in various cell lines, including HL-60 and NB-4 cells. Thus, this combination therapy could potentially be used to treat leukemia. This synergistic interaction was explained by Westin et al., who elucidated the interactions controlling the assembly of heterodimers with their co-activators.²⁷ In the absence of ligand, the activation function (AF-2) domain of RXR was docked in the RAR co-activator interaction site, preventing the binding of RXR ligands. Following ligand binding by RAR, steroid receptor co-activator (SRC-1) was recruited through one of the three LXXLL motifs and displaced the RXR AF-2 domain from RAR, thus relieving the allosteric inhibition and allowing RXR ligands to bind. The binding of the RXR ligand promoted interaction with a second LXXLL motif from the same SRC-1 molecule with RXR, stabilizing the complex. This model explained the selective responsiveness of RAR-RXR heterodimers to RAR ligands and resolved the paradox of why RXR ligands potentiate the effects of RAR ligands. Thus, RXR selective ligands can be clinically beneficial in the treatment of cancer.

As discussed in previous reports, the 6-*s-trans* conformation was preferred for retinoidal activity. Thus by conformationally constraining 9-*cis* RA in the 6-*s-trans* conformation, a new class of synthetic retinoids was developed (Figure 2).²⁸ It was shown that retinoids with bulkier groups at the 5 and 6 positions ((9Z)-UAB8) exhibited increased RXR α binding affinity, as well as improved selectivity for RXR α (Table 1). The next generation of (9Z)-RA analogs, (9Z)-UAB30 and derivatives, were further conformationally constrained by including the R₁ and R₂ substituents in an aromatic ring system.²⁹ This was accomplished by fusion of the cyclohexenyl ring to a phenyl ring.

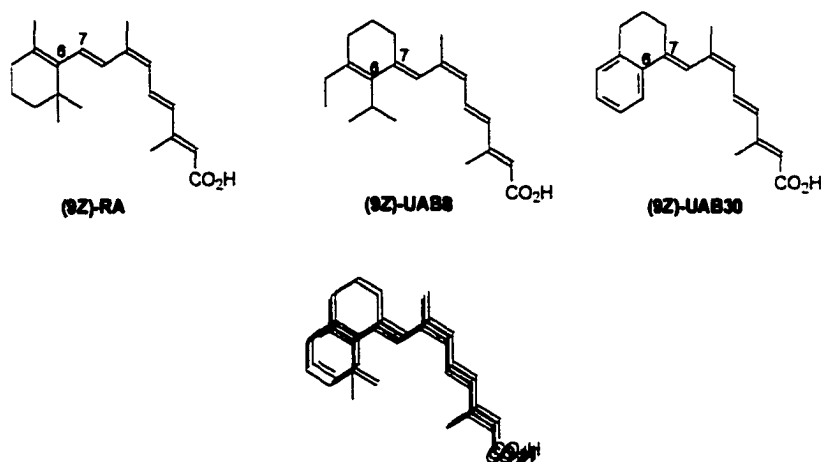


Figure 2. Design strategy for the conformationally constrained 6-*s-trans* analogs of (9Z)-RA.

This strategy resulted in an RXR α agonist (9Z)-UAB30 (IC_{50} = 284 nM; EC_{50} = 118 nM) shown in Table 1 with a four-fold improvement in binding affinity over (9Z)-UAB8 in addition to enhanced RXR-selectivity.

In contrast to previous biological results showing (9Z)-UAB30 as RXR-selective with no RAR affinity,²⁹ recent activation experiments indicated that (9Z)-UAB30 did in fact activate RAR α , but to a lesser extent in comparison to RXR α . Recent studies also revealed a significant difference with regard to the binding affinity (IC_{50} = 960 nM) to RXR α in comparison with the previously reported result (IC_{50} = 268 nM).²⁹ The results from the transcriptional activation assay confirmed the newer binding values. Experiments performed previously also indicated that (9Z)-UAB30 had little affinity for the RAR α /RXR α heterodimer (EC_{50} = >1000 nM), leading our group to believe that (9Z)-UAB30 would affect cells *in vivo* through interaction with the RXR α /RXR α homodimer. However, since (9Z)-UAB30 possesses affinity for RAR α as well as RXR α , the

Table 1. Summary of the IC₅₀ and EC₅₀ Values (nM) for (9Z)-UAB8 and (9Z)-UAB30 Retinoids in Nuclear Receptor Binding and Transcriptional Activation Assays

retinoid	IC ₅₀				EC ₅₀			
	RAR α	RAR β	RAR γ	RXR α	RAR α	RAR β	RAR γ	RXR α
(9Z)-RA	31	8	60	82	18	27	10	27
(9Z)-UAB8	>1000	>1000	>1000	868	>1000	>2000	190	220
(9Z)-UAB30	>2000	>2000	>2000	284	>2000	>2000	>2000	118

biological effects of (9Z)-UAB30 are most likely mediated by the RAR/RXR heterodimers as well as RXR/RXR homodimers. Subsequently, additional biological data are required in order to solve the paradoxical results obtained in the binding and transcriptional activation assays.

In this report, analogs of (9Z)-UAB30 were designed and synthesized in order to enhance the binding affinity for RXRs. At the time, only the apo-RXR α structure was available. The holo-RXR α structure was published after this work had been completed. As shown with RAR γ as well as other hormone nuclear receptors, a substantial conformational change takes place upon ligand binding. Therefore, molecular modeling with the protein was not a straightforward tool in the design of these ligands.

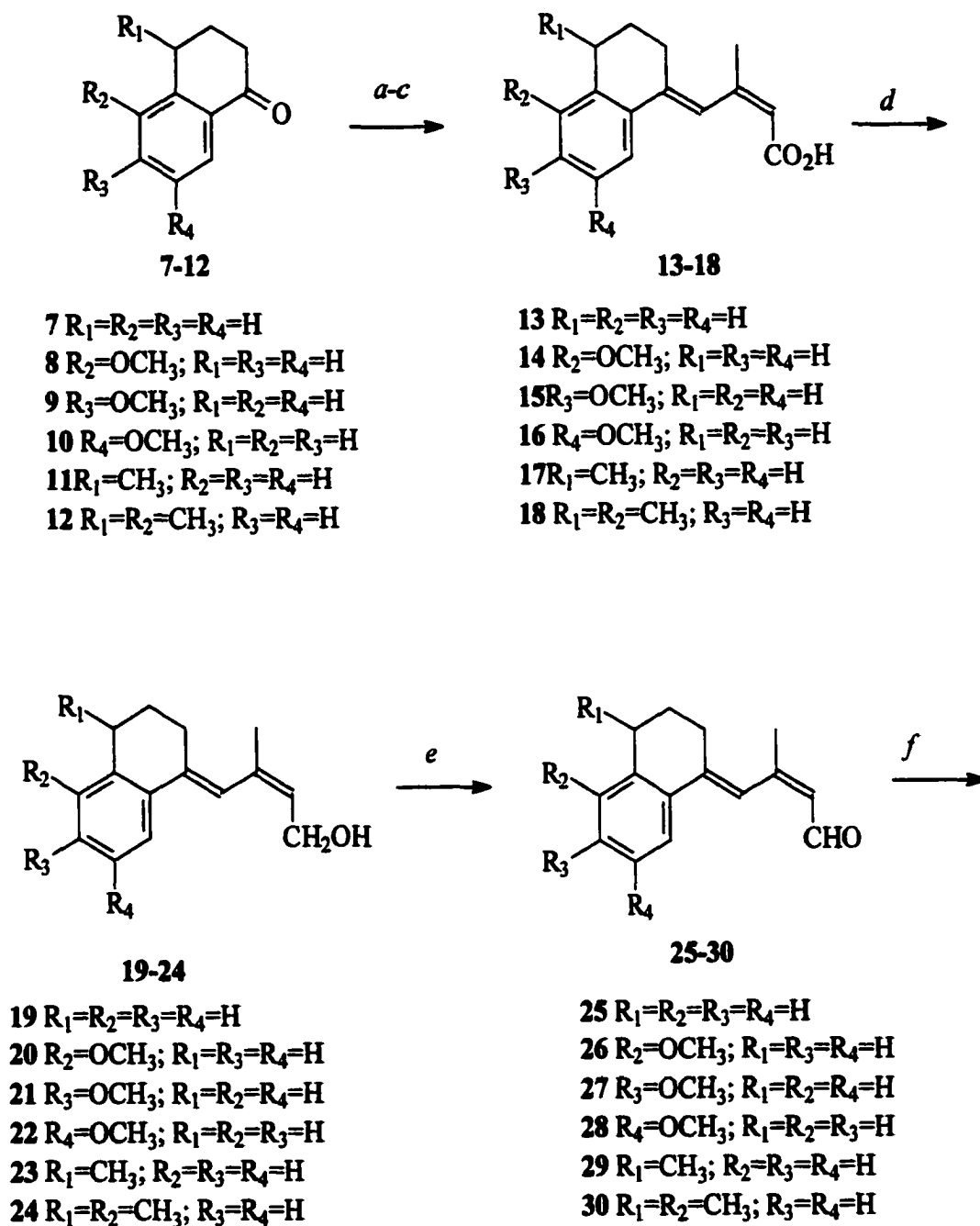
RXR-selectivity could be achieved first with a (9Z)-RA skeleton and second by inducing a twist in the 6-7 single bond.²⁹ Molecular modeling studies performed in our lab indicated that this torsion angle ($\psi_{6,7,8,9}$) of (9Z)-UAB30 was more twisted than that of (9Z)-RA, thus accounting for the increased RXR-selectivity of (9Z)-UAB30. Few RXR-selective ligands have been reported, and the effects of substitution about the region

corresponding to the cyclohexenyl ring on RXR activity and selectivity have not been explored. As shown by the (9Z)-UAB1-8 series of retinoids, additional steric bulk in this region increased RXR activity. We believed that the ligand-binding pocket (LBP) of RXR may accommodate a larger ligand and activity might be enhanced through hydrophobic interactions between RXR and the ligand. Several commercially available starting tetralones substituted with methoxy and methyl groups were selected for this purpose.

Ideally a homologous series should be used to investigate the effects of substitution at each of the positions about the tetralone ring, but this was not possible using commercially available agents. The 2-methyl, 4-methyl, and the 5,7-dimethyl tetralones were commercially available, but not the 5-, 6-, and 7-methyl analogs. Instead, the commercially available 5-, 6-, and 7-methoxy-tetralones were used. In addition to the steric effect of the methyl group, these also included an electronic effect due to the presence of the oxygen in the methoxy substituent.

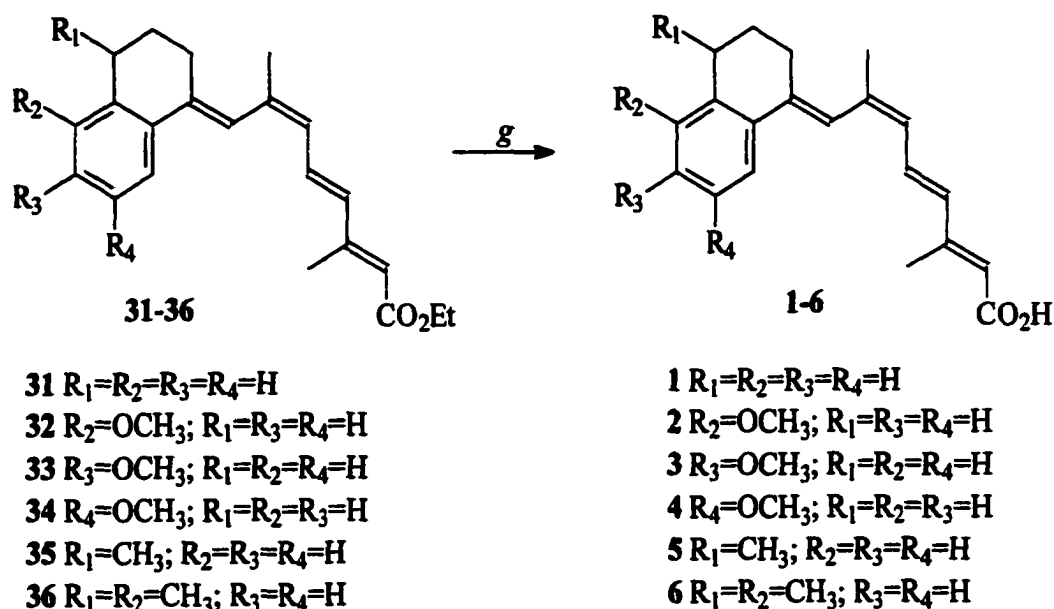
Synthesis

Scheme 1 shows the synthesis of (9Z)-UAB30 **1** and derivatives **2-6**. This synthetic approach was based upon that used previously to synthesize (9Z)-UAB30.²⁹ As shown in Scheme 1, the carboxylic acids **25-30** were prepared from the commercially available 1-tetralone derivatives (**7-12**) via the Reformatsky reaction. The acids (**13-18**) were then reduced with lithium aluminum hydride to give the alcohols (**19-24**) in almost quantitative yields. The alcohols were >95% 9Z, which differed from that reported previously for (9Z)-UAB30. After column purification, Muccio et al.²⁹ obtained the

Scheme 1. Synthesis of analogs of (9Z)-UAB30^a

^a (a) Zn/ HCl; (b) Ethyl 4-bromo-3-methyl-2-butenate, 1,4-dioxane, reflux; (c) 15% HCl work-up; (d) LiAlH₄, diethyl ether, 0 °C; (e) MnO₂, molecular sieves, CH₂Cl₂, 0 °C; (f) NaH, TEPS, DMPU, THF, 0 °C; (g) 0.8 N KOH, MeOH, 60 °C.

Scheme 1 (Continued)



intermediate alcohol ((9Z)-UAB30 synthesis) in a 67% yield with a 1:1 ratio, of Z/ E.²⁹

The result reported here was an obvious improvement in both yield and isomer ratio considering that the 9Z isomer was the desired isomer. The crude alcohols (19-24) were oxidized to the aldehydes (25-30) upon treatment with manganese (IV) oxide in anhydrous dichloromethane. This was a light and heat sensitive reaction, so this step was performed in the dark at 0 °C. In order to drive the reaction to completion, powdered molecular sieves were added to the reaction mixture and stirred vigorously with an overhead stirrer. In the reported synthesis, it was found that sea sand offered an advantage over molecular sieves.²⁹ With these compounds, sea sand caused isomerization of the 9Z-aldehyde. After the reaction reached completion, the reaction mixture was filtered through a pad of flash silica. The filtered solid (MnO₂ and sieves) was transferred to the reaction flask and stirred with 50% ether in CH₂Cl₂ for 30 min. This process was repeated twice more in

order to maximize the yield. Additional washing (>3 times) of the filtered solid did not yield more aldehyde. Even though a 77% yield was obtained for **25**, the typical yield for intermediate aldehydes **26-30** was 60%, and the ratio of 9Z to 9E varied from 4:1 to 5:1. In the published synthesis of (9Z)-UAB30, a 59% yield was reported, and the isomer ratio was 1:1 Z/ E.²⁹ The reported yield for **25** was an improvement, but more importantly, the isomer ratio was enriched in the 9Z isomer. Of course, this was due to the 9Z-enriched alcohol obtained in the reduction.

The (9Z)-aldehydes **25-30** were then olefinated via a Horner-Emmons reaction to yield the crude esters. The crude esters were purified by flash chromatography to yield the purified esters (**31-36**), which were mixtures of geometric isomers in a ratio of 3:1 (9Z) to (9Z, 13Z). In a prior synthesis of (9Z)-UAB30 ester (**31**), high-pressure liquid chromatography (HPLC) on silica was used to separate the two isomers. However, it was discovered that recrystallization of the final product **1** could be utilized to separate the two isomers. The (E,Z)-ester mixtures were thus hydrolyzed to the acid under basic conditions with gentle heating in the absence of light for 1.5 h to yield the crude acid in 90% yield. Longer reaction times resulted in isomerization of the acid and a very crude product that could not be recrystallized. The product was fractionally recrystallized from ether/dichloromethane to yield acids **1-6** in a 40-50% yield. Better yields could be obtained using HPLC at the ester stage rather than recrystallizing the final acid. However, HPLC was time consuming, expensive, and impractical for moderately large-scale synthesis. It should be mentioned that, after this work was completed, a suitable solvent system (30% hexanes in toluene) enabled the flash silica separation of the esters of **1**, thus

making the preparation of (9Z)-UAB30 amenable to large-scale synthesis. A similar system would probably be useful in the separation of the esters (31-36).

Results and Discussion

The binding affinity for the retinoid receptors was measured for four receptor subtypes (RAR α , β , γ and RXR α ; Table 2). Compounds 2-4 and 6 did not possess any appreciable affinity for the RAR α . RXR α affinity was abolished in these compounds as well ($IC_{50} > 2000$ nM). The 4'-methyl substituted analog 5 exhibited affinity for both the RAR α and RXR α receptors. Compared to (9Z)-UAB30, there was a six-fold improvement in RAR α binding affinity accompanied by a four-fold improvement for RXR α .

In order to assess the ability of 1-6 to induce transcription, these compounds were first screened at two concentrations (10^{-6} M and 10^{-7} M) for four receptor subtypes (RAR α , β , γ and RXR α Figures 3-7). Compounds 1 and 2 showed weak activity in both RAR α and RXR α at 10^{-6} M, but activity was greatly diminished at 10^{-7} M. Compound 6 was also active at 10^{-6} M. In fact, 6 was more active than both (9Z)-RA against RXR α and ATRA against RAR α . Surprisingly, activity for 6 was minimal at 10^{-7} M. The most promising of the ring-substituted analogs was 5, which induced transcription in a dose-dependent manner in RXR α , RAR β , and RAR γ and was highly effective at 10^{-7} M.

The purpose of synthesizing these derivatives was to evaluate effects on RXR activity in comparison with (9Z)-UAB30. In this respect, it was determined that substitution at the 4' position enhanced activity. In addition, it seems that substitution at both the 5' and 7' positions enhanced activity, but bulkier groups were required for activity to be maintained at lower concentrations ($\leq 10^{-7}$ M).

Table 2. Inhibition Concentrations at 50% (nM) for the Binding of Retinoids 1-6 and (9Z)-Retinoic Acid (RA) to Mouse Retinoic Acid Receptors (mRARs) and Retinoid X Receptors (mRXRs)

retinoid	IC ₅₀ (nM)			
	mRAR α	mRAR β	mRAR γ	mRXR α
(9Z)-RA	31 ^b	8 ^b	60 ^b	73 ^b
(9Z)-UAB30	980	620	1225	960
(9Z)-2	1505	>500 ^c	>500 ^c	1520
(9Z)-3	>2000 ^d	>500 ^c	>500 ^c	>2000 ^d
(9Z)-4	>2000 ^d	>500 ^c	>500 ^c	>2000 ^d
(9Z)-5	166	285	298	260
(9Z)-6	>2000 ^d	>500 ^c	>500 ^c	1810

^a The IC₅₀ values were determined by the methods of Allenby et al.^{11,30} For IC₅₀ values with RARs, competition of unlabeled test retinoid was determined in the presence of 5 nM of [³H]-(*all-E*)-retinoic acid. For RXRs, competition of unlabeled test retinoid was determined in the presence of 20 nM of [³H]-(9Z)-retinoic acid. ^b Values reported by Allenby et al.³⁰ Based on repeated measurements, the estimated error is 20% of the mean. ^c Doses above 500 nM were not tested, and compound was not active below 500 nM. ^d Doses above 2000 nM were not tested, and compound was not active below 2000 nM.

Experimental Section

Biology. In order to study the ability of the acids 1-6 to recognize RA-binding sites within the protein receptors, the concentrations causing 50% inhibition (IC₅₀) were determined for the RARs and RXRs. The IC₅₀ values for the acids 1-6 were measured for the inhibition of the binding of radiolabeled (*all-E*)-RA to mRAR α , mRAR β , and mRAR γ using methods described previously by Levin and coworkers.¹¹ Similar studies

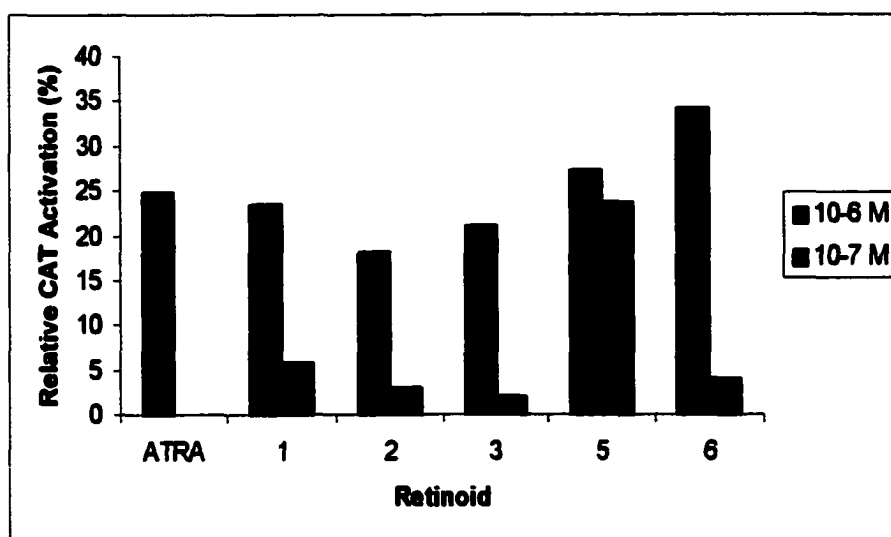


Figure 3. RAR α -receptor transcriptional activation.

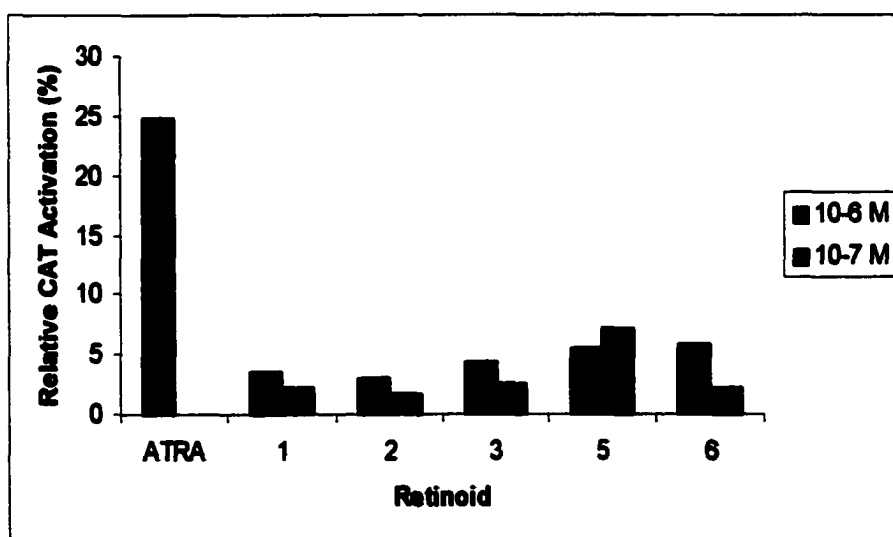


Figure 4. RAR β -receptor transcriptional activation.

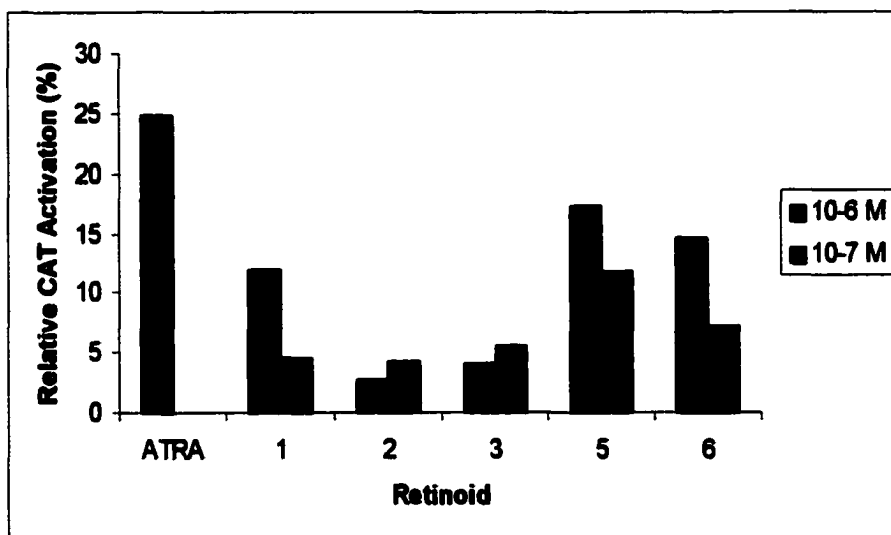


Figure 5. RAR γ -receptor transcriptional activation.

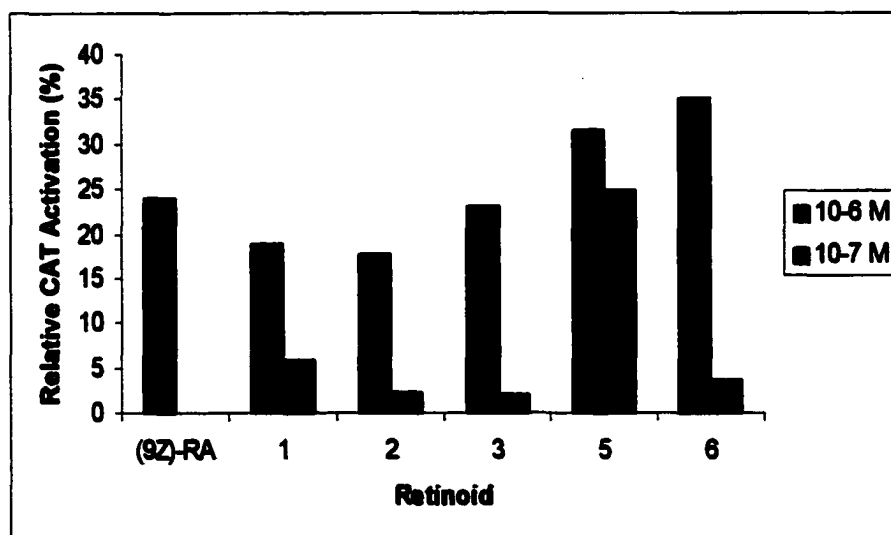


Figure 6. RXR α -receptor transcriptional activation.

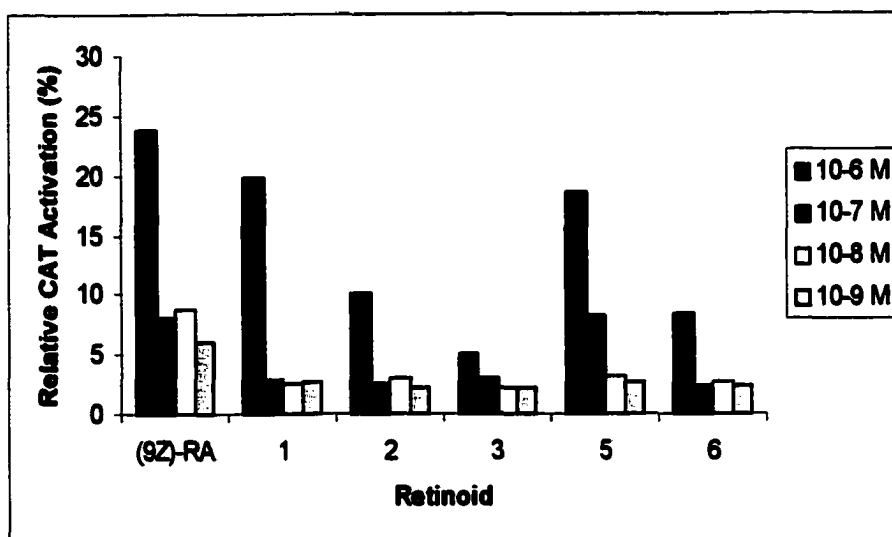


Figure 7. Results from the dose-response assay for RXR α transactivation.

were also performed for the inhibition of binding of (9Z)-RA to mRXR α .³⁰ Finally, each compound was evaluated for the efficiency of activating RAR α , - β , and - γ homodimers, and RXR α homodimers using the chloramphenicol acetyltransferase (CAT) reporter gene containing the thyroid hormone response element (TRE α) according to a method described by Zhang et al.³¹

Chemistry. ¹H NMR spectra were obtained at 300.1 MHz on a Bruker spectrometer in CDCl₃. UV-Vis spectra were recorded on both an AVIV 14DS spectrophotometer and a Hewlett-Packard spectrophotometer in methanol or acetonitrile solutions (Fisher, spectrograde). IR spectra were recorded using a Bomem FTIR spectrometer. TLC was performed on a pre-coated 250 μ m silica gel plates (Analtech, Inc.; 5 x 10 cm). Solvents and liquid starting materials were distilled prior to use. Reactions and purifications were conducted with deoxygenated solvents, under inert gas (N₂) and subdued light-

ing. Melting points were recorded on a Melt-Temp melting point apparatus and were uncorrected. The synthetic procedures are the same as those used in the first manuscript.

(2Z,4E)-4-(5'-Methoxy-3',4'-dihydro-1'(2'H)-naphthalen-1'-ylidene)-3-methyl-2-butenic Acid (14). 6.9 g (86%) yellow solid: mp 140-141 °C (ether/ hexanes); FTIR (KBr) 1681 (C=O), 1592 (C=C) cm^{-1} ; MS m/e 259 (MH^+); UV-Vis (MeOH) λ_{max} 302 nm ($\epsilon=11227$); ^1H NMR (CDCl_3): δ 7.27 (d, 1H, $J=7.98$), 6.76 (d, 1H, $J=7.95$), 5.78 (s, 1H), 2.72 (t, 2H, $J=6.40$), 2.49 (t, 2H, $J=4.80$), 2.11 (s, 3H), 1.83 (p, 2H, $J=6.24$); ^{13}C NMR (CDCl_3) δ 171.71, 157.5, 156.34, 140.6, 137.4, 127.33, 126.60, 122.72, 118.40, 117.61, 55.84, 28.60, 26.17, 23.74, 23.25.

Anal. ($\text{C}_{16}\text{H}_{18}\text{O}_2$) calcd.: C 74.40% H 7.52%. Found: C 74.65%, H 7.10%.

(2Z,4E)-4-(6'-Methoxy-3',4'-dihydro-1'(2'H)-naphthalen-1'-ylidene)-3-methyl-2-butenic Acid (15). 6.0 g (82%) yellow solid: mp 143-144 °C (ether/hexanes); MS m/e 259 (MH^+); FTIR 1680 (C=O) 1600 (C=C) cm^{-1} ; UV-Vis (MeOH) λ_{max} 327 nm ($\epsilon=12590$); ^1H NMR (CDCl_3): δ 7.62 (d, 1H, $J=8.84$), 7.16 (s, 1H), 6.74 (dd, 1H, $J=2.71$ & 6.08), 6.61 (d, 1H, $J=2.64$), 3.79 (s, 3H), 2.77 (t, 2H, $J=6.15$), 2.59 (dt, 2H, $J=1.46$ & 5.45), 2.14 (d, 3H, $J=0.56$), 1.82 (p, 2H, $J=6.27$); ^{13}C NMR (CDCl_3) δ 152.83, 140.69, 137.44, 121.63, 121.28, 110.0, 107.83, 101.60, 98.85, 94.65, 94.08, 36.62, 11.96, 10.28, 7.24, 4.7.

Anal. ($\text{C}_{16}\text{H}_{18}\text{O}_2$) calcd.: C 74.40% H 7.52%. Found: C 74.13% H 7.05%.

(2Z,4E)-4-(7'-Methoxy-3',4'-dihydro-1'(2'H)-naphthalen-1'-ylidene)-3-methyl-2-butenic Acid (16). 5.1 g (70%) pale yellow solid: mp 123-124 °C (ether/hexanes); FTIR (KBr) 3495 (OH), 1680 (C=O), 1607 (C=C) cm^{-1} ; MS m/e 259 (MH^+); UV-Vis (MeOH) λ_{max} 315 nm ($\epsilon=11207$); ^1H NMR (CDCl_3): δ 7.17 (d, 1H, $J=2.31$), 7.00 (d, 1H, $J=8.34$), 6.77 (dd, 1H, $J=2.57$ & 8.47), 5.76 (s, 1H), 3.77 (s, 3H), 2.73 (t, 2H, $J=6.20$), 2.56 (tt, 2H, $J=1.37$ & 5.48), 2.14 (s, 3H), 1.82 (p, 2H, $J=6.25$); ^{13}C NMR (CDCl_3) δ 156.7, 139.3, 137.3, 121.4, 117.95, 112.13, 111.32, 103.52, 99.38, 96.37, 90.12, 36.63, 10.73, 9.92, 7.02, 4.92.

Anal. ($\text{C}_{16}\text{H}_{18}\text{O}_2$) calcd.: C 74.40% H 7.52%. Found: C 74.50% H 7.10%.

(2Z,4E)-4-(4'-Methyl-3',4'-dihydro-1'(2'H)-naphthalen-1'-ylidene)-3-methyl-2-butenic Acid (17). 5.4 g (71%) pale yellow solid: mp 98-99 °C; (ether/hexanes); FTIR (KBr): 1677 (C=O), 1606 (C=C) cm^{-1} ; MS m/e 243 (MH^+); UV-Vis (MeOH) λ_{max} 312 nm ($\epsilon=11498$); ^1H NMR (CDCl_3): δ 7.63 (d, 1H, $J=5.76$), 7.26-7.14 (m, 4H), 5.79 (s, 1H), 2.97-2.89 (m, 1H), 2.71-2.64 (m, 1H), 2.57-2.49 (m, 1H), 2.14 (d, 3H, $J=0.60$), 1.99-1.91 (m, 1H), 1.64-1.53 (m, 1H), 1.29 (d, 3H, $J=5.23$); ^{13}C NMR (CDCl_3): δ 172.18, 156.50, 143.49, 140.71, 135.96, 128.40, 128.07, 126.64, 125.51, 122.71, 118.48, 33.51, 31.24, 26.21, 26.14, 22.07.

Anal. ($\text{C}_{16}\text{H}_{18}\text{O}_2$) calcd.: C 79.31% H 7.49%. Found: C 79.22% H 7.47%.

(2Z,4E)-4-(5',7'-Dimethyl-3',4'-dihydro-1'(2'H)-naphthalen-1'-ylidene)-3-methyl-2-butenic Acid (18). 5.5 g (73%) pale yellow solid: mp 139-141 °C (ether/hexanes); FTIR (KBr) 1679 (C=O), 1619 (C=C) cm^{-1} ; MS m/e 257 (MH^+); UV-Vis

(MeOH): λ_{max} 312 nm ($\epsilon=11273$); ^1H NMR (CDCl_3): δ 7.30 (s, 1H), 6.97 (s, 1H), 6.90 (s, 1H), 5.78 (t, 1H, $J=1.24$), 2.63 (t, 2H, $J=6.37$), 2.47 (tt, 2H, $J=1.22$ & 4.90), 2.26 (s, 3H), 2.18 (s, 3H), 2.09 (d, 3H, $J=0.56$), 1.85 (p, 2H, $J=6.30$); ^{13}C NMR (CDCl_3): δ 172.03, 156.55, 141.43, 136.67, 136.25, 135.32, 133.76, 130.96, 123.79, 122.10, 118.25, 28.68, 27.10, 26.31, 23.89, 21.50, 20.06.

Anal. ($\text{C}_{17}\text{H}_{20}\text{O}_2$) calcd.: C 79.65% H 7.86%. Found: C 79.38% H 7.77%.

(2Z,4E)-4-(5'-Methoxy-3',4'-dihydro-1'(2'H)-naphthalen-1'-ylidene)-3-methyl-2-buten-1-ol (20). 1.8 g (97%) white solid: mp 50-55 °C (ether/ hexanes); FTIR (KBr) 3439 (OH), 1605 (C=C) cm^{-1} ; MS m/e 227 (M-OH); UV-Vis (MeOH) λ_{max} 269 nm ($\epsilon=13541$); ^1H NMR (CDCl_3): δ 7.54 (d, 1H, $J=6.60$), 6.74 (dd, 1H, $J=2.05$ & 4.52), 6.62 (d, 1H, $J=1.93$), 6.24 (s, 1H), 5.54 (t, 1H, $J=4.97$), 4.06 (d, 2H, $J=5.03$), 3.80 (s, 3H), 2.82 (t, 2H, $J=4.71$), 2.33 (tt, 2H, $J=1.03$ & 3.57), 1.86 (s, 3H), 1.81 (p, 2H, $J=4.70$); ^{13}C NMR (CDCl_3): δ 157.26, 137.85, 136.82, 136.13, 126.35, 126.25, 126.07, 122.30, 116.56, 108.51, 60.85, 58.36, 55.41, 27.53, 24.10, 23.50, 23.20, 18.36.

Anal. ($\text{C}_{16}\text{H}_{20}\text{O}_2$) calcd.: C 78.65% H 8.25%. Found: C 78.70 % H 8.21%.

(2Z,4E)-4-(6'-Methoxy-3',4'-dihydro-1'(2'H)-naphthalen-1'-ylidene)-3-methyl-2-buten-1-ol (21). 1.9 g (100%) colorless oil; FTIR (neat) 3393 (OH), 1606 (C=C) cm^{-1} ; MS m/e 227 (M-OH); UV-Vis (MeOH) λ_{max} 273 nm ($\epsilon=11333$); ^1H NMR (CDCl_3): δ 7.53 (d, 1H, $J=8.76$), 6.73 (dd, 1H, $J=2.65$ & 6.11), 6.62 (d, 1H, $J=2.67$), 6.24 (s, 1H), 5.54 (tt, 1H, $J=1.13$ & 6.67), 4.06 (d, 2H, $J=6.70$), 3.80 (s, 3H), 2.81 (t, 2H, $J=6.31$), 2.33 (dt, 2H, $J=1.41$ & 4.65), 1.86 (s, 3H), 1.81 (p, 2H, $J=6.21$); ^{13}C NMR

(CDCl₃): δ 159.3, 139.32, 137.31, 136.77, 128.80, 126.45, 125.93, 120.48, 113.71, 112.98, 61.35, 55.66, 31.00, 28.51, 24.55, 24.05.

Anal. (C₁₆H₂₀O₂) calcd.: C 78.65% H 8.25%. Found: C 78.37% H 8.07%.

(2Z,4E)-4-(7'-Methoxy-3',4'-dihydro-1'(2'H)-naphthalen-1'-ylidene)-3-methyl-2-buten-1-ol (22). 1.9 g (100%) pale yellow oil; FTIR (neat) 3355 (OH), 1605 (C=C) cm⁻¹; MS *m/e* 227 (M-OH); UV-Vis (MeOH) λ_{max} 267 nm (ϵ =11724); ¹H NMR (CDCl₃): δ 7.19 (d, 1H, J=2.36), 7.10 (d, 1H, J=8.36), 6.75 (dd, 1H, J=2.57 & 5.75), 6.34 (s, 1H), 5.55 (t, 1H, J=6.60), 4.05 (d, 2H, J=6.53), 3.80 (s, 3H), 2.76 (t, 2H, J=6.28), 2.32 (t, 2H, J=3.10), 1.86 (s, 3H), 1.79 (p, 2H, J=6.17); ¹³C NMR (CDCl₃): δ 137.89, 136.79, 136.39, 130.53, 130.40, 126.88, 122.61, 114.45, 109.04, 61.23, 55.77, 29.82, 28.35, 24.39, 24.34.

Anal. (C₁₆H₂₀O₂·0.25 H₂O) calcd.: C 77.23% H 8.30%. Found C 77.52% H 8.03%.

(2Z,4E)-4-(4'-Methyl-3',4'-dihydro-1'(2'H)-naphthalen-1'-ylidene)-3-methyl-2-buten-1-ol (23). 1.6 g (96%) cream-colored solid: mp 42-48°C (ether/hexanes); FTIR (KBr): 3347 (OH), 1605 (C=C) cm⁻¹; MS *m/e* 229 (MH⁺); UV-Vis (MeOH) λ_{max} 265nm (ϵ =19165); ¹H NMR: δ 7.55 (d, 1H, J=7.31), 7.23-7.04 (m, 3H), 6.31 (s, 1H), 5.53 (t, 1H, J=6.02), 4.03 (d, 2H, J=6.55), 2.95-2.84 (m, 1H), 2.43-2.37 (m, 1H), 2.33-2.28 (m, 1H), 1.92-1.82 (m, 1H), 1.84 (s, 3H), 1.58-1.52 (m, 1H), 1.26 (d, 3H, J=7.0); ¹³C NMR (CDCl₃): δ 142.80, 138.19, 135.92, 135.78, 128.46, 128.03, 127.28, 126.48, 124.85, 122.72, 60.97, 33.58, 31.87, 25.56, 24.48, 22.62.

Anal. (C₁₆H₁₈O) calcd.: C 84.16%, H 8.83%. Found: C 84.06% H 9.17%.

(2Z,4E)-4-(5',7'-Dimethyl-3',4'-dihydro-1'(2'H)-naphthalen-1'-ylidene)-3-methyl-2-buten-1-ol (24). 1.8 g (95%) yellow oil; FTIR (neat) 3330 (OH), 1606 (C=C) cm⁻¹; MS m/e 257 (MH⁺); UV-Vis (MeOH) λ_{max} 269 nm (ε=4455); ¹H NMR: δ 6.89 (s, 1H), 6.31 (s, 1H), 5.53 (tt, 1H, J=1.07 & 6.63), 4.03 (d, 2H, J=6.63), 2.64 (t, 2H, J=6.36), 2.34-2.25 (m, 5H), 2.18 (s, 3H), 1.88-1.79 (m, 5H); ¹³C NMR (CDCl₃): δ 138.98, 136.89, 136.50, 136.14, 133.24, 130.53, 126.71, 122.22, 122.16, 61.22, 28.05, 27.28, 24.54, 24.32, 21.53, 20.11.

Anal. (C₁₇H₂₂O₂) calcd.: C 84.25% H 9.15%. Found: C 84.22% H 9.23%.

(2Z,4E)-4-(5'-Methoxy-3',4'-dihydro-1'(2'H)-naphthalen-1'-ylidene)-3-methyl-2-buten-1-al ((9Z)-26). 0.67 g (59%) yellow oil; FTIR (neat) 1672 (C=O); 1608 (C=C) cm⁻¹; MS m/e 243 (MH⁺); UV-Vis (MeOH) λ_{max} 332 nm (ε=16533); ¹H NMR (CDCl₃): δ 9.63 (d, 1H, J=8.20), 7.3-7.16 (m, 2H), 6.79 (dd, 1H, J= 0.73 & 7.09), 6.56 (s, 1H), 6.0 (td, 1H, J=0.95 & 6.41), 3.83 (s, 3H), 2.75 (t, 2H, J=6.42), 2.44 (dt, 2H, J=1.33 & 4.81), 2.08 (s, 3H), 1.83 (p, 2H, J=1.83); ¹³C NMR (CDCl₃): δ 193.71, 159.85, 157.76, 142.79, 136.3, 129.42, 127.50, 126.73, 120.92, 117.06, 109.78, 55.85, 28.36, 25.70, 23.83, 23.65.

Anal. (C₁₆H₁₈O₂·0.25 H₂O) calcd.: C 79.31% H 7.49%. Found: C 78.26% H 7.45%.

(2*E*,4*E*)-4-(5'-Methoxy-3',4'-dihydro-1'(2'H)-naphthalen-1'-ylidene)-3-methyl-2-buten-1-al ((*all-E*)-26). 0.035 g (3.0%) yellow oil; FTIR (neat): 1662 (C=O), 1604 (C=C) cm^{-1} ; MS m/e 227 (MH^+); UV-Vis (MeOH) λ_{max} 330 nm ($\epsilon=23036$); ^1H NMR (CDCl_3): δ 10.10 (d, 1H, $J=8.13$), 7.22-7.13 (m, 2H), 6.78 (dd, 1H, $J=1.10$ & 6.54), 6.50 (s, 1H), 6.01 (d, 1H, $J=8.17$), 3.82 (s, 3H), 2.76-2.66 (m, 4H), 2.33 (s, 3H), 1.84 (p, 2H, $J=6.33$); ^{13}C NMR (CDCl_3): δ 191.75, 157.57, 156.96, 143.70, 136.96, 129.56, 128.00, 126.72, 126.08, 117.29, 109.94, 55.86, 28.80, 23.59, 19.11.

(2*E*,4*Z*)-4-(6'-Methoxy-3',4'-dihydro-1'(2'H)-naphthalen-1'-ylidene)-3-methyl-2-buten-1-al ((9*Z*)-27). 0.62 g (54%) yellow oil; FTIR (neat) 1670 (C=O), 1604 (C=C) cm^{-1} ; MS m/e 243 (MH^+); UV-Vis (MeOH) λ_{max} 319 nm ($\epsilon=8837$); ^1H NMR (CDCl_3): δ 9.64 (dd, 1H, $J=0.78$ & 7.47), 7.56 (d, 1H, $J=5.56$), 6.77 (dd, 1H, $J=2.58$ & 6.18), 6.65 (d, 1H, $J=2.03$), 6.45 (s, 1H), 5.99 (dd, 1H, $J=0.91$, 7.31), 3.81 (s, 3H), 2.84 (t, 2H, $J=6.15$), 2.09 (s, 3H), 1.84 (p, 2H, $J=6.21$); ^{13}C NMR (CDCl_3): δ 160.09, 159.93, 142.11, 140.17, 129.15, 127.84, 126.33, 118.71, 113.76, 113.28, 30.84, 29.04, 25.77, 24.10.

Anal. ($\text{C}_{16}\text{H}_{18}\text{O}_2 \cdot 0.25 \text{H}_2\text{O}$) calcd.: C 79.31% H 7.49%. Found: C 77.78% H 7.53%.

(2*E*,4*E*)-4-(6'-Methoxy-3',4'-dihydro-1'(2'H)-naphthalen-1'-ylidene)-3-methyl-2-buten-1-al ((*all-E*)-27). 0.07 g (6.1%) yellow oil; FTIR (neat) 1656 (C=O), 1605 (C=C) cm^{-1} ; MS m/e 243 (MH^+); UV-Vis (MeOH) λ_{max} 358 nm ($\epsilon=13956$); ^1H NMR (CDCl_3): δ 10.08 (d, 1H, $J=8.19$), 7.56 (d, 1H, $J=8.82$), 6.75 (dd, 1H, $J=2.61$ &

6.18), 6.64 (d, 1H, $J=2.39$), 6.39 (s, 1H), 6.02 (d, 1H, $J=8.13$), 3.81 (s, 3H), 2.83-2.72 (m, 4H), 2.35 (s, 3H), 1.84 (p, 2H, $J=6.25$); ^{13}C NMR (CDCl_3): δ 160.23, 157.07, 143.53, 141.01, 129.17, 126.61, 124.06, 113.70, 113.31, 30.85, 29.68, 24.02, 19.34.

Anal. ($\text{C}_{16}\text{H}_{18}\text{O}_2 \cdot 0.25 \text{ H}_2\text{O}$) calcd.: C 79.31% H 7.49%. Found: C 77.64% H 7.23%.

(2Z,4E)-4-(7'-Methoxy-3',4'-dihydro-1'(2'H)-naphthalen-1'-ylidene)-3-methyl-2-buten-1-al ((9Z)-28). 0.62 g (54%) yellow oil; FTIR (neat) 1670 ($\text{C}=\text{O}$), 1609 ($\text{C}=\text{C}$) cm^{-1} ; MS m/e 227 (MH^+); UV-Vis (MeOH) λ_{max} 311 nm ($\epsilon=7913$); ^1H NMR (CDCl_3): δ 9.64 (d, 1H, $J=6.12$), 7.14 (d, 1H, $J=1.95$), 7.05 (d, 1H, $J=3.46$), 6.83 (dd, 1H, 1.98 & 4.32), 6.54 (s, 1H), 6.01 (td, 1H, $J=0.80$ & 5.39), 3.83 (s, 3H), 2.79 (t, 2H, $J=4.73$), 2.47 (dt, 2H, $J=1.15$ & 3.47), 2.09 (s, 3H), 1.84 (p, 2H, $J=6.21$); ^{13}C NMR (CDCl_3): δ 156.96, 132.43, 139.28, 135.77, 133.84, 129.62, 129.57, 128.90, 126.70, 125.93, 125.07, 30.43, 29.42, 23.92, 19.20.

Anal. ($\text{C}_{16}\text{H}_{18}\text{O}_2 \cdot 0.25 \text{ H}_2\text{O}$) calcd.: C 77.86% H 7.56%. Found: C 77.58% H 7.52%.

(2E,4E)-4-(7'-Methoxy-3',4'-dihydro-1'(2'H)-naphthalen-1'-ylidene)-3-methyl-2-buten-1-al ((all-E)-28). 0.07 g (6.1%) yellow oil; FTIR (neat): 1657 ($\text{C}=\text{O}$), 1607 ($\text{C}=\text{C}$) cm^{-1} ; MS m/e 227 (MH^+); UV-Vis (MeOH) λ_{max} 338 nm ($\epsilon=16887$); ^1H NMR (CDCl_3): δ 10.10 (d, 1H, $J=8.13$), 7.11 (d, 1H, $J=2.54$), 7.04 (d, 1H, $J=8.38$), 6.82 (dd, 1H, $J=2.37$ & 5.81), 6.47 (s, 1H), 6.04 (d, 1H, $J=8.12$), 3.82 (s, 3H), 2.76-2.70 (m, 4H), 2.35 (s, 3H), 1.83 (p, 2H, $J=6.28$); ^{13}C NMR (CDCl_3): δ 191.85, 158.37, 156.86,

143.44, 136.60, 131.76, 130.52, 129.64, 126.02, 115.35, 109.66, 55.81, 29.59, 29.34, 24.21, 19.18.

Anal. ($C_{16}H_{18}O_2 \cdot 0.20 H_2O$) calcd.: C 78.15% H 7.54%. Found: C 78.35% H 7.43%.

(2Z,4E)-4-(4'-Methyl-3',4'-dihydro-1'(2'H)-naphthalen-1'-ylidene)-3-methyl-2-buten-1-al ((9Z)-29). 0.44 g (42%) yellow oil; FTIR (neat): 1673 (C=O), 1611 (C=C) cm^{-1} ; MS m/e 227 (MH^+); UV-Vis (MeOH) λ_{max} 303 nm ($\epsilon=8443$); 1H NMR: δ 9.66 (d, 1H, $J=8.25$), 7.61 (d, 1H, $J=7.78$), 7.28-7.14 (m, 3H), 6.57 (s, 1H), 6.57 (td, 1H), 6.01 (td, 1H, $J=1.05$ & 6.19), 3.01-2.93 (m, 1H), 2.62-2.53 (m, 1H), 2.48-2.44 (m, 1H), 2.09 (s, 3H), 2.06-1.92 (m, 1H), 1.64-1.59 (m, 1H), 1.30 (d, 3H, $J=7.02$); ^{13}C NMR ($CDCl_3$): δ 193.59, 159.77, 143.43, 142.69, 134.74, 129.42, 129.02, 128.70, 126.59, 124.97, 120.69, 33.37, 31.74, 25.98, 25.67, 22.46.

(2E,4E)-4-(4'-Methyl-3',4'-dihydro-1'(2'H)-naphthalen-1'-ylidene)-3-methyl-2-buten-1-al ((all-E)-29). 0.15 g (14%) yellow oil; FTIR (neat) 1665 (C=O), 1604 (C=C); MS m/e 227 (MH^+); UV-Vis (MeOH) λ_{max} 335 nm ($\epsilon=19034$); 1H NMR ($CDCl_3$): δ 10.10 (d, 1H, $J=8.13$), 7.60 (d, 1H, $J=11.08$), 7.29-7.16 (m, 3H), 6.46 (s, 1H), 6.06 (d, 1H, $J=8.03$), 2.93-2.89 (m, 1H), 2.85-2.80 (m, 1H), 2.76-2.63 (m, 1H), 2.01-1.91 (m, 1H), 1.67-1.51 (m, 1H), 1.29 (d, 3H, $J=7.07$); ^{13}C NMR ($CDCl_3$): δ 191.91, 156.91, 144.08, 143.99, 135.56, 129.56, 129.11, 128.15, 126.68, 126.17, 125.27, 33.33, 31.36, 26.73, 21.80, 19.21.

Anal. ($C_{16}H_{18}O \cdot 0.5H_2O$) calcd.: C 81.67% H 8.14%. Found: C 81.68% H 7.86%.

(2Z,4E)-4-(5',7'-Dimethyl-3',4'-dihydro-1'(2'H)-naphthalen-1'-ylidene)-3-methyl-2-buten-1-al ((9Z)-30). 0.67 g (59%) yellow oil; FTIR (neat) 1673 (C=O), 1607 (C=C) cm^{-1} ; MS m/e 241 (MH^+); UV-Vis (MeOH) λ_{max} 307 nm ($\epsilon=10343$); ^1H NMR (CDCl_3): δ 9.63 (d, 1H, $J=6.12$), 7.30 (s, 1H), 6.97 (s, 1H), 6.52 (s, 1H), 6.0 (dd, 1H, $J=0.69$ & 4.71), 2.69 (t, 2H, $J=4.81$), 2.32 (s, 3H), 2.21 (s, 3H), 2.09 (s, 3H), 1.87 (p, 2H, $J=7.40$); ^{13}C NMR (CDCl_3): δ 124.63, 118.15, 116.47, 116.22, 114.88, 112.48, 110.30, 104.36, 101.25, 9.40, 8.11, 6.74, 5.28, 2.45, 1.02.

Anal. ($\text{C}_{17}\text{H}_{20}\text{O} \cdot 0.25 \text{H}_2\text{O}$) calcd.: C 84.96% H 8.39%. Found: C 83.77 % H 8.43%.

(2E,4E)-4-(5',7'-Dimethyl-3',4'-dihydro-1'(2'H)-naphthalen-1'-ylidene)-3-methyl-2-buten-1-al ((all-E)-30). 0.08 g (7.1%) yellow oil; FTIR (neat): 1659 (C=O), 1609 (C=C) cm^{-1} ; MS m/e 241 (MH^+); UV-Vis (MeOH) λ_{max} 337 nm ($\epsilon=15064$); ^1H NMR: δ 10.08 (d, 1H, $J=8.13$), 7.25 (s, 1H), 6.95 (s, 1H), 6.36 (s, 1H), 6.00 (d, 1H, $J=8.16$), 2.71-2.64 (m, 4H), 2.34 (s, 3H), 2.30 (s, 3H), 2.20 (s, 3H), 1.87 (p, 2H, $J=6.33$); ^{13}C NMR (CDCl_3) δ 191.77, 157.20, 144.62, 136.90, 135.95, 135.46, 134.48, 131.65, 129.40, 125.62, 123.60, 28.87, 26.93, 24.20, 21.50, 20.04, 19.18.

Anal. ($\text{C}_{17}\text{H}_{20}\text{O} \cdot 0.25 \text{H}_2\text{O}$) calcd.: C 84.96% H 8.39%. Found C: 83.79% H 8.38%.

(2E,4E,6Z,8E)-Ethyl 8-(5'-Methoxy-3',4'-dihydro-1'(2'H)-naphthalen-1'-ylidene)-3,7-dimethyl-2,4,6-octatrienoate (32). 0.71 g (86%) yellow oil; FTIR (neat) 1675 (C=O), 1608 (C=C) cm^{-1} ; MS m/e 353 (MH^+); UV-Vis (MeOH) λ_{max} 332 nm

($\epsilon=16533$); ^1H NMR (CDCl_3): δ 7.16 (t, 1H, $J=8.0$), 6.75 (d, 1H, $J=7.94$), 6.63 (dd, 1H, $J=4.04$ & 11.08), 6.46 (s, 1H), 6.22 (d, 1H, $J=15.32$), 6.10 (d, 1H, $J=11.05$), 5.75 (s, 1H), 4.20-4.10 (m, 2H), 3.83 (s, 3H), 2.75 (t, 2H, $J=6.36$), 2.35 (t, 2H, $J=4.21$), 2.21 (d, 3H, $J=0.80$), 2.00 (s, 3H), 1.80 (p, 2H, $J=6.25$), 1.27 (t, 3H, $J=7.12$); ^{13}C NMR (CDCl_3): δ 167.62, 166.92, 157.70, 153.39, 140.88, 138.93, 137.40, 134.39, 133.38, 127.81, 127.02, 126.55, 123.14, 118.77, 117.18, 116.77, 109.07, 60.03, 55.81, 28.53, 25.13, 23.95, 23.74, 14.77, 14.27.

Anal. ($\text{C}_{23}\text{H}_{28}\text{O}_3 \cdot 0.25 \text{H}_2\text{O}$) calcd.: C 77.39% H 8.05%. Found: C 77.18 % H 8.01%.

(2E,4E,6Z,8E)-Ethyl 8-(6'-Methoxy-3',4'-dihydro-1'(2'H)-naphthalen-1'-ylidene)-3,7-dimethyl-2,4,6-octatrienoate (33). 0.65 g (78%) yellow oil; FTIR (neat) 1700 (C=O), 1603 (C=C); MS m/e 353 (MH^+); UV-Vis (MeOH) λ_{max} 342 nm ($\epsilon=17749$); ^1H NMR (CDCl_3): δ 7.59 (d, 1H, $J=8.78$), 6.76 (dd, 1H, $J=2.56$), 6.65 (tt, 3H, $J=3.37$ & 7.72), 6.35 (s, 3H), 6.21 (d, 1H, $J=20.97$), 6.04 (d, 1H, $J=9.74$), 5.75 (s, 1H), 4.19-4.11 (m, 2H), 3.81 (s, 3H), 2.83 (t, 2H, $J=6.23$), 2.38 (t, 2H, $J=$), 2.23 (s, 3H), 2.05 (s, 3H), 1.97 (s, 3H), 1.81 (p, 2H, $J=6.15$), 1.33-1.24 (m, 3H); ^{13}C NMR (CDCl_3): δ 166.20, 158.06, 152.00, 139.71, 138.21, 136.59, 132.73, 132.06, 127.52, 126.14, 124.76, 119.54, 117.20, 112.30, 111.63, 58.59, 54.25, 29.61, 27.70, 23.80, 22.74, 13.33, 12.85.

Anal. ($\text{C}_{23}\text{H}_{28}\text{O}_3 \cdot 0.25\text{H}_2\text{O}$) calcd.: C 77.42% H 8.04%. Found: C 77.69% H 8.11%.

(2E,4E,6Z,8E)-Ethyl 8-(7'-Methoxy-3',4'-dihydro-1'(2'H)-naphthalen-1'-ylidene)-3,7-dimethyl-2,4,6-octatrienoate (34). 0.62 g (75%) yellow oil; FTIR (neat) 1708 (C=O), 1603 (C=C) cm^{-1} ; MS m/e 353 (MH^+); UV-Vis (MeOH) λ_{max} 335 nm ($\epsilon=27208$); ^1H NMR (CDCl_3): δ 7.17 (d, 1H, $J=2.48$), 7.05 (d, 1H, $J=8.39$), 6.82-6.78 (m, 1H), 6.68-6.59 (m, 1H), 6.45 (s, 1H), 6.23 (d, 1H, $J=15.54$), 5.75 (s, 1H), 4.20-4.11 (m, 2H), 3.83 (s, 3H), 2.79 (t, 2H, $J=6.25$), 2.40-2.36 (m, 2H), 2.23 (s, 3H), 1.98 (s, 3H), 1.81 (p, 2H, $J=6.20$); ^{13}C NMR (CDCl_3): δ 167.60, 158.26, 153.31, 140.77, 138.53, 136.96, 134.51, 133.25, 130.65, 130.56, 127.89, 123.03, 118.85, 114.54, 109.32, 60.05, 55.78, 29.83, 28.91, 25.07, 24.45, 14.76, 14.29.

Anal. ($\text{C}_{23}\text{H}_{28}\text{O}_3 \cdot 0.5 \text{H}_2\text{O}$) calcd.: C 76.42% H 8.09%. Found: C 76.48% H 7.83%.

(2E,4E,6Z,8E)-Ethyl 8-(4'-Methyl-3',4'-dihydro-1'(2'H)-naphthalen-1'-ylidene)-3,7-dimethyl-2,4,6-octatrienoate (35). 0.64 g (86%) yellow oil; FTIR (neat) 1708 (C=O), 1603 (C=C) cm^{-1} ; MS m/e 337 (MH^+); UV-Vis (MeOH) λ_{max} 333 nm ($\epsilon=13394$); ^1H NMR (CDCl_3): δ 7.54 (d, 1H, $J=7.20$), 7.27-7.06 (m, 3H), 6.58 (t, 1H, $J=15.22$), 6.37 (s, 1H), 6.16 (d, 1H, $J=15.48$), 6.03 (d, 1H, $J=10.99$), 6.67 (s, 1H), 4.15-4.00 (m, 2H), 2.94-2.85 (m, 2H), 2.40-2.37 (m, 1H), 2.31-2.20 (m, 1H), 2.15 (s, 3H), 1.90 (s, 3H), 1.55-1.46 (m, 1H), 1.25-1.11 (m, 6H); ^{13}C NMR (CDCl_3): δ 167.62, 153.34, 143.09, 140.91, 138.77, 135.81, 134.46, 133.29, 128.48, 128.18, 127.94, 126.48, 124.97, 123.02, 118.87, 60.06, 33.53, 31.77, 26.00, 25.09, 22.46, 24.80, 14.80, 14.27.

Anal. ($\text{C}_{23}\text{H}_{28}\text{O}_2 \cdot 0.25 \text{H}_2\text{O}$) calcd.: C 81.01% H 8.42%. Found: C 80.62% H 8.35%.

(2E,4E,6Z,8E)-Ethyl 8-(5',7'-Dimethyl-3',4'-dihydro-1'(2'H)-naphthalen-1'-ylidene)-3,7-dimethyl-2,4,6-octatrienoate (36). 0.55 g (76%) yellow oil; FTIR (neat) 1708 (C=O), 1604 (C=C) cm^{-1} ; MS m/e 351 (MH^+); UV-Vis (MeOH) λ_{max} 336 nm ($\epsilon=15404$); ^1H NMR (CDCl_3): δ 7.32 (s, 1H), 6.94 (s, 1H), 6.68-6.58 (m, 1H), 6.47 (s, 1H), 6.22 (d, 1H, $J=15.56$), 6.10 (d, 1H, $J=10.95$), 5.74 (s, 1H), 4.20-4.11 (m, 2H), 2.68 (t, 2H, $J=6.35$), 2.36-2.31 (m, 5H), 2.21 (s, 3H), 2.17 (s, 3H), 1.97 (s, 3H), 1.87-1.81 (m, 2H), 1.31-1.18 (m, 3H); ^{13}C NMR (CDCl_3): δ 166.14, 151.65, 138.21, 137.05, 136.42, 135.52, 134.13, 129.80, 129.04, 127.91, 126.69, 126.27, 125.07, 123.29, 29.19, 27.72, 22.66, 17.31, 13.33, 12.79.

Anal. ($\text{C}_{24}\text{H}_{30}\text{O}_2$) calcd.: C 82.24% H 8.63%. Found: C 82.23% H 8.68%.

(2E,4E,6Z,8E)-8-(5'-Methoxy-3',4'-dihydro-1'(2'H)-naphthalen-1'-ylidene)-3,7-dimethyl-2,4,6-octatrienoic Acid (2). 0.30 g (70%) yellow solid: mp 182-184 °C (ether/ CH_2Cl_2); FTIR (KBr) 1670 (C=O), 1596 (C=C) cm^{-1} ; MS m/e 325 (MH^+); UV-Vis (MeOH) λ_{max} 331 nm ($\epsilon=36514$); ^1H NMR (CDCl_3) δ 7.17 (t, 1H, $J=7.95$), 6.77 (d, 1H, $J=7.96$), 6.67 (dd, 1H, $J=4.06$ & 11.10), 6.46 (s, 1H), 6.25 (d, 1H, $J=15.34$), 6.12 (d, 1H, 11.0), 5.76 (s, 1H), 2.75 (t, 2H, $J=6.30$), 2.34 (t, 2H, $J=5.86$), 2.21 (s, 3H), 1.84 (p, 2H, $J=6.10$); ^{13}C NMR (CDCl_3): δ 172.59, 157.70, 155.98, 141.71, 139.09, 137.37, 134.29, 134.18, 127.72, 127.08, 126.54, 123.10, 117.85, 117.17, 109.10, 55.84, 28.51, 25.19, 23.93, 23.73, 14.45.

Anal. ($\text{C}_{21}\text{H}_{24}\text{O}_3$) calcd.: C 77.75% H 7.46%. Found: C 77.86% H 7.49%.

(2*E*,4*E*,6*Z*,8*E*)-8-(6'-Methoxy-3',4'-dihydro-1'(2'H)-naphthalen-1'-ylidene)-

3,7-dimethyl-2,4,6-octatrienoic Acid (3). 0.45 g (82%) yellow solid: mp 163-164 °C (ether/CH₂Cl₂); FTIR (neat) 1672 (C=O), 1575 (C=C) cm⁻¹; MS m/e 325 (MH⁺); UV-Vis (MeOH) λ_{max} 332 nm (ε=29288); ¹H NMR (CDCl₃): δ 7.16 (d, 1H, J=2.54); 7.06 (d, 1H, J=8.40), 6.80 (dd 1H J=2.56 & 5.81), 6.68 (dd, 1H, J=4.24 & 11.02), 6.45 (s 1H), 6.26 (d 1H J=15.32), 6.13 (d, 1H, J=10.85), 2.79 (t, 2H, J=6.20), 2.38 (t 2H J=5.20), 1.98 (s 3H), 1.81 (p, 2H, J=6.17); ¹³C NMR (CDCl₃): δ 172.10, 158.27, 155.90, 141.60, 138.71, 136.92, 134.92, 134.29, 134.18, 130.69, 130.57, 127.82, 122.98, 117.81, 114.59, 109.34, 55.80, 29.81, 28.92, 25.12, 24.45, 14.46.

Anal. (C₂₁H₂₄O₃) calcd.: C 77.75% H 7.46%. Found: C 77.49% H 7.62%.

(2*E*,4*E*,6*Z*,8*E*)-8-(7'-Methoxy-3',4'-dihydro-1'(2'H)-naphthalen-1'-ylidene)-

3,7-dimethyl-2,4,6-octatrienoic Acid (4). 0.32 g (71%) yellow solid: mp 163-164 °C (ether/CH₂Cl₂); FTIR (KBr) 1672 (C=O), 1575 (C=C) cm⁻¹; MS m/e 325 (MH⁺); UV-Vis (MeOH) λ_{max} 331 nm (ε=23,400); ¹H NMR (CDCl₃): δ 7.16 (d, 1H, J=2.54), 7.06 (d, 1H, J=8.40), 6.80 (dd 1H J=2.56 & 5.81), 6.68 (dd, 1H, J=4.24 & 11.02), 6.45 (s 1H), 6.26 (d 1H J=15.32), 6.13 (d, 1H, J=10.85), 2.79 (t, 2H, J=6.20), 2.38 (t 2H J=5.20), 1.98 (s 3H), 1.81 (p, 2H, J=6.17); ¹³C NMR (CDCl₃): δ 172.10, 158.27, 155.90, 141.60, 138.71, 136.92, 134.92, 134.29, 134.18, 130.69, 130.57, 127.82, 122.98, 117.81, 114.59, 109.34, 55.80, 29.81, 28.92, 25.12, 24.45, 14.46.

Anal. (C₂₁H₂₄O₃) calcd.: C 77.75% H 7.46%. Found: C 77.73% H 7.38%.

(2E,4E,6Z,8E)-8-(4'-Methyl-3',4'-dihydro-1'(2'H)-naphthalen-1'-ylidene)-3,7-dimethyl-2,4,6-octatrienoic Acid (5). 0.39 g (86%) yellow solid: mp 171-172 °C; MS m/e 310 (MH⁺); FTIR (KBr) 1667 (C=O), 1590 (C=C) cm⁻¹; UV-Vis (MeOH) λ_{max} 331 nm (ε=23400); ¹H NMR (CDCl₃): δ 7.63 (d, 1H, J=7.29), 7.26-7.17 (m, 4H), 6.74-6.66 (m, 1H), 6.46 (s, 1H), 6.26 (d, 1H, J=15.35), 6.13 (d, 1H, J=15.35), 5.77 (s, 1H), 3.00-2.92 (m, 2H), 2.54-2.30 (m, 1H), 2.23 (s, 3H), 1.99 (s, 3H), 1.64-1.54 (m, 2H), 1.30 (d, 3H, J=6.98); ¹³C NMR (CDCl₃): δ 172.23, 155.46, 142.71, 141.29, 135.36, 133.81, 132.90, 128.02, 127.77, 127.50, 126.05, 125.83, 124.53, 122.52, 117.54, 33.09, 31.33, 25.57, 24.66, 21.98, 14.02.

Anal. (C₂₁H₂₄O₂) calcd.: C 81.78% H 7.84%. Found 81.63% H 7.82%.

(2E,4E,6Z,8E)-8-(5'7'-Dimethyl-3',4'-dihydro-1'(2'H)-naphthalen-1'-ylidene)-3,7-dimethyl-2,4,6-octatrienoic Acid (6). 0.38 g (82%) yellow solid: mp 198-199 °C (ether/hexanes); FTIR (KBr) 1674 (C=O), 1593 (C=C) cm⁻¹; MS m/e 323 (MH⁺); UV-Vis (MeOH) λ_{max} 333 nm (ε=33719); ¹H NMR (CDCl₃): δ 7.33 (s, 1H), 6.95 (s, 1H), 6.68 (dd, 1H, J=4.23 & 11.04), 6.41 (s, 1H), 6.25 (d, 1H, J=15.33), 6.12 (d, 1H, J=10.98), 5.76 (s, 1H), 2.68 (t, 2H, J=6.36), 2.36-2.27 (m, 5H), 2.22 (s, 3H), 1.97 (s, 3H), 1.85 (p, 2H, J=6.24); ¹³C NMR (CDCl₃): δ 172.99, 156.05, 141.95, 139.84, 137.00, 136.25, 135.35, 134.45, 134.08, 133.53, 130.75, 127.55, 123.42, 122.59, 117.88, 28.58, 27.25, 25.26, 24.39, 21.51, 20.08.

Anal. (C₂₂H₂₆O₂) calcd.: C 81.95% H 8.13%. Found: C 81.65% H 8.11%.

Inhibition Concentrations at 50% (IC₅₀) for the Binding of Retinoids to RARs and RXRs. The procedure for the determination of IC₅₀ values for the isomers of retinoids 1-6 were based on methods previously published by Allenby et al. for (9Z)-RA and (*all-E*)-RA.³⁰ The protocol was performed as described previously.²⁸ Briefly, COS-1 cells were transfected with pSG65 expression plasmids containing cDNAs encoding on of the RARs or RXRs (α , β , or γ - subfamilies). Nucleosol fractions were prepared and stored at -80 °C. Aliquots of these fractions were incubated with assay buffer as described by Levin et al. with tritiated RA or (9Z)-RA and unlabelled ligands in ethanol.^{9a} To survey the binding of test compounds to RARs and RXRs, an initial screen was performed by incubating 5 nM of [³H]-(9Z)-RA and 1000 nM of test compound with the RAR preparation at 4 °C for 4 h or 20 nM of [³H]-(9Z)-RA and 1000 nM of test compound for the RXR preparation. To determine IC₅₀s, this experiment was repeated with nine concentrations of unlabeled ligand (0-10 μ M) in duplicate. Free ligands were separated from the bound ligands using disposable PD-10 desalting columns (Pharmacia LKB Biotechnology Inc.), which were washed as previously described by Levin et al.^{9a} Total activity, specific ligand binding, and nonspecific ligand binding were determined by scintillation counting as previously described by Allenby et al.³⁰ The percent of specific binding was defined as the ratio of observed binding at each concentration of competitive ligand and the specific binding. The IC₅₀ values were calculated by a fit of the 18 data points to the equation: $Y = [A(A-D)/1 + (X/C)^B] + D$, where Y is the percent specific binding, A is the maximal response (set at 100%), D is the minimal response (set at 0%), C is the IC₅₀ value, and B is the slope of the linear portion of the response of the log

dose-response curve. The parameters B and C were adjusted to allow the best fit of the data.

Transient Transfection Assays. CV-1 cells were grown in Dulbecco's modified Eagle's medium (DME) supplemented with 10% fetal bovine serum (FBS). Transient transfection of these cells with a DNA plasmid was performed essentially as described previously by Husmann et al.³¹ and Pfahl et al.³² with minor modifications. Twenty-four hours before transfection, cells were plated at 5×10^4 cells per well in a 24-well plate. Four hours before the addition of DNA-calcium phosphate precipitates, the cells were fed with DNA medium supplemented with charcoal stripped FBS. The DNA used in the transfection consisted of 100 ng of either RAR α , RAR β , RAR γ , or RXR α and 200 ng of the reporter gene (TREpal)₂-tk-chloramphenicol acetyltransferase (CAT), 300 ng of β -galactosidase expression plasmid pCH110, and 400 ng of carrier bluescript plasmid (pBluescript). When RXR homodimer or RAR/RXR heterodimer activities were investigated, 20 ng of RXR α expression vector alone or together with 25 ng of RAR α expression vector was used. After overnight incubation in the presence of the DNA precipitates, cells were washed once with phosphate-buffered saline (PBS) and grown for 24 h in medium containing 10% charcoal- stripped FBS and various concentrations of the 9-*cis* RA or the test retinoids. At the end of the incubation, cells were washed once with PBS and lysed for 10 min at room temperature in 0.25 mL of 100 nM Tris-HCl, pH 7.8, containing 0.5% Triton X-100. The resultant cell extracts were assayed for β -galactosidase and CAT activity as described by Husmann et al.³¹ The CAT activity of

each individual sample was normalized for transfection efficiency by the corresponding β -galactosidase activity.

Gel Retardation Assays. To synthesize RXR α protein *in vitro*, DNA sequences encoding RXR α cloned into pBluescript were transcribed by using T3 RNA polymerase, and the transcripts were translated in the rabbit reticulocyte lysate system (Promega) as described previously by Zhang et al.³³ The relative amount of translated proteins was determined by separating the ³⁵S-methionine-labeled proteins on sodium dodecyl sulfate polyacrylamide gels (SDS-PAGE), quantitating the amounts of incorporated radioactivity, and normalizing it relative to the content of methionine residues in RXR. To perform gel retardation assays, the *in vitro* synthesized RXR α protein was incubated with ³²P-labeled TREpal in a 20 μ L reaction mixture containing 10 mM Hepes buffer, pH 7.9, 50 mM KCl, 1 mM DL-dithiothreitol (DTT), 2.5 mM MgCl₂, 10% glycerol, and 1 μ g of poly (dI-dC) at 25 °C for 20 min. The reaction mixture was loaded on a 5% nondenaturing polyacrylamide gel containing 45.5 mM Tris-borate, 45.5 mM boric acid, and 2 mM ethylenediamine tetraacetic acid (EDTA). When retinoids were used, they were incubated with RXR for 10 min at room temperature prior to performing the DNA binding assay. The TREpal oligonucleotide was labeled by Klenow DNA polymerase and the labeled oligonucleotides were purified by gel electrophoresis and used as probes for the gel retardation assay.

References

- (1) For recent reviews, see: (a) *Chemistry and Biology of Synthetic Retinoids*; Dawson, M. A.; Okamura, W. H., Eds.; CRC Press: Boca Raton, FL, 1990. (b) *THE RETINOIDS: Biology, Chemistry and Medicine*, 2nd ed.; Sporn, M. B.; Roberts, A. B.; Goodman, D. S., Eds. Raven Press: New York, 1994.
- (2) Thaller, C.; Eichele, G. Identification and Spatial Distribution of Retinoids in the Developing Chick Limb Bud. *Nature (London)*, **1987**, *327*, 624-628.
- (3) Moon, R. C.; Mehta, R. G.; Rao, K. V. N. Retinoids and Cancer in Experimental Animals. In *THE RETINOIDS Biology, Chemistry and Medicine*, 2nd ed.; Sporn, M. B.; Roberts, A. B.; Goodman, D. S., Eds.; Raven Press: New York, 1994; pp 573-630.
- (4) (a) Hixson, E. J.; Denine, E. P. Comparative Subacute Toxicity of *All-trans*- and *13-cis*-Retinoic Acid in Swiss Mice. *Toxicol. Appl. Pharmacol.* **1978**, *44*, 29-40. (b) Kamm, J. J. Toxicology, Carcinogenicity, and Teratogenicity of Some Orally Administered Retinoids. *J. Am. Acad. Dermatol.* **1982**, *6*, 652-659. (c) Cohen, M. Tretinoin: A Review of Preclinical Toxicological Studies. *Drug Dev. Res.* **1993**, *30*, 244-51.
- (5) Kochhar, D. M. Teratogenic Activity of Retinoic Acid. *Acta. Pathol. Microbiol. Immunol.* **1967**, *967*, *70*, 398-404. (b) Willhite, C. C. Molecular Correlates in Retinoid Pharmacology and Toxicology. In *Chemistry and Biology of Synthetic Retinoids*; Dawson, M. I., Okamura, W. H., Eds.; CRC Press: Boca Raton, FL, 1990; pp 539-573. (c) Adams, J. Structure-Activity and Dose-Response Relationships in the Neural and Behavioral Teratogenesis of Retinoids, *Neurotoxicol. Teratol.* **1993**, *15*, 193-202.
- (6) (a) Petkovich, M.; Brand, N. J.; Krust, A.; Chambon, P. A Human Retinoic Acid Receptor Which Belongs to the Family of Nuclear Receptors. *Nature (London)* **1987**, *330*, 444-450. (b) Giguere, V.; Ong, E.; Segui, P.; Evans, R. Identification of a Receptor for the Morphogen Retinoic Acid. *Nature (London)* **1987**, *330*, 624-629. (c) Brand, N.; Petkovich, M.; Krust, A.; Chambon, P.; de The, H.; Marchio, A.; Tiollais, P.; Dejean, A. Identification of a Second Human Retinoic Acid Receptor. *Nature (London)*, **1988**, *332*, 850-53. (d) Dejean, A.; Bougueleret, L.; Grzeschik, K.-H.; Tiollais, P. Hepatitis B Virus DNA Integration in a Sequence Homologous to *v-erb-A* and Steroid Receptor Genes in a Hepatocellular Carcinoma. *Nature (London)* **1986**, *322*, 70-72. (e) Krust, A.; Kastner, Ph.; Petkovich, M.; Zelent, A.; Chambon, P. A Third Human Retinoic Acid Receptor, hRAR- γ . *Proc. Natl. Acad. Sci. U.S.A.* **1989**, *86*, 5310-5314. (f) Klaholz, B. P.; Renaud, J.-P.; Mitschler, A.; Zusi, C.; Chambon, P.; Gronemeyer, H.; Moras, D. Conformational Adaptation of Agonists to the Human Nuclear Receptor RAR γ . *Nature Structural Biology* **1998**, *3*, 199-202.

- (7) (a) Mangelsdorf, D.; Ong, E.; Dyck, J.; Evans, R. Nuclear Receptor That Identifies a Novel Retinoic Acid Response Pathway. *Nature (London)* **1990**, *345*, 224-229. (b) Bourget, W.; Ruff, M.; Chambon, P.; Gronemeyer, H.; Moras, D. Crystal Structure of the Ligand-Binding Domain of the Human Nuclear Receptor RXR α . *Nature (London)* **1995**, *375*, 377-382.
- (8) For recent reviews, see: (a) Mangelsdorf, D. J., Umesons, K., Evans, R. M. The Retinoid Receptors. *THE RETINOIDS Biology, Chemistry and Medicine*, 2nd ed.; Sporn, M.B., Roberts, A.B., Goodman, D.S., Eds.; Raven Press: New York, 1994; pp 319-349. (b) Chambon, P. A Decade of Molecular Biology Receptors. *FASEB* **1996**, *10*, 940-54. (c) Mangelsdorf, D.; Thummel, C.; Beato, M.; Herrlich, P.; Schütz, G.; Umesono, K.; Blumberg, B.; Kastner, P.; Mark, M.; Chambon, P.; Evans, R. The Nuclear Receptor Superfamily: The Second Decade. *Cell* **1995**, *83*, 835-39.
- (9) Levin, A. A.; Sturzenbecker, L. J.; Kazmer, S.; Bosakowski, T.; Huselton, C.; Allenby, G.; Speck, J.; Kratzseisen, C.; Rosenberger, M.; Lovey, A.; Grippo, J.F. 9-Cis Retinoic Acid Stereoisomer Binds and Activates the Nuclear Receptor RXR α . *Nature (London)* **1992**, *355*, 359-361. (b) Heyman, R.; Mangelsdorf, D.; Dyck, J.; Stein, R.; Eichele, G.; Evans, R.; Thaller, C. 9-Cis Retinoic Acid is a High Affinity Ligand for the Retinoid X Receptor. *Cell* **1992**, *68*, 397-406.
- (10) Zhang, X.-K.; Lehmann, J. M.; Hoffman, B.; Dawson, M. I.; Cameron, J.; Graupner, G.; Hermann, T.; Tran, P.; Pfahl, M. Homodimer Formation of the Retinoid X Receptor Induced by 9-cis Retinoic Acid. *Nature (London)* **1992**, *358*, 587-591.
- (11) Allenby, G.; Janocha, R.; Kazmer, S.; Speck, J.; Grippo, J.; Levin, A. Binding of 9-cis Retinoic Acid and All-trans-Retinoic Acid to Retinoic Acid Receptors α , β , and γ . *J. Biol. Chem.* **1994**, *269*, 16689-16695.
- (12) For reviews, see: (a) Norum, K. R. Retinoids and Acute Myeloid Leukemia. *Vitamin A in Health and Disease*. Blomhoff, R., Ed.; Dekker Press: New York, 1994; pp 485-501. (b) Chomienne, C.; Fenaux, P.; Degos, L. Retinoid Differentiation Therapy in Acute Promyelocytic Leukemia. *FASEB* **1996**, *10*, 1025-1030. (c) Coco, F.L.; Nerci, C.; Mandelli, F. Acute Promyelocytic Leukemia: A Curable Disease. *Leukemia* **1998**, *12*, 1866-1880.
- (13) (a) Walmsley, S.; Northfelt, D. W.; Melosky, B.; Conant, M.; Friedman, Kien A. E.; Wagner B. Treatment of AIDS-Related Cutaneous Kaposi's Sarcoma With Topical Alitretinoin (9-cis-Retinoic Acid) Gel. *J. Acquir. Immune Defic. Syndr.* **1999**, *22*, 235-246.
- (14) Castleberry, R. P.; Emanuel, P. D.; Zuckerman, K. S.; Cohn, S.; Strauss, L.; Byrd, R. L.; Homans, A.; Chaffee, S.; Nitschke, R.; Gualtieri, R. J. A Pilot Study of Isotretinoin in the Treatment of Juvenile Myelogenous Leukemia. *N. Engl. J. Med.* **1994**, *331*, 1680-1684.

- (15) Carolin, K. A.; Pass, H. A. Bexarotene (Targretin) for Cutaneous T-Cell Lymphoma. *Med. Lett. Drugs Ther.* **2000**, *42*, 31-32.
- (16) (a) Fanjul, A. N.; Piedrafita, J.; Al-Shamma, H.; Pfahl, M. Apoptosis Induction and Potent Antiestrogen Receptor-negative Breast Cancer Activity *in Vivo* by a Retinoid Antagonist. *Cancer Res.* **1998**, *58*, 4607-4610. (b) Shao, Z. M.; Dawson, M. I.; Li, X. S.; Sheikh M. S.; Han, Q. X.; Ordonez, J. V., Shroot, B.; Fontana, J. A. p53 Independent G₀/G₁ Arrest and Apoptosis Induced by a Novel Retinoid in Human Breast Cancer Cells. *Oncogene* **1995**, *11*, 493-504. (c) Green, A.; Shilkaitis, A.; Christov, K. 4-(Hydroxyphenyl)retinamide Selectively Inhibits the Development and Progression of Ductal Hyperplastic Lesions and Carcinoma *In Situ* in Mammary Gland. *Carcinogenesis* **1999**, *20*, 1535-1540.
- (17) Anzano, M. A.; Byers, S. W.; Smith, J. M.; Peer, C. W.; Mullen, L. T.; Brown, C. C.; Roberts, A. B.; Sporn, M. B. Prevention of Breast Cancer in the Rat With 9-*cis*-Retinoic Acid as a Single Agent and in Combination with Tamoxifen. *Cancer Res.* **1994**, *54*, 4614-4617.
- (18) (a) Chang, C. N. A Review of Breast Cancer Chemoprevention. *Biomed. Pharmacother.* **1998**, *52*, 133-136. (b) O'Shaughnessy, J. Chemoprevention and Breast Cancer. *JAMA* **1996**, *275*, 1349-1353. (c) Swan, D. K.; Ford, B. Chemoprevention and Cancer: Review of the Literature. *ONF* **1997**, *24*, 719-727.
- (19) Stearns, V.; Gelmann, E.P. Does Tamoxifen Cause Cancer in Humans? *J. Clin. Oncol.* **1998**, *16*, 779-92.
- (20) Osborne, K.C. Tamoxifen in the Treatment of Breast Cancer. *N. Engl. J. Med.* **1998**, *339*, 1609-1618.
- (21) (a) Dawson, M. I.; Chao, W.; Pine, P.; Jong, L.; Hobbs, P. D.; Rudd, C. K.; Quick, T. C.; Niles, R. M.; Zhang, X.; Lombardo, A.; Ely, K. R.; Shroot, B.; Fontana, J. A. Correlation of Retinoid Binding Affinity to Retinoic Acid Receptor α With Retinoid Inhibition of Growth of Estrogen Receptor Positive MCF-7 Mammary Carcinoma Cells. *Cancer. Res.* **1995**, *55*, 4446-4451.
- (22) Raffo, P.; Emionite, L.; Colucci, L.; Belmondo, F.; Moro, M.; Bollag, W.; Toma, S. Retinoid Receptors: Pathways of Proliferation Inhibition and Apoptosis Induction in Breast Cancer Cell Lines. *Anticancer Res.* **2000**, *20*, 1535-1544.
- (23) Toma, S.; Isnardi, L.; Riccardi, L.; Bollag, W. Induction of Apoptosis in MCF-7 Breast Carcinoma Cell Line by RAR and RXR Selective Retinoids. *Anticancer Res.* **1998**, *18*, 935-942.
- (24) Bischoff, E. D.; Gottardis, M. M.; Moon, T. E.; Heyman, R. A.; Lamph, W. W. Beyond Tamoxifen: The Retinoid X Receptor-Selective Ligand LGD1069 (Tar-

- gretin) Causes Complete Regression of Mammary Carcinoma. *Anticancer Res.* **1998**, *58*, 479-484. (b) Gottardis, M. M.; Bischoff, E. D.; Shirley, M. A.; Wagoner, M. A.; Lamph, W. W.; Heyman, R. A. Chemoprevention of Mammary Carcinoma by LGD1069 (Targretin): An RXR-Selective Ligand. *Cancer Res.* **1996**, *56*, 5566-5570.
- (25) Sherman, S. I.; Gopal, J.; Haugen, B. R.; Chiu, A. C.; Whaley, K.; Nowlakha, P.; Duvic, M. Central Hypothyroidism Associated With Retinoid X Receptor-Selective Ligands. *N. Engl. J. Med.* **1999**, *340*, 1075-1079.
- (26) Roy, B.; Taneja, R.; Chambon, P. Synergistic Activation of Retinoic Acid (RA) Responsive Genes and Induction of Embryonal Carcinoma Cell Differentiation by an RA Receptor α (RAR α), RAR β , or RAR γ -Selective Ligand in Combination with a Retinoid X Receptor-Specific Ligand. *Mol. Cell. Biol.* **1995**, *15*, 6481-6487. (b) Apfel, C. M.; Kamber, M.; Klaus, M.; Mohr, P.; Keidel, S.; LeMotte, P. K. Enhancement of HL-60 Differentiation by a New Class of Retinoids with Selective Activity on Retinoid X Receptor. *J. Biol. Chem.* **1995**, *270*, 30765-30772. (c) Chen, J.-Y.; Clifford, J.; Zusi, C.; Starrett, J.; Tortolani, D.; Ostrowski, J.; Reczek, P. R.; Chambon, P.; Gronemeyer, H. Two Distinct Actions of Retinoid-Receptor Ligands. *Nature* **1996**, *382*, 819-822. (d) Horn, V.; Minucci, S.; Ogryzko, V. V.; Adamson, E. D.; Howard, B. H.; Levin, A. A.; Ozato, K. RAR and RXR Selective Ligands Cooperatively Induce Apoptosis and Neuronal Differentiation in P19 Embryonal Carcinoma Cells. *FASEB J.* **1996**, *10*, 1071-1077. (e) Umemiya, H.; Kagechika, H.; Fukasawa, H.; Kawachi, E.; Ebisawa, M.; Hashimoto, Y.; Eisenmann, G.; Erb, C.; Pornon, A.; Chambon, P.; Gronemeyer, H.; Shudo, K. Action Mechanism of Retinoid-Synergistic Dibenzodiazepines. *Biochem. Biophys. Res. Comm.* **1997**, *233*, 121-125. (f) Umemiya, H.; Fukasawa, H.; Ebisawa, M.; Eyrolles, L.; Kawachi, E.; Eisenmann, G.; Gronemeyer, H.; Hashimoto, Y.; Shudo, K.; Kagechika, H. Regulation of Retinoid Actions by Diazepinylbenzoic Acids. Retinoid Synergists Which Activate the RXR-RAR Heterodimers. *J. Med. Chem.* **1997**, *40*, 4222-4234. (g) Tashimi, T.; Kagechika, H.; Tsuki, M.; Fukasawa, H.; Kawachi, E.; Hashimoto, Y.; Shudo, K. Polyenylenedene Thiazolidene Derivatives with Retinoid Activities. *Chem. Pharm. Bull.* **1997**, *45*, 1805-1813. (h) Ohta, K.; Tsuji, M.; Kawachi, E.; Fukasawa, H.; Hashimoto, Y.; Shudo, K.; Kagechika, H. Potent Retinoid Synergists With Diphenylamine Skeleton. *Biol. Pharm. Bull.* **1998**, *21*, 544-546. (i) Ebisawa, M.; Kawachi, E.; Fukasawa, H.; Hashimoto, Y.; Akiko, I.; Shudo, K.; Kagechika, H. Novel Thiazolidinedione Derivatives With Retinoid Synergistic Activity. *Biol. Pharm. Bull.* **1998**, *21*, 547-549.
- (27) Westin, S.; Kurokawa, R.; Nolte, R. T.; Wisely, G. B.; McInerney, E. M.; Rose, P. W.; Milburn, M. V.; Rosenfeld, M. G.; Glass, C. K. Interactions Controlling Complexes of Nuclear-Receptor Heterodimers and Coactivators. *Nature (London)* **1998**, *395*, 199-202.
- (28) (a) Vaezi, M. F.; Alam, M.; Sani, B. P.; Rogers, T. S.; Simpson-Herren, L.; Wille, J. J.; Hill, D. L.; Doran, T. I.; Brouillette, W. J.; Muccio, D. D. A Conformationally

- Defined 6-*s-trans* Retinoic Acid Isomer. Synthesis, Chemopreventive Activity, and Toxicity. *J. Med. Chem.* **1994**, *37*, 4499-4507. (b) Alam, M.; Zhestkov, V.; Sani, B. P.; Venepally, P.; Levin, A. A.; Kazmer, S.; Li, E.; Norris, A. W.; Zhang, X.-K.; Lee, M. O.; Hill, D. L.; Lin, T.-H.; Brouillette, W. J.; Muccio, D. D.; Conformationally Defined 6-*s-trans*-Retinoic Acid Analogs.2. Selective Agonists for Nuclear Receptor Binding and Transcriptional Activity. *J. Med. Chem.* **1995**, *38*, 2303-2310. (c) Muccio, D. D.; Brouillette, W. J.; Alam, M.; Vaezi, M. F.; Sani, B. P.; Venepally, P.; Reddy, L.; Li, E.; Norris, A. W.; Simpson-Herren, L.; Hill, D. Conformationally Defined 6-*s-trans* Retinoic Acid Analogs.3. Structure-Activity Relationships for Nuclear Receptor Binding, Transcriptional Activity, and Cancer Chemopreventive Activity. *J. Med. Chem.* **1996**, *39*, 3625-3635.
- (29) Muccio, D. D.; Brouillette, W. J.; Breitman, T. R.; Taimi, M.; Emanuel, P. D.; Zhang, X.-K.; Chen, G.-Q.; Sani, B. P.; Venepally, P.; Reddy, L.; Alam, M.; Simpson-Herren, L.; Hill, D. L. Conformationally Defined Retinoic Acid Analogues. 4. Potential New Agents for Acute Promyelocytic and Juvenile Myelomonocytic Leukemias. *J. Med. Chem.* **1998**, *41*, 1679-1687.
- (30) Allenby, G.; Bocquel, M.-T.; Sounders, M.; Karmer, S.; Speck, J.; Rosenberger, M.; Lovey, A.; Kastner, P.; Grippo, J. F.; Chambon, P.; Levin, A. A. Retinoic Acid Receptors and Retinoid X Receptors: Interactions with Endogenous Retinoic Acids. *Proc. Natl. Acad. Sci. U.S.A.* **1993**, *90*, 30-34.
- (31) Husmann, M.; Lehmann, J.; Hoffman, B.; Hermann, T.; Tzuckerman, M.; Pfahl, M. Antagonism Between the Retinoic Acid Receptors. *Mol. Cell. Biol.* **1991**, *11*, 4097-4103.
- (32) Pfahl, M.; Tzuckerman, M.; Zhang, X.-K.; Lehmann, J. M.; Hermann, T.; Wills, K. N.; Graupner, G. Nuclear Retinoic Acid Receptors: Cloning, Analysis, and Function. *Methods Enzymol.* **1990**, *189*, 256-270.
- (33) Zhang, X.-K.; Hoffman, B.; Tran, P.; Graupner, G.; Pfahl, M. Retinoid X Receptor is an Auxilliary Protein for Thyroid Hormone and Retinoic Acid Receptors. *Nature (London)* **1992**, *355*, 441-446.

**CONFORMATIONALLY DEFINED ANALOGUES OF RETINOIC ACID:
SYNTHESIS, NUCLEAR RECEPTOR BINDING AND TRANSCRIPTIONAL
ACTIVATION ACTIVITY OF A RING-EXPANDED DERIVATIVE OF (9Z)-UAB30**

by

**KIMBERLY K. VINES, WAYNE J. BROUILLETTE, DONALD D. MUCCIO,
BRAHMA P. SANI, AND XIAO-KUN ZHANG**

In preparation for Journal of Medicinal Chemistry

Format adapted for dissertation

Abstract

We recently reported the synthesis and biological activity of the conformationally defined 6-*s-trans* retinoic acid (RA) analogue, (9Z)-UAB30 [(2*E*,4*E*,6*Z*,8*E*)-8-(3',4'-dihydro-1'(2'H)-naphthalen-1'-ylidene)-3,7-dimethyl-2,4,6-octatrienoic acid], which is retinoid X receptor (RXR α) selective (IC₅₀ = 284 nM; EC₅₀ = 118 nM) (Muccio et al. *J. Med. Chem.* 1998, 41, 1679). In order to explore the effect of the size of the cyclohexenyl ring on RXR α activity, the ring-enlarged analogue of (9Z)-UAB30 was synthesized. By increasing the size of the cyclohexenyl ring, the range of accessible torsion angles about the C6-C7 bond could be increased, which may affect RXR-selectivity. In this study we prepared homologs of (9Z)-UAB30 that contained a cycloheptenyl ring (2). The transcriptional activation ability of the ring-expanded retinoid 2 revealed significantly increased potency for the activation of both the retinoic acid receptors (RARs) and RXR α , although selectivity for RXR α remained similar to that observed for (9Z)-UAB30.

Introduction

Retinoids control various biological functions, including cell differentiation, proliferation, embryonic development, and apoptosis.^{1,2} Analogs of (*all-trans*) retinoic acid (ATRA) such as Tazarotene³ and Differin⁴ have shown activity in the treatment of the dermatological disorders psoriasis and acne. The naturally occurring retinoid 13-*cis* RA, which *in vivo* is metabolized to ATRA, is currently used in the treatment of acute promyelocytic leukemia (APL).⁵ Preliminary reports have shown that the retinoid pan-agonist 9-*cis* RA⁶ and the RXR-selective retinoid Targretin⁷ exhibit chemopreventive activity in rats. However, retinoid therapy is restricted by a wide range of undesirable side

effects,⁸ including teratogenicity.⁹ Therefore, it is imperative that receptor-subtype selective retinoids be developed in order to elucidate the involvement of receptor subtypes in disease and provide the basis for the design of less toxic action-specific retinoids that could be used in the treatment of disease.

The biological effects of retinoids are mediated through interaction with two classes of receptors (RAR α , β , γ and RXR α , β , γ), both of which belong to the steroid/thyroid superfamily of hormone nuclear receptors. ATRA binds and activates only RARs, while 9-*cis* RA binds both RARs and RXRs. The RARs form heterodimers, while the RXRs can form both heterodimers and homodimers that interact with hormone response elements to affect transcription.

In an effort to elucidate the precise physiological role of each receptor subtype in human disease, both RAR^{10,11} and RXR^{12,13} receptor-selective agonists were developed. Both RAR- and RXR-selective retinoids have shown promise as chemotherapeutic and chemopreventive agents for breast cancer.¹⁴ Breast cancer affects one in ten women in Western Europe and the United States. Mortality remains high despite advances in mammographic screening, adjuvant chemotherapy, and radiotherapy.¹⁵ Approximately 50% of women with existing breast cancer will die of metastatic disease. Therefore, there is a need for new chemopreventive and chemotherapeutic agents. Tamoxifen (TAM) is the current treatment for breast cancer and has been in use since the 1970s and was recently approved by the Food and Drug Administration (FDA) as a mammary chemopreventive agent. TAM exerts its anti-proliferative effect on breast cancer cells through antagonism of the estrogen receptor, thereby blocking estrogen binding and inhibiting estrogen-dependent cell growth.¹⁶ Mammary tumors are classified according to

estrogen receptor expression. Those tumors that express the estrogen receptor are referred to as ER⁺, while those tumors that do not express the estrogen receptor are classified as ER⁻. Although adjuvant use of TAM for more than 2 years has been associated with a 38% reduction in breast cancer recurrence, long-term TAM administration has been associated with blood clots and an increased risk for endometrial cancer and often-times results in drug resistance.¹⁷

The antiproliferative activity of retinoids (9-*cis* RA, ATRA) in ER⁺ breast cancer cells has been attributed to RAR α binding and activation.¹⁸ However, in *in vitro* systems, some ER⁺ cell lines (MDB-MB-231 and MDA-MB-468) are refractory to RAR agonist (ATRA) treatment due to loss of expression of RAR α .¹⁹ Administration of RXR-selective agonists to these ATRA-resistant cells demonstrated that RXR-selective retinoids can induce growth inhibition and apoptosis, whereas RAR-selective retinoids are more effective in ATRA-sensitive cells. RXR ligands mediate these effects not through the RAR/RXR heterodimer but through activation of the RXR/nur77 heterodimer. The RA target gene is retinoic acid response element β RARE, which binds both the RAR/RXR and RXR/nur77 heterodimers. When RAR α receptors are expressed, an RXR specific ligand alone cannot inhibit proliferation, induce differentiation, or induce apoptosis. This is partly due to the inability of RXR ligands to bind the heterodimer in the absence of RAR ligand.²⁰ The activation function (AF-2) helix of the RAR subunit occupies the ligand-binding domain (LBD) of the RXR subunit of the homodimer. Only upon binding of RAR does a conformational change take place to allow for RXR binding. Therefore, RXR-selective retinoids could be useful for ER⁺ breast cancer chemotherapy.

Both the pan-agonist 9-*cis* RA and the RXR-selective agonist Targretin have shown chemopreventive activity in rats in the *N*-methyl nitrosourea (MNU) model for mammary cancer chemoprevention. Anzano et al. reported that the pan-agonist 9-*cis* RA was an effective chemopreventive agent in rats when used alone or in combination with TAM.⁶ In fact, 9-*cis* RA potentiated the chemopreventive activity of TAM. Gottardis reported that the RXR-selective agonist Targretin showed chemopreventive activity when administered alone or in combination with TAM.⁷ A synergistic effect was also observed for the Targretin/TAM combination. Recently, LGD1069 (Targretin) was tested in an *in vivo* assay that mimics the clinical situation where the patient becomes resistant to TAM.^{7c} When used in combination with TAM, LGD1069 reduced the number of tumors in rats. Preliminary results from the *in vivo* testing of (9Z)-UAB30 in the MNU model for mammary cancer chemoprevention indicate that this RXR-selective retinoid also acts as an effective breast cancer chemopreventive agent in rats. Further testing is required to determine the optimal dose and to test in combination with TAM.

Because the crystal structure of holo-RXR was not available until very recently,²⁰ design of RXR-specific ligands followed empirical observations made by us and other groups.^{12,13} The first synthetic retinoid that activated both RARs and RXRs was 3-methyl TTNPB, which is a derivative of 4-[2-(5,6,7,8-tetrahydro-5,5,8,8-tetramethyl-2-naphthalenyl)-1E-propenyl]benzoic acid (TTNPB) and a potent RAR pan-agonist. The only difference between the two structures was the presence of a methyl group at the 3-position, which allowed for binding of RXRs as well as RARs. Molecular modeling showed that the steric repulsion between the 3-methyl and the vinyl hydrogen of the linker resulted in a more bent conformation, which was associated with enhanced RXR

binding. Reported here is a study where the six-membered ring of the dihydronaphthalene moiety in (9Z)-UAB30 was altered to a seven-membered ring in order to explore the effect of the $\psi_{5,6,7,8}$ torsion angle on RXR-selectivity (Figure 1). The larger ring of **2** should enable access to a larger range of torsion angles, which may alter the RXR activity. In this paper, we report the design, synthesis, receptor-binding, and activation activities of this novel retinoid.

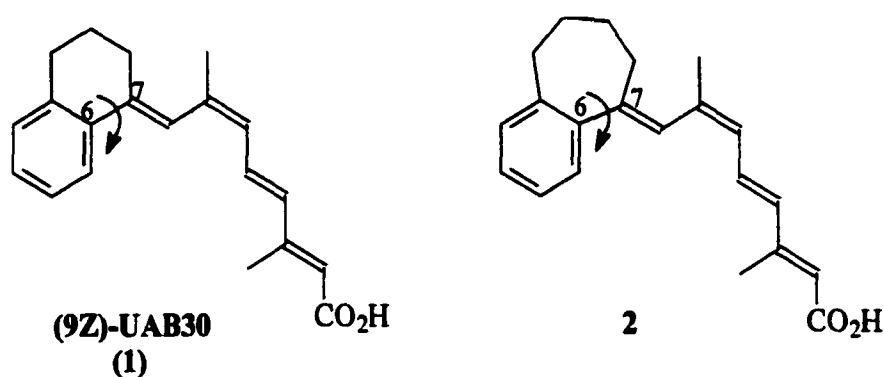
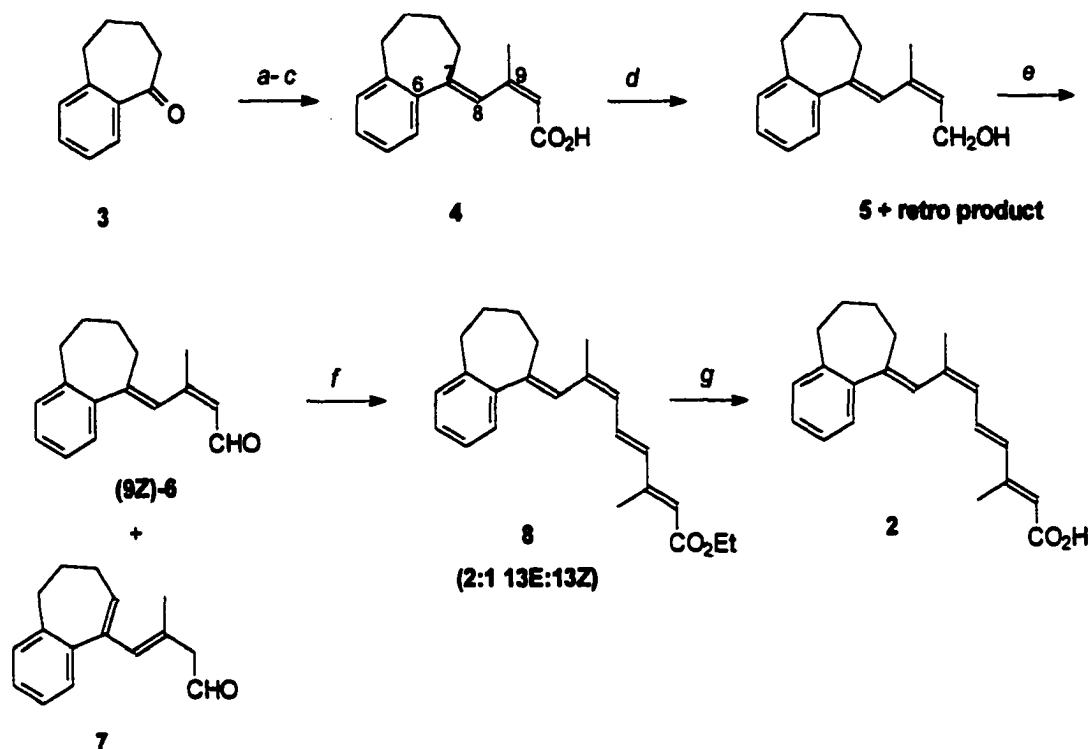


Figure 1. (9Z)-UAB30 (**1**) and ring-expanded analog **2**.

Chemistry

The synthesis of retinoid **2** is summarized in Scheme 1. Starting with commercially available 1-benzosuberone (**3**), a Reformatsky reaction proceeded smoothly to stereospecifically provide the (9Z)-acid **4**. The reduction of the acid **4** yielded the alcohol **5** as expected, which was contaminated with some retro product. The crude mixture of alcohols (**5**) was oxidized, and the crude aldehyde was obtained as a mixture of 9Z (**6**) and retro isomers (**7**) (2:1). The aldehyde **6** was purified on a flash column (10% ethyl acetate/hexanes). In early attempts to synthesize **2**, the aldehyde was carried forward to

Scheme 1. Synthesis of Ring-Expanded Analog (**2**) of (9Z)-UAB30^a

^a (a) Zn/ HCl; (b) ethyl 4-bromo-3-methyl-2-butenate, 1,4-dioxane, reflux; (c) acidic work-up; (d) LiAlH₄, ether, 0 °C; (e) MnO₂, molecular sieves, CH₂Cl₂, 0 °C; (f) NaH, TEPS, DMPU, THF, 0 °C; (g) (aq) KOH, methanol, 60°C.

the next step as a mixture of the (9Z)-aldehyde **6** and retro product **7**, anticipating that the isomers could be separated at the ester stage or the desired isomer could be crystallized at the acid stage. However, the two isomers were inseparable on flash silica chromatography at both the ester and the acid stages. Subsequently, a suitable chromatography solvent (100% CH₂Cl₂) was identified that could separate the (9Z)- and retro-aldehydes although the recovery of **6** was less efficient than anticipated due to the isomerization of the aldehyde during the separation. The pure (9Z)-aldehyde **6** was olefinated in the Horner-Emmons reaction to provide the ester **8** [2:1 (9Z) to (9Z, 13Z)]. The 9Z and diZ

isomers were separated on a flash silica column (30% hexanes/toluene). The pure (9Z, 13E) ester **8** was then hydrolyzed in base to yield the acid **2**.

Results and Discussion

Nuclear Receptor Binding Affinity and Transcriptional Activation Activity.

By expanding the cyclohexenyl ring of (9Z)-UAB30 to a seven-membered ring, greater RXR selectivity was anticipated. As shown by the results from the binding assay (Table 1) and the transcription assay (Figure 2-5), potency for both the RARs and RXR α was enhanced by approximately two-fold, while the goal of enhancing RXR α -selectivity was

Table 1. Inhibition Concentrations at 50% (nM) for the Binding of Retinoids (9Z)-UAB30, (9Z)-Retinoic Acid (RA), and **2** to Mouse Retinoic Acid Receptors (mRARs) and Retinoid X Receptors (mRXR α)

retinoid	IC ₅₀ (nM) ^a			
	mRAR α	mRAR β	mRAR γ	mRXR α
(9Z)-RA	31 ^b	8 ^b	60 ^b	73 ^c
(9Z)-UAB30	980	620	1225	960
[(9Z)-UAB30]	[>2000] ^d	[>2000] ^d	[>2000] ^d	[284] ^d
(9Z)- 2	490	>500 ^e	495	442

^a The IC₅₀ values were determined by the methods of Allenby et al.^{21,22} For IC₅₀ values with RARs, competition of unlabeled test retinoid was determined in the presence of 5 nM of [³H]-(*all-E*)-retinoic acid. For RXRs, competition of unlabeled test retinoid was determined in the presence of 20 nM of [³H]-(9Z)-RA. Based on repeated measurements, the estimated error is 20% of the mean. ^b Values reported by Allenby et al.²¹ ^c Values reported by Allenby et al.²² ^d Values reported in brackets by Muccio et al.¹² The other values are from the present study. ^e Doses greater than 500 nM were not tested.

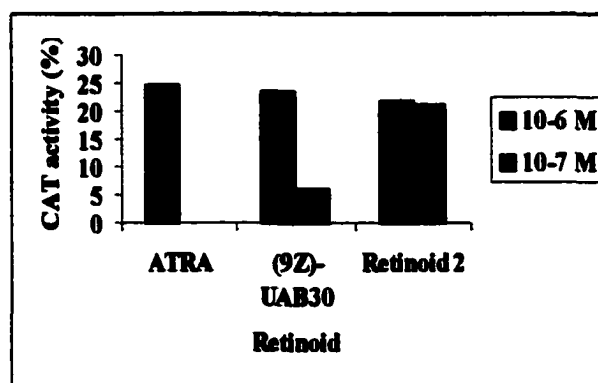


Figure 2. RAR α -receptor transcriptional activation.

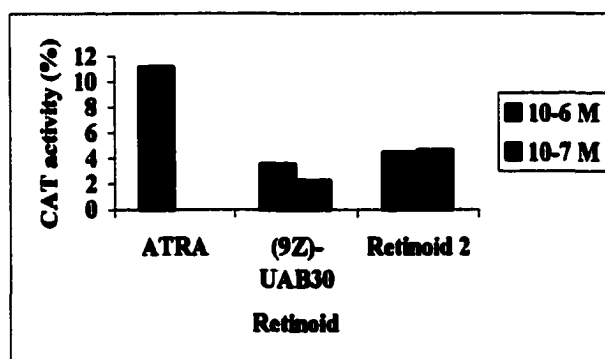


Figure 3. RAR β -receptor transcriptional activation.

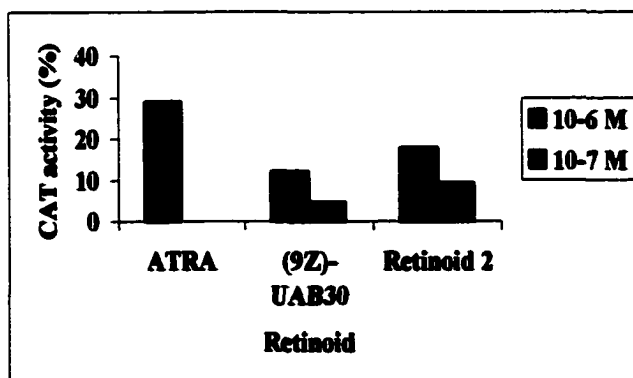


Figure 4. RAR γ -receptor transcriptional activation.

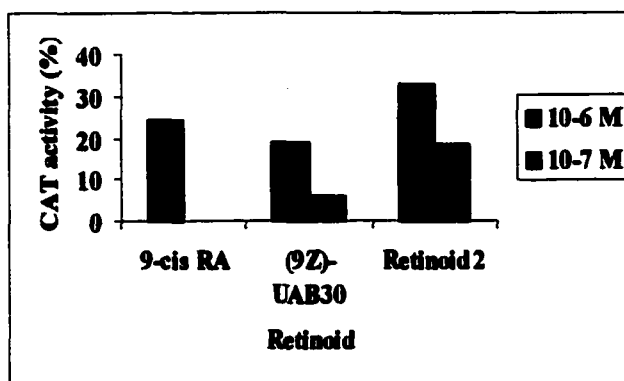


Figure 5. RXR α -receptor transcriptional activation.

not achieved. It is interesting to note that when comparing the chloramphenicol acetyltransferase (CAT) activity at the two doses (10^{-6} M and 10^{-7} M) for **2**, unlike (9Z)-UAB30, there was not a drastic reduction in RAR β and RAR γ activity at the 10^{-7} M dose.

Regarding RXR selectivity, most striking was the RXR α transcriptional activity of **2**, which was more active than 9-*cis* RA at RXR α . In conclusion, UAB retinoid **2** is a potent RXR α agonist that also exhibits significant activity for the RAR α receptor.

Experimental Section

Biology. In order to study the ability **2** to recognize RA-binding sites within the protein receptors, the IC₅₀ values were measured for the inhibition of the binding of (*all-E*)-RA to mRAR α , mRAR β , and mRAR γ using methods described previously by Levin and coworkers.²³ Similar studies were also performed for the inhibition of binding of (9Z)-RA to mRXR α .²¹ Briefly, COS-1 cells were transfected with the pSG5 expression plasmids containing cDNAs encoding one of the RARs or RXRs (α -, β -, or γ -subfamilies). To survey the binding of test compounds to RARs and RXRs, an initial

screen was performed by incubating 5 nM of [^3H]-(*all-E*)-RA and 1000 nM of the test compound with the RAR preparation at 4 °C for 4 h or 20 nM of [^3H]-(*9Z*)-RA and 1000 nM of the test compound with the RXR preparation. To determine IC_{50} values, this experiment was repeated with nine concentrations of unlabeled ligand (0-10 μM) in duplicate. Finally, **2** was evaluated for the efficiency of activating RAR α , - β , and - γ homodimers and RXR α homodimers using the chloramphenicol acetyltransferase (CAT) reporter gene containing the thyroid hormone response element (TRE pal) according to a method described by Zhang et al.²⁴

Chemistry. ^1H and ^{13}C NMR spectra were obtained at 300.1 MHz on a Bruker spectrometer in CDCl_3 . UV-Vis spectra were recorded on both an AVIV 14DS spectrophotometer and a Hewlett-Packard spectrophotometer in methanolic solution (Fisher, spectrograde). IR spectra were recorded using a Bomem FTIR spectrometer. TLC was performed on pre-coated 250 μm silica gel plates (Analtech, Inc.; 5 x 10 cm). Solvents and liquid starting materials were distilled prior to use. Reactions and purifications were conducted with deoxygenated solvents, under inert gas (N_2) and subdued lighting. Melting points were recorded on a MeltTemp melting point apparatus and were uncorrected.

(2*Z*,4*E*)-4-(6',7',8',9'-Tetrahydro-benzocyclohepten-5'-ylidene)-3-methyl-2-butenic Acid (4). Zn dust (13.2 g, 0.200 mol) was stirred with 20% HCl (40 mL) for 20 min at room temperature. The mixture was allowed to settle, and the liquid was carefully removed with a pipet. The Zn was then washed with water (3 x 50 mL), anhydrous acetone (3 x 50 mL), and anhydrous ether (3 x 50 mL). After residual ether was removed

under a stream of N_2 , the flask was gently heated with a heating mantle for 30 min, followed by strong heating with a bunsen burner flame for 1 min. The cooled Zn dust was suspended in anhydrous dioxane (35 mL) and a solution of 1-benzosuberone **3** (5.44 g, 34.0 mmol), ethyl 4-bromo-3-methyl-2-butenolate (7.30 mL, 57.8 mmol), and anhydrous dioxane (45 mL) was added over 10 min, which produced an exothermic reaction. The resulting reaction mixture was stirred at reflux for 3 h then cooled to room temperature. The reaction mixture was diluted with ether (50 mL), and acidified 5% HCl (100 mL) and filtered through a pad of Celite. The filter was washed well with ether (150 mL), and the ether layer from the filtrate was extracted with 1 N NaOH (3 x 200 mL). The pH of the basic aqueous layer was adjusted to pH 1-2 with 5% HCl and extracted with ether (2 x 200 mL). The organic layer was washed with saturated NaCl solution, dried (Na_2SO_4), and concentrated under vacuum to provide a yellow solid **4** (6.2 g, 75%): mp 121-122 °C (ether/hexanes); MS m/e 243 (MH^+); UV-Vis (MeOH) λ_{max} 283 nm ($\epsilon=7316$); 1H NMR ($CDCl_3$): δ 7.32-7.27 (m, 1H), 7.17-7.14 (m, 2H), 7.08-7.05 (m, 1H), 5.80 (t, 1H, $J=1.27$), 2.77 (m, 2H), 2.41-2.39 (m, 2H), 2.17 (s, 3H), 1.75-1.74 (m, 4H); ^{13}C NMR ($CDCl_3$) δ 172.0, 156.95, 146.82, 145.33, 140.41, 129.09, 128.56, 128.19, 127.64, 126.82, 118.29, 35.79, 31.59, 29.63, 27.74, 26.29.

Anal. ($C_{16}H_{18}O_2$) calcd.: C 79.31% H 7.49%. Found: C 79.53% 7.59%.

(2Z,4E)-4-(6',7',8',9'-Tetrahydro-benzocyclohepten-5'-ylidene)-3-methyl-2-butenol (5). A solution of the acid **4** (1.88 g, 7.75 mmol) in anhydrous ether (78 mL) was cooled to -78 °C, and a 1 M solution of $LiAlH_4$ in ether (8.50 mL, 8.50 mmol) was added with stirring under nitrogen atmosphere. After the dry ice-isopropanol bath was

removed, the reaction temperature was brought to 0 °C with an ice water bath and allowed to stir for 3 h. The reaction was quenched with methanol (10 mL) followed by the addition of 5% HCl (100 mL). The mixture was extracted with ether (2 x 100 mL), washed with saturated NaCl solution (100 mL), dried (Na₂SO₄), and concentrated under vacuum to give a pale yellow oil **5** (1.6 g, 93%). The crude oil was purified by flash silica chromatography (30% Et₂O/hexanes) for elemental analysis. FTIR (neat) 3326 (OH), 1710 (C=C), 1660 (C=C) cm⁻¹; MS m/e 211 (MH⁺-H₂O); UV-Vis (MeOH) λ_{max} 239 nm (ε=11263); ¹H NMR (CDCl₃) δ 7.19-7.11 (m, 2H), 7.08-7.03 (m, 1H), 5.91 (s, 1H), 5.53 (tt, 1H, J=1.19 & 6.75), 4.17 (d, 2H, J=6.74), 2.73 (s, 2H), 2.29 (s, 2H), 1.89 (s, 3H), 1.70 (t, 4H, J=2.95); ¹³C NMR (CDCl₃): δ 145.86, 145.32, 140.53, 136.52, 129.21, 128.58, 127.59, 126.75, 126.70, 60.90, 36.19, 30.92, 29.79, 27.87, 24.62.

Anal. (C₁₆H₂₀O) calcd.: C 84.16% H 8.83%. Found: C 83.95% H 8.87%.

(2Z,4E)-4-(6',7',8',9'-Tetrahydro-benzocyclohepten-5'-ylidene)-3-methyl-2-butenal (6). A slurry containing activated MnO₂ (7.57 g, 88.0 mmol), powdered molecular sieves (5.0 g), and anhydrous CH₂Cl₂ (44 mL) was prepared and cooled to 0 °C. A solution of the alcohol **5** (1.50 g, 4.40 mmol) in anhydrous CH₂Cl₂ (44 mL) was added, and the reaction proceeded with vigorous stirring (overhead stirrer) at 0 °C for 3 h. The reaction mixture was filtered through a pad of silica gel, and the filter was washed with a cold 50% ether/CH₂Cl₂ solution (500 mL). The filtrate was concentrated under vacuum to give an oily residue. This was placed on a flash silica gel column (4.5 x 45 cm) and eluted with 100% CH₂Cl₂ to yield (9Z)-aldehyde **6** (0.530 g, 35%) as a colorless oil; FTIR (neat) 1675 (C=O), 1612 (C=C) cm⁻¹; MS m/e 227 (MH⁺); UV-Vis (MeOH) λ_{max}

232nm ($\epsilon=13714$); ^1H NMR (CDCl_3) δ 9.84 (d, 1H, $J=8.23$), 7.12-6.94 (m, 3H), 6.86 (d, 1H, $J=7.25$), 6.57 (s, 1H), 5.64 (d, 1H, $J=8.18$), 2.70-2.66 (m, 2H), 2.39-2.35 (m, 2H), 1.92-1.81 (m, 2H), 1.71-1.65 (m, 2H), 1.61 (s, 3H); ^{13}C NMR (CDCl_3): δ 192.17, 158.87, 152.83, 141.73, 140.73, 129.85, 129.72, 128.71, 128.27, 126.55, 123.80, 39.47, 36.91, 33.06, 27.91, 24.95.

Anal. ($\text{C}_{16}\text{H}_{18}\text{O}\cdot 0.5\text{H}_2\text{O}$) calcd.: C 81.67% H 8.14%. Found C 81.70% H 7.70%.

(2E,4E,6Z,8E)-Ethyl 8-(6',7',8',9'-Tetrahydro-benzocyclohepten-5'-ylidene)-3,7-dimethyl-2,4,6-octatrienoate ((9Z, 13E)-8). In a dry round-bottom flask flushed with N_2 , NaH (60% dispersion in mineral oil) (0.10 g, 3.1 mmol) was washed with hexanes three times to eliminate the mineral oil. At 0 °C, the NaH was suspended in anhydrous tetrahydrofuran (THF) (1 mL) and freshly distilled triethyl phosphonosenecioate (0.74 g, 2.8 mmol) was added followed by distilled 1,3-Dimethyl-3,4,5,6-tetrahydro-2(1H)-pyrimidinone (DMPU) (0.05 mL, 0.47 mmol) and allowed to stir for 20 min. To this mixture was added (9Z)-aldehyde 6 (0.530 g, 2.35 mmol) in THF (4 mL), and the reaction proceeded for 30 min. The reaction was quenched with methanol (2-3 mL), and the reaction mixture was diluted with ether (100 mL). The ether layer was washed with 5% HCl (100 mL) followed by water (100 mL) and brine (100 mL). The product was dried (Na_2SO_4) and concentrated *in vacuo* to give the ester as a mixture of two geometrical isomers. The product was purified by flash chromatography and eluted with 30% hexanes in toluene to yield the (9Z, 13E)-8 and (9Z, 13Z)-8 esters.

For (9Z,13E)-8. 0.33 g (42%) yellow oil; FTIR (neat) 1707 (C=O) 1605 (C=C) cm^{-1} ; MS m/e 337 (MH^+); UV-Vis (MeOH) λ_{max} 324 nm ($\epsilon=28516$); ^1H NMR (CDCl_3) δ 7.25-7.11 (m, 4H), 6.87 (dd, 1H, $J=4.26$ & 11.03), 6.22 (d, 1H, $J=15.37$), 6.16 (d, 1H, $J=14.57$), 6.12 (s, 1H), 5.76 (s, 1H), 4.16 (q, 2H, $J=7.12$), 2.81-2.77 (m, 2H), 2.34 (broad s, 2H), 2.28 (s, 3H), 2.02 (s, 3H), 1.73 (broad s, 4H), 1.28 (t, 3H, $J=7.11$); ^{13}C NMR (CDCl_3) δ 167.62, 153.24, 146.40, 145.30, 140.97, 140.45, 134.21, 132.93, 129.25, 128.41, 127.99, 127.81, 127.68, 126.77, 118.99, 60.06, 35.95, 31.13, 29.22, 27.70, 24.99, 14.78, 14.16.

Anal. ($\text{C}_{23}\text{H}_{28}\text{O}_2$) calcd.: C 82.10% H 8.51%. Found: C 81.86% H 8.51%.

For (9Z, 13Z)-8. 0.22 g (28%) yellow oil; FTIR (neat) 1709 (C=O) 1607 (C=C) cm^{-1} ; MS m/e 337 (MH^+); ^1H NMR (CDCl_3) δ 7.72 (d, 1H, $J=15.62$), 7.25-7.10 (m, 4H), 6.86 (dd, 1H, $J=4.52$ & 11.09), 6.20 (d, 1H, $J=11.07$), 6.06 (s, 1H), 5.63 (s, 1H), 4.16 (q, 2H, $J=7.12$), 2.80-2.76 (m, 2H), 2.35 (broad s, 2H), 2.01 (s, 3H), 1.99 (s, 3H), 1.72 (broad s, 4H), 1.29 (t, 3H, $J=7.10$); ^{13}C NMR (CDCl_3) δ 166.90, 151.73, 146.24, 145.38, 141.22, 140.46, 134.23, 129.24, 128.77, 128.41, 128.34, 127.95, 127.64, 126.75, 116.95, 60.05, 35.97, 31.11, 29.27, 27.72, 25.04, 21.41, 14.79.

(2E,4E,6Z,8E)-8-(6',7',8',9'-Tetrahydro-benzocyclohepten-5'-ylidene)-3,7-dimethyl-2,4,6-octatrienoic Acid (2). The (9Z,13E) ester **8** (0.30 g, 0.89 mmol) was dissolved in HPLC grade methanol (final concentration 0.06 M), and to this solution was added a 2 M aqueous solution of KOH (13 mL). The reaction mixture was heated to reflux for 1 h and then allowed to cool to room temperature. The flask was cooled in an ice

bath (10 °C), and the mixture was acidified with 5% HCl (pH 1-2). The mixture was filtered to yield **2** (0.23 g, 85%) as a yellow solid, which was recrystallized from ether/hexanes to yield 0.12 g (52% recovery) of a creamy white solid: mp 174-175 °C (ether/hexanes); FTIR (KBr) 1669 (C=O), 1595 (C=C) cm^{-1} ; MS m/e 309 (MH^+); UV-Vis (MeOH) λ_{max} 319 nm ($\epsilon=32722$); ^1H NMR (CDCl_3) δ 7.24- 7.17 (m, 3H), 7.12- 7.10 (m, 1H), 6.92 (dd, 1H, $J=11.01$ & 4.27), 6.25 (d, 1H, $J=15.36$), 6.11 (d, 1H, $J=11.07$), 6.07 (s, 1H), 5.79 (s, 1H), 2.81-2.77 (m, 2H), 2.38- 2.34 (m, 2H), 2.29 (s, 3H), 2.03 (s, 3H), 1.73 (broad s, 4H); ^{13}C NMR (CDCl_3) δ 172.63, 155.83, 146.55, 145.24, 141.81, 140.45, 133.99, 133.86, 129.27, 128.40, 127.94, 127.75, 127.71, 126.77, 35.94, 31.13, 29.21, 27.68, 25.04, 14.37.

Anal. ($\text{C}_{21}\text{H}_{24}\text{O}_2$) calcd.: C 81.78% H 7.84%. Found C 81.65% H 7.84%.

References

- (1) For recent reviews, see: (a) *Chemistry and Biology of Synthetic Retinoids*; Dawson, M.A.; Okamura, W.H., Eds.; CRC Press: Boca Raton, FL, 1990. (b) *THE RETINOIDS: Biology, Chemistry and Medicine*, 2nd ed.; Sporn, M.B.; Roberts, A.B.; Goodman, D.S., Eds.; Raven Press: New York, 1994.
- (2) Thaller, C.; Eichele, G. Identification and Spatial Distribution of Retinoids in the Developing Chick Limb Bud. *Nature (London)* **1987**, *327*, 624-628.
- (3) Chandraratna, R. A. S. Tazarotene: The First Receptor-Selective Topical Retinoid for the Treatment of Psoriasis. *Journal of the American Academy of Dermatology* **1997**, *37*, S12-17.
- (4) Nagpal, S.; Chandraratna, R.A.S. Recent Developments in Receptor-Selective Retinoids. *Current Pharmaceutical Design* **2000**, *6*, 919-931.
- (5) Hansen, L. A.; Sigman, C. C.; Andreola, F.; Ross, S. A.; Kelloff, G. J.; De Luca, L. M. Retinoids in Chemoprevention and Differentiation Therapy. *Carcinogenesis* **2000**, *21*, 1271-1279.

- (6) Anzano, M. A.; Byers, S. W.; Smith, J. M.; Peer, C. W.; Mullen, L. T.; Brown, C. C.; Roberts, A. B.; Sporn, M. B. Prevention of Breast Cancer in the Rat With 9-*cis*-Retinoic Acid as a Single Agent and in Combination With Tamoxifen. *Cancer Res.* 1994, 54, 4614-4617.
- (7) Bischoff, E. D.; Gottardis, M. M.; Moon, T. E.; Heyman, R. A.; Lamph, W. W. Beyond Tamoxifen: The Retinoid X Receptor-Selective Ligand LGD1069 (Targretin) Causes Complete Regression of Mammary Carcinoma. *Anticancer Res.* 1998, 58, 479-484. (b) Gottardis, M. M.; Bischoff, E. D.; Shirley, M. A.; Wagoner, M. A.; Lamph, W. W.; Heyman, R. A. Chemoprevention of Mammary Carcinoma by LGD1069 (Targretin): An RXR-Selective Ligand. *Cancer Res.* 1996, 56, 5566-5570. (c) Bischoff, E. D.; Heyman, R. A.; Lamph, W. W. Effect of the Retinoid X Receptor-Selective Ligand LGD1069 on Mammary Carcinoma After Tamoxifen Failure. *J. Natl. Cancer Inst.* 1999, 91, 2118-2123.
- (8) (a) Hixson, E.J.; Denine, E.P. Comparative Subacute Toxicity of *All-trans*- and 13-*cis*-Retinoic Acid in Swiss Mice. *Toxicol. Appl. Pharmacol.* 1978, 44, 29-40. (b) Kamm, J.J. Toxicology, Carcinogenicity, and Teratogenicity of Some Orally Administered Retinoids. *J. Am. Acad. Dermatol.* 1982, 6, 652-659. (c) Cohen, M. Tretinoin: A Review of Preclinical Toxicological Studies. *Drug Dev. Res.* 1993, 30, 244-51.
- (9) Kochhar, D. M. Teratogenic Activity of Retinoic Acid. *Acta. Pathol. Microbiol. Immunol.* 1967, 967, 70, 398-404. (b) Willhite, C. C. Molecular Correlates in Retinoid Pharmacology and Toxicology. In *Chemistry and Biology of Synthetic Retinoids*; Dawson, M.I., Okamura, W.H., Eds.; CRC Press: Boca Raton, FL, 1990; pp 539-573. (c) Adams, J. Structure-Activity and Dose-Response Relationships in the Neural and Behavioral Teratogenesis of Retinoids. *Neurotoxicol. Teratol.* 1993, 15, 193-202.
- (10) (a) Kagechika, H.; Kawachi, E.; Hashimoto, Y.; Shudo, K. Retinobenzoic Acids. 2. Structure-Activity Relationships of Chalcone-4-carboxylic Acids and Flavone-4'-carboxylic Acids. *J. Med. Chem.* 1989, 32, 834-840. (b) Delecleuse, C.; Cavey, M.T.; Martin, B.; Bernard, B.A.; Reichert, U.; Maignan, J.; Shroot, B. Selective High Affinity Retinoic Acid Receptor α or β - γ Ligands. *Molec. Pharmacol.* 1991, 40, 556-562. (c) Teng, M.; Duong, T.; Klein, E.; Pino, M.; Chandraratna, R. Identification of Retinoic Acid Receptor α Subtype Specific Agonist. *J. Med. Chem.* 1996, 39, 3035-3038. (d) Kikuchi, K.; Hibi, S.; Yoshimura, H.; Tokuhara, N.; Tai, K.; Hida, T.; Yamauchi, T.; Nagai, M. Syntheses and Structure-Activity Relationships of 5,6,7,8-Tetrahydro-5,5,8,8,-Tetramethyl-2-Quinoxaline Derivatives With Retinoic Acid Receptor α Agonistic Activity. *J. Med. Chem.* 2000, 43, 409-419.
- (11) (a) Vaezi, M. F.; Alam, M.; Sani, B. P.; Rogers, T. S.; Simpson-Herren, L.; Wille, J. J.; Hill, D. L.; Doran, T. I.; Brouillette, W. J.; Muccio, D. D. A Conformationally Defined 6-*s-trans*-Retinoic Acid Isomer. Synthesis, Chemopreventive Activity, and Toxicity. *J. Med. Chem.* 1994, 37, 4499-4507. (b) Alam, M.; Zhestkov, V.; Sani, B.

- P.; Venepally, P.; Levin, A. A.; Kazmer, S.; Li, E.; Norris, A. W.; Zhang, X.-K.; Lee, M. O.; Hill, D. L.; Lin, T.-H.; Brouillette, W. J.; Muccio, D. D. Conformationally Defined 6-*s-trans*-Retinoic Acid Analogs. 2. Selective Agonists for Nuclear Receptor Binding and Transcriptional Activity. *J. Med. Chem.* **1995**, *38*, 2303-2310. (c) Muccio, D. D.; Brouillette, W. J.; Alam, M.; Vaezi, M. F.; Sani, B. P.; Venepally, P.; Reddy, L.; Li, E.; Norris, A.; Simpson-Herren, L.; Hill, D. Conformationally Defined 6-*s-trans* Retinoic Acid Analogs. 3. Structure-Activity Relationships for Nuclear Receptor Binding, Transcriptional Activity, and Cancer Chemopreventive Activity. *J. Med. Chem.* **1996**, *39*, 3625-3635.
- (12) Muccio, D. D.; Brouillette, W. J.; Breitman, T. R.; Taimi, M.; Emanuel, P. D.; Zhang, X.-K.; Chen, G.-Q.; Sani, B. P.; Venepally, P.; Reddy, L.; Alam, M.; Simpson-Herren, L.; Hill, D. L. Conformationally Defined Retinoic Acid Analogues. 4. Potential New Agents for Acute Promyelocytic and Juvenile Myelomonocytic Leukemias. *J. Med. Chem.* **1998**, *41*, 1679-1687.
- (13) (a) Jong, L.; Lehmann, J. M.; Hobbs, P. D.; Harlev, E.; Huffman, J. C.; Pfahl, M.; Dawson, M. I. Conformational Effects on Retinoid Receptor Selectivity. 1. Effect of 9-Double Bond Geometry on Retinoid X Receptor Activity. *J. Med. Chem.* **1993**, *36*, 2605-2613. (b) Dawson, M. I.; Jong, L. J.; Hobbs, P. D.; Cameron, J. F.; Chao, W.-R.; Pfahl, M.; Lee, M.-O.; Shroot, B.; Pfahl, M. Conformational Effects on Retinoid Receptor Selectivity. 2. Effects of Retinoid Bridging Group on Retinoid X Receptor Activity and Selectivity. *J. Med. Chem.* **1995**, *38*, 3368-3383. (c) Beard, R.L.; Gil, D.W.; Marler, D.K.; Henry, E.; Colon, D.F.; Gillett, S.J.; Arefieg, T.; Breen, T.S.; Krauss, H.; Davies, P.J.A.; Chandraratna, R. Structural Basis of the Differential RXR and RAR Activity of Stilbene Retinoid Analogs. *Bioorg. Med. Chem. Lett.* **1994**, *4*, 1447-1452. (d) Boehm, M. F.; Zhang, L.; Badea, B. A.; White, S.K.; Mais, D. E.; Berger, E.; Suto, C. M.; Goldman, M.E.; Heyman, R. A. Synthesis and Structure-Activity Relationships of Novel Retinoid X Receptor-Selective Retinoids. *J. Med. Chem.* **1994**, *37*, 2930-2941. (e) Beard, R. L.; Colon, D. F.; Klein, E. S.; Vorse, K. A.; Chandraratna, R. A. S. Differential RXR and RAR Activity of Stilbene Retinoid Analogs Bearing Thiazole and Imidazole Carboxylic Acids. *Bioorg. Med. Chem. Lett.* **1995**, *5*, 2729-2734.
- (14) (a) O'Shaughnessy, J. Chemoprevention and Breast Cancer. *JAMA* **1996**, *275*, 1349-1353. (b) Swan, D. K.; Ford, B. Chemoprevention and Cancer: Review of the Literature. *ONF* **1997**, *24*, 719-727.
- (15) Chang, C. N. A Review of Breast Cancer Chemoprevention. *Biomed. Pharmacother.* **1998**, *52*, 133-136.
- (16) Osborne, K. C. Tamoxifen in the Treatment of Breast Cancer. *N. Engl. J. Med.* **1998**, *339*, 1609-1618.
- (17) Carmichael, P. L. Mechanisms of Action of Antiestrogens: Relevance to Clinical Benefits and Risks. *Cancer Investigation* **1998**, *16*, 604-611.

- (18) Dawson, M. I.; Chao, W.-R.; Pine, P.; Jong, L.; Hobbs, P.D.; Rudd, C.K.; Quick, T.C.; Niles, R.M.; Zhang, X.-K.; Lombardo, A.; Ely, K.R.; Shroot, B.; Fontana, J.A. Correlation of Retinoid Binding Affinity to Retinoic Acid Receptor α With Retinoid Inhibition of Growth of Estrogen Receptor-Positive MCF-7 Mammary Carcinoma Cells. *Cancer Res.* **1995**, *55*, 4446-4451.
- (19) Wu, Q.; Dawson, M. I.; Zheng, Y.; Hobbs, P. D.; Agadir, A.; Jong, L.; Li, Y.; Liu, R.; Lin, B.; Zhang, X.-K. Inhibition of *trans*-Retinoic Acid-Resistant Human Breast Cancer Cell Growth by Retinoid X Receptor-Selective Retinoids. *Molec. Cell Biol.* **1997**, *17*, 6598-6608.
- (20) (a) Egea, P. F.; Klaholz, B. P.; Moras, D. Ligand-Protein Interactions in Nuclear Receptors of Hormones. *FEBS Letters* **2000**, *476*, 62-67. (b) Egea, P. F.; Mitschler, A.; Rochel, N.; Ruff, M.; Chambon, P.; Moras, D. Crystal Structure of the Human RXR α Ligand-Binding Domain Bound to its Natural Ligand: 9-*Cis* Retinoic Acid. *EMBO J.* **2000**, *19*, 2592-2601.
- (21) Allenby, G.; Bocquel, M.-T.; Sounders, M.; Karmer, S.; Speck, J.; Rosenberger, M.; Lovey, A.; Kastner, P.; Grippo, J. F.; Chambon, P.; Levin, A. A. Retinoic Acid Receptors and Retinoid X Receptors: Interactions With Endogenous Retinoic Acids. *Proc. Natl. Acad. Sci. U.S.A.* **1993**, *90*, 30-34.
- (22) Allenby, G.; Janocha, R.; Kazmer, S.; Speck, J.; Grippo, J.; Levin, A. Binding of 9-*Cis* Retinoic Acid and All-*trans*-Retinoic Acid to Retinoic Acid Receptors α , β , and γ . *J. Biol. Chem.* **1994**, *269*, 16689-16695.
- (23) (a) Levin, A. A.; Sturzenbecker, L.J.; Kazmer, S.; Bosakowski, T.; Huselton, C.; Allenby, G.; Speck, J.; Kratzeisen, C.; Rosenberger, M.; Lovey, A.; Grippo, J. F. 9-*Cis* Retinoic Acid Stereoisomer Binds and Activates the Nuclear Receptor RXR α . *Nature (London)* **1992**, *355*, 359-361. (b) Heyman, R.; Mangelsdorf, D.; Dyck, J.; Stein, R.; Eichele, G.; Evans, R.; Thaller, C. 9-*Cis* Retinoic Acid is a High Affinity Ligand for the Retinoid X Receptor. *Cell* **1992**, *68*, 397-406.
- (24) Zhang, X.-K.; Hoffman, B.; Tran, P.; Graupner, G.; Pfahl, M. Retinoid X Receptor is an Auxilliary Protein for Thyroid Hormone and Retinoic Acid Receptors. *Nature (London)* **1992**, *355*, 441-446.

**CONFORMATIONALLY DEFINED RETINOIC ACID ANALOGUES: SYNTHESIS
AND NUCLEAR RECEPTOR TRANSCRIPTIONAL ACTIVATION ACTIVITY FOR
AMIDE DERIVATIVES OF (9Z)-UAB30, RAR γ -SELECTIVE LIGANDS**

by

**KIMBERLY K. VINES, WAYNE J. BROUILLETTE,
DONALD D. MUCCIO, AND XIAO-KUN ZHANG**

In preparation for Journal of Medicinal Chemistry

Format adapted for dissertation

Abstract

We recently reported the synthesis and biological activity of the conformationally defined 6-*s-trans* retinoic acid (RA) analogue, (9Z)-UAB30 [(2*E*,4*E*,6*Z*,8*E*)-8-(3',4'-dihydro-1'(2'H)-naphthalen-1'-ylidene)-3,7-dimethyl-2,4,6-octatrienoic acid], which is retinoid X receptor (RXR α) selective (IC₅₀ = 284 nM; EC₅₀ = 118 nM) (Muccio et al. *J. Med. Chem.* 1998, 41, 1679). In an effort to enhance RXR α activity, analogues were synthesized possessing both an amide linkage and a benzoic acid terminus to explore the effects of these structural alterations on receptor selectivity. The transcriptional activation ability of these retinoids was measured for the retinoic acid receptor (RARs - α , - β , - γ) and RXR α . Although these structural alterations to (9Z)-UAB30 resulted in the loss of RAR α and RXR α activation, RAR γ activation was enhanced, revealing a new class of RAR γ -selective ligands.

Introduction

Retinoids are involved in the regulation of cell processes such as proliferation, differentiation, and apoptosis via the activation of retinoid receptors, which are members of the hormone nuclear receptor superfamily.^{1,2} These retinoid nuclear receptors function as transcription factors and are comprised of the retinoic acid receptors (RARs) and retinoid X receptors (RXRs). These two classes of retinoid receptors each include three isoforms (α , β , γ). RARs are activated by both the 9-*cis* and (*all-trans*) isomers of retinoic acid (RA),³ while RXRs are activated by 9-*cis* RA. The RARs function *in vivo* as RXR heterodimers, which bind the promoter regions of RA responsive genes and mediate gene transcription upon ligand-binding of the RARs. RXR can also form heterodimers with

other hormone nuclear receptors peroxisome proliferator activation receptor (PPAR γ), vitamin D receptor (VDR), and thyroid receptor (TR), in addition to forming homodimers. Both (*all-trans*)-RA (ATRA) and 9-*cis* RA are used clinically, but therapeutic use is hampered by toxicity³ and teratogenicity.⁴ Because each retinoid receptor has a characteristic tissue distribution pattern,⁵ toxicity can be reduced by selectively activating individual retinoid receptors. Several RAR-^{6,7,8} and RXR-^{9,10} selective agonists and antagonists have been reported, which have helped elucidate the physiological role of each receptor subtype. Thus, considerable effort has been directed toward identifying retinoids with receptor subtype selectivity.

Common structural features are often found in receptor-selective retinoids. For example, substitution of the dienoic acid terminus of ATRA with a benzoic acid terminus resulted in the potent RAR pan-agonist 4-[2-(5,6,7,8-tetrahydro-5,5,8,8-tetramethyl-2-naphthalenyl)-1E-propenyl]benzoic acid (TTNPB) (Figure 1).¹¹ Kagechika et al. altered the structure of TTNPB by inserting an amide linkage in place of the propenyl linker to yield Am80, a RAR α -selective agonist.⁷ Similarly, Targretin, which is an RXR-selective

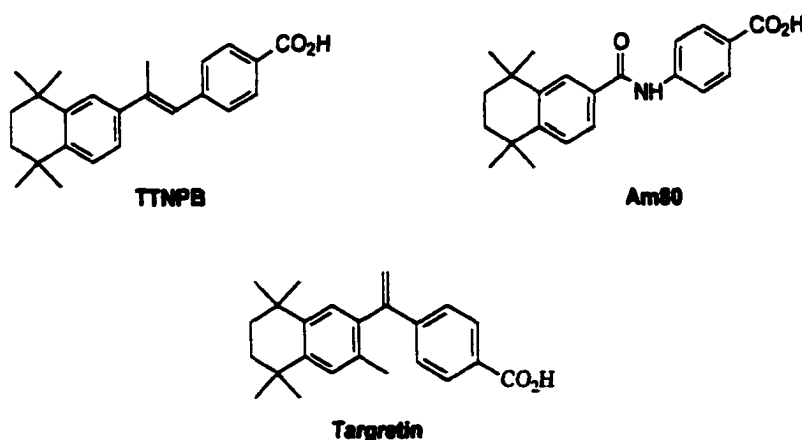


Figure 1. Pan-agonist TTNPB, RAR α -selective retinoid Am80, and RXR-selective retinoid Targretin.

retinoid, is also a derivative of TTNPB. In this case, replacement of the propenyl linker with a methylene linker resulted in a central “cis-oid” geometry and RXR selectivity. Thus, retinoid receptor selectivity may be modified in compounds possessing a benzoic acid terminus. We previously reported the synthesis and receptor binding and activation profile of the 9-*cis* RA analog, (9Z)-UAB30, which is an RXR-selective ligand. We sought to explore the effect of replacing the dienolic acid terminus of (9Z)-UAB30 with an amide-linked benzoic acid terminus as in compound **2** (Figure 2). In addition, if the receptor subtype selectivity and potency for these agents were maintained or enhanced, the synthesis of the amide derivative would make these compounds attractive because it is much simpler and higher yielding than the synthesis of (9Z)-UAB30. Also targeted were the p-aminobenzoic acid amides of substituted (9Z)-UAB30 analogs (**3-8**, Scheme 1).

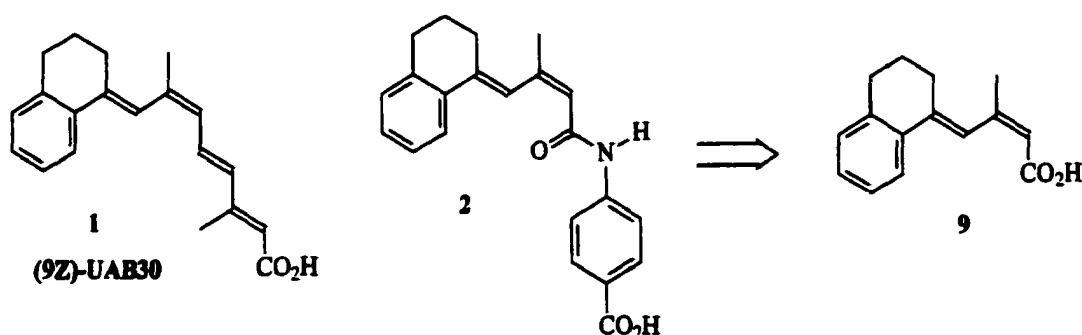
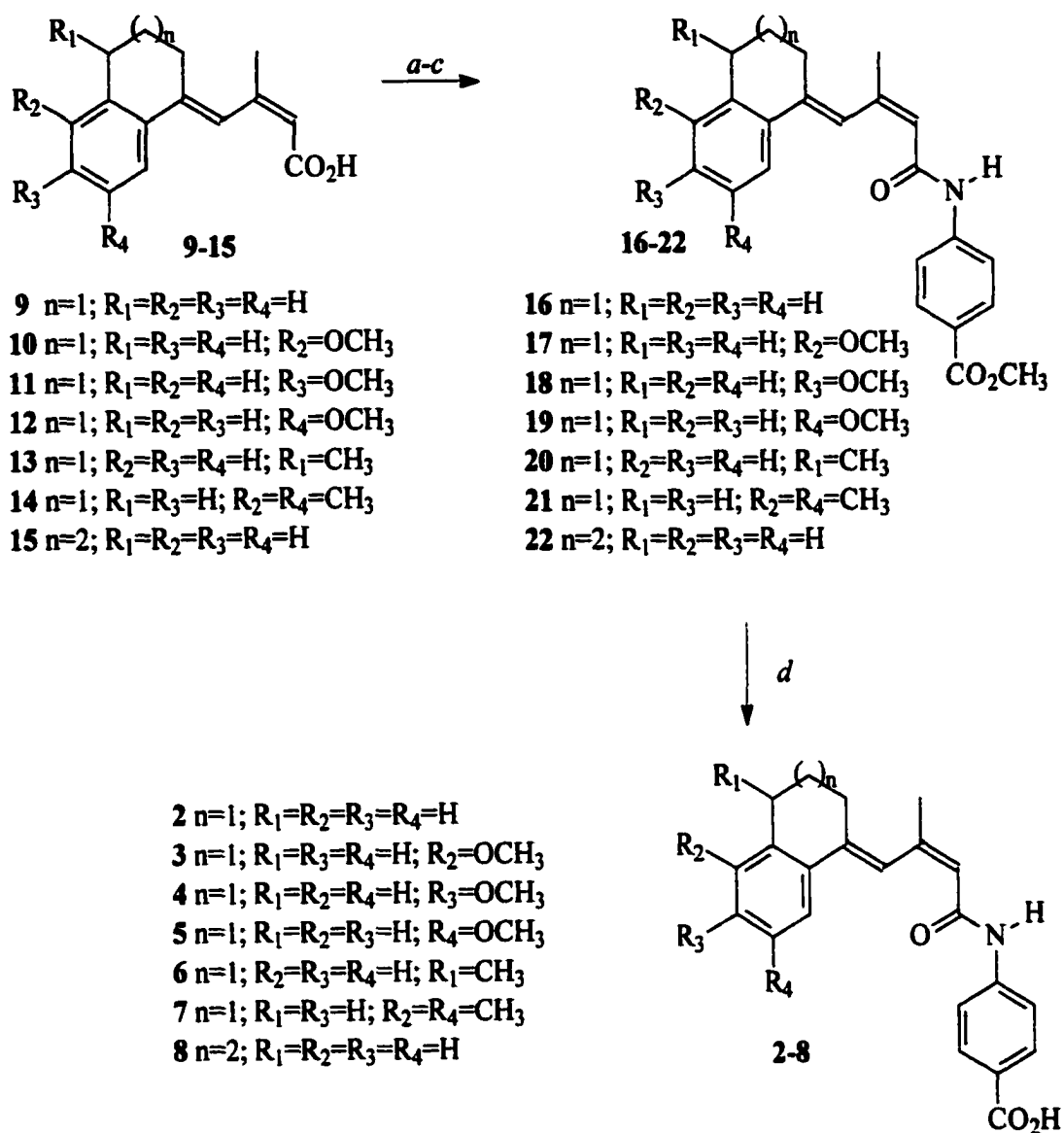


Figure 2. Structures of (9Z)-UAB30 **1** and the amide derivative **2**.

Chemistry

The synthesis of **2** and analogs was proposed as the straightforward amidation of (9Z)-acid **9**, which is made in one step from 1-tetralone as described in the first manu-

Scheme 1. Synthesis of Amides 2-8^a

^a (a) hexachloroacetone, PPh_3 , THF, $-78^\circ C$; (b) methyl 4-aminobenzoate, $-78^\circ C$; (c) pyridine, $-78^\circ C$; (d) 0.8 N KOH, methanol, $60^\circ C$.

script. The first attempt involved the acid chloride intermediate. Conventional methods utilizing reagents such as PCl_3 ¹² and SOCl_2 ⁷ failed to convert the acid to acid chloride. Phosphorous trichloride required elevated reaction temperatures and caused decomposition of the acid. A similar decomposition was obtained with thionyl chloride. Milder procedures were then utilized to activate the carboxyl group. Activation of the carboxylic acid with each of the reagents carbodiimidazole (CDI),¹³ 1-(3-Dimethyl-aminopropyl)-3-ethylcarbodiimide hydrochloride (EDI),^{7c} and dicyclohexylcarbodiimide (DCC)/4-Dimethylaminopyridine (DMAP)¹⁴ was attempted and appeared promising. The first two methods were successful in activating the carboxyl group as evidenced by the evolution of CO_2 (g), and the third method was also successful in activating the carboxyl group due to the disappearance of starting material on TLC. However, methyl 4-aminobenzoate was unreactive with these intermediates. This was confirmed by performing the reaction of the acid **9** with aniline under the same reaction conditions to form the corresponding amide.

In addition, several peptide-coupling reagents, including EEDQ,¹⁵ diphenylphosphorylazide (DPPA),¹⁶ and Bis(2-oxo-3-oxazolidinyl)phosphinic chloride (BOPCl)¹⁷ also failed to provide product. Finally, Villeneuve and Chan¹⁸ reported a modification of a mild procedure used to synthesize retinamides from an acid and methyl-4-aminobenzoate as first reported by Magid et al.¹⁹ Using benzoic acid and methyl 4-aminobenzoate, a quantitative yield of the resulting amide was obtained. This procedure was then used to prepare amides **16-22** from the corresponding acids **9-15**, which were synthesized as described previously.¹⁰ The amides **16-22** were prepared by reaction of the appropriate carboxylic acid **9-15** with hexachloroacetone, triphenylphosphine, and methyl 4-amino-

benzoate in tetrahydrofuran (THF) at -78°C using the method reported by Villeneuve and Chan.¹⁸ The acid chloride formed almost immediately, and the formation of the amide was complete within 30 min. A nonpolar side product was also formed for reactions longer than 30 min. For reaction times shorter than this, yields between 60-70% were obtained.

Formation of the amide bond could result in two conformers (-cis and -trans amides). As reported by Kagechika et al., the trans-amide predominates due to increased thermodynamic stability unless the amide nitrogen is substituted.^{7c,d} The trans conformation of the amide bond was confirmed using Nuclear Overhauser Effect Spectroscopy (NOESY).

Three key interactions define the stereochemistry of the trans conformation of the amides (2-8). Cross-peaks observed for H5/H8 and H2'/C9-methyl indicate an *s-trans* conformation about the C8-C9 bond (Figure 3). The third key interaction defines the conformation of the amide bond. A cross-peak was observed for H10 and the amide hydrogen (N-H), which indicates that the amide is trans.

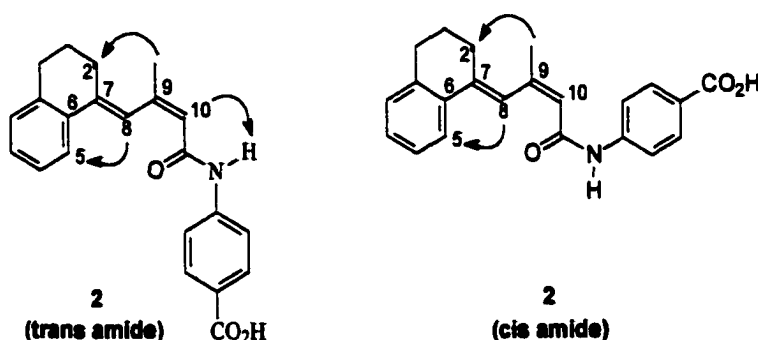


Figure 3. Key interactions in the trans and cis amides.

Results and Discussion

The results from the nuclear receptor transactivation assays are summarized in Figures 4-7. As shown, replacement of the tetraene chain with the amide functionality and benzoic acid terminus abolished RAR α and RXR α activity, while RAR β activity was unaffected. The decrease in RXR α activity may be due to the increased distance between the hydrophobic ring and the carboxyl terminus of the amide ligand when compared to the corresponding tetraenoic acid. However, as shown in Figure 6, comparison of the benzoic acids 2-8 with the corresponding tetraenoic acids (1, 23-28) (structures shown in Figure 8) showed that the introduction of the p-aminobenzoic acid amide resulted in increased RAR γ activation. This was especially true for amides 2, 6, and 8. The enhanced RAR γ activation may be due to the interaction of the amide proton with Met272 of the RAR γ ligand-binding pocket.

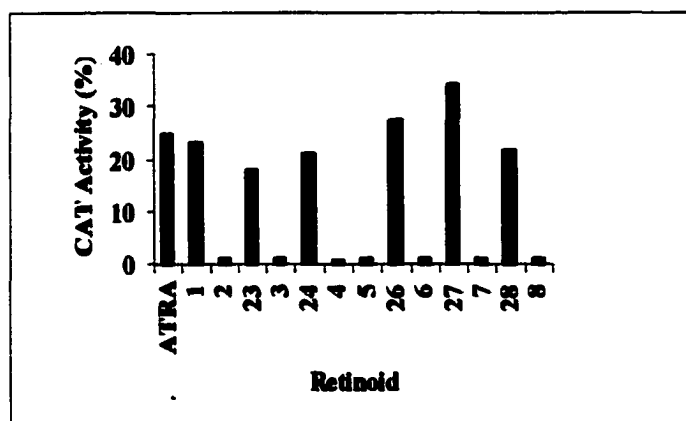


Figure 4. RAR α -receptor transcriptional activation (10^{-6} M).

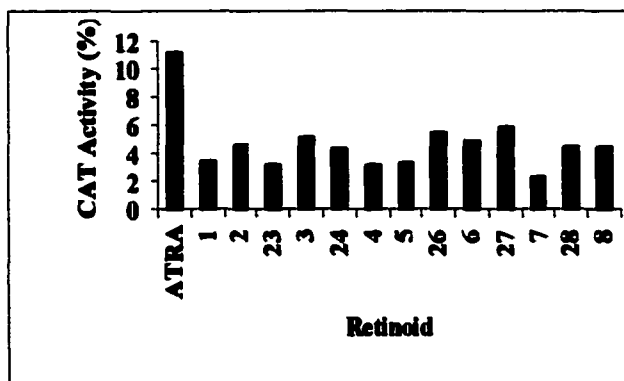


Figure 5. RAR β -receptor transcriptional activation (10^{-6} M).

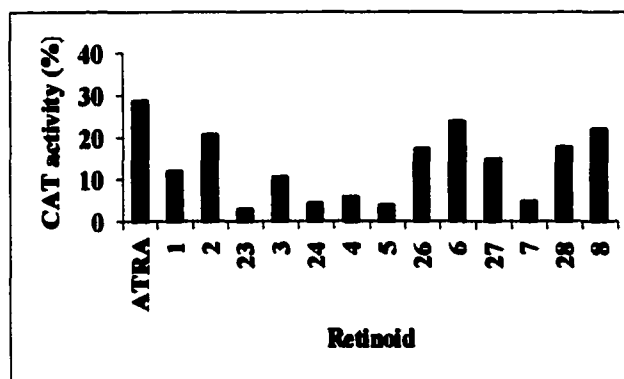


Figure 6. RAR γ -receptor transcriptional activation (10^{-6} M).

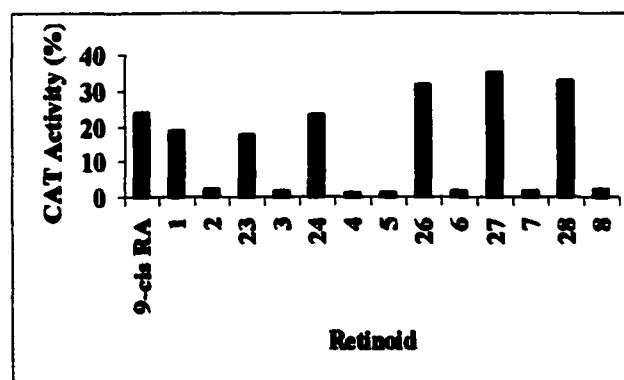


Figure 7. RXR α -receptor transcriptional activation (10^{-6} M).

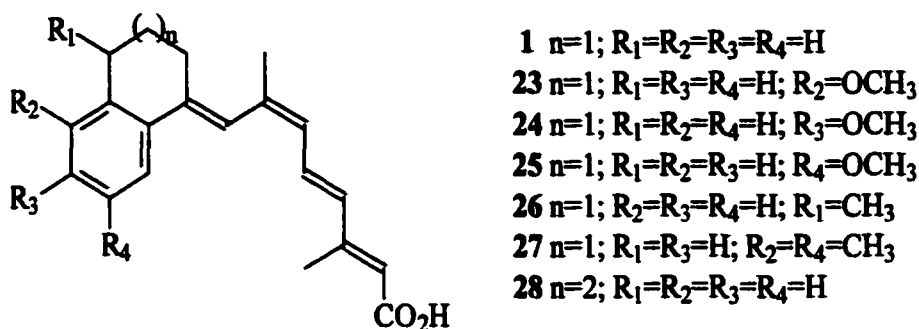


Figure 8. Previously synthesized (9Z)-UAB30 analogs.

In summary, these studies have revealed a new class of compounds with high selectivity for RAR γ receptors. RAR γ -selective retinoids have been used clinically for the treatment of proliferative skin diseases (Figure 9). Tazarotene, a RAR β,γ -selective acetylenic retinoid, is used to treat psoriasis.²⁰ Differin, also an RAR γ agonist, is used to treat *acne vulgaris*.²¹ Therefore, **2** and analogs may have similar utility in the treatment of skin disease.

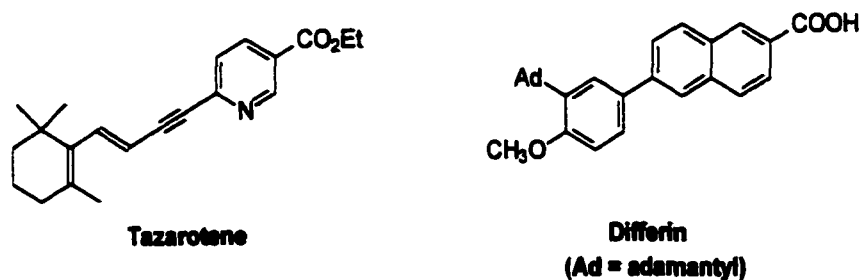


Figure 9. Receptor subtype selective retinoids used to treat proliferative skin disease.

Experimental Section

Biology. Each amide was evaluated for the efficiency of activating RAR α , - β , and - γ homodimers and RXR α homodimers using the chloramphenicol acetyltransferase

(CAT) reporter gene containing thyroid hormone response element (TREpal) according to a method described by Zhang et al.²² Briefly, CV-1 cells were transiently transfected with a DNA plasmid as described previously by Husmann et al.²³ and Pfahl et al.,²⁴ with minor modifications as described by Alam et al.^{8b} The DNA used in the transfection consisted of either RAR α , RAR β , or RAR γ and (TRE-pal)₂-*tk*-CAT, β -galactosidase expression plasmid pCH110, and carrier bluescript plasmid. The transfected cells were treated with ATRA or the test retinoid. After an incubation of 24 h, the resultant cell extracts were assayed for β -galactosidase and CAT activity as described by Husmann et al.²³ The CAT activity was normalized for transfection efficiency by the corresponding β -galactosidase activity.

Chemistry. ¹H NMR spectra were obtained at 300.1 MHz on a Bruker spectrometer in CDCl₃ or DMSO-*d*₆. NOE experiments were obtained at 400.1 MHz (Bruker DRX spectrometer) using 2D phase-sensitive NOESY experiments with different mixing times (between 250 and 2000 ms). Typically, 1 s mixing times were used with 16 pulses for phase cycling and two dummy scans. The spectra were processed with line broadening of 0.3 Hz in each dimension and zero-filled to yield 512 x 4096 2D contour plots. The integrated intensities of the negative cross-peaks were determined using standard Bruker NMR software features.

UV-Vis spectra were recorded on both an AVIV 14DS spectrophotometer and a Hewlett-Packard spectrophotometer in methanol or acetonitrile solutions (Fisher, spectrograde). IR spectra were recorded using a Bomem FTIR spectrometer. TLC was performed on pre-coated 250 μ m silica gel plates (Analtech, Inc.; 5 x 10 cm). Solvents and

liquid starting materials were distilled prior to use. Reactions and purifications were conducted with deoxygenated solvents, under inert gas (N_2) and subdued lighting. Melting points were recorded on a MeltTemp melting point apparatus and were uncorrected.

General Procedure for the Preparation of Amides 16-22. At $-78\text{ }^\circ\text{C}$, under N_2 , hexachloroacetone (0.30 mL, 1.9 mmol) was added to a solution of acids (second manuscript) **9-15** (3.9 mmol) in anhydrous THF (15 mL) with stirring. A solution of triphenylphosphine (1.0 g, 3.9 mmol) in anhydrous THF (4 mL) was added dropwise over 10 min. The bright yellow reaction mixture was diluted with THF (4 mL), and methyl 4-aminobenzoate (0.60 g, 3.9 mmol) was added followed by the dropwise addition of a solution of anhydrous pyridine (1.9 mL, 23 mmol) in THF (4 mL). After 0.5 h, the reaction mixture was diluted with ether (200 mL) and extracted with 5% HCl (200 mL). The ether layer was washed with saturated NaCl, dried (Na_2SO_4), and concentrated *in vacuo* to yield an oily residue. The crude product was purified on a flash silica gel column (4.5 x 45cm) using 30% ethyl acetate/hexanes to yield the amides **16-22**.

Methyl 4-[(1Z,3E)-4-(3',4'-dihydro-1'(2'H)-naphthalen-1'-ylidene)-3-methylbut-2-enoylamino]-benzoate (16) 0.97g white solid (61%): mp $141\text{-}142\text{ }^\circ\text{C}$ (MeOH/ether); FTIR (KBr) 3339 (NH), 1697 (C=O), 1667 (C=O), 1605 (C=C) cm^{-1} ; MS m/e 362 (MH^+); UV-Vis (MeOH) λ_{max} 296 nm ($\epsilon=8312$); ^1H NMR ($DMSO-d_6$): δ 10.18 (s, 1H), 7.89 (d, 2H, $J=8.37$), 7.67 (d, 2H, $J=8.56$), 7.57 (m, 1H), 7.38 (s, 1H), 7.12-6.99 (m, 3H), 3.71 (s, 3H), 2.63 (t, 2H, $J=6.12$), 2.48 (t, 2H, $J=5.93$), 2.03 (s, 3H), 1.63 (p, 2H, $J=6.16$); ^{13}C NMR ($DMSO-d_6$): δ 166.20, 164.70, 149.96, 144.32, 138.20, 138.16, 136.08, 130.58,

129.26, 127.83, 126.50, 124.83, 123.90, 123.47, 122.11, 118.67, 29.98, 28.46, 25.33, 23.23.

Anal. (C₂₃H₂₂NO₃) calcd.: C 76.43% H 6.41% N 3.88%. Found C 76.14% H 6.41 N 3.87%.

Methyl 4-[(1Z,3E)-5'-Methoxy-4-(3',4'-dihydro-1'(2'H)-naphthalen-1'-ylidene)-3-methyl-but-2-enoylamino]-benzoate (17) 1.2 g (75%) white solid: mp 148-149 °C (MeOH/ether); FTIR (KBr) 3358 (NH), 1703 (C=O), 1677 (C=O) cm⁻¹; UV-Vis (MeOH) λ_{max} 298 nm (ε=22666); MS m/e 392 (MH⁺); ¹H NMR (DMSO-*d*₆) δ 10.28 (s, 1H), 7.90 (d, 2H, J=8.75), 7.77 (d, 2H, J=8.78), 7.40 (s, 1H), 7.28 (d, 1H, J=7.95), 7.17 (t, 1H, J=7.99), 6.86 (d, 1H, J=7.94), 6.02 (s, 1H), 2.63 (t, 2H, J=6.30), 2.50 (t, 2H, J=5.73), 2.12 (s, 3H), 1.74 (p, 2H, J=6.20); ¹³C NMR (DMSO-*d*₆) δ 167.05, 164.96, 157.75, 148.28, 142.69, 142.22, 135.95, 131.23, 127.48, 126.92, 125.49, 123.53, 121.19, 118.86, 116.81, 109.87, 55.83, 52.36, 28.22, 26.11, 23.69, 23.18.

Anal. (C₂₄H₂₅NO₄) calcd.: C 73.64% H 6.44% N 3.58%. Found C 73.39% H 6.55% N 3.59%.

Methyl 4-[(1Z,3E)-6'-Methoxy-4-(3',4'-dihydro-1'(2'H)-naphthalen-1'-ylidene)-3-methyl-but-2-enoylamino]-benzoate (18). 1.2 g (75%) yellow solid: mp 128-129 °C (EtOAc/hexanes); FTIR (KBr) 3336 (NH), 1708 (C=O), 1656 (C=O), 1607 (C=C) cm⁻¹; MS m/e 392 (MH⁺); UV-Vis (MeOH) λ_{max} 283 nm (ε=25341); ¹H NMR (CDCl₃) δ 8.30 (s, 1H), 7.90 (d, 2H, J=8.94), 7.67 (d, 1H, J=8.80), 7.42 (d, 2H, J=8.65), 6.79 (dd, 1H, J=2.60 & 6.21), 6.74 (s, 1H), 6.65 (d, 1H, J=2.45), 5.91 (s, 1H), 3.83 (s,

3H), 3.80 (s, 3H), 2.78 (t, 2H, $J=6.19$), 2.52 (t, 2H, $J=5.82$), 2.05 (s, 3H), 1.88-1.76 (m, 2H); ^{13}C NMR (CDCl_3) δ 167.06, 165.06, 160.10, 148.58, 142.78, 141.50, 140.34, 131.25, 127.48, 126.12, 125.45, 123.28, 118.87, 118.81, 113.89, 113.46, 55.69, 52.36, 30.89, 28.00.

Anal. ($\text{C}_{24}\text{H}_{25}\text{NO}_4$) calcd.: C 73.64% H 6.44% N 3.58%. Found C 73.54% H 6.53% N 3.60%.

Methyl 4-[(1*Z*,3*E*)-7'-Methoxy-4-(3',4'-dihydro-1'(2'H)-naphthalen-1'-ylidene)-3-methyl-but-2-enoylamino]-benzoate (19). 1.1 g (74%) yellow solid: mp 128-129 °C (MeOH/ether); FTIR (KBr) 3351 (NH), 1703 (C=O), 1669 (C=O), 1600 (C=C) cm^{-1} ; MS m/e 392 (MH^+); UV-Vis (MeOH) λ_{max} 291 nm ($\epsilon=23574$); ^1H NMR (CDCl_3): δ 8.22 (s, 1H), 7.91 (d, 2H, $J=8.69$), 7.45 (d, 2H, $J=8.70$), 7.21 (d, 1H, $J=2.48$), 7.05 (d, 1H, $J=8.41$), 6.85 (d, 1H, $J=2.53$), 6.82 (d, 1H, $J=2.37$), 5.94 (s, 1H), 3.86 (s, 2H), 3.83 (s, 3H), 2.74 (t, 2H, $J=6.22$), 2.52 (t, 2H, $J=5.58$), 2.08 (s, 3H), 1.80 (p, 2H, $J=6.24$); ^{13}C NMR (CDCl_3): δ 167.02, 164.84, 158.46, 148.29, 142.67, 141.59, 135.53, 131.24, 130.81, 125.55, 123.56, 121.16, 118.83, 115.31, 109.14, 55.81, 52.36, 29.63, 28.57, 26.01, 23.87.

Anal. ($\text{C}_{24}\text{H}_{25}\text{NO}_4$) calcd.: C 73.64% H 6.44% N 3.58%. Found: C 73.43% H 6.47% N 3.54%.

Methyl 4-[(1*Z*,3*E*)-4'-Methyl-4-(3',4'-dihydro-1'(2'H)-naphthalen-1'-ylidene)-3-methyl-but-2-enoylamino]-benzoate (20). 0.93 g (60%) white solid: mp 153-155 °C (MeOH/ether); FTIR (KBr) 3346 (NH), 1683 (C=O), 1632 (C=O), 1606

(C=C) cm^{-1} ; MS m/e 376 (MH^+); UV-Vis (MeOH) λ_{max} 292 nm ($\epsilon=19228$); ^1H NMR ($\text{DMSO}-d_6$): δ 10.21 (s, 1H), 7.81 (d, 2H, $J=8.63$), 7.69 (d, 2H, $J=8.47$), 7.57-7.54 (m, 1H), 7.40 (s, 1H), 7.15-7.10 (m, 3H), 5.94 (s, 1H), 3.73 (s, 3H), 2.85-2.74 (m, 1H), 2.65-2.56 (m, 1H), 2.50-2.43 (m, 1H), 1.83-1.72 (m, 1H), 1.49-1.38 (m, 1H), 1.14 (d, 3H, $J=6.90$); ^{13}C NMR ($\text{DMSO}-d_6$): δ 166.20, 164.72, 149.96, 144.32, 142.98, 138.60, 135.79, 130.58, 128.06, 127.90, 126.46, 125.00, 123.90, 123.56, 122.12, 118.67, 52.17, 32.78, 30.67, 25.49, 25.32, 21.76.

Anal. ($\text{C}_{24}\text{H}_{25}\text{NO}_3$) calcd.: C 76.77% H 6.49% N 3.73%. Found: C 76.49% H 6.68% N 3.65%.

Methyl 4-[(1*Z*,3*E*)-5',7'-Dimethyl-4-(3',4'-dihydro-1'(2'H)-naphthalen-1'-ylidene)-3-methyl-but-2-enoylamino]-benzoate (21). 1.2 g (80%) white solid: mp 180-181 °C (MeOH/ether); FTIR (KBr) 3334 (NH), 1685 (C=O), 1630 (C=O), 1597 (C=C) cm^{-1} ; MS m/e 390 (MH^+); ^1H NMR ($\text{DMSO}-d_6$): δ 10.25 (s, 1H), 7.86 (d, 2H, $J=8.74$), 7.74 (d, 2H, $J=8.77$), 7.27 (s, 1H), 7.21 (s, 1H), 6.90 (s, 1H), 6.00 (s, 1H), 2.58 (t, 2H, $J=6.22$), 2.47-2.43 (m, 2H), 2.25 (s, 3H), 2.14 (s, 3H), 2.10 (s, 3H), 1.75 (p, 2H, $J=6.19$); ^{13}C NMR ($\text{DMSO}-d_6$): δ 166.20, 164.67, 149.97, 144.35, 139.17, 136.12, 136.08, 134.38, 133.27, 130.57, 130.35, 123.86, 123.26, 123.05, 121.93, 118.65, 52.18, 28.06, 26.35, 25.47, 23.35, 21.15, 19.62.

Anal. ($\text{C}_{25}\text{H}_{27}\text{NO}_3$) calcd.: C 77.09% H 6.99% N 3.60%. Found C 76.79% H 7.01% N 3.27%.

Methyl 4-[(1Z,3E)-4-(6',7',8',9'-Tetrahydro-benzocyclohepten-5'-ylidene)-3-methyl-but-2-enoylamino]-benzoate (22) 0.99 g (64%) white solid: mp 153-154 °C (EtOAc/hexanes); FTIR (KBr) 3339 (NH), 1699 (C=O), 1669 (C=O), 1604 (C=C) cm^{-1} ; MS m/e 376 (MH^+); UV-Vis (MeOH) λ_{max} 299 nm ($\epsilon=24656$); ^1H NMR ($\text{DMSO}-d_6$): δ 10.28 (s, 1H), 7.90 (d, 2H, $J=8.82$), 7.76 (d, 2H, $J=8.80$), 7.31-7.28 (m, 1H), 7.22-7.09 (m, 3H), 6.90 (s, 1H), 6.00 (s, 1H), 2.70 (broad s, 2H), 2.43 (broad s, 2H), 2.17 (s, 3H), 1.67 (broad s, 4H); ^{13}C NMR ($\text{DMSO}-d_6$): δ 166.21, 164.66, 149.77, 145.54, 145.34, 144.28, 139.66, 130.61, 129.00, 128.64, 128.03, 127.48, 126.65, 123.95, 122.04, 118.69, 34.75, 31.05, 28.60, 21.11, 25.34.

Anal. ($\text{C}_{24}\text{H}_{25}\text{NO}_3$) calcd.: C 76.77% H 6.71% N 3.73%. Found: C 76.77% H 6.85% N 3.65%.

General Procedure for Ester Hydrolysis. The amide (16-22, 1.55 mmol) was dissolved in HPLC grade methanol (67 mL) followed by the addition of an aqueous solution of KOH (0.8 M, 23 mL). The reaction mixture was heated (60 °C) for 2 h after which the hot solution was allowed to cool to room temperature. The flask was cooled to 10 °C in an ice bath and acidified with 5% HCl (pH 1-2). The mixture was then filtered, and the filtered solid was dissolved in ether, dried (Na_2SO_4), and concentrated *in vacuo*. The residue was recrystallized to give the acid (2, 4-9).

4-[(1Z,3E)-4-(3',4'-dihydro-1'(2'H)-naphthalen-1'-ylidene)-3-methyl-but-2-enoylamino]-benzoic acid (2). 0.46 g (85%) white solid: mp 145-146 °C (ether/hexanes); FTIR (KBr) 3463 (OH), 1670 (C=O), 1592 (C=C) cm^{-1} ; MS m/e 347

(MH⁺); UV-Vis (MeOH) λ_{max} 298 nm ($\epsilon=22666$); ¹H NMR (DMSO-*d*₆) δ 12.65 (s, 1H), 10.24 (s, 1H), 7.86 (d, 2H, *J*=8.69), 7.73 (d, 2H, *J*=8.69), 7.68-7.64 (m, 1H), 7.47 (s, 1H), 7.23-7.10 (m, 4H), 6.01 (s, 1H), 2.74 (t, 2H, *J*=6.13), 2.59 (t, 2H, *J*=5.58), 2.50 (t, 3H, *J*=1.64), 2.13 (s, 3H), 1.74 (p, 2H, *J*=6.21) ¹³C NMR (DMSO-*d*₆) δ 138.31, 138.24, 136.20, 130.69, 129.37, 127.94, 126.62, 124.93, 124.04, 123.58, 122.22, 118.80, 30.08, 28.54, 25.43, 23.34.

Anal. (C₂₂H₂₁NO₃·0.25 H₂O) calcd.: C 75.09% H 6.16% N 3.98%. Found: C 75.14% H 6.33% N 3.89%.

4-[(1*Z*,3*E*)-5'-Methoxy-4-(3',4'-dihydro-1'(2'H)-naphthalen-1'-ylidene)-3-methyl-but-2-enoylamino]-benzoic acid (3). 0.43 g (75%) yellow solid: mp 150-151 °C (ether/hexanes); FTIR (KBr) 1679 (C=O), 1591 (C=C) cm⁻¹; MS *m/e* 378 (MH⁺); UV-Vis (MeOH) λ_{max} 298 nm ($\epsilon=22781$); ¹H NMR (DMSO-*d*₆) δ 12.65 (s, 1H), 10.23 (s, 1H), 7.86 (d, 2H, *J*=8.64), 7.72 (d, 2H, *J*=8.64), 7.39 (s, 1H), 7.27 (d, 1H, *J*=8.12), 7.17 (t, 1H, *J*=7.99), 6.87 (d, 1H, *J*=7.97), 6.02 (s, 1H), 3.78 (s, 3H), 3.34 (s, 2H), 2.63 (t, 2H, *J*=6.29), 2.47-2.50 (m, 3H), 2.12 (s, 3H), 1.73 (p, 2H, *J*=6.21); ¹³C NMR (DMSO-*d*₆): δ 167.30, 164.64, 157.02, 149.63, 143.94, 138.38, 137.17, 130.71, 126.63, 126.23, 125.09, 123.68, 122.21, 118.57, 117.10, 109.42, 55.70, 27.96, 25.37, 23.27, 22.78.

Anal. (C₂₃H₂₃NO₄) calcd.: C 73.19% H 6.14% N 3.71%. Found: C 72.77% H 6.07% N 3.63%.

4-[(1*Z*,3*E*)-6'-Methoxy-4-(3',4'-Dihydro-1'(2'H)-naphthalen-1'-ylidene)-3-methyl-but-2-enoylamino]-benzoic acid (4). 0.48 g (82%) yellow solid: mp 184-186

$^{\circ}\text{C}$ (ether/hexanes); FTIR (KBr) 3325.9 (NH), 1695 (C=O), 1643 (C=O), 1586 (C=C) cm^{-1} ; MS m/e 378 (MH^+); UV-Vis (MeOH) λ_{max} 340 nm ($\epsilon=20121$); ^1H NMR ($\text{DMSO}-d_6$) δ 12.67 (s, 1H), 10.22 (s, 1H), 7.87 (d, 2H, $J=8.54$), 7.74 (d, 2H, $J=8.54$), 7.61 (d, 1H, $J=8.81$), 7.50 (s, 1H), 6.81 (dd, 1H, $J=2.40$ & 6.32), 6.69 (d, 1H, $J=2.27$), 5.96 (s, 1H), 3.75 (s, 3H), 2.72 (t, 2H, $J=6.01$), 2.60 (t, 2H, $J=5.69$), 2.14 (s, 3H), 1.73 (p, 2H, $J=5.99$); ^{13}C NMR ($\text{DMSO}-d_6$) δ 167.32, 164.83, 159.11, 149.98, 144.01, 139.95, 138.55, 130.70, 128.81, 126.38, 125.04, 121.59, 121.32, 118.54, 113.37, 113.25, 30.33, 28.69, 25.52, 23.25.

Anal. ($\text{C}_{23}\text{H}_{23}\text{NO}_4$) calcd. C 73.19% H 6.14% N 3.71%. Found C 72.92% H 6.15% N 3.67%.

4-[(1Z,3E)-7'-Methoxy-4-(3',4'-dihydro-1'(2'H)-naphthalen-1'-ylidene)-3-methyl-but-2-enoylamino]-benzoic acid (5). 0.43 g (74%) yellow solid: mp 189-190 $^{\circ}\text{C}$ (ether/hexanes); FTIR (KBr) 3328 (NH), 1689 (C=O), 1596 (C=C) cm^{-1} ; UV-Vis (MeOH) λ_{max} 298 nm ($\epsilon=20691$); ^1H NMR ($\text{DMSO}-d_6$) δ 12.67 (s, 1H), 10.25 (s, 1H), 7.86 (d, 2H, $J=8.73$), 7.73 (d, 2H, $J=8.75$), 7.40 (s, 1H), 7.17 (d, 1H, $J=2.54$), 7.05 (d, 1H, $J=8.39$), 6.82 (dd, 1H, $J=2.52$ & 5.83), 3.76 (s, 3H), 2.67 (t, 2H, $J=6.11$), 2.56-2.50 (m, 3H), 2.12 (s, 3H), 1.72 (p, 2H, $J=6.16$); ^{13}C NMR ($\text{DMSO}-d_6$) δ 167.30, 164.64, 157.03, 149.63, 143.94, 138.38, 137.16, 130.70, 126.64, 126.23, 125.09, 123.68, 122.21, 118.56, 117.11, 109.43, 27.96, 25.38, 23.27, 22.78.

Anal. ($\text{C}_{23}\text{H}_{23}\text{NO}_4$) calcd. C 73.19% H 6.14% N 3.71%. Found: C 72.80% H 6.13% N 3.66%.

4-[(1Z,3E)-4'-Methyl-4-(3',4'-dihydro-1'(2'H)-naphthalen-1'-ylidene)-3-methyl-but-2-enoylamino]-benzoic acid. (6). 0.47 g (85%) pale yellow solid: mp 151-152 °C (acetone/hexanes); UV-Vis (MeOH) λ_{max} 291 nm ($\epsilon=18364$); FTIR (KBr) (NH) 1685 (C=O), 1657 (C=O), 1596 (C=C) cm^{-1} ; MS m/e 362 (MH^+); ^1H NMR ($\text{DMSO}-d_6$) δ 12.83 (s, 1H), 10.40 (s, 1H), 8.02 (d, 2H, $J=8.71$), 7.88 (d, 2H, $J=8.75$), 7.79-7.76 (m, 1H), 7.62 (s, 1H), 7.37-7.32 (m, 3H), 6.16 (s, 1H), 3.07-2.97 (m, 1H), 2.87-2.80 (m, 1H), 2.78-2.65 (m, 1H), 2.29 (s, 3H), 2.07-1.95 (m, 1H), 1.71-1.61 (m, 1H), 1.36 (d, 3H, $J=6.96$); ^{13}C NMR ($\text{DMSO}-d_6$): δ 167.32, 164.70, 149.79, 143.96, 142.98, 138.55, 135.80, 130.71, 128.06, 127.91, 126.47, 125.10, 125.00, 123.60, 122.21, 118.57, 32.79, 30.67, 25.49, 25.33, 21.79.

Anal. ($\text{C}_{23}\text{H}_{23}\text{NO}_3 \cdot 0.25 \text{H}_2\text{O}$) calcd.: C 75.49% H 6.47% N 3.82%. Found C 75.16% H 6.35% N 3.74%.

4-[(1Z,3E)-5',7'-Dimethyl-4-(3',4'-dihydro-1'(2'H)-naphthalen-1'-ylidene)-3-methyl-but-2-enoylamino]-benzoic acid (7). 0.51 g (88%) white solid: mp 180-181 °C (acetone/hexanes); FTIR (KBr) 3311 (NH), 1687 (C=O), 1656 (C=O), 1607 (C=C) cm^{-1} ; MS m/e 376 (MH^+); UV-Vis (MeOH) λ_{max} 293 nm ($\epsilon=18372$); ^1H NMR ($\text{DMSO}-d_6$): δ 10.21 (s, 1H), 7.85 (d, 1H, $J=8.75$), 7.72 (d, 1H, $J=8.79$), 7.24 (d, 1H, $J=17.21$), 6.89 (s, 1H), 6.01 (s, 1H), 2.57 (t, 2H, $J=6.23$), 2.46-2.42 (m, 2H), 2.24 (s, 3H), 2.13 (s, 3H), 2.09 (s, 3H), δ 1.82-1.71 (m, 2H); ^{13}C NMR ($\text{DMSO}-d_6$): δ 167.30, 164.63, 149.77, 145.46, 143.96, 139.14, 136.11, 136.10, 134.37, 133.26, 130.68, 130.33, 125.07, 123.25, 123.06, 122.00, 118.54, 28.05, 25.35, 25.45, 23.35, 21.14, 19.62, 19.03.

Anal. ($C_{24}H_{25}NO_3 \cdot H_2O$) calcd.: C 73.26% H 6.92% N 3.56%. Found: C 72.96% H 7.07% N 3.47%.

4-[(1Z,3E)-4-(6',7',8',9'-Tetrahydro-benzocyclohepten-5'-ylidene)-3-methyl-but-2-enoylamino]-benzoic acid (8). 0.41 g (73%) white solid: mp 170-172 °C (acetone/hexanes); FTIR (KBr) 3238 (NH), 1683 (C=O), 1662 (C=O), 1604 (C=C) cm^{-1} ; MS m/e 376 (MH^+); UV-Vis: (MeOH) λ_{max} 298 nm ($\epsilon=22765$); 1H NMR (DMSO- d_6): δ 12.69 (s, 1H), 10.27 (s, 1H), 7.90 (d, 2H, $J=8.63$), 7.76 (d, 2H, $J=8.68$), 7.30 (d, 1H, $J=6.86$), 7.22-7.11 (m, 3H), 6.91 (s, 1H), 6.01 (s, 1H), 2.71 (s, 2H), 2.44 (s, 2H), 2.18 (s, 3H), 1.69 (s, 4H); ^{13}C NMR (DMSO- d_6): δ 167.32, 164.64, 149.62, 145.46, 145.36, 145.90, 139.69, 130.74, 129.03, 128.67, 128.04, 127.51, 126.68, 125.15, 122.11, 118.60, 34.76, 31.06, 28.62, 27.12, 23.35.

Anal. ($C_{23}H_{23}NO_3 \cdot 0.25 H_2O$) calcd.: C 75.49% H 6.47% N 3.83%. Found C 75.66% H 6.55% N 3.62%.

References

- (1) For recent reviews, see: (a) *Chemistry and Biology of Synthetic Retinoids*; Dawson, M. A.; Okamura, W. H., Eds.; CRC Press: Boca Raton, FL, 1990. (b) *THE RETINOIDS Biology, Chemistry and Medicine*, 2nd ed.; Sporn, M. B.; Roberts, A. B.; Goodman, D. S., Eds.; Raven Press: New York, 1994.
- (2) Thaller, C.; Eichele, G. Identification and Spatial Distribution of Retinoids in the Developing Chick Limb Bud. *Nature (London)* **1987**, *327*, 624-628.
- (3) (a) Hixson, E.J.; Denine, E.P. Comparative Subacute Toxicity of *All-trans*- and 13-*cis*-Retinoic Acid in Swiss Mice. *Toxicol. Appl. Pharmacol.* **1978**, *44*, 29-40. (b) Kamm, J. J. Toxicology, Carcinogenicity, and Teratogenicity of Some Orally Administered Retinoids. *J. Am. Acad. Dermatol.* **1982**, *6*, 652-659. (c) Cohen, M. Tretinoin: A Review of Preclinical Toxicological Studies. *Drug Dev. Res.* **1993**, *30*, 244-51.

- (4) (a) Kochhar, D. M. Teratogenic Activity of Retinoic Acid. *Acta. Pathol. Microbiol. Immunol.* **1967**, *70*, 398-404. (b) Willhite, C. C. Molecular Correlates in Retinoid Pharmacology and Toxicology. In *Chemistry and Biology of Synthetic Retinoids*; Dawson, M.I.; Okamura, W.H., Eds.; CRC Press: Boca Raton, FL, 1990; pp 539-573. (c) Adams, J. Structure-Activity and Dose-Response Relationships in the Neural and Behavioral Teratogenesis of Retinoids, *Neurotoxicol. Teratol.* **1993**, *15*, 193-202.
- (5) (a) Fisher, G. J.; Talwar, H. S.; Xiao, J.-H.; Datta, S. C.; Reddy, A. P.; Gaub, M.-P.; Rochette-Egly, C.; Chambon, P.; Voorhees, J. J. Immunological Identification and Functional Quantitation of Retinoic Acid and Retinoid X Receptor Proteins in Human Skin. *J. Biol. Chem.* **1994**, *269*, 20629-20635. (b) Dolle, P.; Ruberte, E.; Leroy, P.; Morriss-Kay, G.; Chambon, P. Retinoic Acid Receptors and Cellular Retinoid Binding Proteins. 1. A Systematic Study of Their Differential Pattern of Transcription During Mouse Oncogenesis. *Development* **1990**, *110*, 1133-1151.
- (6) (a) Kagechika, H.; Kawachi, E.; Hashimoto, Y.; Shudo, K. Retinobenzoic Acids. 2. Structure-Activity Relationships of Chalcone-4-Carboxylic Acids and Flavone-4'-Carboxylic Acids. *J. Med. Chem.* **1989**, *32*, 834-840. (b) Delecluse, C.; Cavey, M. T.; Martin, B.; Bernard, B. A.; Reichert, U.; Maignan, J.; Shroot, B. Selective High Affinity Retinoic Acid Receptor α or β - γ Ligands. *Molec. Pharmacol.* **1991**, *40*, 556-562. (c) Teng, M.; Duong, T.; Klein, E.; Pino, M.; Chandraratna, R. Identification of Retinoic Acid Receptor α Subtype Specific Agonist. *J. Med. Chem.* **1996**, *39*, 3035-3038. (d) Kikuchi, K.; Hibi, S.; Yoshimura, H.; Tokuhara, N.; Tai, K.; Hida, T.; Yamauchi, T.; Nagai, M. Syntheses and Structure-Activity Relationships of 5,6,7,8-Tetrahydro-5,5,8,8-Tetramethyl-2-Quinoxaline Derivatives With Retinoic Acid Receptor α Agonistic Activity. *J. Med. Chem.* **2000**, *43*, 409-419. (e) Johnson, A.; Klein, E.; Wang, L.; Pino, M.; Chandraratna, R. Identification of Retinoic Acid Receptor β Subtype Specific Agonists. *J. Med. Chem.* **1996**, *39*, 5027-5030. (g) Vuligonda, V.; Lin, Y.; Thacher, S.; Standeven, A.; Kochar, D.; Chandraratna, R. A New Class of RAR Subtype Selective Retinoids: Correlation of Pharmacological Effects with Receptor Activity. *Bioorg. Med. Chem. Lett.* **1999**, *7*, 263-270.
- (7) (a) Kagechika, H.; Kawachi, E.; Shudo, K. New Type of Inducers of Differentiation of Human HL-60 Promyelocytic Leukemia Cells. *Chem. Pharm. Bull.* **1984**, *32*, 4209-4212. (b) Kagechika, H.; Kawachi, E.; Hashimoto, Y.; Shudo, K. Differentiation Inducers of Human Promyelocytic Leukemia Cells HL-60. Phenylcarbamoylbenzoic Acids and Polyene Amides. *Chem. Pharm. Bull.* **1986**, *34*, 2275-2278. (c) Kagechika, H.; Kawachi, E.; Hashimoto, Y.; Himi, T.; Shudo, K. Retinobenzoic Acids. 1. Structure-Activity Relationships of Aromatic Amides With Retinoidal Activity. *J. Med. Chem.* **1988**, *31*, 2182-2192. (d) Kagechika, H.; Himi, T.; Kawachi, E.; Hashimoto, Y.; Shudo, K. Retinobenzoic Acids. 4. Conformation of Aromatic Amides With Retinoidal Activity. Importance of *trans*-Amide Structure for the Activity. *J. Med. Chem.* **1989**, *32*, 2292-2296.

- (8) (a) Vaezi, M. F.; Alam, M.; Sani, B. P.; Rogers, T. S.; Simpson-Herren, L.; Wille, J. J.; Hill, D. L.; Doran, T. I.; Brouillette, W. J.; Muccio, D. D. A Conformationally Defined 6-*s-trans*-Retinoic Acid Isomer. Synthesis, Chemopreventive Activity, and Toxicity. *J. Med. Chem.* **1994**, *37*, 4499-4507. (b) Alam, M.; Zhestkov, V.; Sani, B. P.; Venepally, P.; Levin, A. A.; Kazmer, S.; Li, E.; Norris, A. W.; Zhang, X.-K.; Lee, M. O.; Hill, D. L.; Lin, T.-H.; Brouillette, W. J.; Muccio, D. D.; Conformationally Defined 6-*s-trans*-Retinoic Acid Analogs. 2. Selective Agonists for Nuclear Receptor Binding and Transcriptional Activity. *J. Med. Chem.* **1995**, *38*, 2303-2310. (c) Muccio, D. D.; Brouillette, W. J.; Alam, M.; Vaezi, M. F.; Sani, B. P.; Venepally, P.; Reddy, L.; Li, E.; Norris, A. W.; Simpson-Herren, L.; Hill, D. Conformationally Defined 6-*s-trans* Retinoic Acid Analogs. 3. Structure-Activity Relationships for Nuclear Receptor Binding, Transcriptional Activity, and Cancer Chemopreventive Activity. *J. Med. Chem.* **1996**, *39*, 3625-3635.
- (9) (a) Jong, L.; Lehmann, J. M.; Hobbs, P. D.; Harlev, E.; Huffman, J. C.; Pfahl, M.; Dawson, M. I. Conformational Effects on Retinoid Receptor Selectivity. 1. Effect of 9-Double Bond Geometry on Retinoid X Receptor Activity. *J. Med. Chem.* **1993**, *36*, 2605-2613. (b) Dawson, M. I.; Jong, L. J.; Hobbs, P. D.; Cameron, J. F.; Chao, W.-R.; Pfahl, M.; Lee, M.-O.; Shroot, B.; Pfahl, M. Conformational Effects on Retinoid Receptor Selectivity. 2. Effects of Retinoid Bridging Group on Retinoid X Receptor Activity and Selectivity. *J. Med. Chem.* **1995**, *38*, 3368-3383. (c) Beard, R. L.; Gil, D. W.; Marler, D. K.; Henry, E.; Colon, D. F.; Gillett, S. J.; Arefieg, T.; Breen, T. S.; Krauss, H.; Davies, P. J. A.; Chandraratna, R. Structural Basis of the Differential RXR and RAR Activity of Stilbene Retinoid Analogs. *Bioorg. Med. Chem. Lett.* **1994**, *4*, 1447-1452. (d) Boehm, M. F.; Zhang, L.; Badea, B. A.; White, S. K.; Mais, D. E.; Berger, E.; Suto, C. M.; Goldman, M. E.; Heyman, R. A. Synthesis and Structure-Activity Relationships of Novel Retinoid X Receptor-Selective Retinoids. *J. Med. Chem.* **1994**, *37*, 2930-2941. (e) Boehm, M. F.; Zhang, L.; McClurg, M. R.; Berger, E.; Wagoner, M.; Mais, D. E.; Suto, C. M.; Davies, P. J. A.; Heyman, R. A.; Nadzan, A. M. Design and Synthesis of Potent Retinoid X Receptor Selective Ligands That Induce Apoptosis in Leukemia Cells. *J. Med. Chem.* **1995**, *38*, 3146-3155. (f) Vuligonda, V. S.; Garst, M. E.; Chandraratna, R. A. S. Stereoselective Synthesis and Receptor Activity of Conformationally Defined Retinoid X Receptor Selective Ligands. *Bioorg. Med. Chem. Lett.* **1999**, *9*, 589-594.
- (10) Muccio, D. D.; Brouillette, W. J.; Breitman, T. R.; Taimi, M.; Emanuel, P. D.; Zhang, X.-K.; Chen, G.-Q.; Sani, B. P.; Venepally, P.; Reddy, L.; Alam, M.; Simpson-Herren, L.; Hill, D. L. Conformationally Defined Retinoic Acid Analogues. 4. Potential New Agents for Acute Promyelocytic and Juvenile Myelomonocytic Leukemias. *J. Med. Chem.* **1998**, *41*, 1679-1687.
- (11) Loeliger, P.; Bollag, W.; Mayer, H. Arotonoids, A New Class of Highly Active Retinoids. *Euro. J. Med. Chem.* **1980**, *15*, 9-15.

- (12) *The Chemistry of Carboxylic Acids and Esters*; Patai, S., Ed.; Interscience: New York, 1969.
- (13) Staab, H. A. New Methods of Preparative Organic Chemistry. IV. Syntheses Using Heterocyclic Amides (Azolides). *Angew. Chem. Int. Ed. Engl.* **1962**, *1*, 351-367.
- (14) Hassner, A.; Alexanian, V. Direct Room Temperature Esterification of Carboxylic Acids. *Tetrahedron Lett.* **1978**, 4475-4478.
- (15) Belleau, B.; Malek, G. A New Convenient Reagent for Peptide Synthesis. *J. Am. Chem. Soc.* **1968**, *90*, 1651-1652.
- (16) Shiori, T.; Ninomiya, K.; Yamada, S. Diphenylphosphoryl Azide. A New Convenient Reagent for the Modified Curtius Reaction and for Peptide Synthesis. *J. Am. Chem. Soc.* **1972**, *94*, 6203-6205.
- (17) Cabré, J.; Palomo, A. L. New Experimental Strategies in Amide Synthesis Using N,N-Bis [2-oxo-3-oxazolidinyl]phosphoramidic Chloride. *Synthesis* **1984**, 413-417.
- (18) Villeneuve, G.B. and Chan, T.H. A Rapid, Mild and Acid-Free Procedure for the Preparation of Acyl Chlorides Including Formyl Chloride. *Tetrahedron Lett.* **1997**, *38*, 6489-6492.
- (19) Magid, R.M.; Fruchey, O.S.; Johnson, W.L.; Allen, T.G. Title? *J. Org. Chem.* **1979**, *44*, 359-363.
- (20) (a) Chandraratna, R.; Gillett, S.; Song, T.; Attard, J.; Vuligonda, S.; Garst, M.; Arefieg, T.; Gil, D.; Wheeler, L. Synthesis and Pharmacological Activity of Conformationally Restricted, Acetylenic Retinoid Analogs. *Bioorg. Med. Chem. Lett.* **1995**, *5*, 523-527. (b) Chandraratna, R. A. S. Tazarotene-First of a New Generation of Receptor-Selective Retinoids. *Br. J. Derm.* **1996**, *135*, 18-25.
- (21) Charpentier, B.; Bernardon, J.-M.; Eustache, J.; Millois, C.; Martin, B.; Michel, G.; Shroot, B. Synthesis, Structure-Affinity Relationships, and Biological Activities of Ligands Binding to Retinoid Acid Receptor Subtypes. *J. Med. Chem.* **1995**, *38*, 4993-5006.
- (22) Zhang, X.-K.; Hoffman, B.; Tran, P.; Graupner, G.; Pfahl, M. Retinoid X Receptor is an Auxilliary Protein for Thyroid Hormone and Retinoic Acid Receptors. *Nature (London)* **1992**, *355*, 441-446.
- (23) Husmann, M.; Lehmann, J. M.; Hoffman, B.; Hermann, T.; Tzukerman, M. Antagonism Between Retinoic Acid Receptors. *Mol. Cell. Biol.* **1991**, *11*, 4097-4103.

- (24) Pfahl, M.; Tzukerman, M.; Zhang, X.-K.; Lehmann, J. M.; Hermann, T.; Wills, K. N.; Graupner, G. Nuclear Retinoic Acid Receptors: Cloning, Analysis, and Function. *Methods Enzym.* **1990**, *189*, 256-270.

UNPUBLISHED DATA

Synthesis of Derivatives of (*all-E*)-UAB30

The naturally occurring retinoids (ATRA, 9-*cis* RA, and 13-*cis* RA) have been used to treat disease,¹⁵⁷ but their clinical use is hampered by toxicity¹⁵⁸ and teratogenicity.¹⁵⁹ However, receptor-selective retinoids have been utilized in the treatment of diseases with limited side effects. For example, Kikuchi et al. reported the design and synthesis of potent RAR α agonists (Figure 1), which exhibit immunosuppressive effects, especially in the inhibition of antibody production.¹⁰⁴ The RAR α agonist ER-38925 (Figure 1) and similar derivatives are currently being evaluated for immunosuppressive activity, pharmacokinetics, and safety to select a clinical candidate suitable for use as an immunosuppressive agent. An acetylenic RAR β,γ selective agonist (Tazarotene, Figure 1) with no affinity for the RAR α or the RXR α receptors is currently used to treat psoriasis.^{108,109} The RAR γ agonist Differin (also called Adapalene, Figure 1) has been used in the treatment of *acne vulgaris*.¹¹³ The RXR agonist LGD1069 (Targretin, also called Bexarotene, Figure 1) is currently used to treat T-cell lymphoma¹⁶⁰ and has also shown promise as a mammary cancer chemopreventive agent.^{138,139} Therefore, we sought to explore the requirements for RXR-selectivity for (9Z)-UAB30 (1).¹⁴³

Even though the focus of this research project was the synthesis of derivatives of (9Z)-UAB30, some of the analogs of (*all-E*)-UAB30 were also synthesized. The detailed synthetic procedure is the same described in the first manuscript. In the synthesis of

(9Z)-UAB30 (Scheme 1), the oxidation of the alcohol resulted in two isomers [(9Z)- and (*all-E*)], which were separable by flash column chromatography. For the synthesis of (9Z)-UAB30, the (9Z)-aldehyde was carried forward to the Horner Emmons reaction. Depending on the amount of (*all-E*)-aldehydes available, the (*all-E*)-esters (14-19) were also synthesized. As shown in Scheme 1, additional (*all-E*)-aldehyde (13) could be obtained by the isomerization of the (9Z)-aldehyde (11) in the presence of I₂ in ether. Unfortunately, the extent of isomerization was only about 10%, and it was difficult to remove all of the iodine from the reaction mixture, which was often present even after the column chromatography separation, thus causing further isomerization and decomposition of each isomer. Only two (*all-E*)-UAB30 esters (14-19) were obtained in sufficient

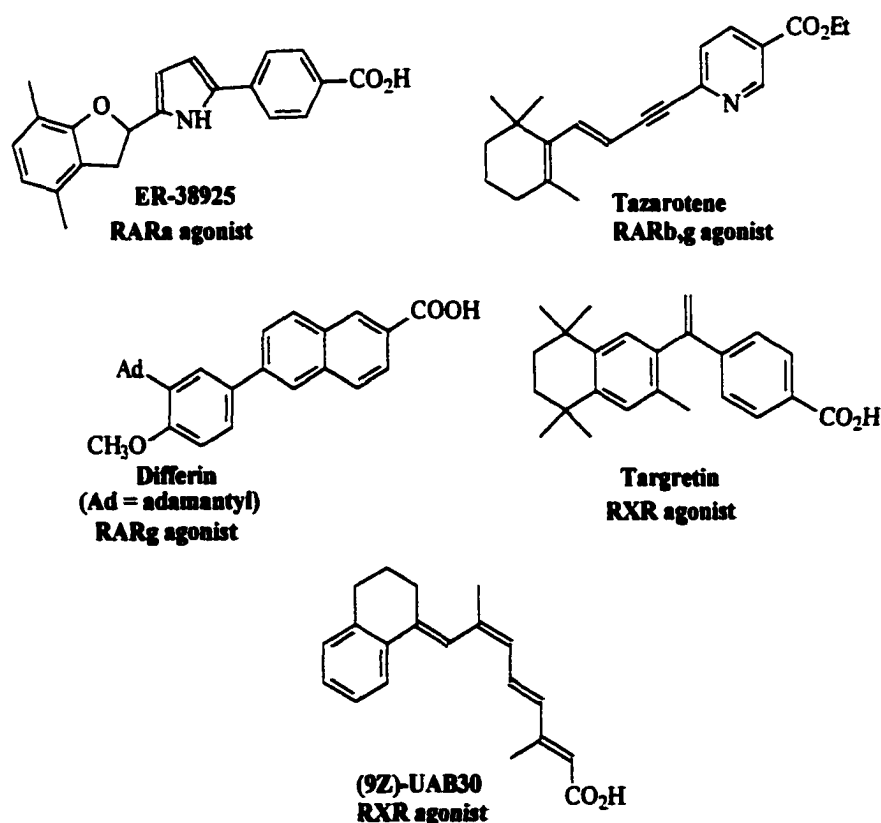
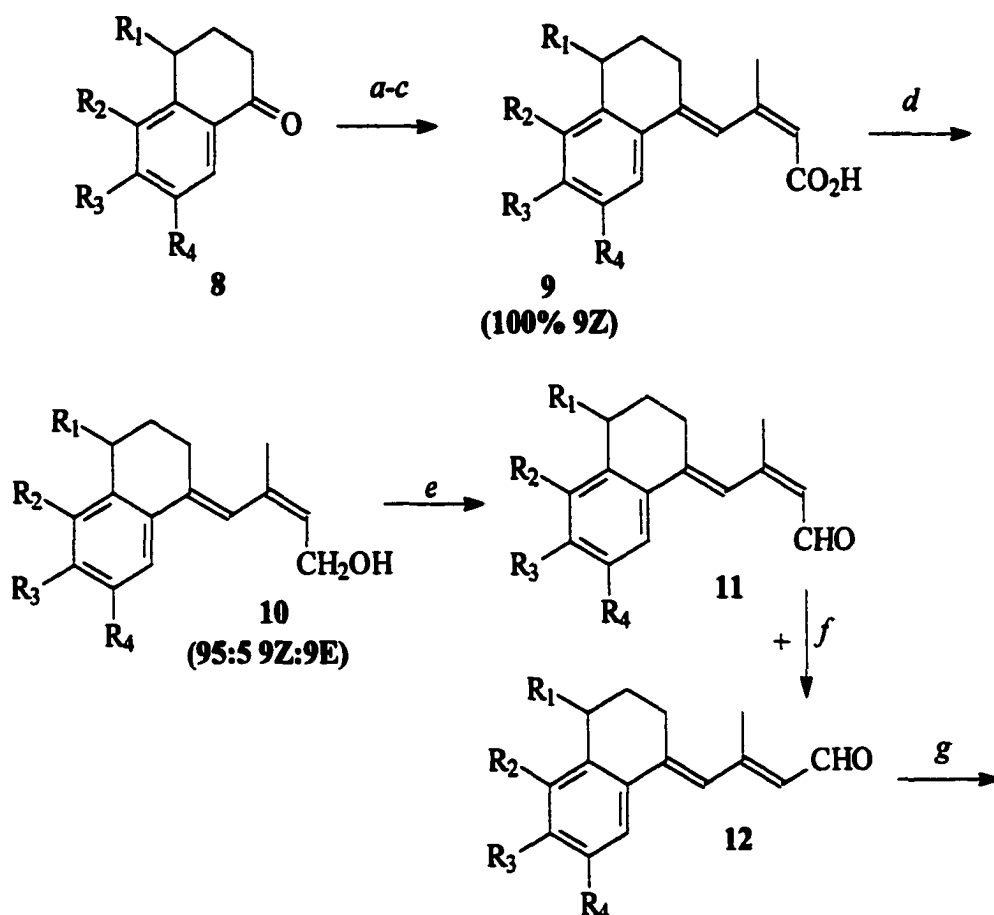
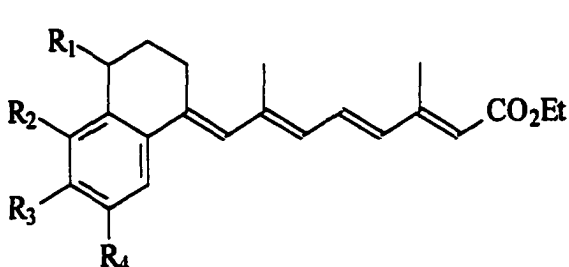


Figure 1. Receptor-selective retinoids.

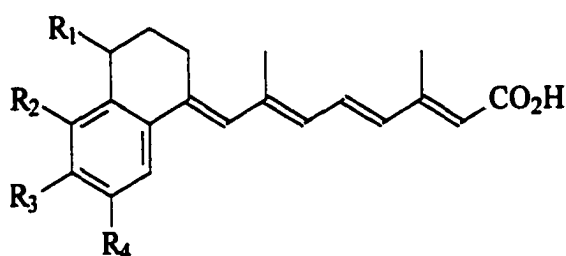
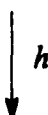
Scheme 1. Synthetic Strategy for (9Z)- and (*all-E*)-UAB30^a

^a (a) Zn/HCl; (b) ethyl 4-bromo-3-methyl-2-butenolate, 1,4 dioxane, reflux; (c) HCl work-up; (d) LiAlH₄, ether, 0 °C; (e) MnO₂, molecular sieves, CH₂Cl₂, 0 °C; (f) I₂, ether, 0 °C; (g) NaH, TEPS, DMPU, THF, 0 °C; (h) 0.8 N KOH, MeOH, reflux.

Scheme 1 (Continued)



- 13 $R_1=R_2=R_3=R_4=H$
 14 $R_2=OCH_3$; $R_1=R_3=R_4=H$
 15 $R_3=OCH_3$; $R_1=R_2=R_4=H$
 16 $R_4=OCH_3$; $R_1=R_2=R_3=H$
 17 $R_1=CH_3$; $R_2=R_3=R_4=H$
 18 $R_1=R_2=CH_3$; $R_3=R_4=H$



- 2 $R_1=R_2=R_3=R_4=H$ (*all-E*)-UAB30
 3 $R_2=OCH_3$; $R_1=R_3=R_4=H$
 4 $R_3=OCH_3$; $R_1=R_2=R_4=H$
 5 $R_4=OCH_3$; $R_1=R_2=R_3=H$
 6 $R_1=CH_3$; $R_2=R_3=R_4=H$
 7 $R_1=R_2=CH_3$; $R_3=R_4=H$

quantities to carry the synthesis forward to the final acids (2-7). These acids were screened for retinoidal activity. The 7'-methoxy derivative 5 was screened for nuclear receptor binding and exhibited potent RAR binding (Table 1). The 5',7'-dimethyl derivative 7 was screened for activation of RAR α , β , γ , and RXR α and possessed RAR pan-agonist activity with slightly higher RAR γ activity (Figure 2). Because of the limited amount of the available esters (14-19) and acids (5 and 7), full characterization of each analog was not accomplished.

Table 1. Nuclear Receptor Binding Profile for Retinoid **5**

retinoid	IC ₅₀ (nM)			
	RAR α	RAR β	RAR γ	RXR α
ATRA	6 ^a	5 ^a	4 ^a	>2000 ^a
(all-E)-UAB30	35 ^a	49 ^a	55 ^a	>2000 ^a
5	52	56	48	>2000

^a As previously reported by Muccio et al.¹⁴⁴

Experimental Section

General Procedure for the Olefination of Individual Aldehyde Isomers. In a dry round-bottom flask flushed with N₂ (g), NaH (60% dispersion in mineral oil) (0.10 g, 3.0 mmol) was washed with hexanes three times to eliminate the mineral oil. At 0 °C, the NaH was suspended in anhydrous tetrahydrofuran (THF) (1 mL), and freshly distilled triethyl phosphonosencioate (0.70 mL, 2.8 mmol) was added followed by distilled 1,3-Dimethyl-3,4,5,6-tetrahydro-2(1*H*)-pyrimidinone (DMPU) (0.10 mL, 0.020 mmol) and stirred for 20 min. To this mixture was added (*all-E*)- aldehyde **12** (2.4 mmol) in THF (4 mL), and the reaction proceeded for 30 min. The reaction was quenched with methanol (2-3 mL), and the reaction mixture was diluted with ether (100mL). The ether layer was washed with saturated NaHCO₃ (100 mL) followed by brine (100 mL). The product was dried (Na₂SO₄) and concentrated *in vacuo* to yield the ester as a mixture of two geometrical isomers [3:1 (*all-E*): (13*Z*)]. Separation of the (*all-E*)- and (13*Z*)-isomers was attempted via flash chromatography (5% ether/hexanes). The isomers could not be completely separated, thus flash chromatography could only enrich the ester in (*all-E*) composition.

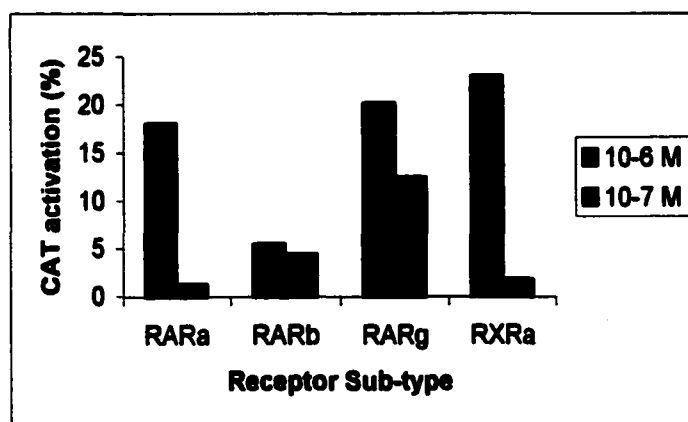


Figure 2. Transcriptional activation for retinoid 7.

(2*E*,4*E*,6*E*,8*E*)-Ethyl 8-(5'-Methoxy-3',4'-dihydro-1'(2'H)-naphthalen-1'-ylidene)-3,7-dimethyl-2,4,6-octatrienoate (14). Yellow oil (42%); FTIR (neat) 1707 (C=O), 1600 (C=C) cm⁻¹; ¹H NMR (CDCl₃): δ 7.79 (d, 1H, J=15.33), 7.20 (dd, 1H, J=8.02 & 10.08), 6.94 (dd, 1H J=3.54 & 11.46), 6.74 (d, 1H, J=7.81), 6.52 (s, 1H), 6.30 (d, 1H, J=11.37), 5.65 (s, 1H), 4.20-4.14 (m, 2H), 3.82 (s, 3H), 2.76-2.69 (m, 4H), 2.09 (s, 3H), 2.06 (s, 3H), 1.82-1.78 (m, 2H), 1.31-1.25 (m, 3H); ¹³C NMR (CDCl₃): δ 167.64, 157.46, 153.14, 139.67, 138.67, 138.43, 135.51, 131.27, 130.30, 128.74, 128.21, 127.16, 126.49, 119.07, 117.17, 60.08, 55.81, 28.60, 23.75, 23.66, 18.75, 14.77, 14.23.

(2*E*,4*E*,6*E*,8*E*)-Ethyl 8-(6'Methoxy-3',4'-dihydro-1'(2'H)-naphthalen-1'-ylidene)-3,7-dimethyl-2,4,6-octatrienoate (16). ¹H NMR (CDCl₃): δ 7.50-7.47 (m, 1H), 7.09-6.99 (m, 3H), 2.47 (dd, 1H, J=11.39), 6.42 (s, 1H), 6.20 (d, 1H, J=15.21), 6.14 (d, 1H, J=11.51), 5.77 (s, 1H), (q, 2H, J=7.10), 2.71 (t, 2H, J=6.28), 2.28 (s, 3H), 1.98 (s, 3H), 1.75 (p, 2H, J=6.23), 1.20 (t, 3H, J=7.11); ¹³C NMR (CDCl₃): δ 166.14, 151.65,

138.21, 137.05, 136.42, 135.52, 134.13, 129.80, 129.04, 127.91, 126.69, 126.27, 125.07, 123.29, 117.67, 58.61, 29.19, 27.72, 22.66, 17.31, 13.33, 12.79.

(2*E*,4*E*,6*E*,8*E*)-Ethyl 8-(4'-Methyl-3',4'-dihydro-1'(2'H)-naphthalen-1'-ylidene)-3,7-dimethyl-2,4,6-octatrienoate (17). 0.51 g (70%) yellow oil; MS *m/e* 337 (MH^+); FTIR (neat) 1708 (C=O), 1603 (C=C) cm^{-1} ; UV-Vis (MeOH) λ_{max} 272 nm ($\epsilon=14199$); λ_{max} 333 nm ($\epsilon=13394$); 1H NMR ($CDCl_3$): δ 7.54 (d, 1H, $J=6.86$), 7.23-7.16 (m, 3H), 6.96 (dd, 1H, $J=11.42$ & 3.51), 6.48 (s, 1H), 6.32-6.23 (m, 1H), 5.79 (s, 1H), 4.21-4.13 (m, 2H), 2.97-2.70 (m, 4H), 2.37 (s, 3H), 2.17 (s, 3H), 2.08 (s, 3H), 1.99-1.93 (m, 1H), 1.66-1.56 (m, 1H), 1.31-1.23 (m, 3H); ^{13}C NMR ($CDCl_3$) δ 167.61, 153.11, 143.35, 139.74, 138.25, 135.59, 131.28, 130.50, 128.39, 127.90, 126.50, 124.96, 119.11, 60.07, 33.45, 31.57, 26.33, 21.86, 18.76, 14.78, 14.25.

Anal. ($C_{23}H_{28}O_2 \cdot 0.5 H_2O$) calcd.: C 76.42% H 8.09%. Found: 76.83% C 7.83%.

(2*E*,4*E*,6*E*,8*E*)-Ethyl 8-(5',7'-Dimethyl-3',4'-dihydro-1'(2'H)-naphthalen-1'-ylidene)-3,7-dimethyl-2,4,6-octatrienoate (18). 0.67 g (93%) yellow oil; FTIR (neat) 1711 (C=O), 1604 (C=C) cm^{-1} ; MS *m/e* 351 (MH^+); UV-Vis (MeOH) λ_{max} 359 nm ($\epsilon=22693$); 1H NMR ($CDCl_3$): δ 7.24 (s, 1H), 7.00-6.86 (m, 2H), 6.47 (s, 1H), 6.28 (d, 1H, $J=15.11$), 6.20 (d, 1H, $J=11.43$), 5.78 (s, 1H), 4.21-4.09 (m, 2H), 2.72-2.64 (m, 2H), 2.37 (s, 3H), 2.30 (s, 3H), 2.21 (s, 3H), 2.10-2.05 (m, 5H), 1.92-1.82 (m, 2H); ^{13}C NMR ($CDCl_3$): δ 167.67, 153.20, 139.90, 139.22, 137.10, 136.60, 135.34, 135.25, 133.73, 131.35, 130.55, 130.09, 127.76, 123.37, 118.97, 60.08, 28.62, 27.00, 24.37, 21.51, 20.06, 18.77, 14.77, 14.25.

Anal. ($C_{24}H_{30}O_2 \cdot 0.5 H_2O$) calcd.: C 80.18% H 8.69%. Found C 79.91% H 8.63%.

(2*E*,4*E*,6*E*,8*E*)-Ethyl 8-(7'-Methoxy-3',4'-dihydro-1'(2'H)-naphthalen-1'-ylidene)-3,7-dimethyl-2,4,6-octatrienoic Acid (5). (77%) yellow solid: mp 203-204 °C (EtOAc/hexanes); 1H NMR ($CDCl_3$): δ 7.60-7.56 (m, 1H), 7.23-7.06 (m, 4H), 7.01-6.97 (m, 1H), 6.52 (s, 1H), 6.33 (d, 1H, $J=15.06$), 6.25 (d, 1H, $J=11.32$), 5.82 (s, 1H), 2.83-2.76 (m, 4H), 2.39 (s, 3H), 2.09 (s, 3H), 1.85 (p, 2H, $J=6.29$); ^{13}C NMR ($CDCl_3$): δ 162.5, 140.07, 138.17, 137.81, 136.51, 134.87, 131.80, 129.91, 128.97, 127.66, 127.39, 126.13, 124.36, 117.53, 30.20, 28.78, 23.68, 18.43, 14.05.

(2*E*,4*E*,6*E*,8*E*)-Ethyl 8-(5'7'-Dimethyl-3',4'-dihydro-1'(2'H)-naphthalen-1'-ylidene)-3,7-dimethyl-2,4,6-octatrienoic Acid (7). (87%) yellow solid: mp 195-199 °C (ether/hexanes); FTIR (KBr) 1677 (C=O), 1574 (C=C) cm^{-1} ; MS m/e 323 (MH^+); UV-Vis (MeOH) λ_{max} 367 nm ($\epsilon=31434$); 1H NMR ($CDCl_3$): δ 7.01 (dd, 1H, $J=11.48$ & 3.47), 6.87 (s, 1H), 6.57 (s, 1H), 6.32 (d, 1H, $J=15.04$), 6.21 (d, 1H, $J=11.25$), 5.81 (s, 1H), 2.77-2.64 (m, 4H), 2.38 (s, 3H), 2.30 (s, 3H), 2.21 (s, 3H), 2.08 (s, 3H), 1.91-1.83 (m, 2H); ^{13}C NMR ($CDCl_3$): δ 172.66, 155.81, 140.70, 139.56, 136.63, 135.28, 135.07, 133.78, 132.30, 130.62, 129.98, 127.68, 123.39, 118.00, 28.65, 27.00, 24.36, 21.52, 20.07, 18.85, 14.48.

A Ring-Contracted Analog of (9*Z*)-UAB30

Previously reported results from nuclear receptor binding and transcription assays indicated that the conformationally restricted 6-*s-trans* retinoid (9*Z*)-UAB30 (1) was

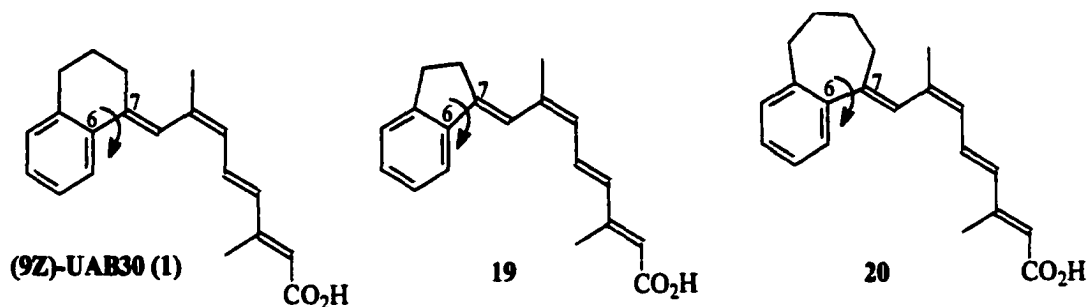


Figure 3. RXR-selective (9Z)-UAB30 **1** and the ring-altered analogs **19** and **20**.

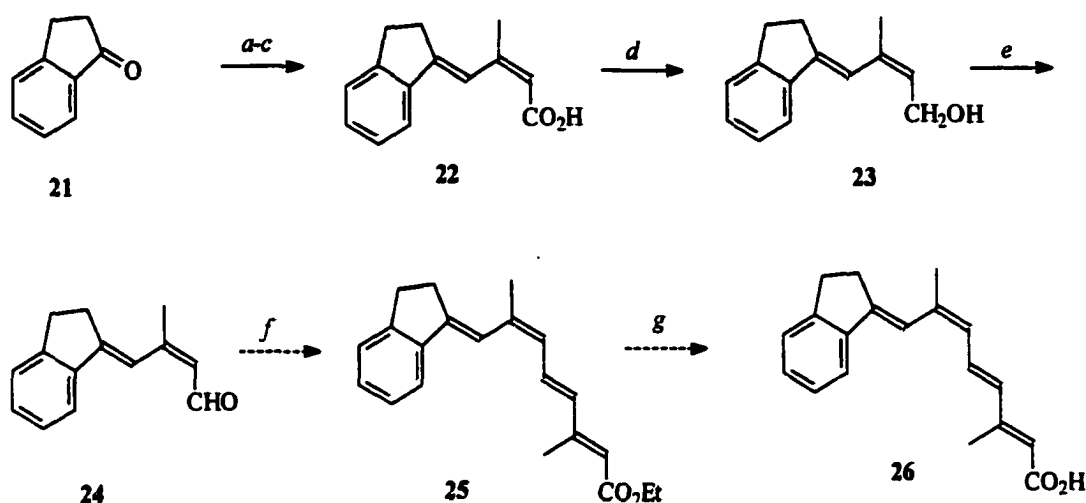
RXR-selective (Figure 3).¹⁴³ Because the crystal structure of holo-RXR was not available until very recently,¹⁴⁹ design of RXR-specific ligands followed empirical observations made by us¹⁴³⁻¹⁴⁴ and other groups.^{134-137,141,161}

The first synthetic retinoid that activated both RARs and RXRs was 3-methyl TTNPB, which is a derivative of TTNPB and a potent RAR pan-agonist. The only difference between the two structures was the presence of a methyl group at the 3-position, which allowed for binding of RXRs as well as RARs. Molecular modeling showed that the steric repulsion between the 3-methyl and the vinyl hydrogen of the linker resulted in a more bent conformation, which was associated with enhanced RXR binding. Reported here is a study in which the six-membered ring of the dihydronaphthalene moiety in (9Z)-UAB30 was altered to a five-membered ring in order to explore the effect of the $\psi_{5,6,7,8}$ torsion angle on RXR-selectivity (Figure 3). The ring-contracted analog was a member of a homologous series of compounds, which included (9Z)-UAB30 (**1**) and a ring-expanded analog (**20**) (Manuscript III). This smaller ring should restrict the range of accessible torsion angles, which may alter the RXR activity. However, because the synthesis of **19** proved problematic, the ring-contracted analog **19** was neither synthesized nor

tested for retinoid receptor binding and transactivation. The various approaches used in the attempted synthesis of **19** are presented here.

As shown in Scheme 2, a previously reported synthesis was used as the first approach to prepare the ring-contracted analog **19** (second manuscript).¹⁴³ The Reformatsky reaction using 1-indanone yielded the acid in very poor yield (10%). The problem was not that the 1-indanone was unreactive, because, by TLC, the spot corresponding to the 1-indanone disappeared. An explanation for the poor yield may be attributed to the instability of the γ -lactone intermediate. Because the Reformatsky reaction proceeds through a γ -lactone intermediate, the five-membered ring spiro lactone may have possessed a significant amount of ring strain. This explanation for the poor yielding Reformatsky reaction is supported by TLC evidence. Although some acid was obtained, formation of the γ -lactone intermediate was not observed by TLC. Therefore, the γ -lactone was most likely not very stable and decomposed. Decomposition was indicated by the presence of a baseline spot on TLC. This spot was not the hydroxyl ester because the corresponding spot for other analogs typically was not a baseline spot. Further, the acid was obtained as a crude oil that was purified by column chromatography unlike the acid of (9Z)-UAB30, which following work-up was obtained as a solid. The remainder of the mass stuck to the column and attempts to elute the material with polar solvents, such as ethyl acetate and methanol, were unsuccessful.

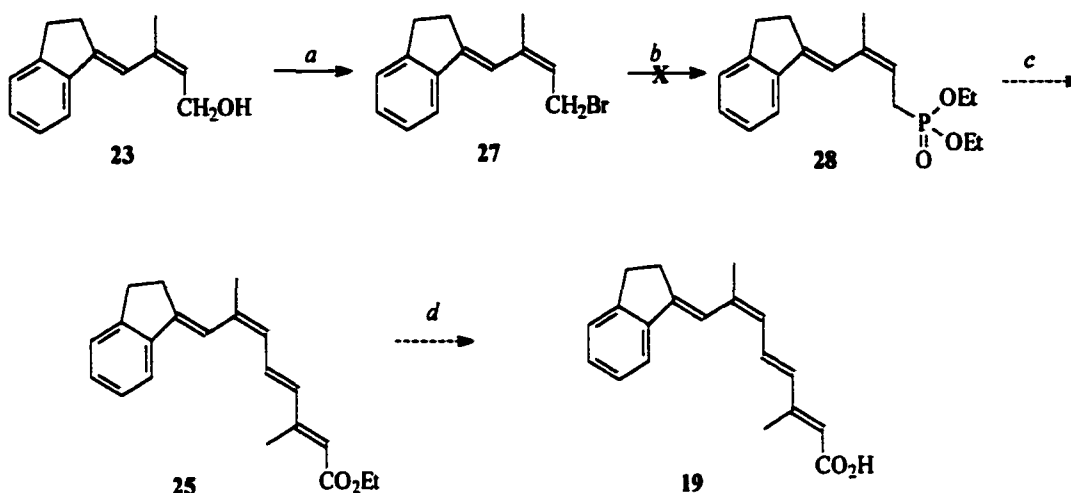
The reduction of **22** with lithium aluminum hydride proceeded smoothly to yield the very stable alcohol **23** (86%, 9:1 9Z/9E). Oxidation of the alcohol to the aldehyde with MnO_2 , however, was problematic. Following the reaction by TLC showed the

Scheme 2. Attempted Synthesis of 19^a

^a (a) Zn/ HCl; (b) ethyl 4-bromo-3-methyl-2-butenate, 1,4-dioxane, reflux; (c) 5% HCl; (d) LiAlH_4 , ether, -78°C ; (e) MnO_2 , sieves, CH_2Cl_2 , 0°C ; (f) NaH, TEPS, THF, -78°C ; (g) 0.8 N KOH, methanol, 60°C .

formation of a major new spot with an R_f value consistent with the aldehyde. Repeated washing of the filtered solid (MnO_2 and molecular sieves) with a large volume of solvent was necessary in order to maximize yield. However, the aldehyde was so unstable that it could not be isolated before it decomposed.

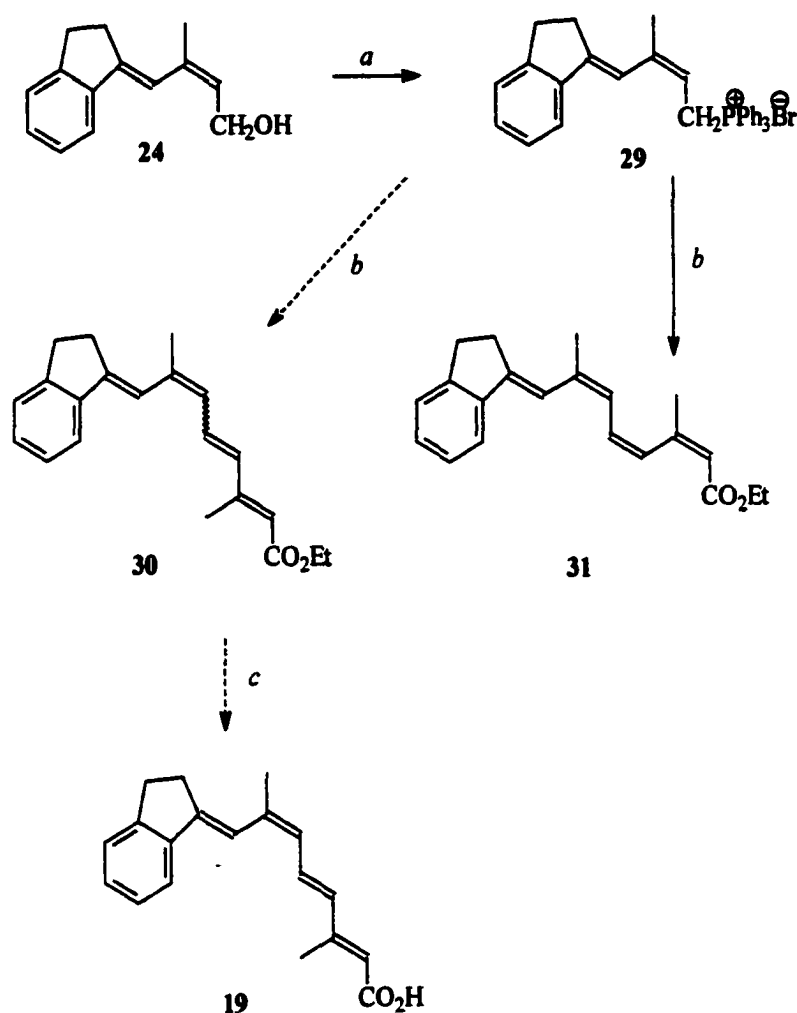
Different approaches were attempted to avoid the aldehyde. The first approach was to change the direction of the olefination reaction.⁴ As shown in Scheme 3, one approach in synthesizing 19 was to first form the Horner-Emmons reagent 28 from the alcohol and react it with commercially available methyl-3-oxo-crotonate. This was the reverse of the Horner-Emmons reaction employed in the past. The alcohol 23 was converted to the bromide 27 successfully, but it was not possible to form the phosphonate

Scheme 3. Attempted Horner-Emmons Reaction^a

^a (a) Br_2 , CCl_4 ; (b) triethylphosphite 80°C ; (c) NaH , THF, DMPU, methyl-4-oxocrotonate; (d) 0.8 N KOH , MeOH, 60°C .

ester **28**. The reaction progress of **27** with triethylphosphite at 80°C was monitored by mass spectrometry, but no product had formed after 12 h. Therefore, this approach was abandoned.

Another approach utilized the Wittig reaction of the triphenylphosphine adduct of the alcohol with methyl-3-oxocrotonate (Scheme 4). Even though the triphenylphosphine ylide should favor *cis* double bonds, this approach was attempted with the expectation that a mixture of *cis* and *trans* isomers would result. The triphenylphosphine ylide of **29** was easily formed upon treatment with PBr_3 / PPh_3 followed by deprotonation with NaH . Following the addition of the methyl-3-oxocrotonate, the ester product was obtained. Unfortunately, NMR analysis showed that the resulting ester was the 11-*cis* isomer **31** and not a mixture as anticipated (**30** and **31**).

Scheme 4. Synthetic Strategy for the Preparation of **19** Using the Wittig Reaction^a

^a (a) PBr_3 , PPh_3 ; (b) NaH , methyl 3-oxocrotonate, THF, 0°C ; (c) 0.8 N KOH , methanol, 60°C .

Very recently, Wei and Taylor reported an *in situ* MnO_2 oxidation/Wittig reaction that produced the ester without isolating the aldehyde.¹⁶² This procedure was attempted, but, instead of using the Wittig reaction, the Horner-Emmons reaction was used to olefinate the aldehyde. The procedure required long reaction times at room temperature, but because of the potential for isomerization of the double bonds of the aldehyde, this

reaction had to be performed in the cold room (4 °C). The reaction did not proceed past the formation of the aldehyde and was abandoned.

Common structural features are often found in receptor-selective retinoids. For example, substitution of the dienolic acid terminus of ATRA with a benzoic acid terminus resulted in the potent RAR pan-agonist TTNPB (Figure 4).⁸² Kagechika et al. altered the structure of TTNPB by inserting an amide linkage in place of the propenyl linker to yield Am80, which is a RAR α -selective agonist.⁹⁵ Similarly, Targretin, an RXR-selective retinoid, is also a derivative of TTNPB.¹⁶³ In this case, replacement of the propenyl linker with a methylene linker resulted in a central “cis-oid” geometry and RXR selectivity. Thus, retinoid receptor selectivity may be modified in compounds possessing a benzoic acid terminus.

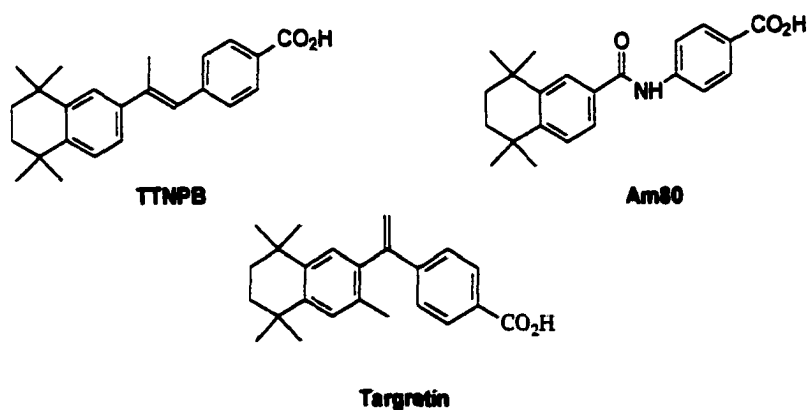


Figure 4. Structures of TTNPB, Am80 and Targretin.

A Ring-Contracted Amide Analog of (9Z)-UAB30

As discussed previously (fourth manuscript), we sought to explore the effect of replacing the dienolic acid terminus of (9Z)-UAB30 with an amide-linked benzoic acid

terminus as in compound **32**. In addition, if the receptor subtype selectivity and potency for these agents were maintained or enhanced, the synthesis of the amide derivative would make these compounds attractive because it is much simpler and higher yielding than the synthesis of (9Z)-UAB30.¹⁴³ Also targeted were the p-aminobenzoic acid amides of substituted (9Z)-UAB30 analogs, including the amide of the ring-contracted analog of (9Z)-UAB30 (**33**) (Figure 5, Scheme 5). Because of the limited amount of starting material available, this ring-contracted amide (**33**) was not synthesized or screened for retinoid receptor binding. However, the ester intermediate (**34**) was synthesized, as described previously (fourth manuscript), and partially characterized.

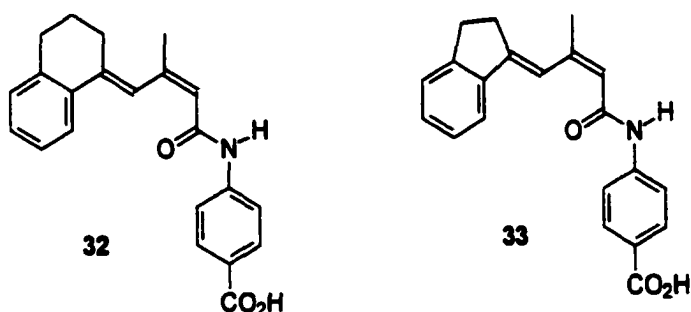
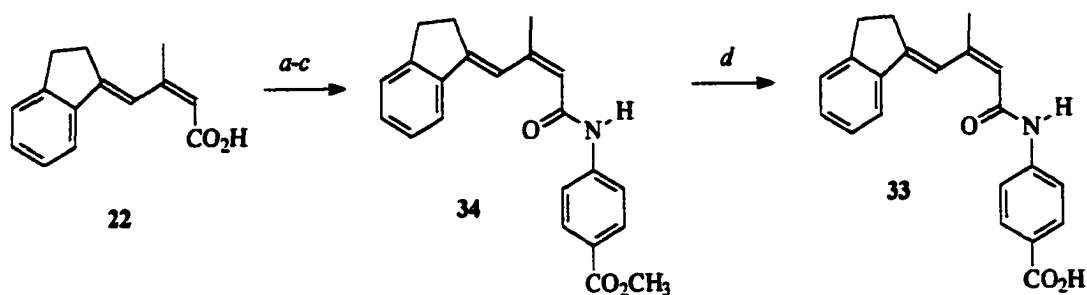


Figure 5. Structures of the (9Z)-UAB30 amide (**32**) and the ring-contracted amide (**33**).

Experimental Section

Chemistry. ¹H NMR spectra were obtained at 300.1 MHz on a Bruker spectrometer in CDCl₃ or DMSO-*d*₆. UV-Vis spectra were recorded on both an AVIV 14DS spectrophotometer and a Hewlett-Packard spectrophotometer in methanolic solution (Fisher, spectrograde). IR spectra were recorded using a Bomem FTIR spectrometer. TLC was performed on precoated 250 μm silica gel plates (Analtech, Inc.; 5 x 10 cm).

Scheme 5. Synthetic Scheme for the Preparation of the Amide 33^a



^a (a) hexachloroacetone, PPh₃, THF, -78 °C; b) methyl 4-aminobenzoate -78 °C; c) pyridine, -78 °C; (g) 0.8 N KOH, methanol, 60 °C.

Solvents and liquid starting materials were distilled prior to use. Reactions and purifications were conducted with deoxygenated solvents, under inert gas (N_2) and subdued lighting. Melting points were recorded on a MeltTemp melting point apparatus and are uncorrected.

(2Z,4E)-4-(Indan-1'-ylidene)-3-methyl-2-butenic Acid (22). 0.73 g (10%)
white solid: mp 168-170 °C (ether/hexanes); FTIR (KBr) 1667 (C=O), 1613 (C=C) cm^{-1} ;
MS m/e 215 (MH^+); UV-Vis (MeOH) λ_{max} 333 nm ($\epsilon = 22946$); ^1H NMR ($\text{DMSO}-d_6$)
 δ 11.96 (s, 1H), 8.20 (s, 1H), 7.53-7.49 (m, 1H), 7.32-7.22 (m, 3H), 5.62 (s, 1H), 3.0 (s,
4H), 2.16 (s, 3H); ^{13}C NMR ($\text{DMSO}-d_6$) δ 167.58, 152.14, 149.94, 147.14, 142.36,
129.53, 127.12, 125.76, 120.98, 117.91, 117.11, 30.75, 30.54, 24.37.

(2Z,4E)-4-(Indan-1'-ylidene)-3-methyl-2-butenol (23). 1.3 g (83%) white solid: mp 75-76 °C (ether/hexanes); FTIR (KBr) 3407 (OH), 1615 (C=C) cm^{-1} ; MS m/e

183 (M-OH); UV-Vis (MeOH) λ_{max} 239 nm (ϵ = 11384); ^1H NMR (CDCl_3) δ 7.51-7.44 (m, 1H), 7.27-7.13 (m, 3H), 5.51 (t, 1H, J =6.88), 4.25 (d, 2H, J =6.87), 3.00-2.95 (m, 2H), 2.88-2.78 (m, 2H), 2.01 (s, 3H); ^{13}C NMR (CDCl_3) δ 146.50, 144.87, 142.63, 136.63, 128.63, 128.20, 126.97, 125.69, 120.71, 116.77, 60.04, 31.08, 24.10.

Anal. ($\text{C}_{14}\text{H}_{16}\text{O}$) calcd.: C 83.96% H 8.05%. Found C 83.84% H 7.98%.

Methyl 4-[(1Z,3E)-4-(Indan-1'-ylidene)-3-methyl-2-butenoylamino]-benzoate

(34). 0.36 g (66%) yellow solid: mp 174-175 °C (ether/hexanes); FTIR (KBr) 3350 (N-H), 1697 (C=O), 1667 (C=C) cm^{-1} ; UV-Vis (MeOH) λ_{max} 239 nm (ϵ = 11384); ^1H NMR ($\text{DMSO}-d_6$): δ 10.31 (s, 1H), 8.36 (s, 1H), 7.92 (d, 2H, J =8.71), 7.73 (d, 2H, J =8.42), 7.58-7.49 (m, 1H), 7.36-7.27 (m, 3H), 5.88 (s, 1H), 3.82 (s, 3H), 3.08 (s, 2H), 3.05 (s, 2H), 2.23 (s, 3H).

CONCLUSIONS

By developing receptor subtype selective retinoids, retinoid associated toxicity may be greatly reduced. In addition, receptor-subtype selective retinoids have found new therapeutic applications. Recently, both the pan-agonist 9-*cis* RA¹⁵⁶ and the RXR agonist LGD1069¹³⁸ exhibited chemopreventive activity when used as a single agent or in combination with the estrogen antagonist Tamoxifen in rats.

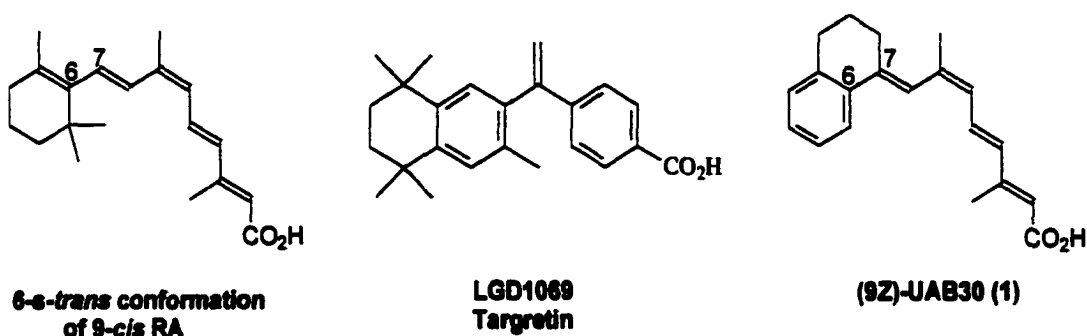


Figure 1. Structures of 9-*cis* RA, Targretin, and (9Z)-UAB30.

We recently reported that (9Z)-UAB30 is an RXR-selective retinoid. In order to assess the chemopreventive ability of (9Z)-UAB30 (Figure 1) in the *N*-methyl nitrosourea (MNU) rat mammary chemoprevention assay, multigram quantities were required (10-75 g). The first goal of this dissertation was to scale up the synthesis of (9Z)-UAB30 in order to provide the necessary quantities, including optimization of synthetic.⁹⁸

The synthesis was made amenable to large-scale synthesis primarily by eliminating the HPLC purification of the ester intermediate by separating the geometric isomers via flash column chromatography. Preliminary results from the MNU chemoprevention assay indicate that (9Z)-UAB30 is an effective chemopreventive agent at the 200 mg/kg dose.

A second goal of this proposal was to prepare analogs of (9Z)-UAB30 to determine if RXR selectivity and potency could be improved. Three classes of analogs were proposed. First, the ring-substituted analogs were synthesized and screened for retinoid receptor binding and transactivation. The 4'-methyl analog (6) exhibited enhanced binding and transcription for both the RAR α and RXR α retinoid receptors.

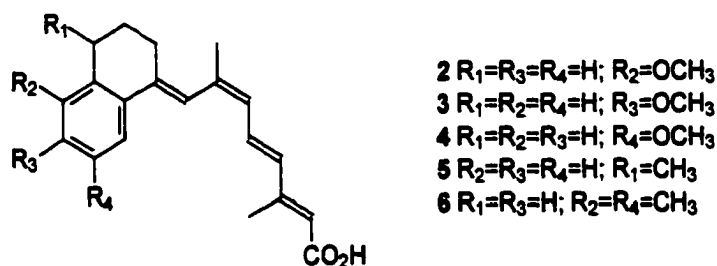


Figure 2. Ring-substituted analogs of (9Z)-UAB30.

It was believed that, when bound to the RXR receptor, 9-*cis* RA adopted a bent conformation.^{137,141} This was later confirmed by Egea et al.¹⁴⁹ when the crystal structure of 9-*cis* RA bound to RXR α was published. Therefore, we proposed that, by altering the torsion angle of the C6-C7 bond of (9Z)-UAB30, RXR-selectivity and potency might be enhanced. Thus the synthesis of ring-altered analogs of (9Z)-UAB30 was proposed, in which the torsion angle about the C6-C7 bond would be varied via a more conformation-

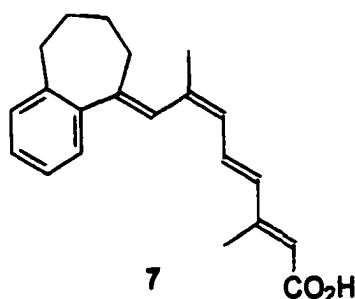


Figure 3. Ring-expanded analog of (9Z)-UAB30.

ally constrained or flexible ring to yield a second class of (9Z)-UAB30 derivatives. The synthesis of the ring-contracted analog was problematic, but the ring-expanded analog (7) was synthesized and screened for retinoid receptor binding and transactivation. The benzocycloheptenyl analog 7 possessed enhanced RAR α and RXR α potency, but selectivity was unaffected.

Examples of potent RXR-selective ligands from the literature, such as LGD1069, contain a terminal benzoic acid.¹³⁷ Also, it had been shown that inclusion of an internal amide group changed the selectivity of the potent pan-agonist TTNPB and resulted in a RAR α -selective retinoid Am80.^{93,96} Using a similar strategy, we proposed to alter the structure of (9Z)-UAB30 by replacing the carboxy terminus of (9Z)-UAB30 with an amide linked p-amino benzoic acid (Figure 4). Even if this does not enhance potency and/or selectivity, these retinoids would be dramatically simpler to synthesize and would be more resistant to oxidation as compared to (9Z)-UAB30. Results from retinoid receptor binding and transcription assays showed abrogation of both the RAR α and RXR α activity. The amides exhibited enhanced RAR γ binding and transcription perhaps through interaction of the amide bond with the Ser232 of RAR γ .

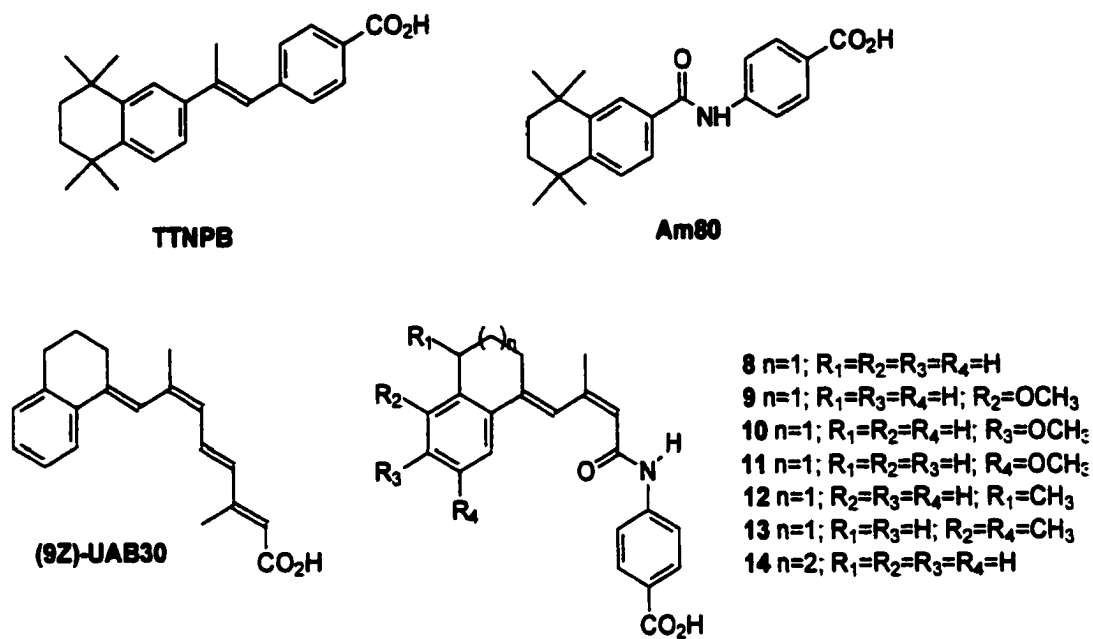


Figure 4. Structures of TTNPB, Am80, and (9Z)-UAB30 and the amide derivatives of (9Z)-UAB30.

LIST OF REFERENCES

- (1) IUPAC-IUB Joint Commission on Biochemical Nomenclature. Nomenclature of Retinoids. *Europ. J. Biochem.* **1982**, *129*, 1-5.
- (2) Schweiter, U; Isler, O. The Synthesis and Labeling of Vitamin A and Related Compounds. In *Vitamins and Hormones*, Academic Press: New York, 1970; pp295-311.
- (3) Stepp, W. Versuche über Fütterang mit Lipidfreier Nahrung. *Biochem. Z.* **1909**, *22*, 452-460.
- (4) McCollum, E. V.; Davis, M. The Necessity of Certain Lipids in the Diet During Growth. *J. Biol Chem.* **1913**, *15*, 167-175.
- (5) Drummond, J. C. The Nomenclature of the So-Called Accessory Food Factors. *Biochem. J.* **1920**, *14*, 660.
- (6) (a) Wald, G. Carotenoids and the Visual Cycle. *J. Gen. Physiol.* **1935**, *19*, 351-371. (b) Wald, G. Pigments of the Retina. I. The Bullfrog. *J. Gen. Physiol.* **1936**, *19*, 781-794.
- (7) Karrer, P.; Morf, R.; Schöpp, K. Zur Kenntnis des Vitamins-A aus Fischtranen II. *Helv. Chim. Acta.* **1931**, *14*, 1431-1437.
- (8) Kuhn, R.; Morris, C. J. O. R. Synthese von Vitamin A. *Chem. Ber.* **1937**, *70*, 853-855.
- (9) Isler, O. History and Industrial Application of Carotenoids and Vitamin A. *Pure Appl. Chem.* **1979**, *51*, 447-462.
- (10) Schweiter, U; Isler, O. Chemistry. In *The Vitamins (Volume I)*, Academic Press: New York, 1967; pp102-103.
- (11) (a) Saucy, G.; Marbet, R.; Lindlar, H.; Isler, O. Synthesis of Citral and Related Compounds. *Chimia* **1958**, *12*, 326-327. (b) Saucy, G.; Marbet, R. New Type of β -Oxallene Synthesis by Reaction with Tertiary Acetylene Carbinols with Vinyl Ethers. A Method for Preparation of Pseudoionone and Related Compounds. *Helv. Chim. Acta.* **1967**, *50*, 1158-67. (c) Saucy, G.; Marbet, R. Reaction of Tertiary Vinylcarbinols with Isoprenyl Ether. New Method for the Preparation of γ,δ -Unsaturated Ketones. *Helv. Chim. Acta.* **1967**, *50*, 2091-2095.

- (12) Isler, O.; Huber, W.; Ronco, A.; Kofler, M. Synthese des Vitamin A. *Helv. Chim. Acta*. **1947**, *30*, 1911.
- (13) Eiter, K.; Truscheit, E. A New Vitamin A Synthesis. *Med. Chem. Abhandl. Med. Chem. Forschungsstaetten Farbenfabriken Bayer A.-G.* **1963**, *7*, 719-734.
- (14) Wittig, G.; Geisler, G. Reactions of Pentaphenyl Phosphorous and Derivatives. *Liebigs Ann. Chem.* **1953**, *580*, 44-57.
- (15) (a) Pommer, H.; Nürrenbach, A. Industrial Synthesis of Terpene Compounds. *Pure Appl. Chem.* **1975**, *43*, 527-551. (b) Pommer, H. Synthesen in der Carotenoid-Reihe. *Angew. Chem.* **1960**, *72*, 811-819. (c) Pommer, H. The Wittig Reaction in Practice. *Angew. Chem.* **1977**, *89*, 437-443.
- (16) Oroshnik, W.; Mebane, A. D. The Nef Reaction With α,β -Unsaturated Ketones. *J. Am. Chem. Soc.* **1949**, *71*, 2062-2069.
- (17) Matsui, M.; Okano, S.; Yamashita, M.; Miyamo, S.; Kitamura, S.; Kobayashi, A.; Sato, T.; Mikami, R. Synthesis of Vitamin A. *Proc. Japan Acad.* **1958**, *34*, 220-222.
- (18) Wendler, N. L.; Slates, H. L.; Trenner, N. R.; Tishler, M. Synthesis of Vitamin A. *J. Am. Chem. Soc.* **1951**, *73*, 719-724.
- (19) Cheeseman, G. W. H.; Heilbron, I.; Jones, E. R. H.; Sondmeier, F.; Weedon, B. C. L.; Julia, M. Polyene Synthesis (XXVIII) Structure of β -C14 Aldehyde Derived From β -Ionone and its Use for the Synthesis of Vitamin A. *J. Chem. Soc.* **1949**, *44*, 2031-2035.
- (20) Attenburrow, J.; Cameron, A. F. B.; Chapman, J. H.; Evans, R. M.; Hems, B. A.; Jansen, A. B. A.; Walker, T. Synthesis of Vitamin A From Cyclohexanone. *J. Chem. Soc.* **1952**, 1094-1111.
- (21) Colombi, L.; Bosshard, A.; Schinz, H.; Seidel, C. F. Cyclocitral, Dihydro-cyclocitral, Dihydronone. *Helv. Chim. Acta* **1951**, *34*, 265.
- (22) Badische Anilin-und Soda-Fabrik A. G. Acetals and Methylglyoxal Ketals. Ger. Patent, DE 1008729, **1957**.
- (23) Badische Anilin-und Soda-Fabrik A. G. Conjugated Unsaturated Aldehydes or Ketones. Ger. Patent DE 1031301, **1958**.
- (24) Badische Anilin-und Soda-Fabrik A. G. C40 Carotenoids. Ger. Patent, DE 1068707, **1960**.
- (25) Giguere, V.; Ong, E.; Segui, P.; Evans, R. Identification of a Receptor for the Morphogen Retinoic Acid. *Nature (London)* **1987**, *330*, 624-629.

- (26) Petkovich, M.; Brand, N. J.; Krust, A.; Chambon, P. A Human Retinoic Acid Receptor, Which Belongs to the Family of Nuclear Receptors. *Nature (London)* **1987**, *330*, 444-450.
- (27) Brand, N.; Petkovich, M.; Krust, A.; Chambon, P.; de The, H.; Marchio, A.; Tiollais, P.; Dejean, A. Identification of a Second Human Retinoic Acid Receptor. *Nature (London)* **1988**, *332*, 850-53.
- (28) Benbrook, D.; Lernhardt, E.; Pfahl, M. A New Retinoic Acid Receptor Identified From Hepatocellular Carcinoma. *Nature (London)* **1988**, *333*, 669-672.
- (29) Dejean, A.; Bougueleret, L.; Grzeschik, K.-H.; Tiollais, P. Hepatitis B Virus DNA Integration in a Sequence Homologous to *v-erb-A* and Steroid Receptor Genes in a Hepatocellular Carcinoma. *Nature (London)* **1986**, *322*, 70-72.
- (30) Krust, A.; Kastner, P.; Petkovich, M.; Zelent, A.; Chambon, P. A Third Human Retinoic Acid Receptor, hRAR- γ . *Proc. Natl. Acad. Sci. U.S.A.* **1989**, *86*, 5310-5314.
- (31) Mangelsdorf, D.; Ong, E.; Dyck, J.; Evans, R. Nuclear Receptor that Identifies a Novel Retinoic Acid Response Pathway. *Nature (London)* **1990**, *345*, 224-229.
- (32) Heyman, R.; Mangelsdorf, D.; Dyck, J.; Stein, R.; Eichele, G.; Evans, R.; Thaller, C. 9-*Cis* Retinoic Acid is a High Affinity Ligand for the Retinoid X Receptor. *Cell* **1992**, *68*, 397-406.
- (33) Levin, A. A.; Sturzenbecker, L. J.; Kazmer, S.; Bosakowski, T.; Husehlon, C.; Allenby, G.; Speck, J.; Kratzeisen, C.; Rosenberger, M.; Lovey, A.; Grippo, J. F. 9-*Cis* Retinoic Acid Stereoisomer Binds and Activates the Nuclear Receptor RXRa. *Nature (London)* **1992**, *355*, 359-361.
- (34) (a) Kliewer, S. A.; Umesono, K.; Mangelsdorf, D. J.; Evans, R. M. Retinoid X Receptor Interacts With Nuclear Receptors in Retinoic Acid, Thyroid Hormone and Vitamin D₃ Signalling. *Nature (London)* **1992**, *335*, 446-449. (b) Kliewer, S. A.; Umesono, K.; Noonan, D. J.; Heyman, R. A.; Evans, R. M. Convergence of 9-*Cis* Retinoic Acid and Peroxisome Proliferator Pathways through Heterodimer Formation of their Receptors. *Nature (London)* **1992**, *358*, 771-774.
- (35) Zhang, X.-K.; Hoffman, B.; Tram, P. B.; Graupner, G.; Pfahl, M. Retinoid X Receptor is an Auxiliary Protein for Thyroid Hormone and Retinoic Acid Receptors. *Nature (London)* **1992**, *355*, 441-446.
- (36) Zhang, X.-K.; Lehmann, J. M.; Hoffman, B.; Dawson, M. I.; Cameron, J.; Graupner, G.; Hermann, T.; Tran, P.; Pfahl, M. Homodimer formation of the Retinoid X Receptor induced by 9-*cis* Retinoic Acid. *Nature (London)* **1992**, *358*, 587-591.
- (37) (a) Mangelsdorf, D. J., Umesons, K., Evans, R. M. The Retinoid Receptors. In *THE RETINOIDS: Biology, Chemistry and Medicine*, 2nd ed.; Sporn, M. B.; Rob-

- erts, A. B.; Goodman, D. S., Eds.; Raven Press: New York, 1994; pp 319-349. (b) Mangelsdorf, D.; Thummel, C.; Beato, M.; Herrlich, P.; Schütz, G.; Umesono, K.; Blumberg, B.; Kastner, P.; Mark, M.; Chambon, P.; Evans, R. The Nuclear Receptor Superfamily: The Second Decade. *Cell* **1995**, *83*, 835-39.
- (38) Chambon, P. A Decade of Molecular Biology Receptors. *FASEB* **1996**, *10*, 940-54.
- (39) (a) Knegtel, R. M.; Katahira, M.; Schilthuis, J. G.; Bonvin, A. M.; Boelens, R.; Eib, D.; Van der Saag, P. T.; Kaptein, R. The Solution Structure of the Human Retinoic Acid Receptor-Beta DNA-Binding Domain. *J. Biomolec. NMR*. **1993**, *3*, 1-17. (b) Knegtel, R.M.; Van Tilborg, M.A.; Boelens, R.; Kaptein, R. NMR Structural Studies on the Zinc Finger Domains of Nuclear Hormone Receptors. *EXS*. **1995**, *73*, 279-95.
- (40) Lee, M. S.; Klierer, S. A.; Provencal, J.; Wright, P. E.; Evans, R. M. Structure for the Retinoid X receptor Alpha DNA Binding Domain: A Helix Required for Homodimeric DNA Binding. *Science* **1993**, *260*, 1117-1121.
- (41) Mangelsdorf, D.; Ong, E.; Dyck, J.; Evans, R. Nuclear Receptor that Identifies a Novel Retinoic Acid Response Pathway. *Nature (London)* **1990**, *345*, 224-229.
- (42) Umesono, K.; Evans, R. M. Direct Repeats as Selective Response Elements for the Thyroid Hormone, Retinoic Acid and Vitamin D₃ Receptors. *Cell* **1991**, *65*, 1255-1266.
- (43) Umesono, K.; Giguère, V.; Glass, C. K.; Rosenfield, M. G.; Evans, R. M. Retinoic Acid and Thyroid Hormone Induce Gene Expression Through Common Response Element. *Nature (London)* **1988**, *336*, 262-265.
- (44) (a) Kersten, S.; Kelleher, D.; Chambon, P.; Gronemeyer, H.; Noy, N. Retinoid X Forms Tetramers in Solution. *Proc. Natl. Acad. Sci., U.S.A.* **1995**, *92*, 8645-8649. (b) Kersten, S.; Pan, L.; Chambon, P.; Gronemeyer, H.; Noy, N. Role of Ligand in Retinoid Signaling. 9-*cis*-Retinoic Acid Modulates the Oligomeric State of the Retinoid X Receptor. *Biochem.* **1995**, *34*, 13717-13721. (c) Kersten, S.; Pan, L.; Noy, N. On the Role of Ligand in Retinoid Signaling: Positive Cooperativity in the Interactions of 9-*cis* Retinoic Acid with Tetramers of the Retinoid X Receptor. *Biochem.* **1995**, *34*, 14263-14269.
- (45) Kersten, S.; Reczek, P. R.; Noy, N. The Tetramerization Region of the Retinoid X Receptor Is Important to the Transcriptional Activation by the Receptor. *J. Biol. Chem.* **1997**, *272*, 29759-29768.
- (46) Dong, D.; Noy, N. Heterodimer Formation by the Retinoid X Receptor: Regulation by Ligands and by the Receptor's Self-Association Properties. *Biochem.* **1998**, *37*, 10691-10700.

- (47) Kersten, S.; Dong, D.; Lee, W.-Y.; Reczek, P. R.; Noy, N. Auto-Silencing by the Retinoid X Receptor. *J. Mol. Biol.* **1998**, *284*, 21-32.
- (48) Bourget, W.; Ruff, M.; Chambon, P.; Gronemeyer, H.; Moras, D. Crystal Structure of the Ligand-Binding Domain of the Human Nuclear Receptor RXRa. *Nature (London)* **1995**, *375*, 377-382
- (49) Gampe, R. T., Jr.; Montana, V. G.; Lambert, M. H.; Wisely, G. B.; Milburn, M. V.; Xu, H. E. Structural Basis for Autorepression of Retinoid X Receptor by Tetramer Formation and the AF-2 Helix. *Genes and Dev.* **2000**, *14*, 2229-2241.
- (50) Perissi, V.; Staszewski, L. M.; McInerney, E. M.; Kurokawa, R.; Krones, A.; Rose, D. W.; Lambert, M. H.; Milburn, M. V.; Glass, C. K.; Rosenfield, M. G. Molecular Determinants of Nuclear Co-Repressor Interaction. *Genes and Dev.* **1999**, *13*, 3198-3208.
- (51) Pazin, M. J.; Kadanaga, J. T. What's Up and Down with Histone Deacetylation and Transcription? *Cell* **1997**, *89*, 325-328.
- (52) Lin, B. C.; Hong, S. H.; Krig, S.; Yoh, S. M.; Privalsky, M. L. A Conformational Switch in Nuclear Hormone Receptors Is Involved in Coupling Hormone Binding to Co-Repressor Release. *Mol. Cell. Biol.* **1997**, *17*, 6131-6138.
- (53) Chen, J. D. and Evans, R. M. A Transcriptional Co-Repressor that Interacts with Nuclear Hormone Receptors. *Nature (London)* **1995**, *377*, 454-457.
- (54) Horlein, A. J.; Naar, A. M.; Heinzel, T.; Torchia, J.; Gloss, R.; Kurokawa, A.; Ryan, Y.; Kamei, M.; Soderstrom, M.; Glass, C. K.; Rosenfeld, M. G. Ligand-Independent Repression by the Thyroid Hormone Receptor Mediated by a Nuclear Receptor Co-Repressor. *Nature (London)* **1997**, *377*, 397-404.
- (55) Seol, W.; Mahon, M. J.; Le, Y.-K.; Moore, D. D. Two Receptor Interacting Domains in the Nuclear Hormone Receptor Co-Repressor RIP13/N-CoR. *Mol. Endocrinol.* **1996**, *10*, 1646-1655.
- (56) Zamir, I.; Harding, H. P.; Atkins, G. B.; Horlein, A. Glass, C. K.; Rosenfeld, M. G.; Lazar, M. A. A Nuclear Hormone Receptor Co-Repressor Mediates Transcriptional Silencing by Receptors with Different Repression Domains. *Proc. Natl. Acad. Sci., U.S.A.* **1996**, *16*, 5458-5465.
- (57) Klein, E. S.; Pino, M. E.; Johnson, A. T.; Davies, P. J. A.; Nagpal, S.; Thacher, S. M.; Krasinski, G.; Chandraratna, R. A. S. Identification and Functional Separation of Retinoic Acid Receptor Neutral Antagonists and Inverse Agonists. *J. Biol. Chem.* **1996**, *271*, 22692-22696.
- (58) Renaud, J. P.; Rochel, N.; Ruff, M.; Vivat, V.; Chambon, P.; Gronemeyer, H.; Moras, D. Crystal Structure of the RAR γ Ligand-Binding Domain Bound to All-Trans Retinoic Acid. *Nature (London)* **1995**, *378*, 681-689.

- (59) Nagpal, S.; Friant, S.; Nakshatri, H.; Chambon, P. RARs and RXRs: Evidence for Two Autonomous Transactivation Functions (AF-1 and AF-2) and Heterodimerization *In Vivo*. *EMBO J.* **1993**, *12*, 2349-2360.
- (60) Heery, D. M.; Kalkoven, E.; Hoare, S.; Parker, M. G. A Signature Motif in Co-Activators Mediates Binding to Nuclear Receptors. *Nature (London)* **1997**, *387*, 733-736.
- (61) McInerney, E. M.; Rose, D. W.; Flynn, S. E.; Westin, S.; Mullen, T.-M.; Krones, A.; Inostroza, J.; Torchia, J.; Nolte, R. T.; Assa-Munt, N.; Milburn, M. V.; Glass, C. K.; Rosenfeld, M. G. Determinants of Co-Activator LXXLL Motif Specificity in Nuclear Receptor Transcriptional Activation. *Genes and Dev.* **1998**, *12*, 3357-3368.
- (62) Nagy, L.; Thomázy, V. A.; Shipley, G. L.; Fésűs, L.; Lamph, W.; Heyman, R. A.; Chandraratna, R. A. S.; Davies, P. J. A. Activation of Retinoid X Receptors Induces Apoptosis in HL-60 Cell Lines. *Molec. Cell. Biol.* **1995**, *15*, 3540-3551.
- (63) Nolte, R. T.; Wisely, G. B.; Westin, S.; Cobb, J. E.; Lambert, M. H.; Kurokawa, R.; Rosenfeld, M. G.; Wilson, T. M.; Glass, C. K.; Milburn, M. V. Ligand Binding and Co-Activator Assembly of the Peroxisome Proliferator-Activated Receptor γ . *Nature (London)* **1998**, *395*, 137-143.
- (64) Darimont, B. D.; Wagner, R. L.; Apriletti, J. W.; Stallcup, M. R.; Krushner, P. J.; Baxter, J. D.; Fletterick, R. J.; Yamamoto, K. R. Structure and Specificity of Nuclear Receptor-Co Activator Interactions. *Genes and Dev.* **1998**, *12*, 3343-3356.
- (65) Torchia, J.; Glass, C.; Rosenfeld, M. G. Co-Activators and Co-Repressors in the Integration of Transcriptional Responses. *Curr. Opinion Cell. Biol.* **1998**, *10*, 373-383.
- (66) Sporn, M. B.; Dunlop, N. M.; Newton, D. L.; Smith, J. M. Prevention of Chemical Carcinogenesis by Vitamin A and its Synthetic Analogs (Retinoids). *Fed. Proc.* **1976**, *35*, 1332-1338.
- (67) Yob, E. H.; Pochi, P. E. Side Effects and Long-Term Toxicity of Synthetic Retinoids. *Arch. Dermatol.* **1987**, *123*, 1375-1378.
- (68) Pawson, B. A.; Ehmann, C. W.; Itri, L. M.; Sherman, M. I. Retinoids at the Threshold: Their Biological Significance and Therapeutic Potential. *J. Med. Chem.* **1982**, *25*, 1269-1277.
- (69) Frickel, F. Retinoids: An Overview of Some Natural Carotenoid Metabolites and Their Synthetic Metabolites. *Pure Appl. Chem.* **1985**, *57*, 709.

- (70) Sporn, M. B.; Roberts, A. B. Biological Methods for Analysis and Assay of Retinoids-Relationship Between Structure and Activity. In *The Retinoids*, Academic Press: Orlando, FL, 1984, pp 250-253.
- (71) Mori, S. The Changes in the Para-Ocular Glands Which Follow the Administration of Diets Low in Fat-Soluble A; With Notes of the Effect of the Same Diets on the Salivary Glands and the Mucosa of the Larynx and Trachea. *Bull. Johns Hopkins Hosp.* **1922**, *32*, 357-359.
- (72) Wolbach, S. B.; Howe, P. R. Tissue Changes Following Deprivation of Fat-Soluble A Vitamin. *J. Exp. Med.* **1925**, *42*, 753-777.
- (73) (a) Verma, A. K.; Boutwell, R. K. Vitamin A Acid (Retinoic Acid), A Potent Inhibitor of 12-*O*-Tetradecanoyl-Phorbol-13-Acetate-Induced Ornithine Decarboxylase Activity in Mouse Epidermis. *Cancer Res.* **1977**, *37*, 2196-2201. (b) Verma, A. K.; Boutwell, R. K. Inhibition of 12-*O*-Tetradecanoyl-Phorbol-13-Acetate-Induced Ornithine Decarboxylase Activity in Mouse Epidermis by Vitamin A Analogs (Retinoids). *Cancer Res.* **1978**, *38*, 793-801. (c) Verma, A. K.; Boutwell, R. K. Correlation of the Inhibition by Retinoids of Tumor Promoter-Induced Mouse Epidermal Ornithine Decarboxylase Activity and of the Skin Tumor Promotion. *Cancer Res.* **1979**, *39*, 419-425.
- (74) Russell, D. H. Polyamines in Growth-Normal and Neoplastic. In *Polyamines in Normal and Neoplastic Growth*, Raven Press: New York, 1973, p 1.
- (75) Bachrach, U. Polyamines as Chemical Markers for Malignancy. *Italian J. Biochem.* **1976**, *25*, 77-93.
- (76) Durie, B. G. M.; Salmon, S. E.; Russell, D. H. Polyamines as Markers of Response and Disease Activity in Cancer Chemotherapy. *Cancer Res.* **1977**, *37*, 214-221.
- (77) O'Brien, T. G.; Simsiman, R. C.; Boutwell, R. K. Induction of the Polyamine-Biosynthetic Enzymes in Mouse Epidermis by Tumor Promoting Agents. *Cancer Res.* **1975**, *35*, 1662-1670.
- (78) Murray, A. E.; Verma, A. K.; Froschio, M. Effect of Carcinogens and Tumor Promoters on Epidermal Cyclic 3':5'-Monophosphate Metabolism. In *Control Mechanisms in Cancer*, Raven Press: New York, 1976, pp 217-219.
- (79) Van Duuren, B. L. Tumor-Promoting Agents in Two-Stage Carcinogenesis. *Progr. Exp. Tumor Res.* **1969**, *11*, 31-68.
- (80) Bollag, W. Therapeutic Effects of an Aromatic Retinoic Acid Analog on Chemically Induced Skin Papillomas and Carcinomas of Mice *Euro. J. Cancer* **1974**, *10*, 731-737.

- (81) Bollag, W. Therapy of Epithelial Tumors With an Aromatic Retinoic Acid Analog *Chemotherapy* 1975, 21, 236-247.
- (82) Loeliger, P.; Bollag, W.; Mayer, H. Arotonoids, A New Class of Highly Active Retinoids. *Euro. J. Med. Chem.* 1980, 15, 9-15.
- (83) Frolick, C. A. Metabolism of Retinoids. In *The Retinoids*, Sporn, M. B.; Roberts, A. B.; Dewitt, S. G., Eds.; Academic Press: Orlando, FL, 1984; p177.
- (84) Stephens-Jarnigen, A.; Miller, D. A.; DeLuca, H. F. The Growth-Supporting Activity of a Retinoidal Benzoic Acid Derivative and 4,4-Difluororetinoic Acid. *Arch. Biochem. Biophys.* 1985, 237, 11-16.
- (85) Dawson, M. I.; Hobbs, P. D.; Chan, R. L.-S.; Chao, W.-R. Retinoic Acid Analogs With Ring Modifications. Synthesis and Pharmacological Activity. *J. Med. Chem.* 1981, 24, 1214-1223.
- (86) Sporn, M. B.; Newton, D. L. Chemoprevention of Cancer With Retinoids. *Fed. Proc.* 1979, 38, 2528-2534.
- (87) Newton, D. L.; Henderson, W. R.; Sporn, M. B. Structure-Activity Relationship of Retinoids in Hamster Tracheal Organ Culture. *Cancer Res.* 1980, 40, 3413-3425.
- (88) Dawson, M. I.; Hobbs, P. D.; Chan, R. L.; Chao, W.; Fung, V. A. Aromatic Retinoid Analogues. Synthesis and Pharmacological Activity. *J. Med. Chem.* 1981, 24, 583-592.
- (89) Dawson, M. I.; Chan, R. L.-S.; Derdzinski, K.; Hobbs, P. D.; Chao, W.-R.; Schiff, L. J. Synthesis and Pharmacological Activity of 6-[(E)-2-(2,6,6-Trimethyl-1-cyclohexen-1-yl)ethen-1-yl]- and 6-(1,2,3,4-tetrahydro-1,1,4,4-tetramethyl-6-naphthyl)-2-naphthalenecarboxylic Acids. *J. Med. Chem.* 1983, 26, 1653-1656.
- (90) Dawson, M. I.; Hobbs, P. D.; Derdzinski, K.; Chan, R. L.-S.; Gruber, J.; Chao, W.-R.; Smith, S. S.; Thies, R. W.; Schiff, L. J. Conformationally Restricted Retinoids. *J. Med. Chem.* 1984, 27, 1516-1531.
- (91) Baas, J. L.; Davies-Fidder, A.; Visser, F.R.; Huisman, H.O. Synthesis of 4-Thia-Vitamin A. *Tetrahedron* 1966, 22, 265-275.
- (92) (a) Breitman, T. R.; Selonick, S. E.; Collins, S. J. Induction of Differentiation of the Human Promyelocytic Leukemia Line (HL-60) by Retinoic Acid. *Proc. Natl. Acad. Sci. U.S.A.* 1980, 77, 2936-40. (b) Breitman, T. R. Growth and Differentiation of Human Myeloid Leukemia Cell Line HL60. In *Methods in Enzymology*, Academic Press: San Diego, CA, 1990; Vol. 190, pp 118-130.

- (93) Kagechika, H.; Kawachi, E.; Shudo, K. New Type Inducers of Differentiation of Human HL-60 Promyelocytic Leukemia Cells. *Chem Pharm. Bull.* **1984**, *32*, 4209-4212.
- (94) Kagechika, H.; Kawachi, E.; Hashimoto, Y.; Shudo, K. Differentiation Inducers of Human Promyelocytic Leukemia Cells HL-60. Phenylcarbamoylbenzoic Acids and Polyene Amides. *Chem. Pharm. Bull.* **1986**, *34*, 2275-2278.
- (95) Kagechika, H.; Kawachi, E.; Hashimoto, Y.; Himi, T.; Shudo, K. Retinobenzoic Acids. 1. Structure-Activity Relationships of Aromatic Amides With Retinoidal Activity. *J. Med. Chem.* **1988**, *31*, 2182-2192.
- (96) (a) Kagechika, H.; Himi, T.; Kawachi, E.; Hashimoto, Y.; Shudo, K. Retinobenzoic Acids. 4. Conformation of Aromatic Amides with Retinoidal Activity. Importance of *trans*-Amide Structure for the Activity. *J. Med. Chem.* **1989**, *32*, 2292-2296. (b) Kagechika, H.; Kawachi, E.; Hashimoto, Y.; Shudo, K. Retinobenzoic Acids. 2. Structure-Activity Relationships of Chalcone-4-Carboxylic Acids and Flavone-4'-Carboxylic Acids. *J. Med. Chem.* **1989**, *32*, 834-840.
- (97) Vaezi, M. F.; Alam, M.; Sani, B. P.; Rogers, T. S.; Simpson-Herren, L.; Wille, J. J.; Hill, D. L.; Doran, T. I.; Brouillette, W. J.; Muccio, D. D. A Conformationally Defined 6-*s-trans*-Retinoic Acid Isomer. Synthesis, Chemopreventive Activity, and Toxicity. *J. Med. Chem.* **1994**, *37*, 4499-4507.
- (98) Alam, M.; Zhestkov, V.; Sani, B. P.; Venepally, P.; Levin, A. A.; Kazmer, S.; Li, E.; Norris, A. W.; Zhang, X.-K.; Lee, M. O.; Hill, D. L.; Lin, T.-H.; Brouillette, W. J.; Muccio, D. D.; Conformationally Defined 6-*s-trans*-Retinoic Acid Analogs. 2. Selective Agonists for Nuclear Receptor Binding and Transcriptional Activity. *J. Med. Chem.* **1995**, *38*, 2303-2310.
- (99) Honig, B.; Hudson, B.; Sykes, B.; Karplus, M. Ring Orientation in β -Ionone and Retinals. *Proc. Natl. Acad. Sci. U.S.A.* **1971**, *68*, 1289-1293.
- (100) Deleccluse, C.; Cavey, M. T.; Martin, B.; Bernard, B. A.; Reichert, U.; Maignan, J.; Shroot, B. Selective High Affinity Retinoic Acid Receptor α or β - γ Ligands. *Molec. Pharmacol.* **1991**, *40*, 556-562.
- (101) Tobita, T.; Takeshita, A.; Kitamura, K.; Ohnishi, K.; Yanagi, M.; Hiraoka, A.; Karasuno, T.; Takeuchi, M.; Miyawaki, S.; Ueda, R.; Naoe, T.; Ohno, R. Treatment with a New Synthetic Retinoid, Am80, of Acute Promyelocytic Leukemia Relapsed from Complete Remission Induced by *All-trans* Retinoic Acid. *Blood* **1997**, *90*, 967-973.
- (102) Teng, M.; Duong, T. T.; Johnson, A. T.; Klein, E. S.; Wang, L.; Khalifa, B.; Chandraratna, R. A. S. Identification of Highly Potent Retinoic Acid Receptor α -Selective Antagonists. *J. Med. Chem.* **1997**, *30*, 2445-2451.

- (103) Isnardi, L.; Raffo, P.; Emionite, L.; Chandraratna, R. A. S.; Toma, S. Different Effects of the Treatment with AGN 193836 and 9-*Cis* Retinoic Acid in Breast Cancer Cells. *Anticancer Res.* **1999**, *19*, 3083-3092.
- (104) (a) Kikuchi, K.; Hibi, S.; Yoshimura, H.; Tai, K.; Hida, T.; Tokuhara, N.; Yamauchi, T.; Nagai, M. Novel Retinoic Acid Receptor α Agonists: Syntheses and Evaluation of Pyrazole Derivatives. *Bioorg. Med. Chem. Lett.* **2000**, *10*, 619-622. (b) Hibi, S.; Tagami, K.; Kikuchi, K.; Yoshimura, H.; Tai, K.; Hida, T.; Tokuhara, N.; Yamauchi, T.; Nagai, M. Syntheses and Evaluation of Naphthalenyl- and Chromenyl-Pyrrolyl-Benzonic Acids as Potent and Selective Retinoic Acid Receptor α Agonists. *Bioorg. Med. Chem. Lett.* **2000**, *10*, 623-625. (c) Kikuchi, K.; Hibi, S.; Yoshimura, H.; Tokuhara, N.; Tai, K.; Hida, T.; Yamauchi, T.; Nagai, M. Syntheses and Structure-Activity Relationships of 5,6,7,8-Tetrahydro-5,5,8,8-tetramethyl-2-quinoxaline Derivatives With Retinoic Acid Receptor α Agonistic Activity. *J. Med. Chem.* **2000**, *43*, 409-419.
- (105) Badische Anilin und Soda Fabrik. New Diaryl Heterocyclic Compounds Useful as Retinoid Medicaments. Eur. Patent EP 0382077A, **1990**.
- (106) Apfel, C.; Bauer, F.; Crettaz, M.; Forni, L.; Kamber, M.; Kaufmann, F.; LeMotte, P.; Pirson, W.; Klaus, M. A Retinoic Acid Receptor α Antagonist Selectively Counteracts Retinoic Acid Effects. *Proc. Natl. Acad. Sci. U.S.A.* **1992**, *89*, 7129-7133.
- (107) Barrero, A. F.; Sanchez, J. F.; Oltra, J. E.; Teva, D.; Ferrol, R. R.; Elmerabet, J.; Del Moral, R. G.; Lucena, M. A.; O'Valle, F. Synthesis of Some Retinoids Bearing Different Heterocyclic Rings With Anticancer Activity. *Euro. J. Med. Chem.* **1994**, *29*, 773.
- (108) Chandraratna, R.; Gillett, S.; Song, T.; Attard, J.; Vuligonda, S.; Garst, M.; Arefig, T.; Gil, D.; Wheeler, L. Synthesis and Pharmacological Activity of Conformationally Restricted, Acetylenic Retinoid Analogs. *Bioorg. Med. Chem. Lett.* **1995**, *5*, 523-527.
- (109) Chandraratna, R. A. S. Tazarotene-First of a New Generation of Receptor-Selective Retinoids. *Br. J. Derm.* **1996**, *135*, 18-25.
- (110) Johnson, A.; Klein, E.; Wang, L.; Pino, M.; Chandraratna, R. Identification of Retinoic Acid Receptor β Subtype Specific Agonists. *J. Med. Chem.* **1996**, *39*, 5027-5030.
- (111) (a) Vuligonda, V. S.; Garst, M. E.; Chandraratna, R. A. S. Stereoselective Synthesis and Receptor Activity of Conformationally Defined Retinoid X Receptor Selective Ligands. *Bioorg. Med. Chem. Lett.* **1999**, *9*, 589-594. (b) Vuligonda, V.; Standeven, A. M.; Escobar, M.; Chandraratna, R. A. S. A New Class of Potent

- RAR Antagonists: Dihydroanthracenyl, Benzochromenyl and Benzothiochromenyl Retinoids. *Bioorg. Med. Chem. Lett.* **1999**, 9, 743-748. (c) Vuligonda, V.; Lin, Y.; Thacher, S.; Standeven, A.; Kochar, D.; Chandraratna, R. A New Class of RAR Subtype Selective Retinoids: Correlation of Pharmacological Effects With Receptor Activity. *Bioorg. Med. Chem. Lett.* **1999**, 7, 263-270.
- (112) Kistler, A.; Howard, B. W. Teratogenicity of Retinoids: Mechanistic Studies. In *Methods in Enzymology*, Academic Press: San Diego, CA, 1990; Vol. 190, pp 418-433.
- (113) Charpentier, B.; Bernardon, J.-M.; Eustache, J.; Millois, C.; Martin, B.; Michel, G.; Shroot, B. Synthesis, Structure-Affinity Relationships, and Biological Activities of Ligands Binding to Retinoid Acid Receptor Subtypes. *J. Med. Chem.* **1995**, 38, 4993-5006.
- (114) Graupner, G.; Malle, G.; Maignan, J.; Lang, G.; Pruni  ras, M.; Pfahl, M. 6'-Substituted Naphthalene-2-Carboxylic Acid Analogs, A New Class of Retinoic Acid Receptor Subtype-Specific Ligands. *Biochem. Biophys. Res. Comm.* **1991**, 179, 1554-1561.
- (115) Yu, K.-L.; Spinazze, P.; Ostrowski, J.; Currier, S.; Pack, E.; Hammer, L.; Roalsvig, T.; Honeyman, J.; Tortolani, D.; Reczek, P.; Mansuri, M.; Starrett, J., Jr. Retinoic Acid Receptor β , γ -Selective Ligands: Synthesis and Biological Activity of 6-Substituted 2-Naphthoic Acid Retinoids. *J. Med. Chem.* **1996**, 39, 2411-2421.
- (116) Renaud, J. P.; Rochel, N.; Ruff, M.; Vivat, V.; Chambon, P.; Gronemeyer, H.; Moras, D. Crystal Structure of the RAR γ Ligand-Binding Domain Bound to All-Trans Retinoic Acid. *Nature (London)* **1995**, 378, 681-689.
- (117) Klaholz, B. P.; Renaud, J.-P.; Mitschler, A.; Zusi, C.; Chambon, P.; Gronemeyer, H.; Moras, D. Conformational Adaptation of Agonists to the Human Nuclear Receptor RAR Gamma. *Nature Struct. Biol.* **1998**, 5, 199-202.
- (118) Klaholz, B. P.; Mitschler, A.; Belema, M.; Zusi, C.; Moras, D. Enantiomer Discrimination Illustrated by High Resolution Crystal Structures of the Human Nuclear Receptor hRAR Gamma. *Proc. Natl Acad. Sci. U.S.A.* **2000**, 97, 6322-6327.
- (119) Klaholz, B. P.; Mitschler, A.; Moras, D. Structural Basis for Isotype Selectivity of the Human Retinoic Acid Nuclear Receptor. *J. Molec. Biol.* **2000**, 302, 155-170.
- (120) Wahl, M. C.; Sundaralingam, M. C-H...O Hydrogen Bonding in Biology. *Trends Biochem. Sci.* **1997**, 22, 97-102.
- (121) Eryolles, L.; Kagechika, H.; Kawachi, E.; Fukasawa, H.; Iijima, T.; Matsushima, Y.; Hashimoto, Y.; Shudo, K. Retinobenzoic Acids. 6. Retinoid Antagonists With a Heterocyclic Ring. *J. Med. Chem.* **1994**, 37, 1508-1517.

- (122) Fanjul, A. N.; Piedrafita, J.; Al-Shamma, H.; Pfahl, M. Apoptosis Induction and Potent Antiestrogen Receptor-Negative Breast Cancer Activity *in Vivo* by a Retinoid Antagonist. *Cancer Res.* **1998**, *58*, 4607-4610.
- (123) Pfahl, M. Nuclear Receptor/AP-1 Interaction. *Endocrine Rev.* **1993**, *14*, 651-658.
- (124) Yoshimura, H.; Nagai, M.; Hibi, S.; Kikuchi, K.; Abe, S.; Hida, T.; Higashi, S.; Hishinuma, I.; Yamanaka, T. A Novel Type of Retinoic Acid Receptor Antagonist: Synthesis and Structure-Activity Relationships of Heterocyclic Ring-Containing Benzoic Acid Derivatives. *J. Med. Chem.* **1995**, *38*, 3163-3173.
- (125) Ueno, H.; Kizaki, M.; Matsushita, H.; Muto, A.; Yamato, K.; Nishihara, T.; Hida, T.; Yoshimura, H.; Koeffler, H.P.; Ikeda, Y. A Novel Retinoic Acid Receptor (RAR)-Selective Antagonist Inhibits Differentiation and Apoptosis of HL-60 Cells: Implications of RAR α -Mediated Signals in Myeloid Leukemic Cells. *Leukemia Res.* **1998**, *22*, 517-522.
- (126) Johnson, A. T.; Klein, E. S.; Gillett, S. J.; Wang, L.; Song, T. C.; Pino, M. E.; Chandraratna, R. A. S. Synthesis and Characterization of Highly Potent and Effective Antagonists of Retinoic Acid Receptors. *J. Med. Chem.* **1995**, *38*, 4764-4767.
- (127) Johnson, A. T.; Wang, L.; Standeven, A. M.; Escobar, M.; Chandraratna, R. A. S. Synthesis and Biological Activity of High-Affinity Retinoic Acid Receptor Antagonists. *Bioorg. Med. Chem. Lett.* **1999**, *7*, 1321-1338.
- (128) (a) Vuligonda, V.; Standeven, A. M.; Escobar, M.; Chandraratna, R. A. S. A New Class of Potent RAR Antagonists: Dihydroanthracenyl, Benzochromenyl and Benzoethiochromenyl Retinoids. *Bioorg. Med. Chem. Lett.* **1999**, *9*, 743-748. (b) Vuligonda, V.; Lin, Y.; Thacher, S.; Standeven, A.; Kochar, D.; Chandraratna, R. A. S. New Class of RAR Subtype Selective Retinoids: Correlation of Pharmacological Effects With Receptor Activity. *Bioorg. Med. Chem. Lett.* **1999**, *7*, 263-270.
- (129) Apfel, C.; Bauer, F.; Crettaz, M.; Forni, L.; Kamber, M.; Kaufmann, F.; LeMotte, P.; Pirson, W.; Klaus, M. A Retinoic Acid Receptor α Antagonist Selectively Counteracts Retinoic Acid Effects. *Proc. Natl. Acad. Sci. U.S.A.* **1992**, *89*, 7129-7133.
- (130) Toma, S.; Isnardi, L.; Raffo, P.; Dastoli, G.; Apfel, C.; LeMotte, P.; Bollag, W. RAR α Antagonist Ro-415253 Inhibits Proliferation and Induces Apoptosis in Breast Cancer Cell Lines. *Int. J. Cancer* **1998**, *78*, 86-94.
- (131) Teng, M.; Duong, T. T.; Johnson, A. T.; Klein, E. S.; Wang, L.; Khalifa, B.; Chandraratna, R. A. S. Identification of Highly Potent Retinoic Acid Receptor α -Selective Antagonists. *J. Med. Chem.* **1997**, *30*, 2445-2451.

- (132) Bourget, W.; Vivat V.; Wurtz, J.-M.; Chambon, P.; Gronemeyer, H.; Moras, D. Crystal Structure of the Heterodimeric Complex of RAR and RXR Ligand-Binding Domains *Molecular Cell* **2000**, *5*, 289-298.
- (133) Johnson, A. T.; Wang, L.; Standeven, A. M.; Escobar, M.; Chandraratna, R. A. S. Lehmann, J. M.; Jong, L.; Fanjul, A.; Cameron, J. F.; Lu, X. P.; Haefner, P.; Dawson, M. I.; Pfahl, M. Retinoids Selective for Retinoid X Receptor Response Pathways. *Science* **1992**, *258*, 1944-1946.
- (134) Jong, L.; Lehmann, J. M.; Hobbs, P. D.; Harlev, E.; Huffman, J. C.; Pfahl, M.; Dawson, M. I. Conformational Effects on Retinoid Receptor Selectivity. 1. Effect of 9-Double Bond Geometry on Retinoid X Receptor Activity. *J. Med. Chem.* **1993**, *36*, 2605-2613.
- (135) Beard, R. L.; Gil, D. W.; Marler, D. K.; Henry, E.; Colon, D. F.; Gillett, S. J.; Arefieg, T.; Breen, T. S.; Krauss, H.; Davies, P. J. A.; Chandraratna, R. A. S. Structural Basis for the Differential RXR and RAR Activity of Stilbene Retinoid Analogs. *Bioorg. Med. Chem. Lett.* **1994**, *4*, 1447-1452.
- (136) Beard, R. L.; Chandraratna, R. A. S.; Colon, D. F.; Gillett, S. J.; Henry, E.; Marler, D. K.; Song, T.; Denys, L.; Garst, M. E.; Arefieg, T. Synthesis and Structure-Activity Relationships of Stilbene Retinoid Analogs Substituted With Heteroaromatic Carboxylic Acids. *J. Med. Chem.* **1995**, *38*, 2820-2829.
- (137) Boehm, M. F.; Zhang, L.; Badea, B. A.; White, S. K.; Mais, D. E.; Berger, E.; Suto, C. M.; Goldman, M. E.; Heyman, R. A. Synthesis and Structure-Activity Relationships of Novel Retinoid X Receptor-Selective Retinoids. *J. Med. Chem.* **1994**, *37*, 2930-2941.
- (138) Gottardis, M. M.; Bischoff, E. D.; Shirley, M. A.; Wagoner, M. A.; Lamph, W. W.; Heyman, R. A.; Chemoprevention of Mammary Carcinoma by LGD1069 (Targretin): An RXR-Selective Ligand. *Cancer Res.* **1996**, *56*, 5566-5570.
- (139) Bischoff, E. D.; Gottardis, M. M.; Moon, T. E.; Heyman, R. A.; Lamph, W. W.; Beyond Tamoxifen: The Retinoid X Receptor-Selective Ligand LGD1069 (Targretin) Causes Complete Regression of Mammary Carcinoma. *Anticancer Res.*, **1998**, *58*, 479-484.
- (140) Sherman, S. I.; Gopal, J.; Haugen, B. R.; Chiu, A. C.; Whaley, K.; Nowlakha, P.; Duvic, M. Central Hypothyroidism Associated with Retinoid X Receptor-Selective Ligands. *N. Engl. J. Med.* **1999**, *340*, 1075-9.
- (141) Dawson, M. I.; Jong, L.; Hobbs, P. D.; Cameron, J. F.; Chao, W.-R.; Pfahl, M.; Lee, M.-O.; Shroot, B.; Pfahl, M. Conformational Effects on Retinoid Receptor Selectivity. 2. Effects of Retinoid Bridging Group on Retinoid X Receptor Activity and Selectivity. *J. Med. Chem.* **1995**, *38*, 3368-3383.

- (142) Muccio, D. D.; Brouillette, W. J.; Alam, M.; Vaezi, M. F.; Sani, B. P.; Venepally, P.; Reddy, L.; Li, E.; Norris, A. W.; Simpson-Herren, L.; Hill, D. Conformationally Defined 6-*s-trans* Retinoic Acid Analogs. 3. Structure-Activity Relationships for Nuclear Receptor Binding, Transcriptional Activity, and Cancer Chemopreventive Activity. *J. Med. Chem.* **1996**, *39*, 3625-3635.
- (143) Muccio, D.D.; Brouillette, W.J.; Breitman, T.R.; Taimi, M.; Emanuel, P.D.; Zhang, X.-K.; Chen, G.-Q.; Sani, B. P.; Venepally, P.; Reddy, L.; Alam, M.; Simpson-Herren, L.; Hill, D. L. Conformationally Defined Retinoic Acid Analogues. 4. Potential New Agents for Acute Promyelocytic and Juvenile Myelomonocytic Leukemias. *J. Med. Chem.* **1998**, *41*, 1679-1687.
- (144) Vuligonda, V.; Lin, Y.; Chandraratna, R. A. S. Synthesis of Highly Potent RXR-Specific Retinoids: The Use of a Cyclopropyl Group as a Double Bond Isostere. *Bioorg. Med. Chem. Lett.* **1996**, *6*, 213-218.
- (145) Vuligonda, V. S.; Garst, M. E.; Chandraratna, R. A. S. Stereoselective Synthesis and Receptor Activity of Conformationally Defined Retinoid X Receptor Selective Ligands. *Bioorg. Med. Chem. Lett.* **1999**, *9*, 589-594.
- (146) (a) Farmer, L. J.; Jeong, S.; Kallel, A.; Koch, S. S. C.; Croston, G. E.; Flatten, K. S.; Heyman, R. A.; Nadzan, A. M. Synthesis and Structure-Activity Relationships of Potent Retinoid X Receptor Ligands. *Bioorg. Med. Chem. Lett.* **1997**, *7*, 2393-2398.
- (147) Farmer, L. J.; Zhi, L.; Jeong, S.; Kallel, A.; Croston, G.; Flatten, K. S.; Heyman, R. A.; Nadzan, A. M. Synthesis and Structure-Activity Relationships of Potent Conformationally Restricted Retinoid X Receptor Ligands. *Bioorg. Med. Chem. Lett.* **1997**, *7*, 2747-2752.
- (148) Hibi, S.; Kikuchi, K.; Yoshimura, H.; Nagai, M.; Tai, K.; Hida, T. Syntheses and Structure-Activity Relationships of Novel Retinoid X Receptor Agonists. *J. Med. Chem.* **1998**, *41*, 3245-3252.
- (149) Egea, P. F.; Mitschler, A.; Rochel, N.; Ruff, M.; Chambon, P.; Moras, D. Crystal Structure of the Human RXR α Ligand-Binding Domain Bound to its Natural Ligand: 9-*Cis* Retinoic Acid. *EMBO J.* **2000**, *19*, 2592-2601.
- (150) Nagy, L.; Thomázy, V. A.; Shipley, G. L.; Fésüs, L.; Lamph, W.; Heyman, R. A.; Chandraratna, R. A. S.; Davies, P. J. A. Activation of Retinoid X Receptors Induces Apoptosis in HL-60 Cell Lines. *Molec. Cell. Biol.* **1995**, *15*, 3540-3551.
- (151) Roy, B.; Taneja, R.; Chambon, P. Synergistic Activation of Retinoic acid (RA)-Responsive Genes and Induction of Embryonal Carcinoma Cell Differentiation by an RA Receptor α (RAR α)-, RAR β -, or RAR γ -Selective Ligand in Combination with a Retinoid X Receptor-Specific Ligand. *Molec. Cell. Biol.* **1995**, *15*, 6481-6487.

- (152) Apfel, C. M.; Kamber, M.; Klaus, M.; Mohr, P.; Keidel, S.; LeMotte, P. K. Enhancement of HL-60 Differentiation by a New Class Retinoids With Selective Activity on Retinoid X Receptor. *J. Biol. Chem.* **1995**, *270*, 30765-30772.
- (153) Chen, J.-Y.; Clifford, J.; Zusi, C.; Starrett, J.; Tortolani, D.; Ostrowski, J.; Reczek, P. R.; Chambon, P.; Gronemeyer, H. Two Distinct Actions of Retinoid-Receptor Ligands. *Nature (London)* **1996**, *382*, 819-822.
- (154) Minucci, S.; Leid, M.; Toyama, R.; Saint-Jeannet, J.-P.; Peterson, V. J.; Horn, V.; Ishmael, J. E.; Bhattacharyya, A. D.; Dawid, I. B.; Ozato, K. Retinoid X Receptor (RXR) Within the RXR-Retinoic Acid Receptor Heterodimer Binds Its Ligand and Enhances Retinoid-Dependent Gene Expression. *Molec. Cell. Biol.* **1997**, *17*, 644-655.
- (155) (a) Umemiya, H.; Kagechika, H.; Fukasawa, H.; Kawachi, E.; Ebisawa, M.; Hashimoto, Y.; Eisenmann, G.; Erb, C.; Pornon, A.; Chambon, P.; Gronemeyer, H.; Shudo, K. Action Mechanism of Retinoid-Synergistic Dibenzodiazepines. *Biochem. Biophys. Res. Comm.* **1997**, *233*, 121-125. (b) Umemiya, H.; Kagechika, H.; Fukasawa, H.; Ebisawa, M.; Eryolles, L.; Kawachi, E.; Eisenmann, G.; Gronemeyer, H.; Hashimoto, Y.; Shudo, K.; Kagechika, H. Regulation of Retinoid Actions by Diazepinylbenzoic Acids. Retinoid Synergists Which Activate the RXR-RAR Heterodimers. *J. Med. Chem.* **1997**, *40*, 4222-4234.
- (156) Anzano, M. A.; Byers, S. W.; Smith, J. M.; Peer, C. W.; Mullen, L. T.; Brown, C. C.; Roberts, A. B.; Sporn, M. B. Prevention of Breast Cancer in the Rat With 9-*cis*-Retinoic Acid as a Single Agent and in Combination with Tamoxifen. *Cancer Res.* **1994**, *54*, 4614-4617.
- (157) (a) Chomienne, C.; Fenaux, P.; Degos, L. Retinoid Differentiation Therapy in Acute Promyelocytic Leukemia. *FASEB* **1996**, *10*, 1025-1030. (b) Walmsley, S.; Northfelt, D. W.; Melosky, B.; Conant, M.; Friedman, Kien A. E.; Wagner B. Treatment of AIDS-Related Cutaneous Kaposi's Sarcoma With Topical Alitretinoin (9-*cis*-Retinoic Acid) Gel. *J. Acquir. Immune Defic. Syndr.* **1999**, *22*, 235-246. (c) Castleberry, R. P.; Emanuel, P. D.; Zuckerman, K. S.; Cohn, S.; Strauss, L.; Byrd, R. L.; Homans, A.; Chaffee, S.; Nitschke, R.; Gualtieri, R. J. A Pilot Study of Isotretinoin in the Treatment of Juvenile Myelogenous Leukemia. *N. Engl. J. Med.* **1994**, *331*, 1680-1684.
- (158) (a) Hixson, E. J.; Denine, E. P. Comparative Subacute Toxicity of *All-trans*- and 13-*cis*-Retinoic Acid in Swiss Mice. *Toxicol. Appl. Pharmacol.* **1978**, *44*, 29-40. (b) Kamm, J. J. Toxicology, Carcinogenicity, and Teratogenicity of Some Orally Administered Retinoids. *J. Am. Acad. Dermatol.* **1982**, *6*, 652-659. (c) Cohen, M. Tretinoin: A Review of Preclinical Toxicological Studies. *Drug Dev. Res.* **1993**, *30*, 244-51.

- (159) Kochhar, D. M. Teratogenic Activity of Retinoic Acid. *Acta. Pathol. Microbiol. Immunol.* **1967**, 967, 70, 398-404. (b) Willhite, C. C. Molecular Correlates in Retinoid Pharmacology and Toxicology. In *Chemistry and Biology of Synthetic Retinoids*, Dawson, M. I., Okamura, W. H., Eds.; CRC Press: Boca Raton, FL, 1990; pp 539-573. (c) Adams, J. Structure-Activity and Dose-Response Relationships in the Neural and Behavioral Teratogenesis of Retinoids, *Neurotoxicol. Teratol.* **1993**, 15, 193-202.
- (160) Carolin, K. A.; Pass, H. A. Bexarotene (Targretin) for Cutaneous T-Cell Lymphoma. *Med. Lett. Drugs Ther.* **2000**, 42, 31-32.
- (161) Beard, R. L.; Colon, D. F.; Klein, E. S.; Vorse, K. A.; Chandraratna, R. A. S. Differential RXR and RAR Activity of Stilbene Retinoid Analogs Bearing Thiazole and Imidazole Carboxylic Acids. *Bioorg. Med. Chem. Lett.* **1995**, 5, 2729-2734.
- (162) Wei, X.; Taylor, R. J. K. In Situ Manganese Dioxide Alcohol Oxidation-Wittig Reactions: Preparation of Bifunctional Dienyl Building Blocks. *J. Org. Chem.*, **2000**, 65, 616-620.
- (163) Boehm, M. F.; Zhang, L.; Zhi, L.; McClurg, M. R.; Berger, E.; Wagoner, M.; Mais, D. E.; Suto, C. M.; Davies, P. J. A.; Heyman, R. A.; Nadzan, A. M. Design and Synthesis of Potent Retinoid X Receptor Selective Ligands That Induce Apoptosis in Leukemia Cells. *J. Med. Chem.* **1995**, 38, 3146-3155.

APPENDIX A

Spectroscopic Data for Compounds in “The Large Scale Synthesis of (9Z)-UAB30 and the Effect on Prevention of Chemically-Induced Mammary Tumors”

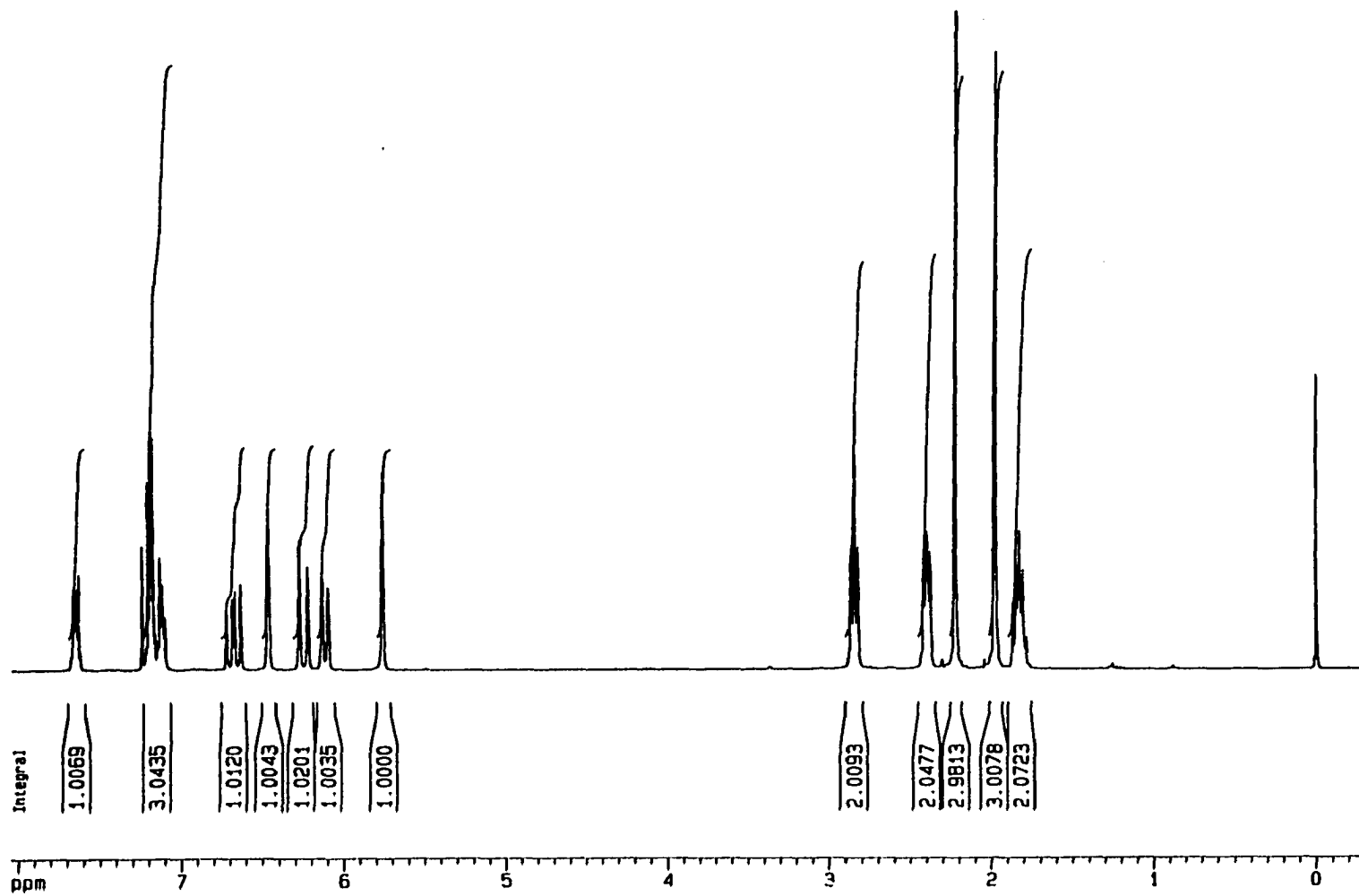


Figure 1. ^1H NMR Spectrum (300 MHz) of Compound I-1 (CDCl_3).

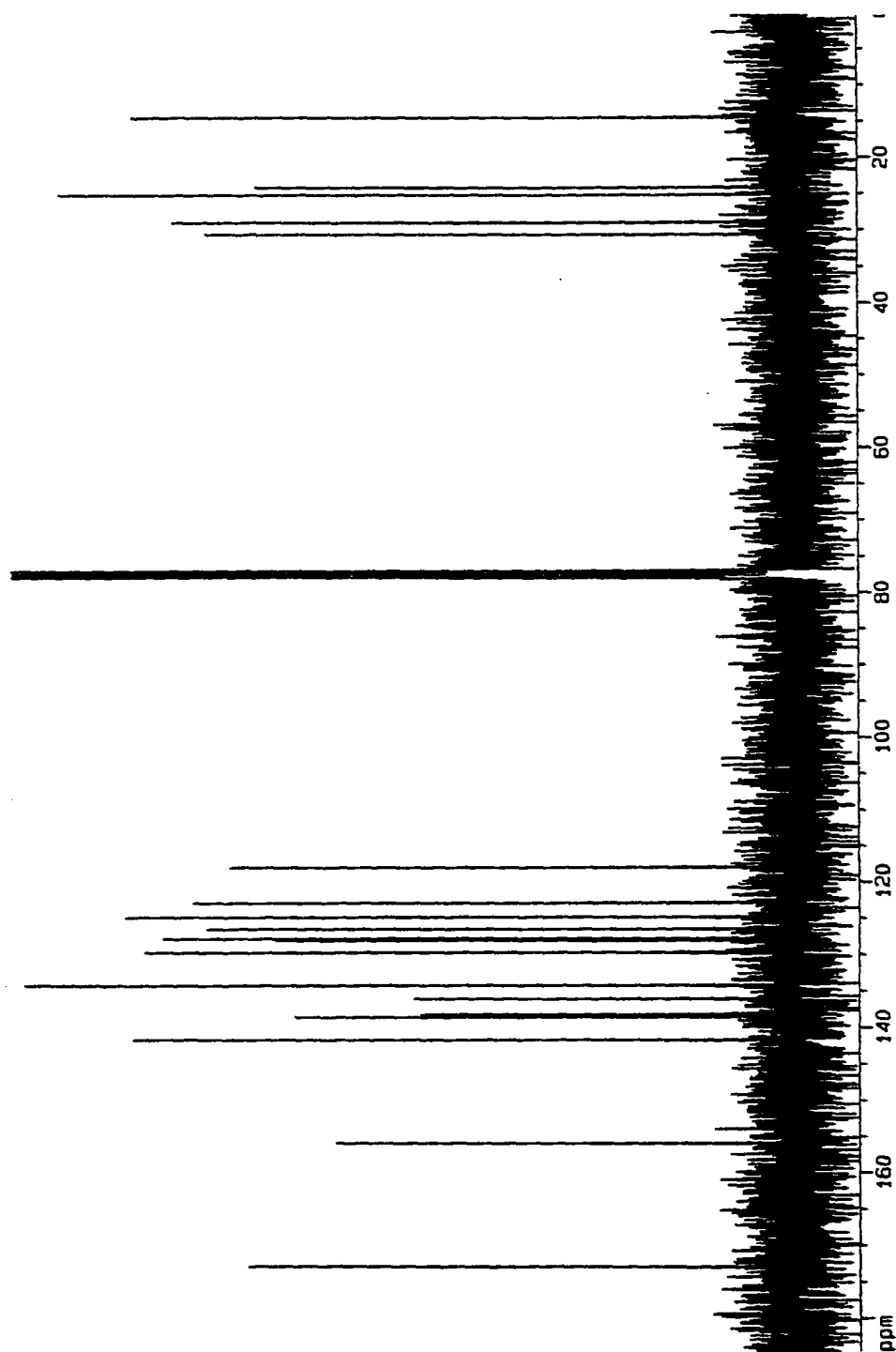


Figure 2. ^{13}C NMR (300 MHz) of Compound I-1 (CDCl_3).

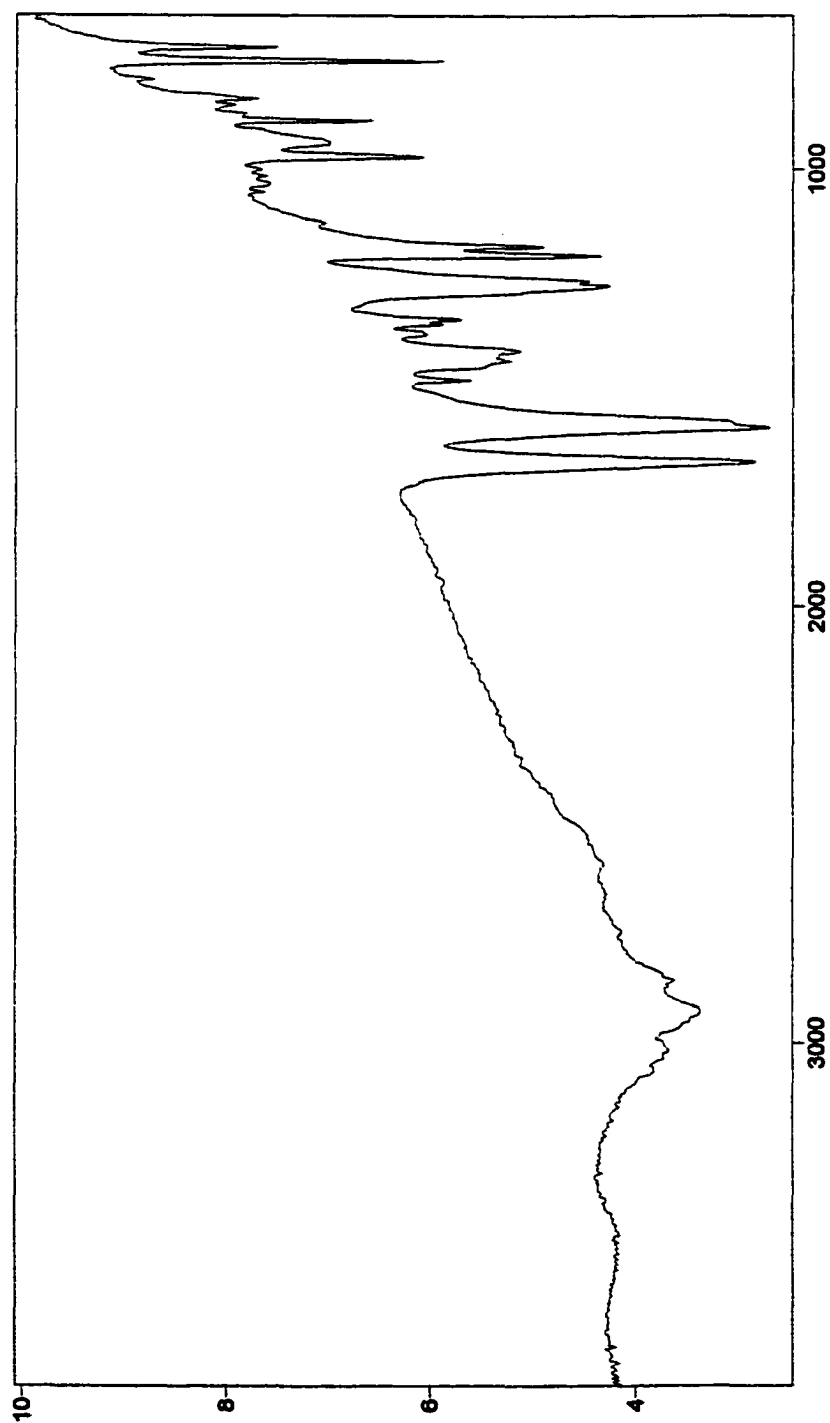


Figure 3. FTIR of Compound I-1 (KBr).

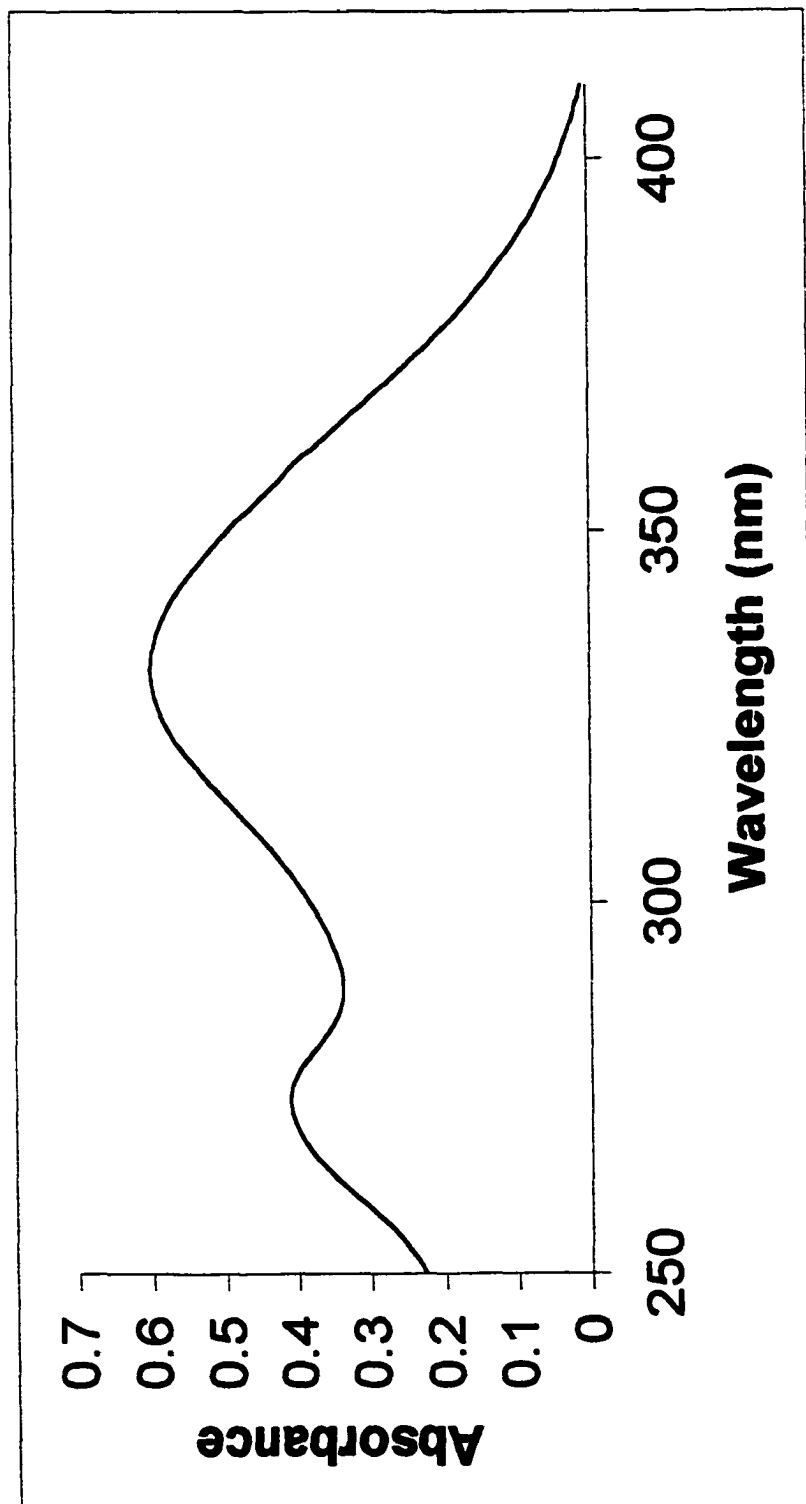


Figure 4. UV-Vis of Compound I-1 (MeOH).

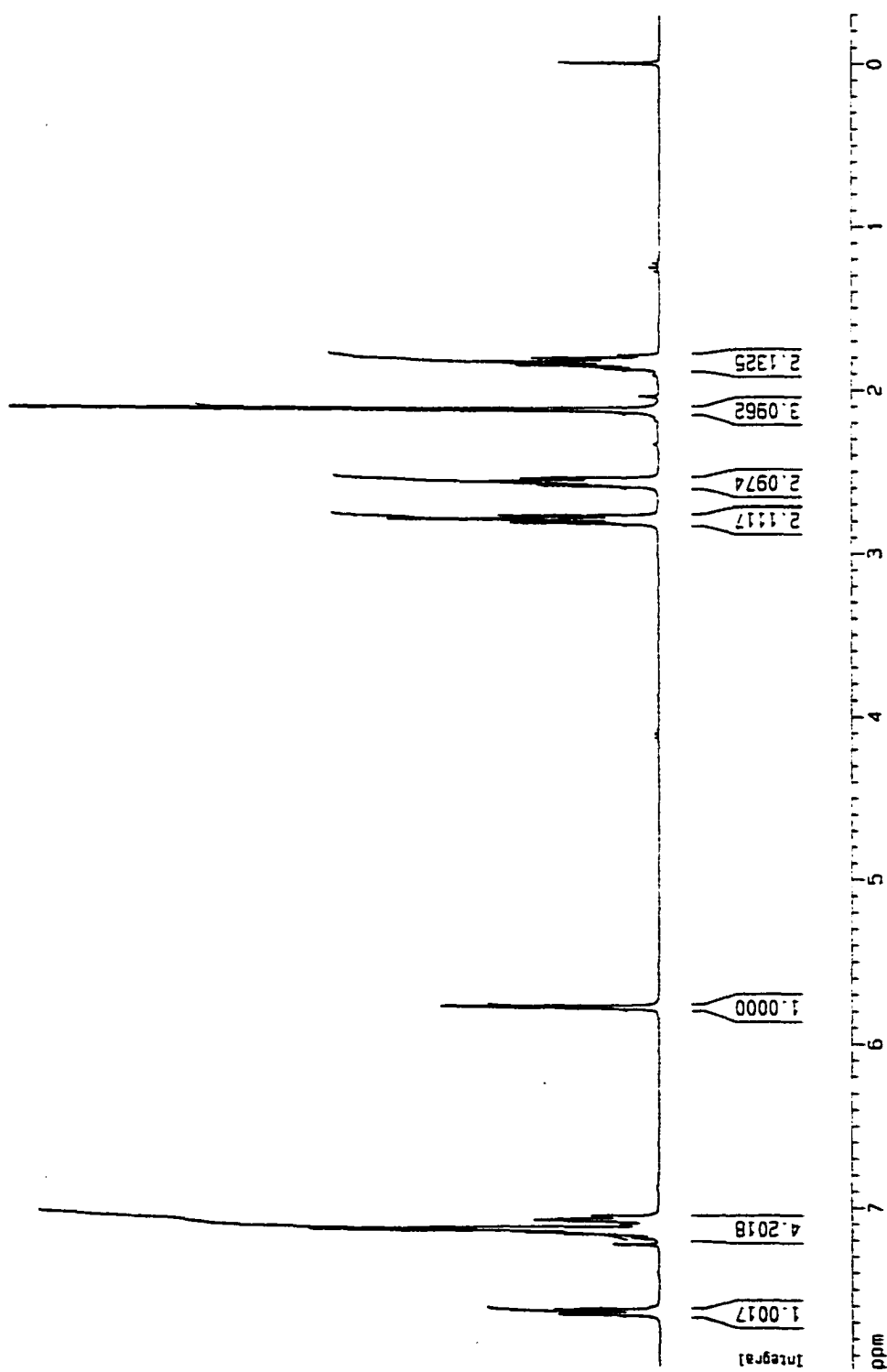


Figure 5. ^1H NMR (300 MHz) of Compound I-3 (CDCl_3).

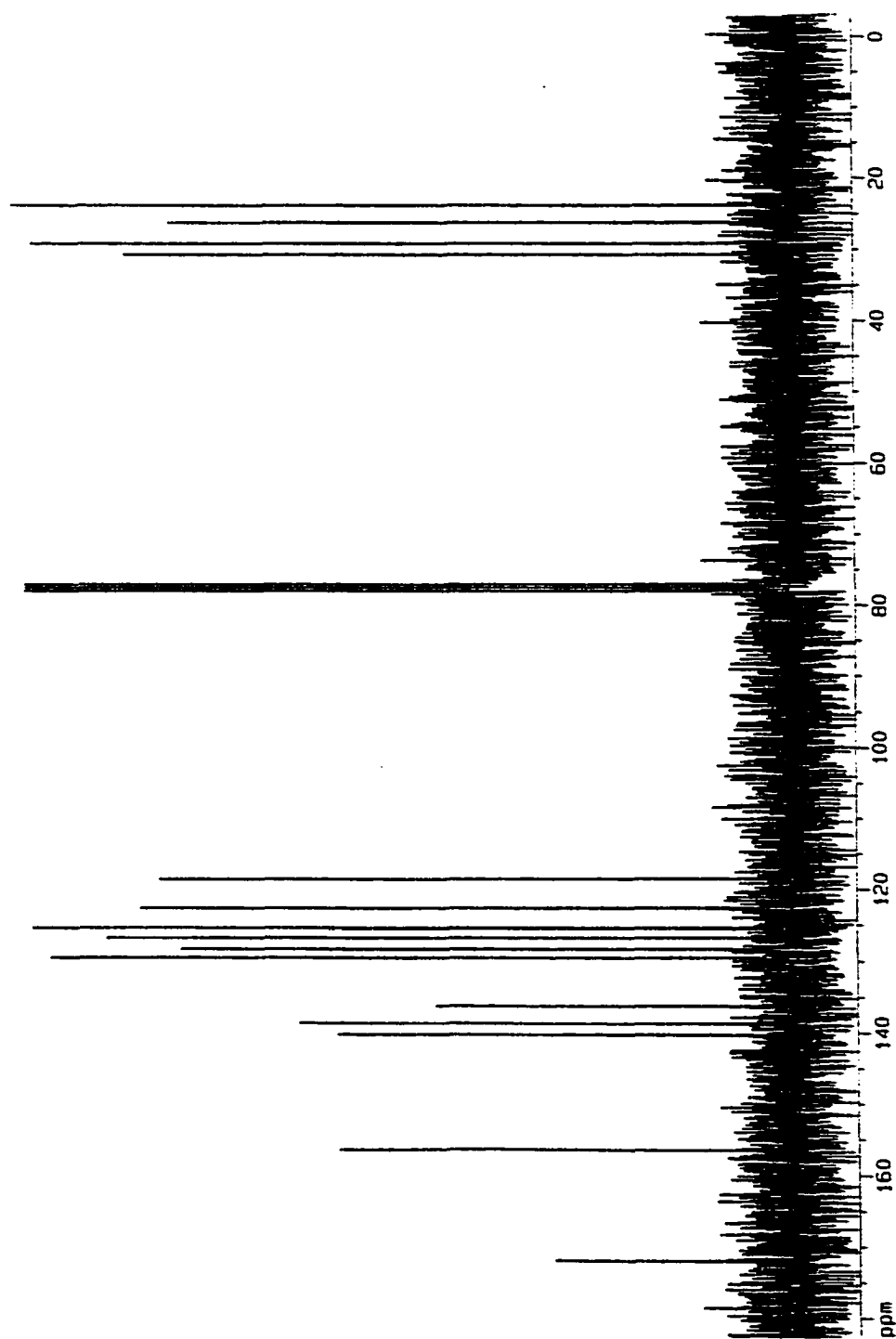


Figure 6. ^{13}C NMR (300 MHz) of Compound I-3 (CDCl_3).

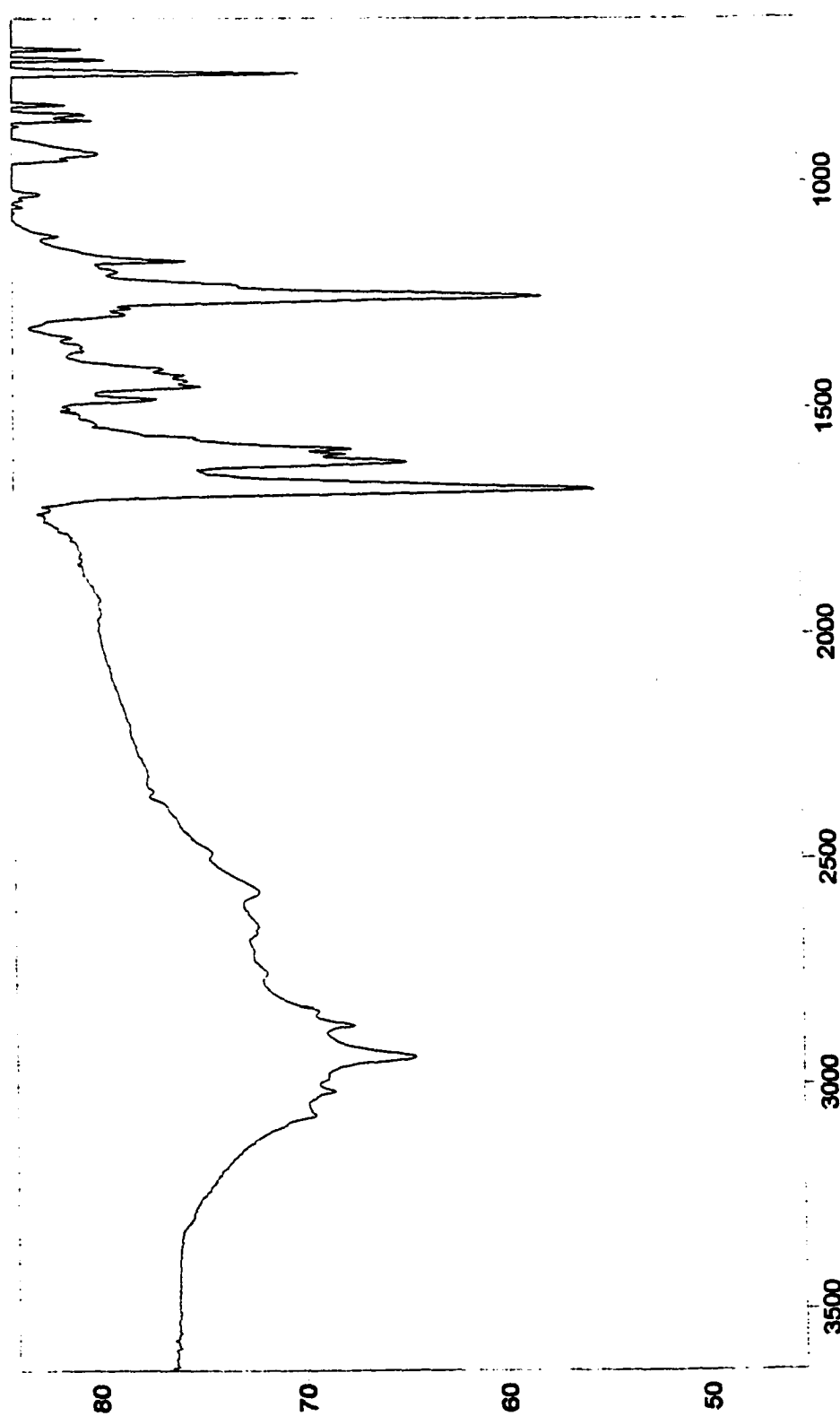


Figure 7. FTIR of Compound I-3 (KBr).

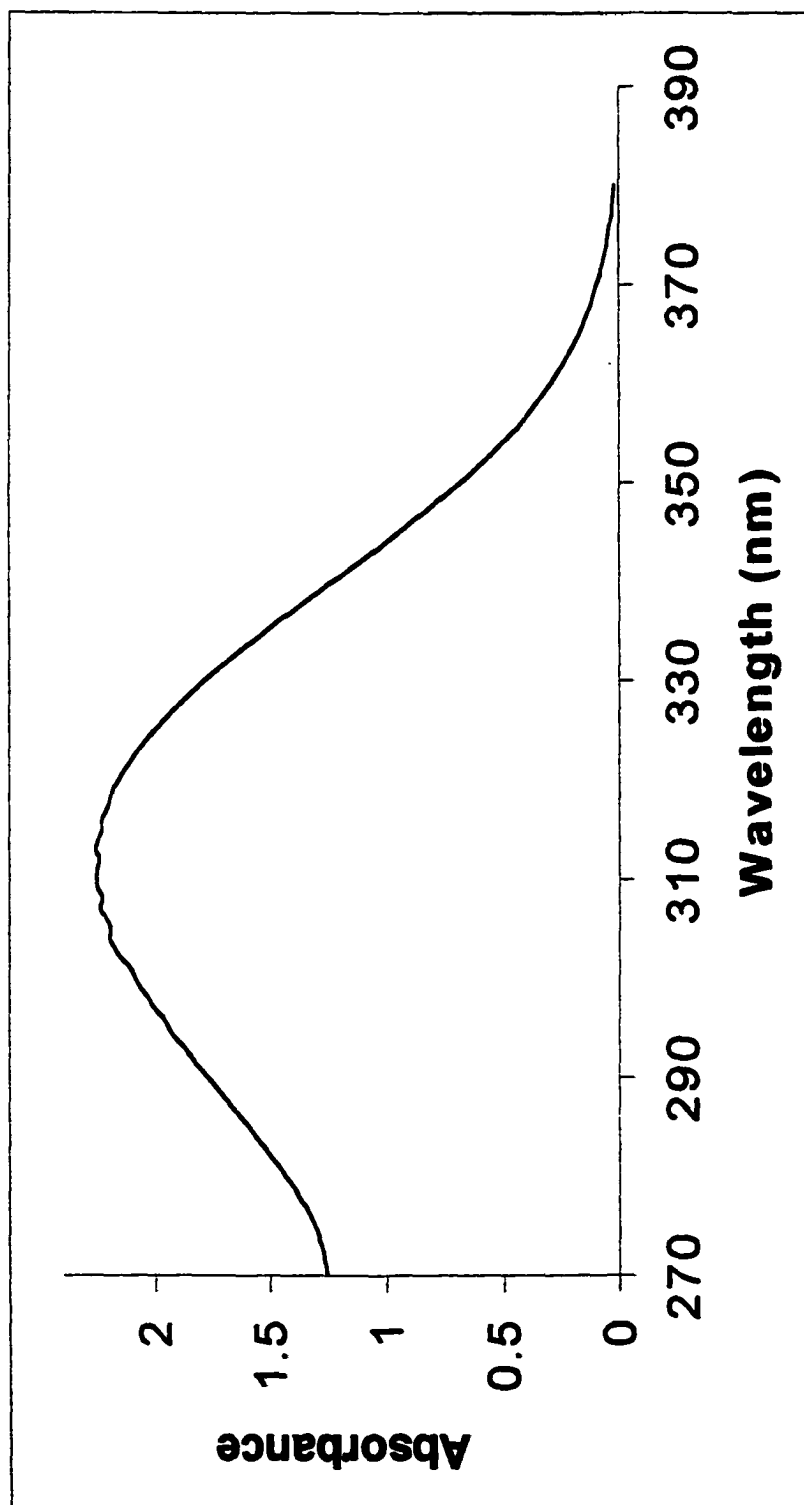


Figure 8. UV-Vis of Compound 1-3 (MeOH).

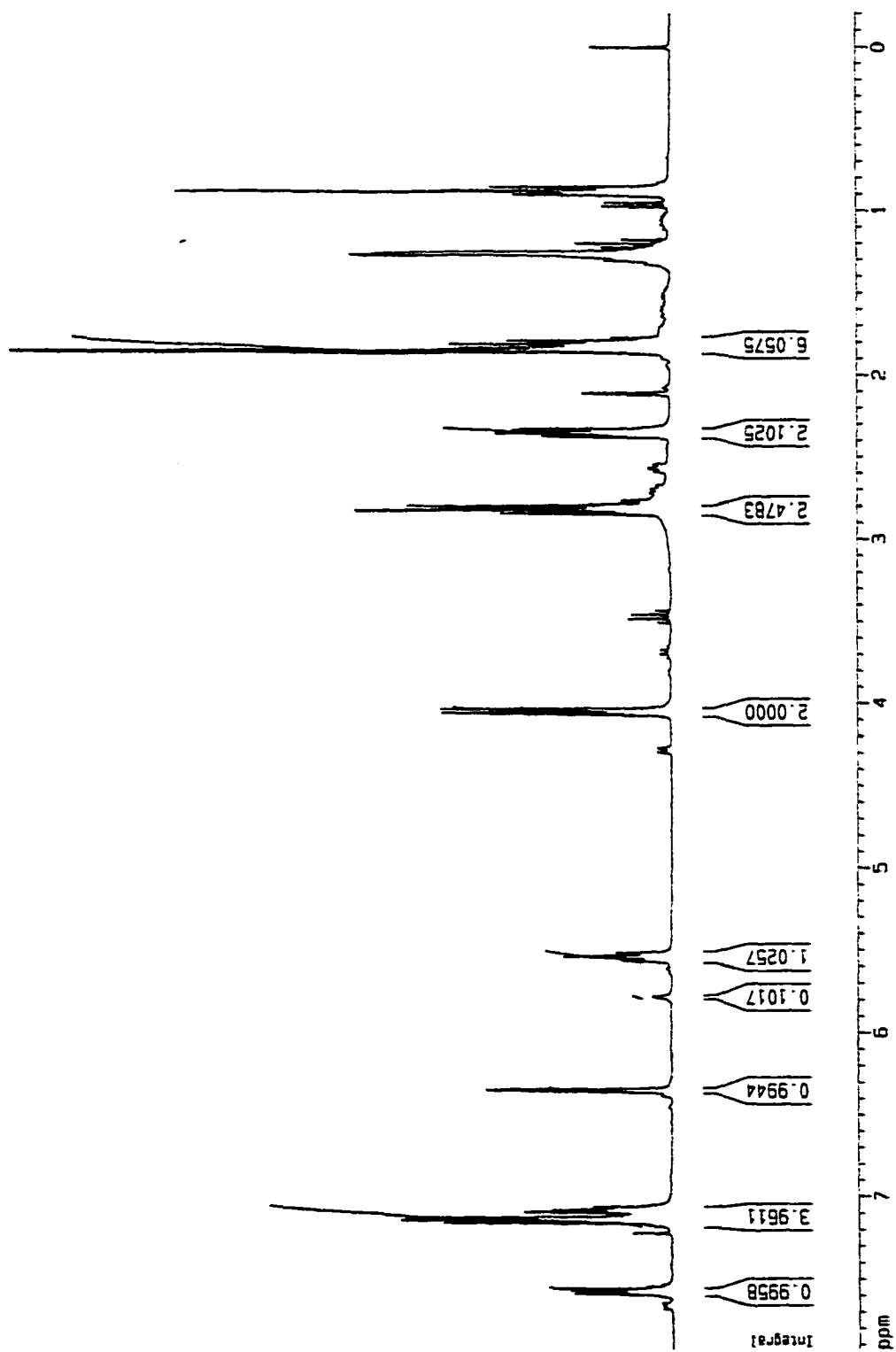


Figure 9. ^1H NMR (300 MHz) of Compound 1-4 (CDCl_3).

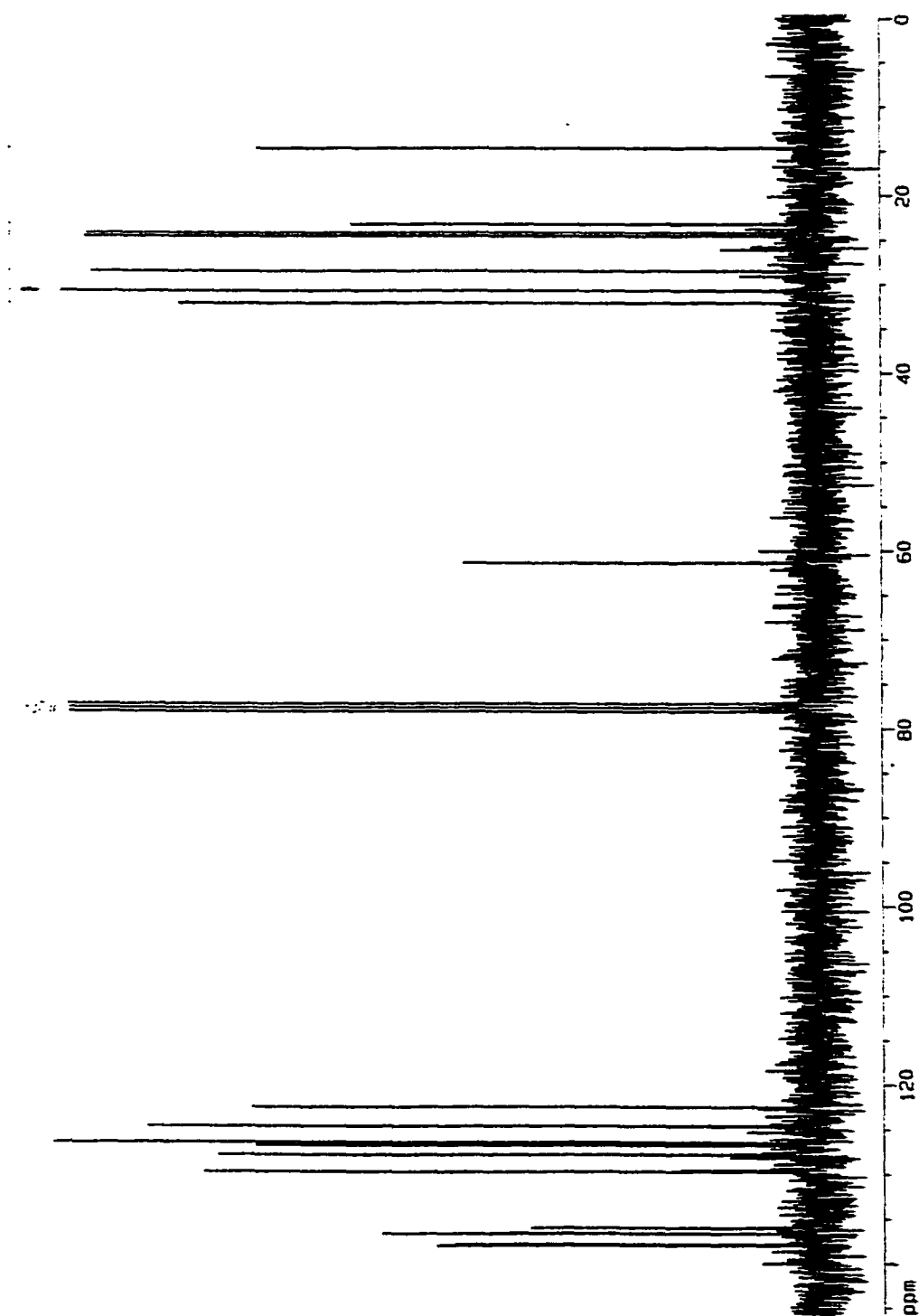


Figure 10. ^{13}C NMR (300 MHz) of Compound I-4 (CDCl_3).

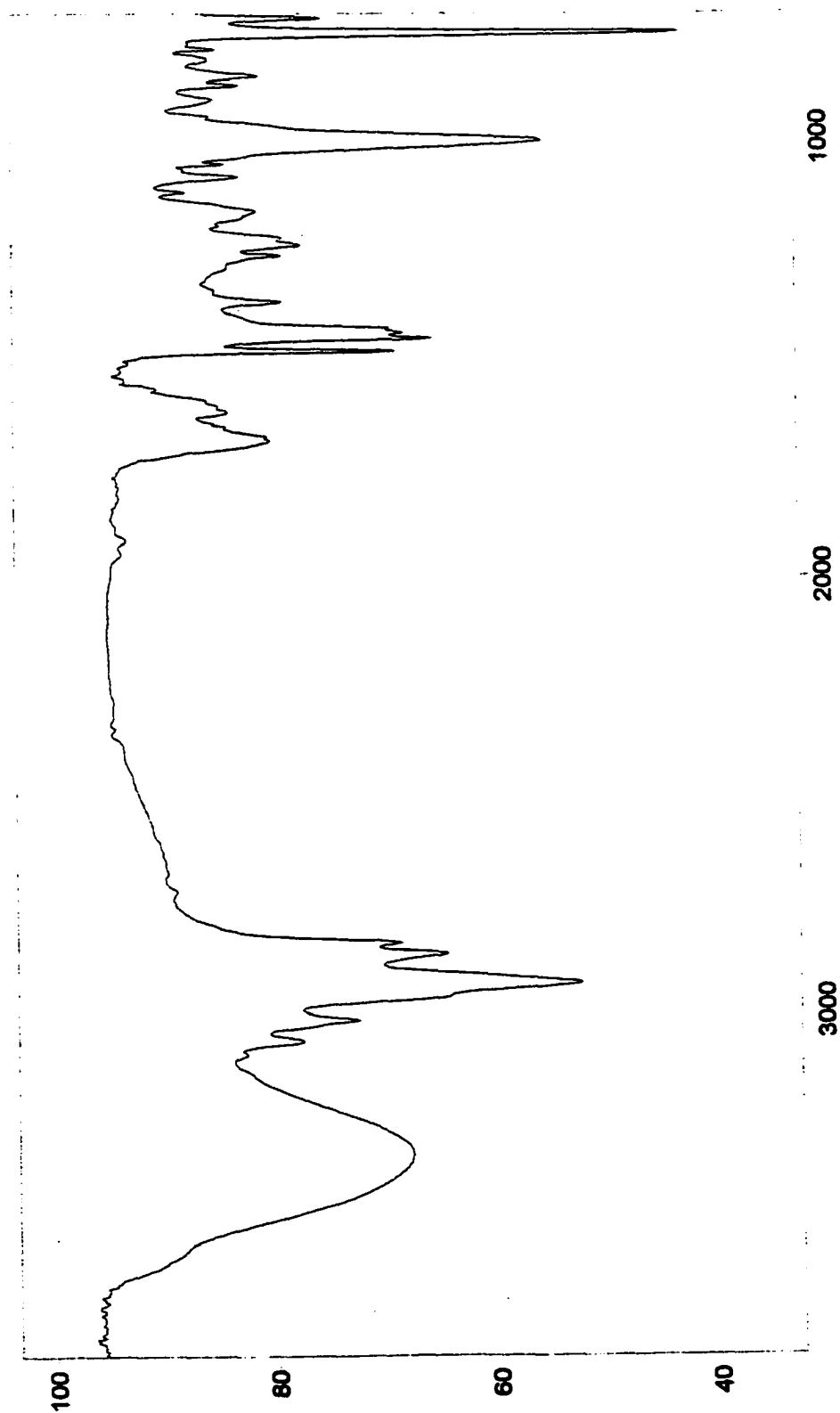


Figure 11. FTIR of Compound I-4 (KBr).

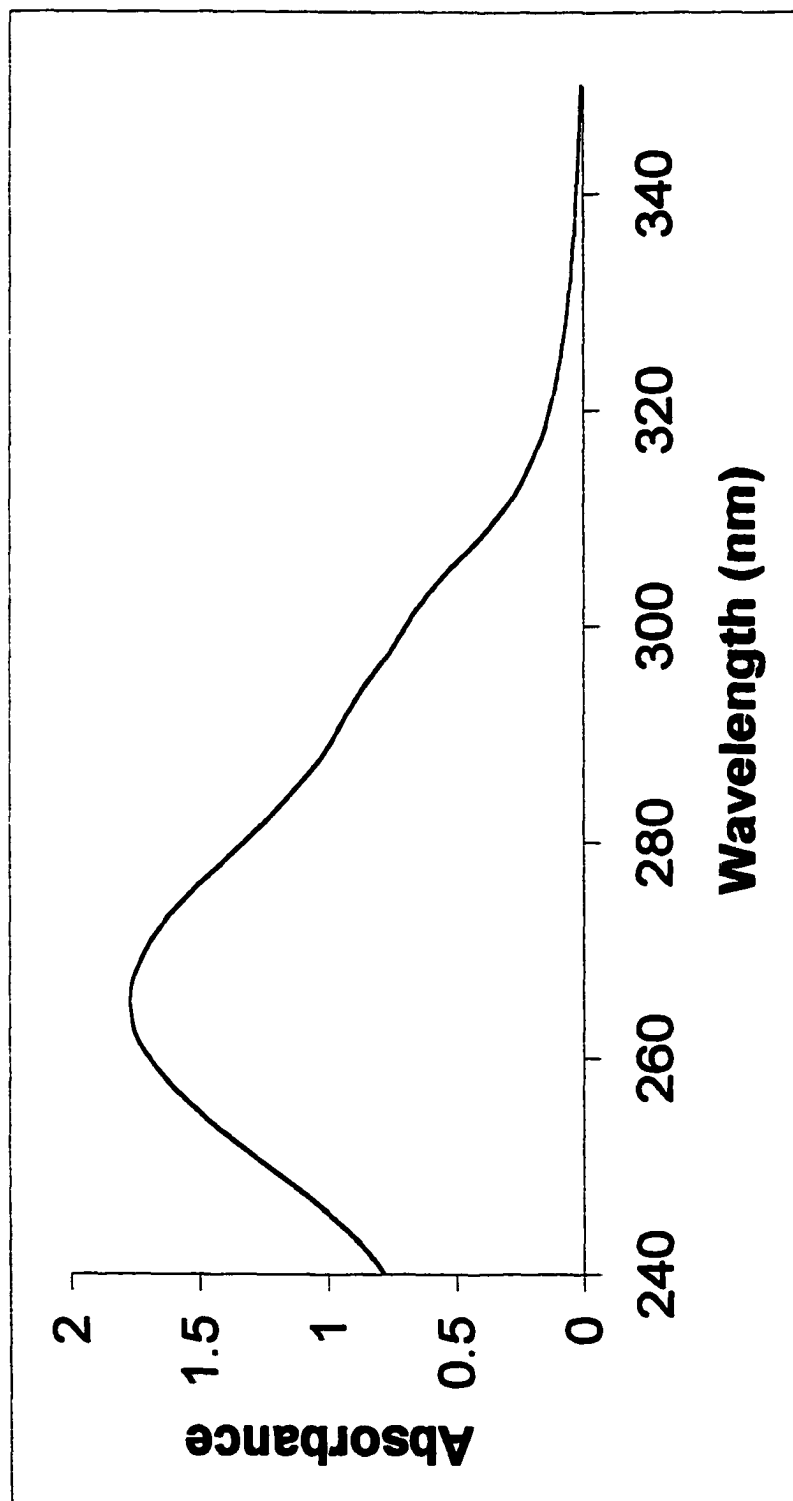


Figure 12. UV-Vis of Compound I-4 (MeOH).

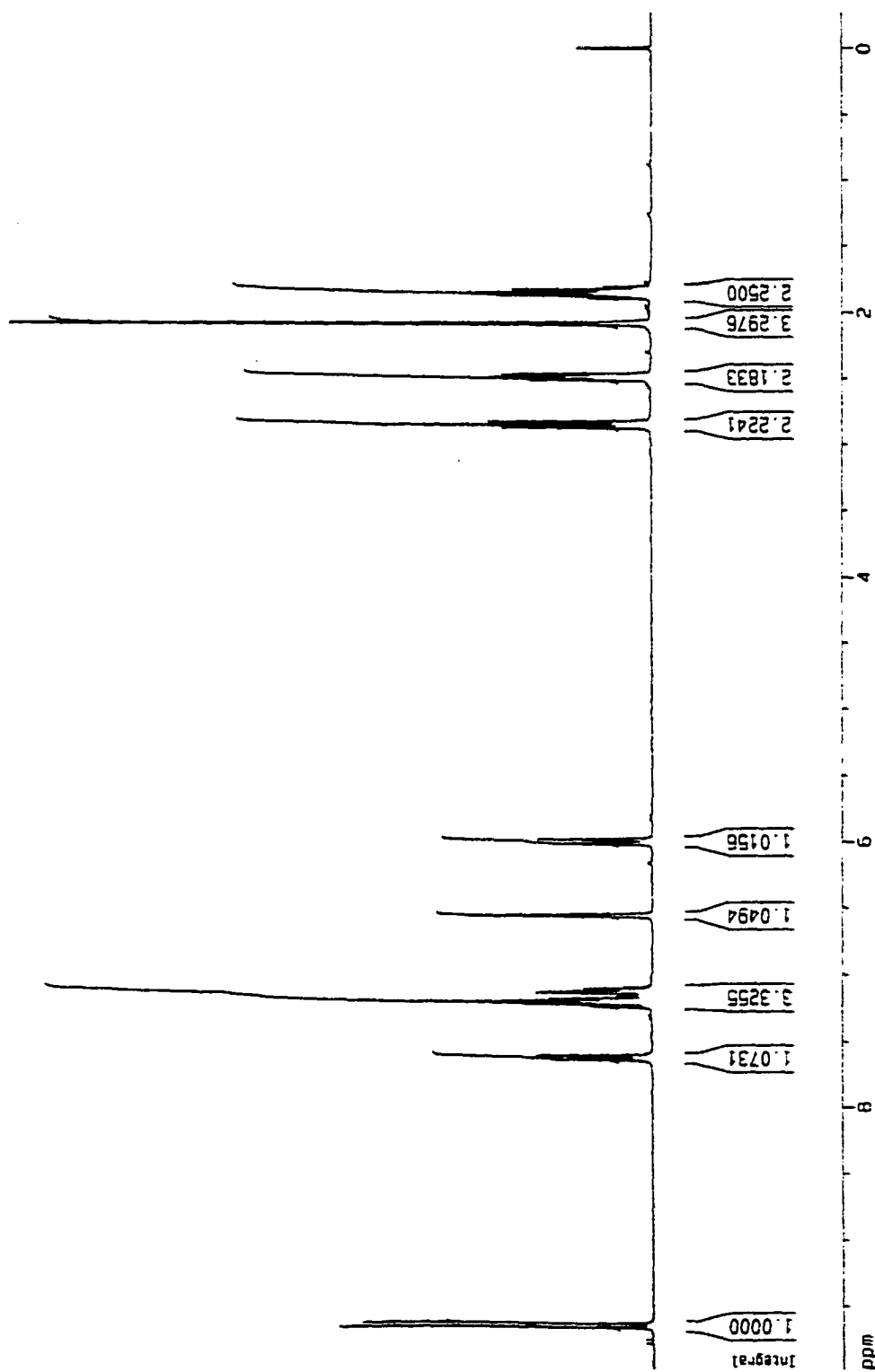


Figure 13. ^1H NMR (300 MHz) of Compound 1-(9Z)-5 (CDCl_3).

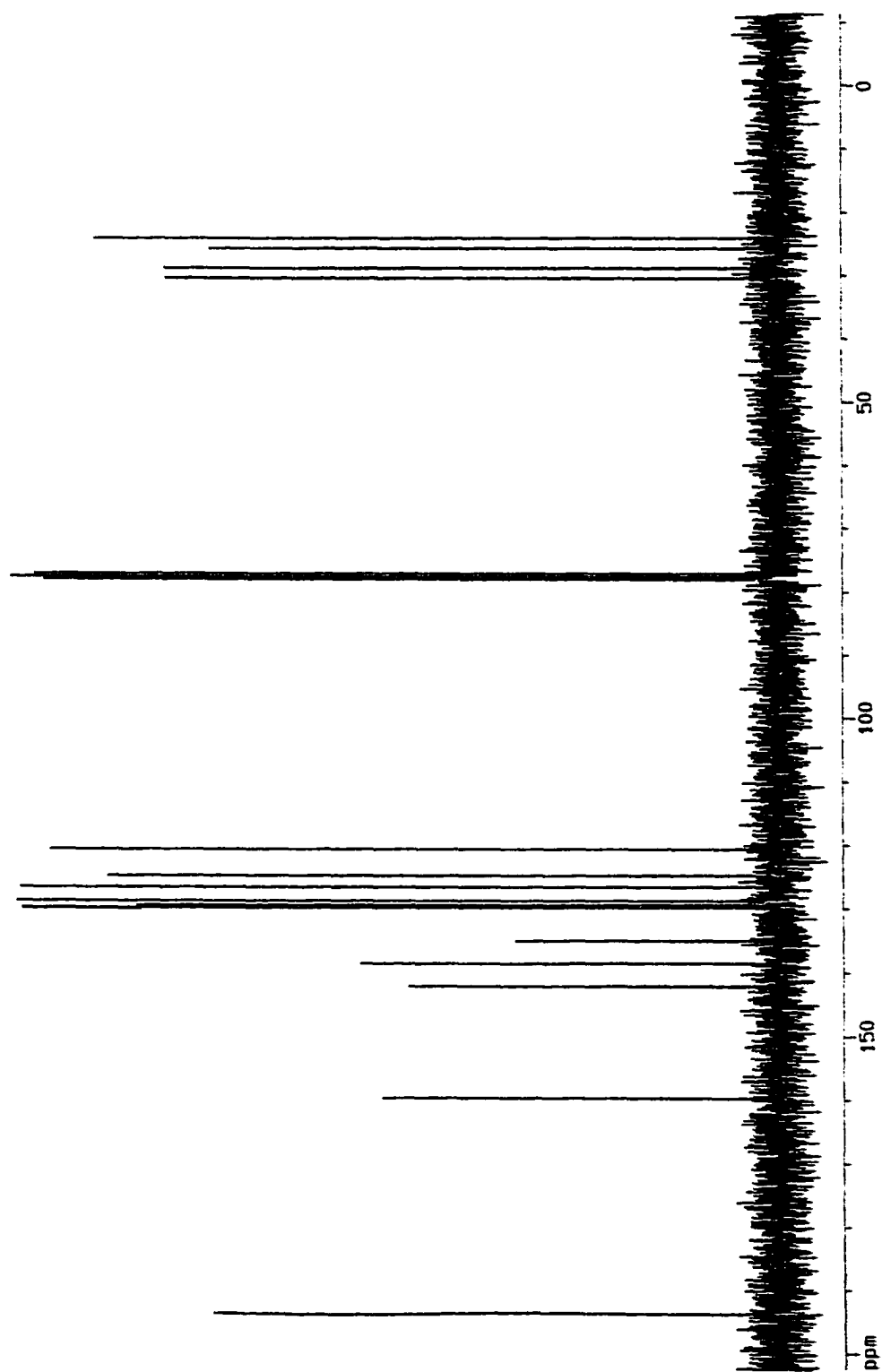


Figure 14. ^{13}C NMR (300 MHz) of Compound 1-(9Z)-5 (CDCl_3).

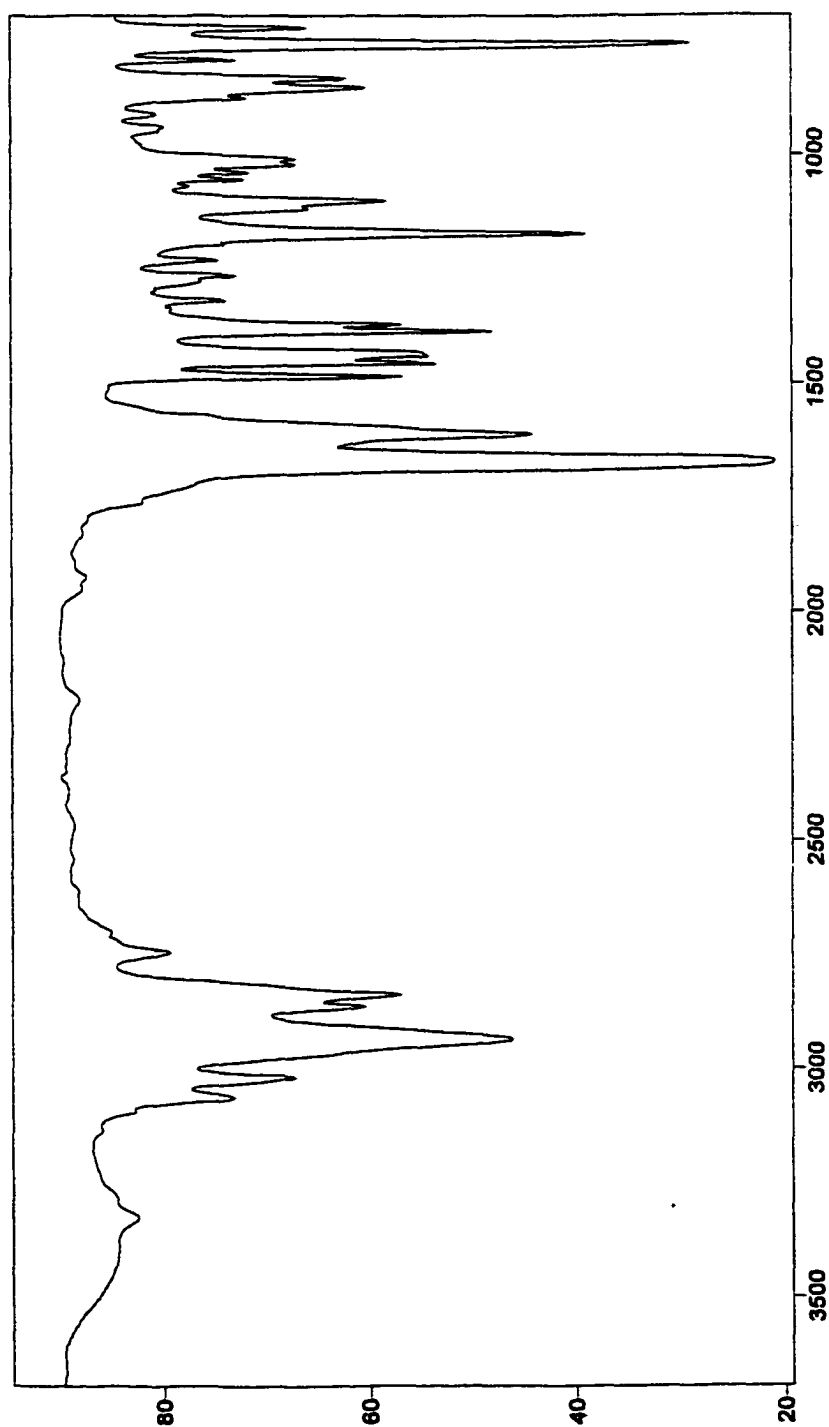


Figure 15. FTIR of Compound **1-(9Z)-5** (KBr).

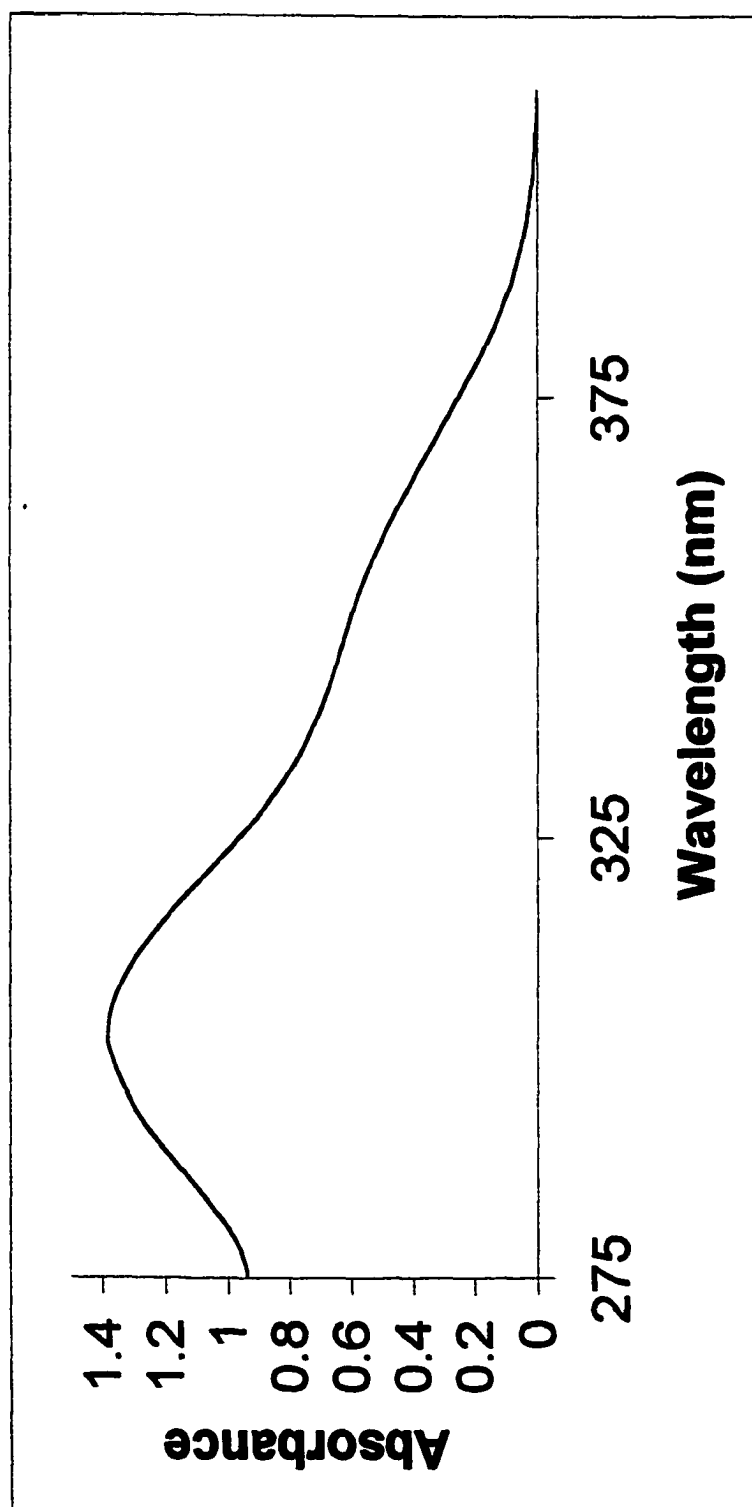


Figure 16. UV-Vis of Compound **1-(9Z)-5** (MeOH).

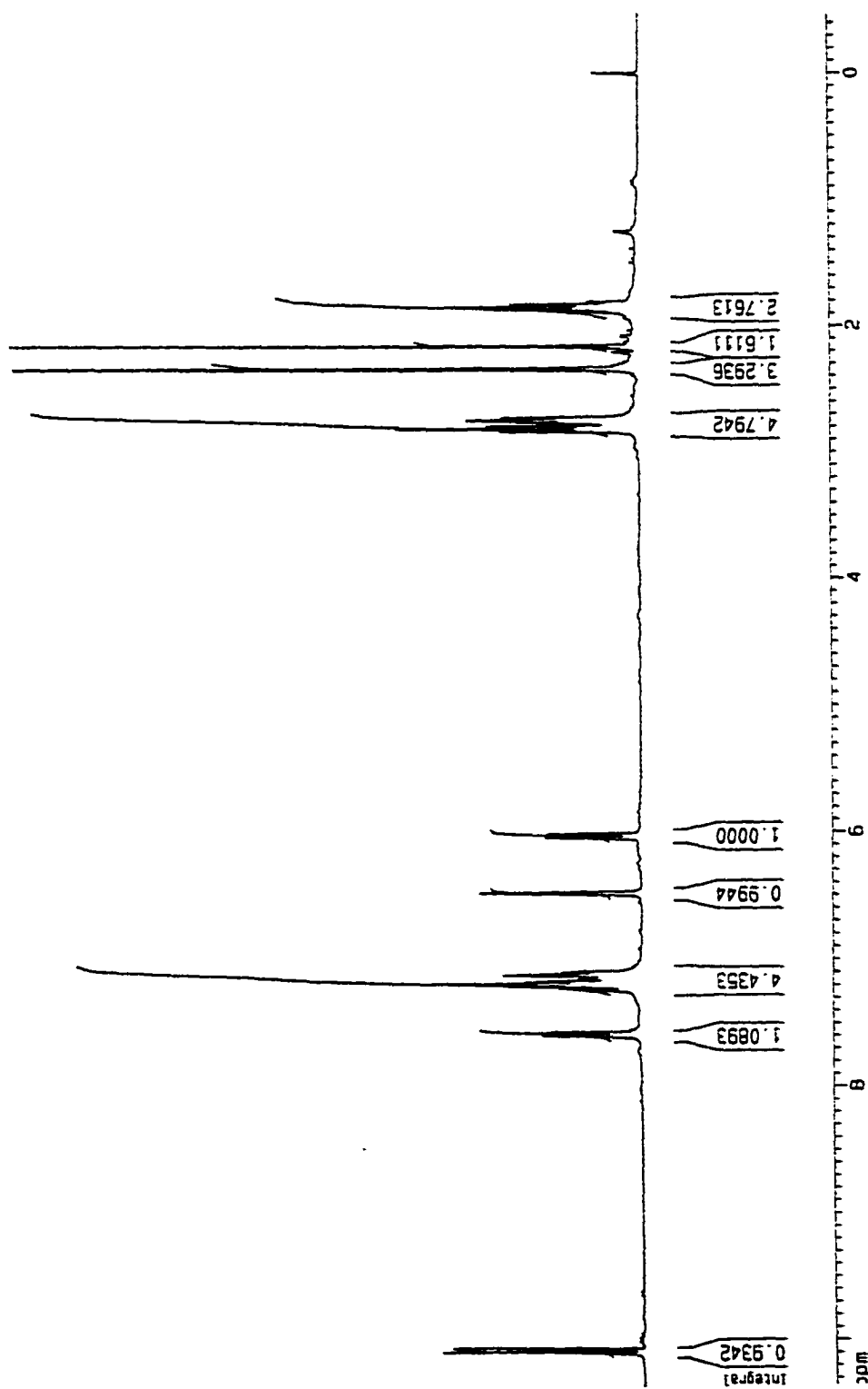


Figure 17. ^1H NMR (300 MHz) of Compound 1-(*all-E*)-5 (CDCl_3).

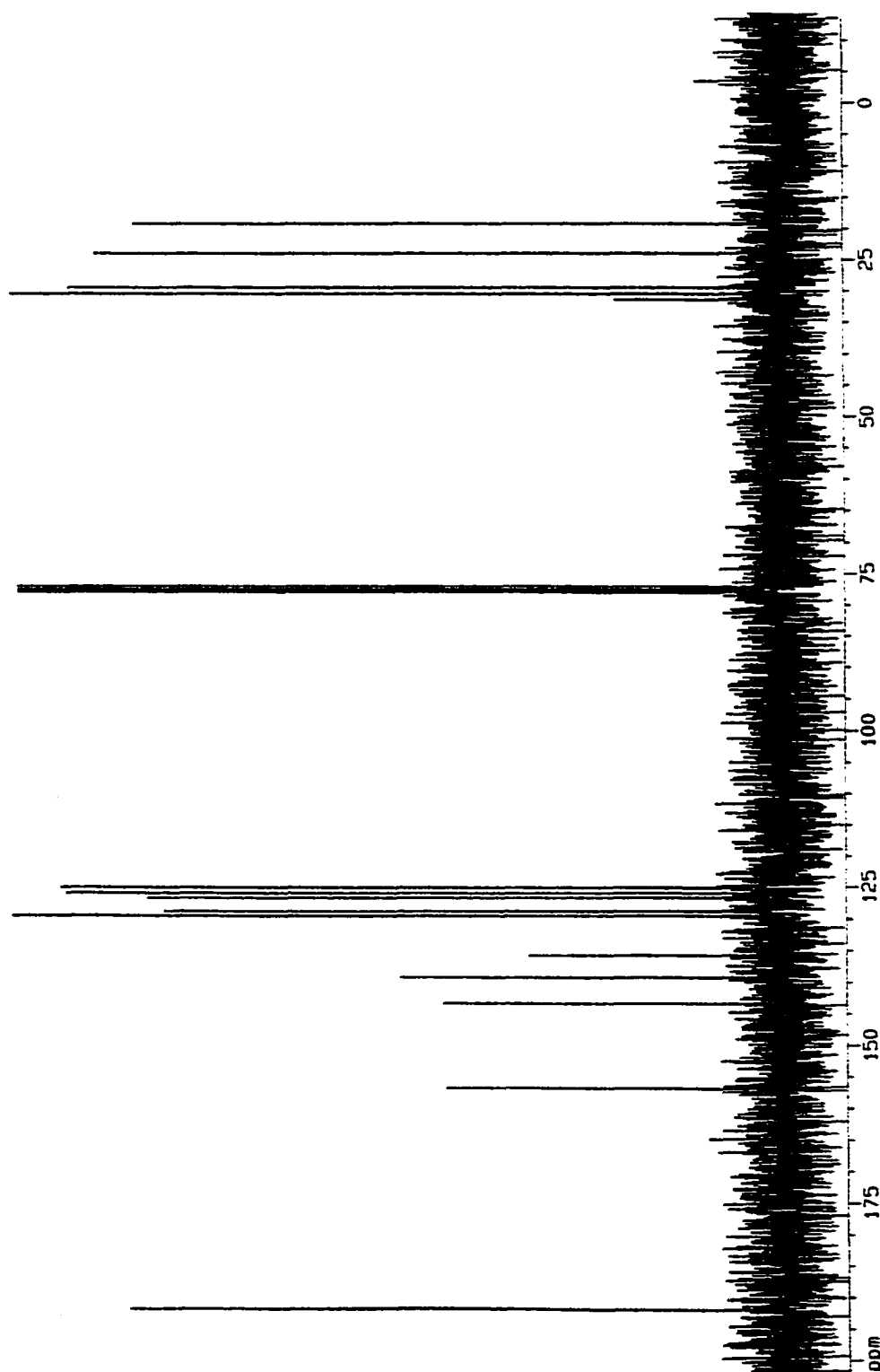


Figure 18. ^{13}C NMR (300 MHz) of Compound 1-(*all-E*)-5 (CDCl_3).

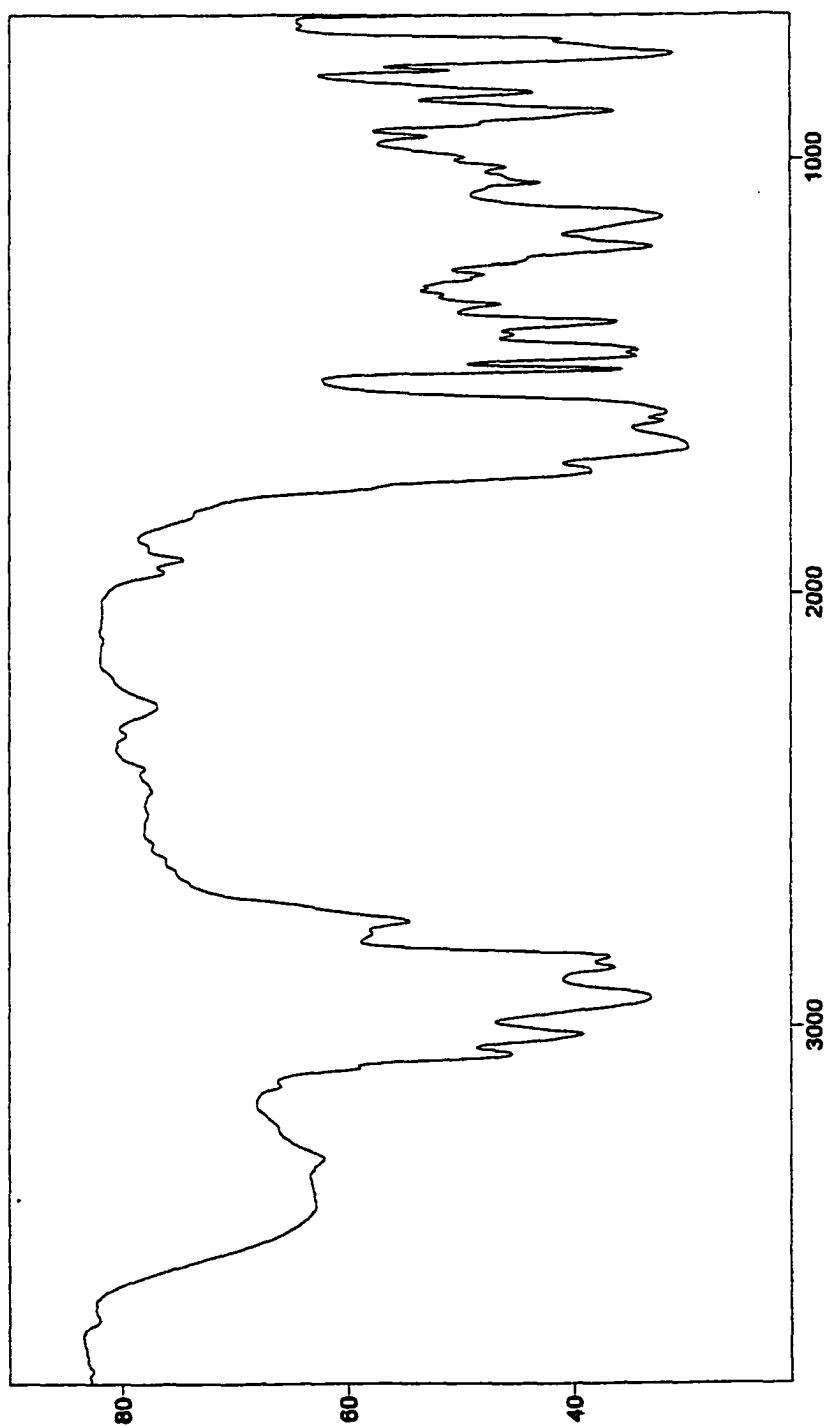


Figure 19. FTIR of Compound **1-(*all-E*)-5** (KBr).

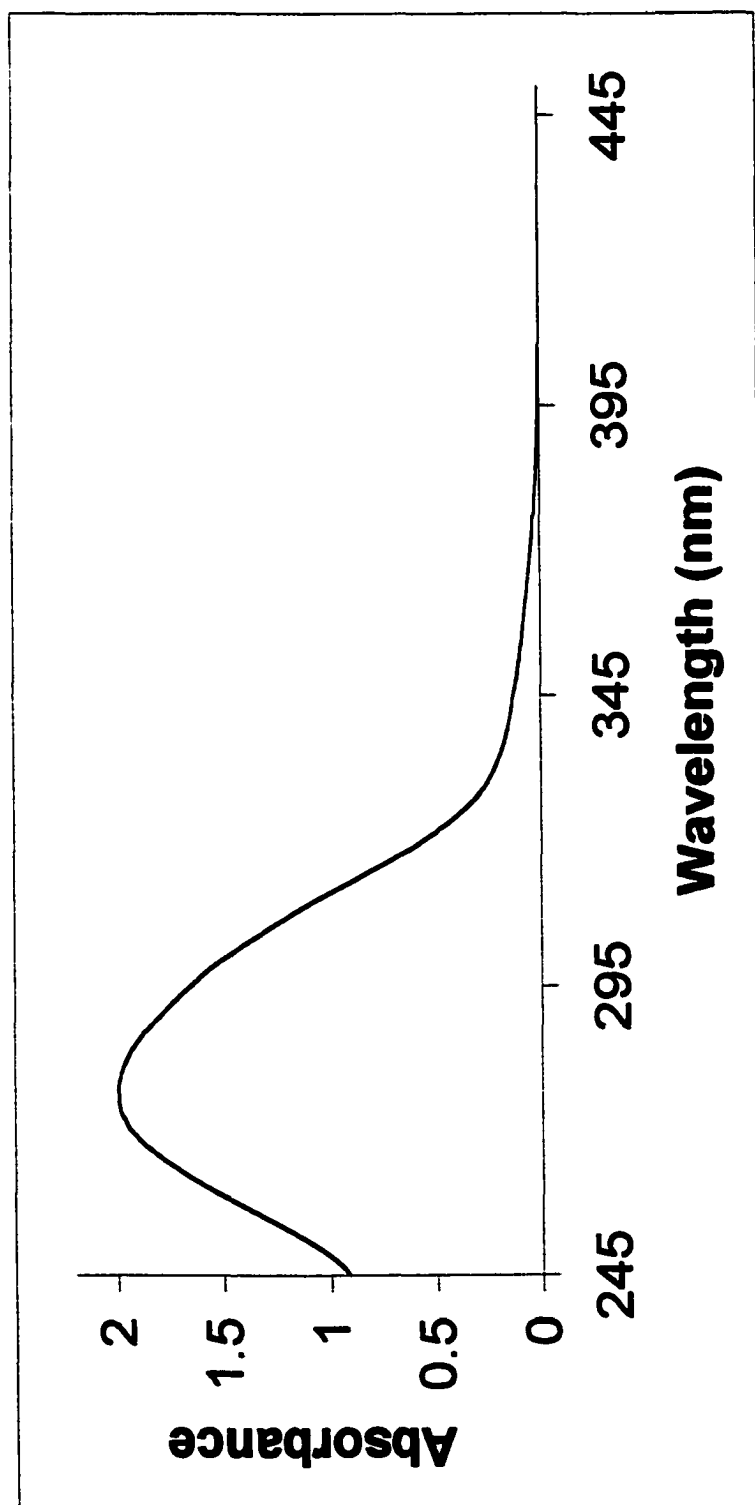


Figure 20. UV-Vis of Compound 1-(*all-E*)-5 (MeOH).

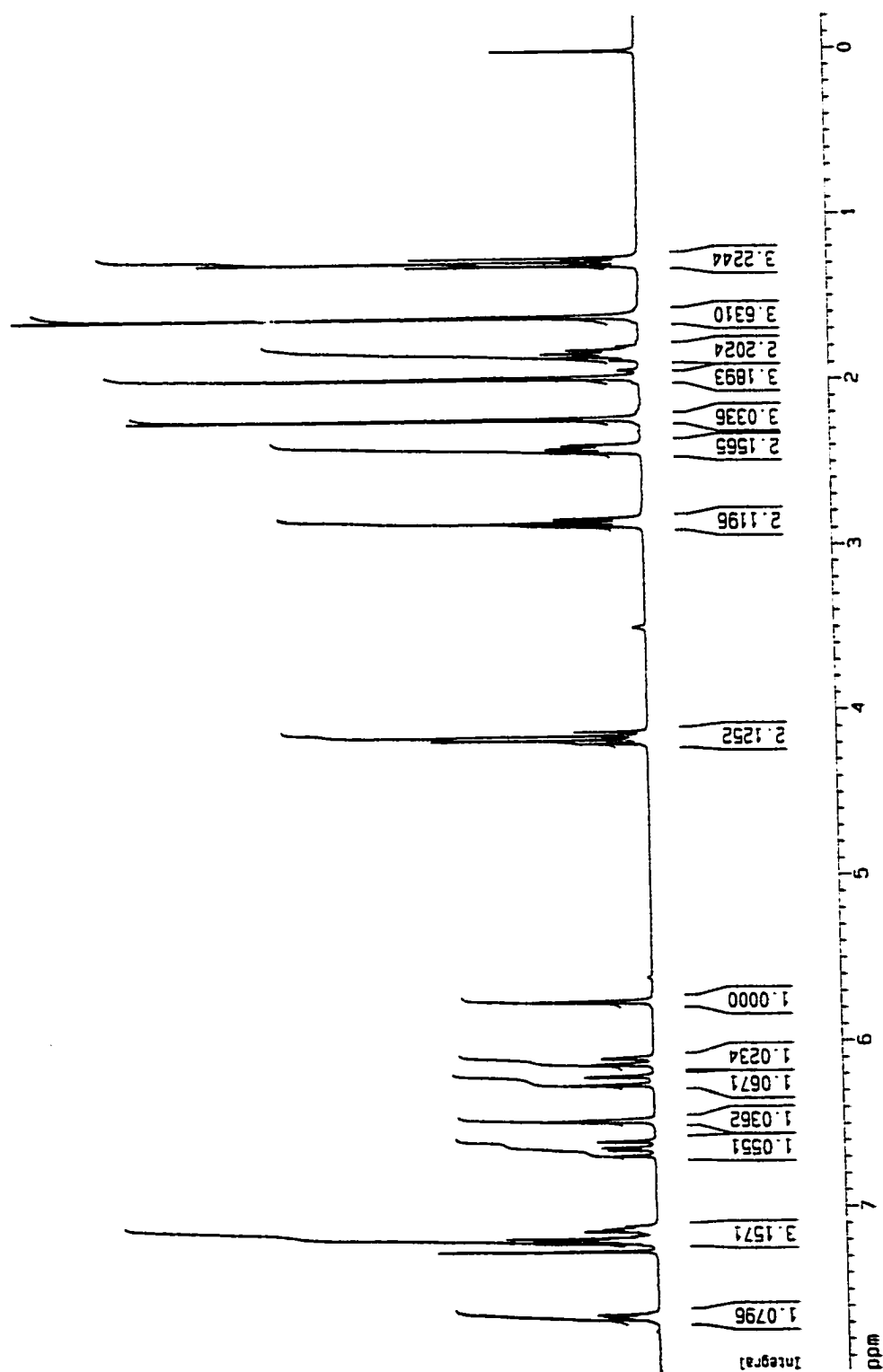


Figure 21. ^1H NMR Spectrum (300 MHz) of Compound 1-6 (CDCl_3).

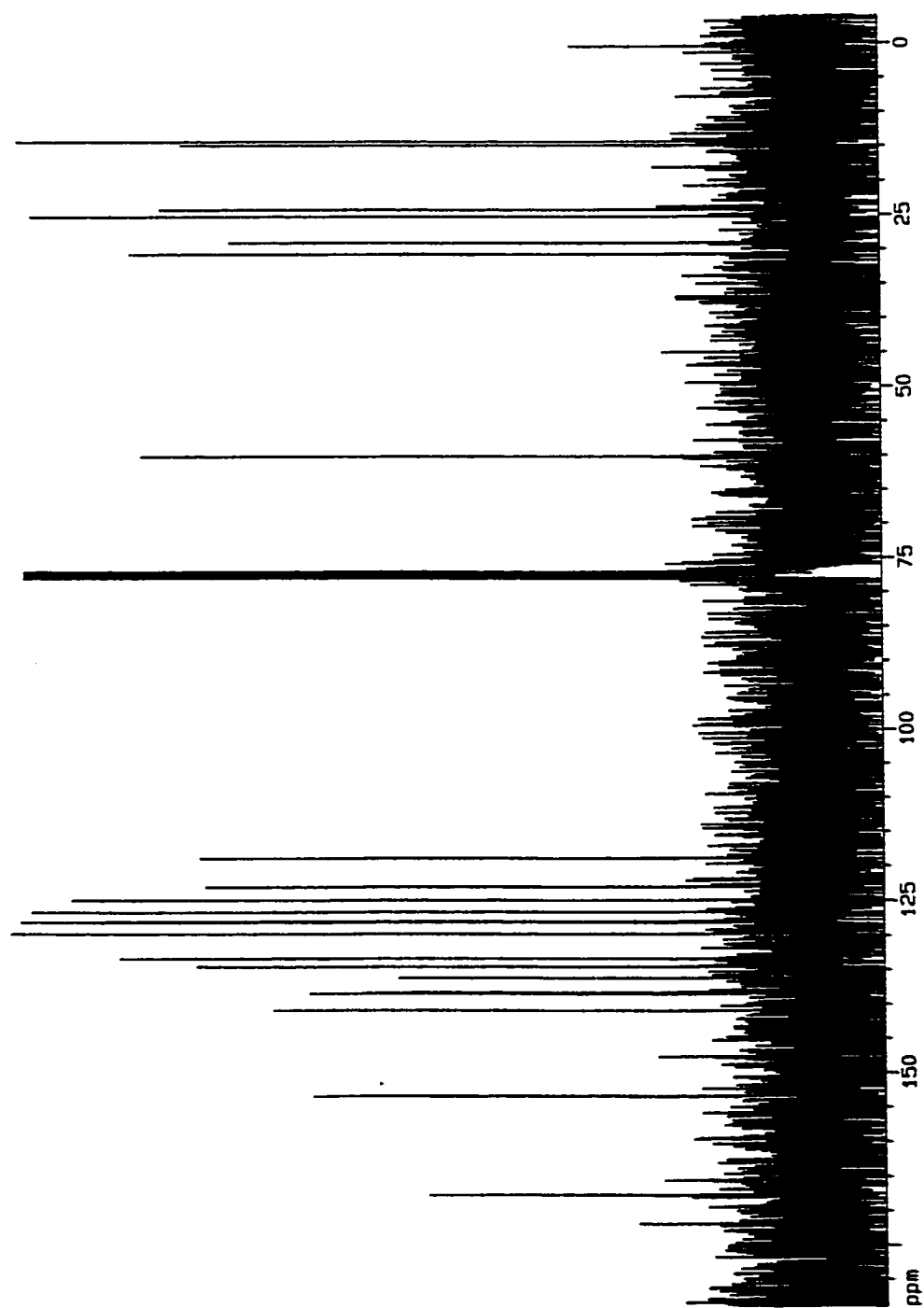


Figure 22. ^{13}C NMR (300 MHz) of Compound 1-6 (CDCl_3).

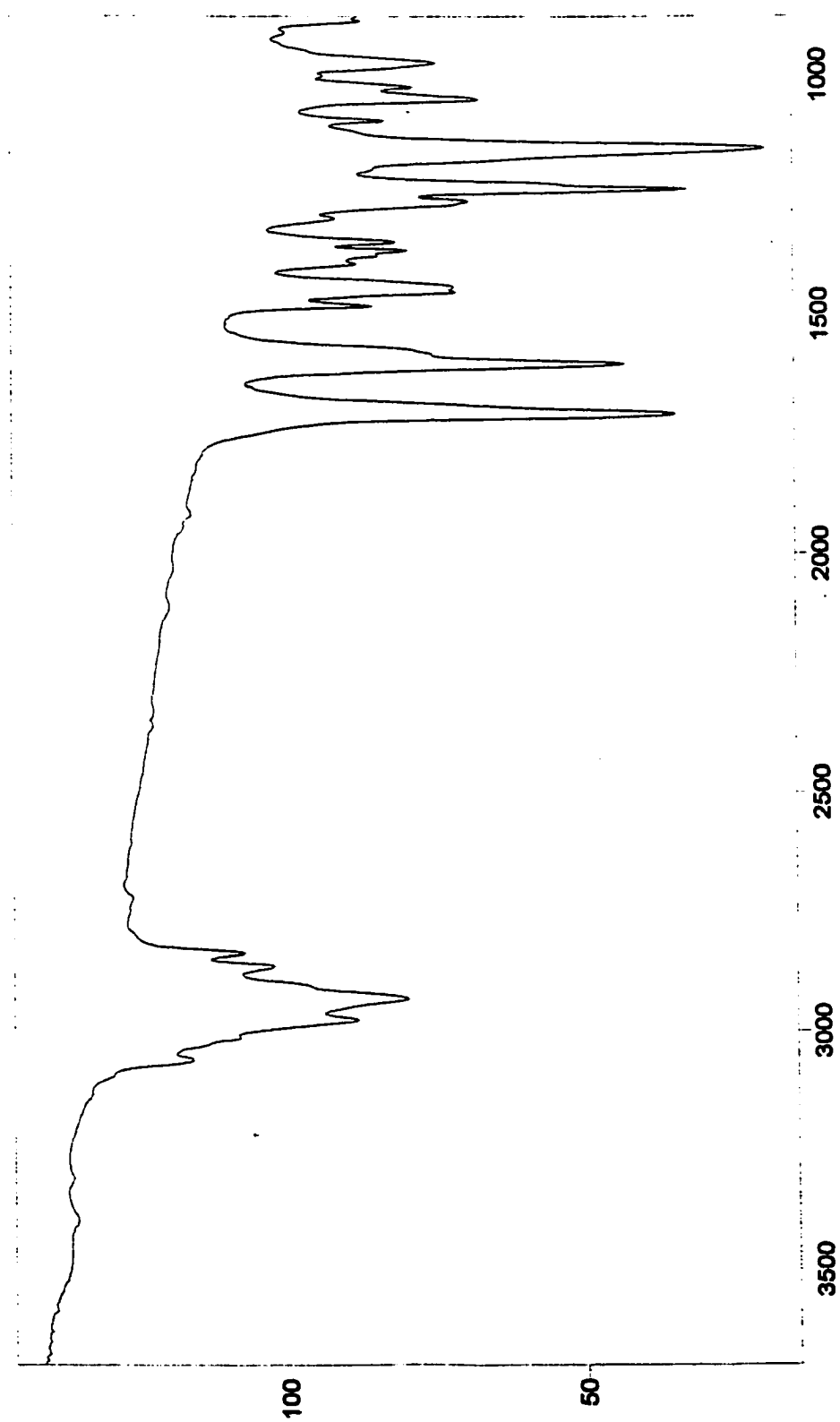


Figure 23. FTIR of Compound 1-6 (KBr).

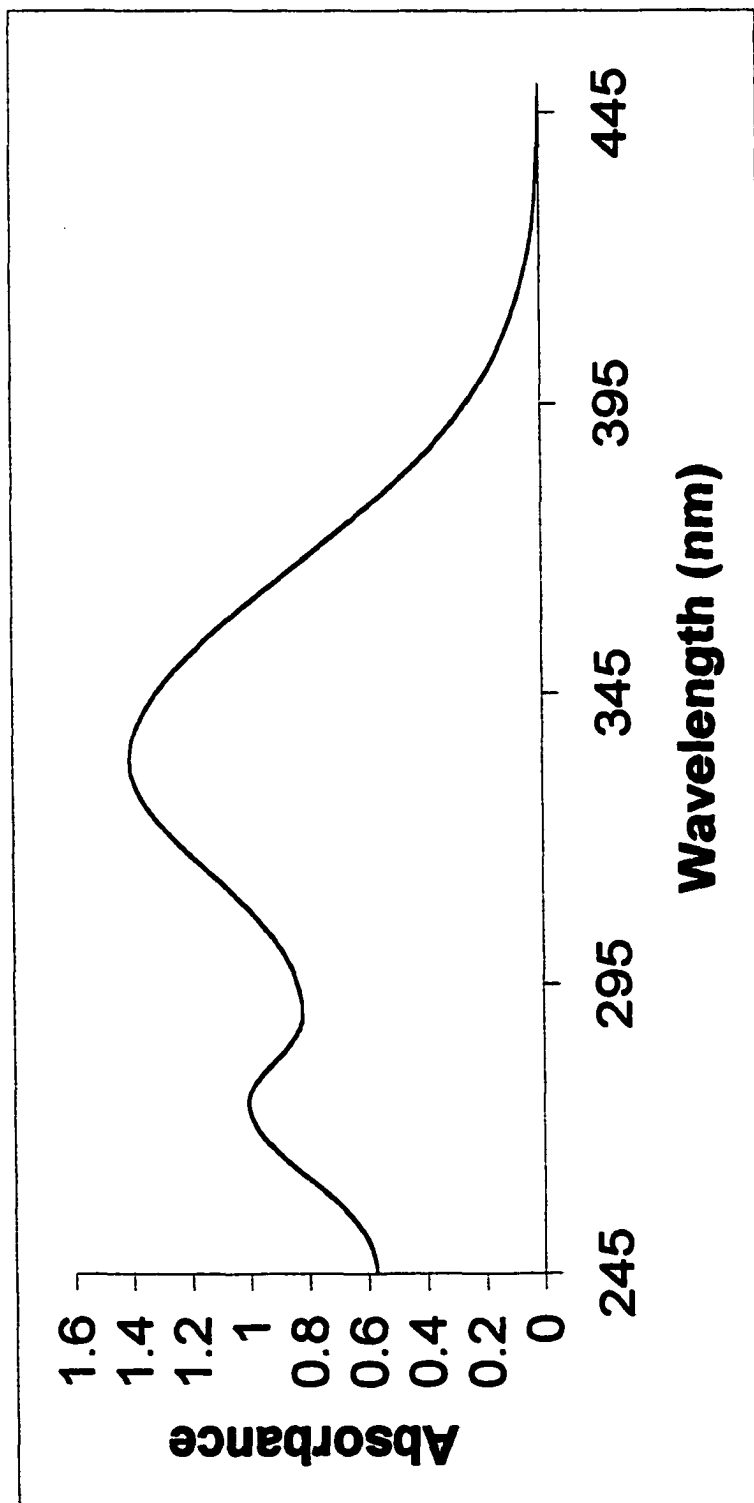


Figure 24. UV-Vis of Compound I-6 (MeOH).

APPENDIX B

Spectroscopic Data for Compounds in “Conformationally Defined Retinoic Acid Analogues. Synthesis, Nuclear Receptor Binding, and Transcriptional Activation Activity of Derivatives of RXR-Selective (9Z)-UAB30”

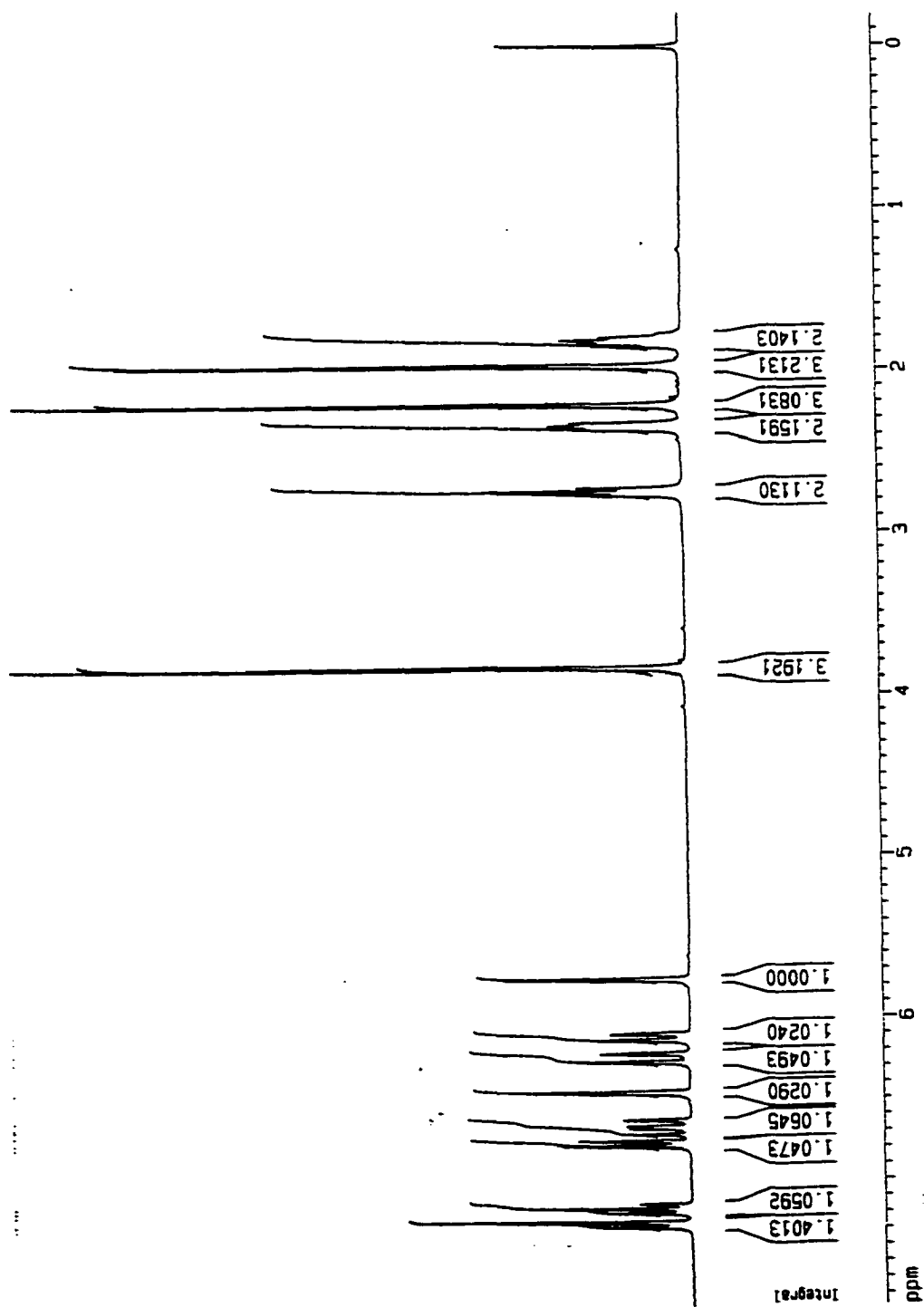


Figure 1. ^1H NMR (300 MHz) of Compound II-2 (CDCl_3).

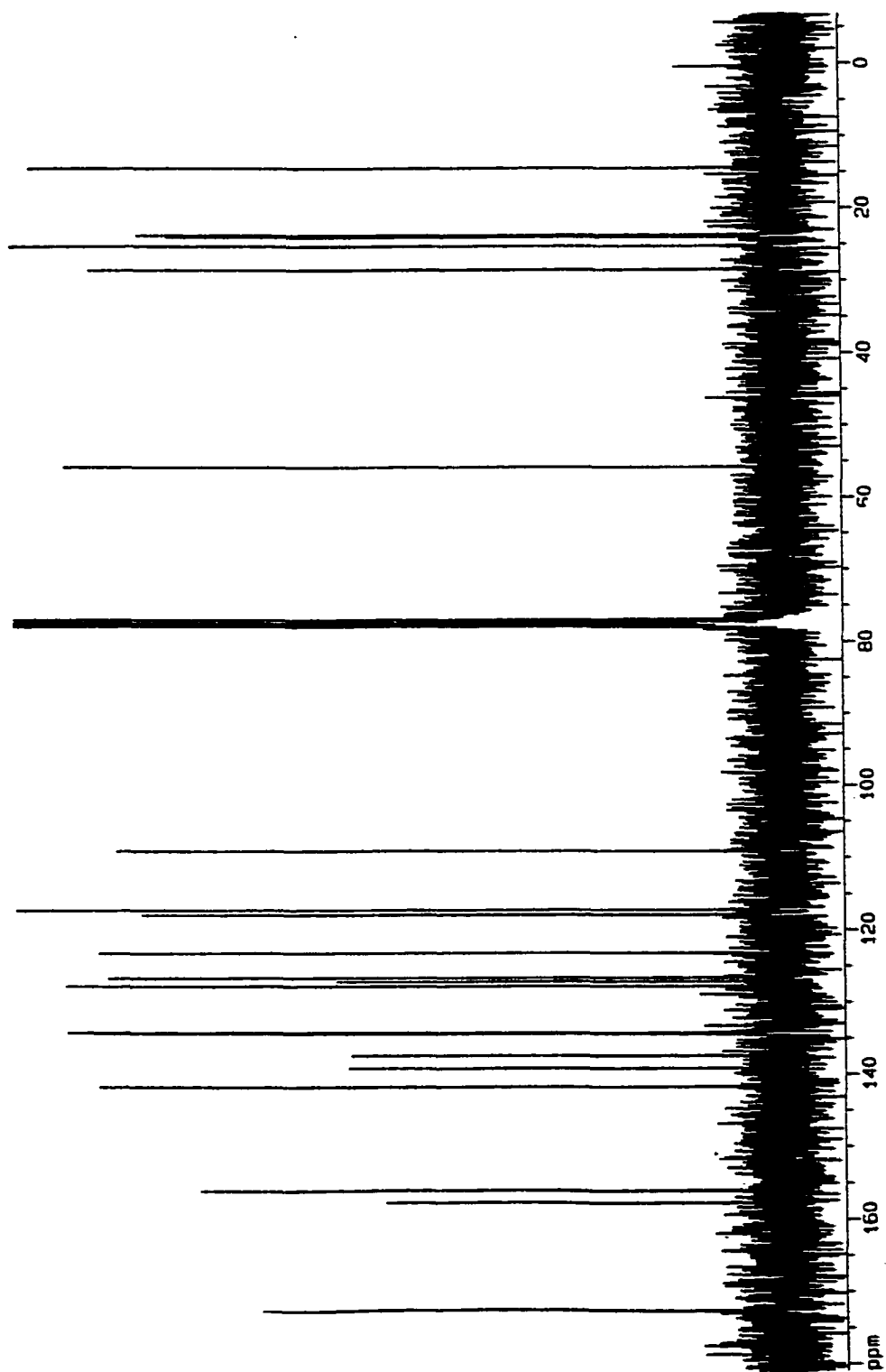


Figure 2. ^{13}C NMR (300 MHz) of Compound II-2 (CDCl_3).

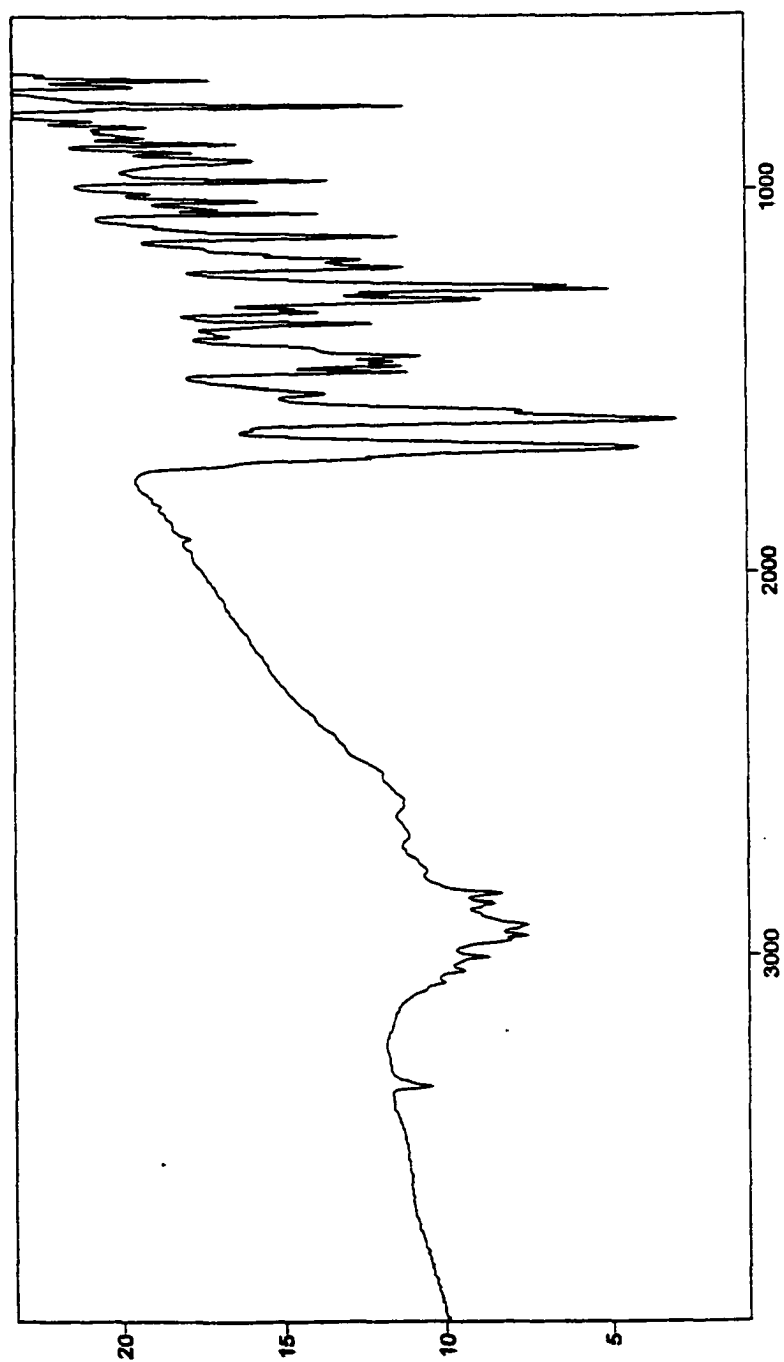


Figure 3. FTIR of Compound II-2 (KBr).

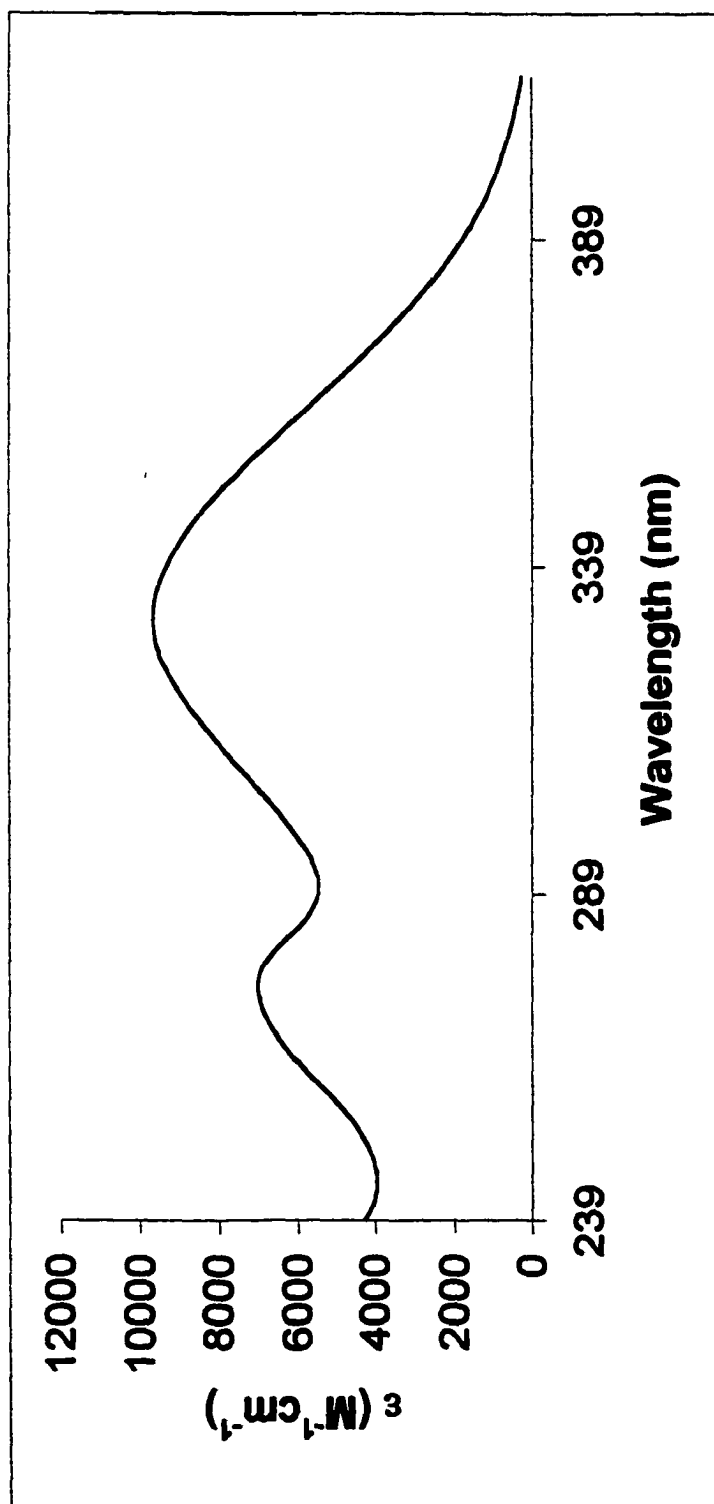


Figure 4. UV-Vis of Compound **II-2** (MeOH).

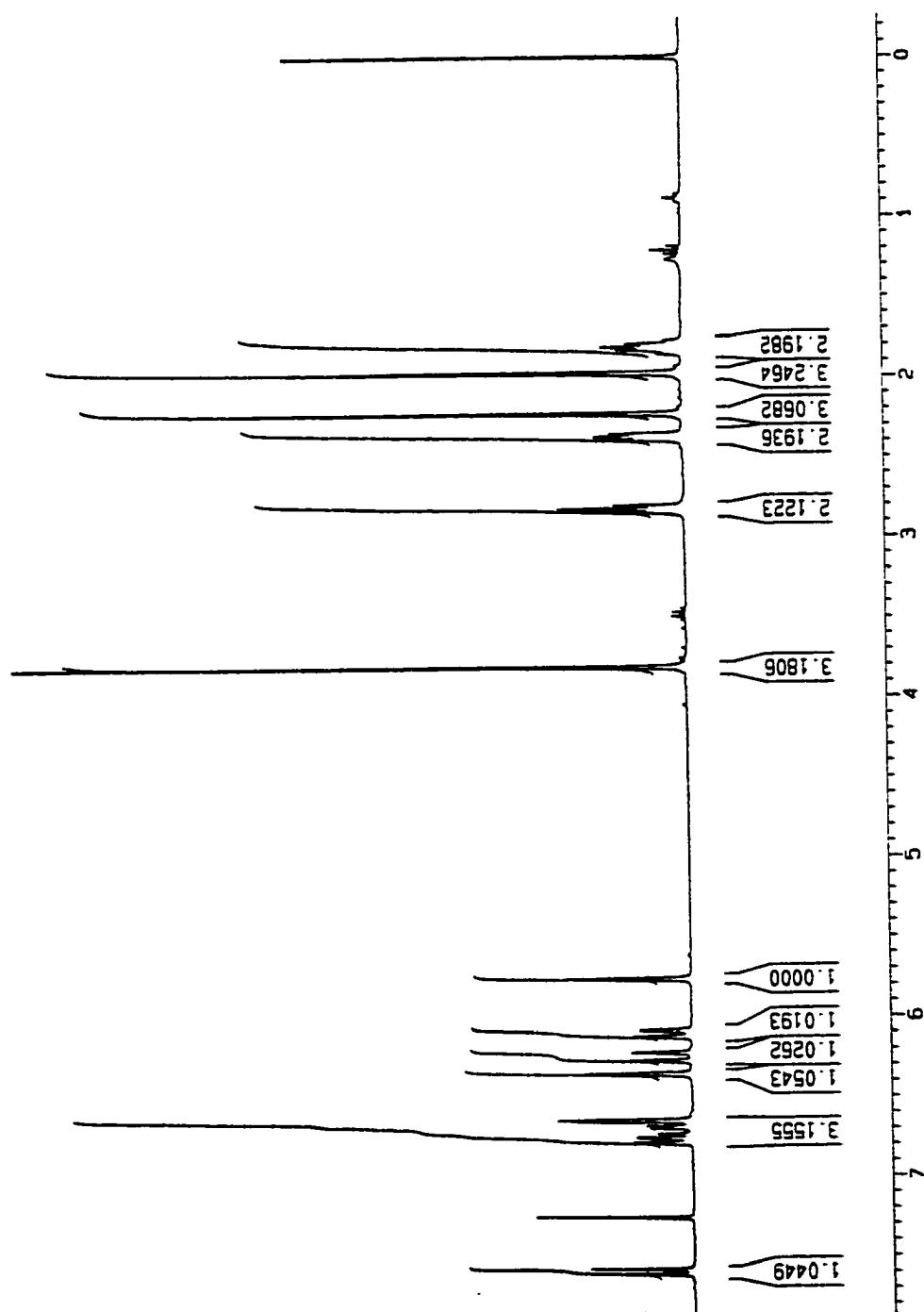


Figure 5. ^1H NMR (300 MHz) of Compound II-3 (CDCl_3).

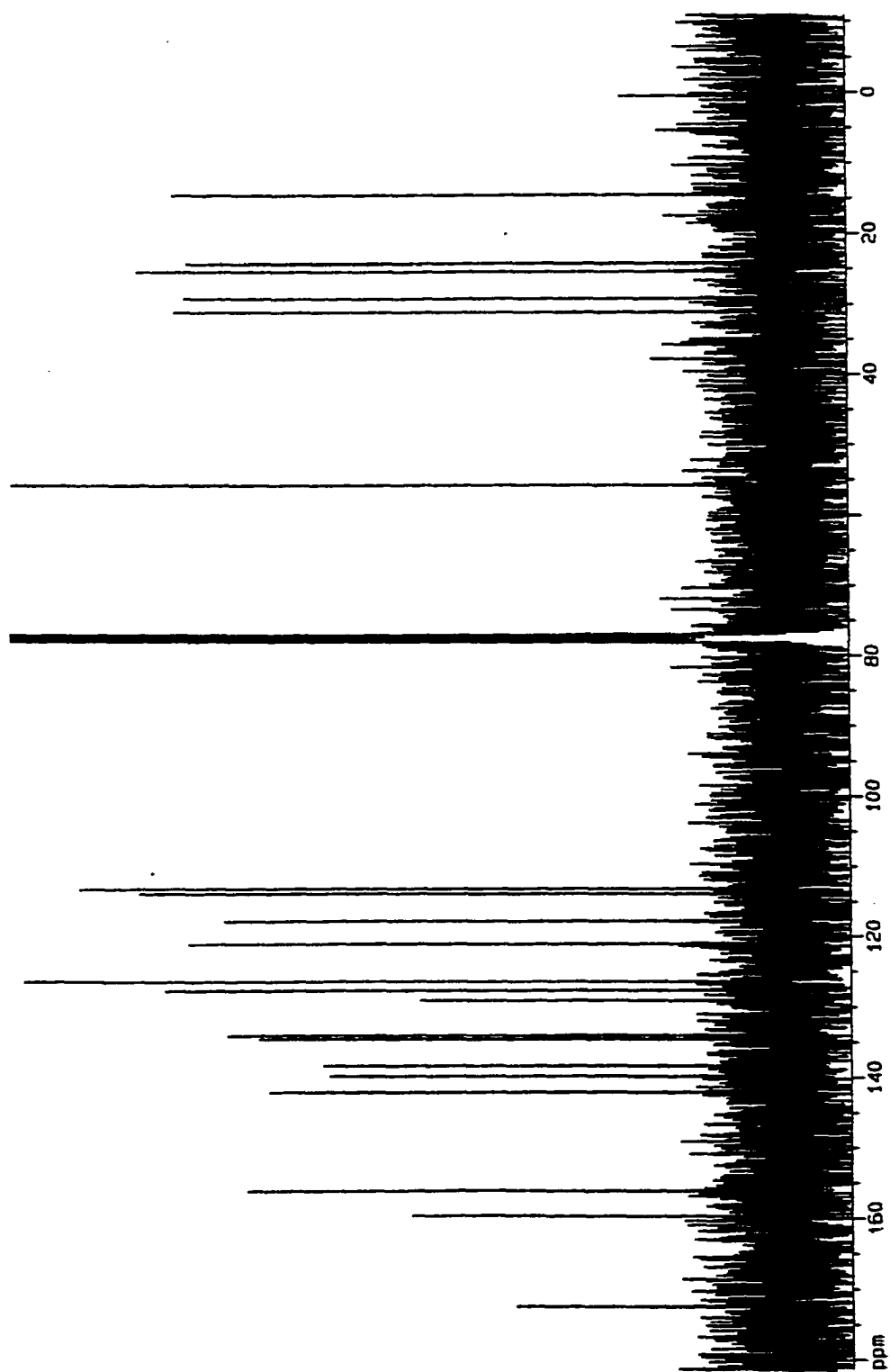


Figure 6. ^{13}C NMR (300 MHz) of Compound II-3 (CDCl_3).

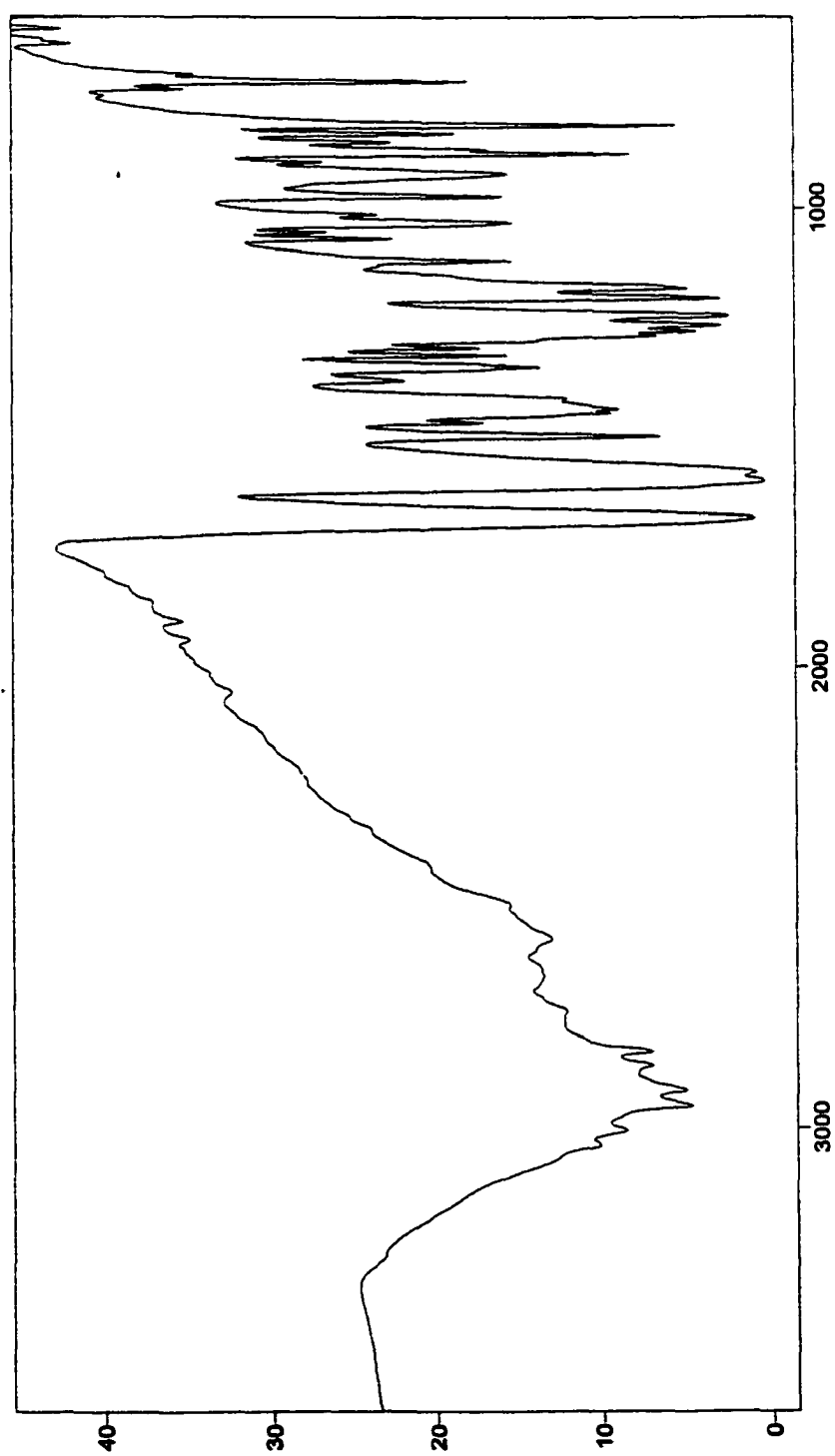


Figure 7. FTIR of Compound II-3 (KBr).

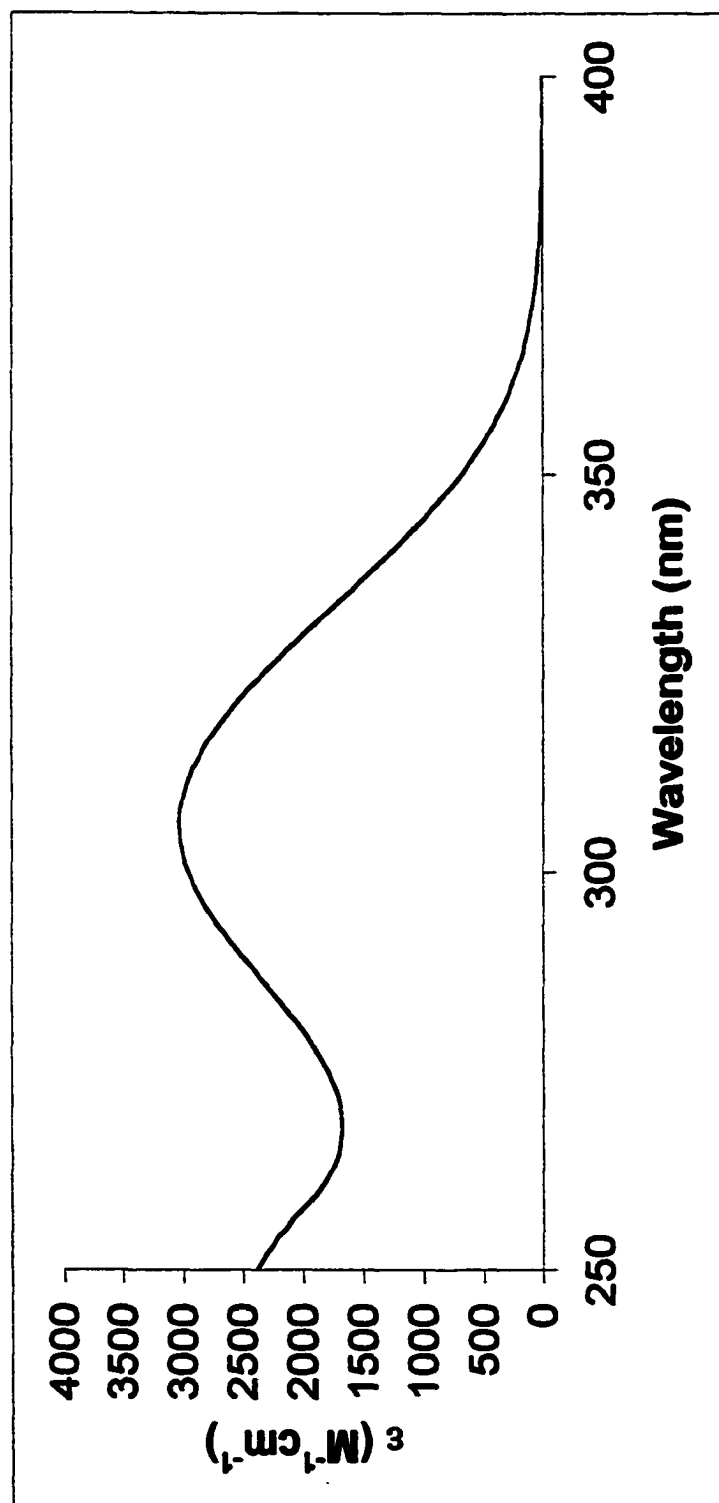


Figure 8. UV-Vis of Compound II-3 (MeOH).

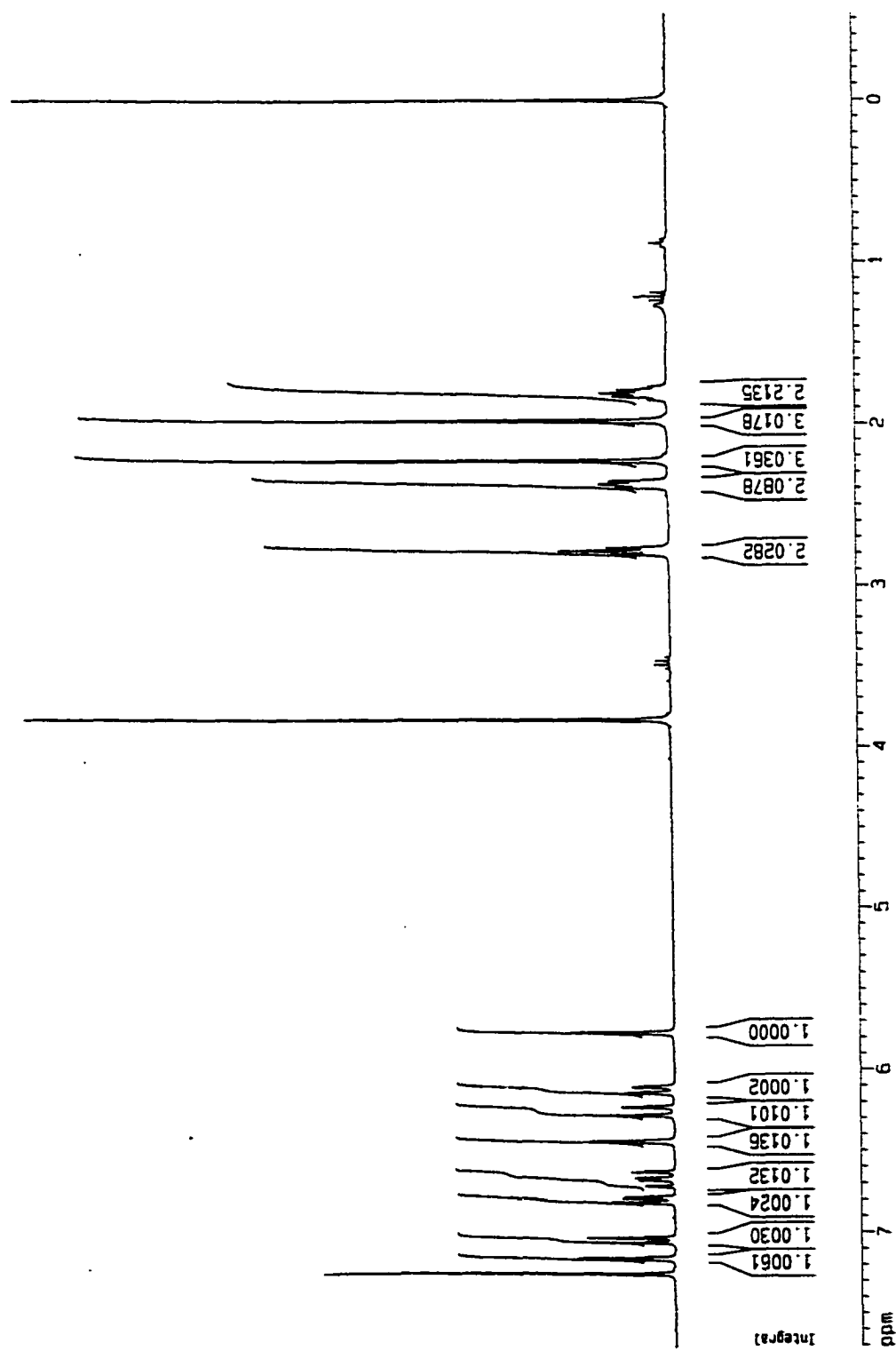


Figure 9. ¹H NMR (300 MHz) of Compound II-4 (CDCl₃).

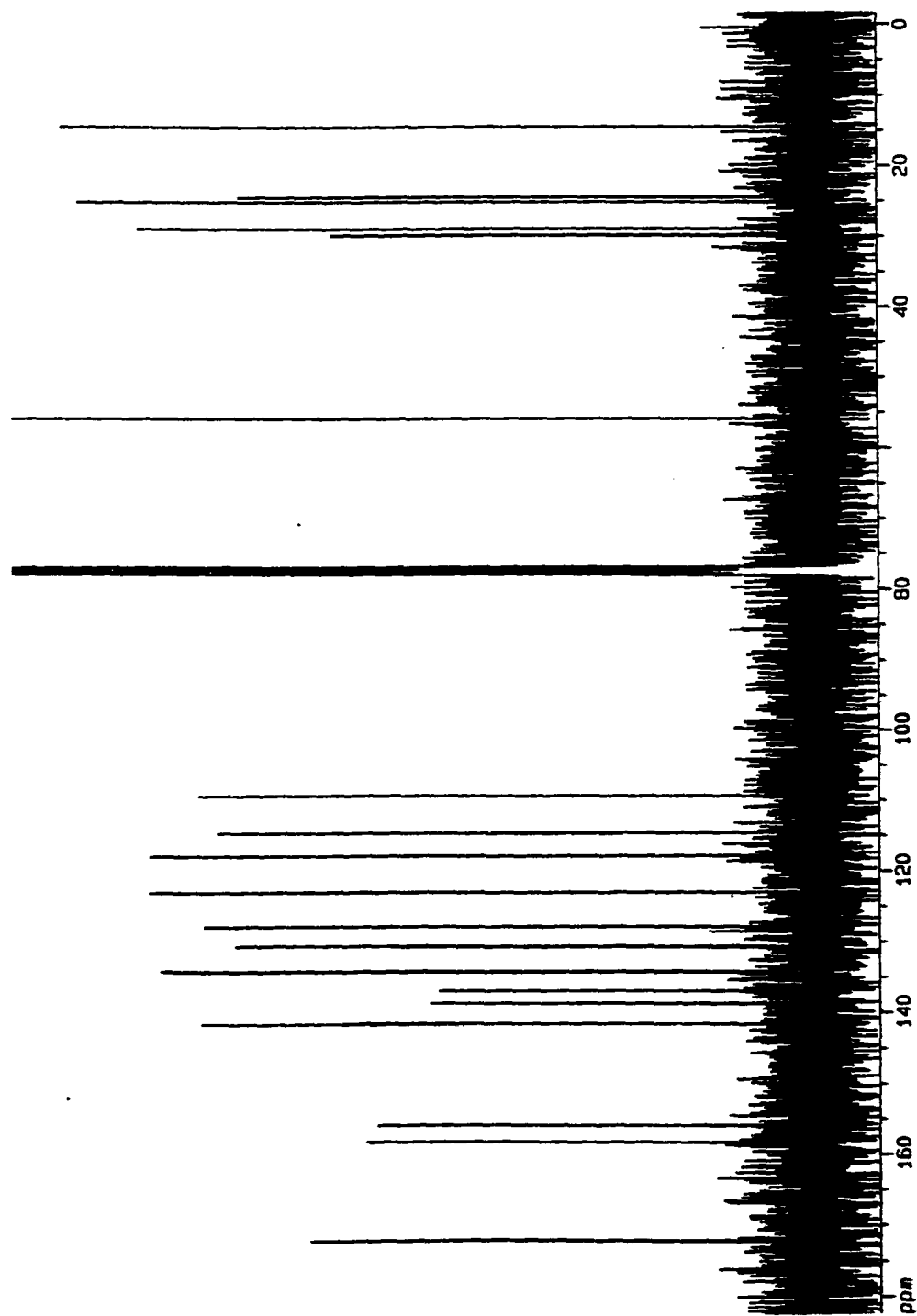


Figure 10. ^{13}C NMR (300 MHz) of Compound II-4 (CDCl_3).

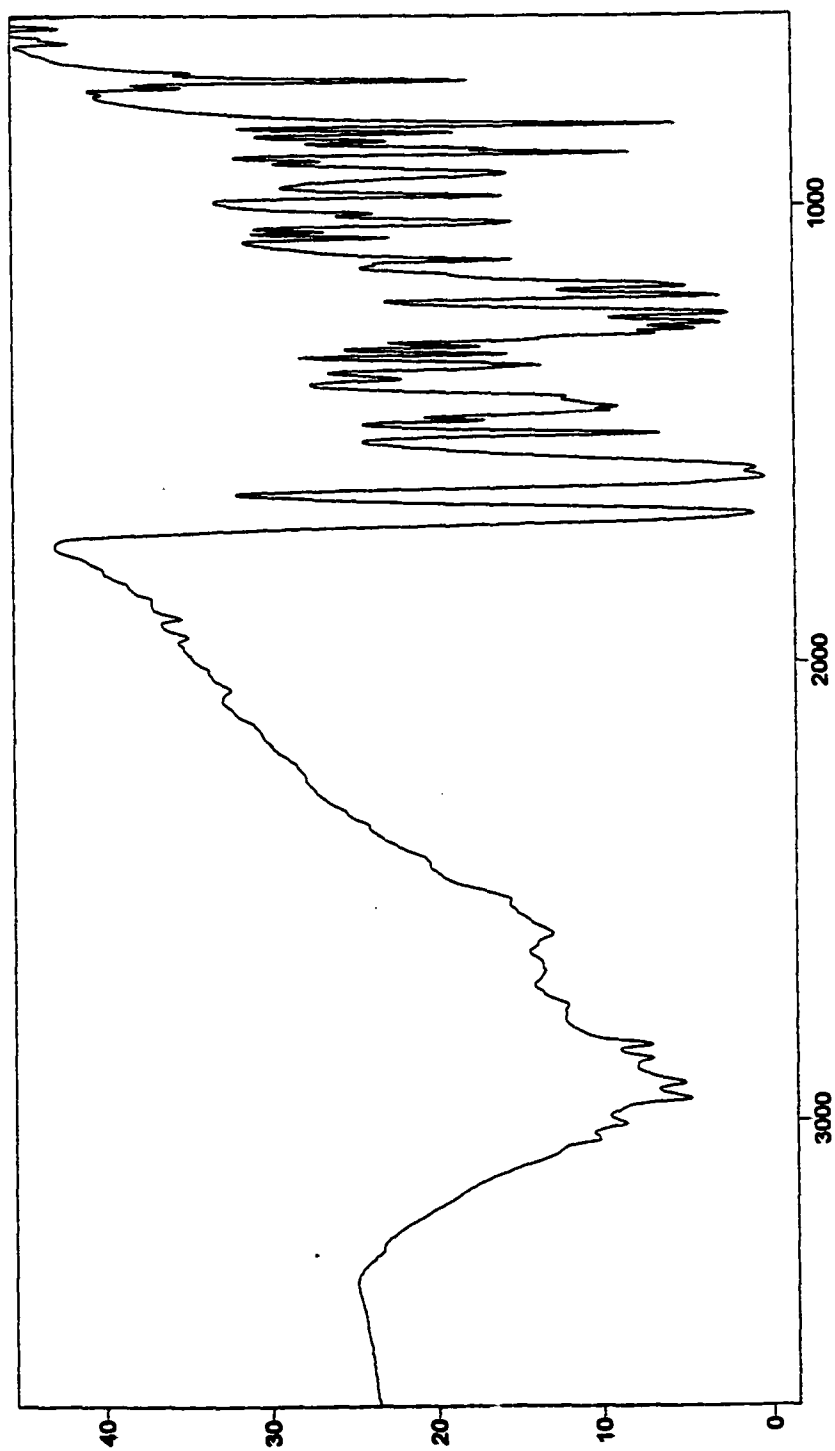


Figure 11. FTIR of Compound II-4 (KBr).

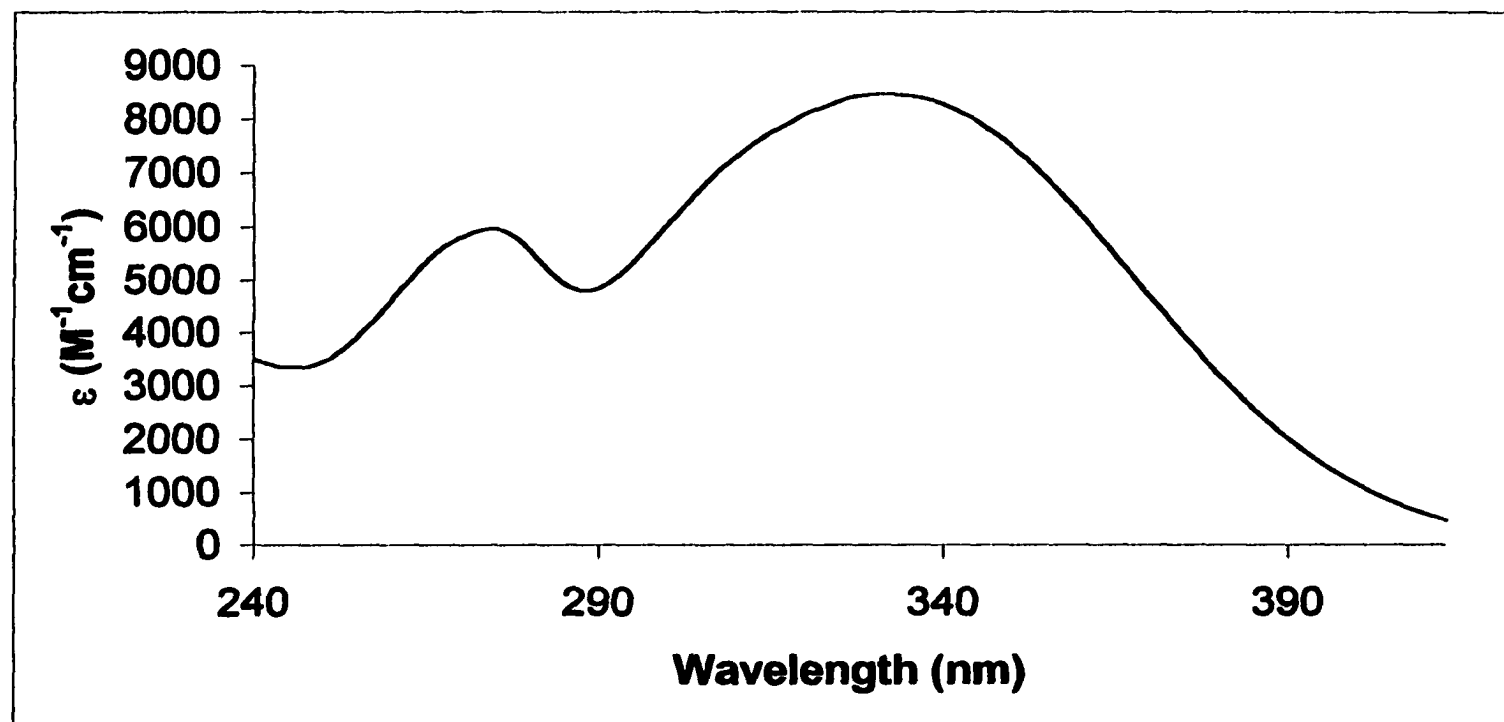


Figure 12. UV-Vis of Compound II-4 (MeOH).

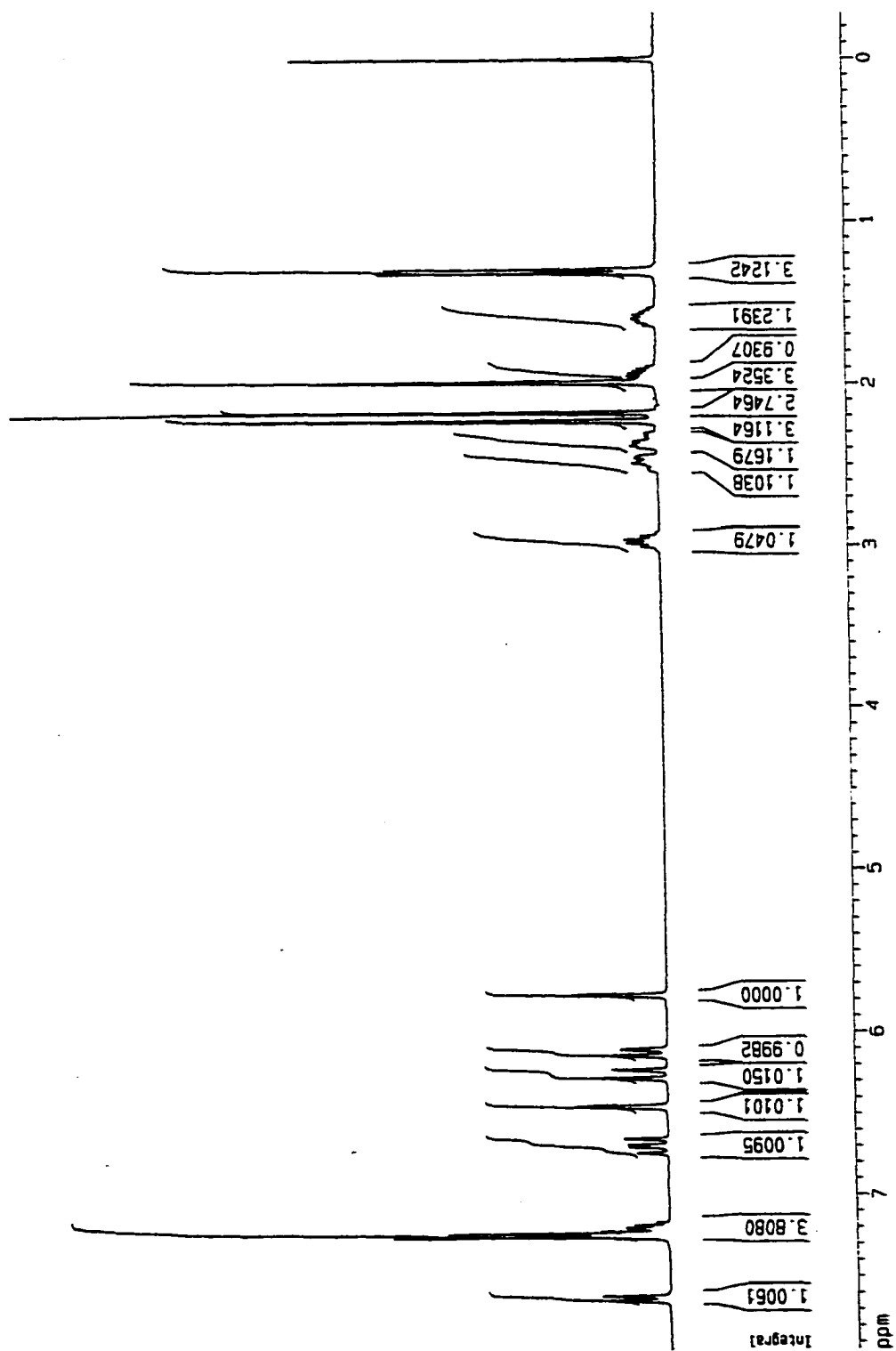


Figure 13. ¹H NMR (300 MHz) of Compound II-5 (CDCl₃).

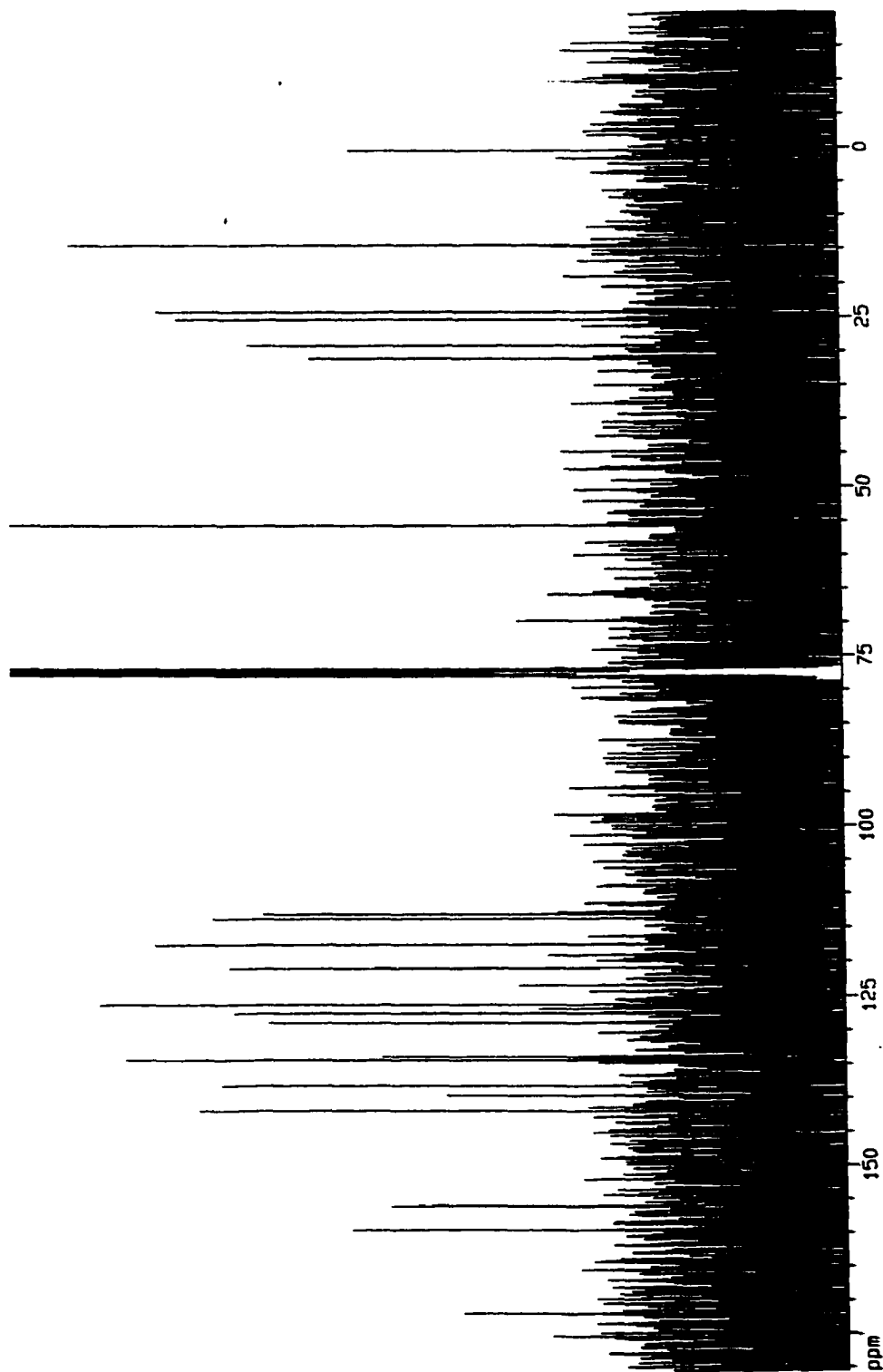


Figure 14. ^{13}C NMR (300 MHz) of Compound II-5 (CDCl_3).

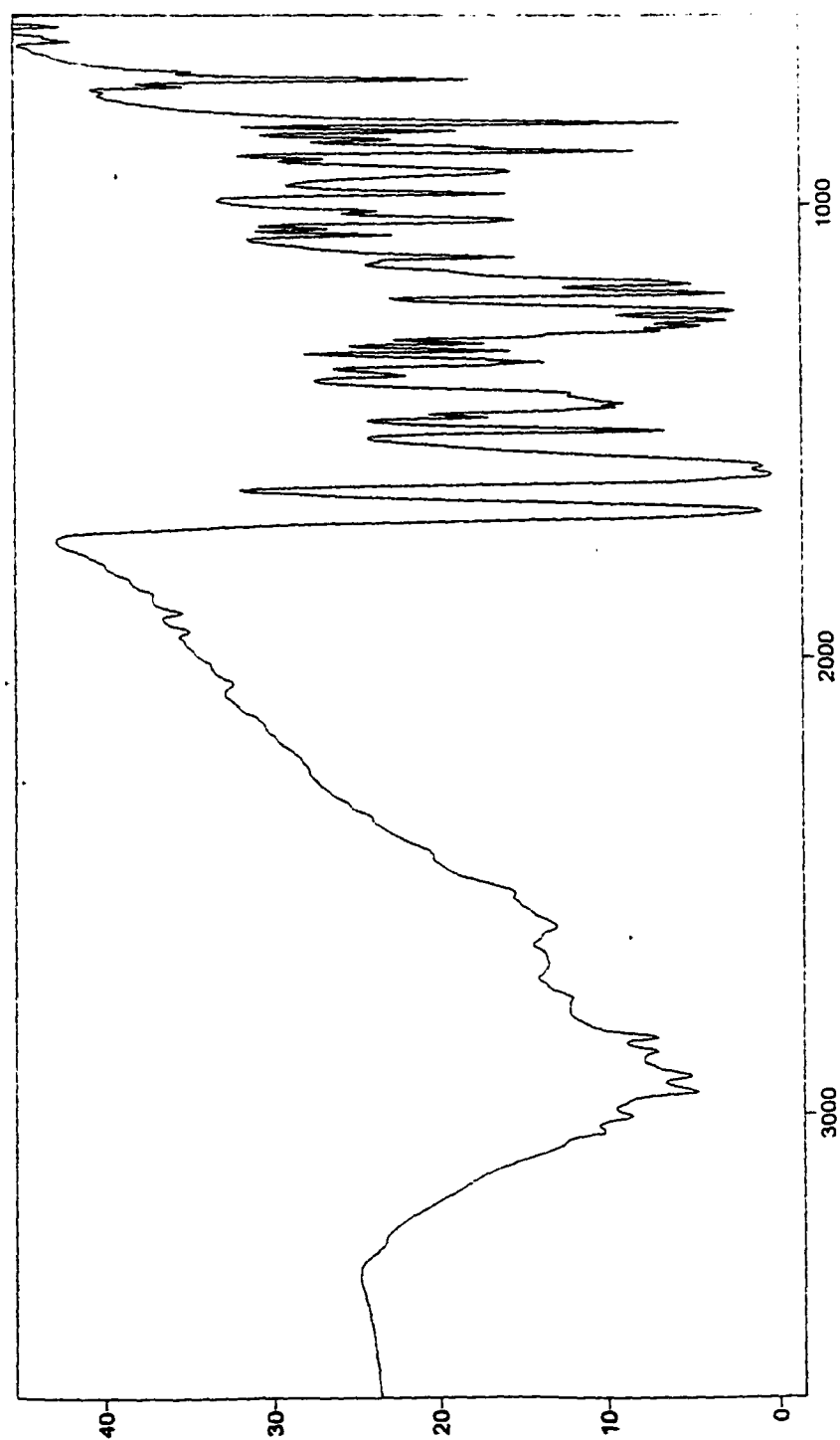


Figure 15. FTIR of Compound II-5 (KBr).

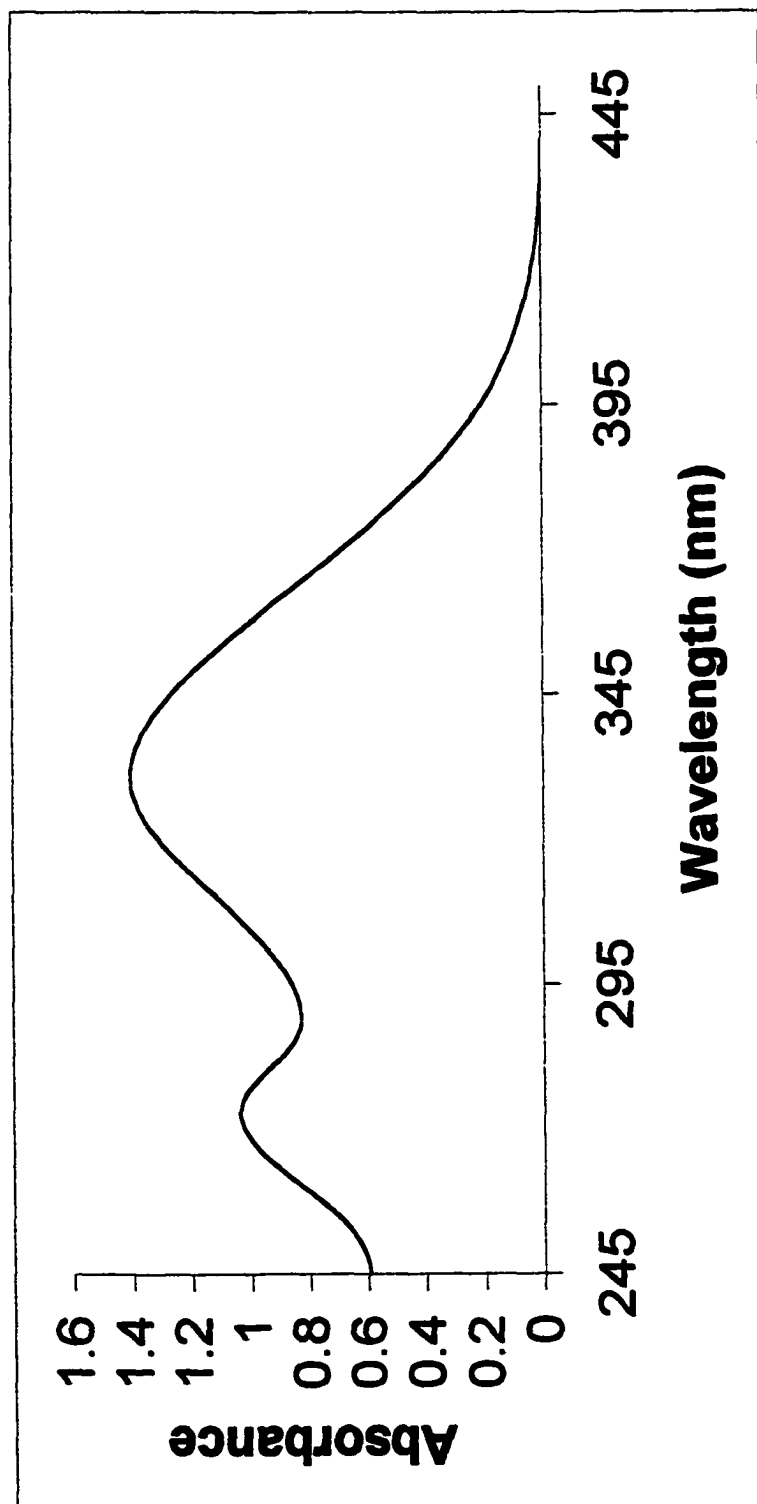


Figure 16. UV-Vis of Compound II-5 (MeOH).

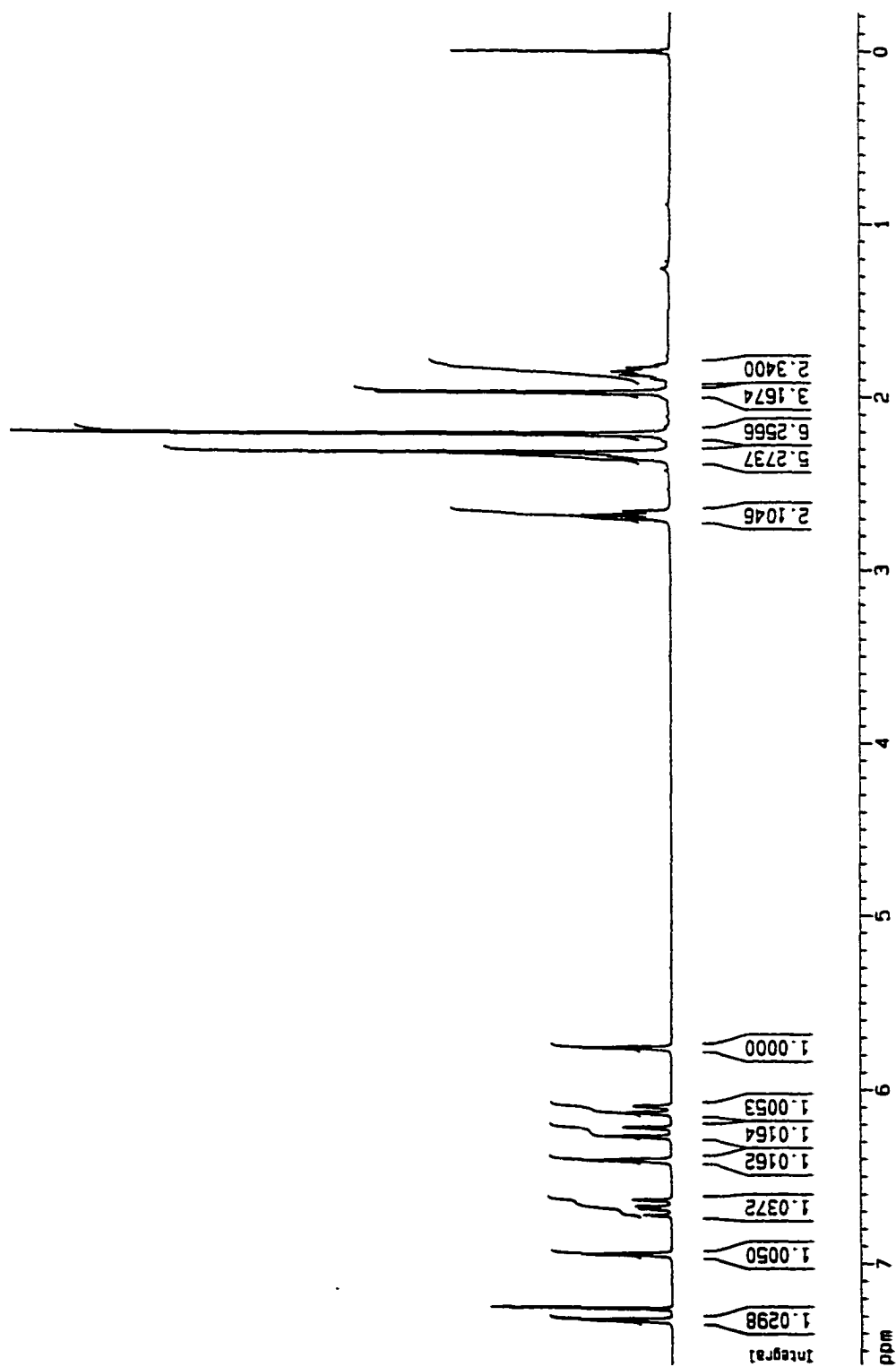


Figure 17. ^1H NMR (300 MHz) of Compound II-6 (CDCl_3).

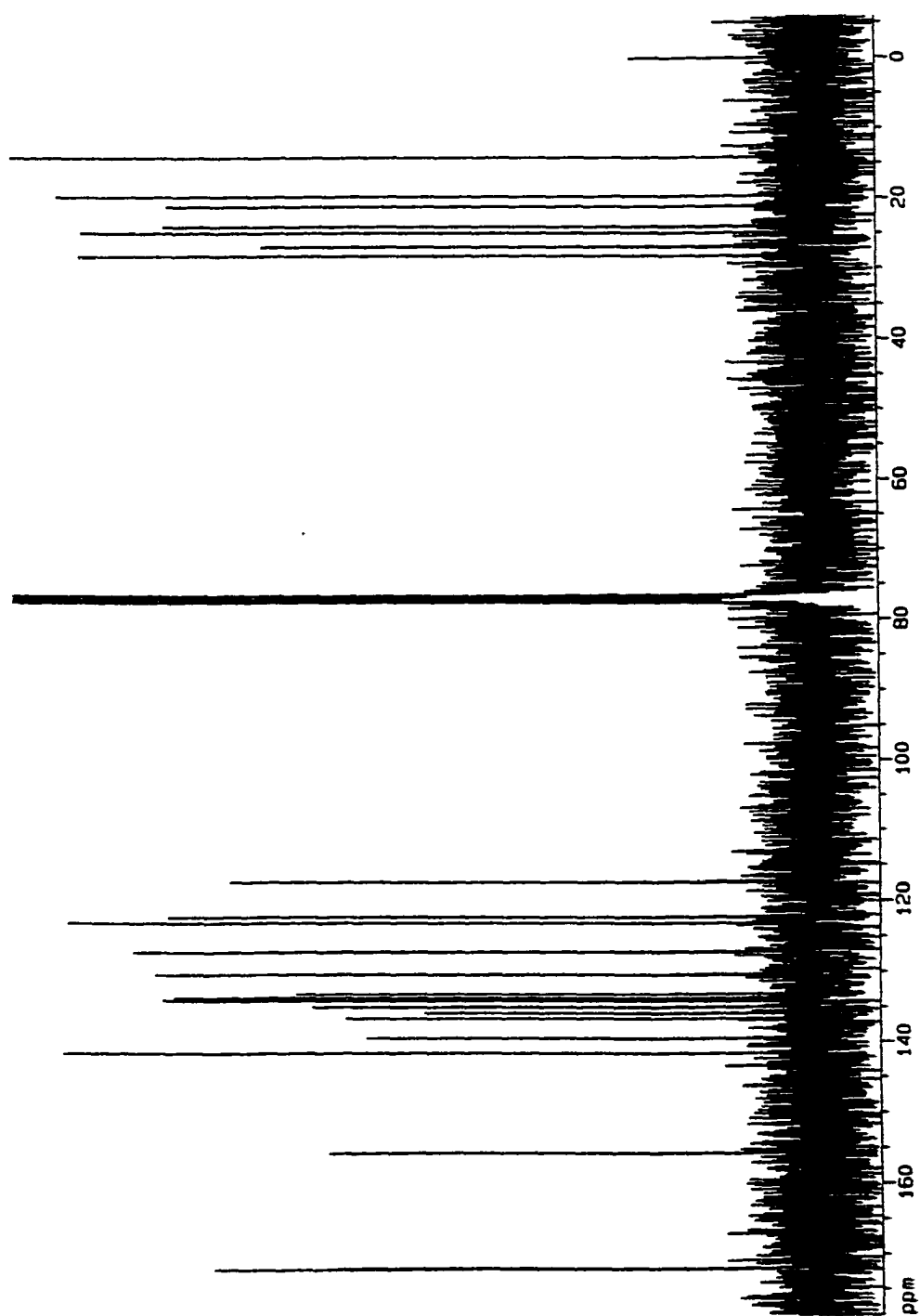


Figure 18. ^{13}C NMR (300 MHz) of Compound 11-6 (CDCl_3).

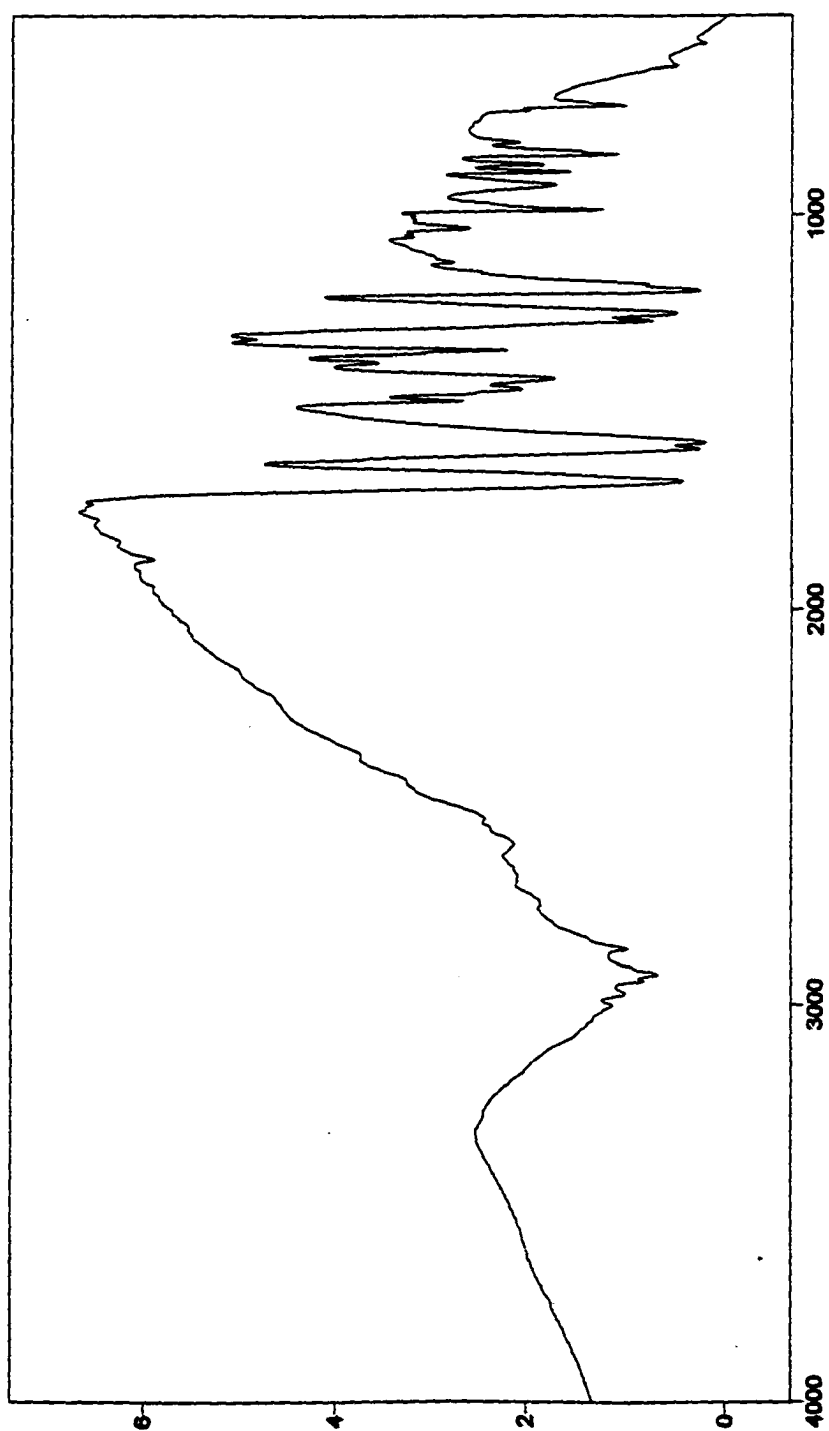


Figure 19. FTIR of Compound II-6 (KBr).

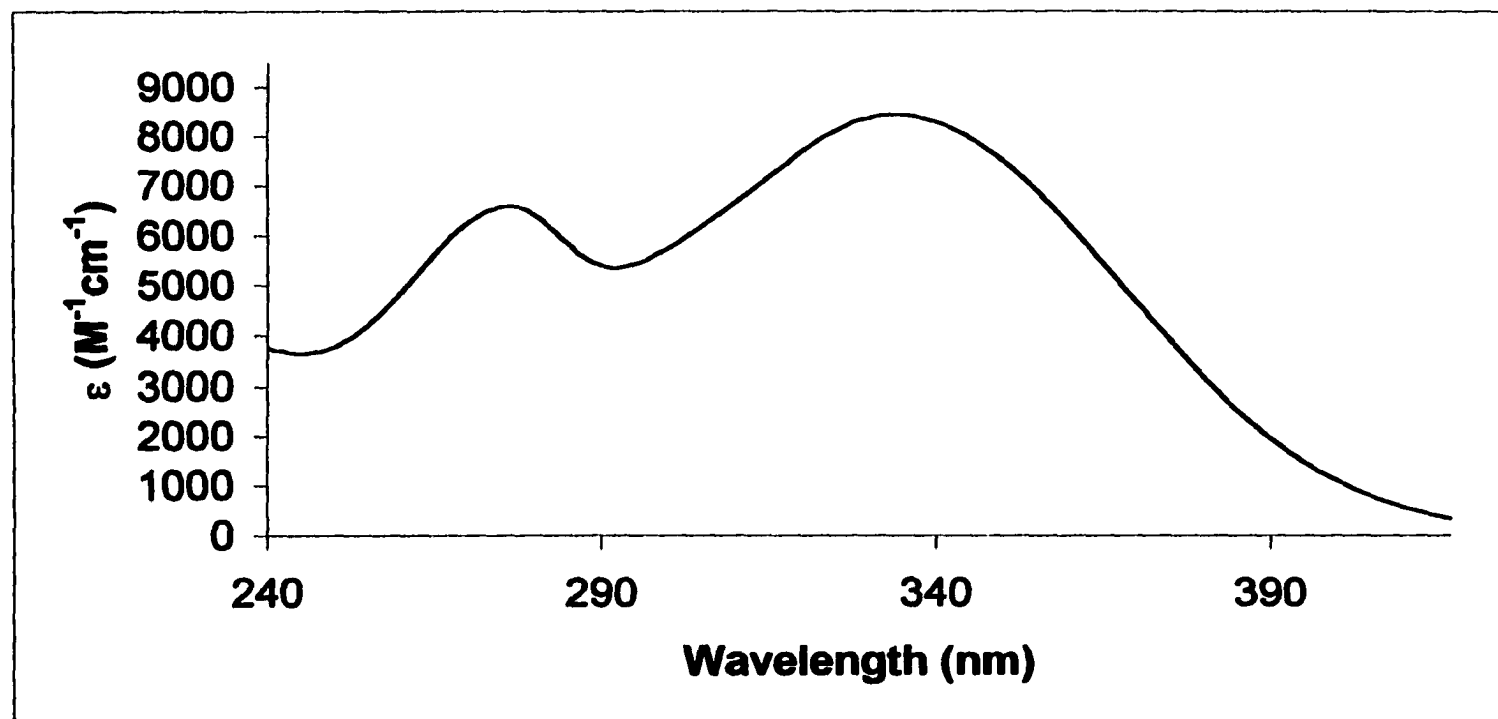


Figure 20. UV-Vis of Compound II-6 (MeOH).

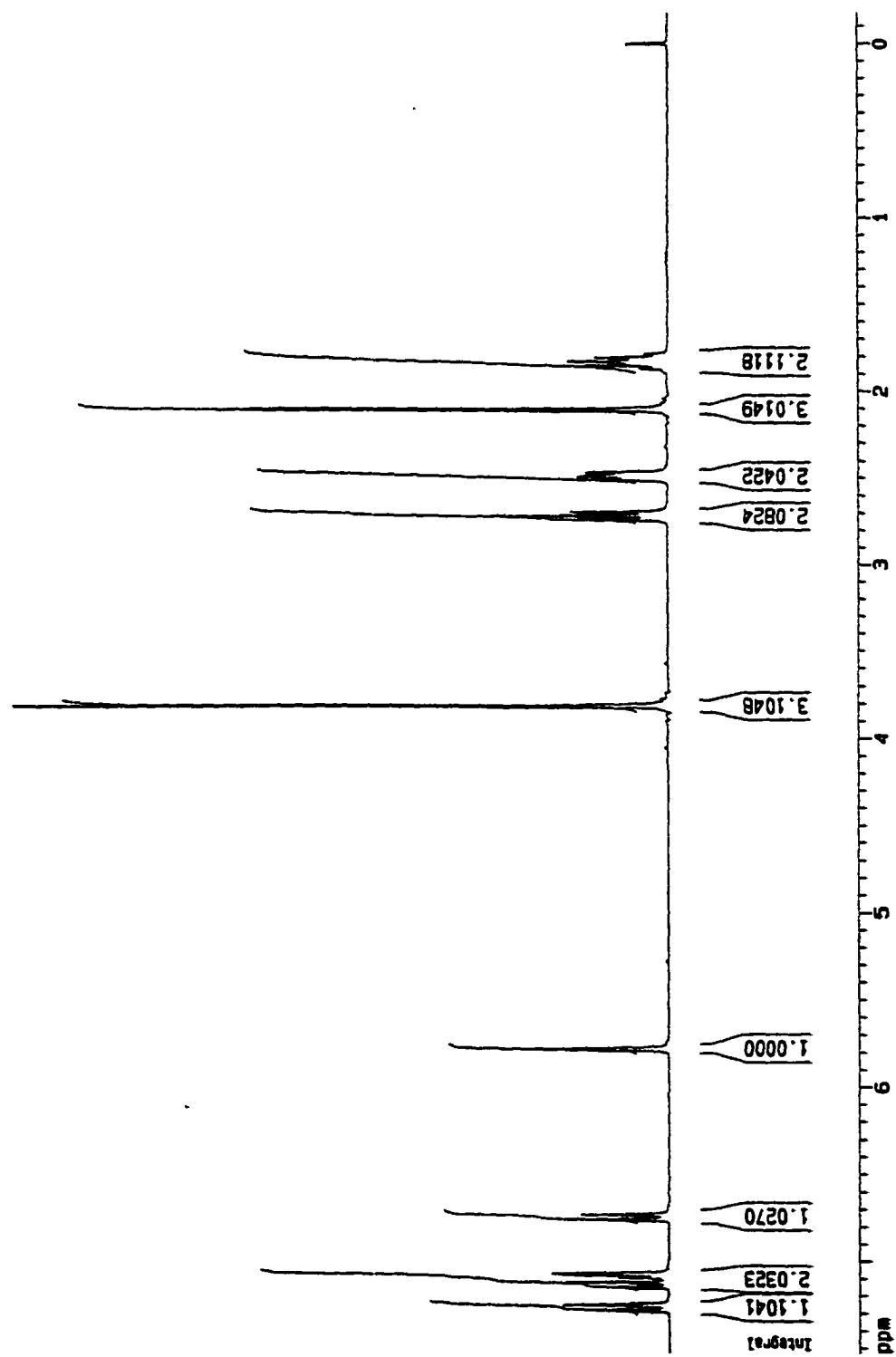


Figure 21. ¹H NMR (300 MHz) of Compound II-14 (CDCl₃).

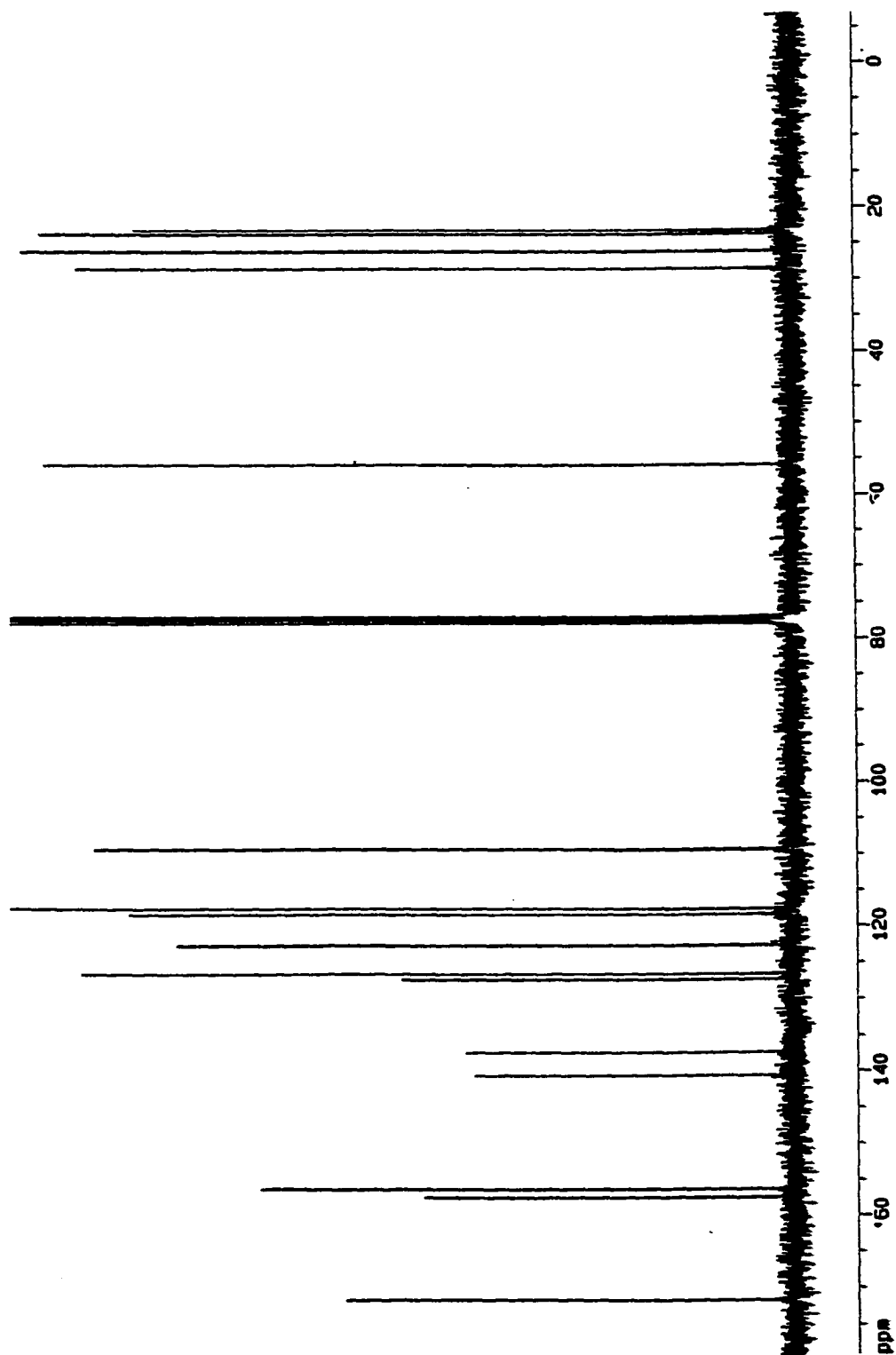


Figure 22. ^{13}C NMR (300 MHz) of Compound II-14 (CDCl_3).

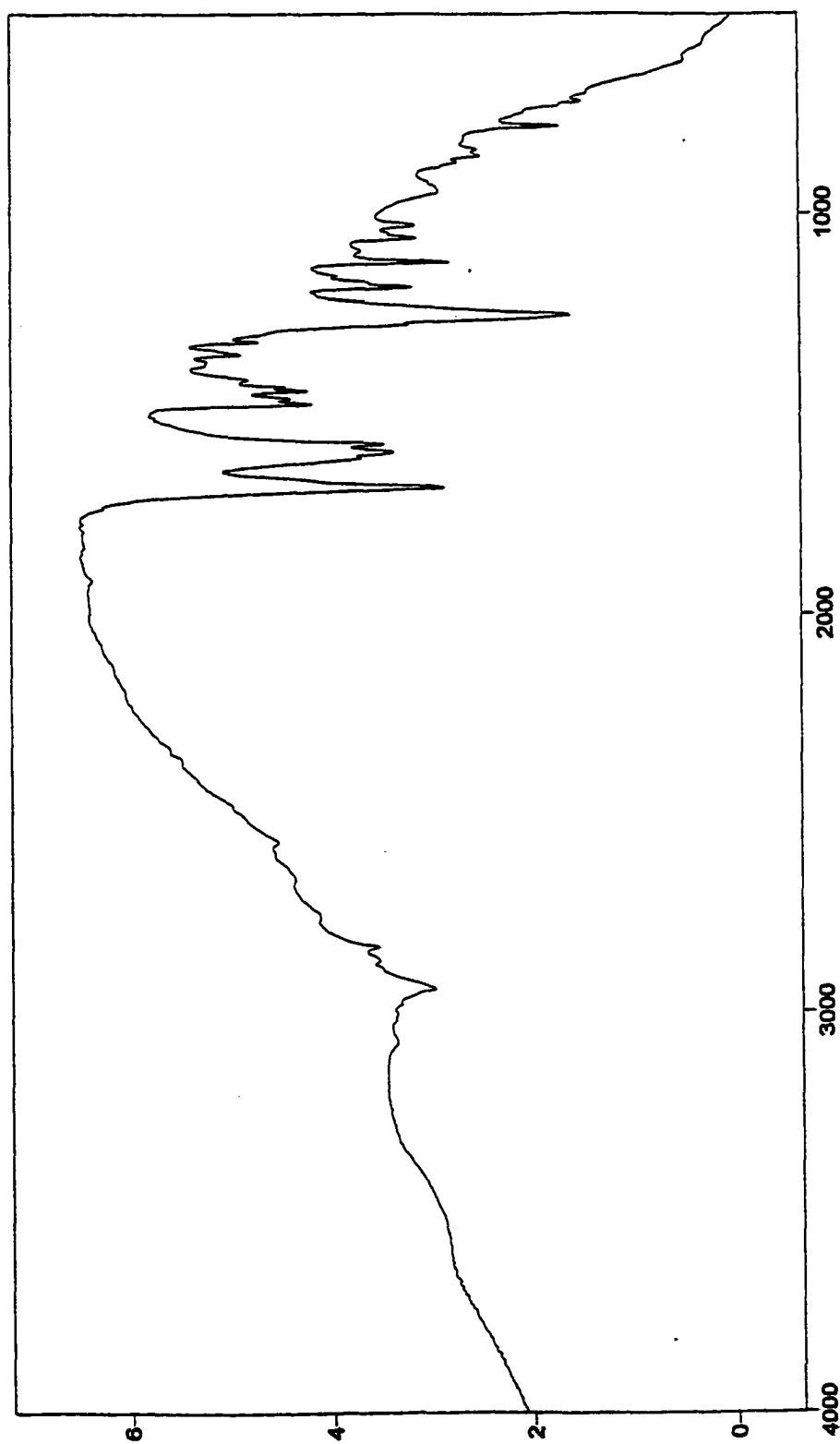


Figure 23. FTIR of Compound II-14 (KBr).

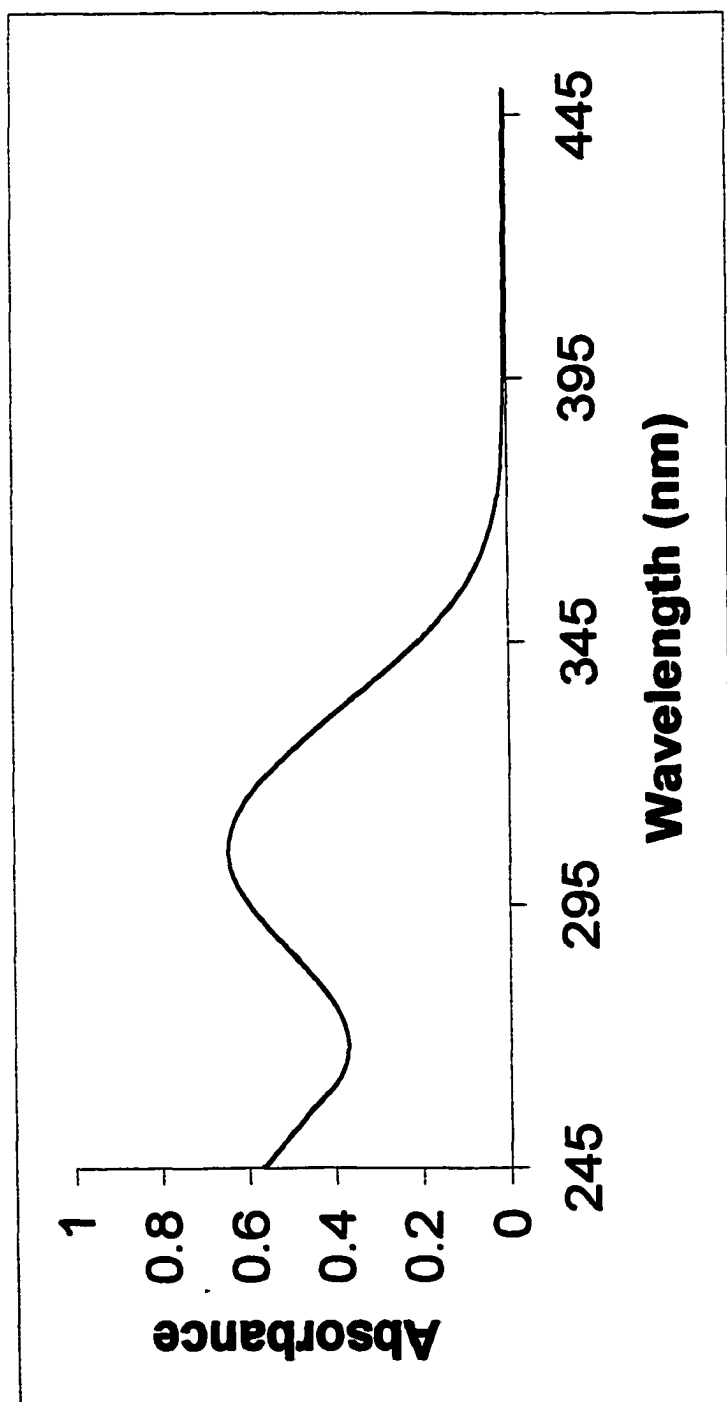


Figure 24. UV-Vis of Compound II-14 (MeOH).

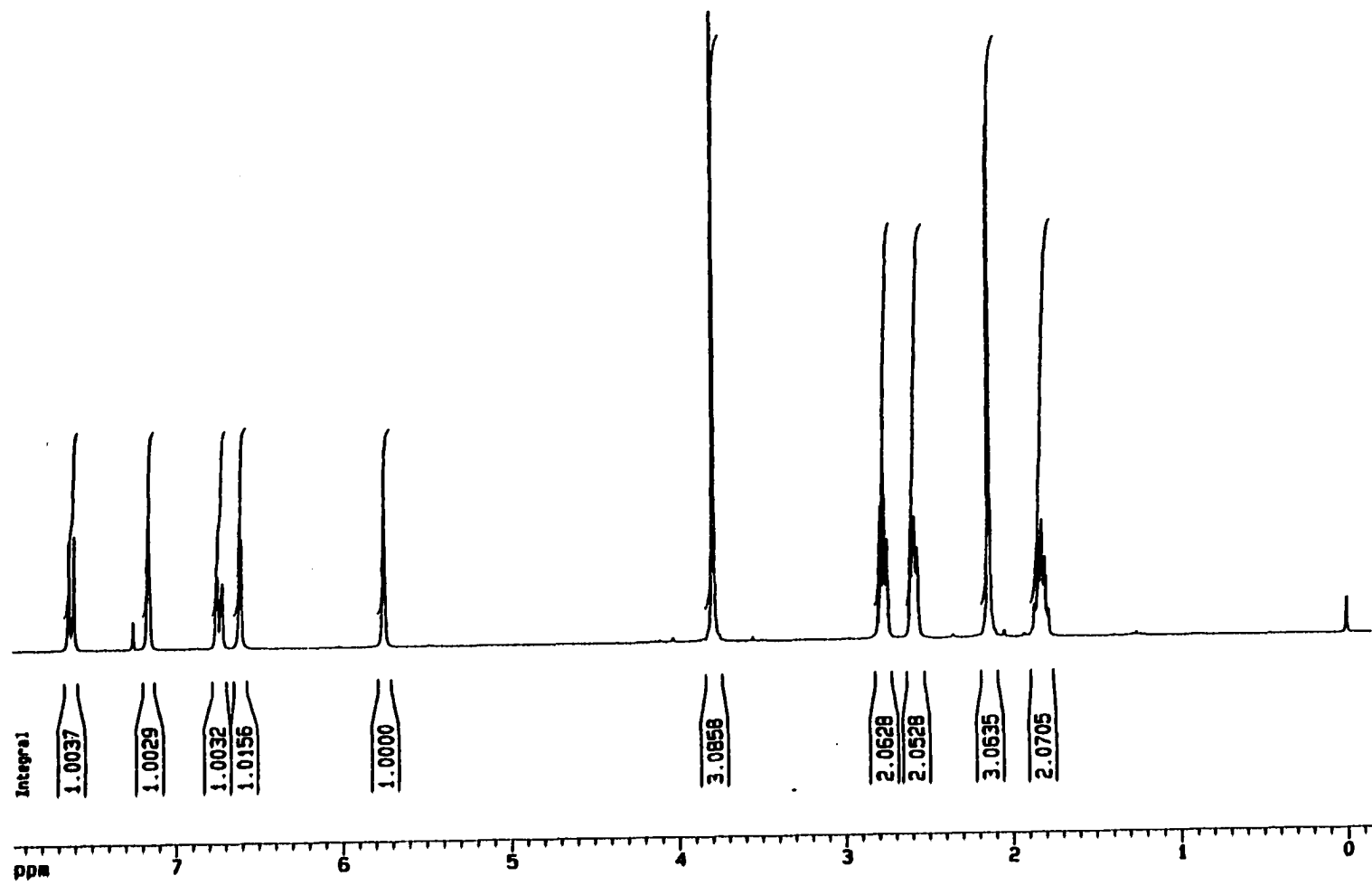


Figure 25. ¹H NMR (300 MHz) of Compound II-15 (CDCl₃).

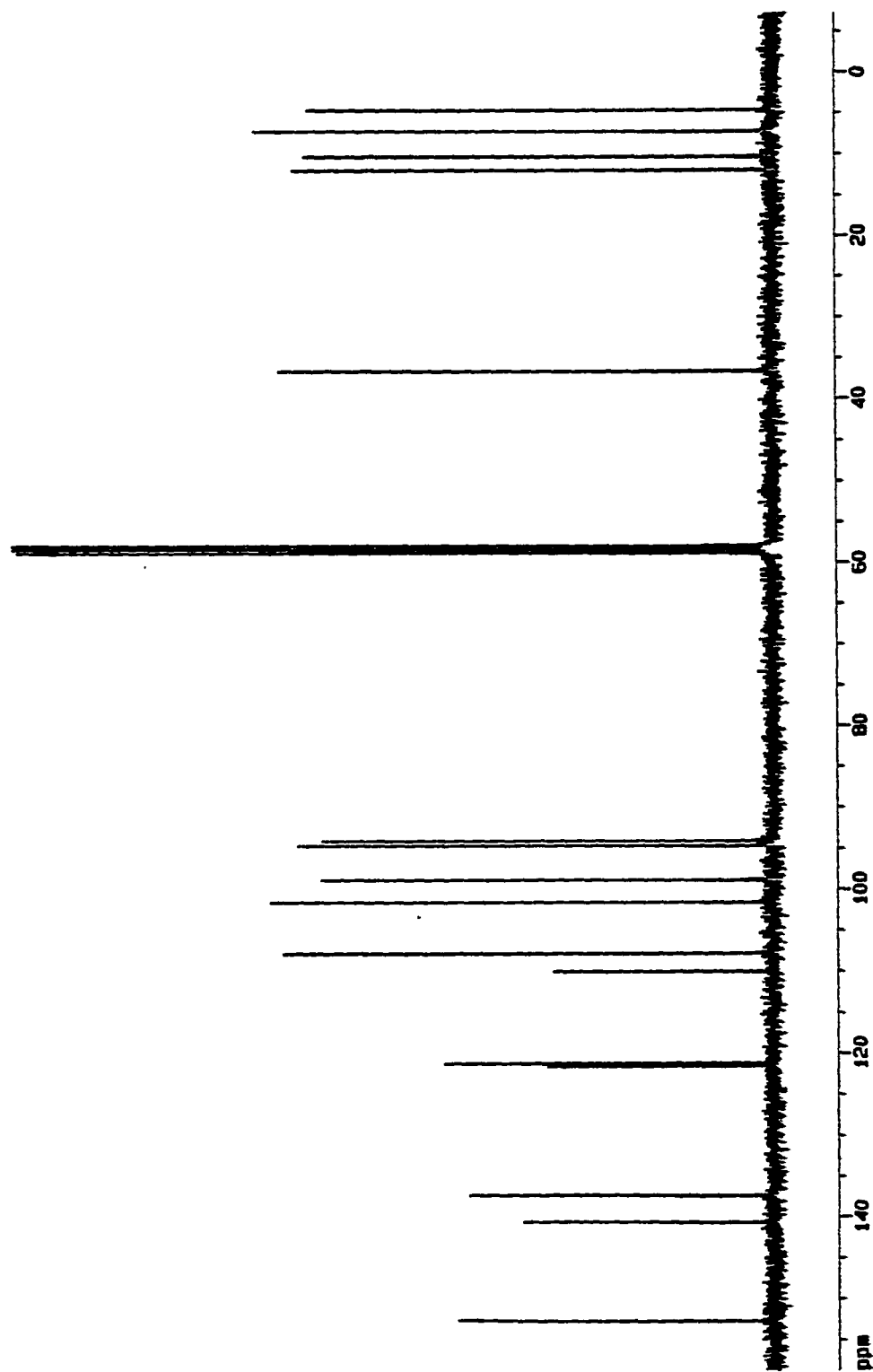


Figure 26. ^{13}C NMR (300 MHz) of Compound II-15 (CDCl_3).

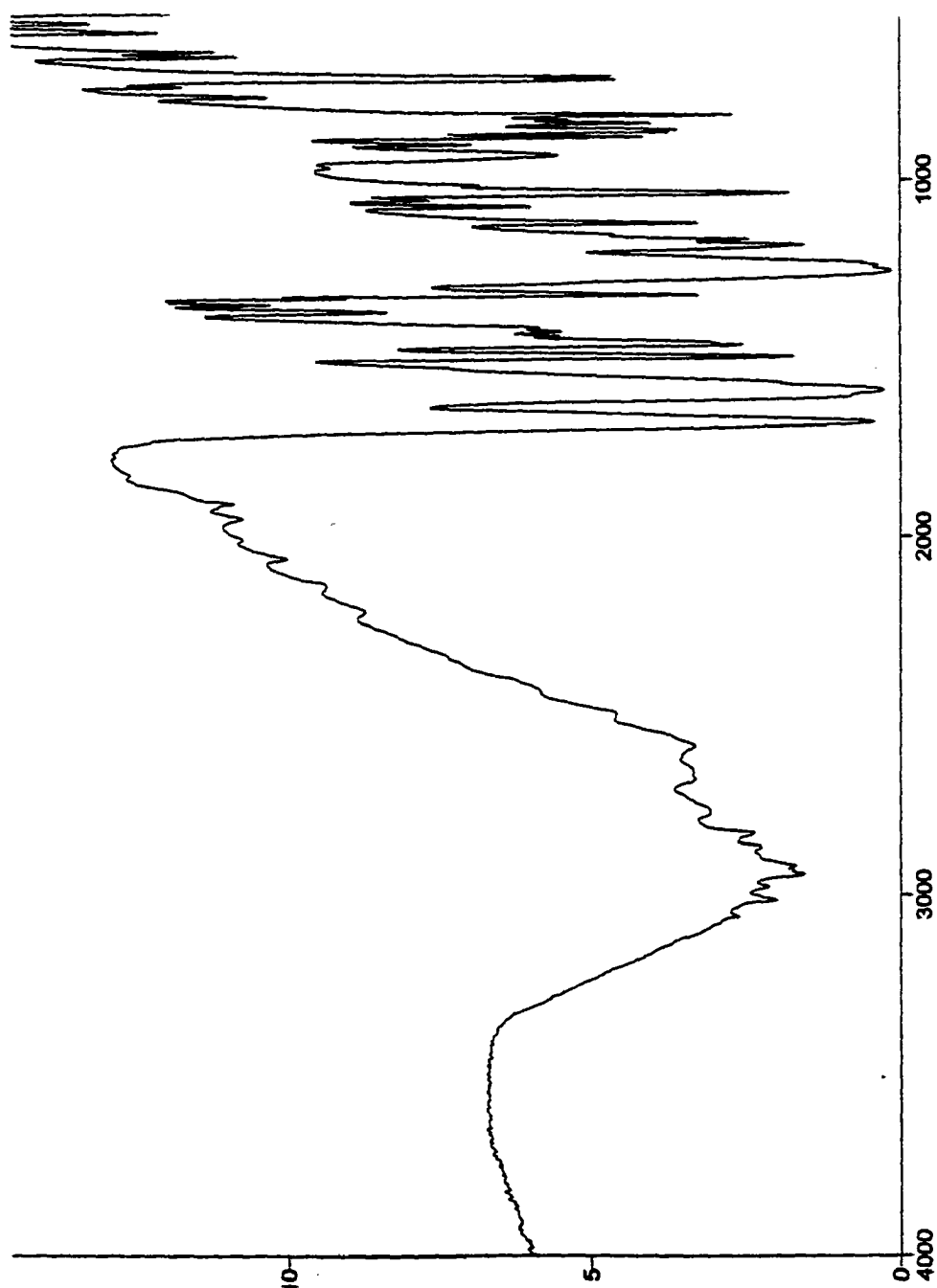


Figure 27. FTIR of Compound II-15 (KBr).

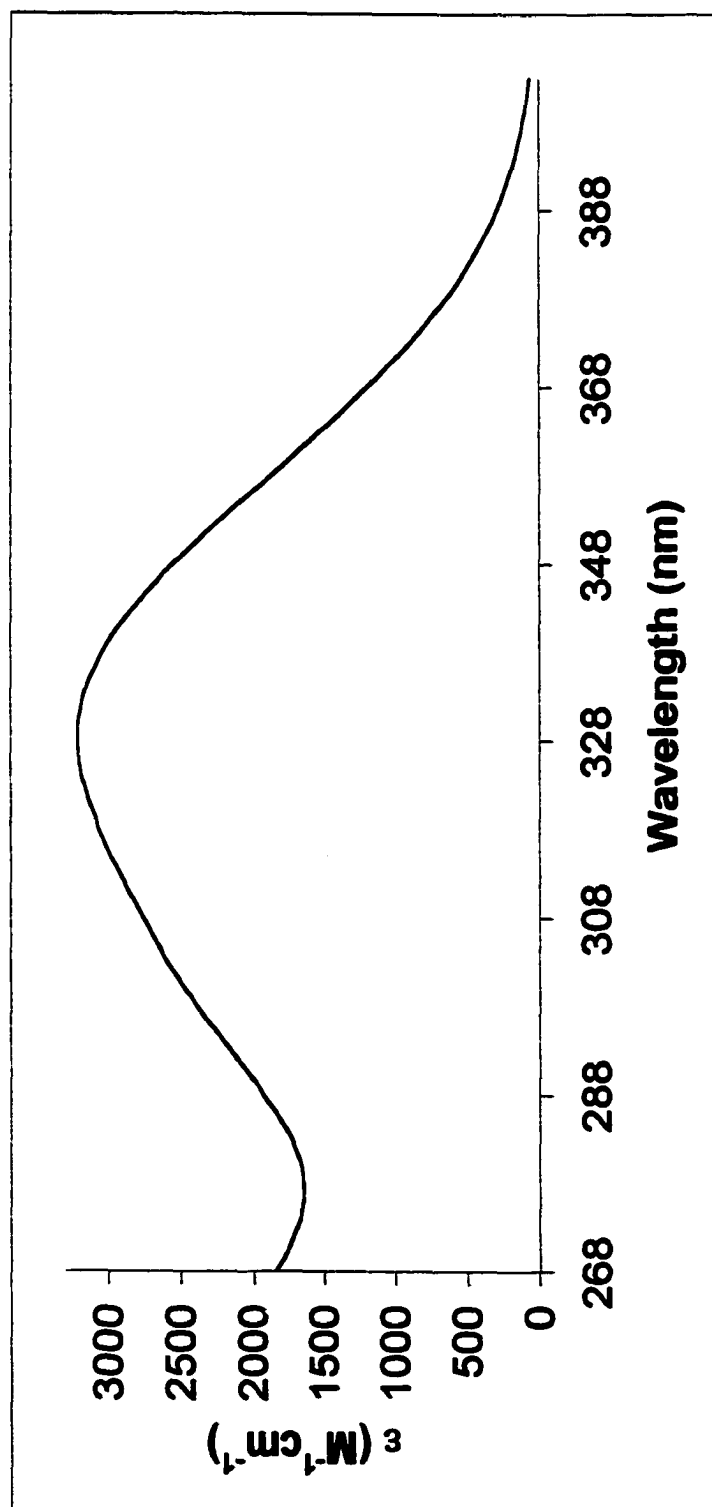


Figure 28. UV-Vis of Compound II-15 (MeOH).

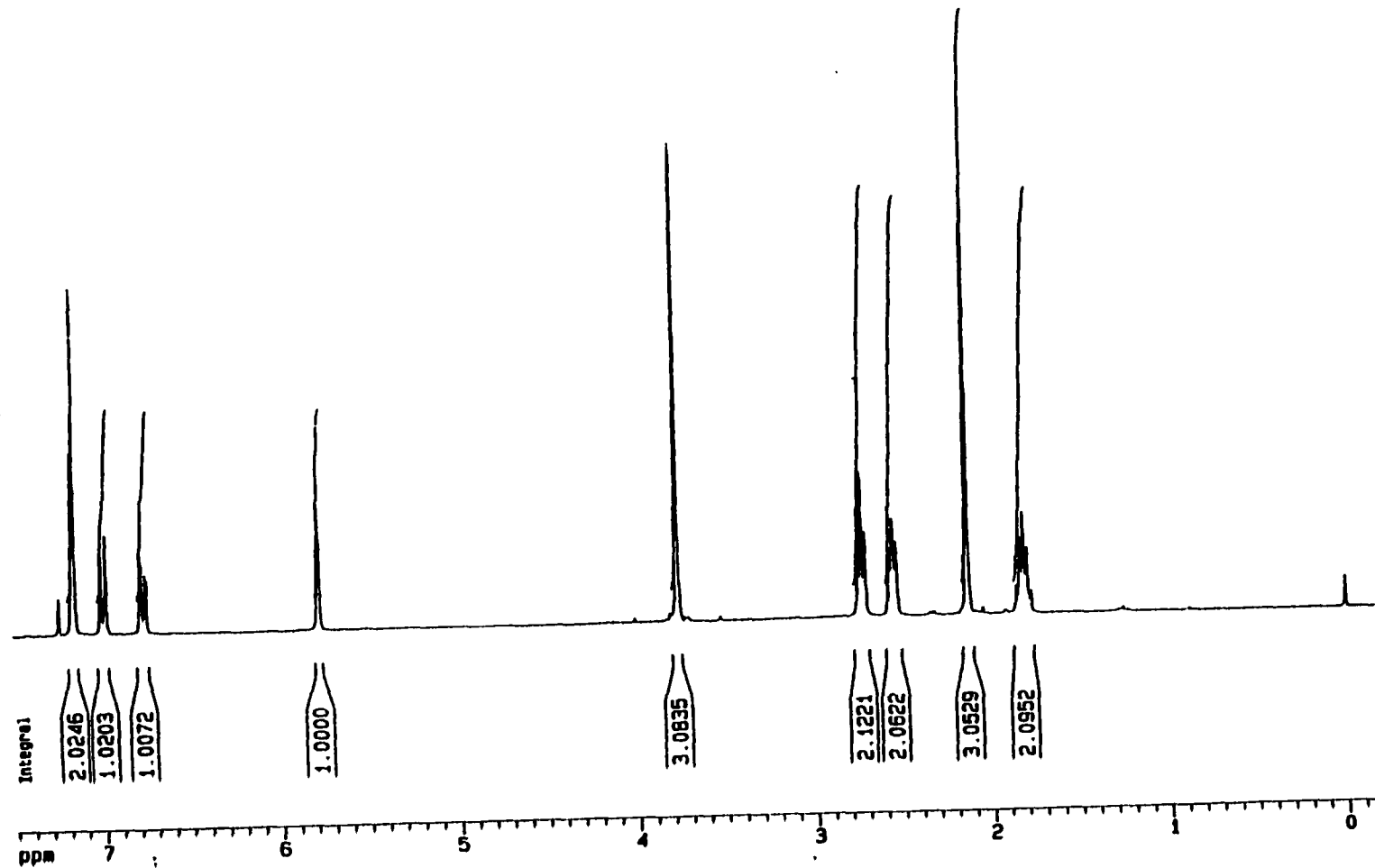


Figure 29. ^1H NMR (300 MHz) of Compound II-16 (CDCl_3).

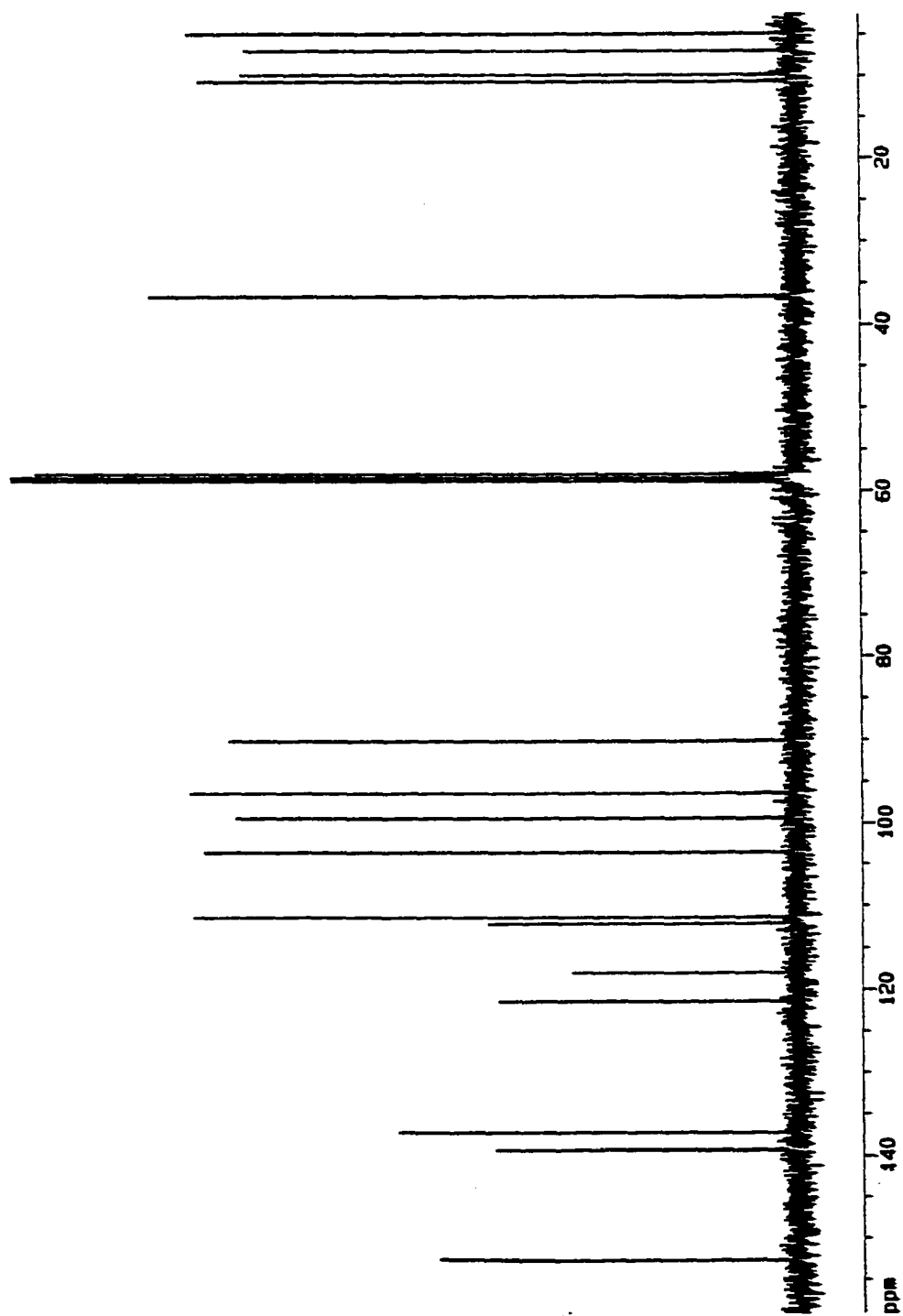


Figure 30. ^{13}C NMR (300 MHz) of Compound II-16 (CDCl_3).

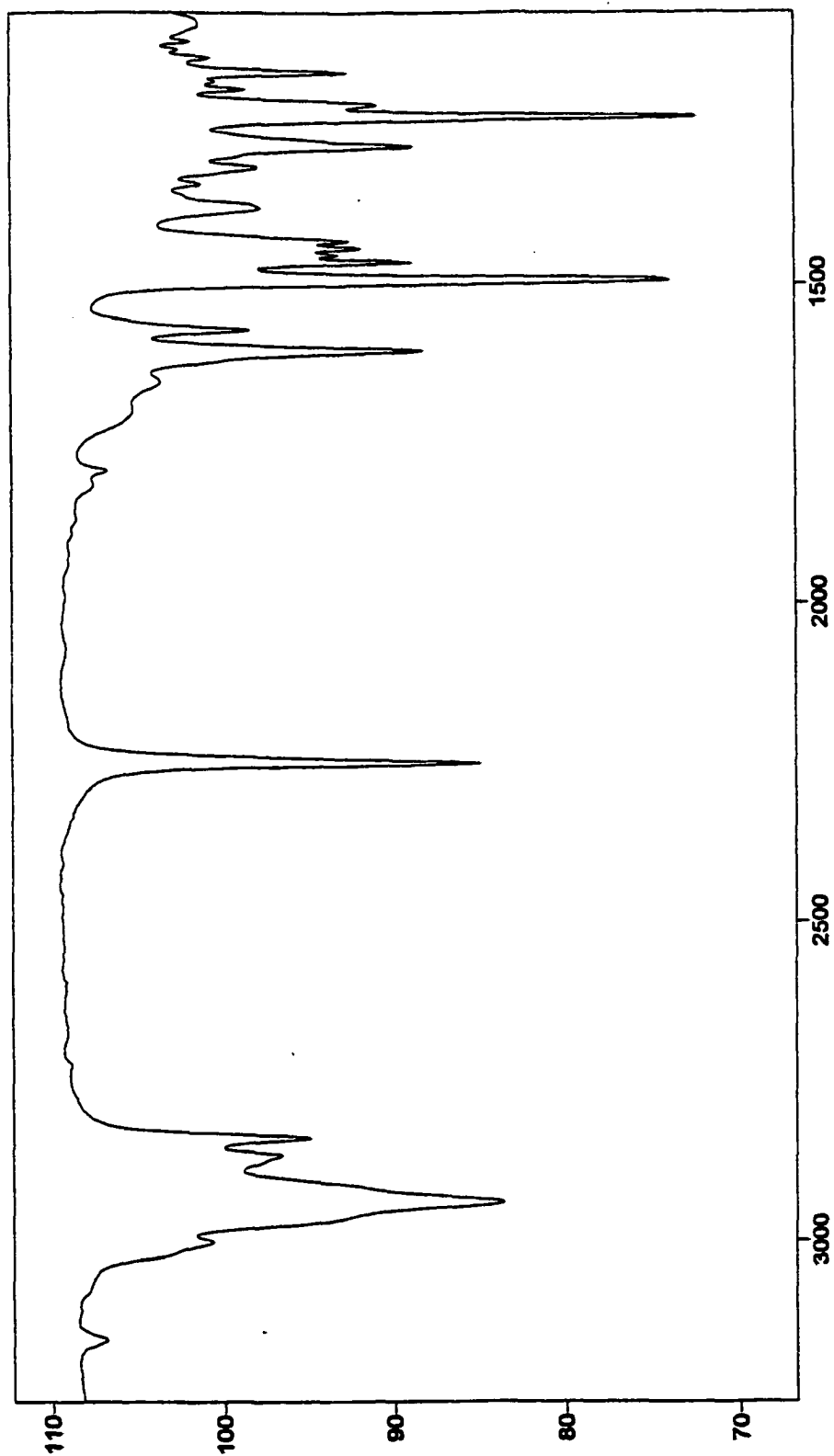


Figure 31. FTIR of Compound II-16 (KBr).

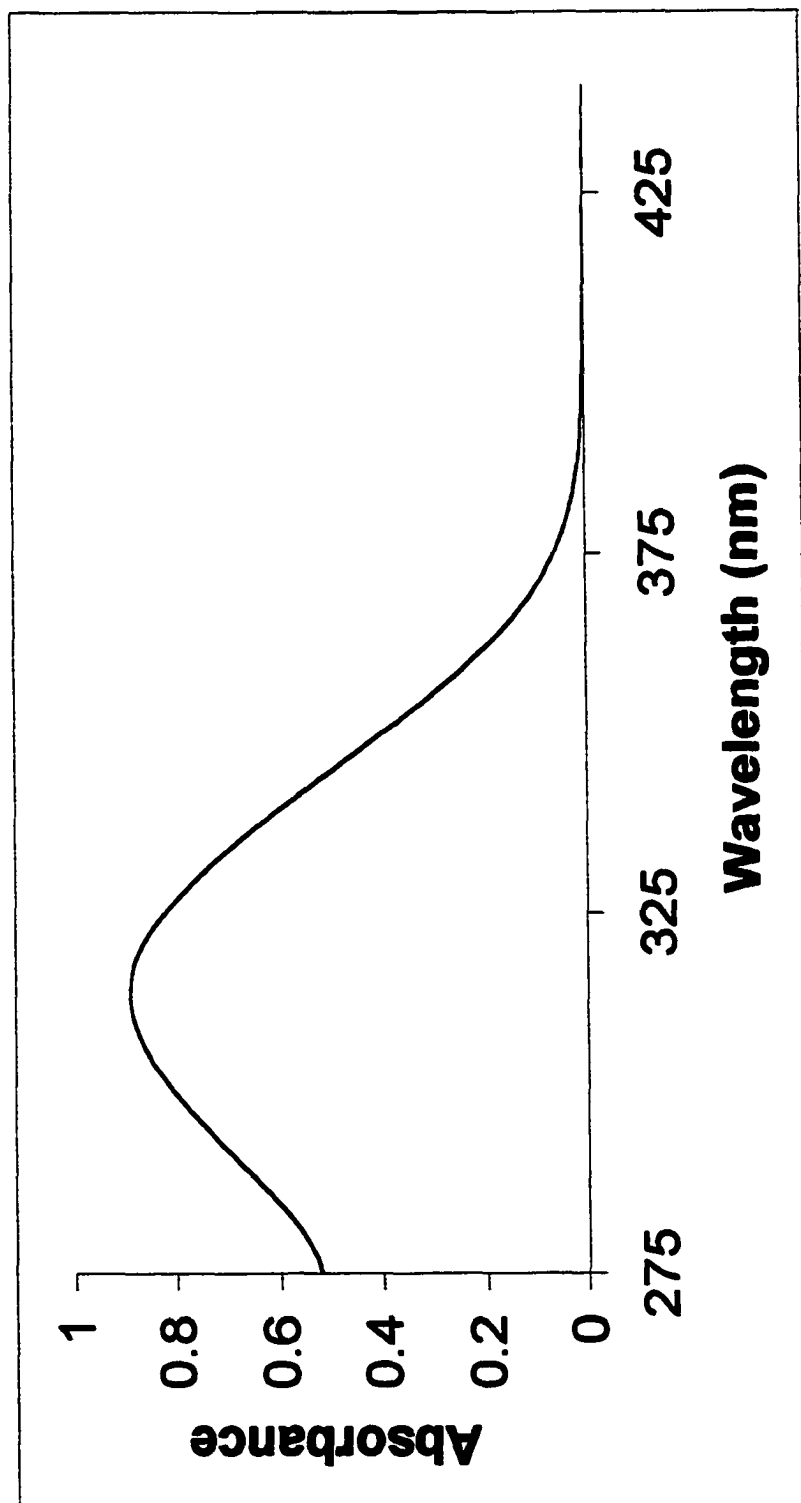


Figure 32. UV-Vis of Compound **II-16** (MeOH).

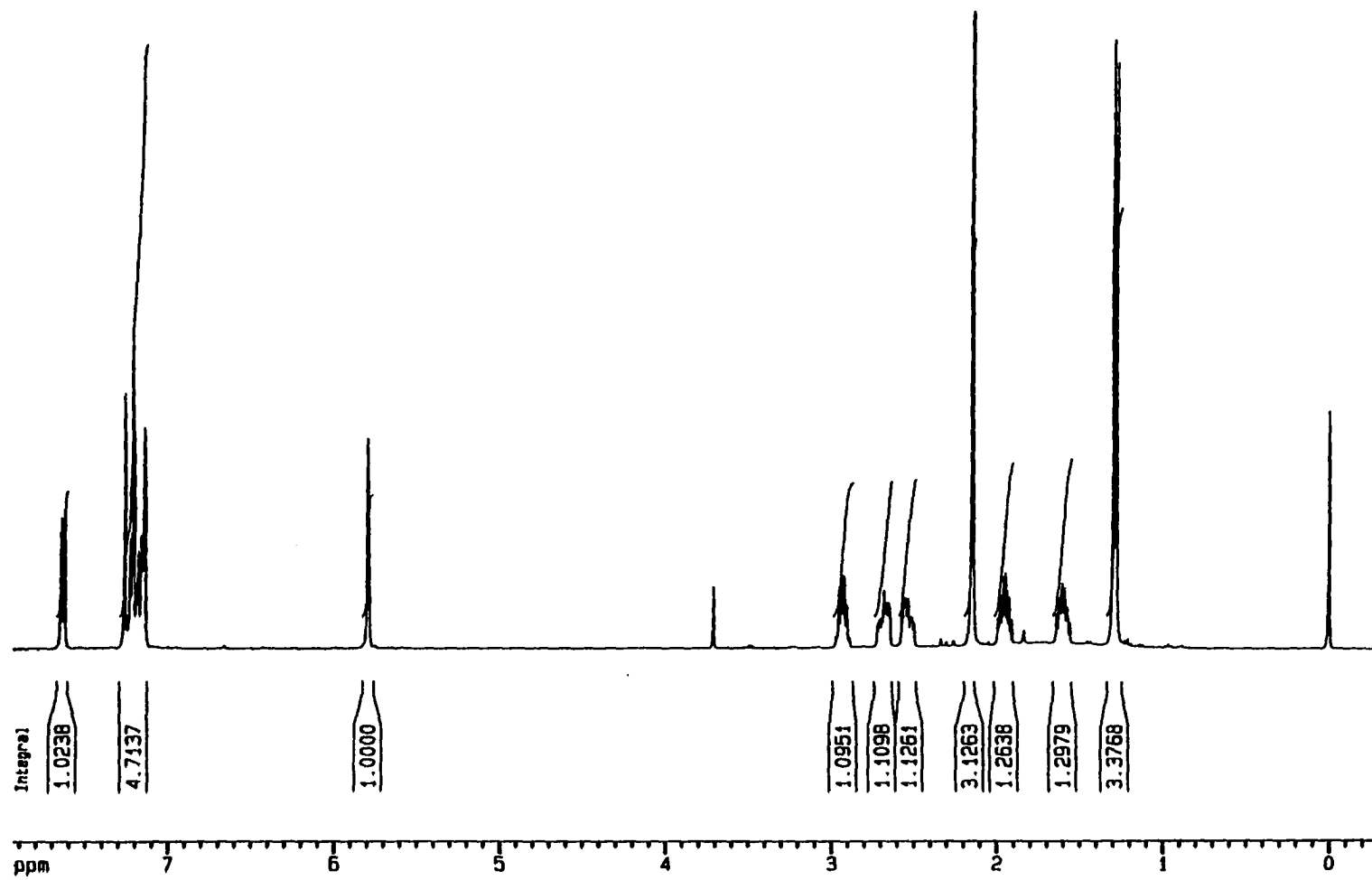


Figure 33. ^1H NMR (300 MHz) of Compound II-17 (CDCl_3).

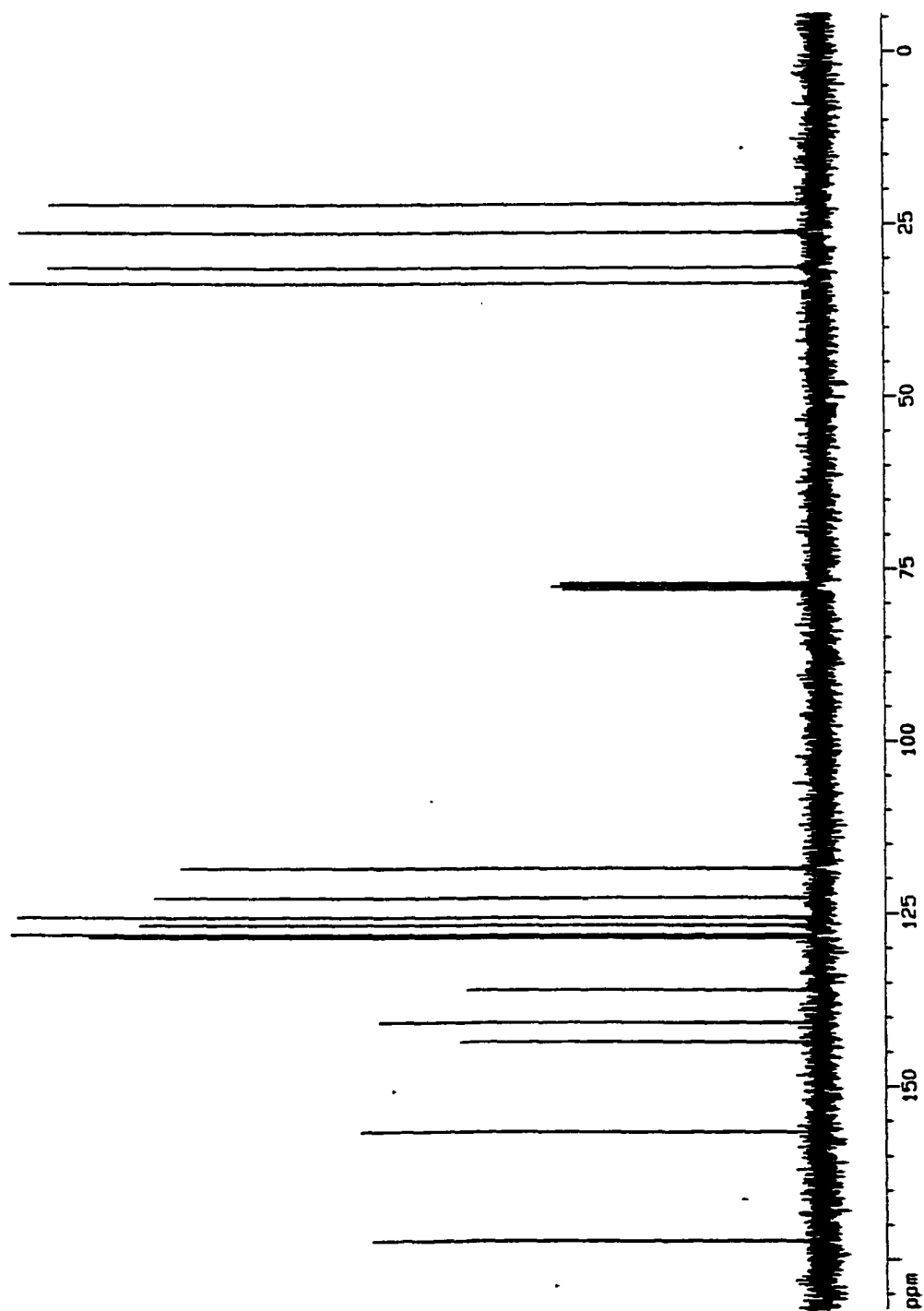


Figure 34. ^{13}C NMR (300 MHz) of Compound II-17 (CDCl_3).

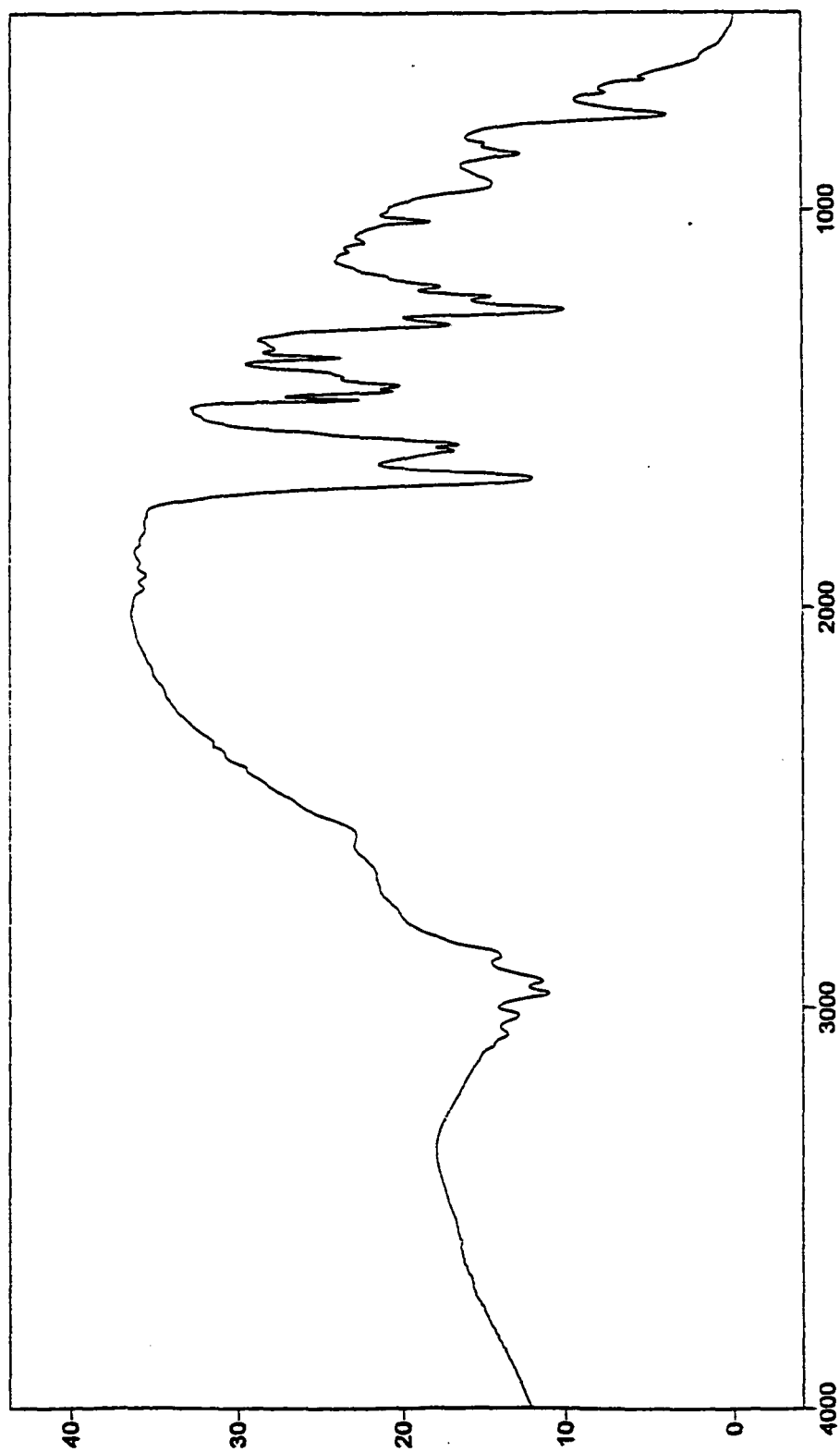


Figure 35. FTIR of Compound II-17 (KBr).



Figure 36. UV-Vis of Compound II-17 (MeOH).

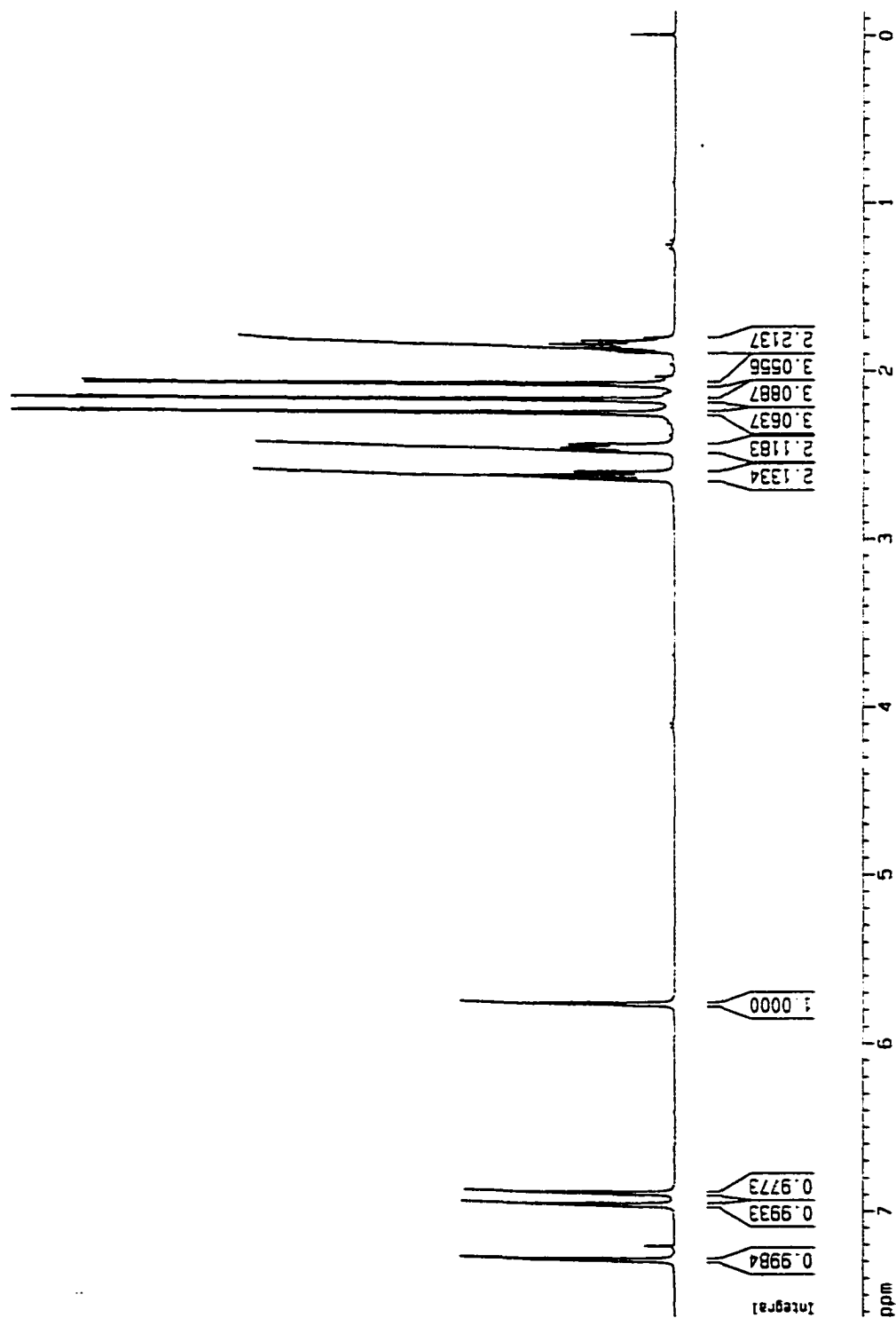


Figure 37. ¹H NMR (300 MHz) of Compound II-18 (CDCl₃).

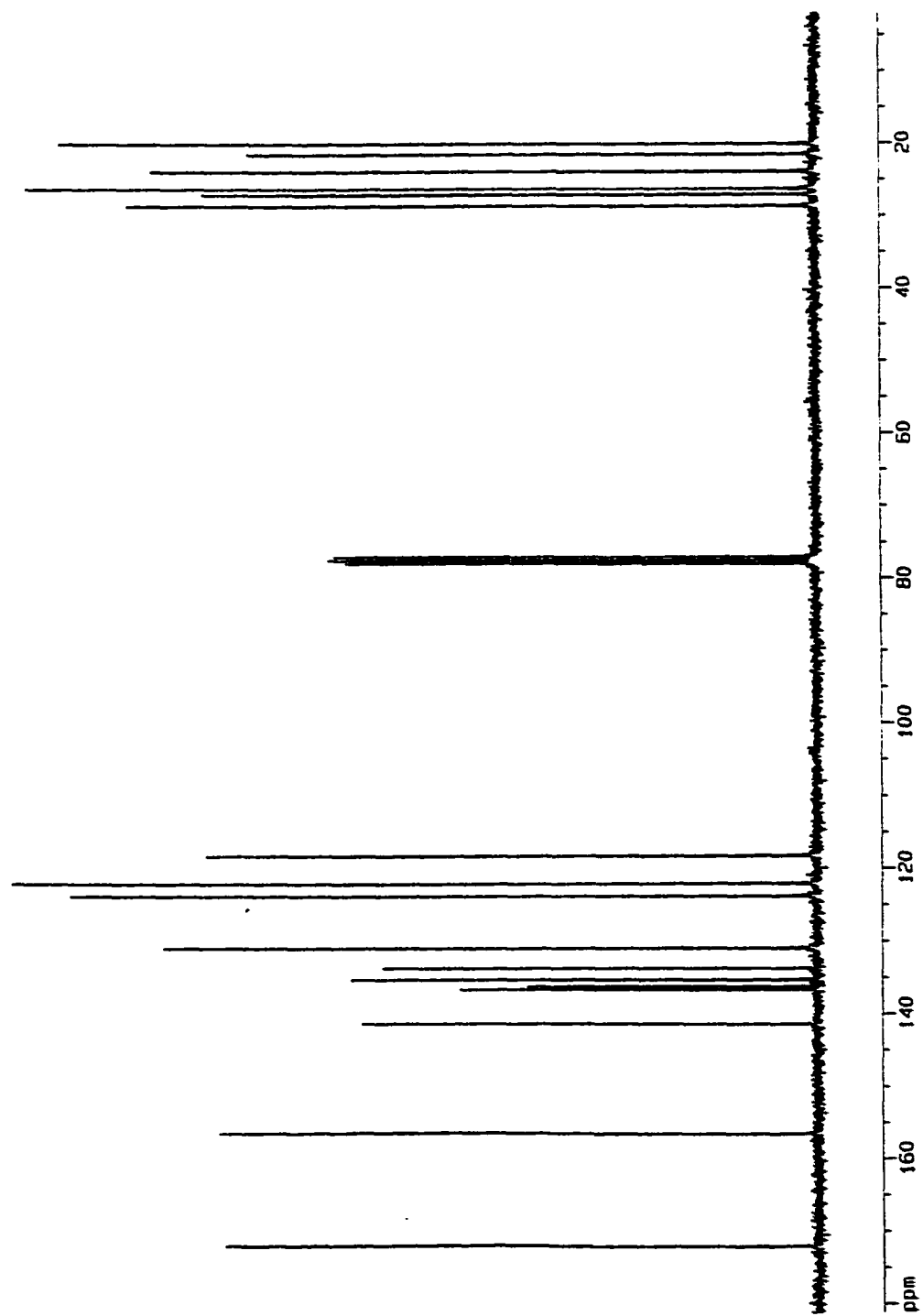


Figure 38. ^{13}C NMR (300 MHz) of Compound **II-18** (CDCl_3).

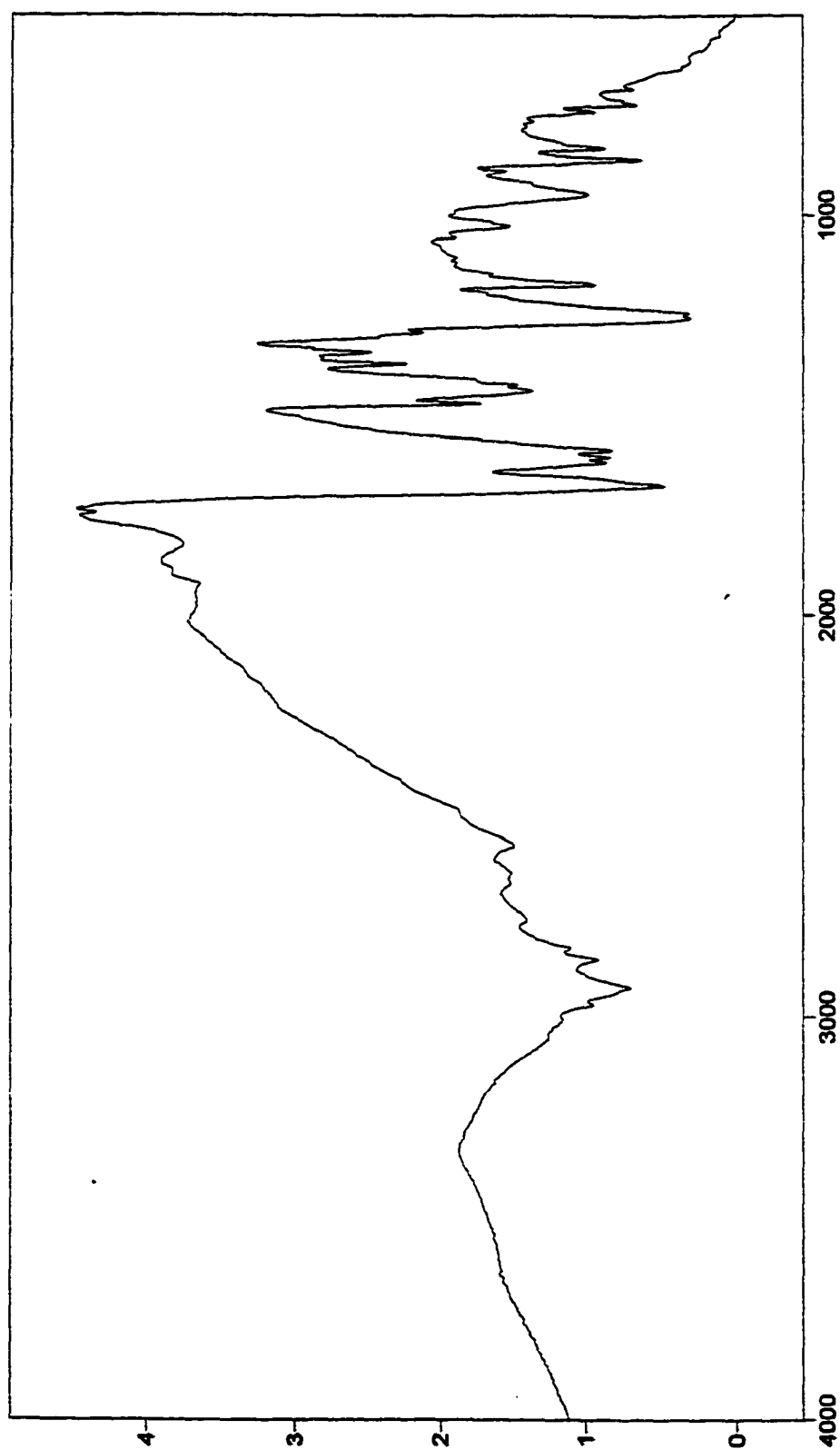


Figure 39. FTIR of Compound II-18 (KBr).

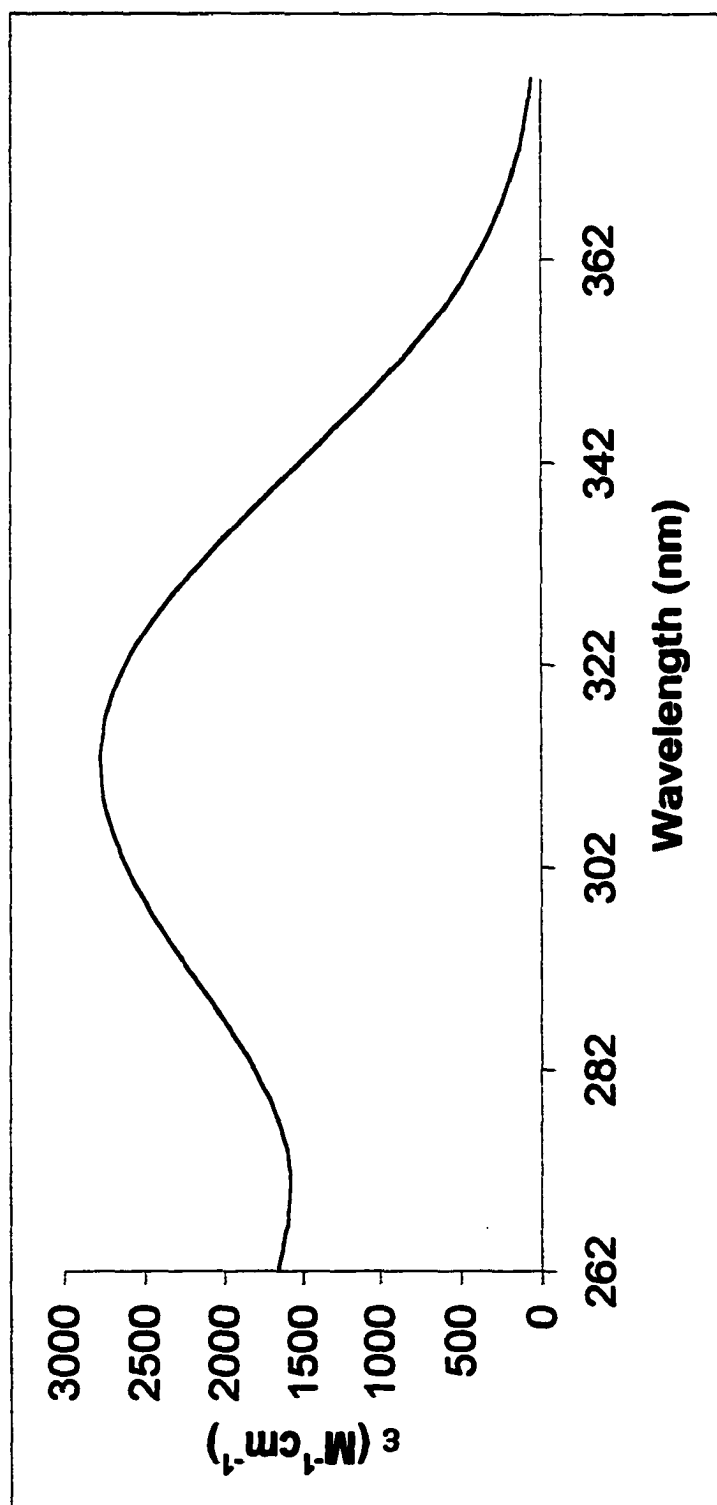


Figure 40. UV-Vis of Compound 11-18 (MeOH).

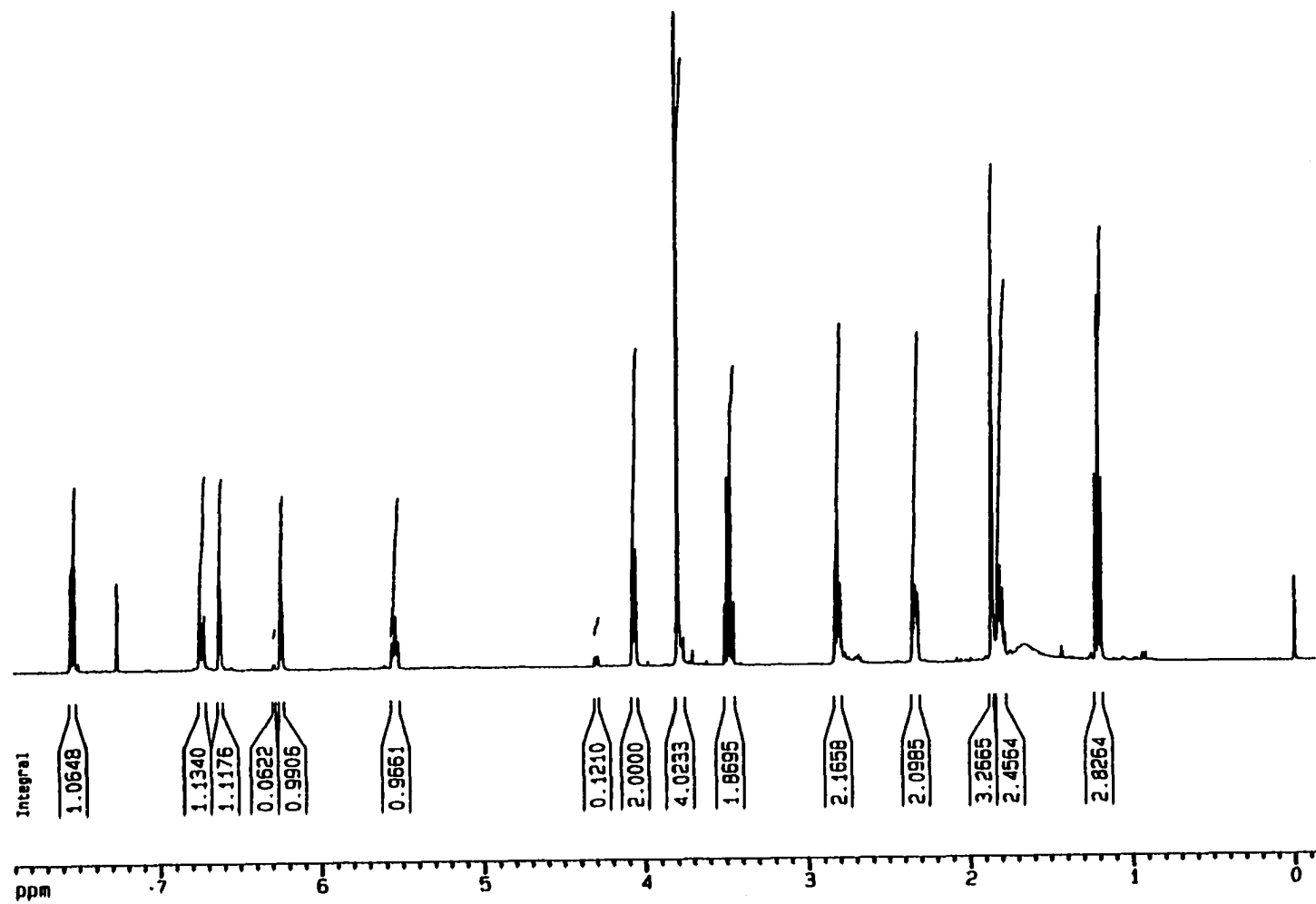


Figure 41. ^1H NMR (300 MHz) of Compound II-20 (CDCl_3).

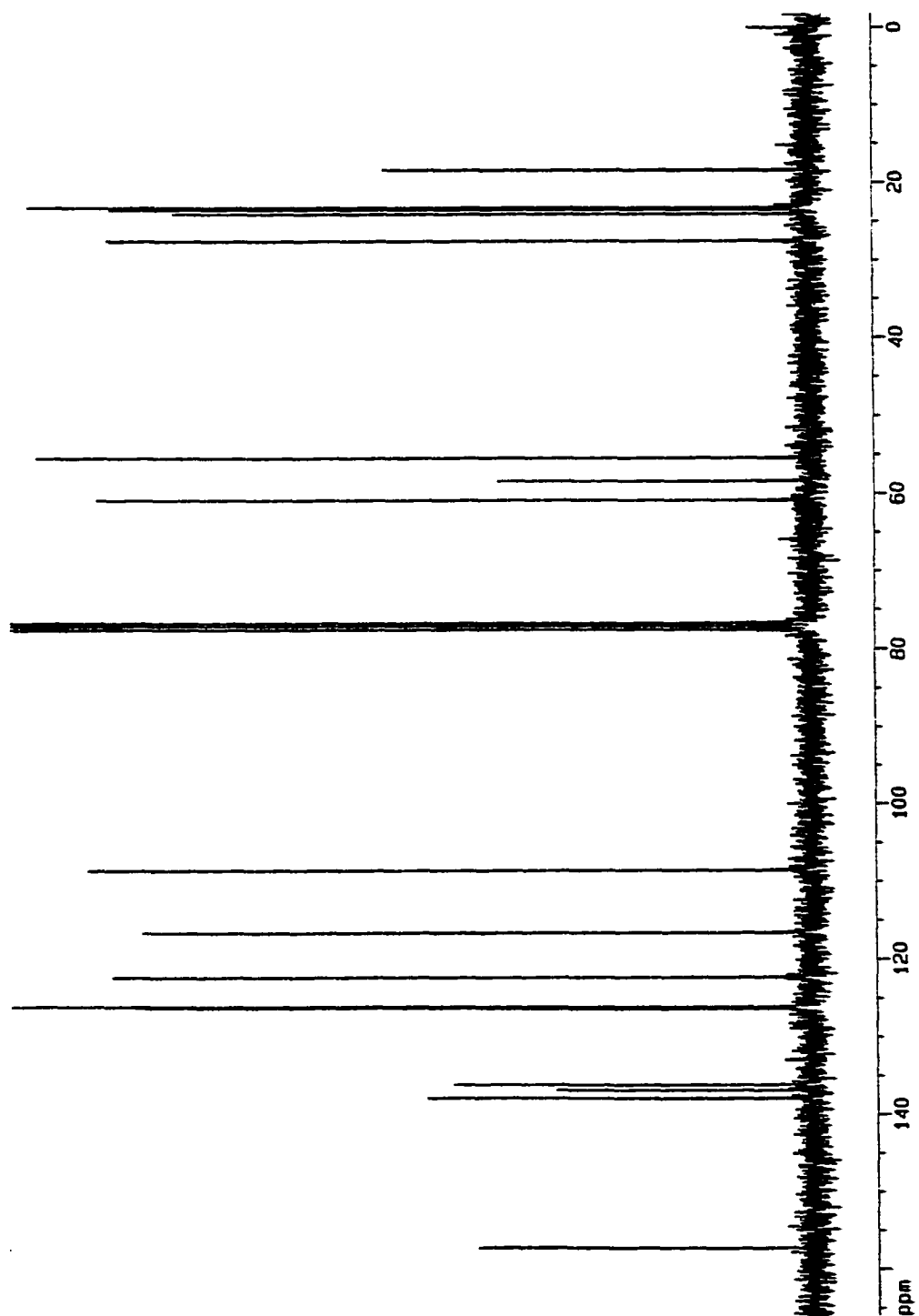


Figure 42. ^{13}C NMR (300 MHz) of Compound 11-20 (CDCl_3).

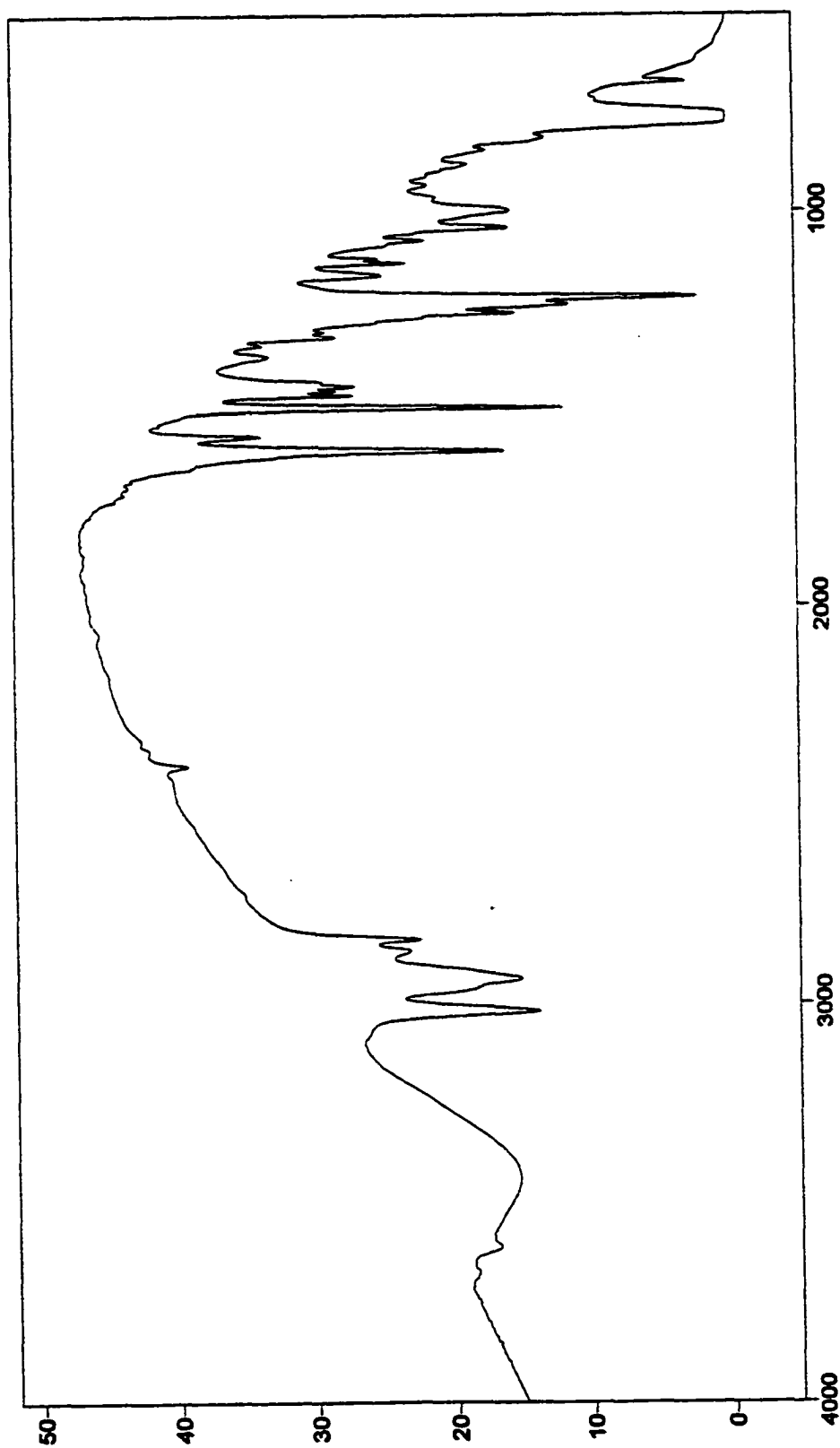


Figure 43. FTIR of Compound II-20 (KBr).

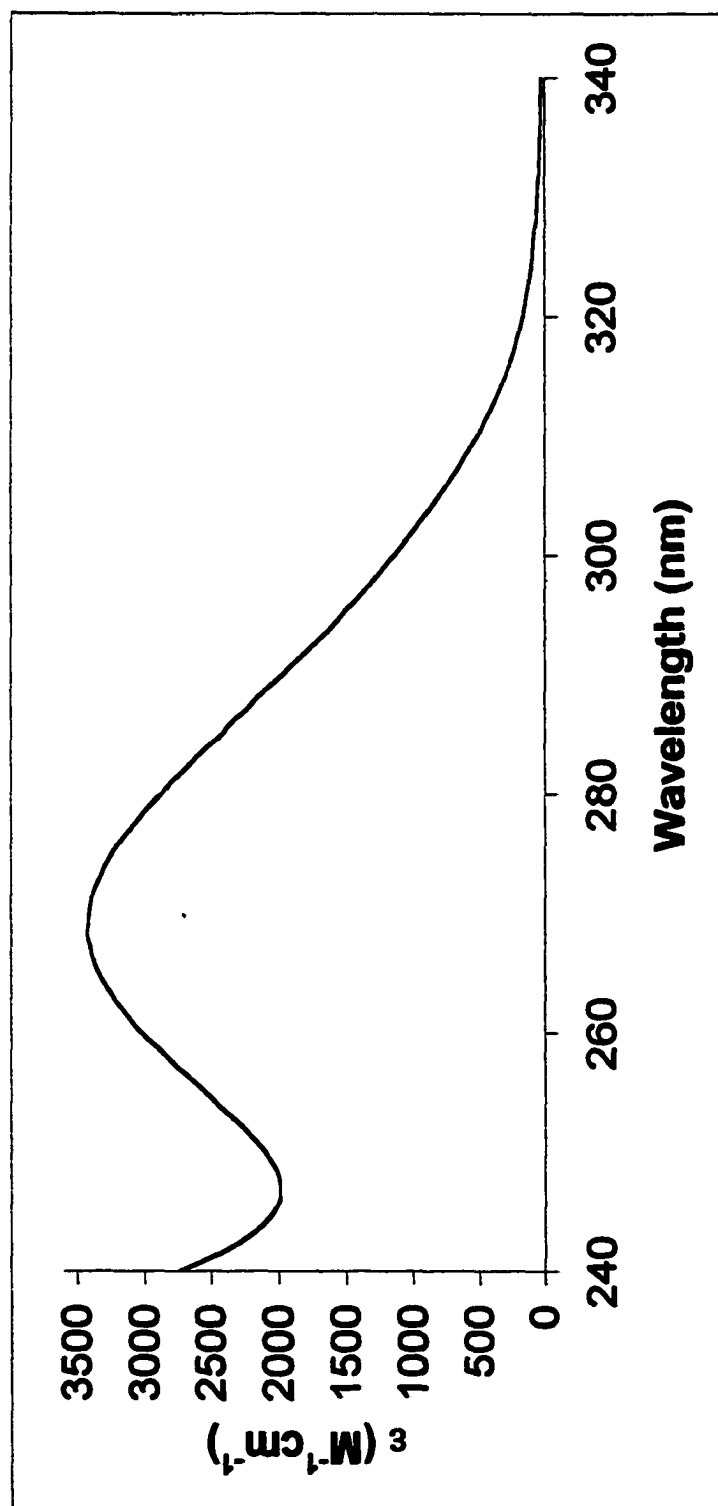


Figure 44. UV-Vis of Compound II-20 (MeOH).

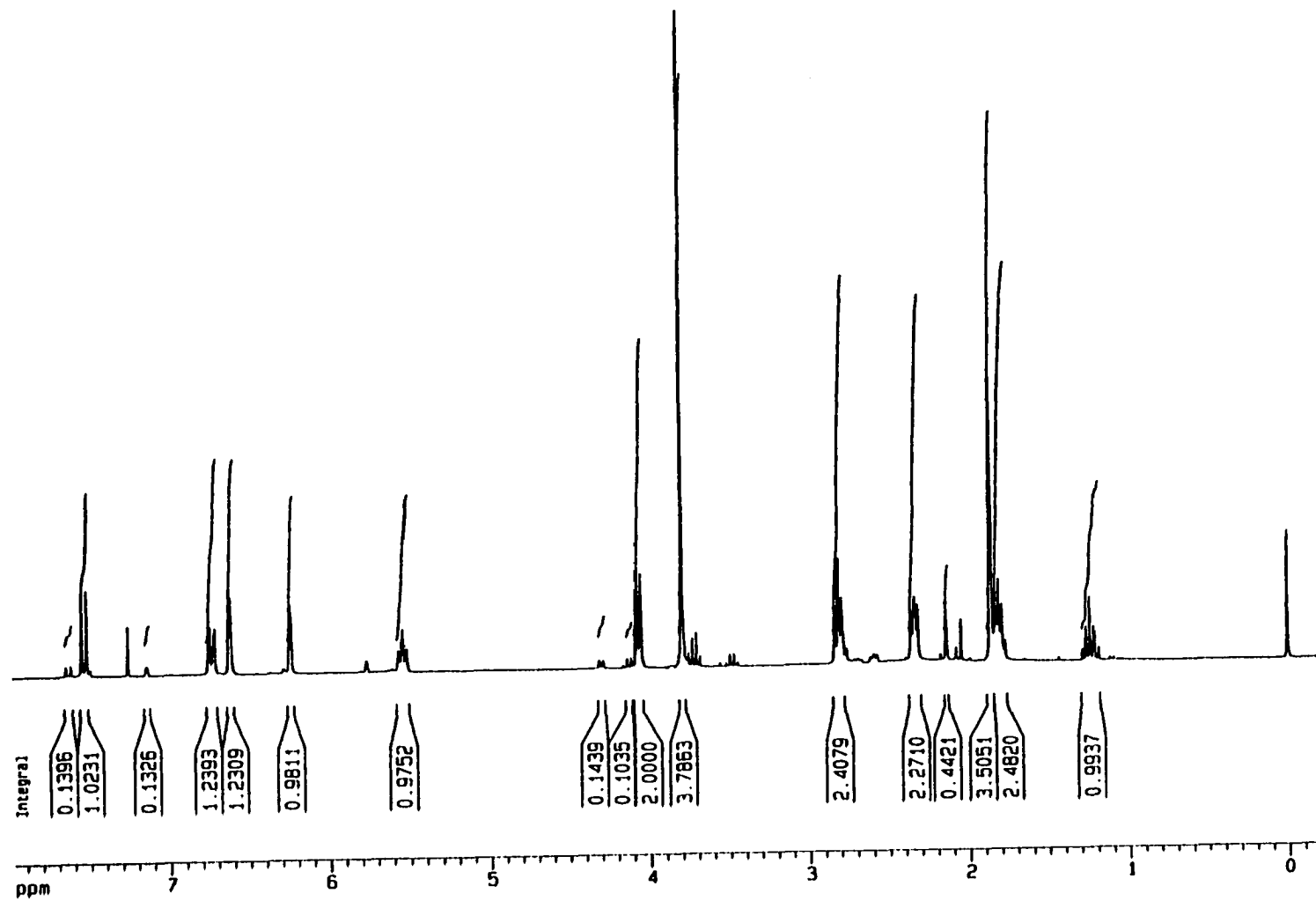


Figure 45. ^1H NMR (300 MHz) of Compound II-21 (CDCl_3).

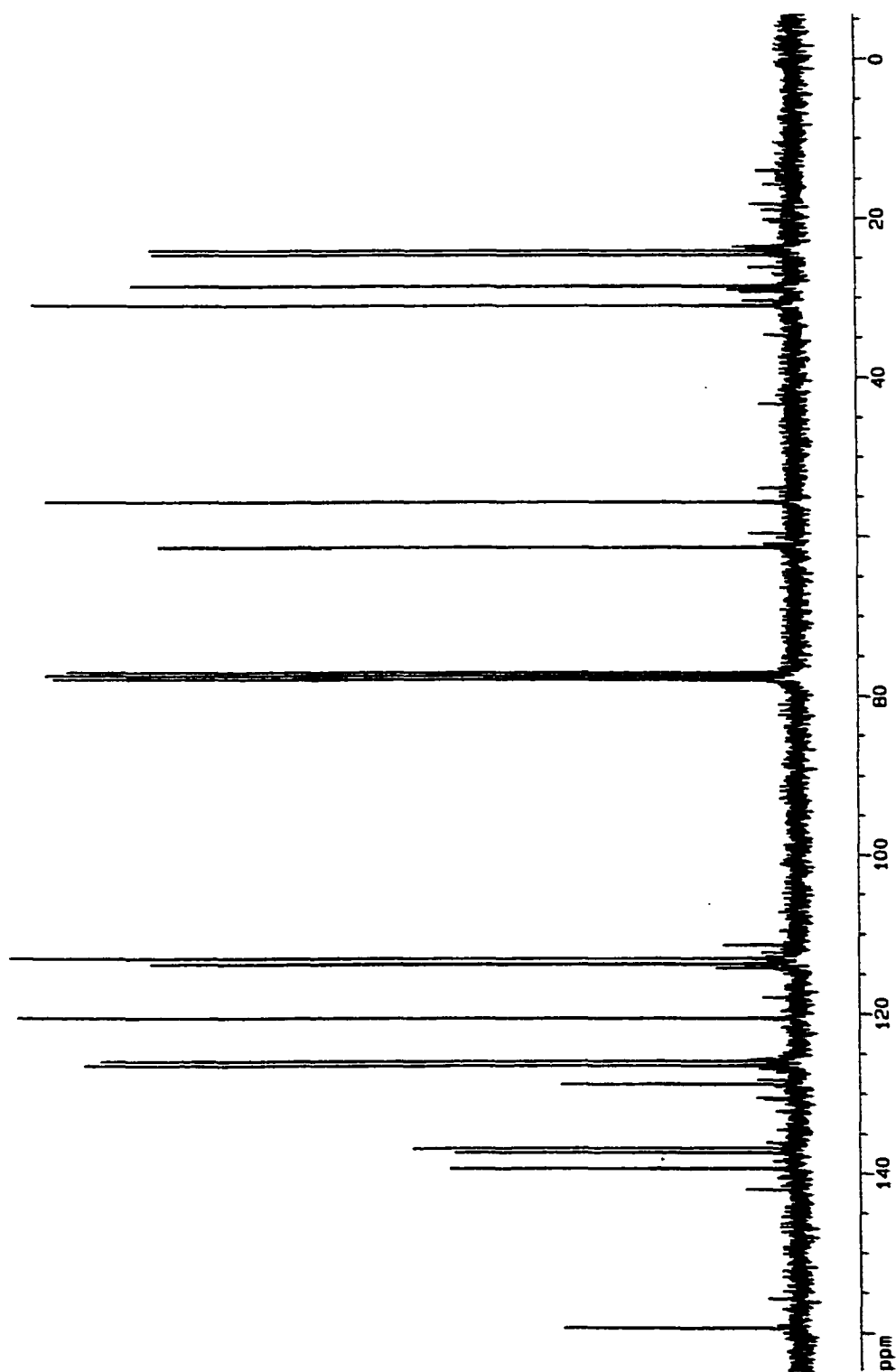


Figure 46. ^{13}C NMR (300 MHz) of Compound II-21 (CDCl_3).

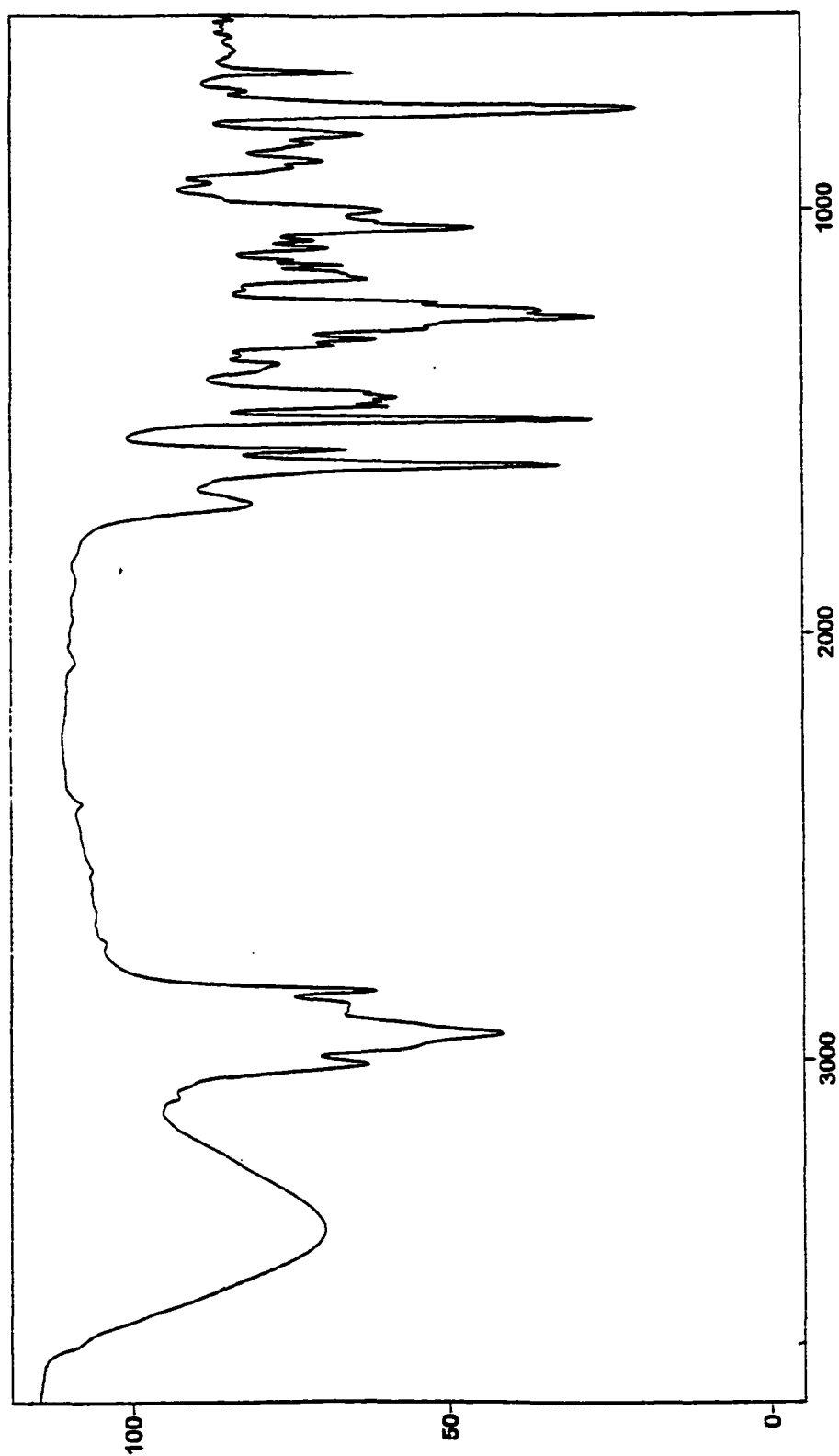


Figure 47. FTIR of Compound II-21 (neat)

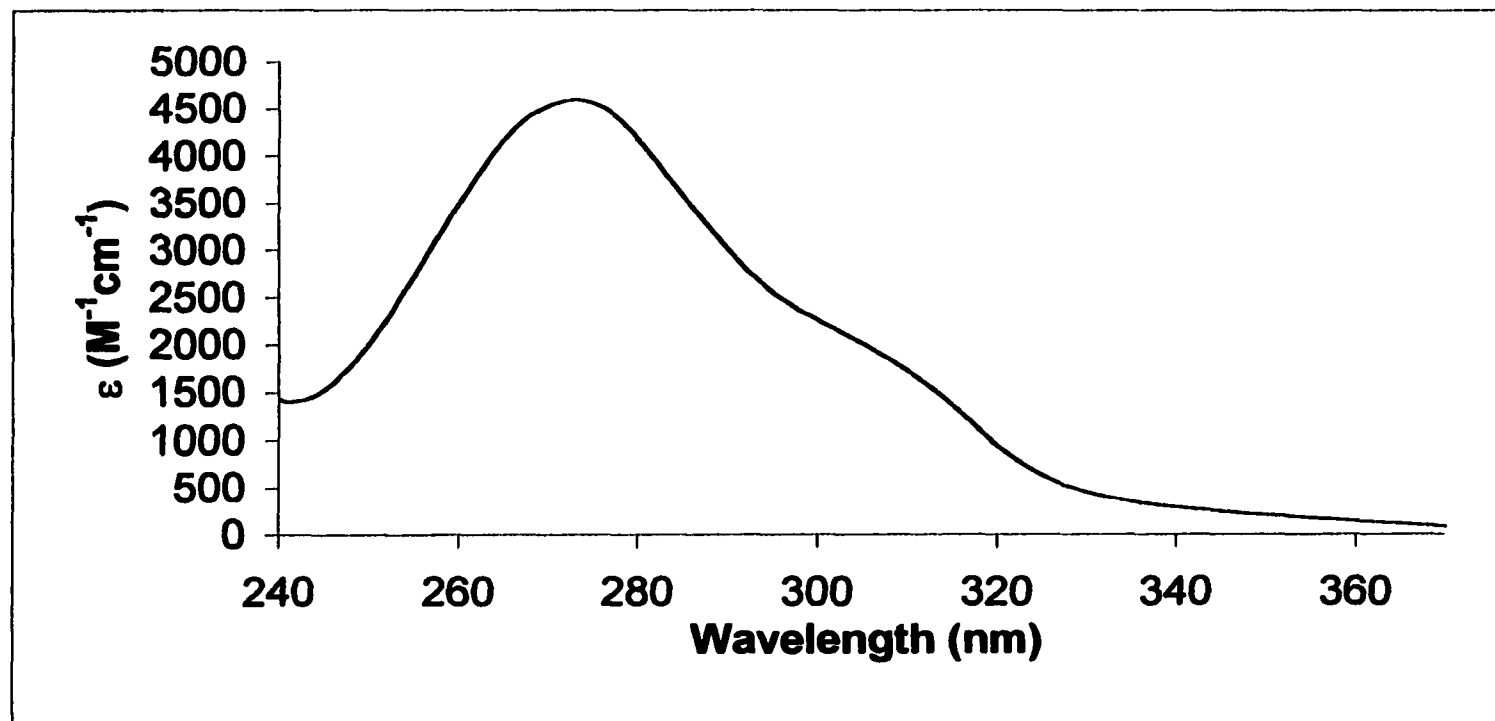


Figure 48. UV-Vis of Compound **II-21** (MeOH).

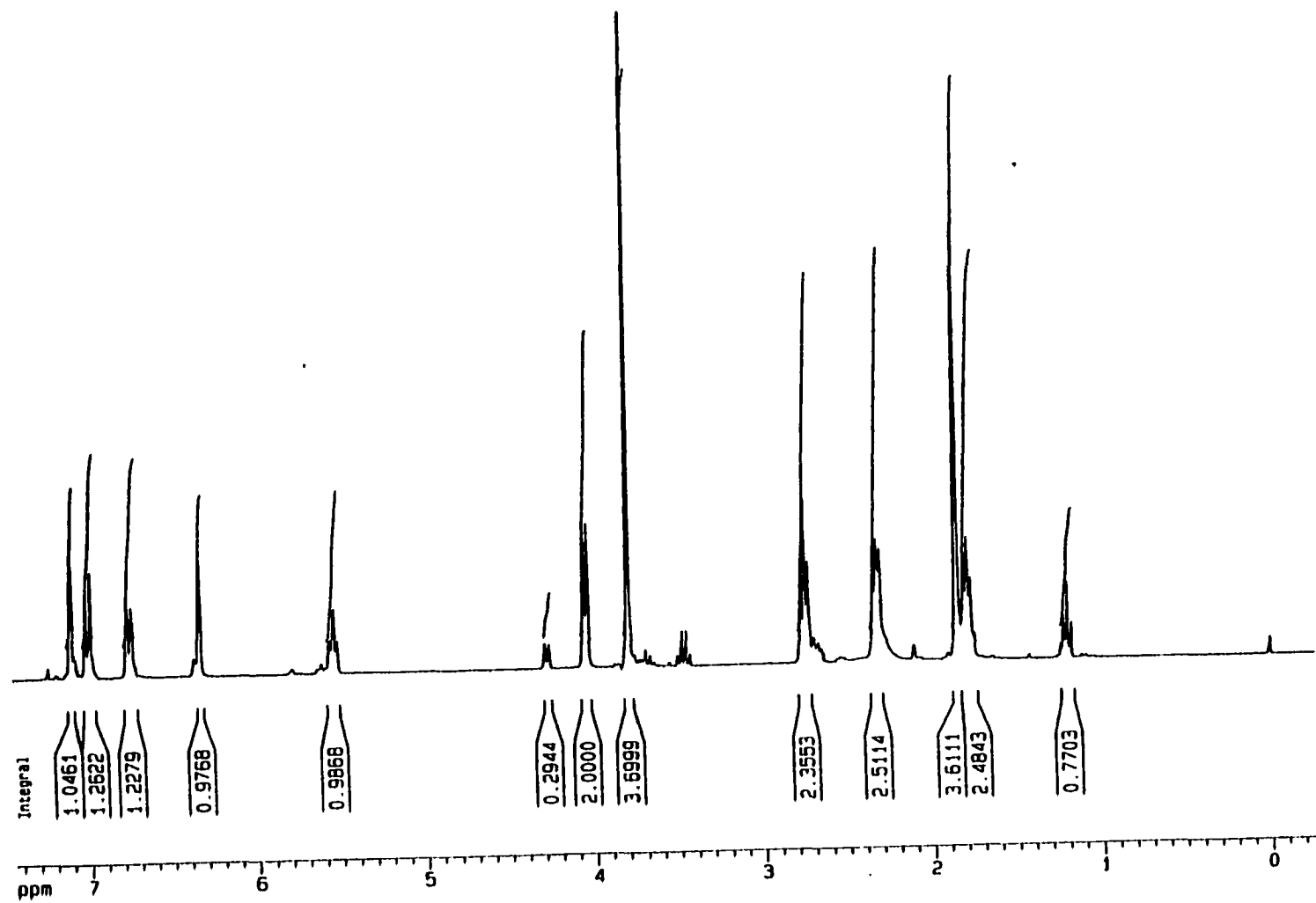


Figure 49. ^1H NMR (300 MHz) of Compound II-22 (CDCl_3).

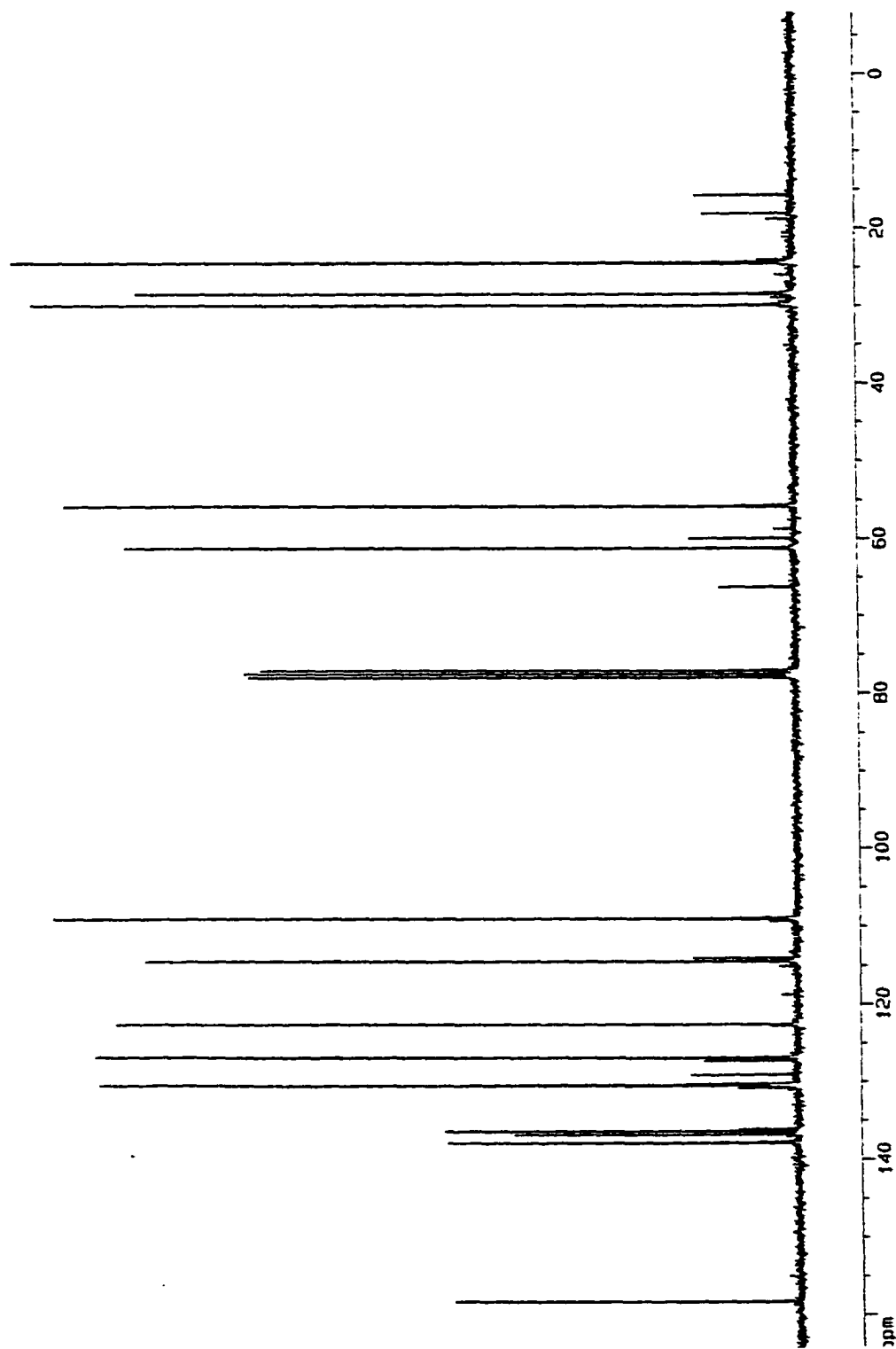


Figure 50. ^{13}C NMR (300 MHz) of Compound II-22 (CDCl_3).

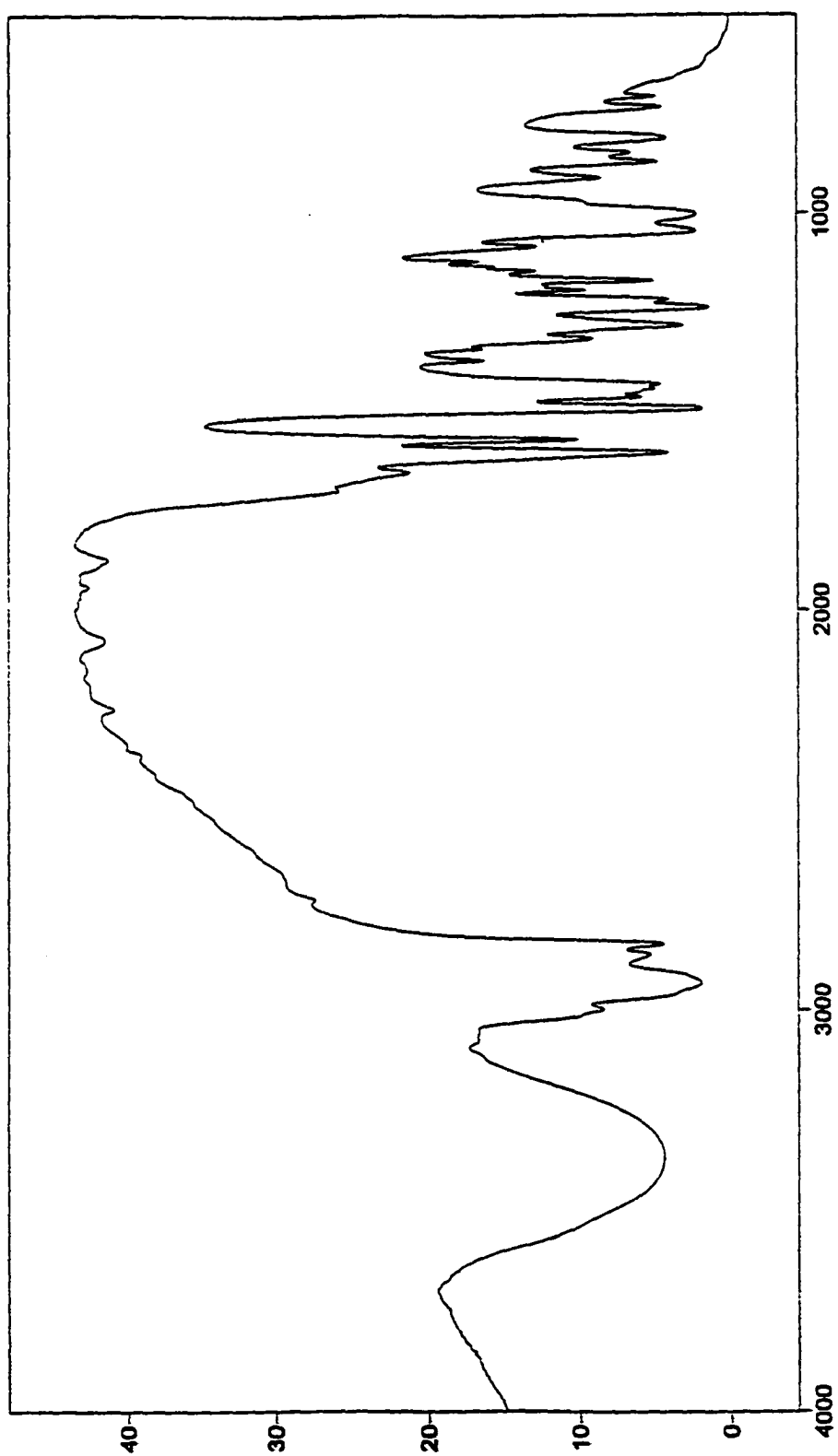


Figure S1. FTIR of Compound II-22 (neat).

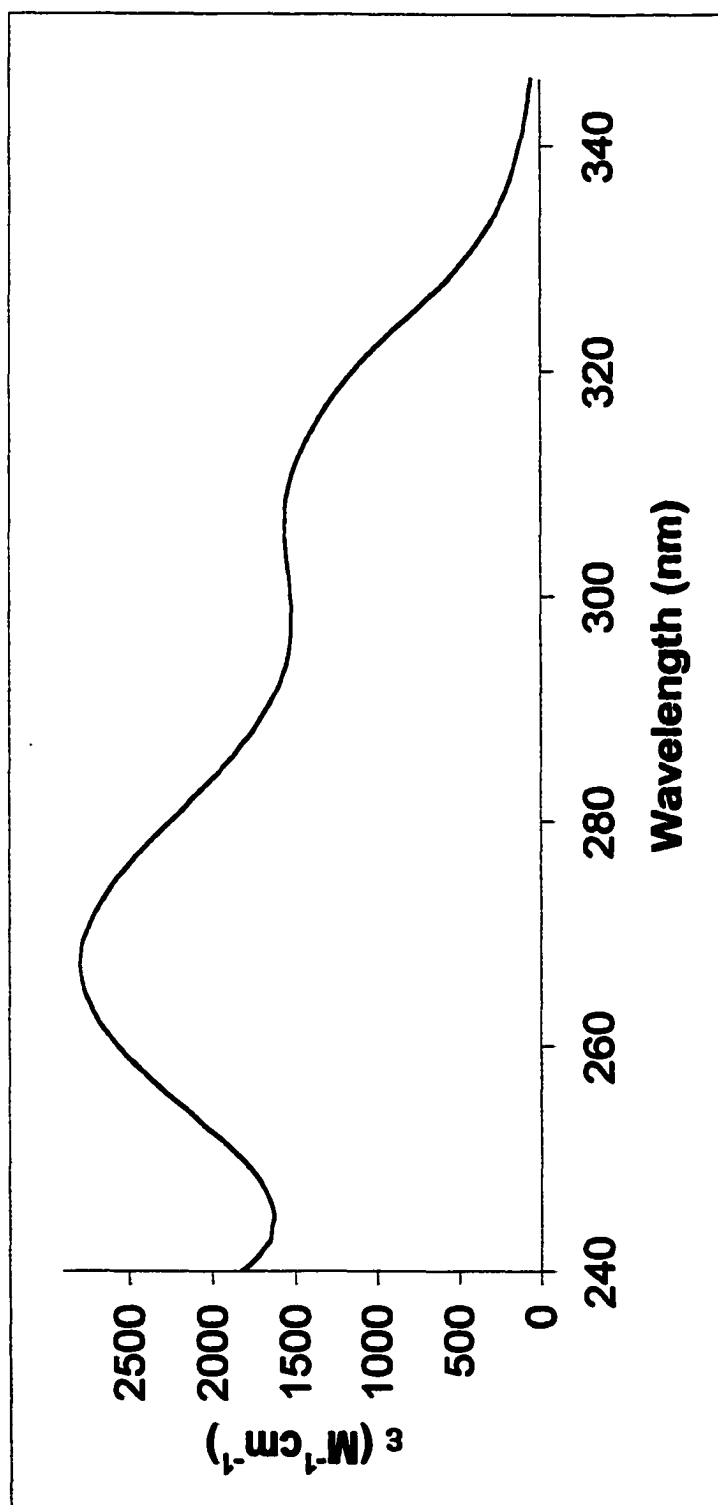


Figure 52. UV-Vis of Compound II-22 (MeOH).

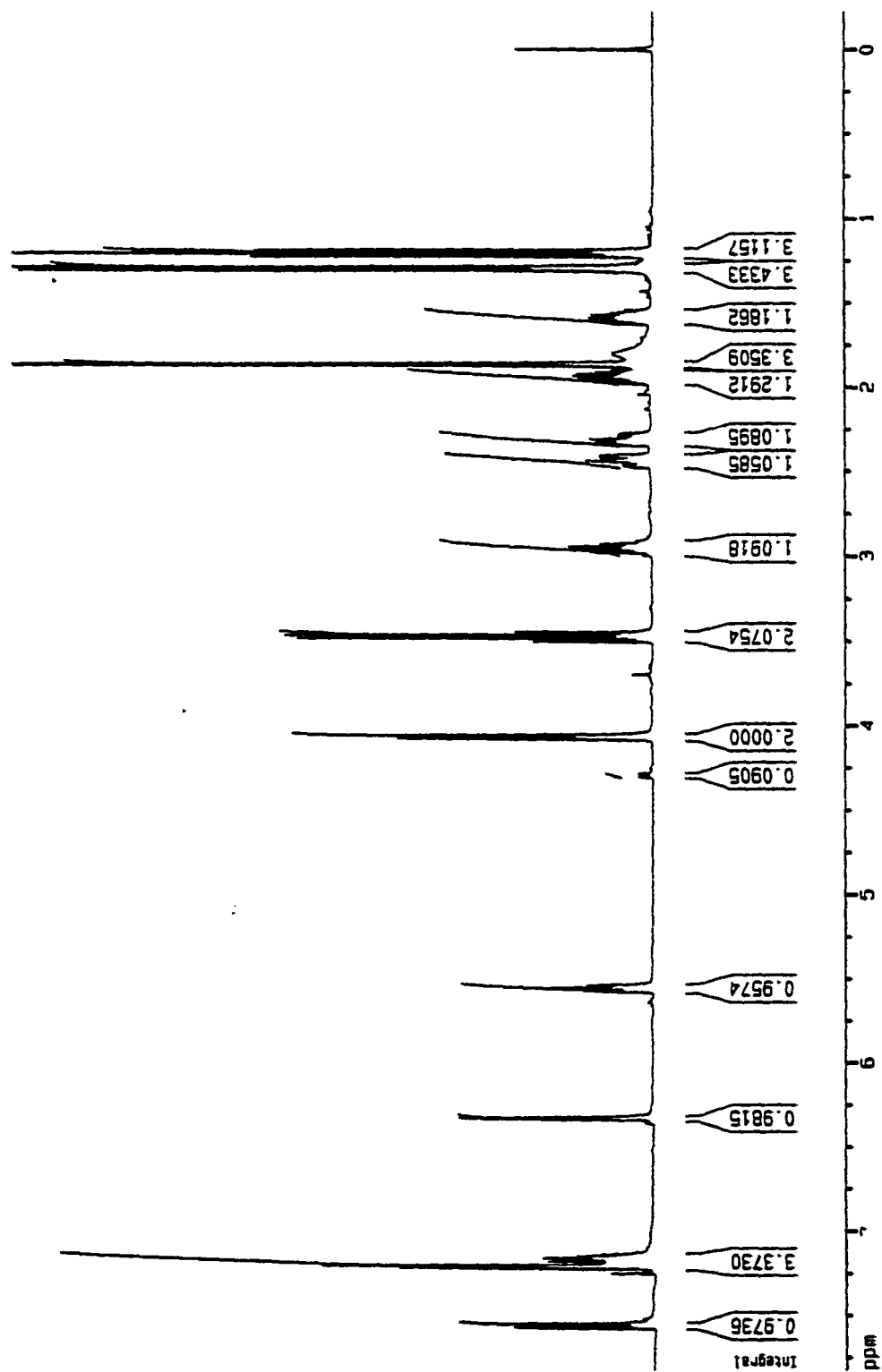


Figure 53. ¹H NMR (300 MHz) of Compound II-23 (CDCl₃).

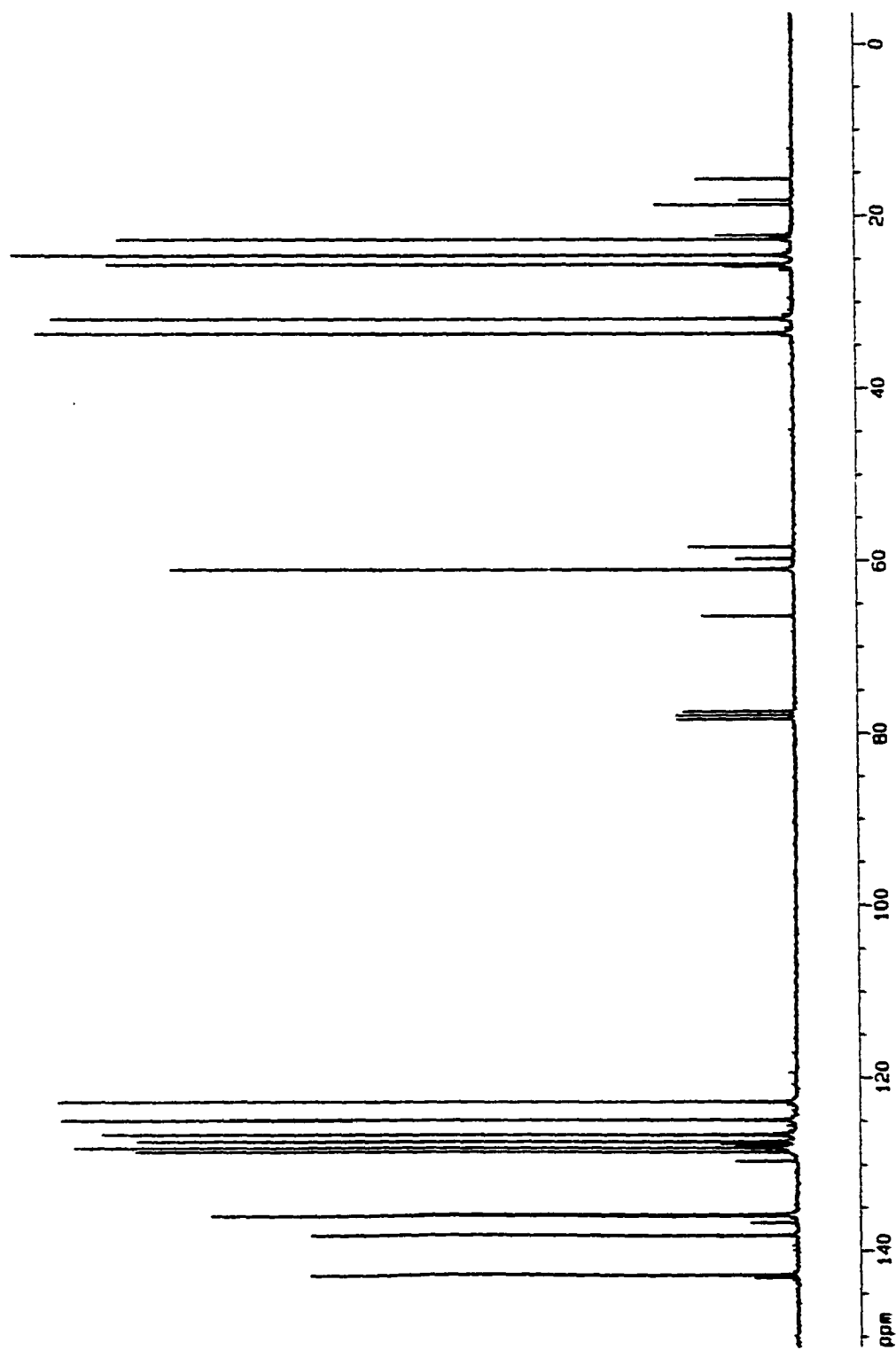


Figure 54. ^{13}C NMR (300 MHz) of Compound II-23 (CDCl_3).

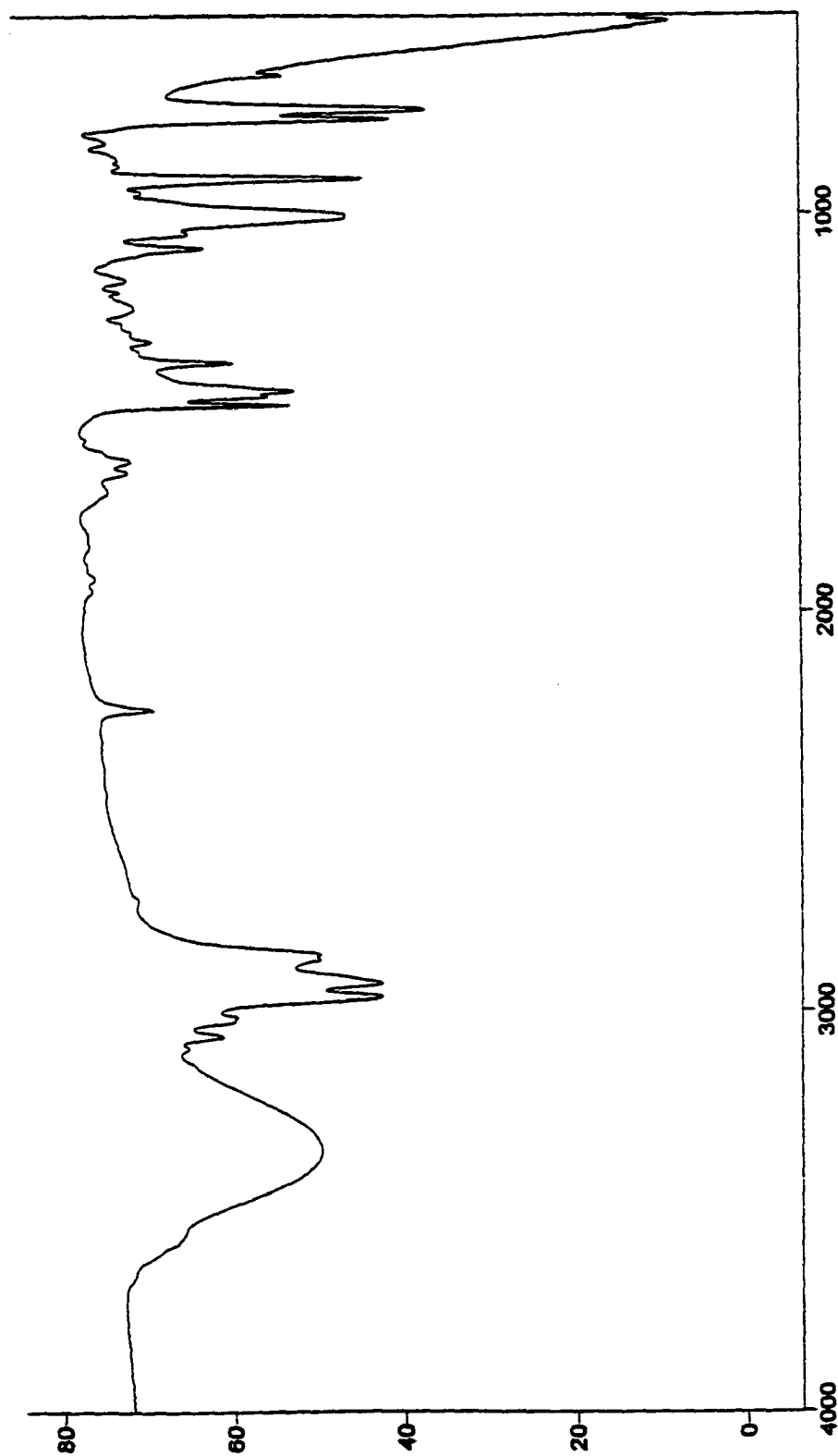


Figure 55. FTIR of Compound II-23 (neat).

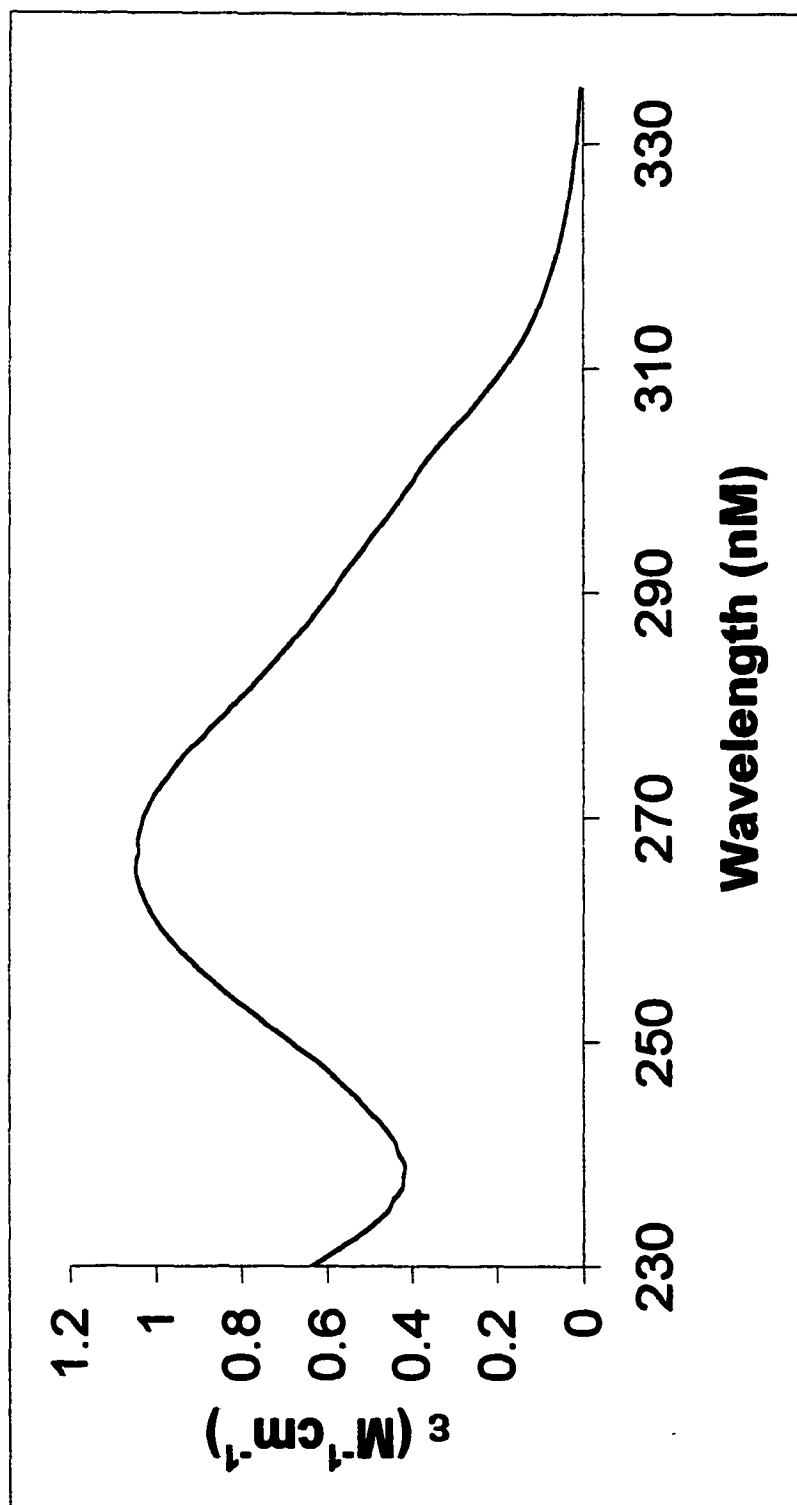


Figure S6. UV-Vis of Compound **II-23** (MeOH).

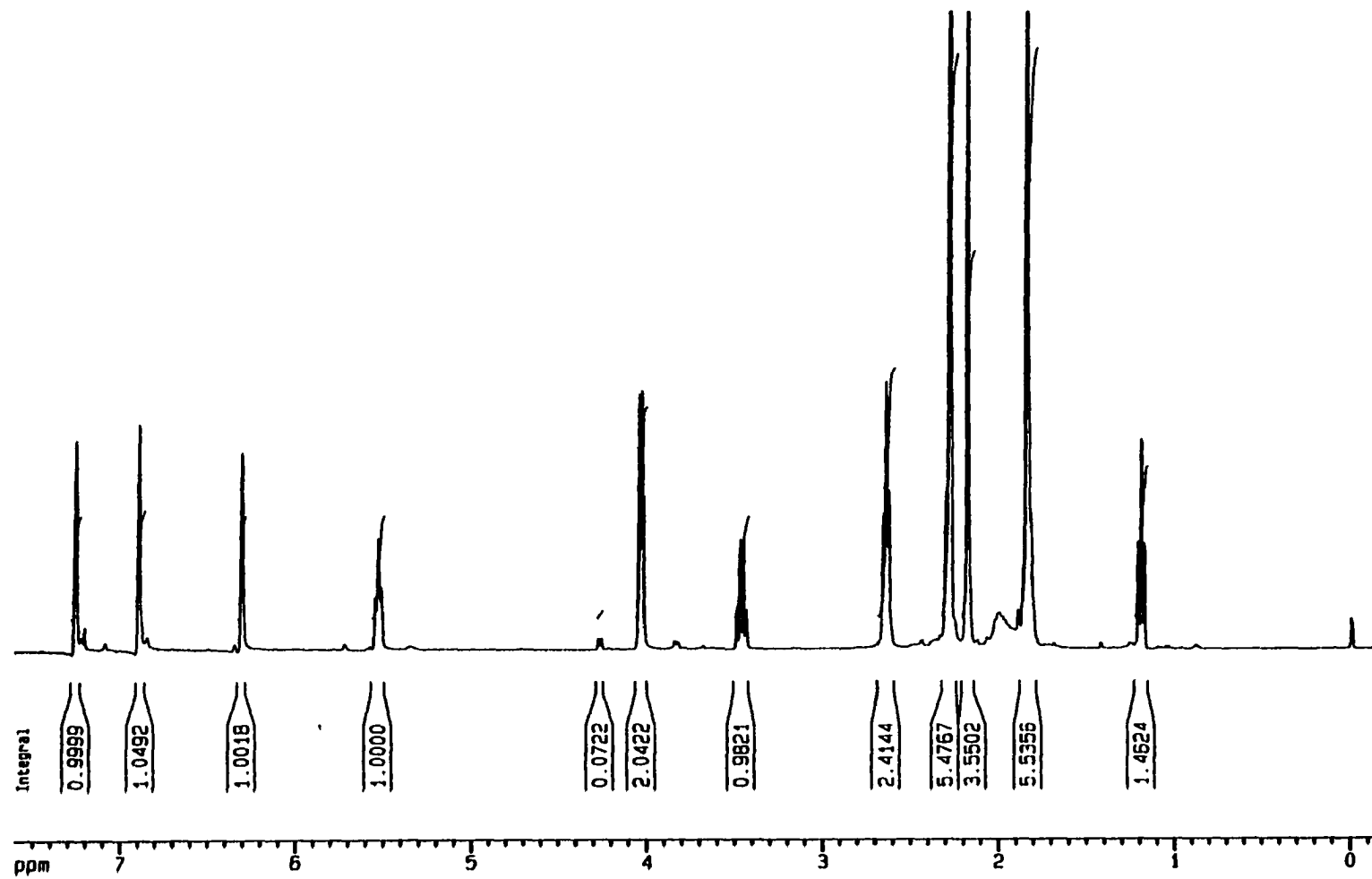


Figure 57. ^1H NMR (300 MHz) of Compound II-24 (CDCl_3).

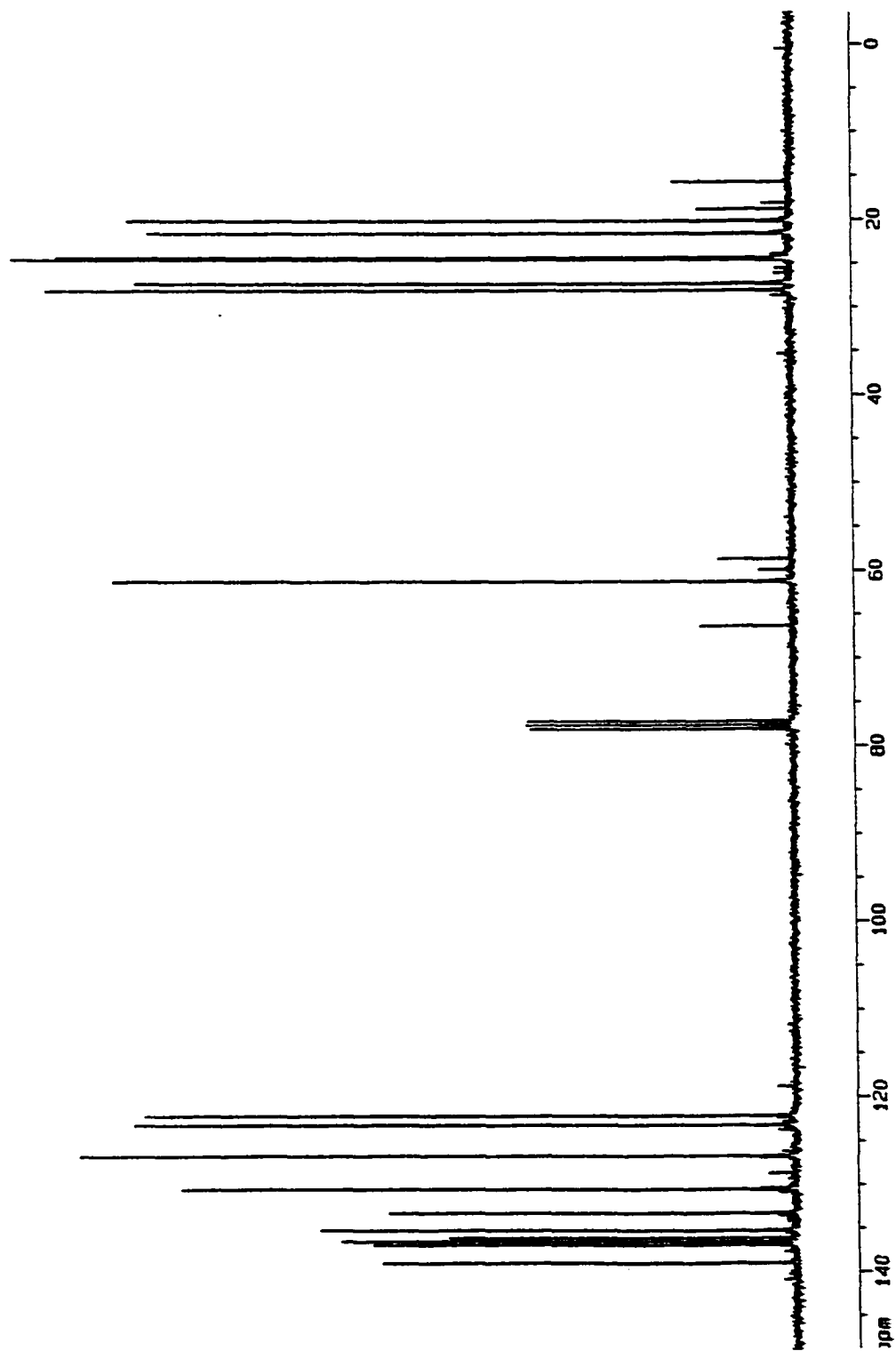


Figure 58. ^{13}C NMR (300 MHz) of Compound II-24 (CDCl_3).

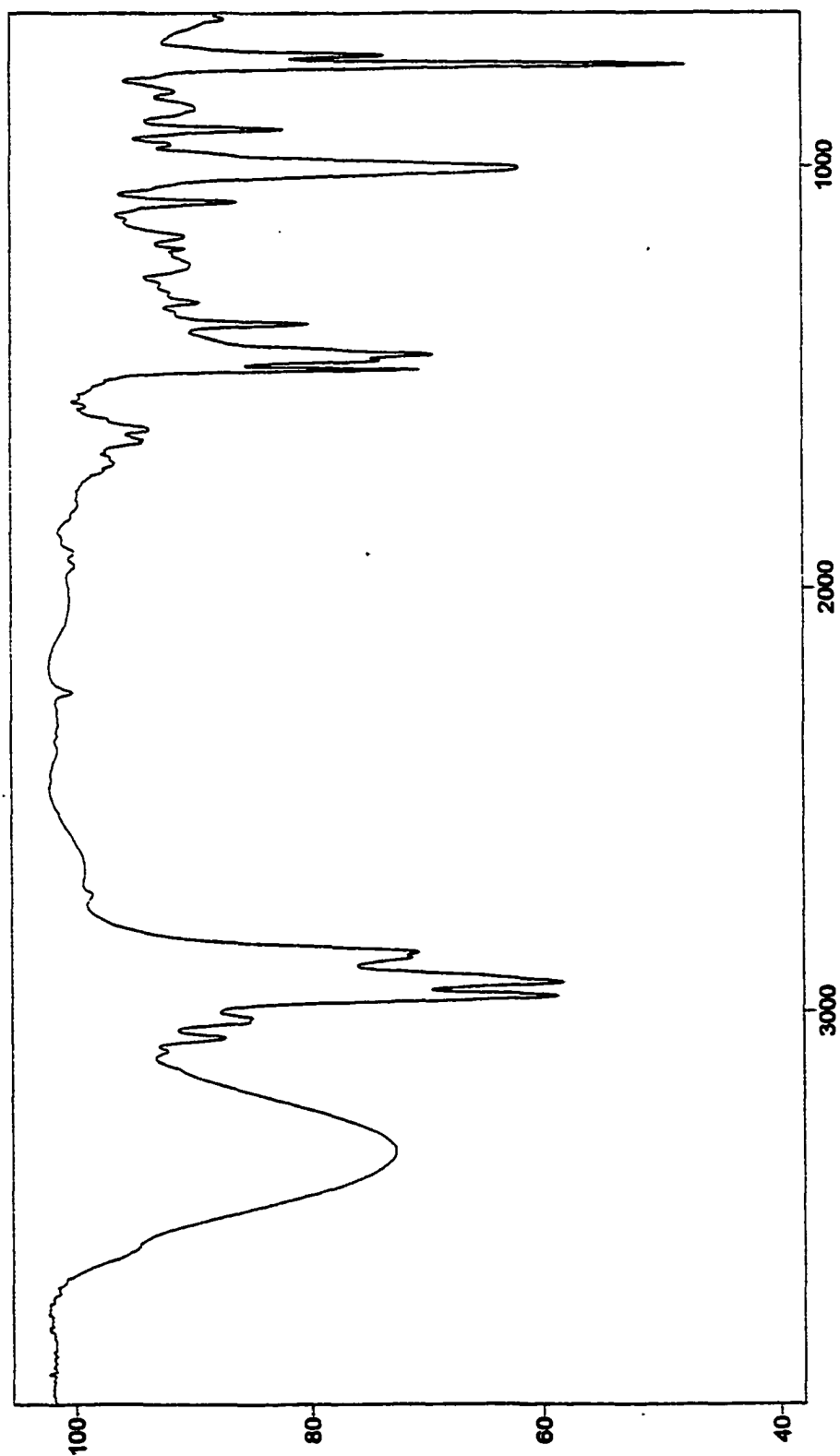


Figure 59. FTIR of Compound II-24 (neat).

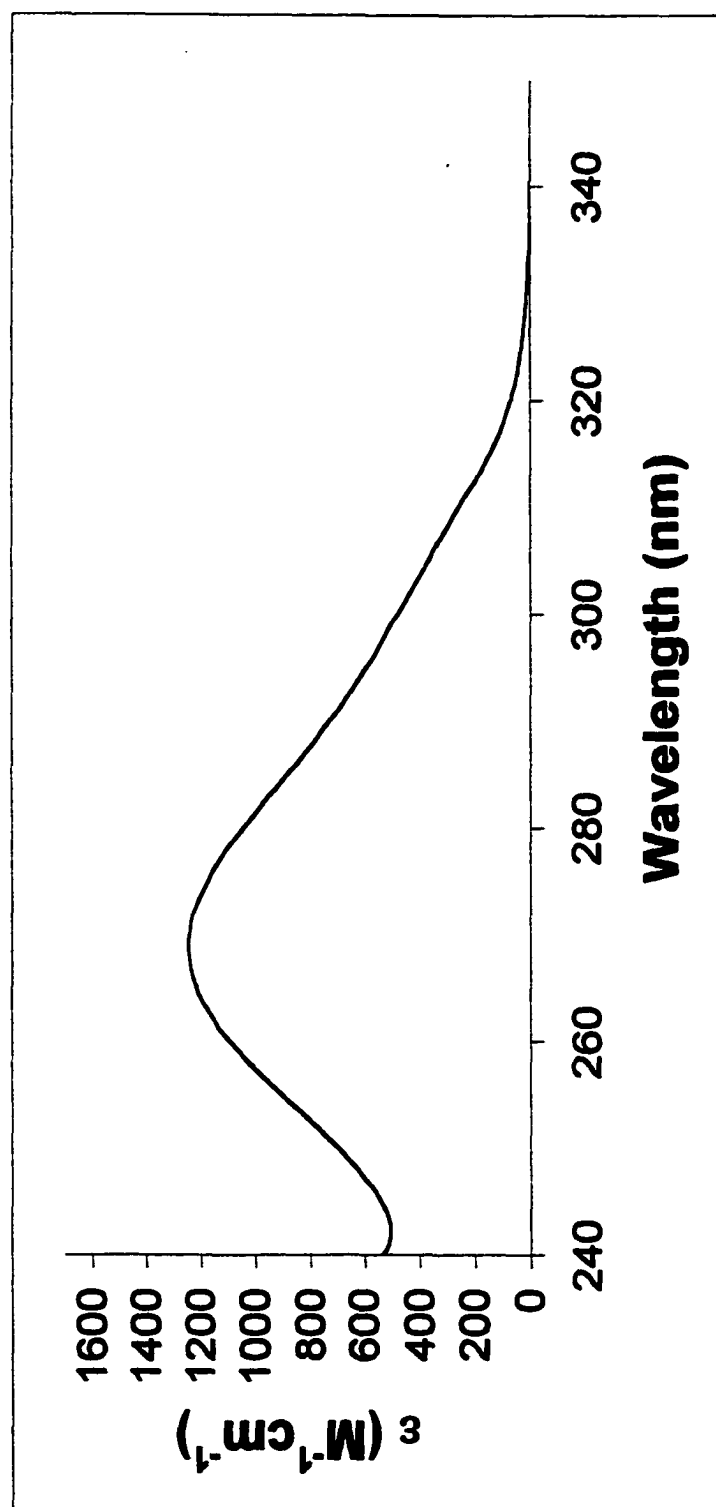


Figure 60. UV-Vis of Compound II-24 (MeOH).

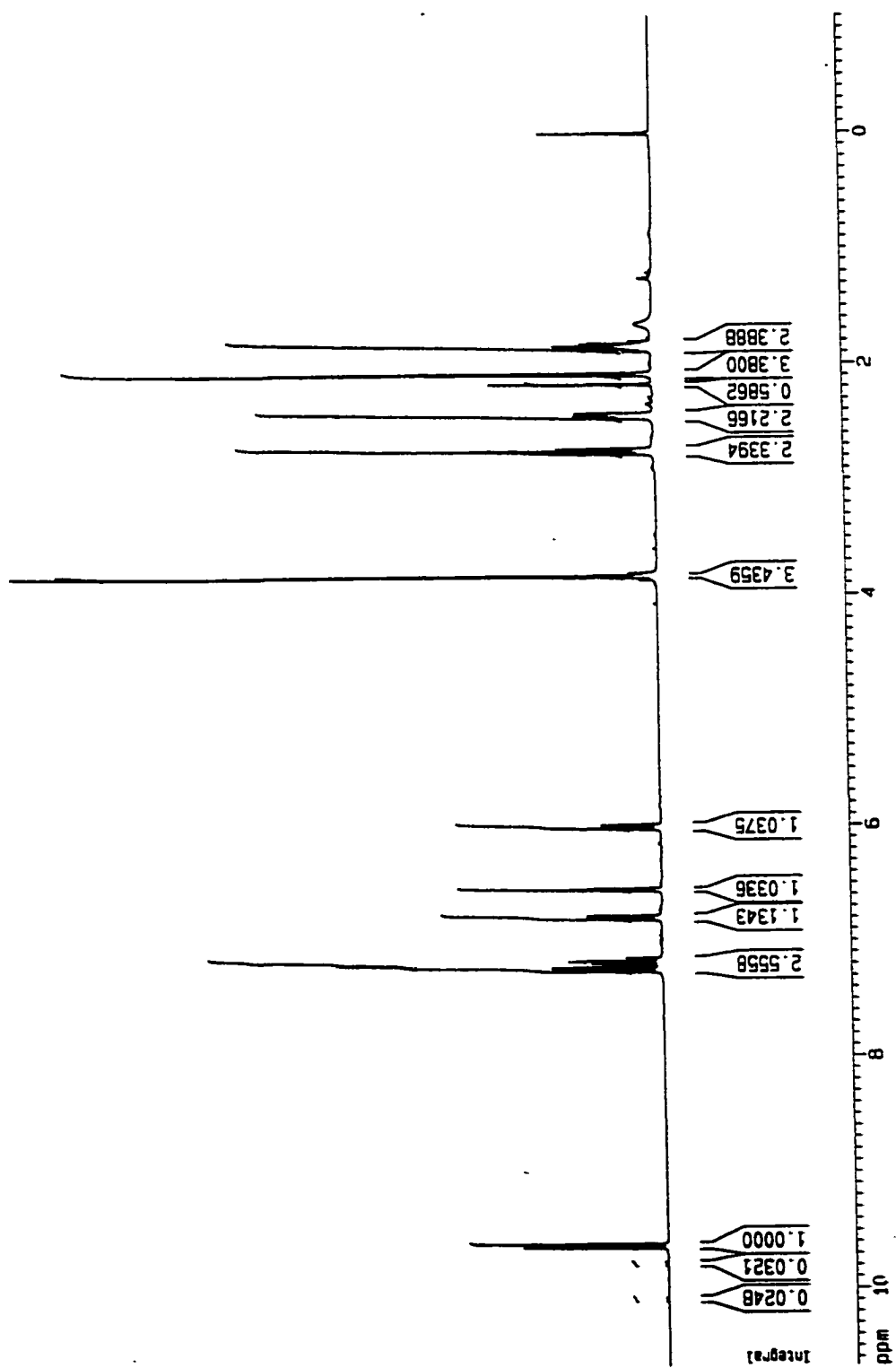


Figure 61. ^1H NMR (300 MHz) of Compound II-(9Z)-26 (CDCl_3).

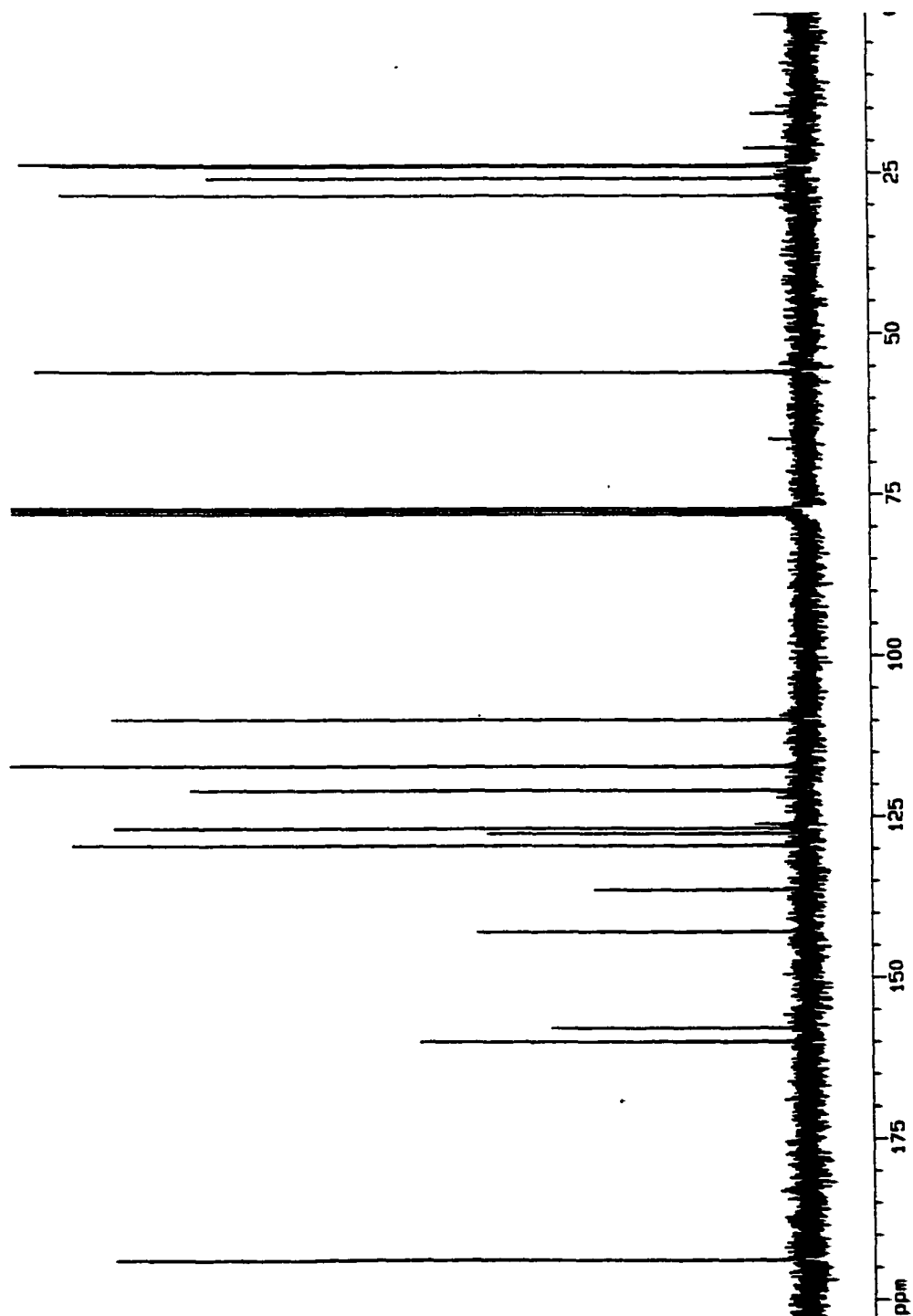


Figure 62. ^{13}C NMR (300 MHz) of Compound II-(9Z)-26 (CDCl_3).

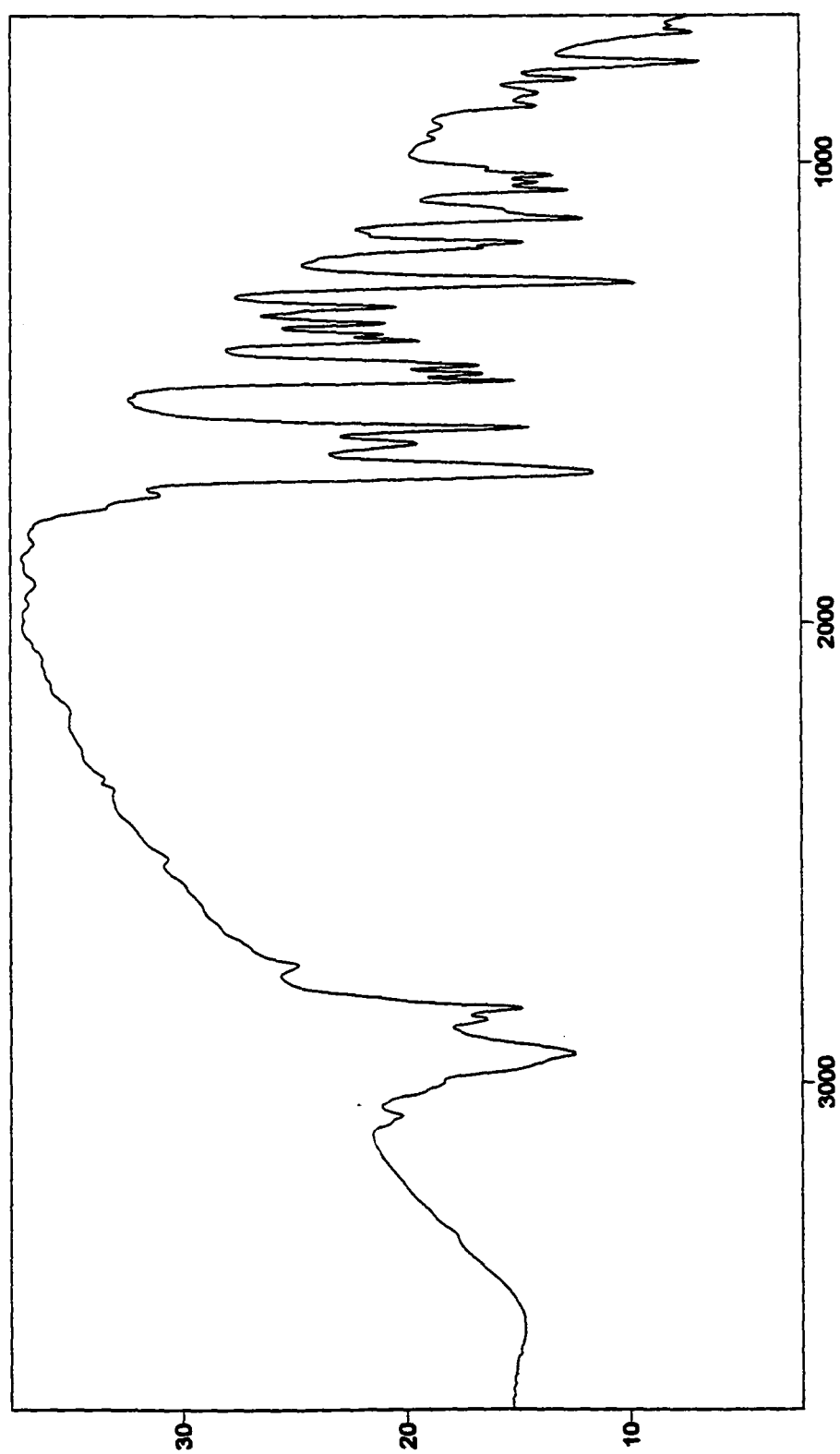


Figure 63. FTIR of Compound II-(9Z)-26 (neat).

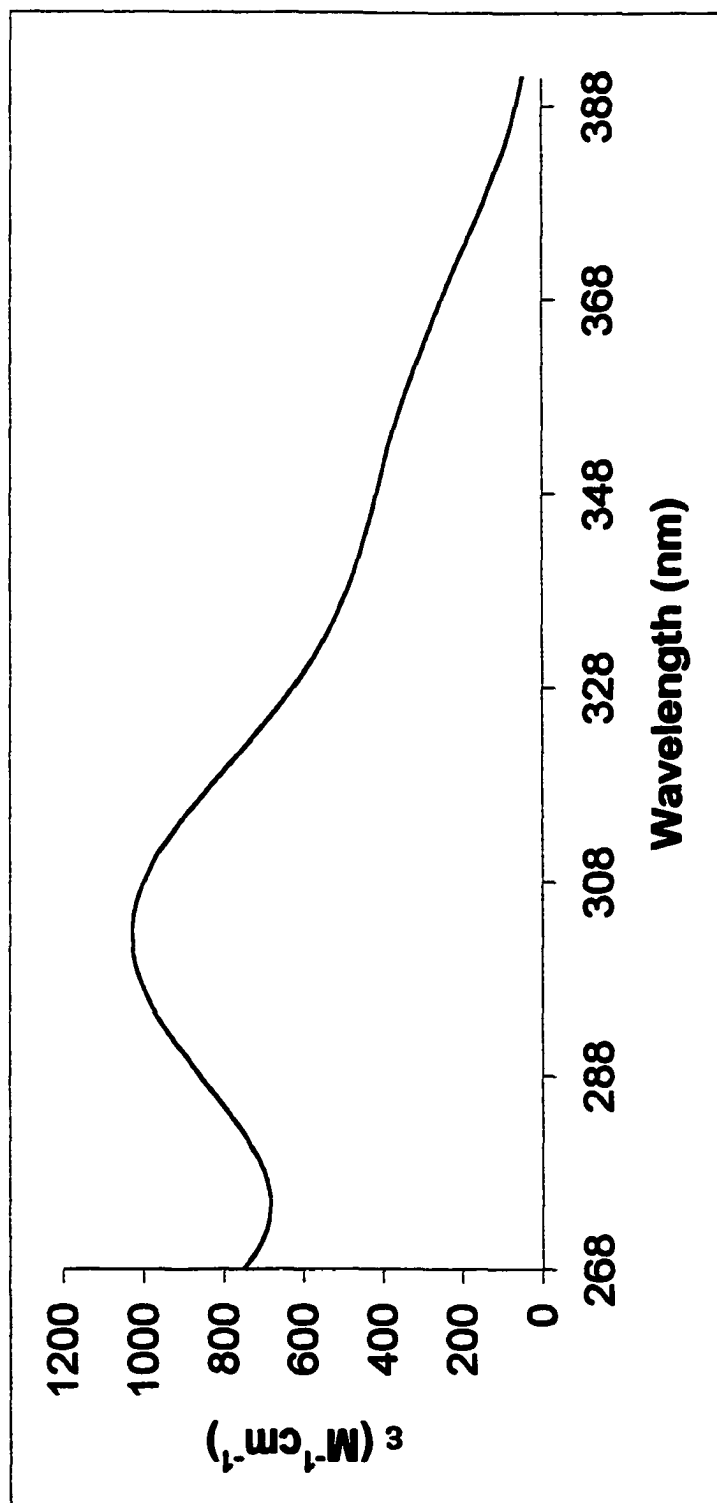


Figure 64. UV-Vis of Compound II-(9Z)-26 (MeOH).

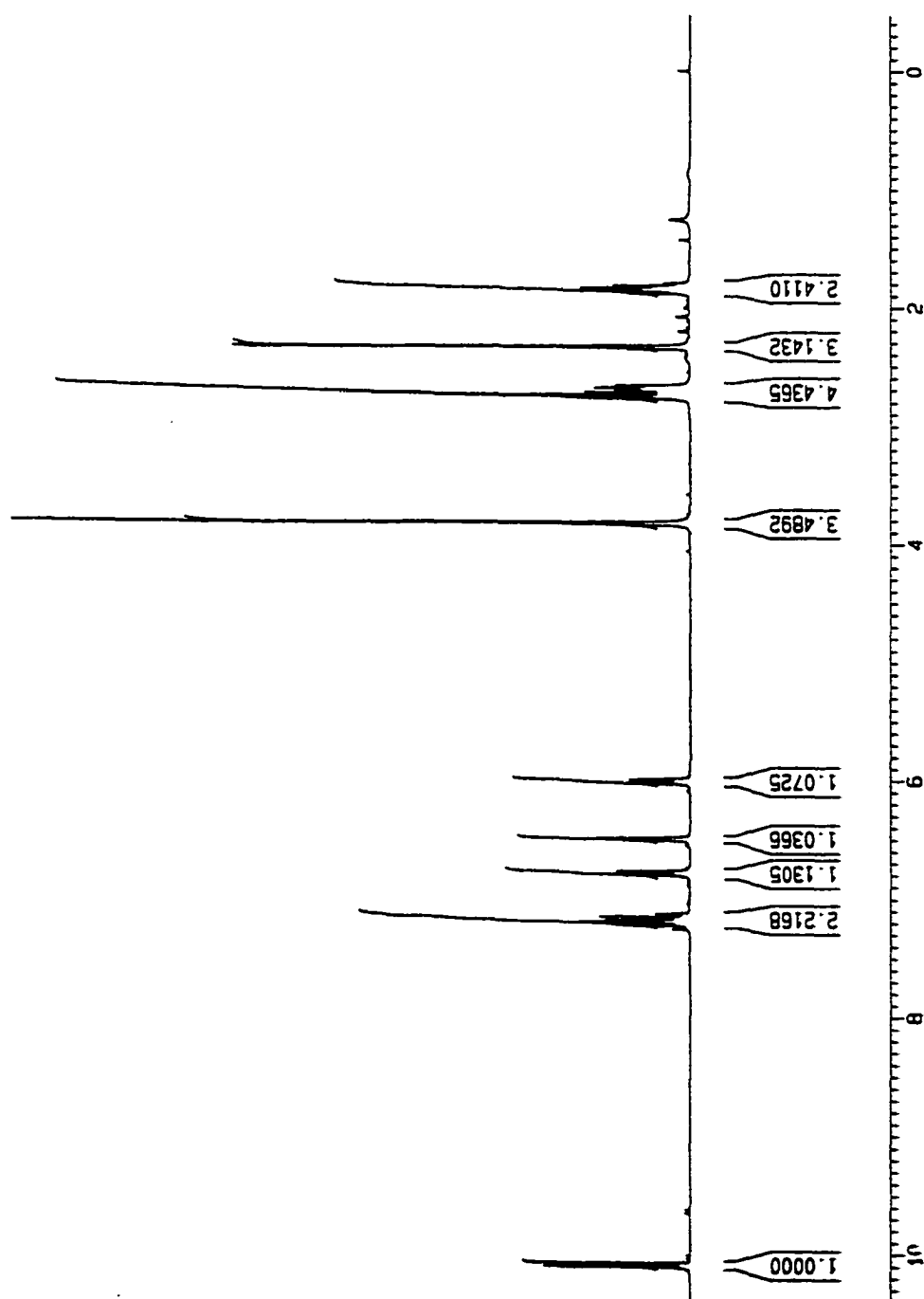


Figure 65. ^1H NMR (300 MHz) of Compound II-(*all-E*)-26 (CDCl_3).

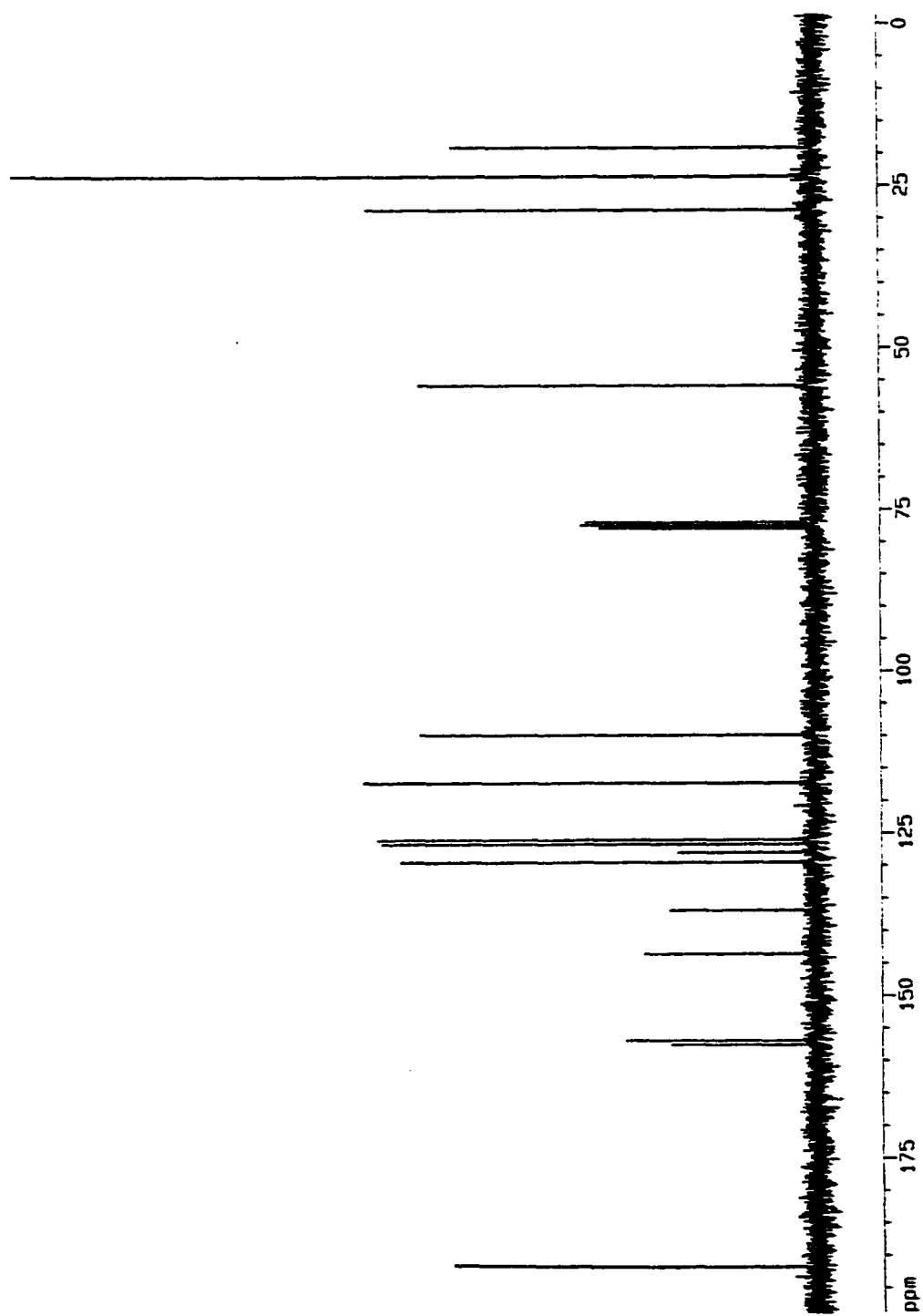


Figure 66. ^{13}C NMR (300 MHz) of Compound II-(*all-E*)-26 (CDCl_3).

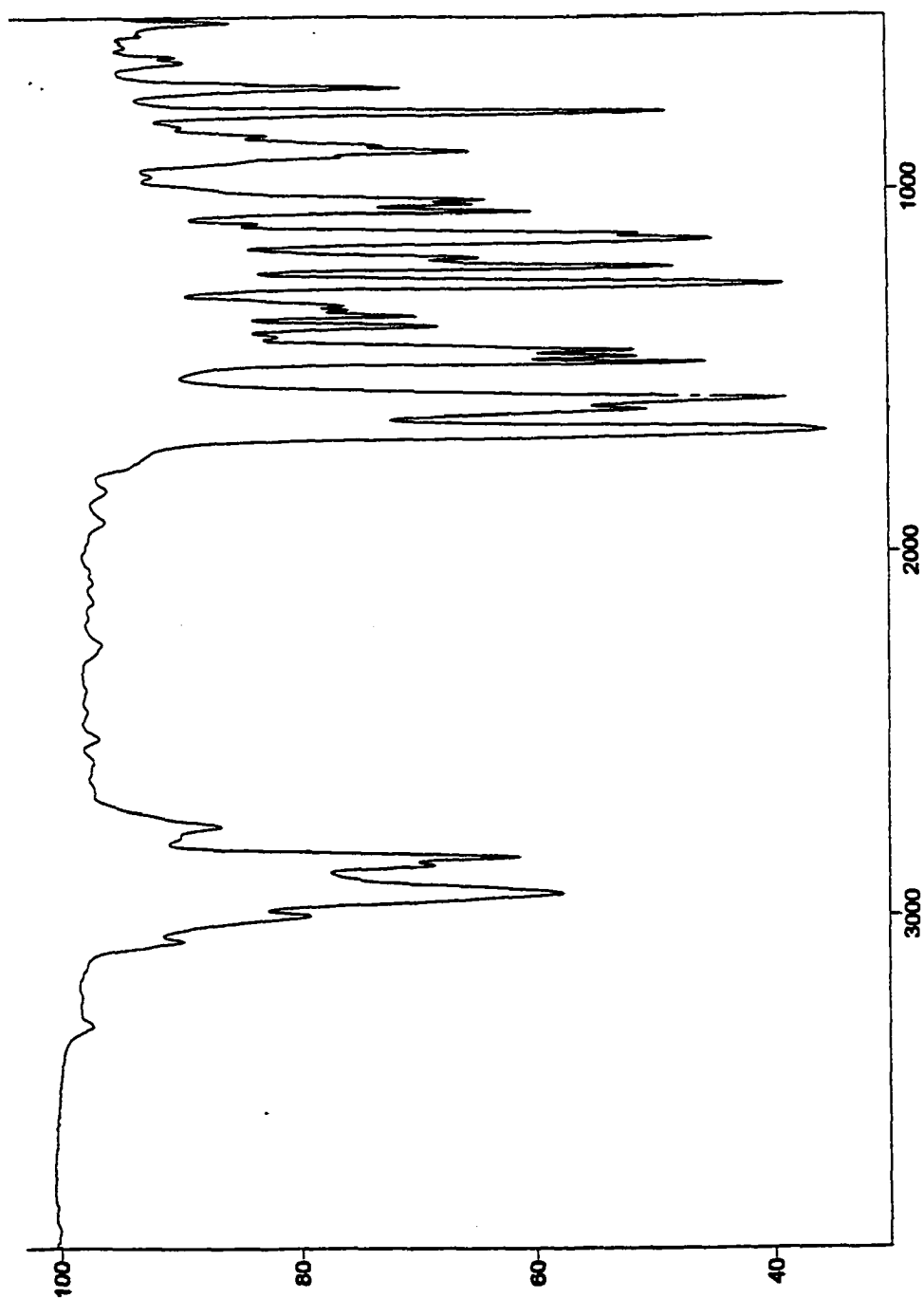


Figure 67. FTIR of Compound II-(*all-E*)-26 (neat).

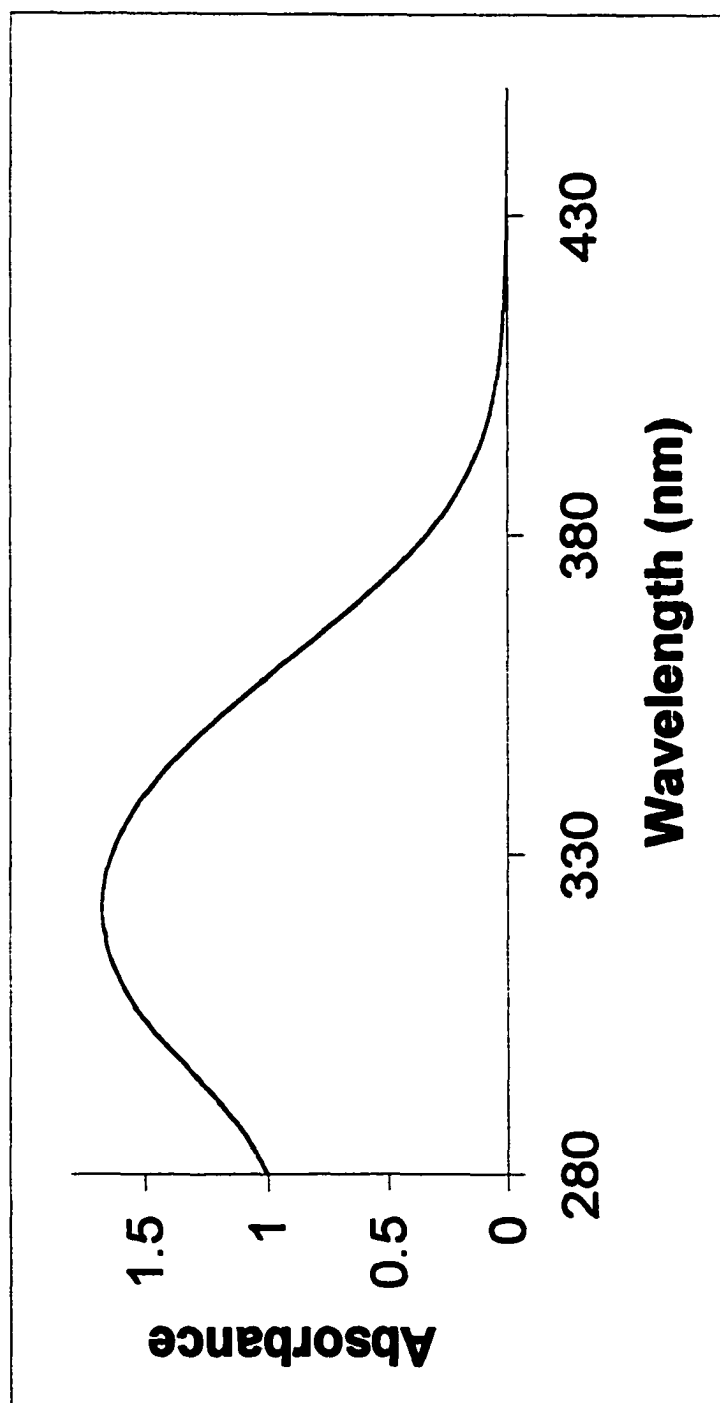


Figure 68. UV-Vis of Compound 11-(*all-E*)-26 (MeOH).

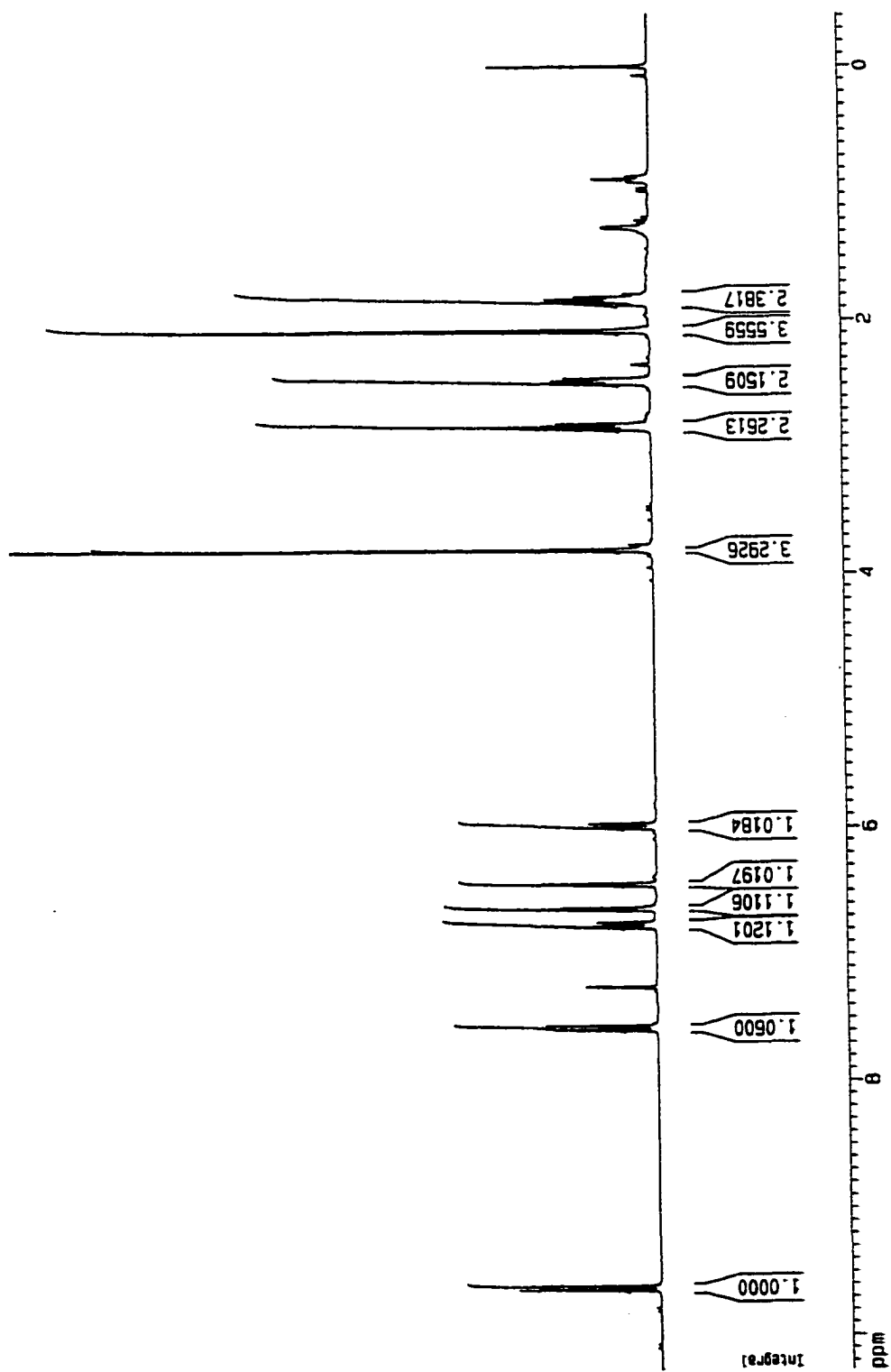


Figure 69. ^1H NMR (300 MHz) of Compound II-(9Z)-27 (CDCl_3).

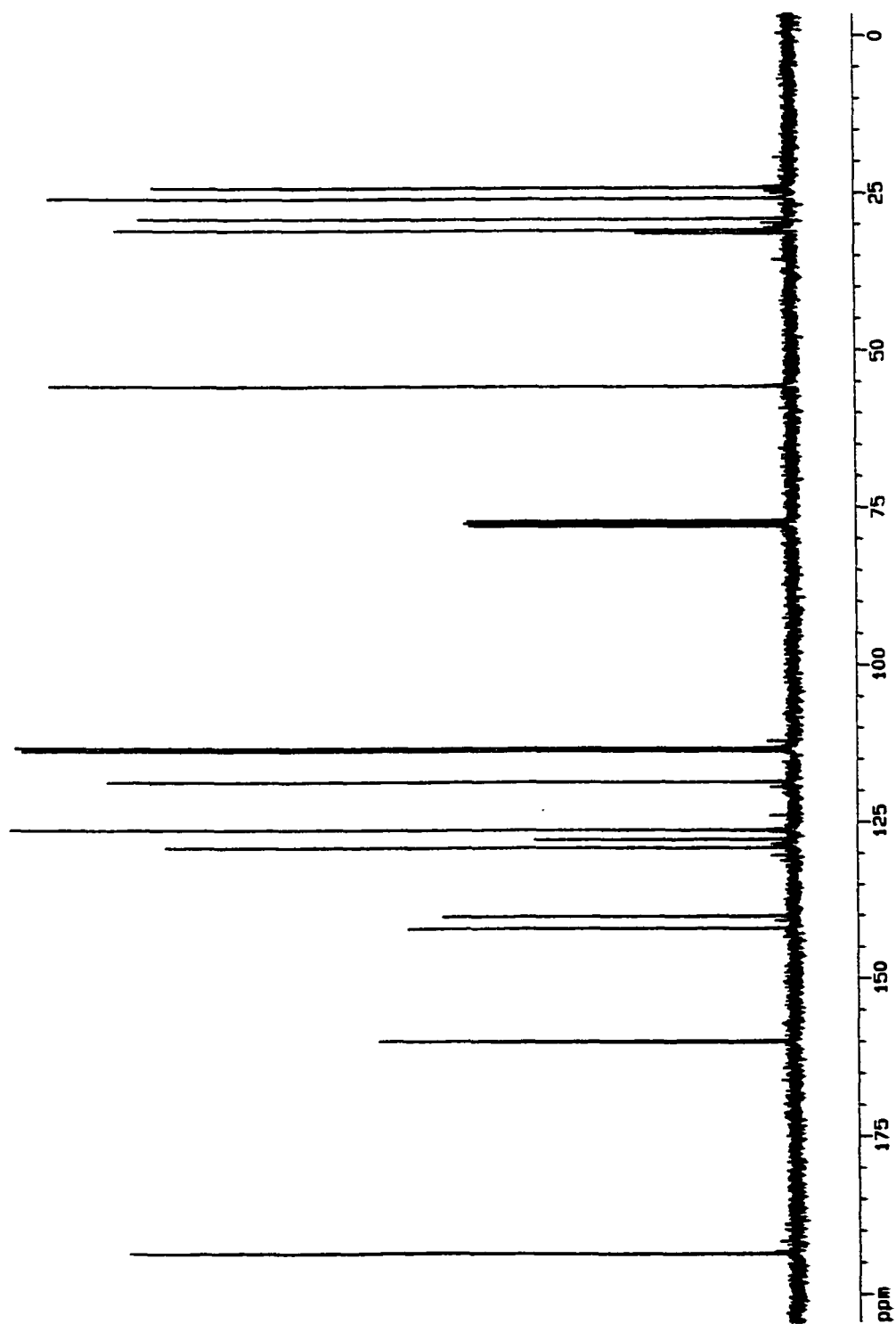


Figure 70. ^{13}C NMR (300 MHz) of Compound II-(9Z)-27 (CDCl_3).

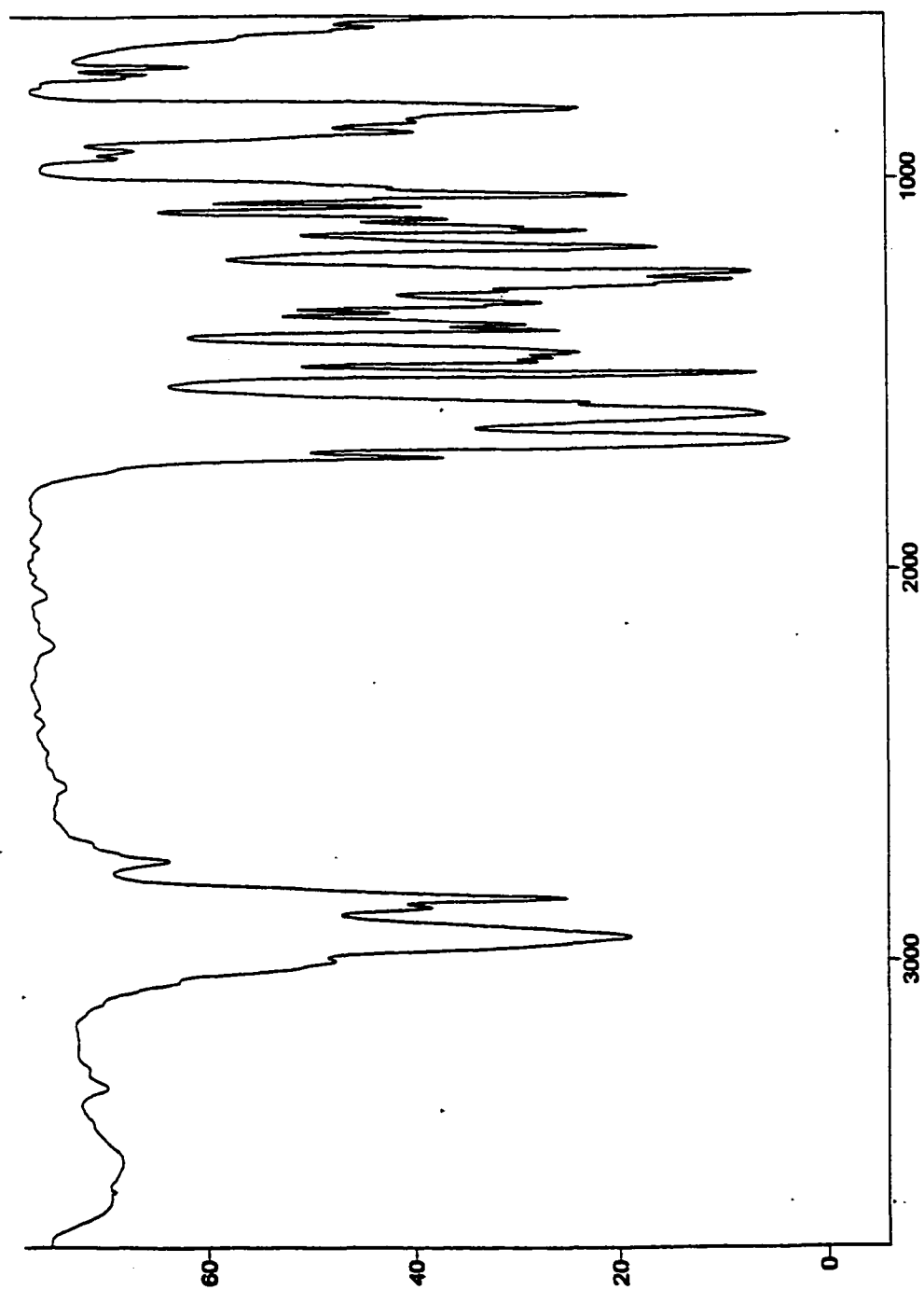


Figure 71. FTIR of Compound II-(9Z)-27 (neat).

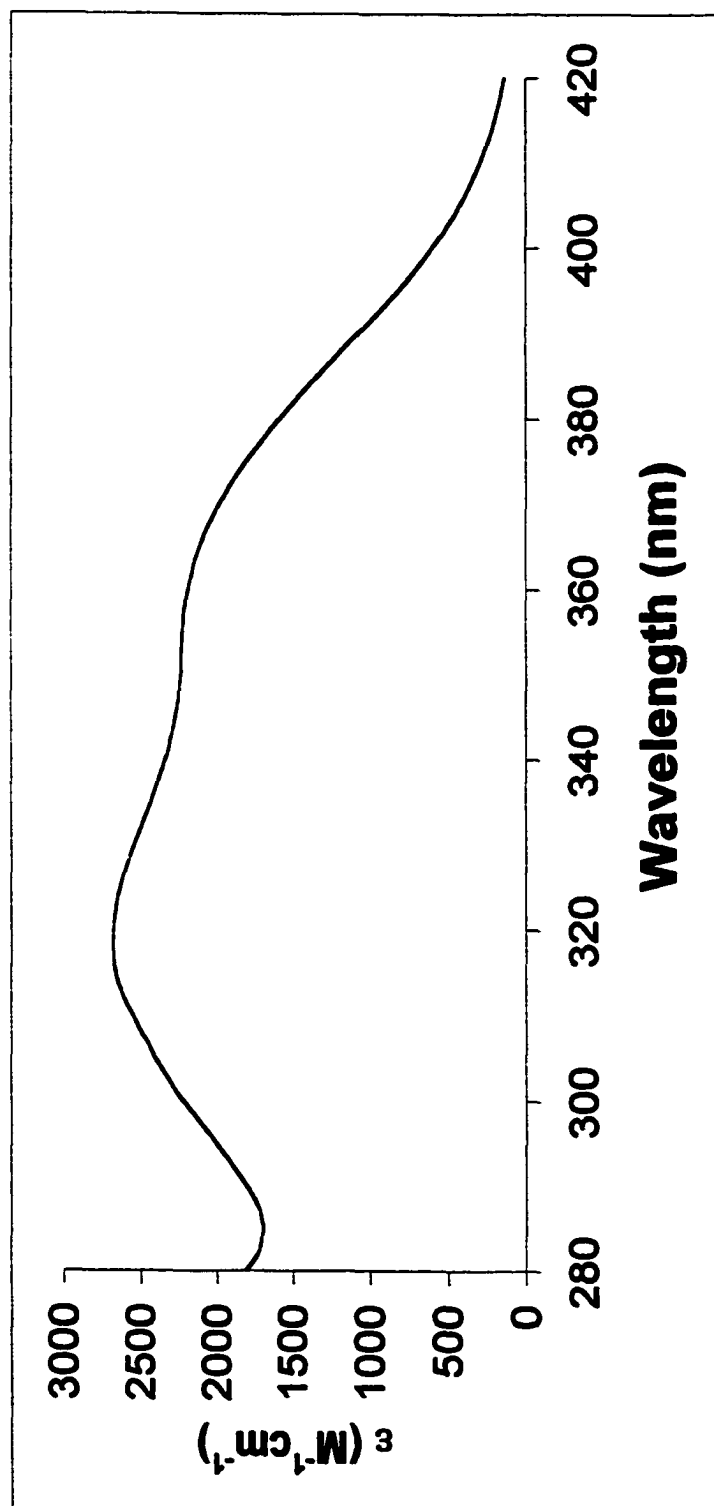


Figure 72. UV-Vis of Compound II-(9Z)-27 (MeOH).

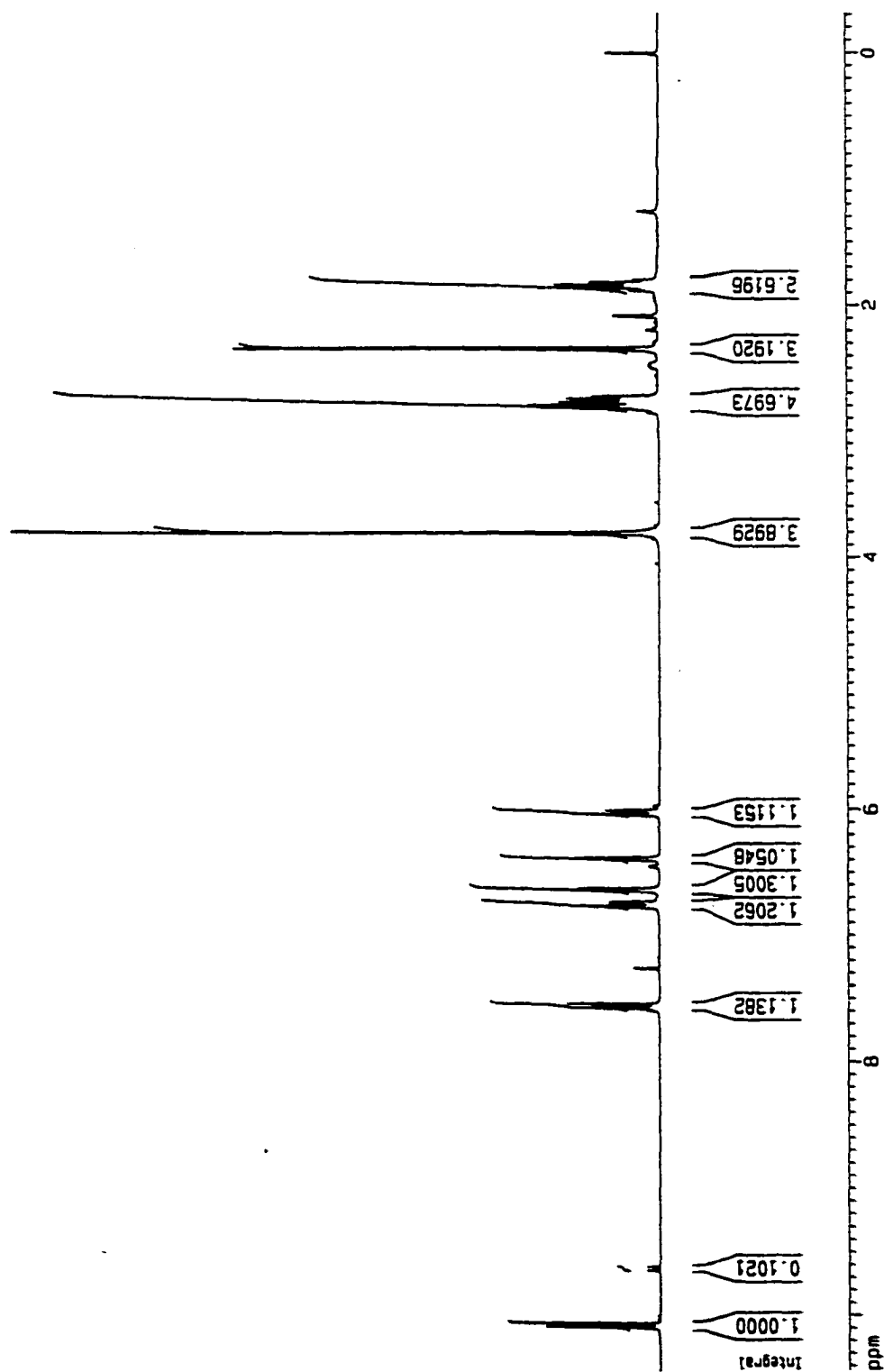


Figure 73. ^1H NMR (300 MHz) of Compound II-(all-E)-27 (CDCl_3).

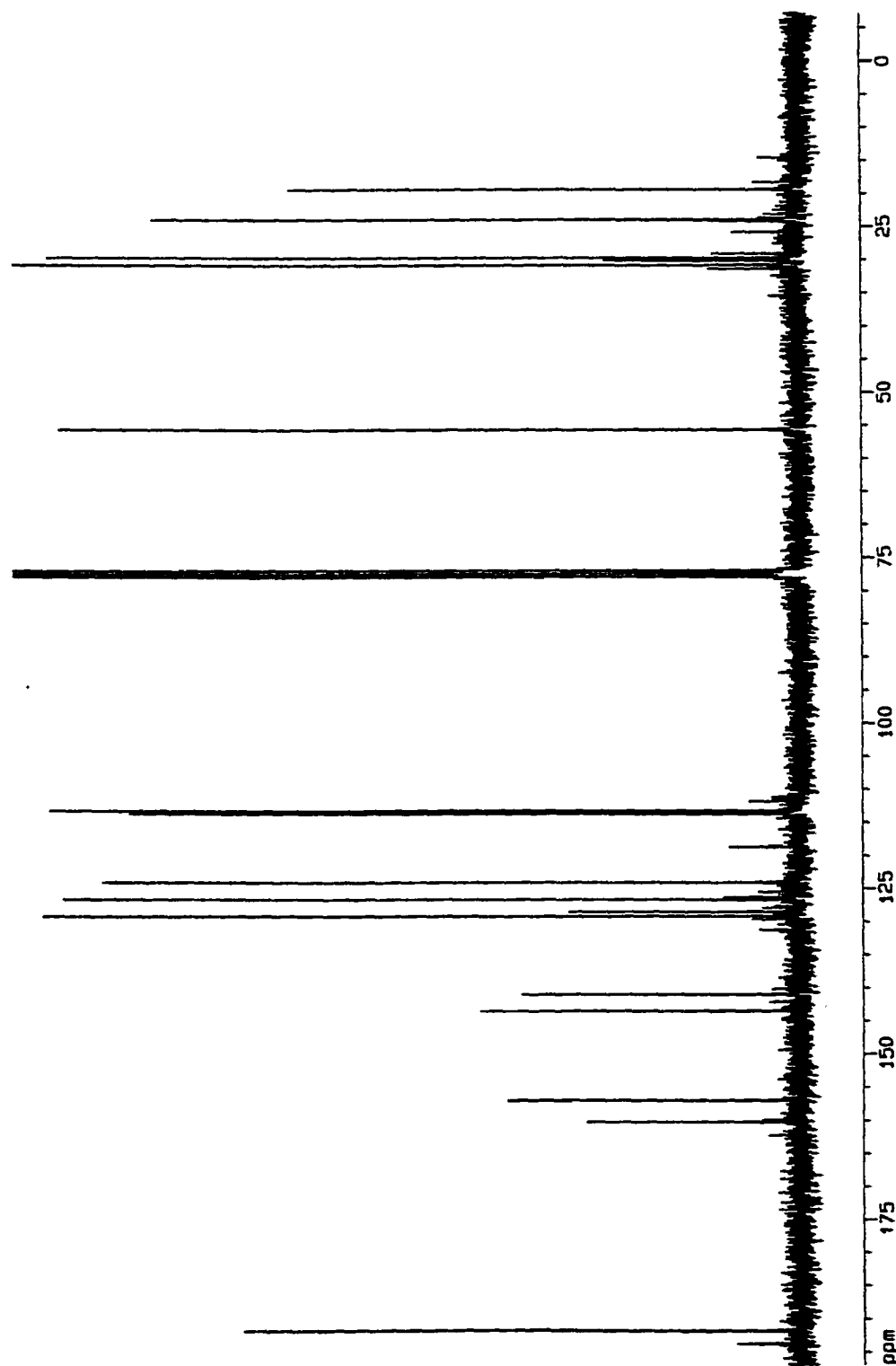


Figure 74. ^{13}C NMR (300 MHz) of Compound **11-(all-E)-27** (CDCl_3).

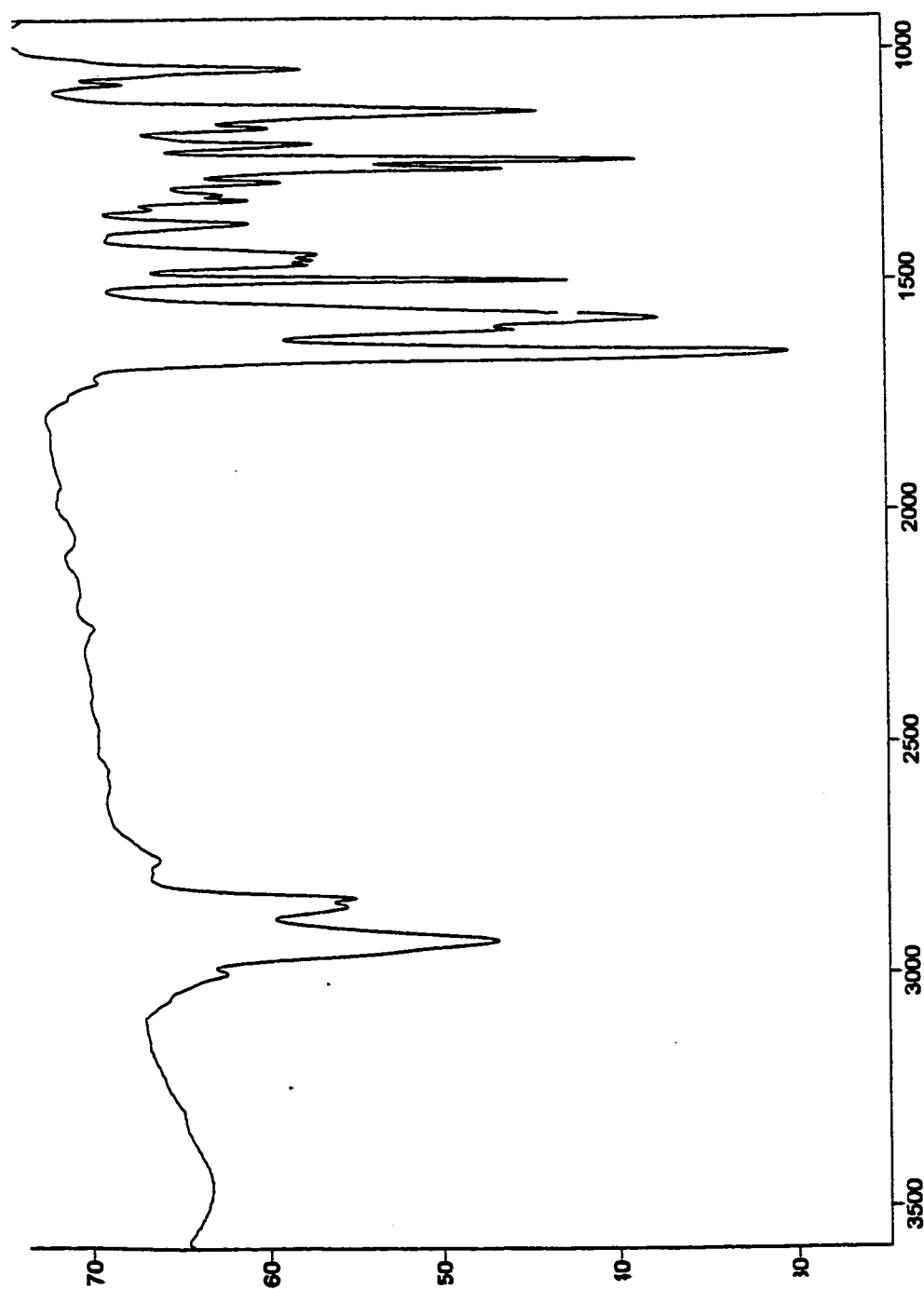


Figure 75. FTIR of Compound II-(*all-E*)-27 (neat).

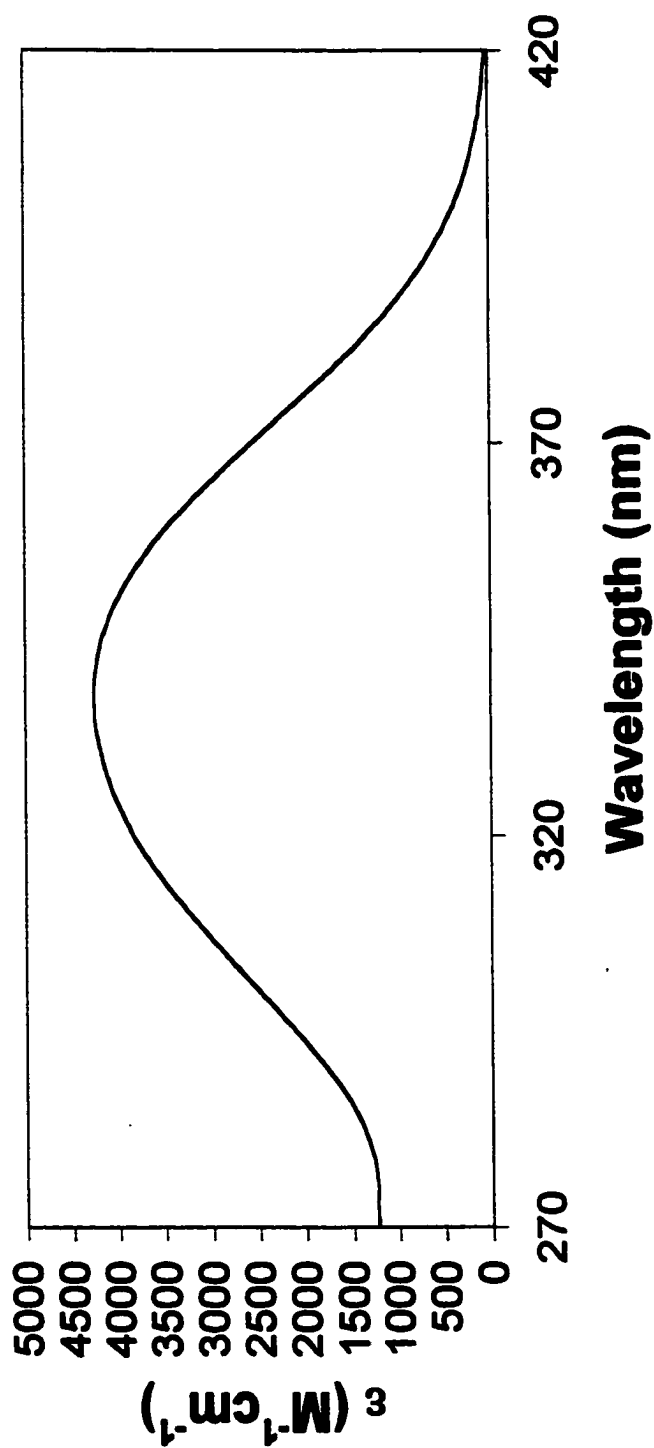


Figure 76. UV-Vis of Compound II-(*all-E*)-27 (MeOH).

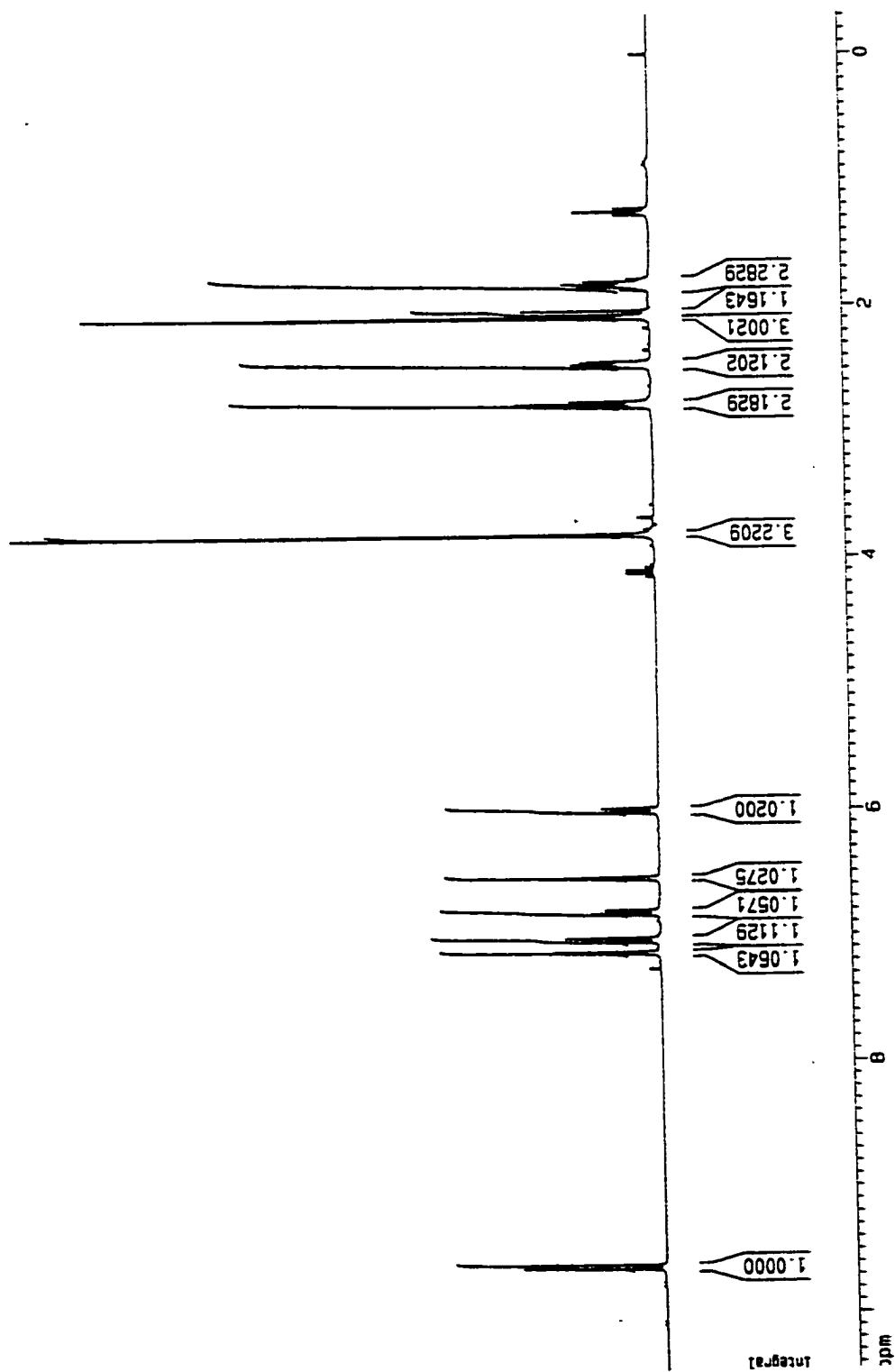


Figure 77. ¹H NMR (300 MHz) of Compound II-(9Z)-28 (CDCl₃).

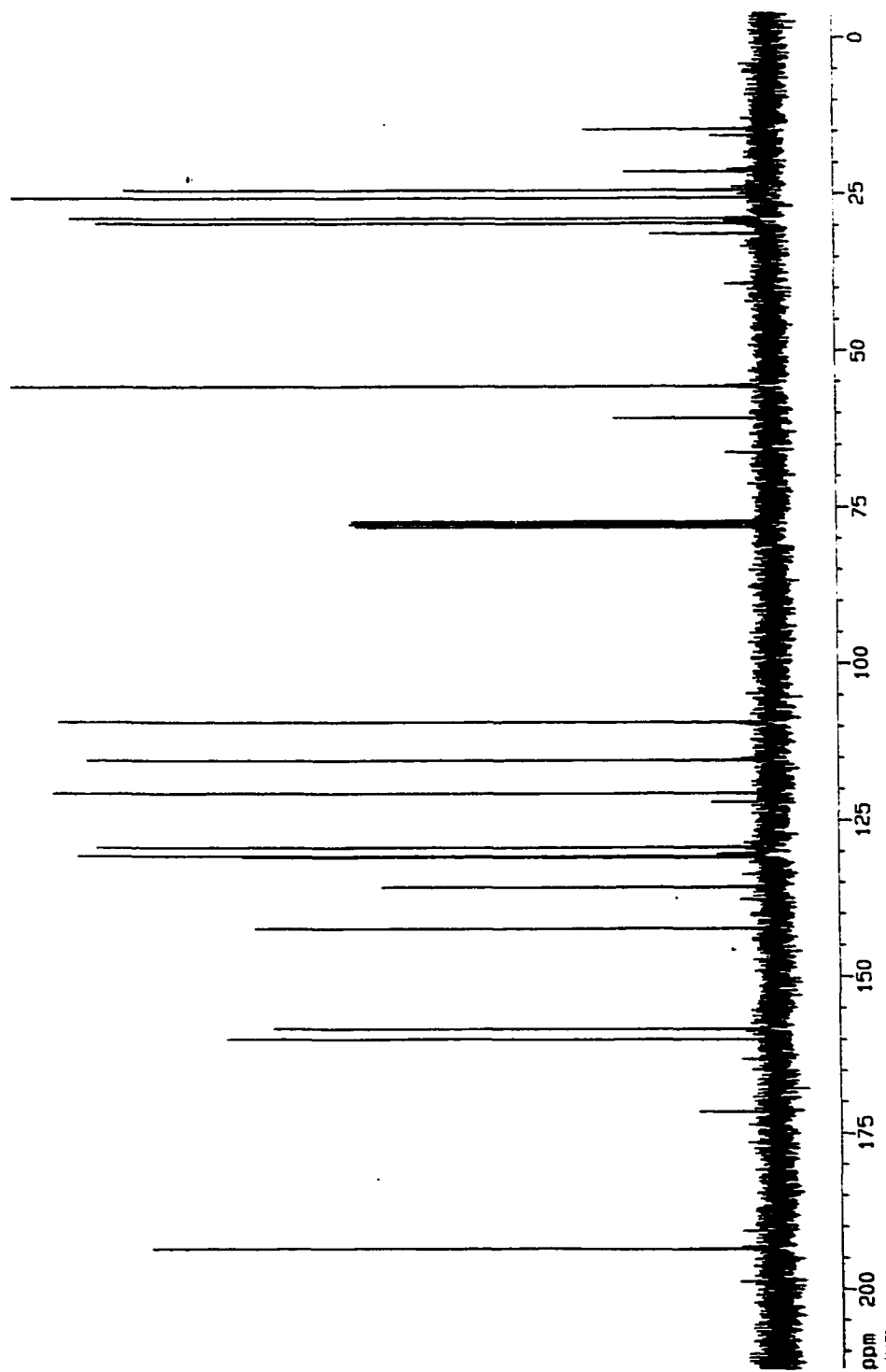


Figure 78. ^{13}C NMR (300 MHz) of Compound II-(9Z)-28 (CDCl_3).

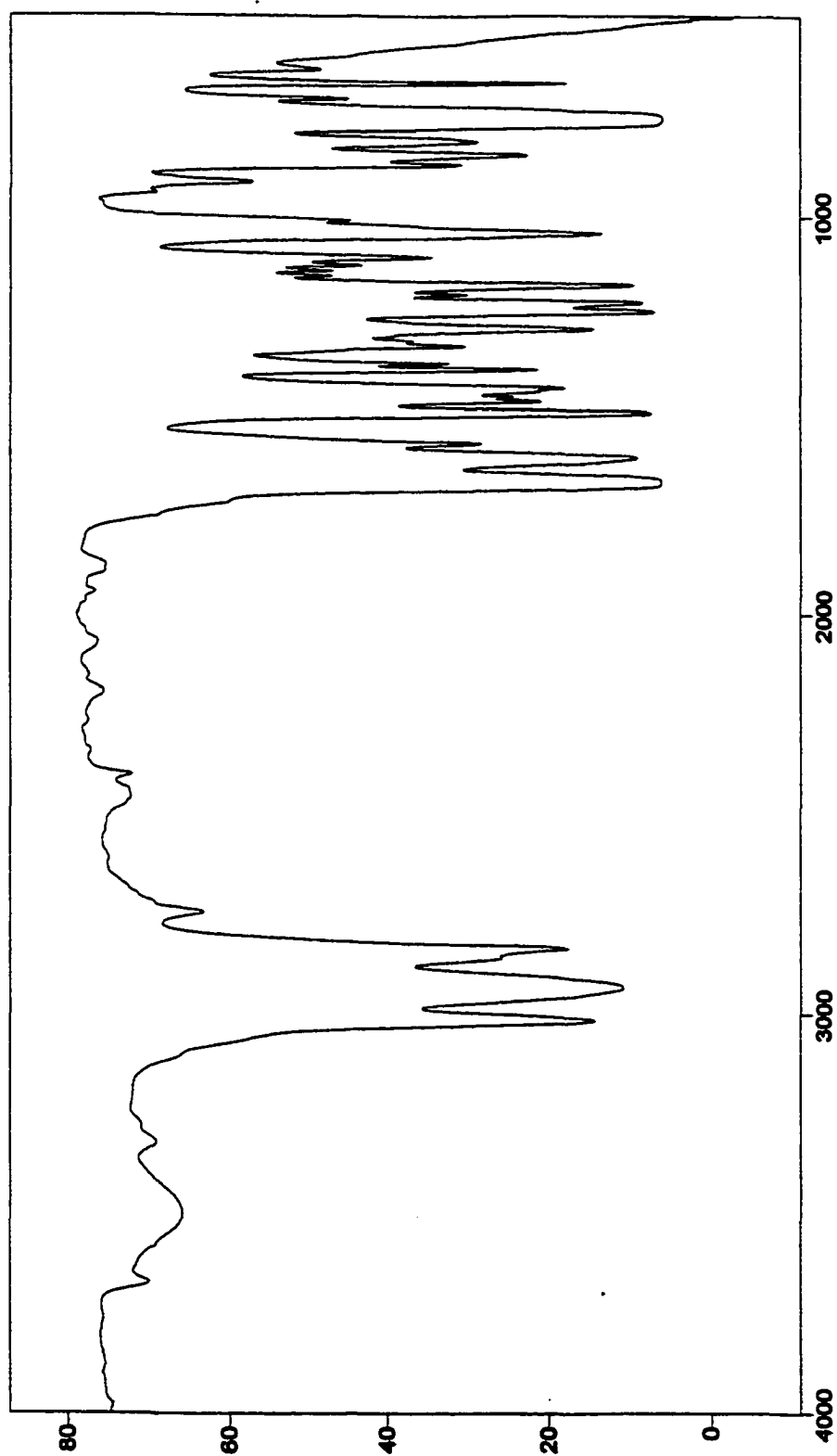


Figure 79. FTIR of Compound II-(9Z)-28 (neat).

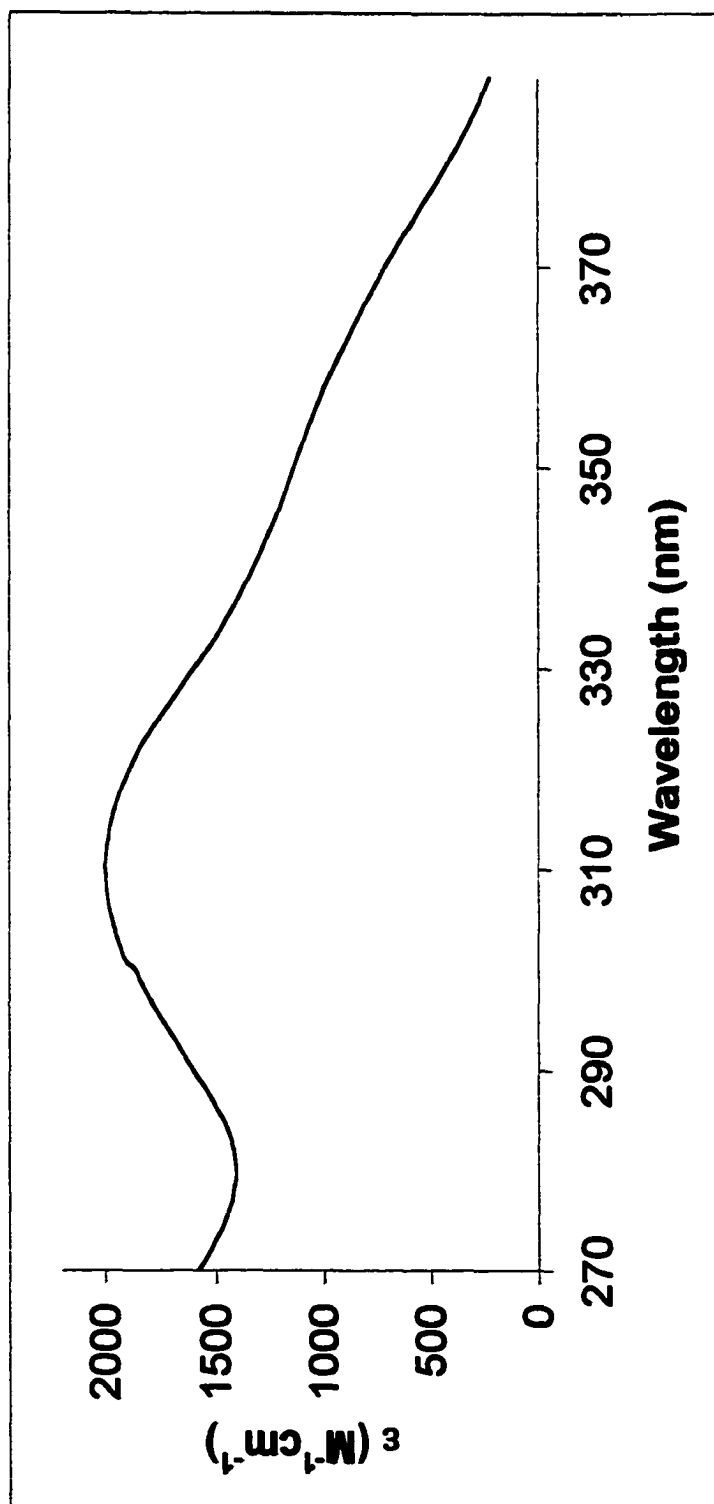


Figure 80. UV-Vis of Compound II-(9Z)-28 (MeOH).

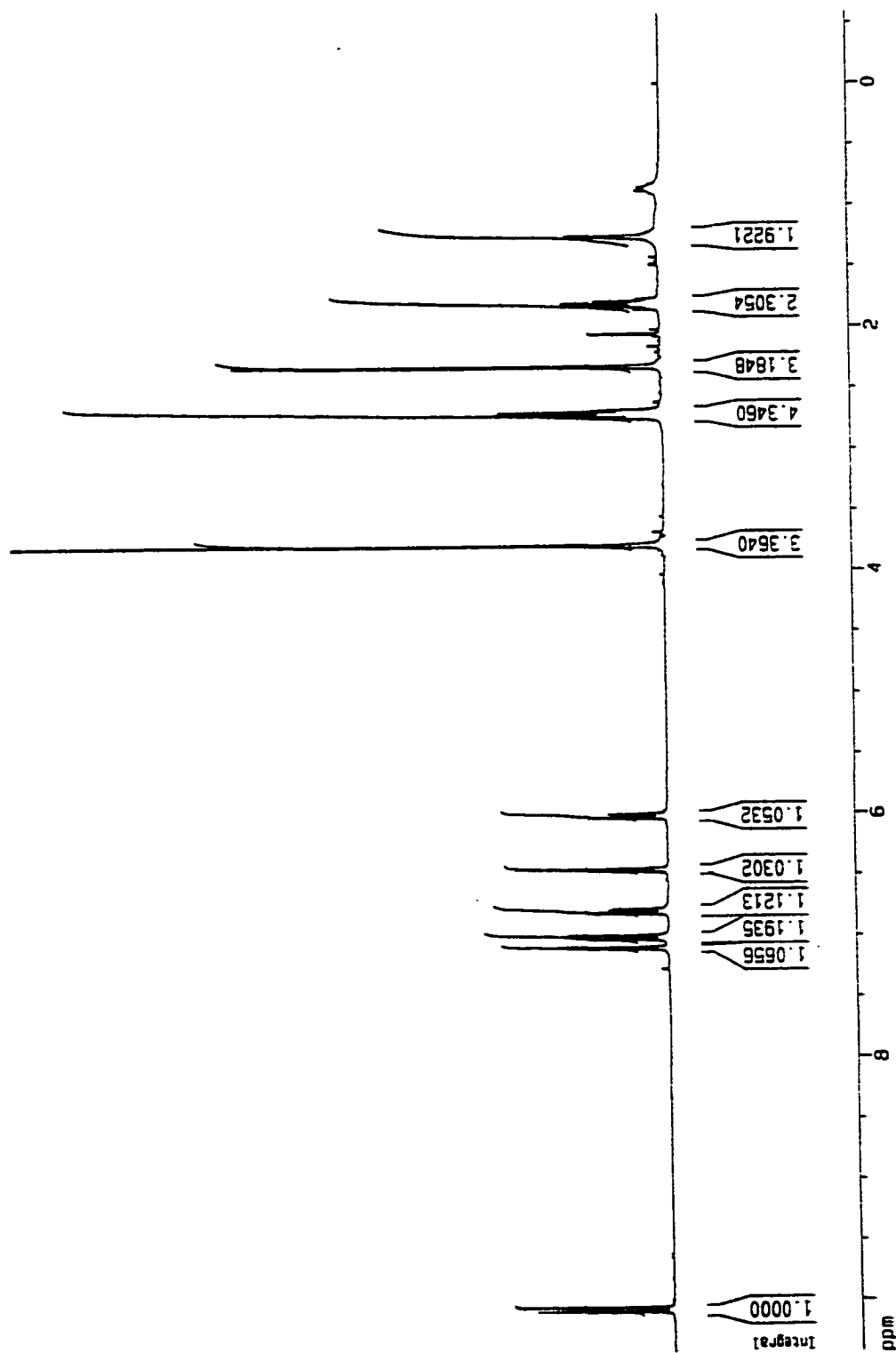


Figure 81. ^1H NMR (300 MHz) of Compound II-(*all-E*)-28 (CDCl_3).

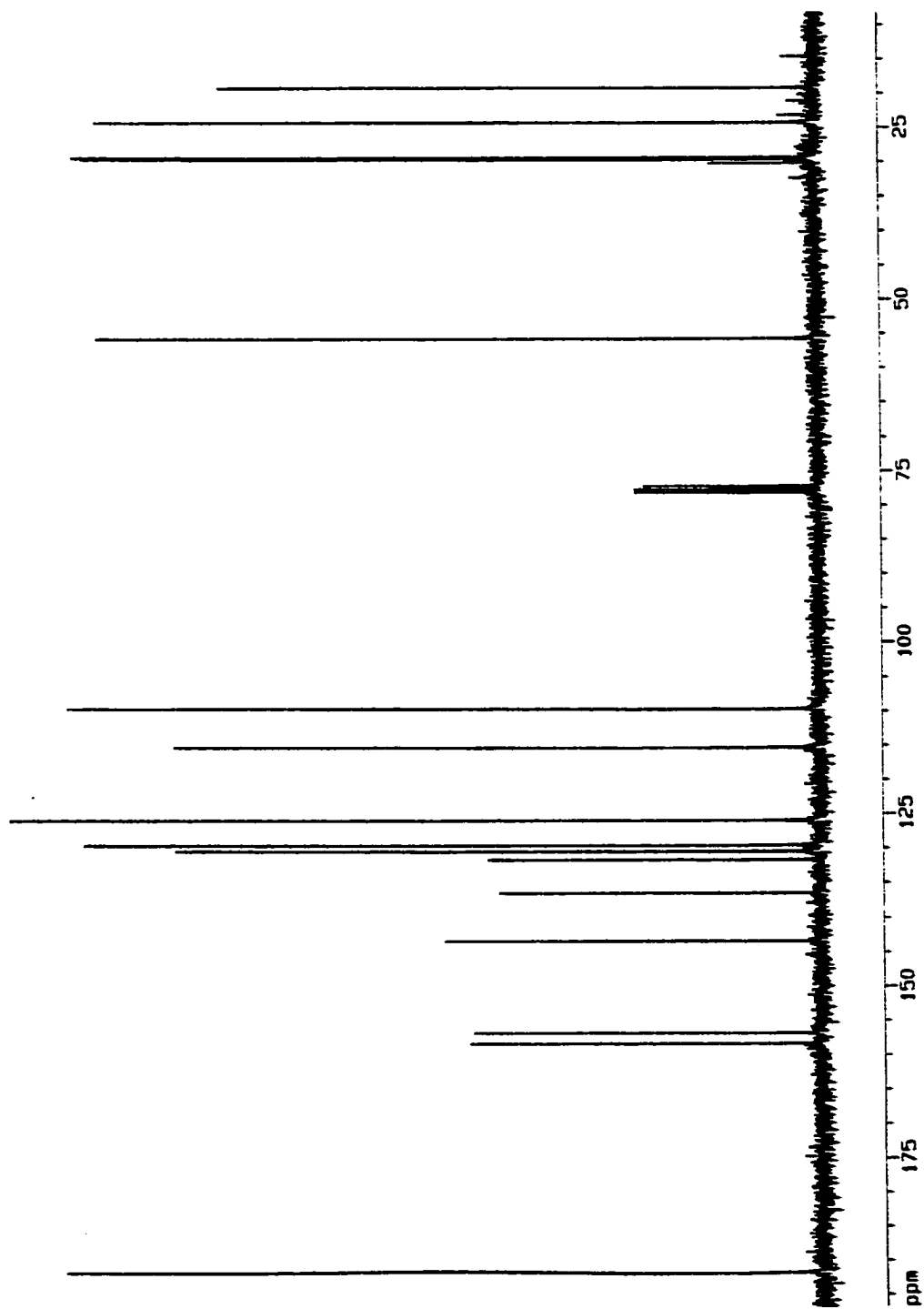


Figure 82. ^{13}C NMR (300 MHz) of Compound II-(*all-E*)-28 (CDCl_3).

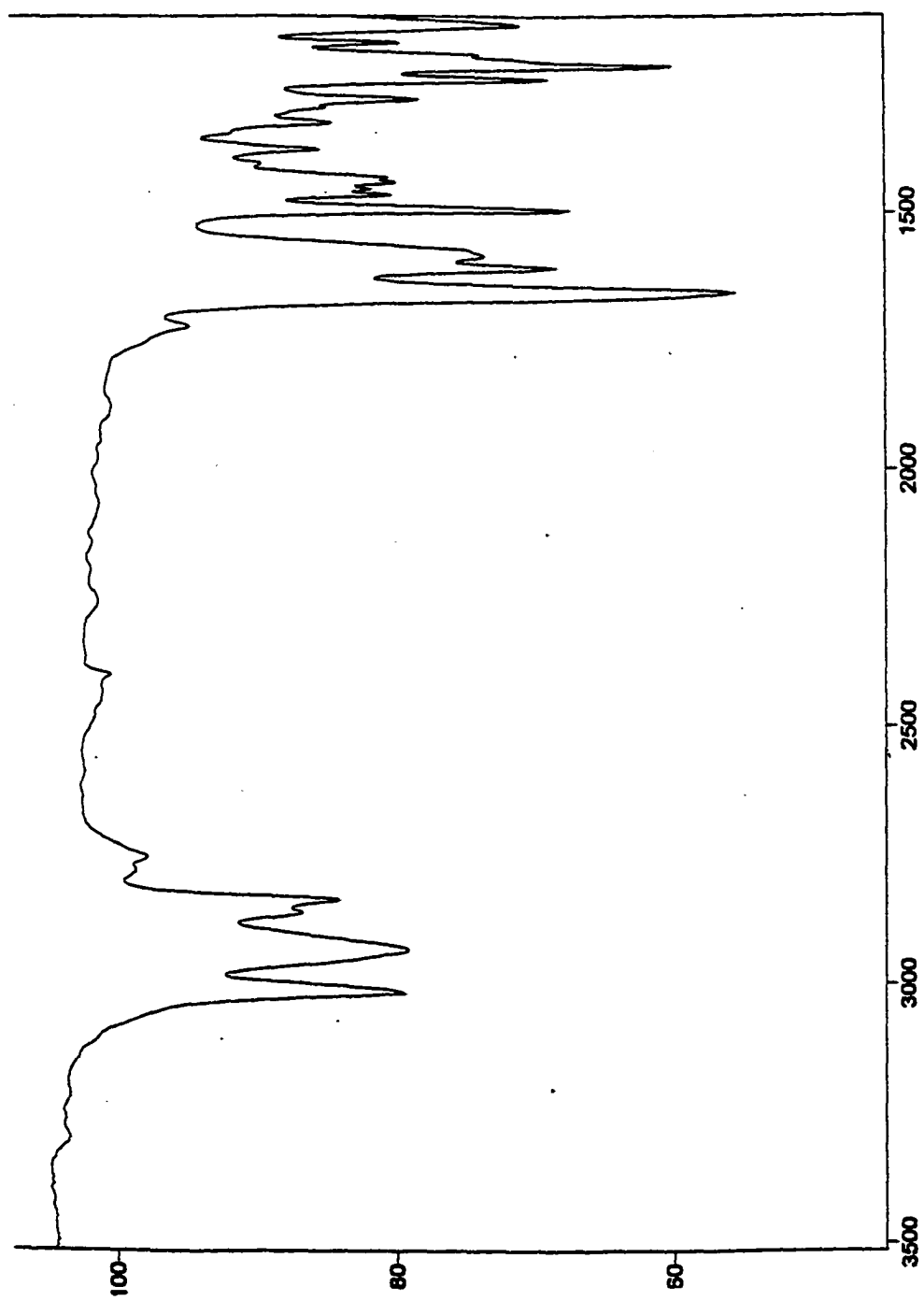


Figure 83. FTIR of Compound II-(*all-E*)-28 (neat).

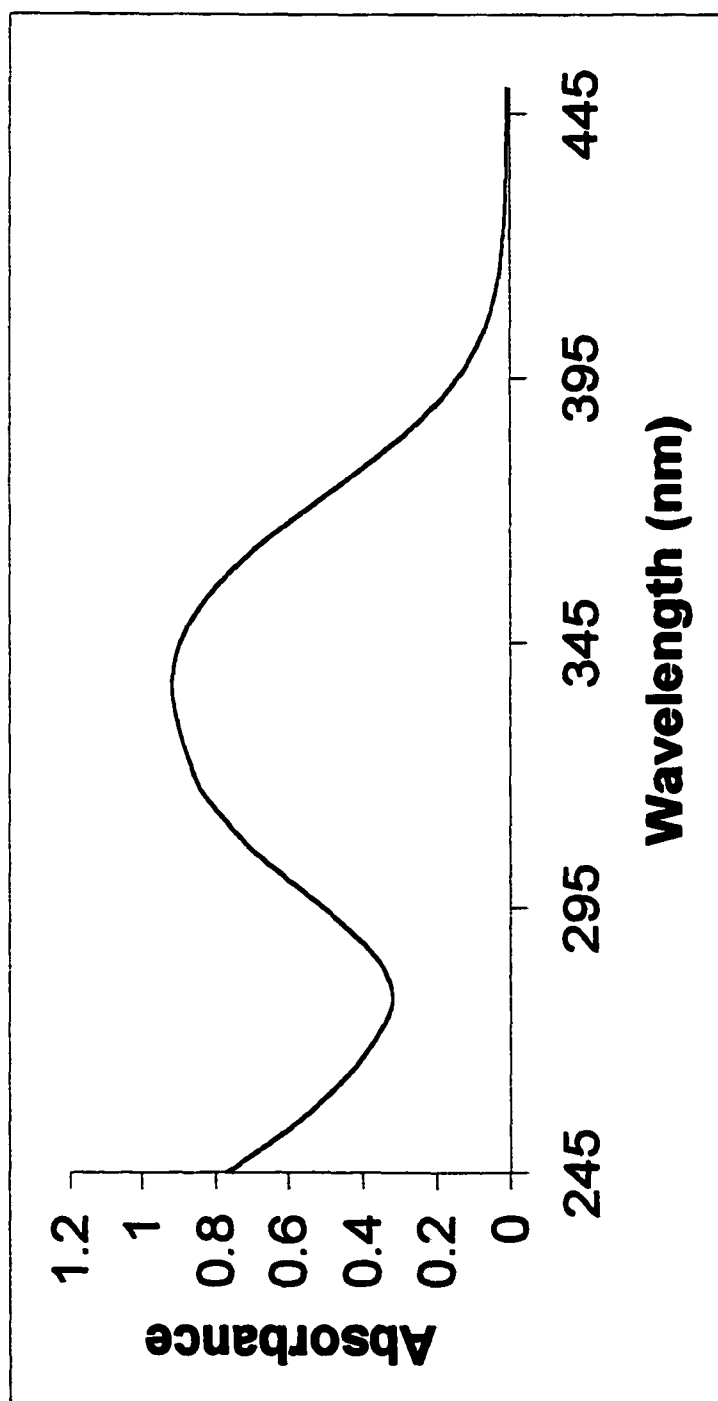


Figure 84. UV-Vis of Compound II-(*all-E*)-28 (MeOH).

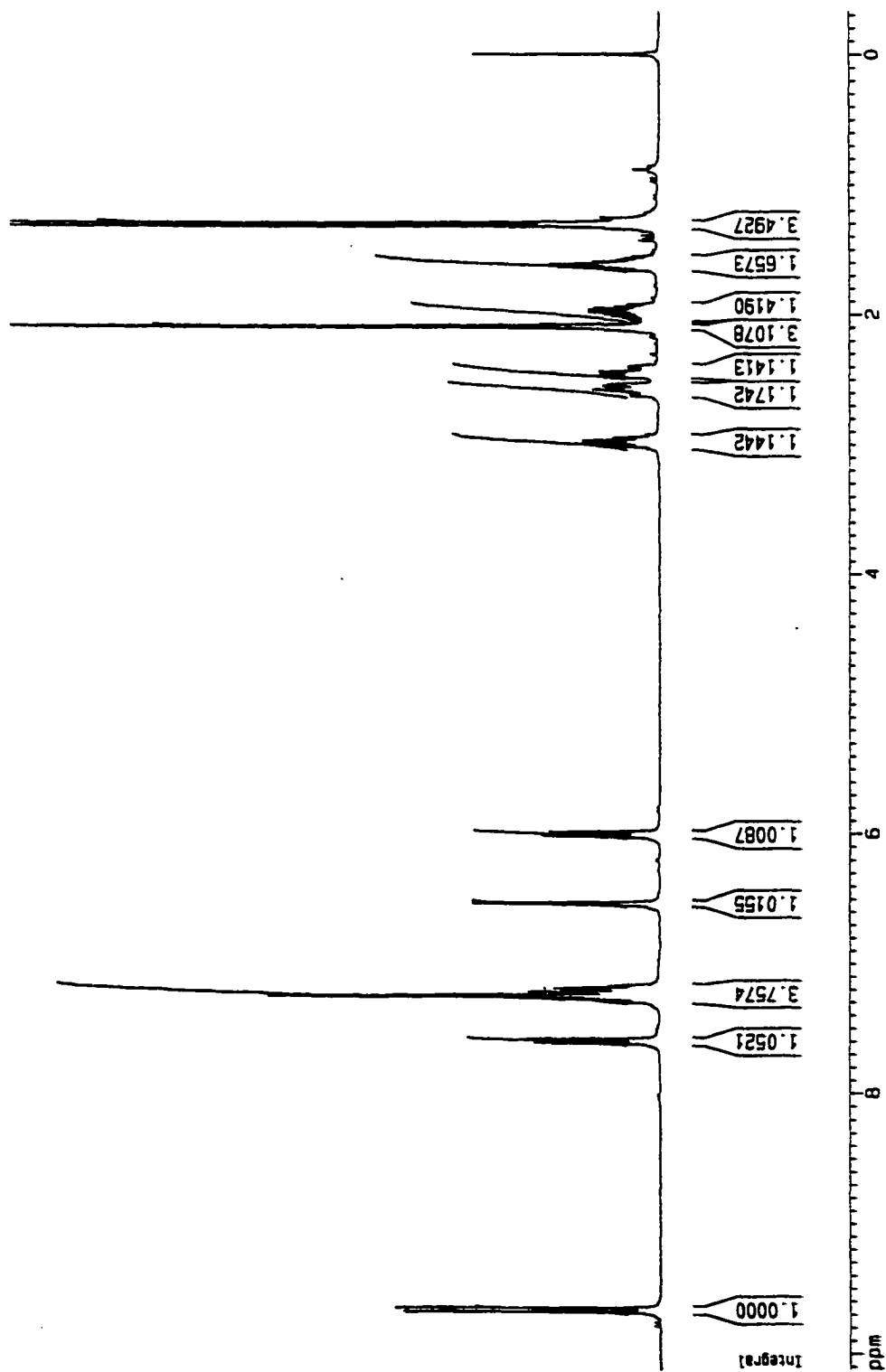


Figure 85. ^1H NMR (300 MHz) of Compound II-(9Z)-29 (CDCl_3).

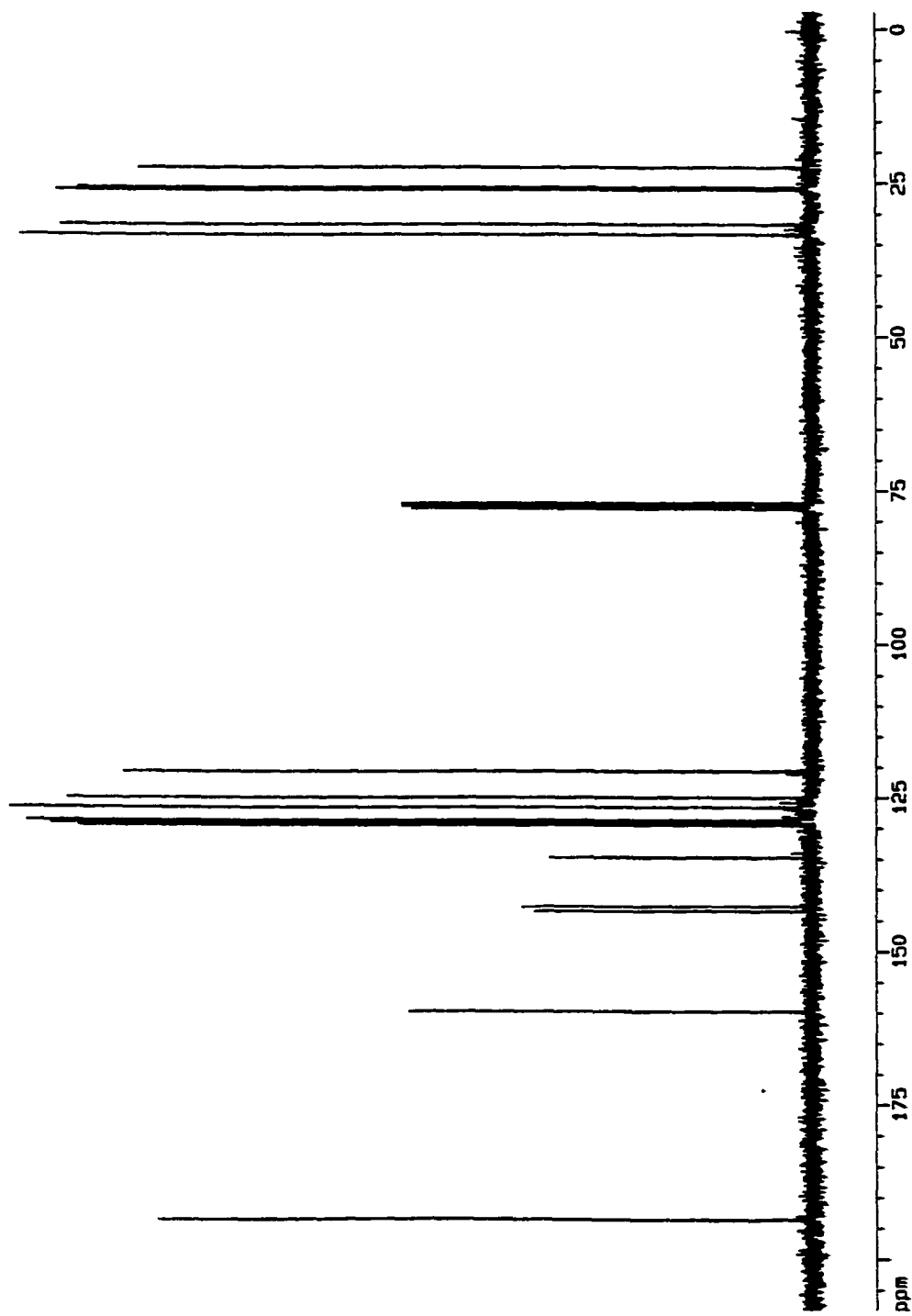


Figure 86. ^{13}C NMR (300 MHz) of Compound II-(9Z)-29 (CDCl_3).

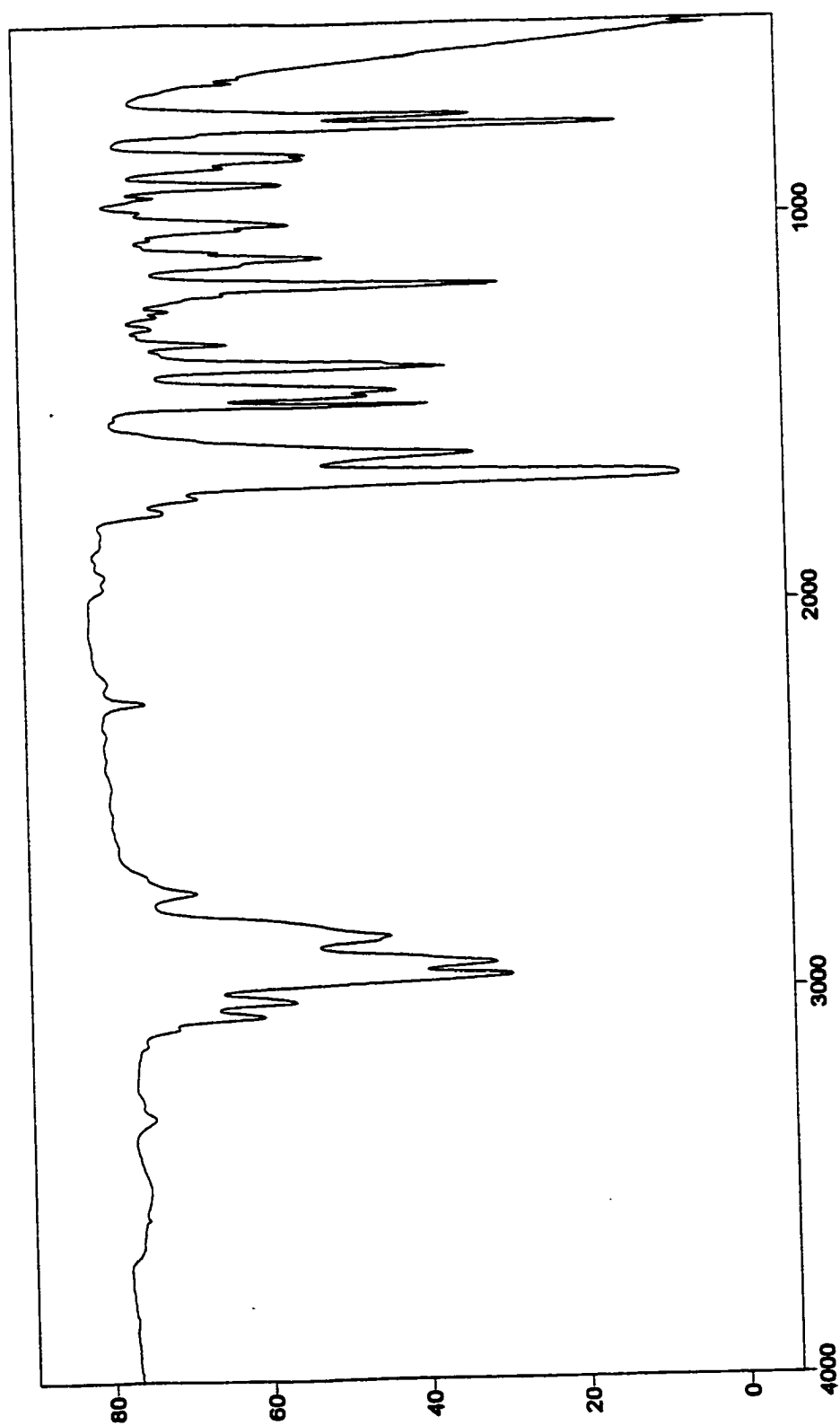


Figure 87. FTIR of Compound II-(9Z)-29 (neat).

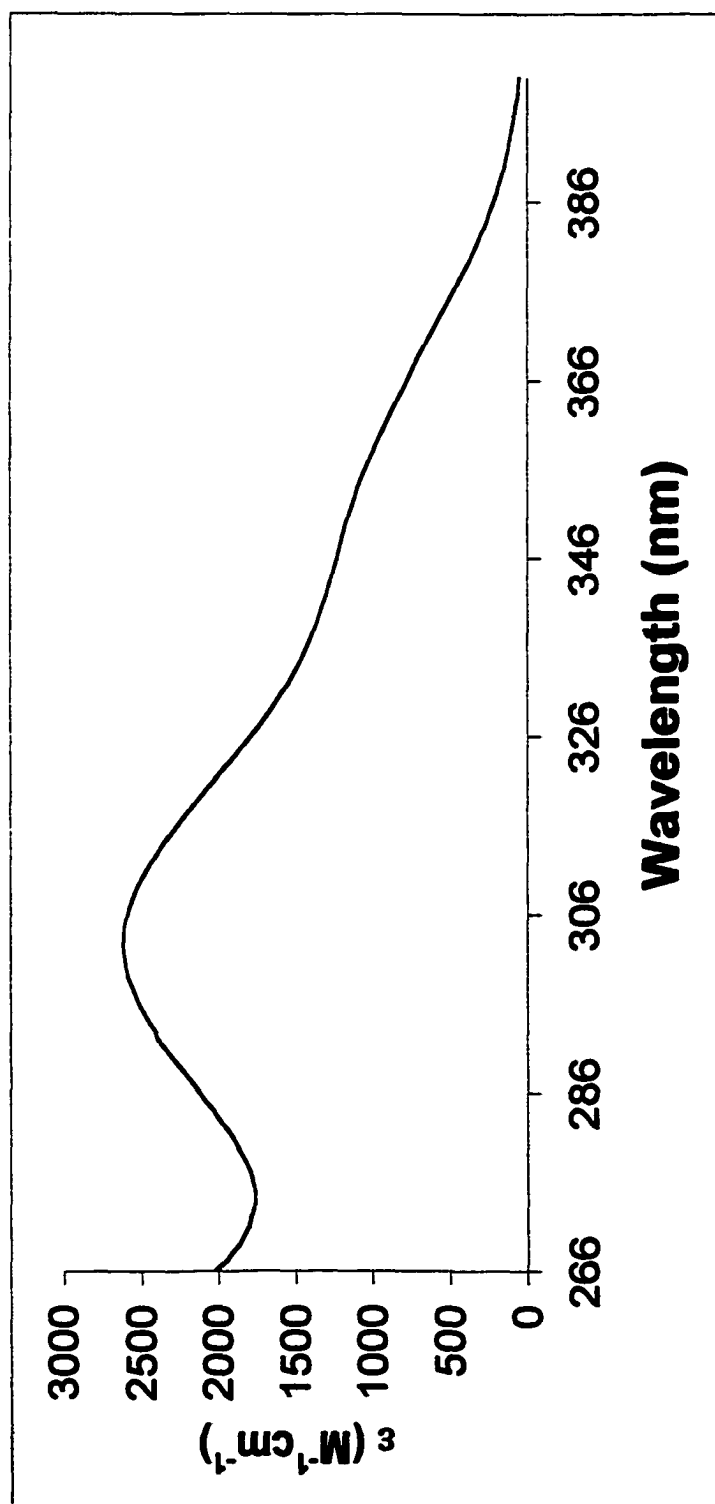


Figure 88. UV-Vis of Compound II-(9Z)-29 (MeOH).

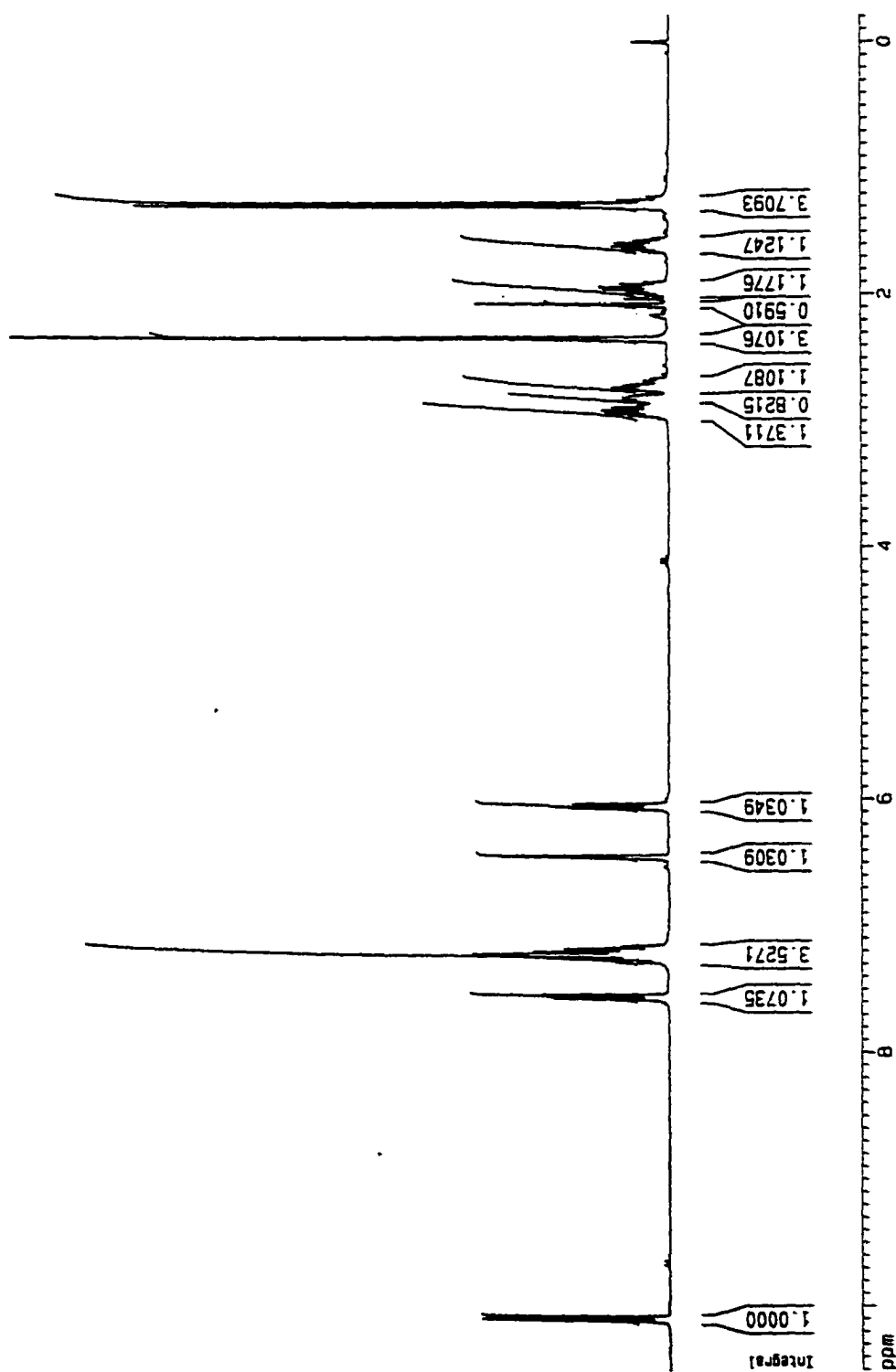


Figure 89. ^1H NMR (300 MHz) of Compound II-(all-E)-29 (CDCl_3).

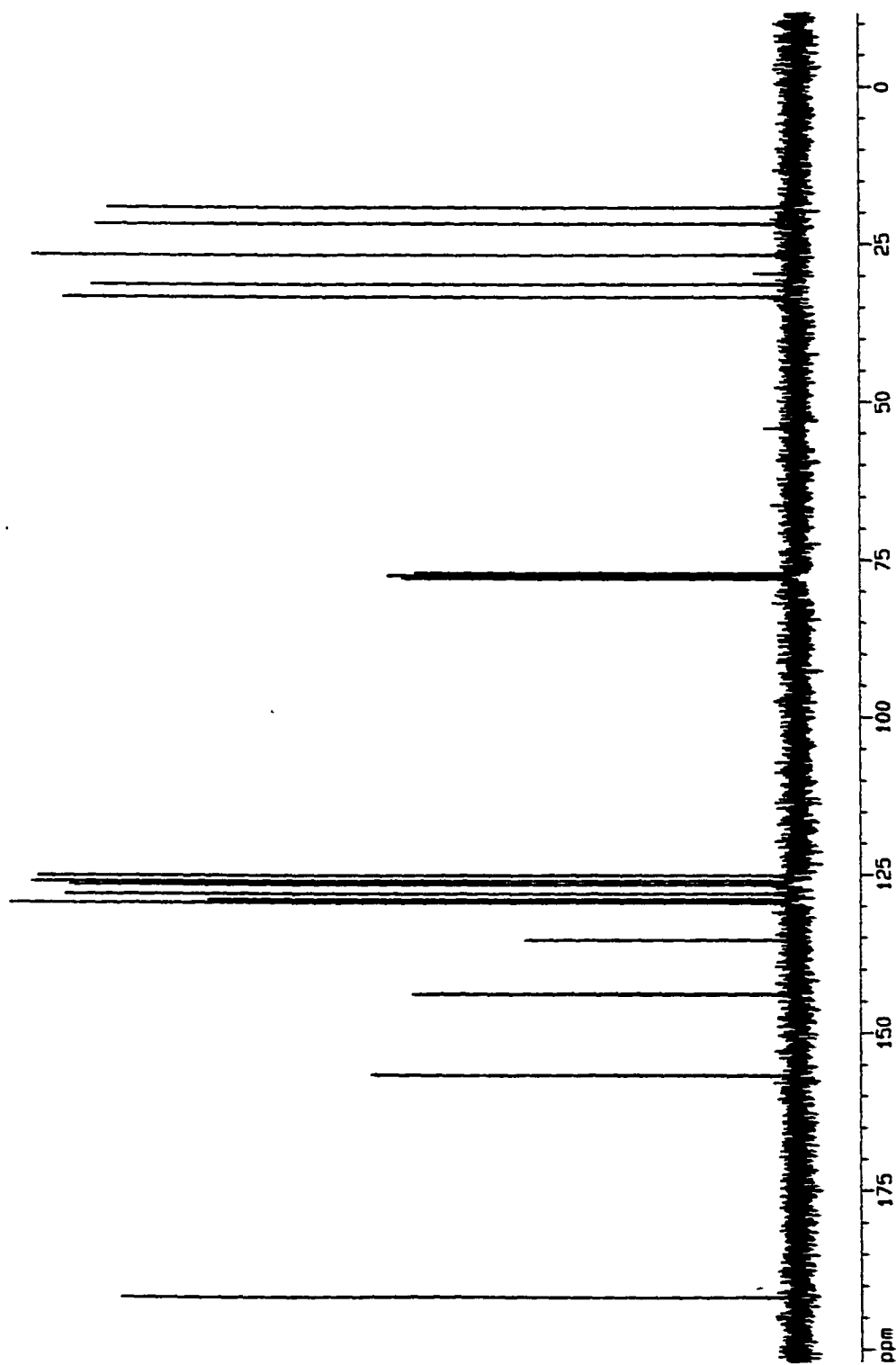


Figure 90. ^{13}C NMR (300 MHz) of Compound 11-(*all-E*)-29 (CDCl_3).

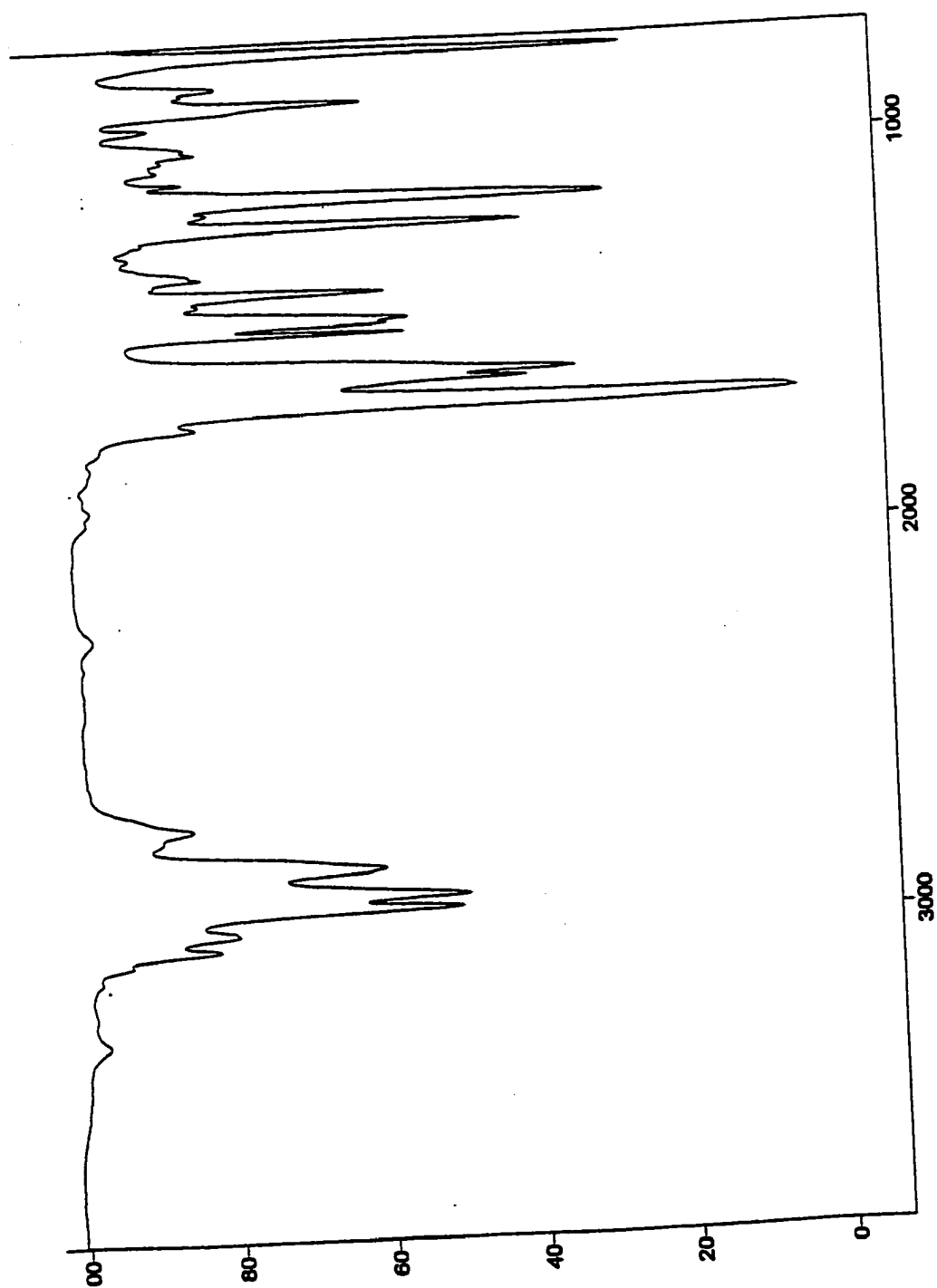


Figure 91. FTIR of Compound II-(*all-E*)-29 (neat).

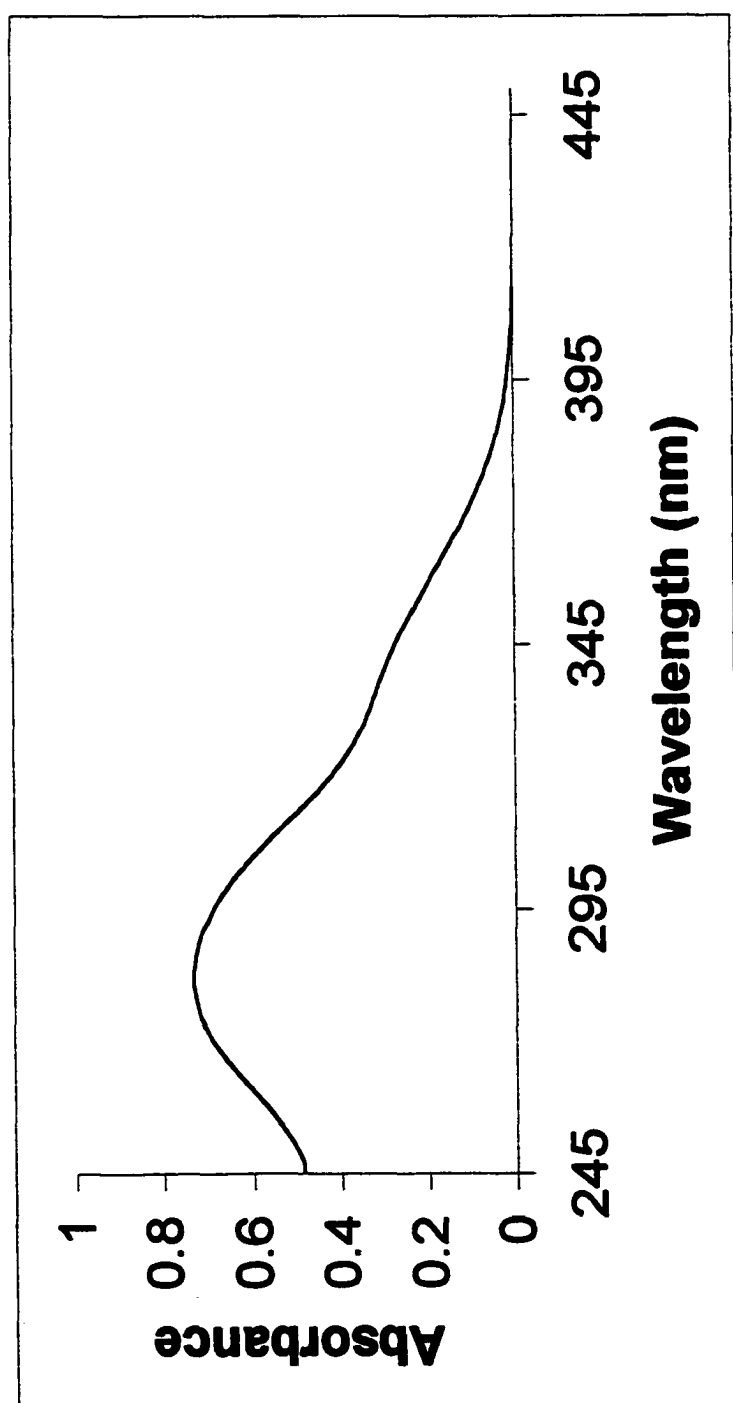


Figure 92. UV-Vis of Compound II-(*all-E*)-29 (MeOH).

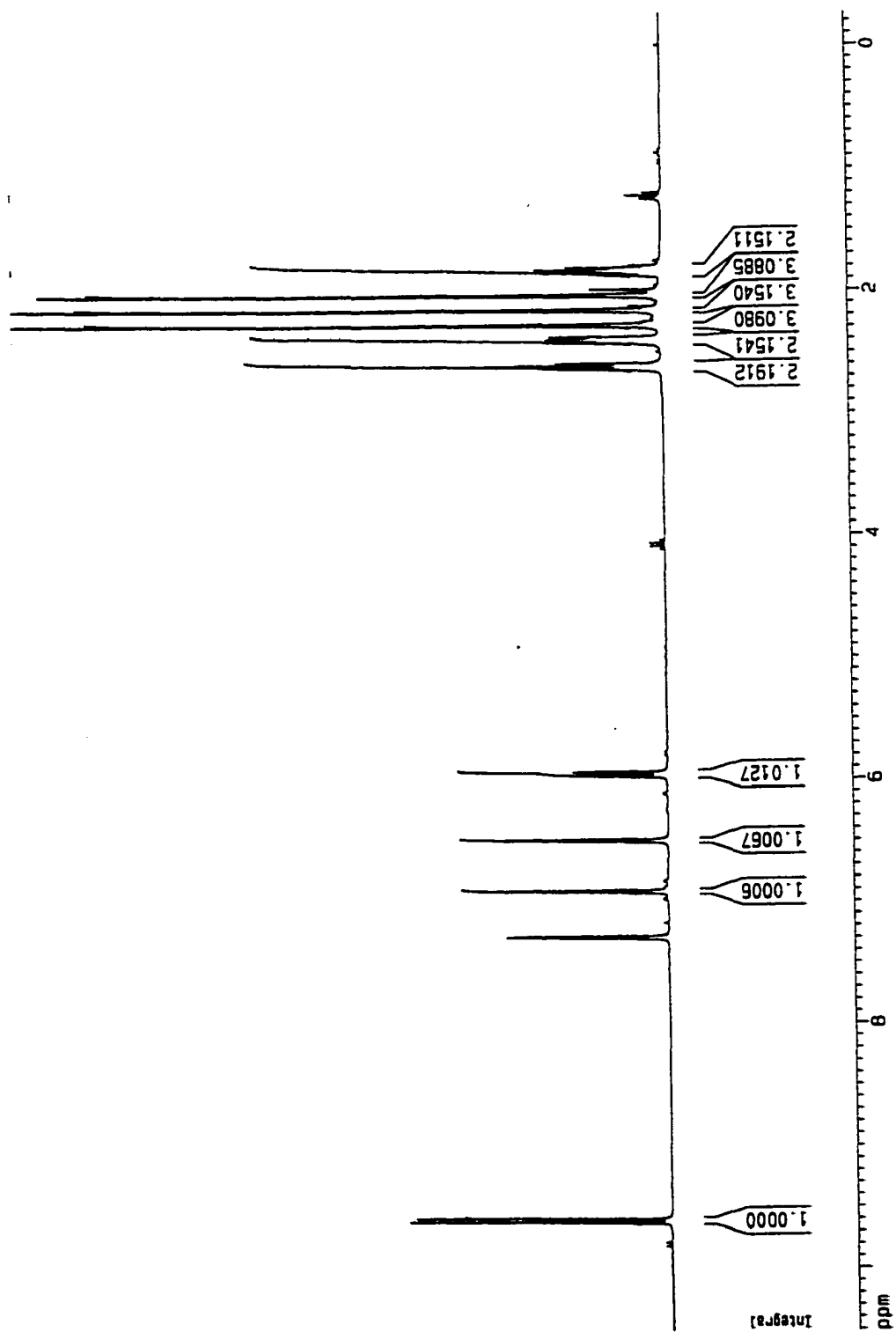


Figure 93. ¹H NMR (300 MHz) of Compound 11-(9Z)-30 (CDCl₃).

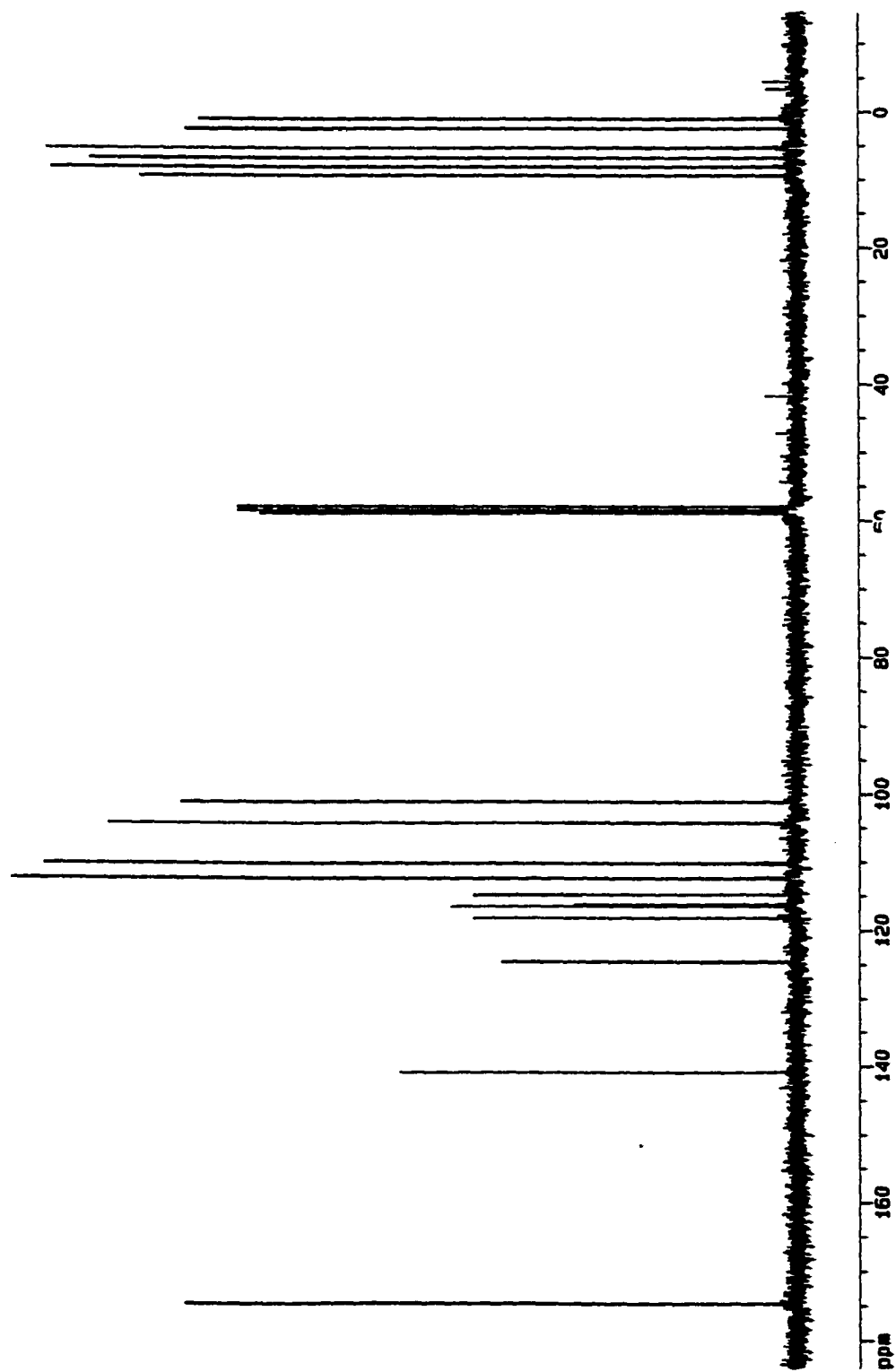


Figure 94. ^{13}C NMR (300 MHz) of Compound II-(9Z)-30 (CDCl_3).

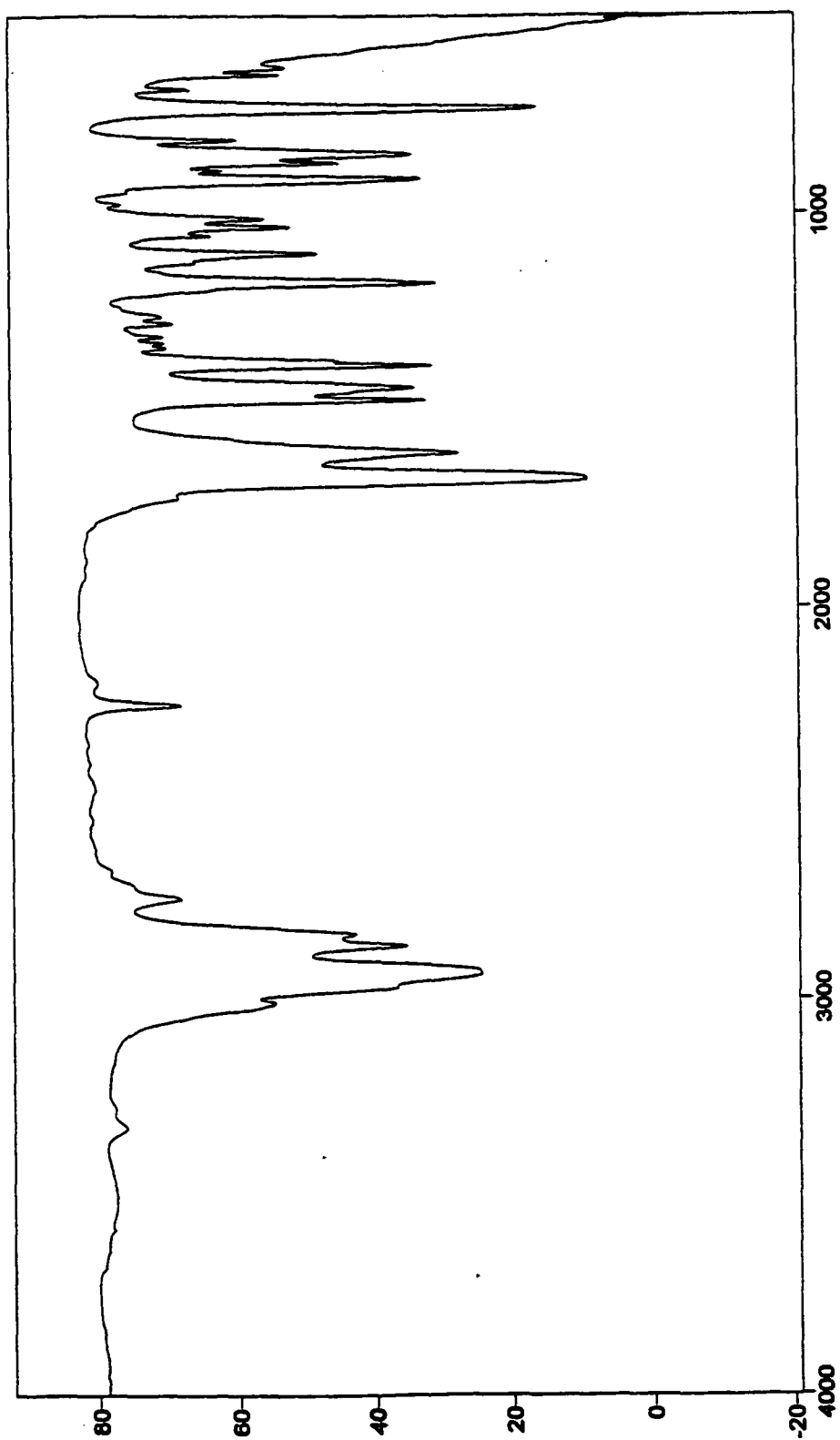


Figure 95. FTIR of Compound II-(9Z)-30 (neat).

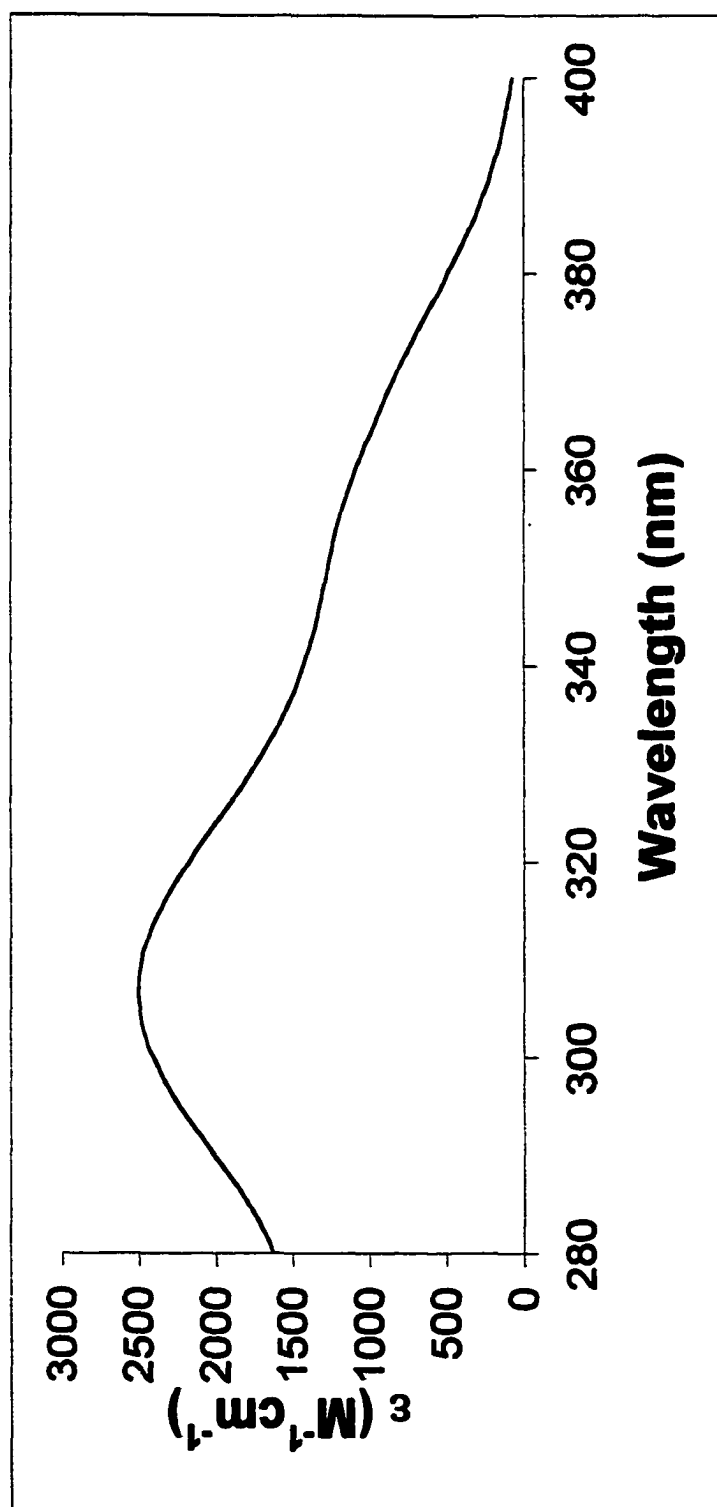


Figure 96. UV-Vis of Compound II-(9Z)-30 (MeOH).

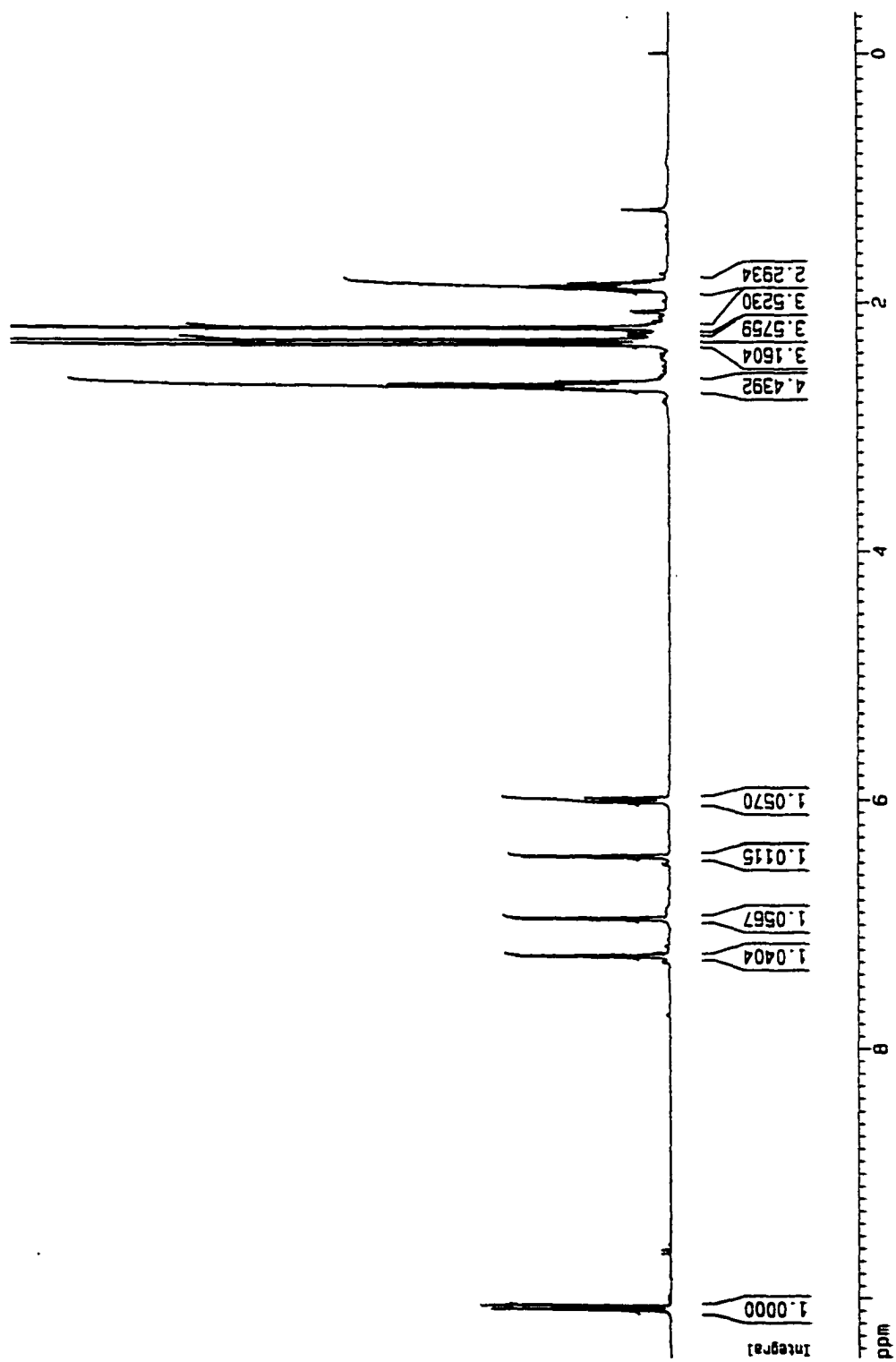


Figure 97. ¹H NMR (300 MHz) of Compound II-(*all-E*)-30 (CDCl₃).

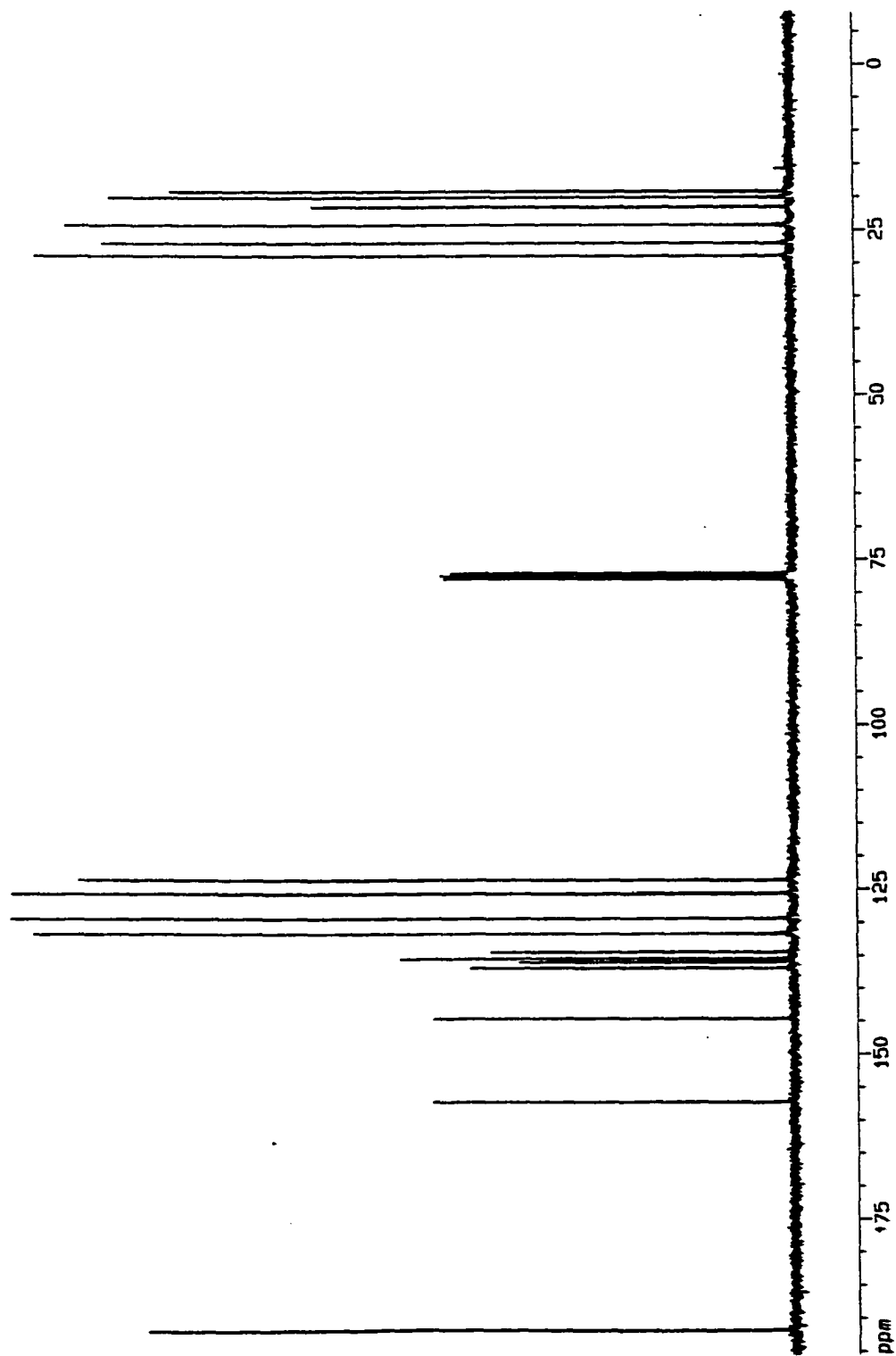


Figure 98. ^{13}C NMR (300 MHz) of Compound **II-(all-E)-30** (CDCl_3).

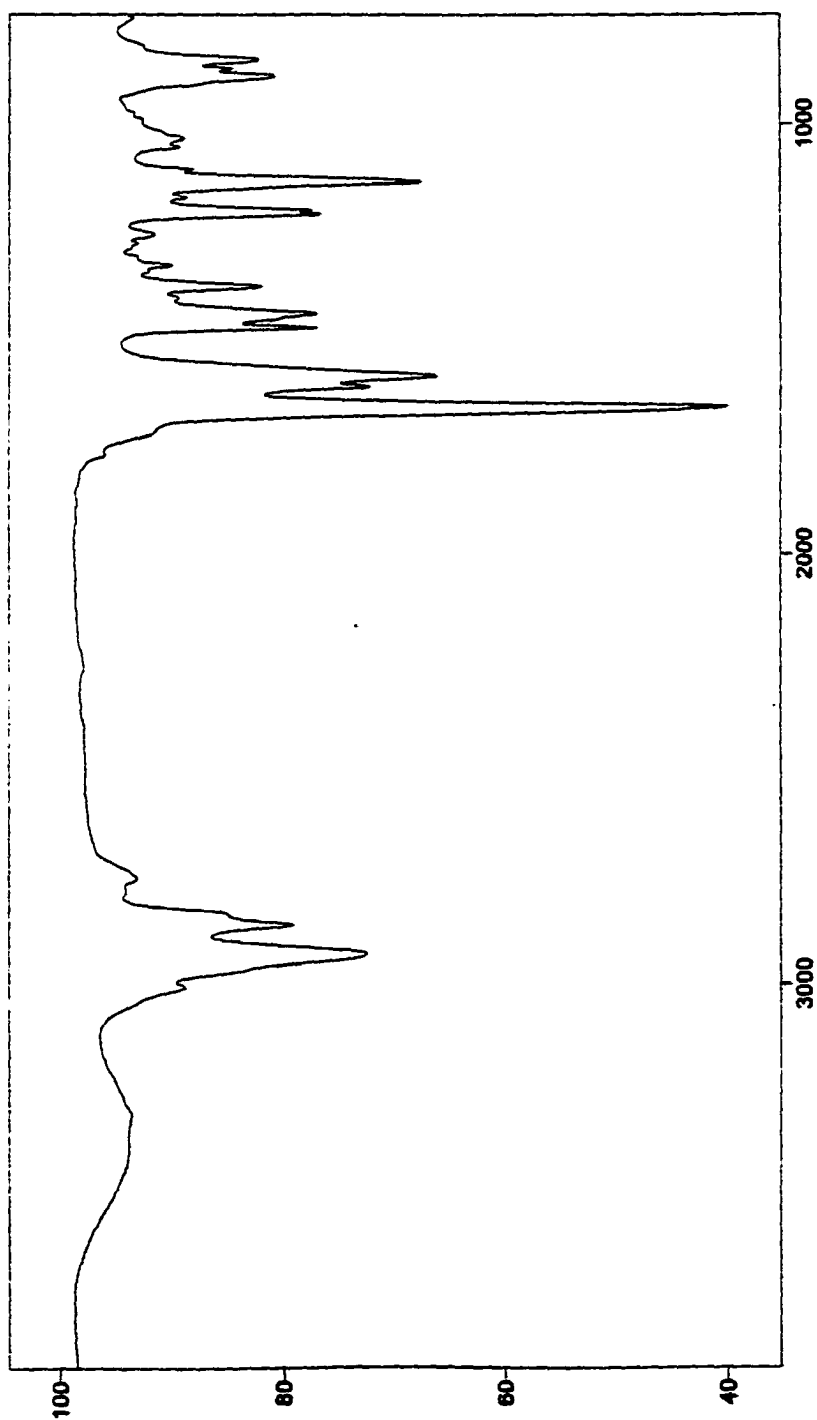


Figure 99. FTIR of Compound II-(*all-E*)-30 (neat).

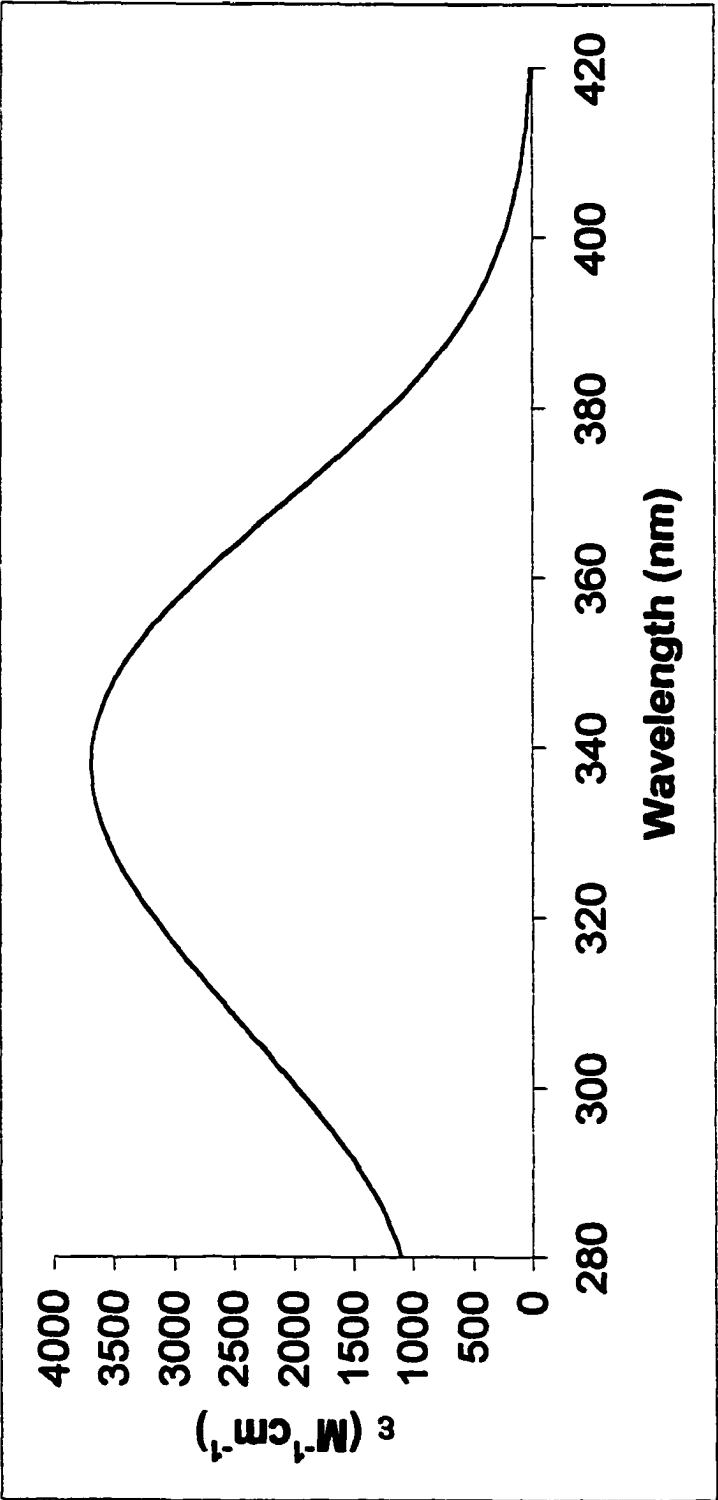


Figure 100. UV-Vis of Compound II-(*all-E*)-30 (MeOH).

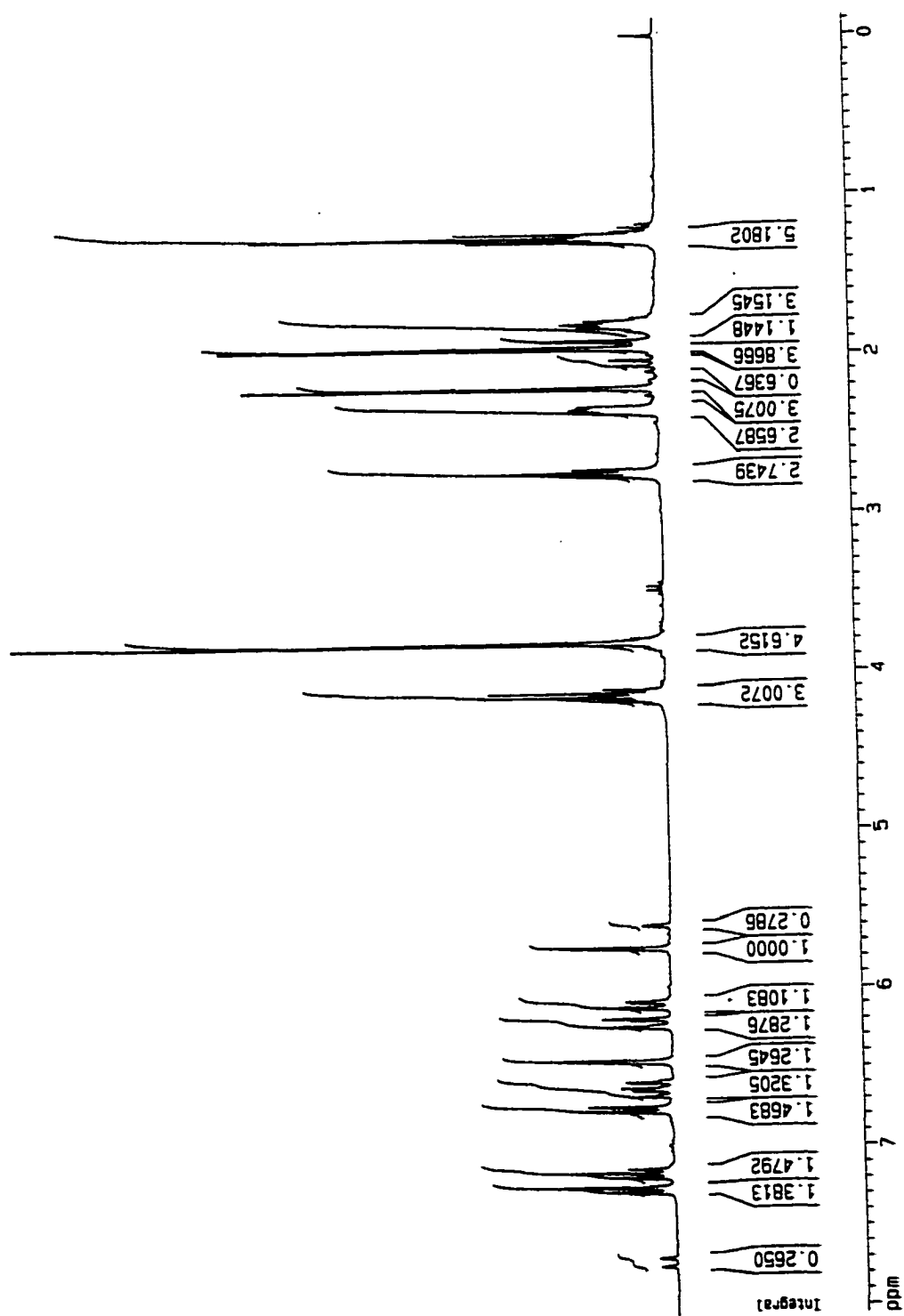


Figure 101. ¹H NMR (300 MHz) of Compound II-32 (CDCl₃).

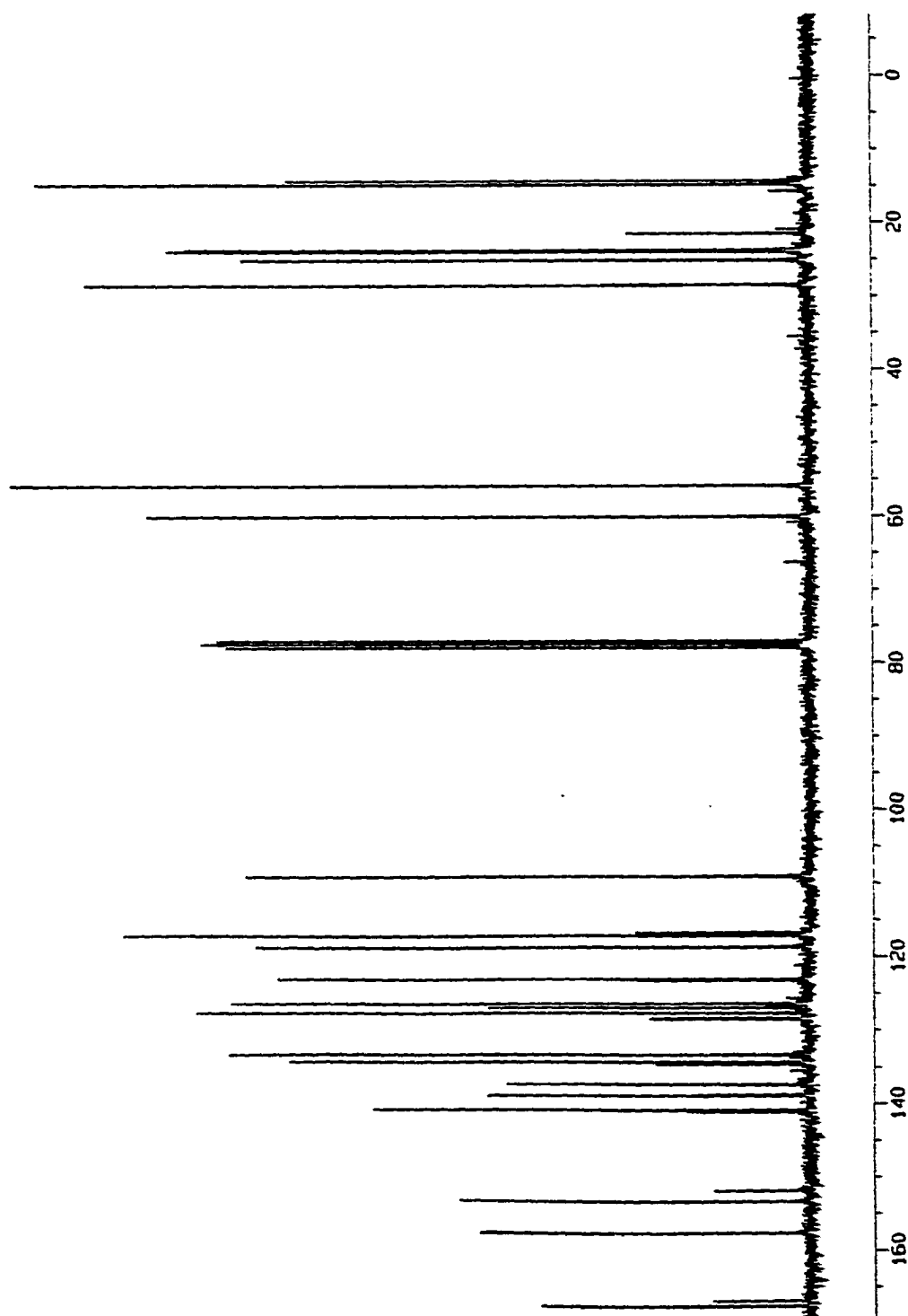


Figure 102. ^{13}C NMR (300 MHz) of Compound 11-32 (CDCl_3).

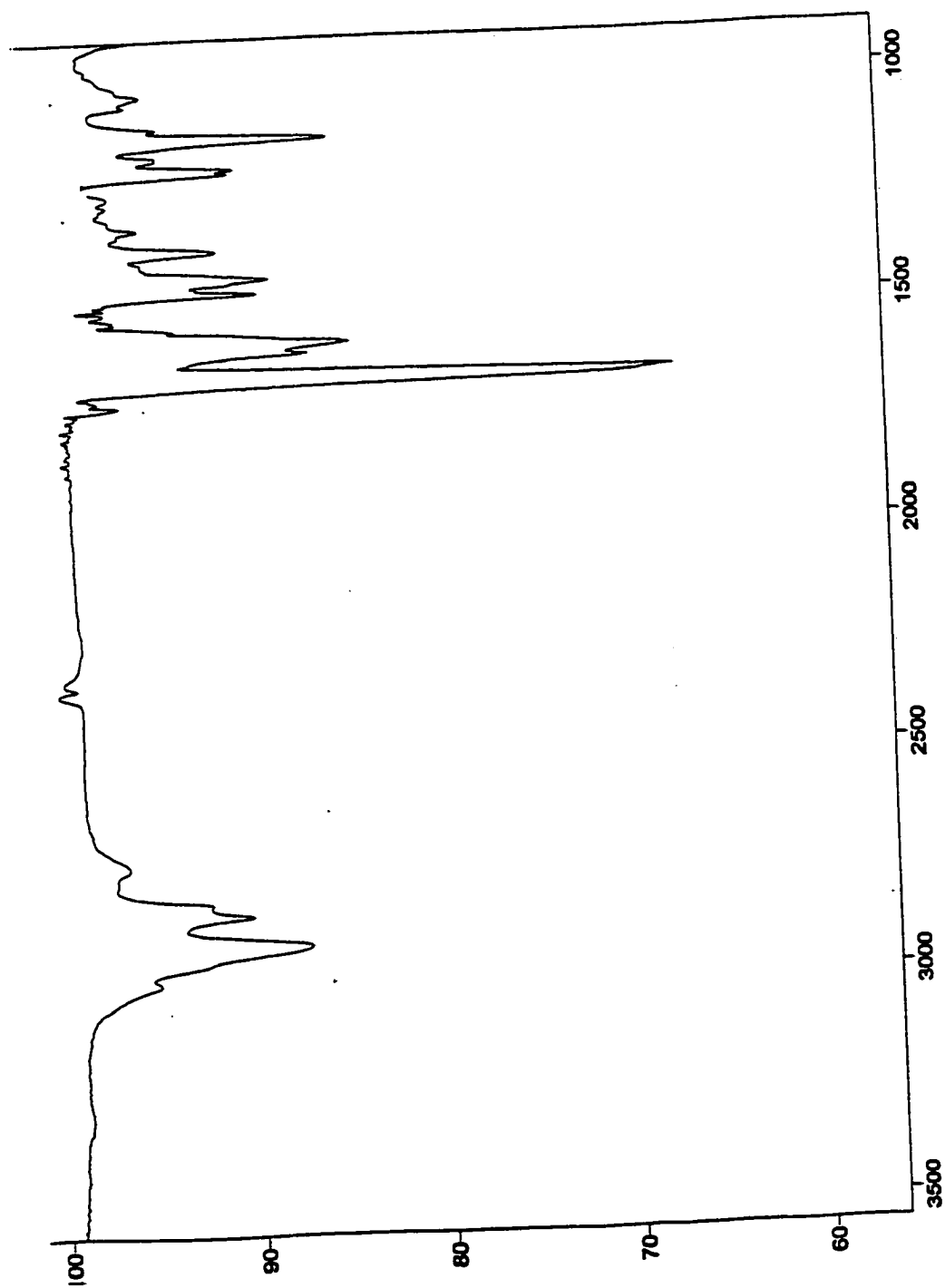


Figure 103. FTIR of Compound II-32 (neat).

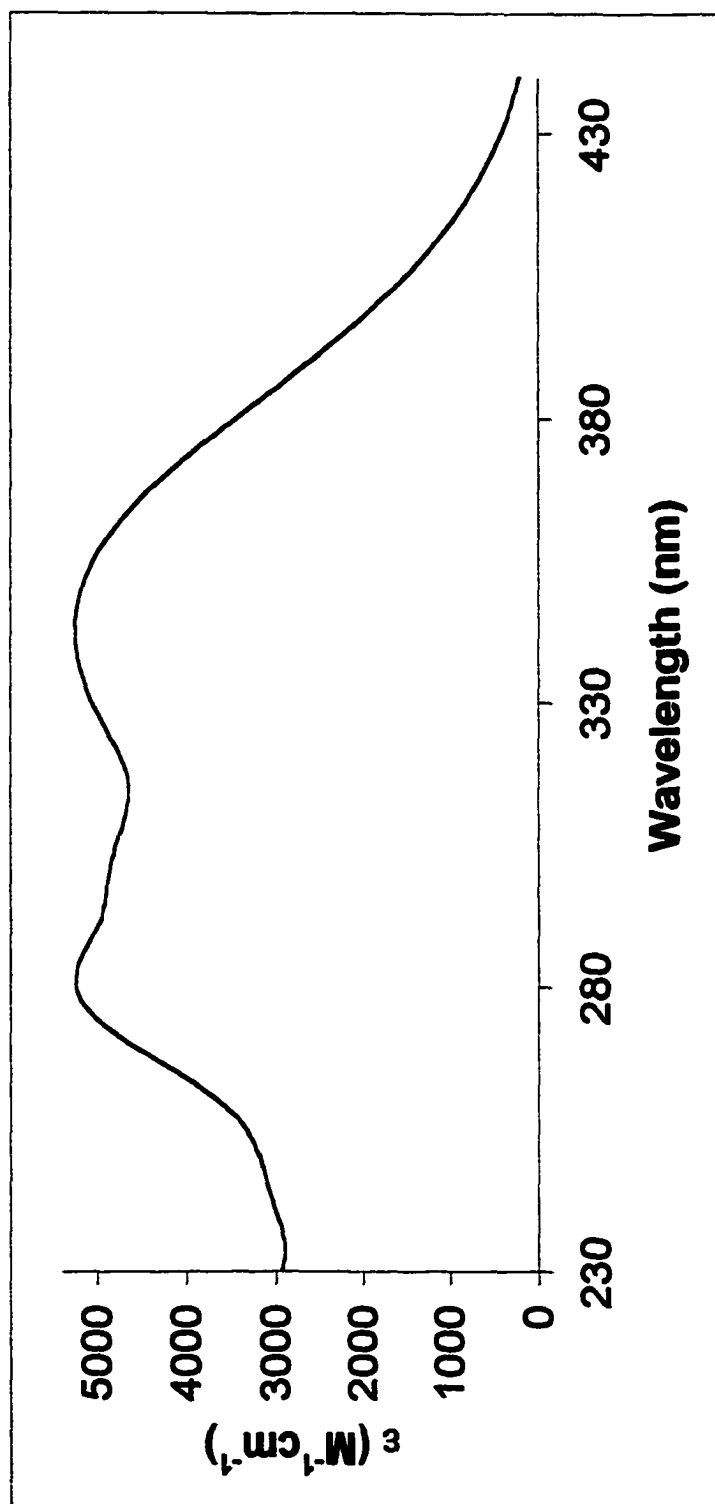


Figure 104. UV-Vis of Compound II-32 (MeOH).

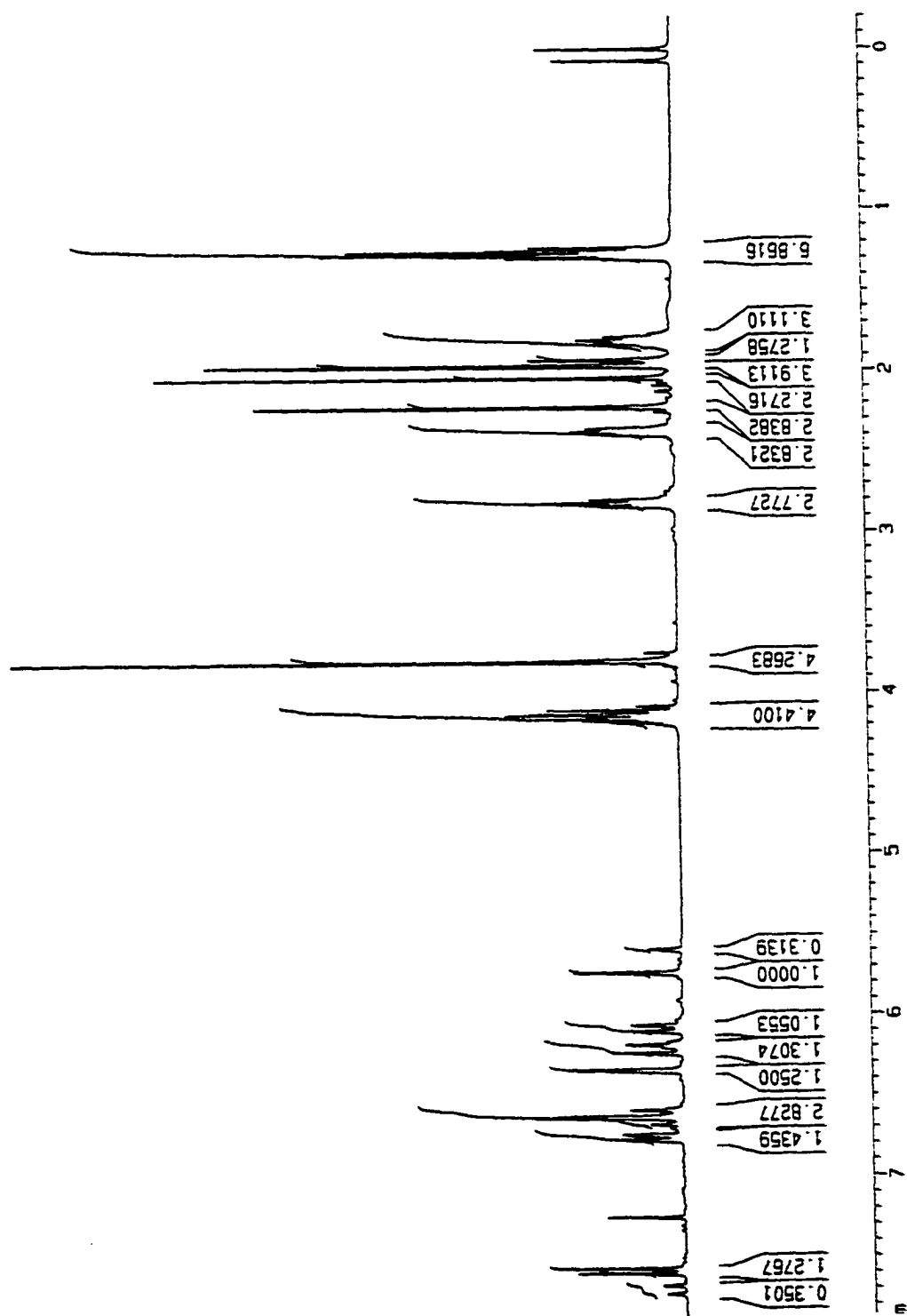


Figure 105. ¹H NMR (300 MHz) of Compound II-33 (CDCl₃).

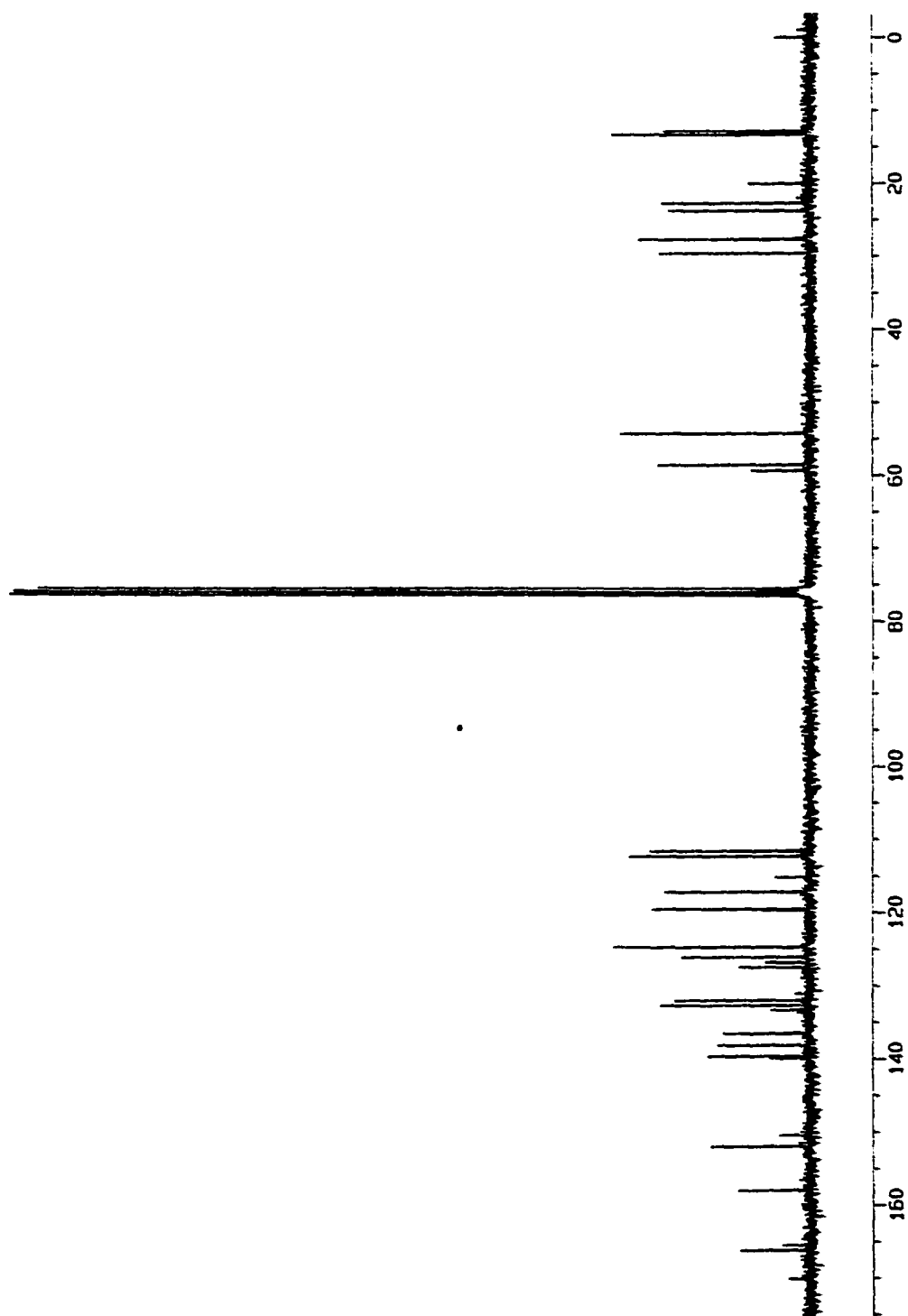


Figure 106. ^{13}C NMR (300 MHz) of Compound II-33 (CDCl_3).

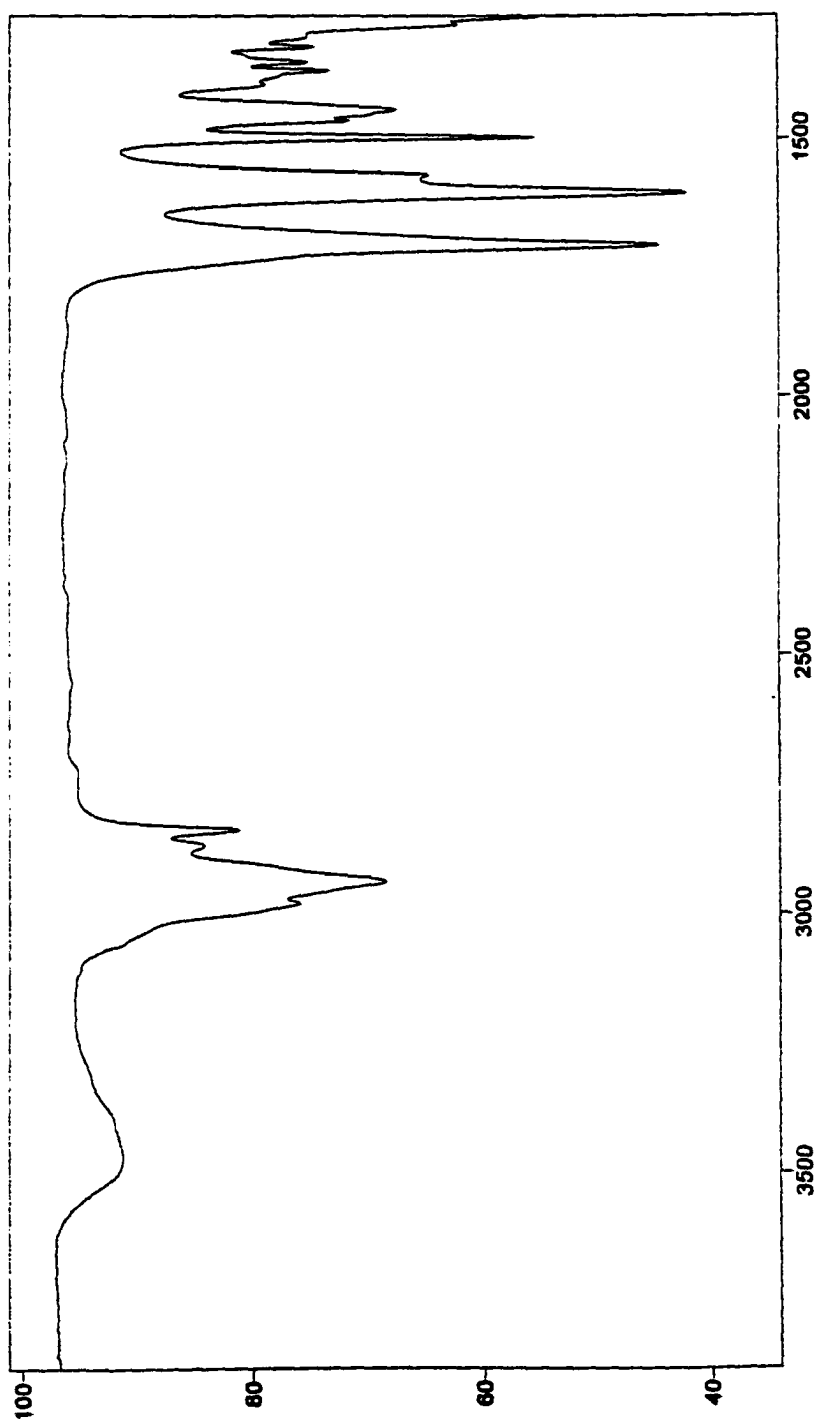


Figure 107. FTIR of Compound **II-33** (neat).

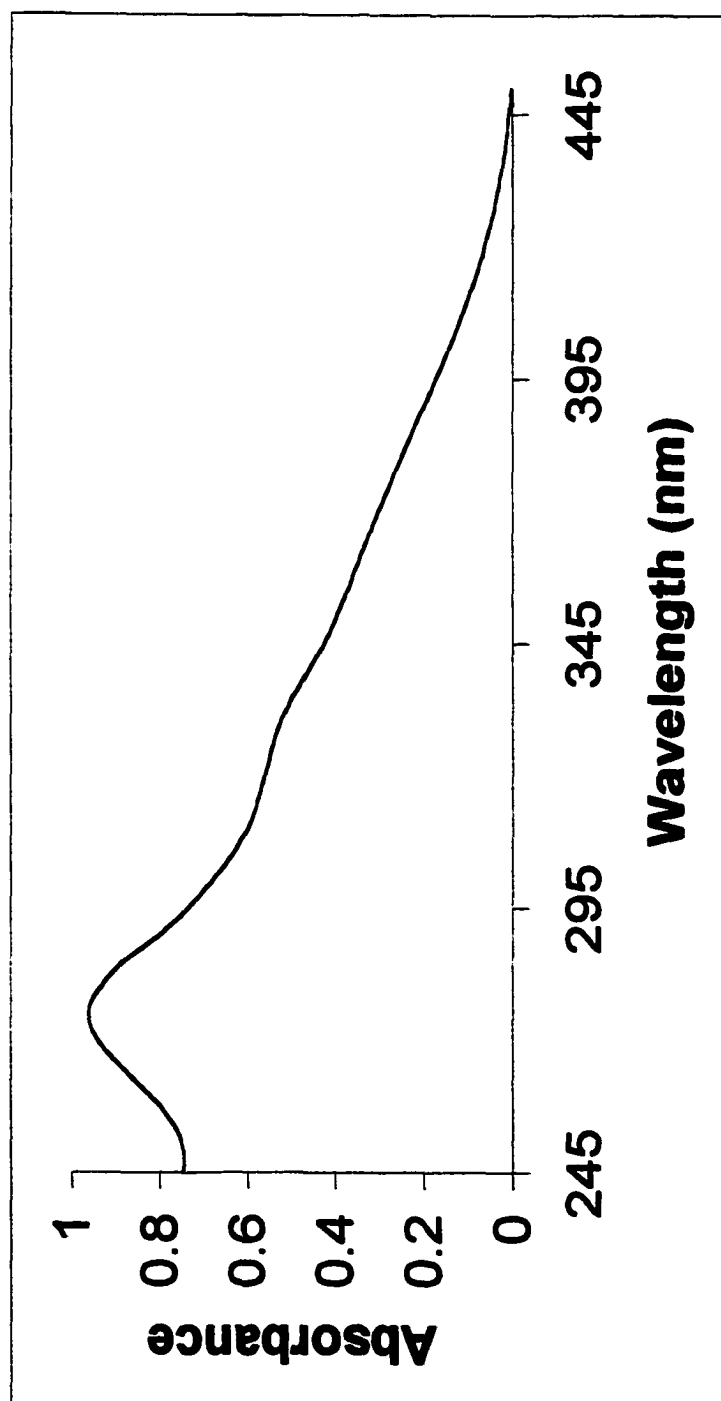


Figure 108. UV-Vis of Compound II-33 (MeOH)

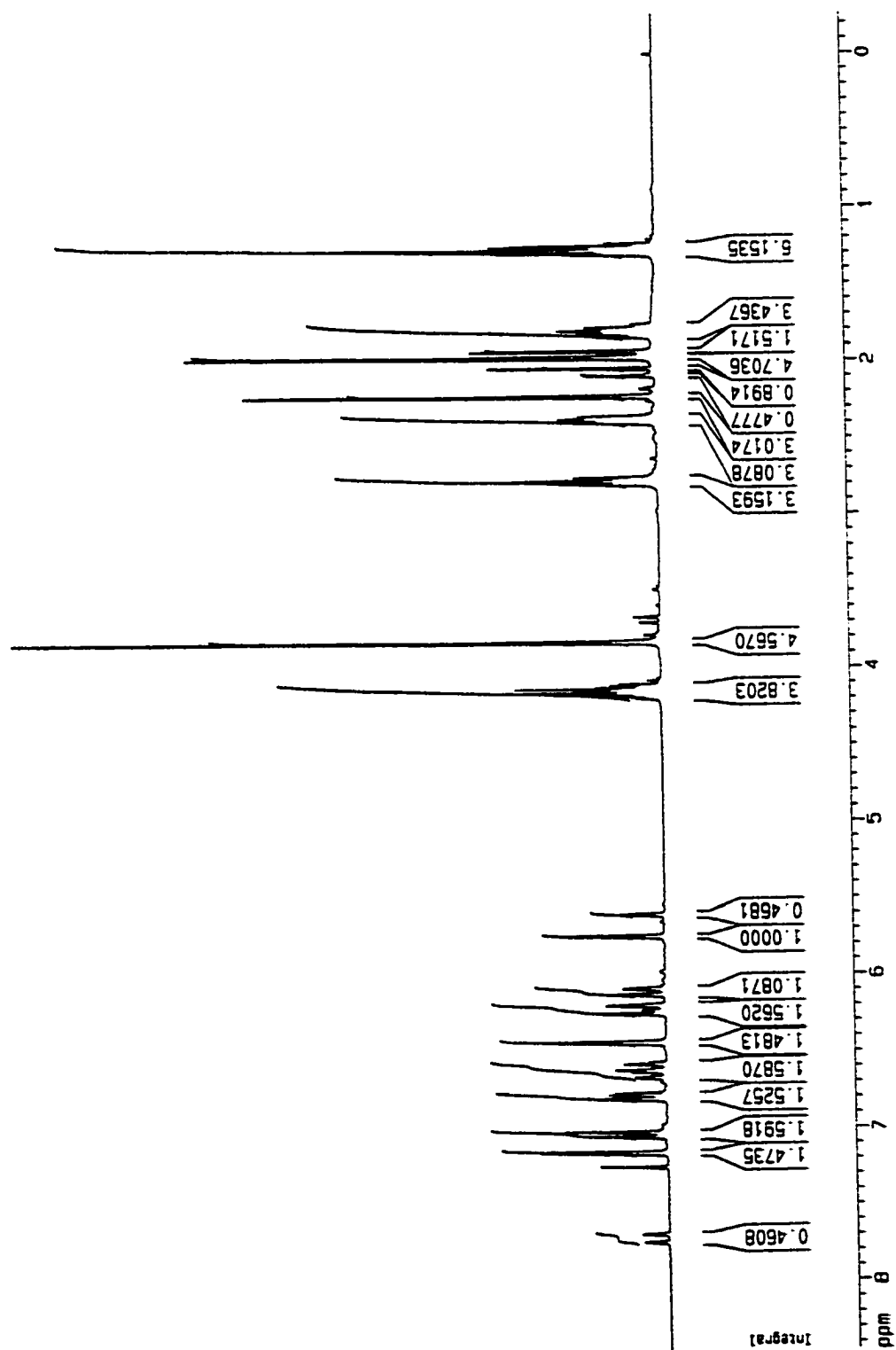


Figure 109. ¹H NMR (300 MHz) of Compound II-34 (CDCl₃).

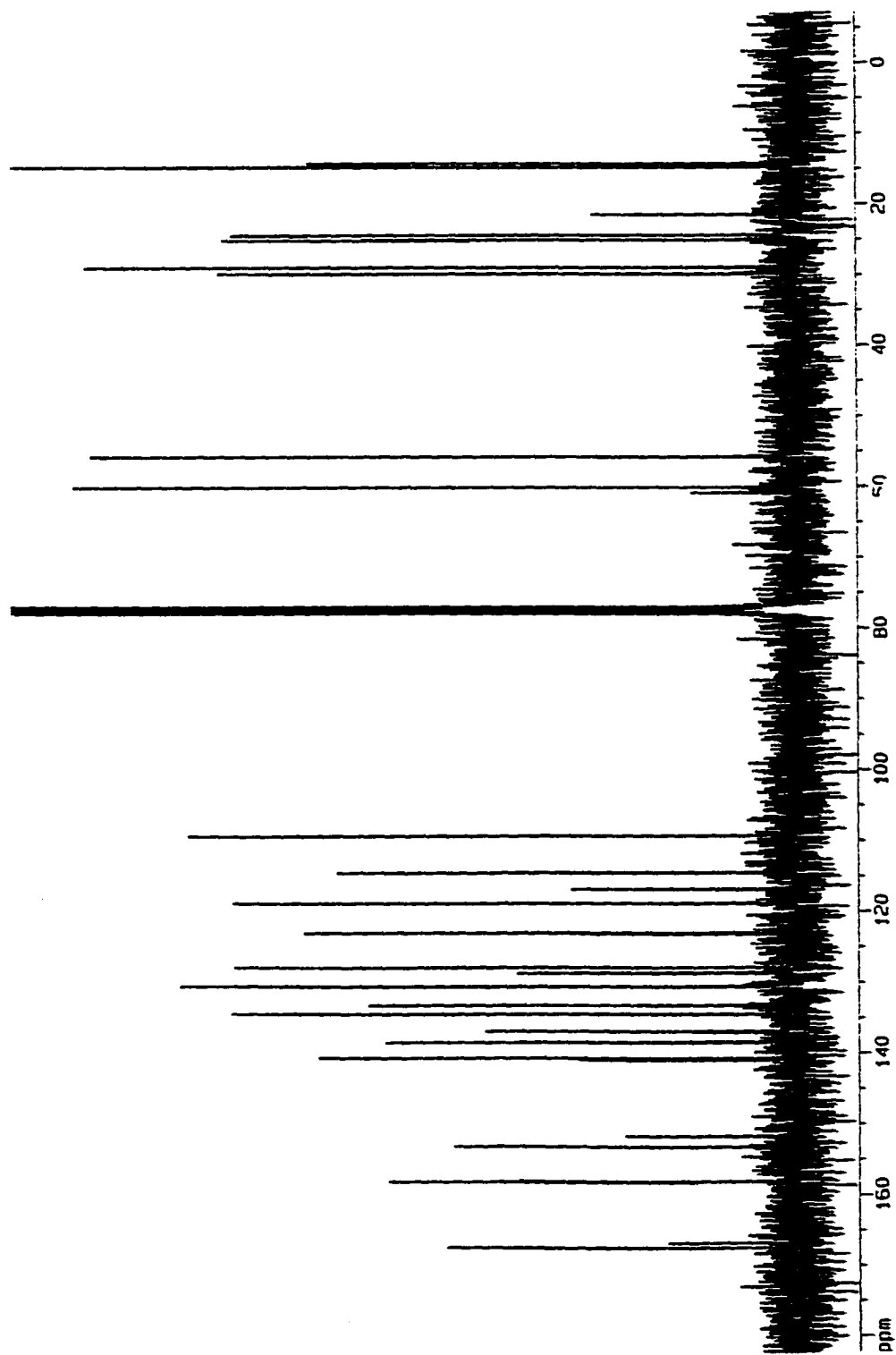


Figure 110. ^{13}C NMR (300 MHz) of Compound II-34 (CDCl_3).

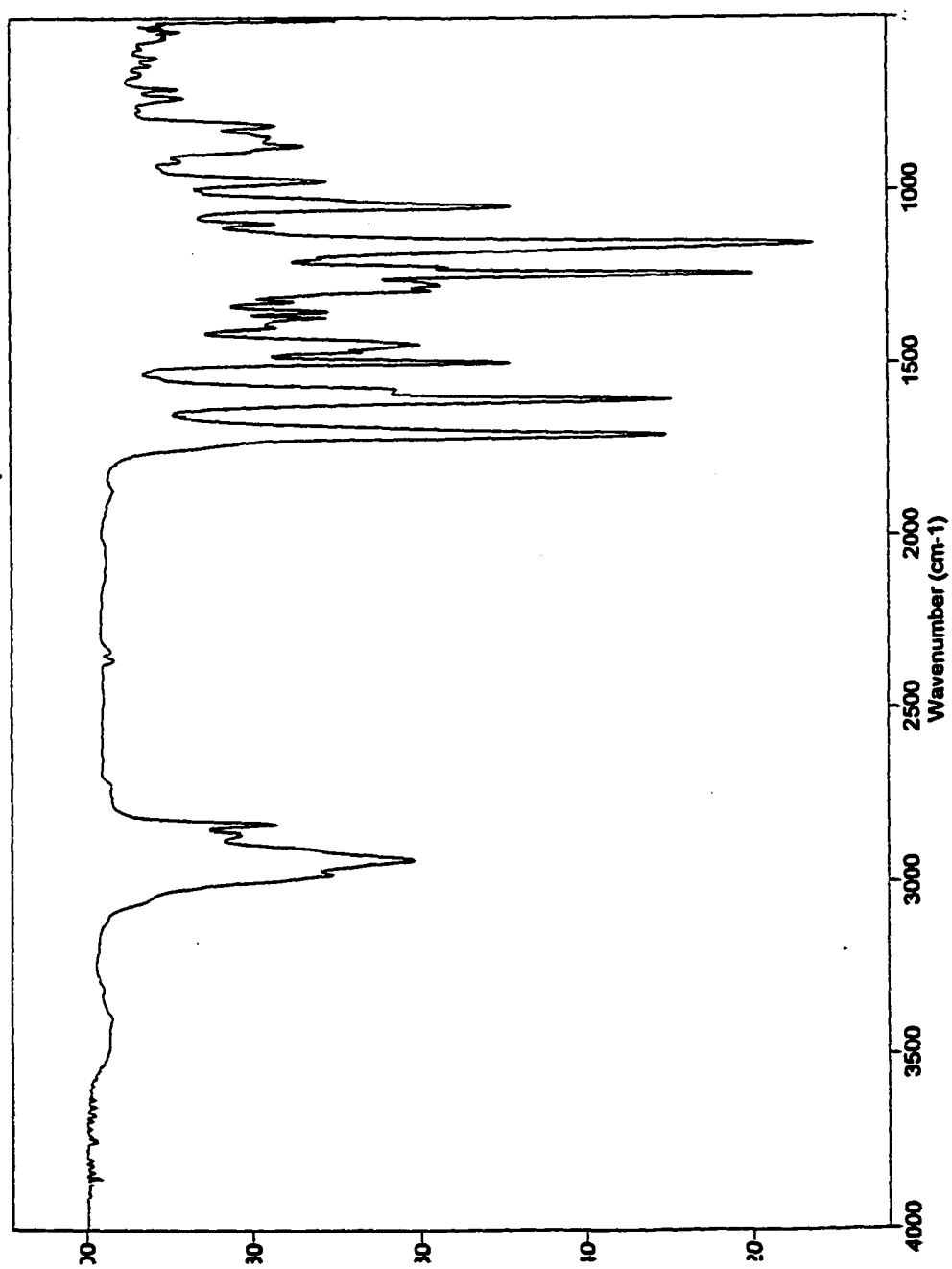


Figure 111. FTIR of Compound II-34 (neat).

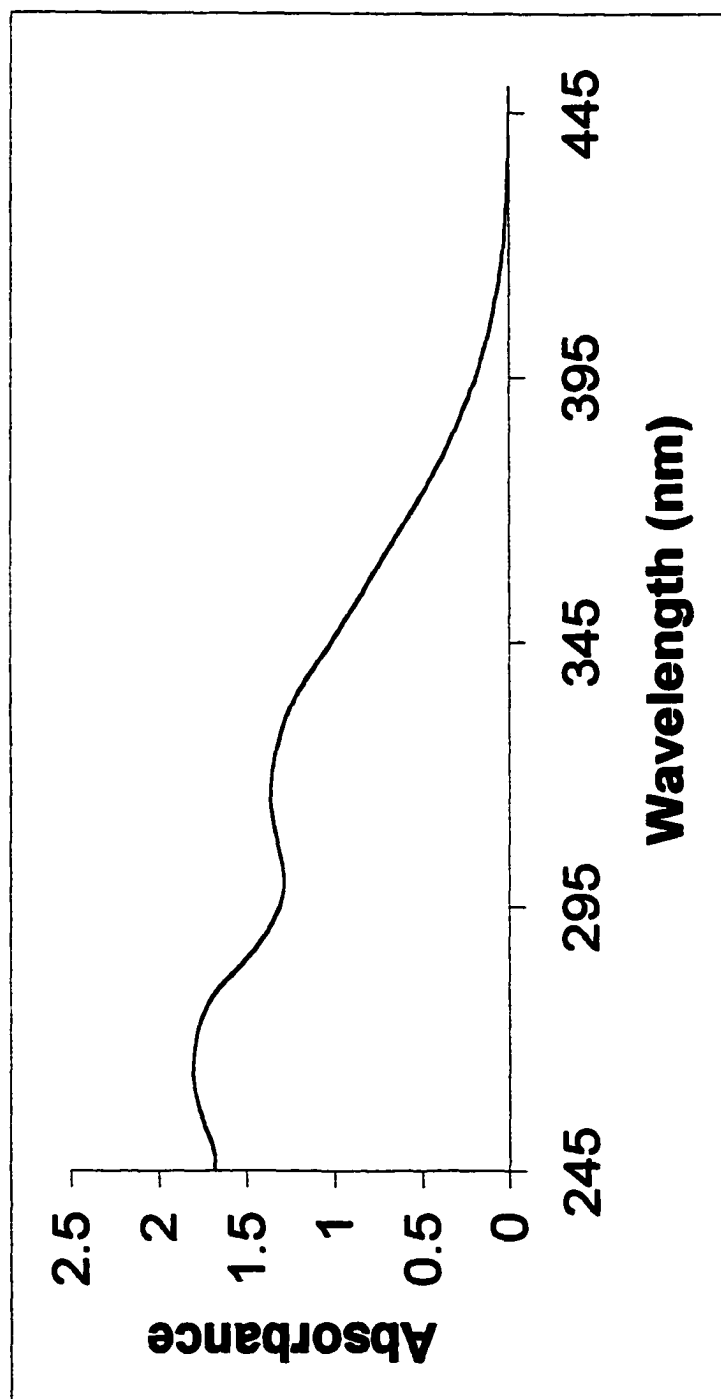


Figure 112. UV-Vis of Compound II-34 (MeOH)

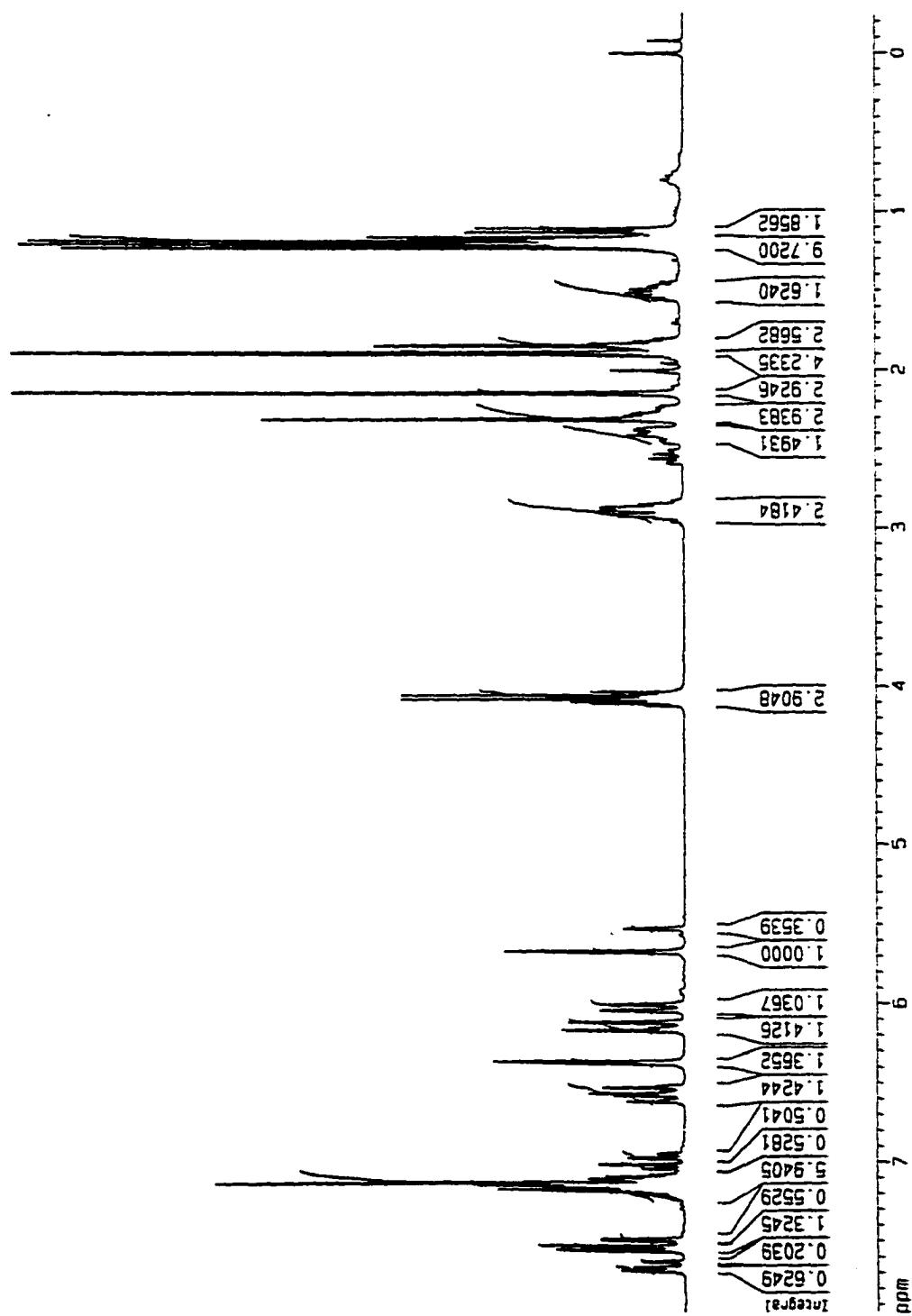


Figure 113. ¹H NMR (300 MHz) of Compound II-35 (CDCl₃).

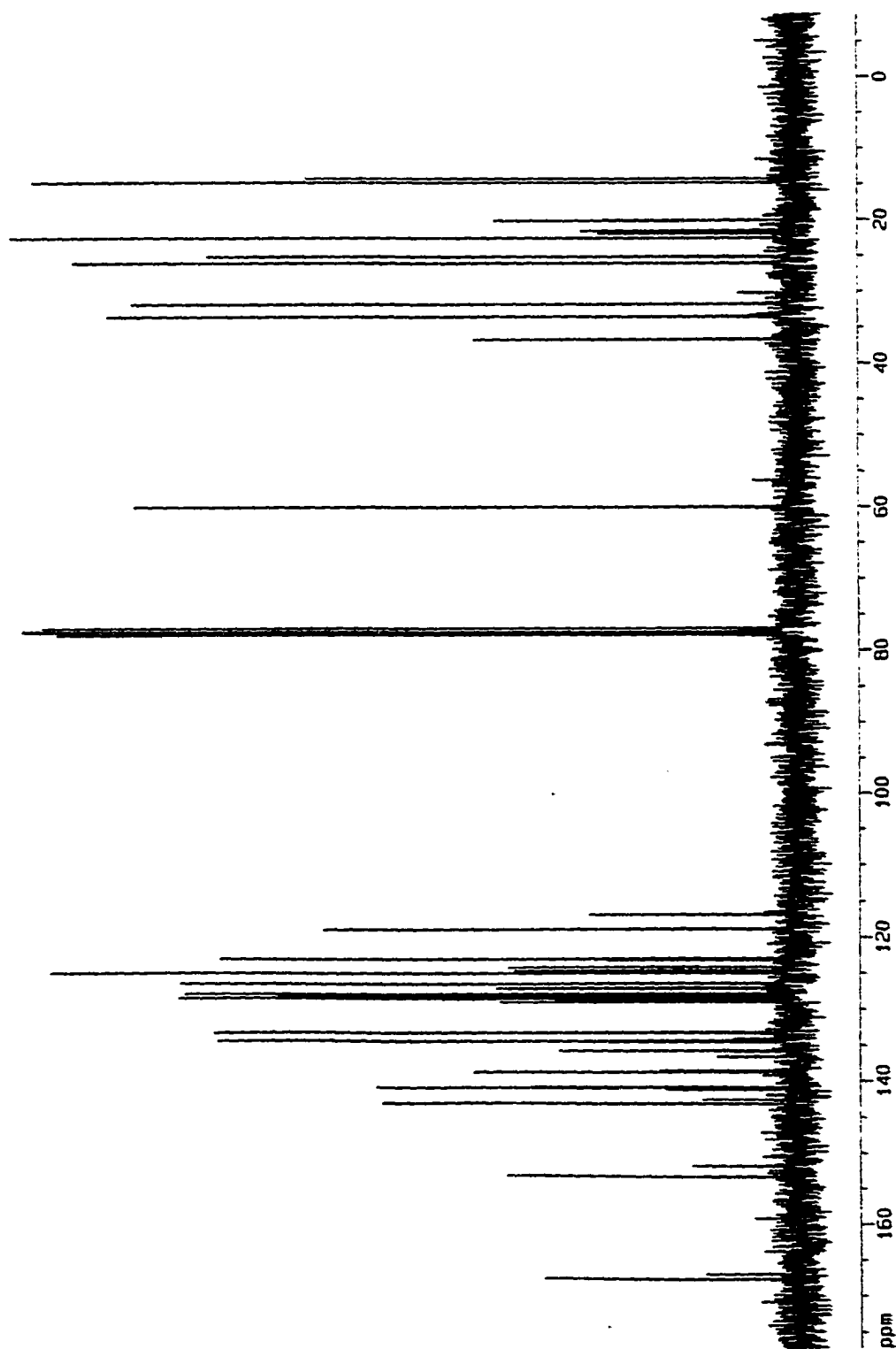


Figure 114. ^{13}C NMR (300 MHz) of Compound II-35 (CDCl_3).

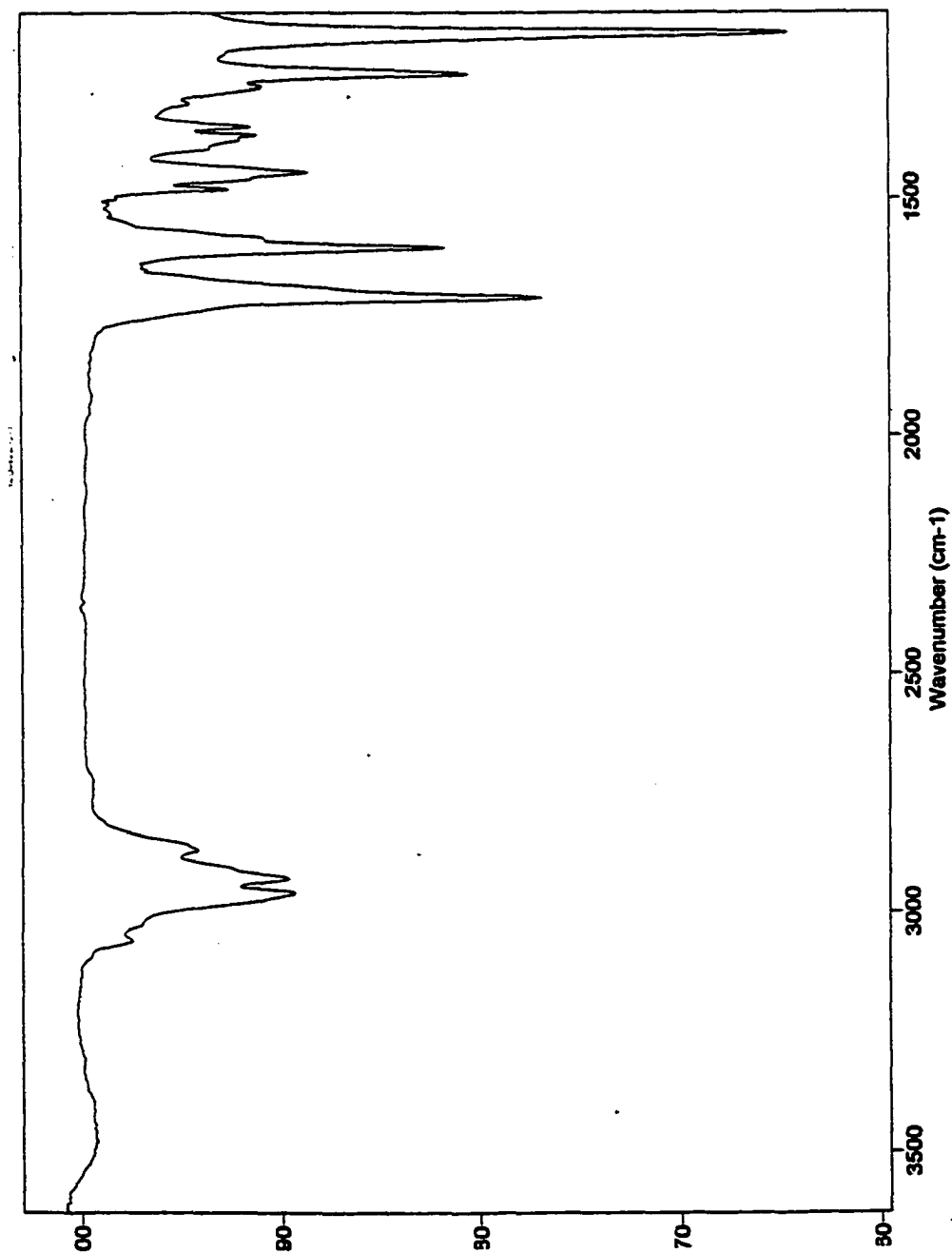


Figure 115. FTIR of Compound II-35 (neat).

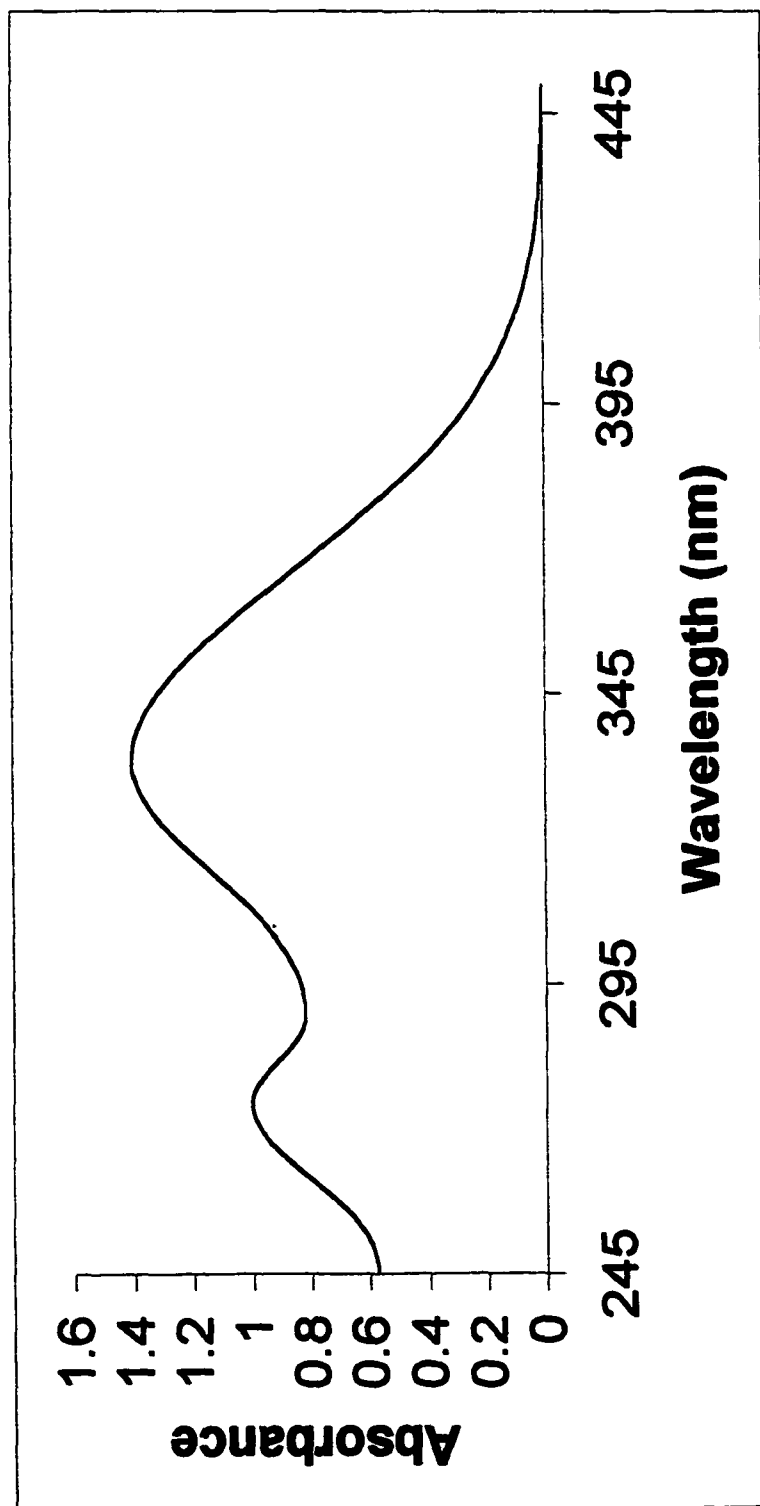


Figure 116. UV-Vis of Compound II-35 (MeOH).

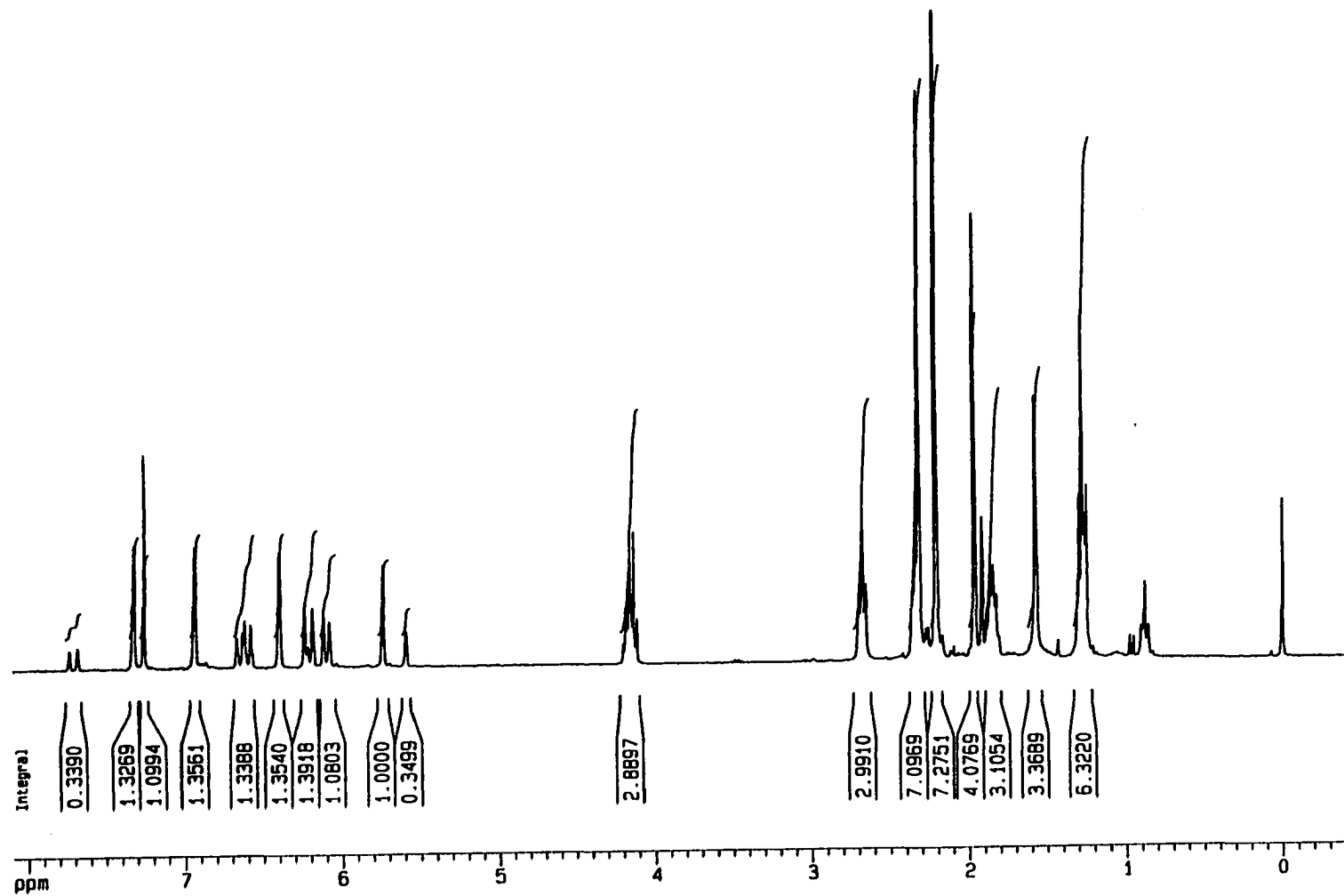


Figure 117. ¹H NMR (300 MHz) of Compound II-36 (CDCl₃).

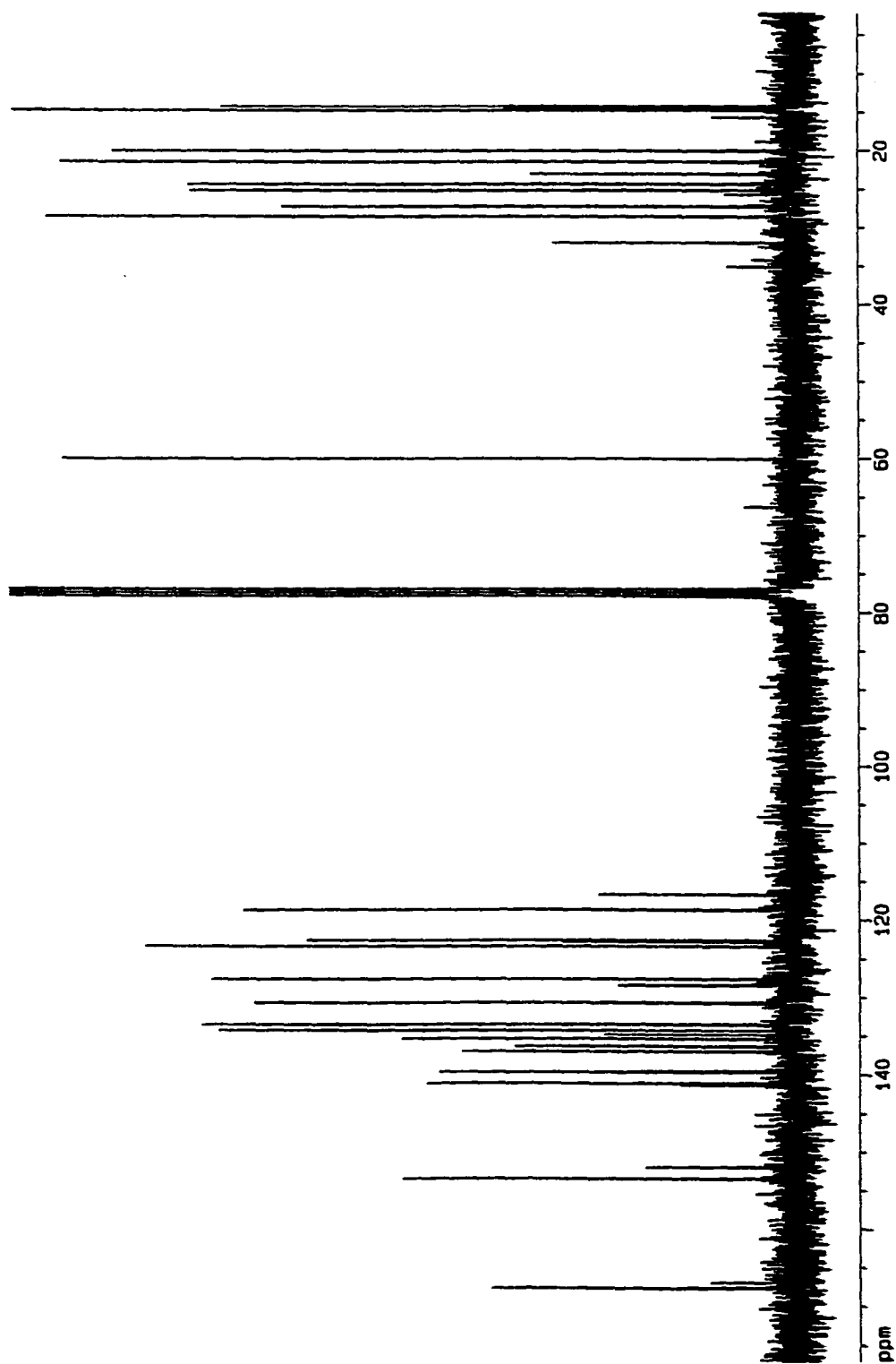


Figure 118. ^{13}C NMR (300 MHz) of Compound II-36 (CDCl_3).

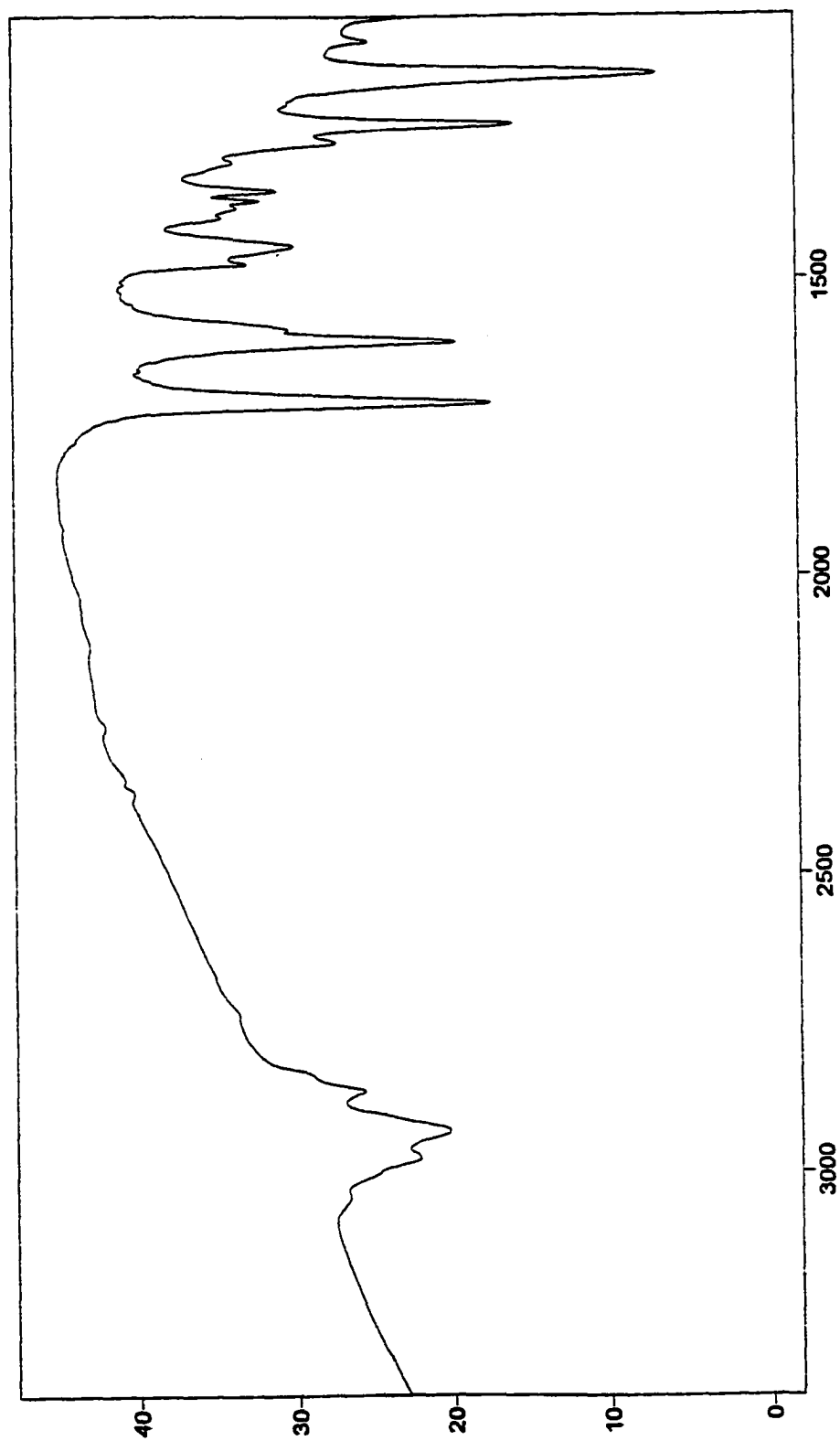


Figure 119. FTIR of Compound II-36 (neat).

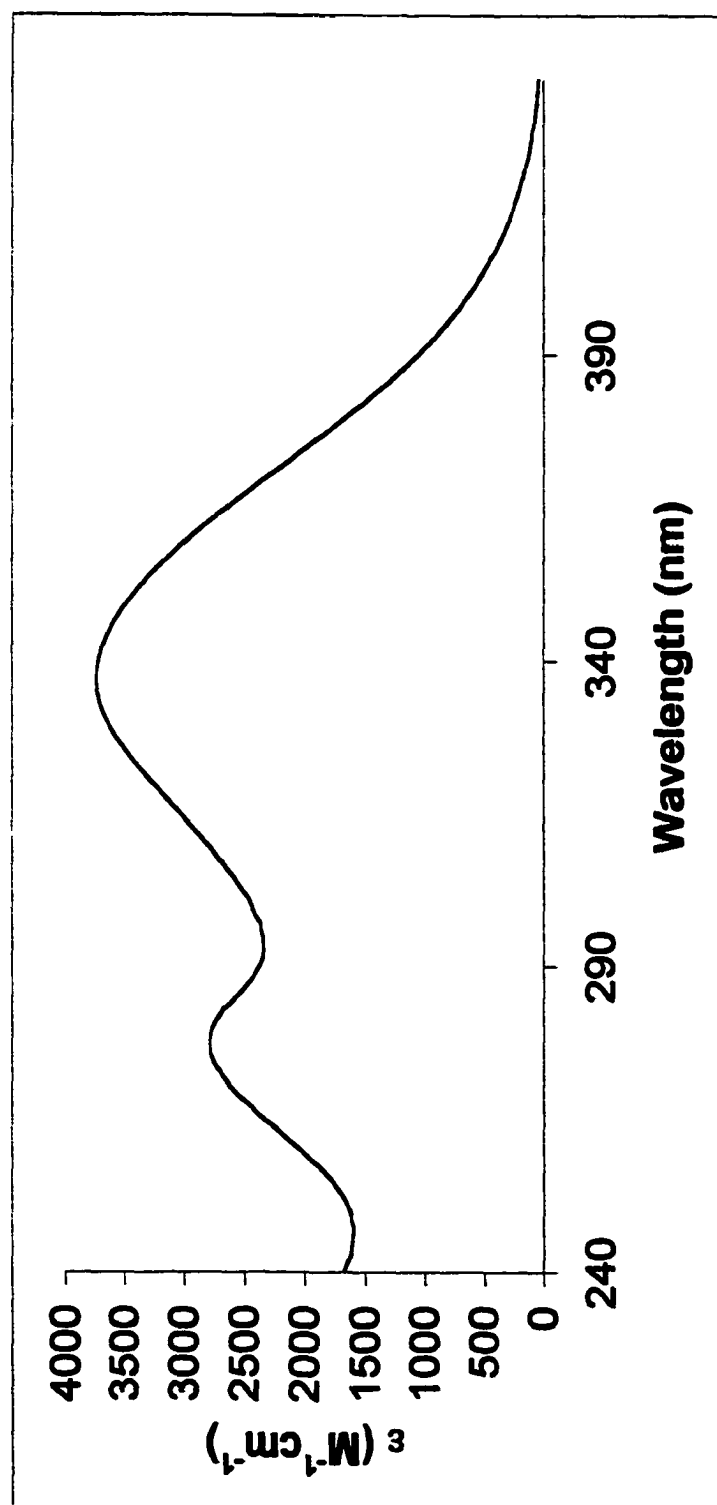


Figure 120. UV-Vis of Compound II-36 (MeOH).

APPENDIX C

Spectroscopic Data for Compounds in “Conformationally Defined Analogues of Retinoic Acid. Synthesis, Nuclear Receptor Binding and Transcriptional Activation Activity of a Ring-Expanded Derivative of (9Z)-UAB30”

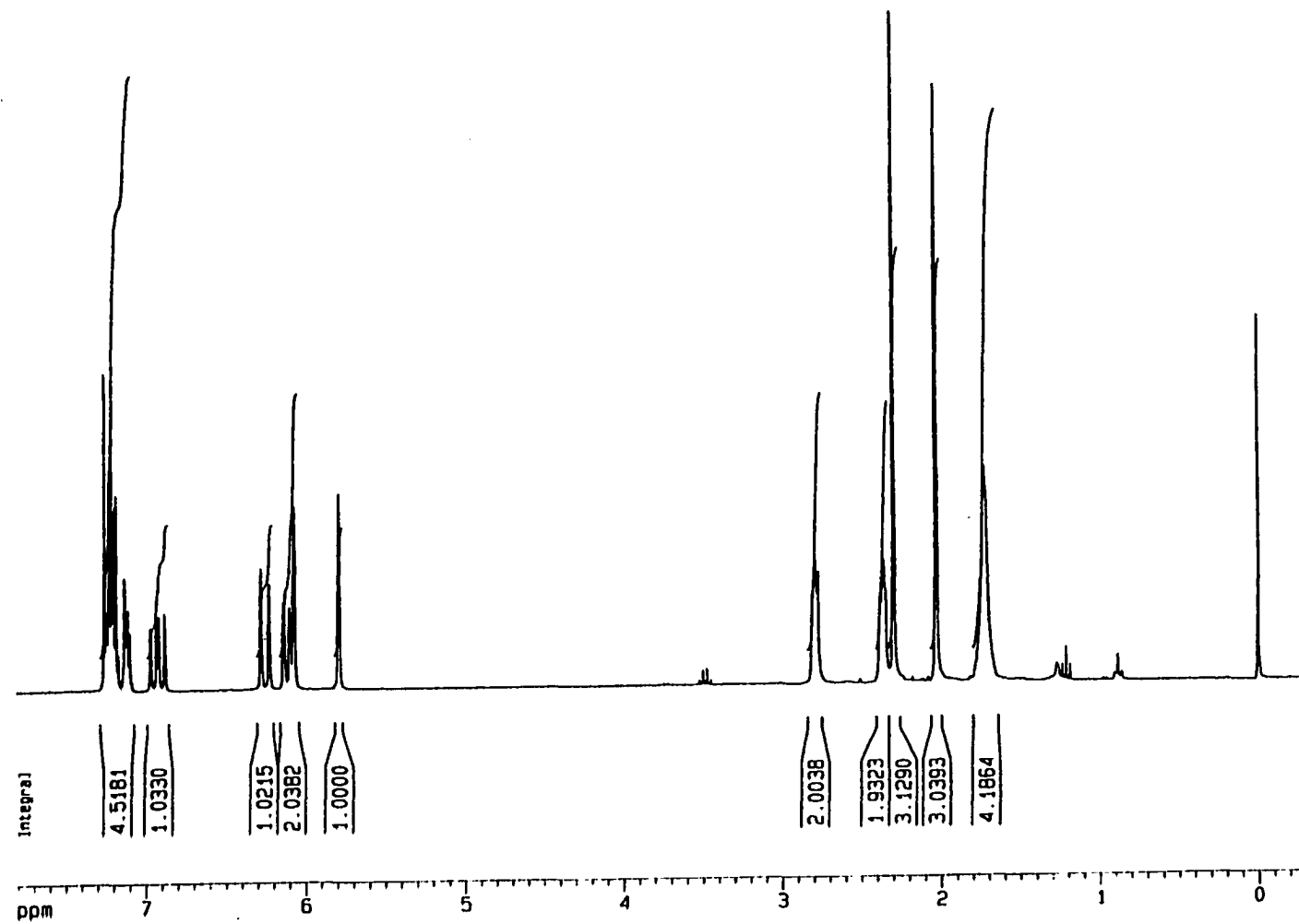


Figure 1. ^1H NMR Spectrum (300 MHz) of Compound III-2 (CDCl_3).

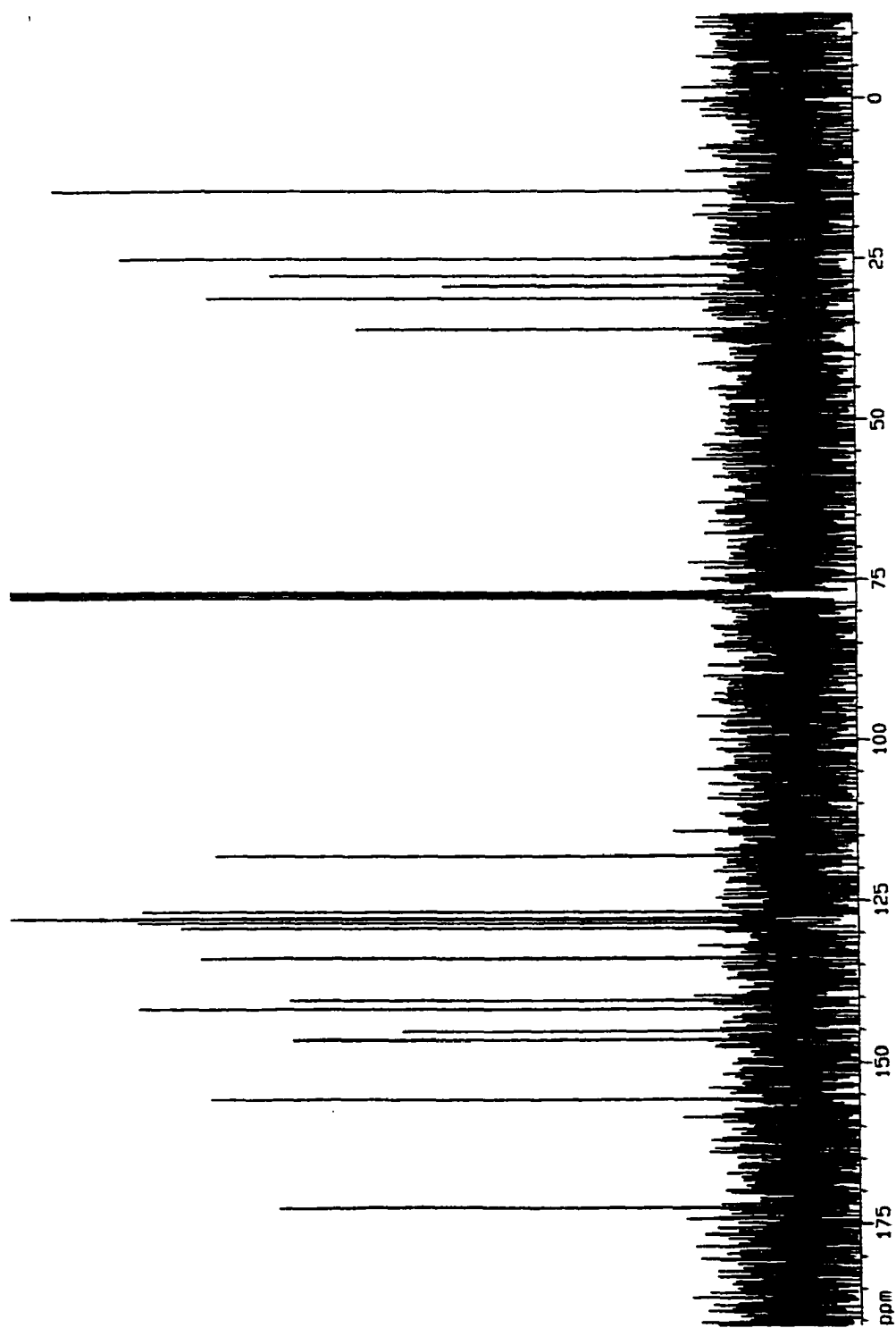


Figure 2. ^{13}C NMR (300 MHz) of Compound III-2 (CDCl_3).

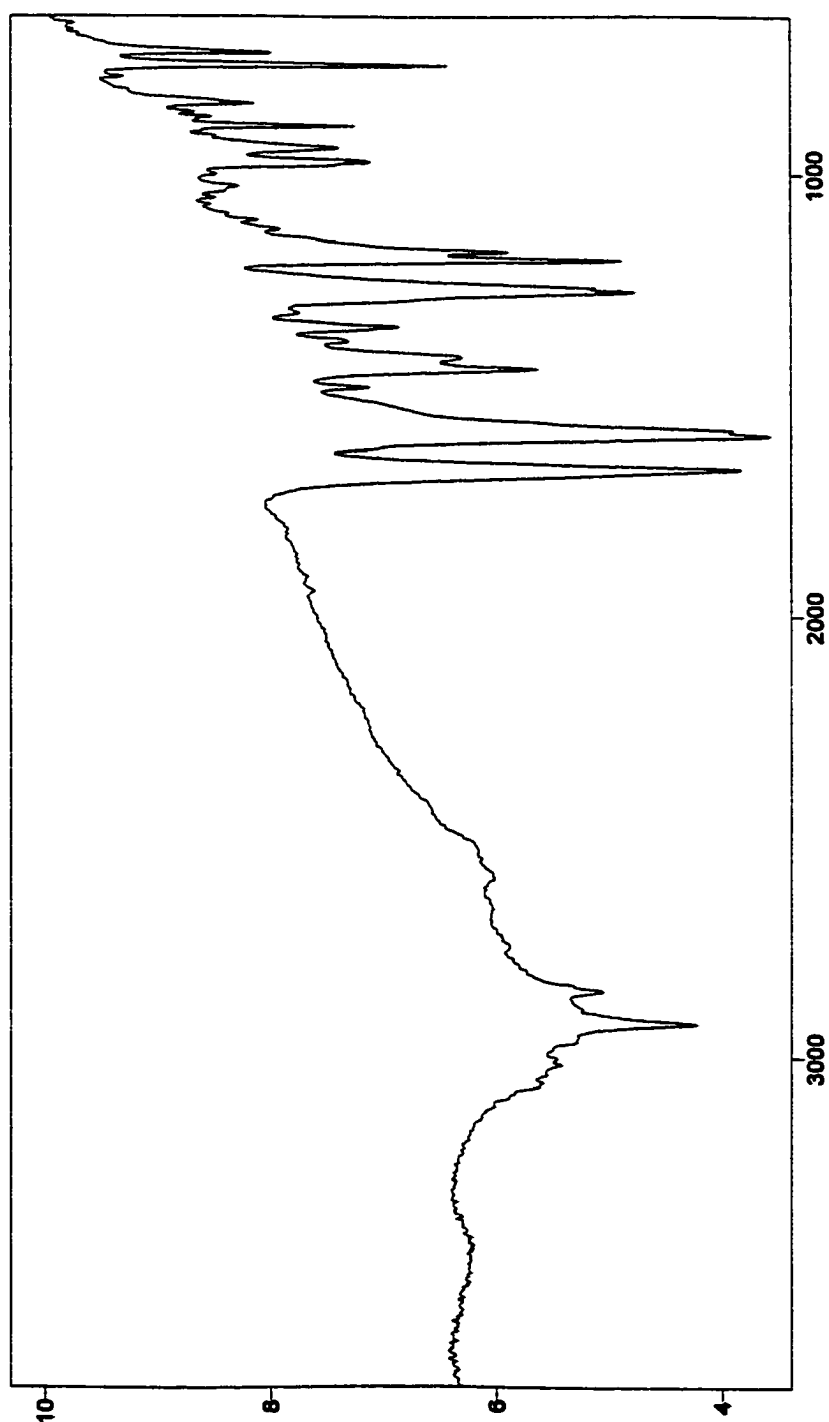


Figure 3. FTIR of Compound III-2 (KBr)

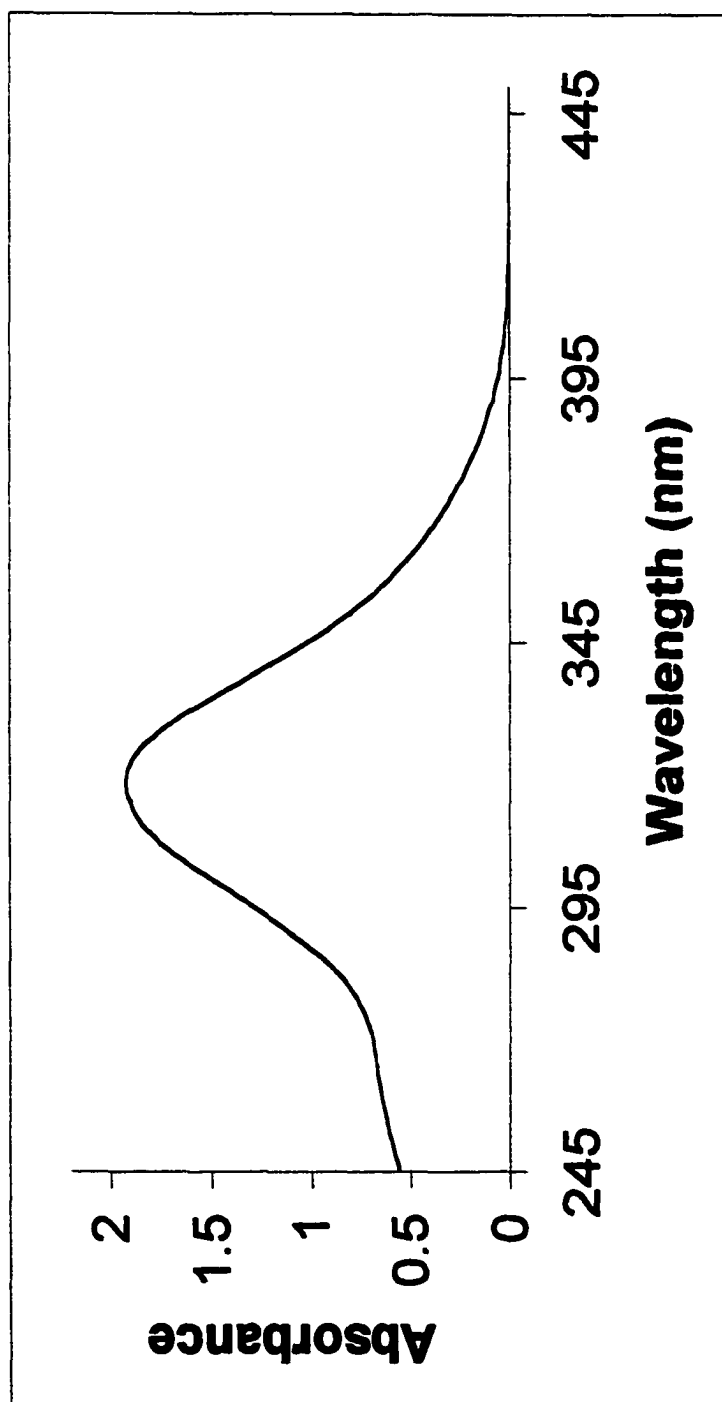


Figure 4. UV-Vis of Compound III-2 (MeOH).

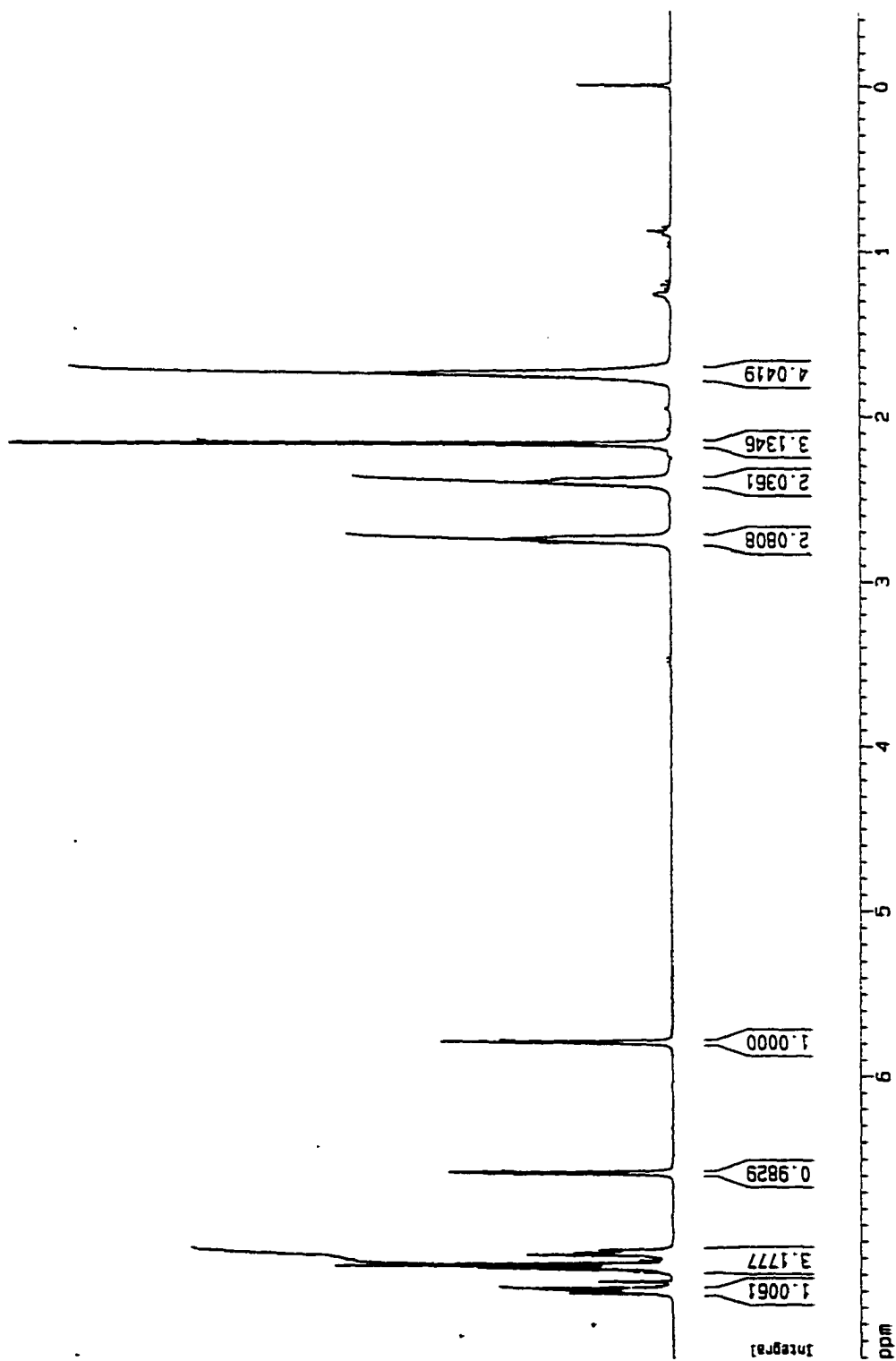


Figure 5. ^1H NMR Spectrum (300 MHz) of Compound III-4 (CDCl_3).

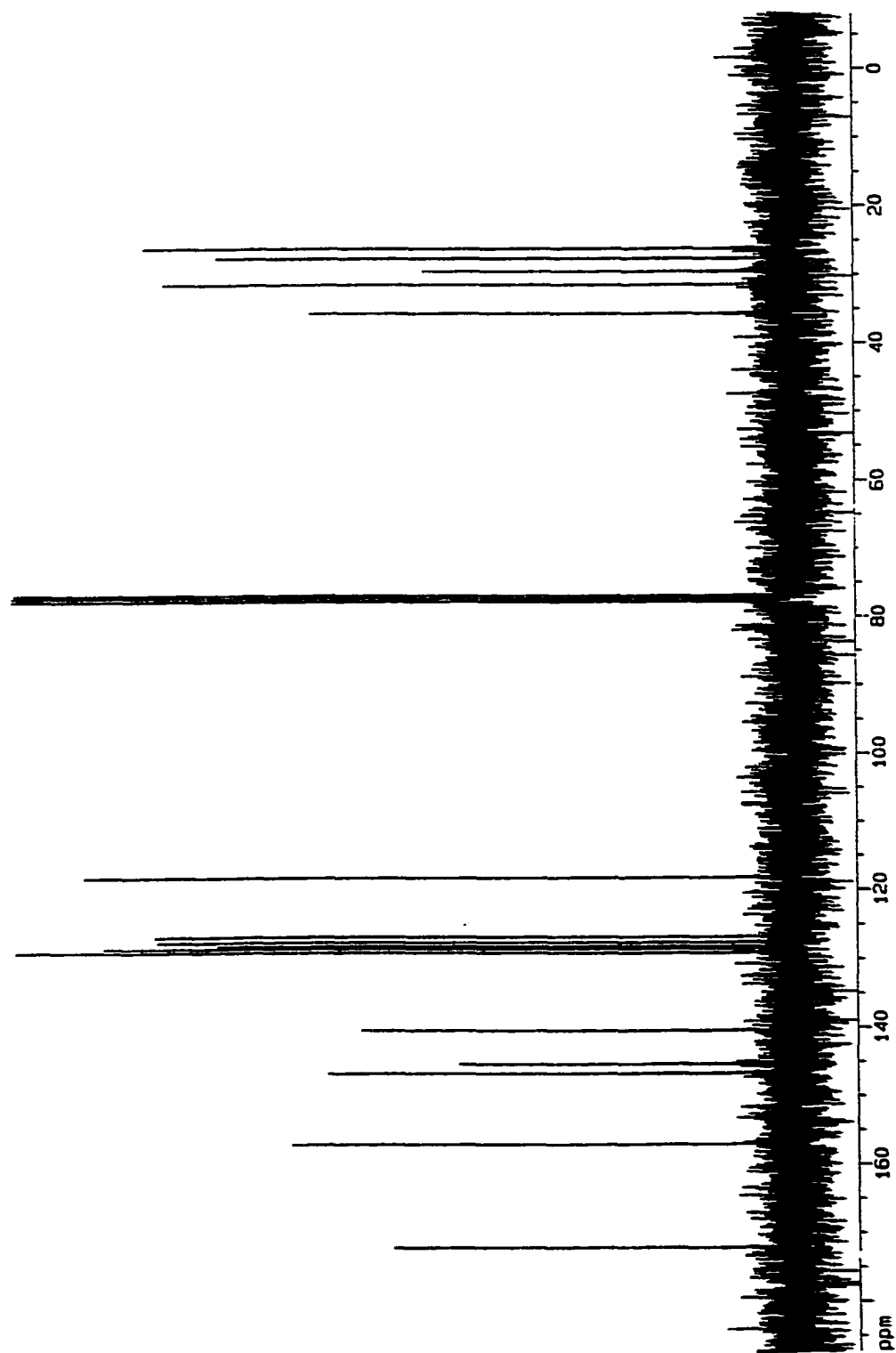


Figure 6. ^{13}C NMR (300 MHz) of Compound III-4 (CDCl_3).

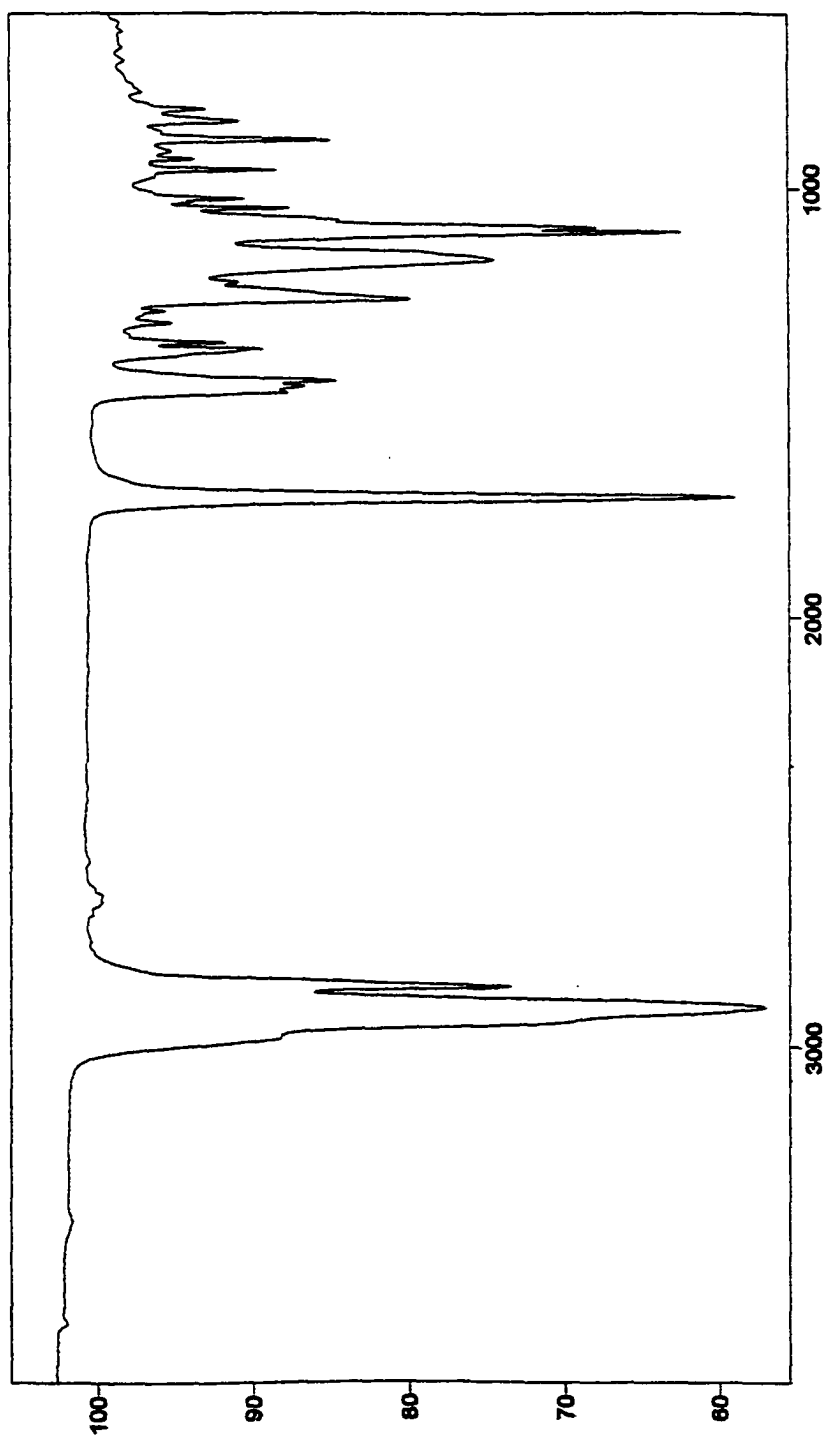


Figure 7. FTIR of Compound III-4 (KBr).

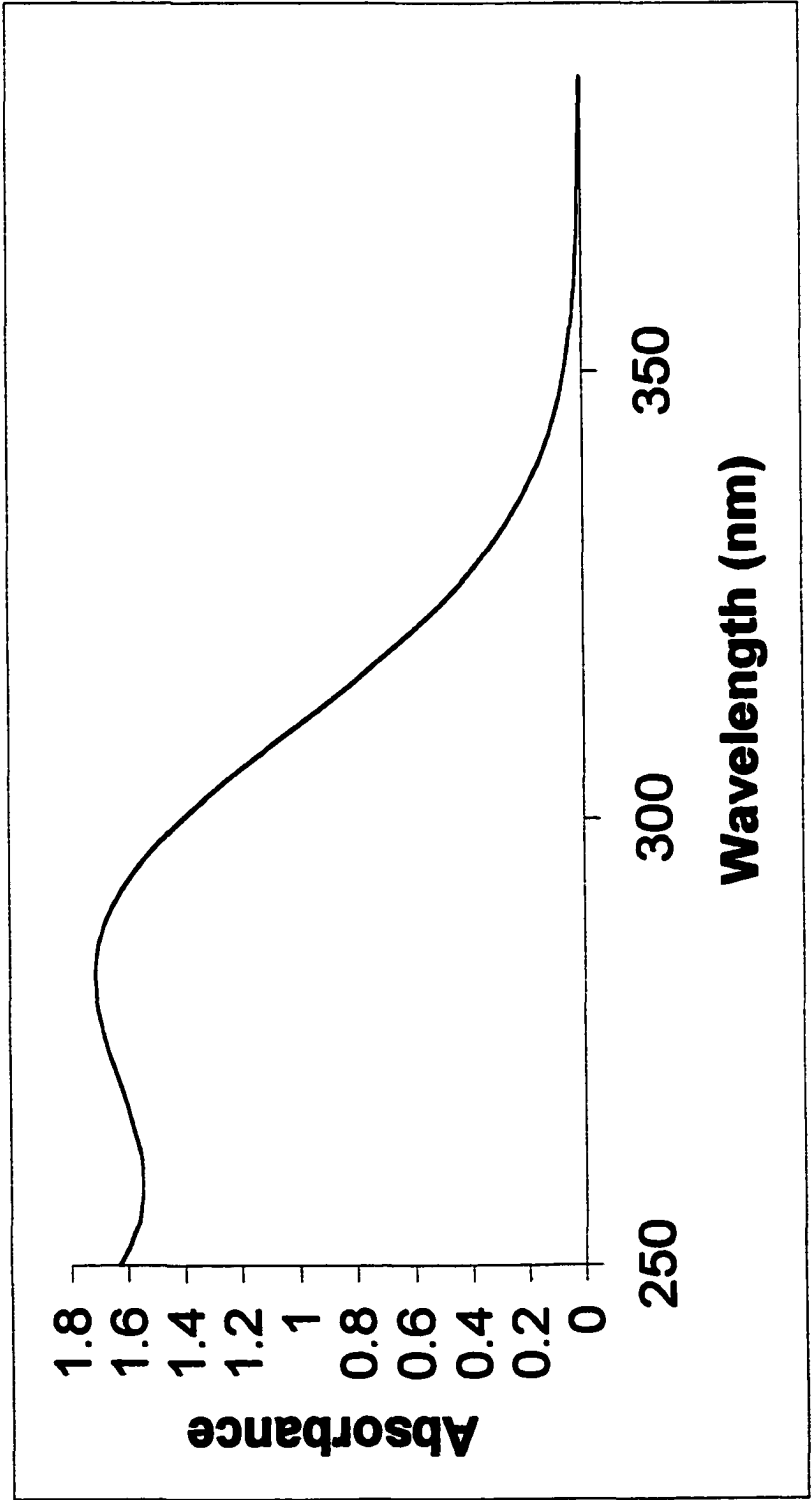


Figure 8. UV-Vis of Compound **III-4** (MeOH).

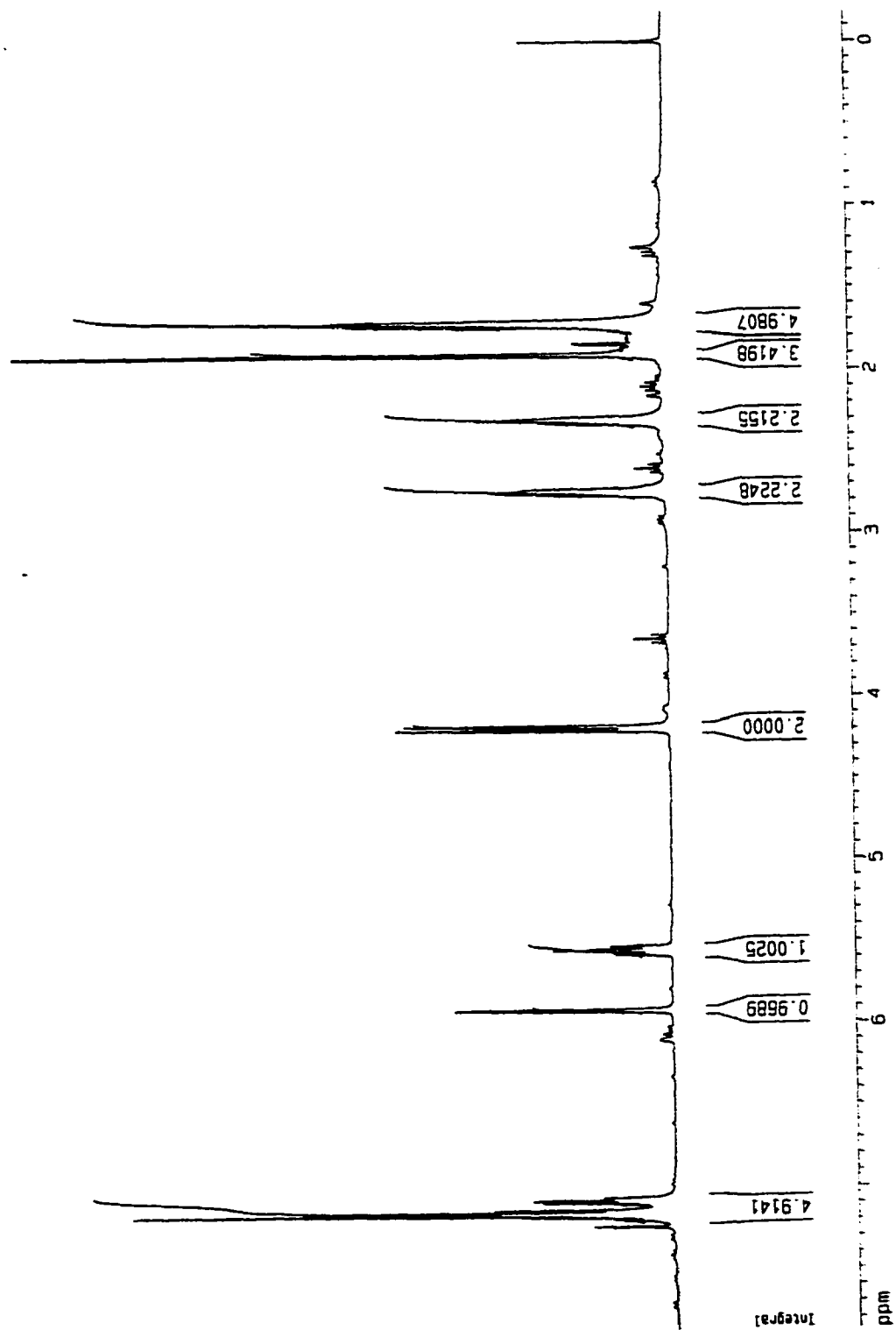


Figure 9. ^1H NMR Spectrum (300 MHz) of Compound III-5 (CDCl_3).

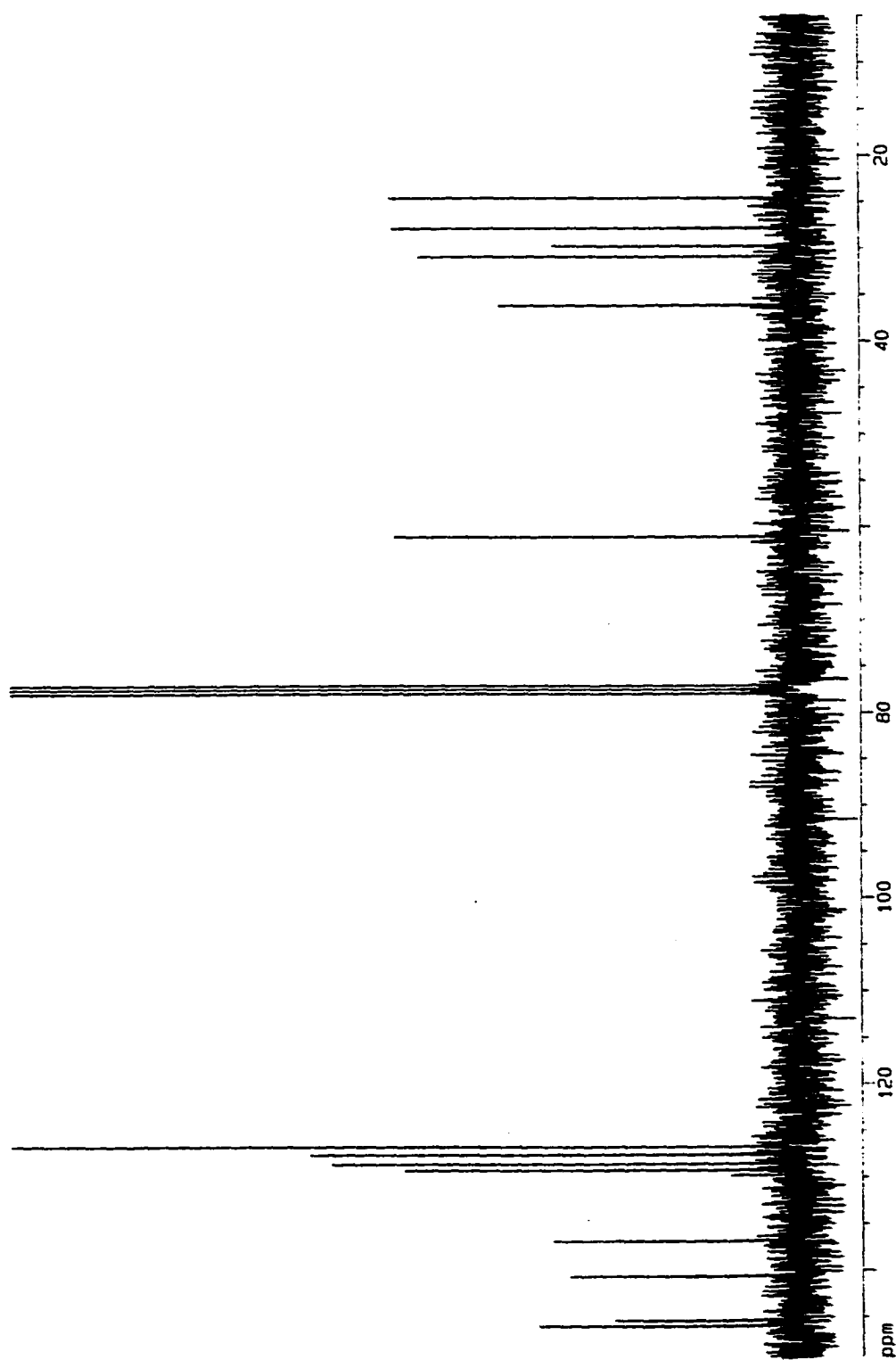


Figure 10. ^{13}C NMR (300 MHz) of Compound III-5 (CDCl_3).

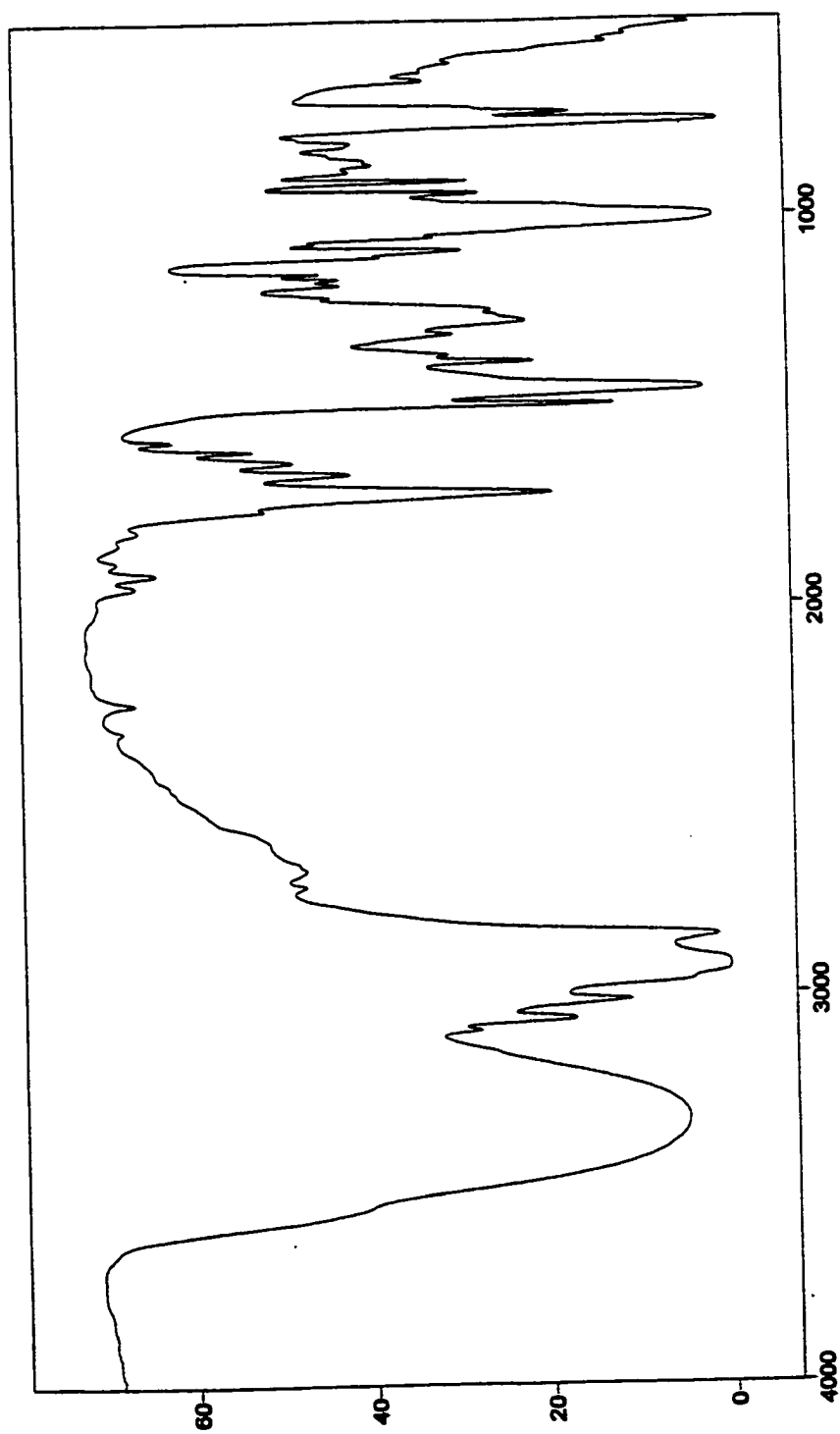


Figure 11. FTIR of Compound III-5 (neat).

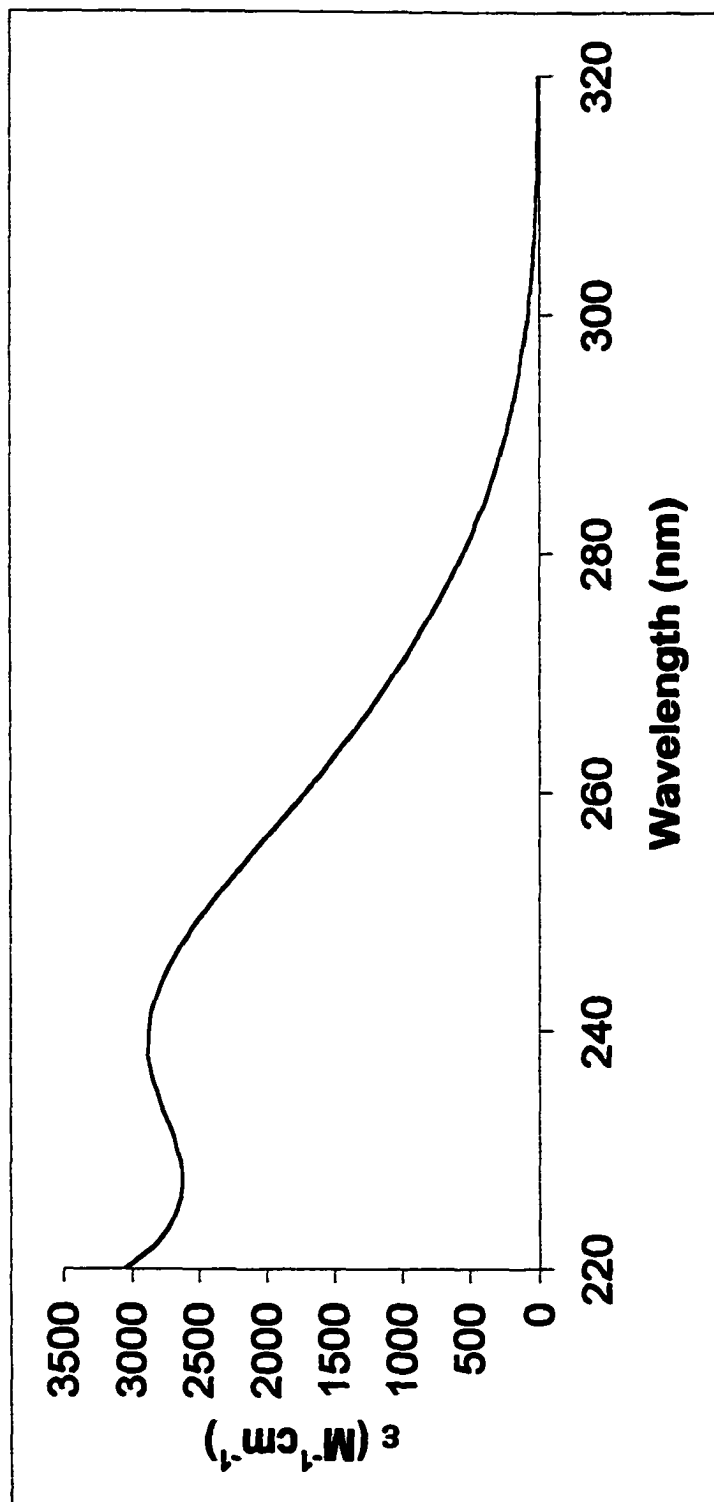


Figure 12. UV-Vis of Compound III-5 (MeOH).

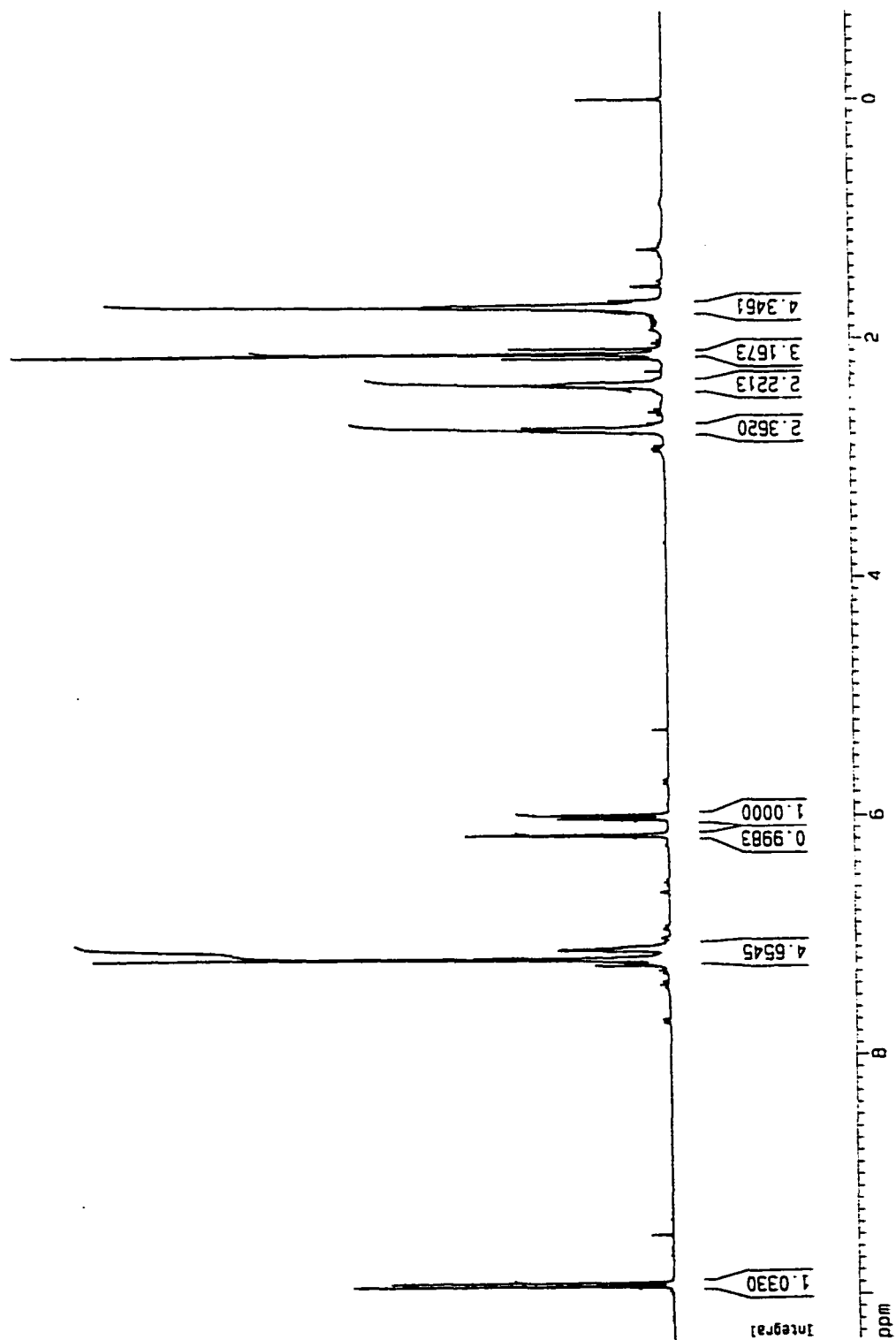


Figure 13. ^1H NMR Spectrum (300 MHz) of Compound III-6 (CDCl_3).

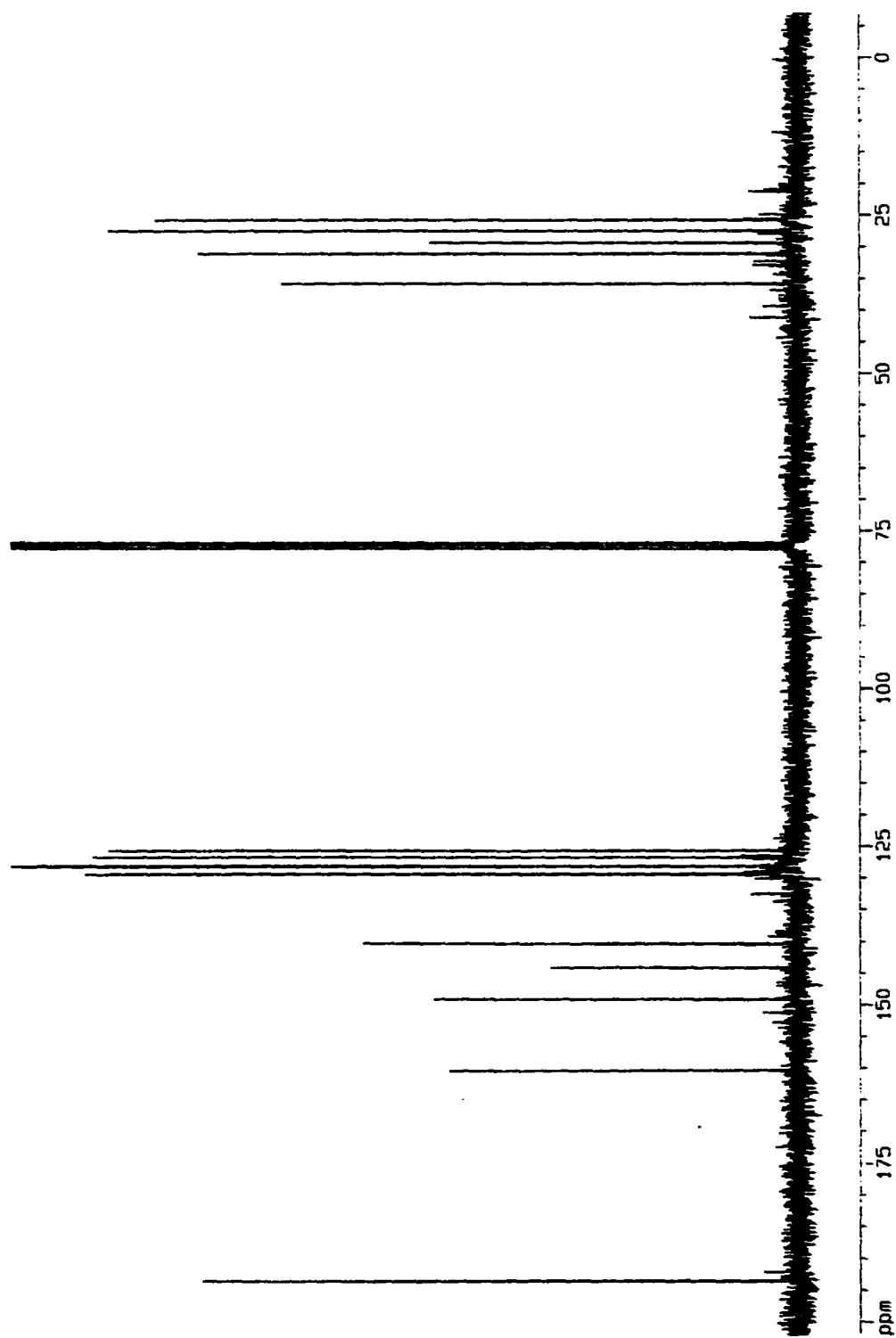


Figure 14. ^{13}C NMR (300 MHz) of Compound III-6 (CDCl_3).

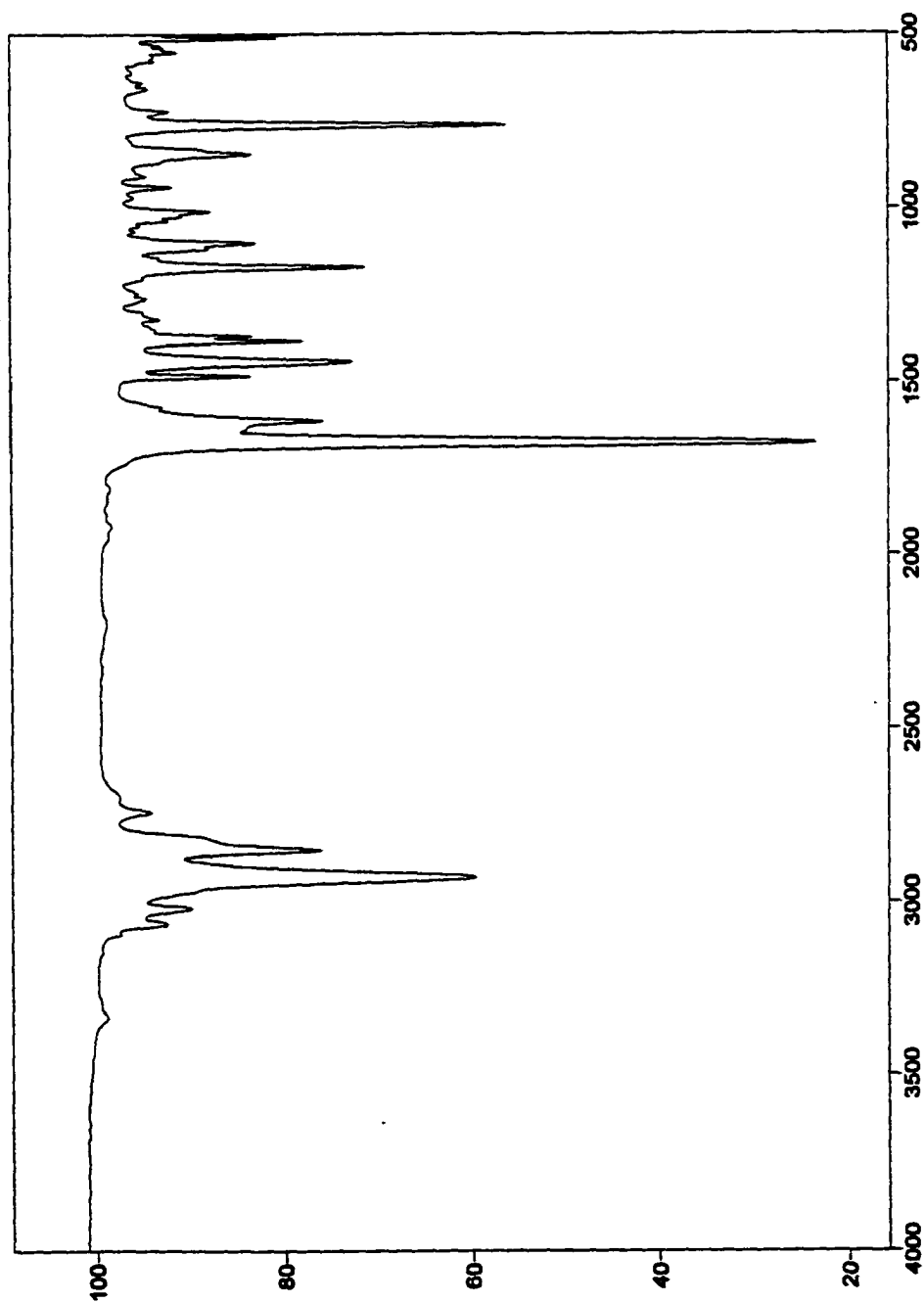


Figure 15. FTIR of Compound III-6 (neat).

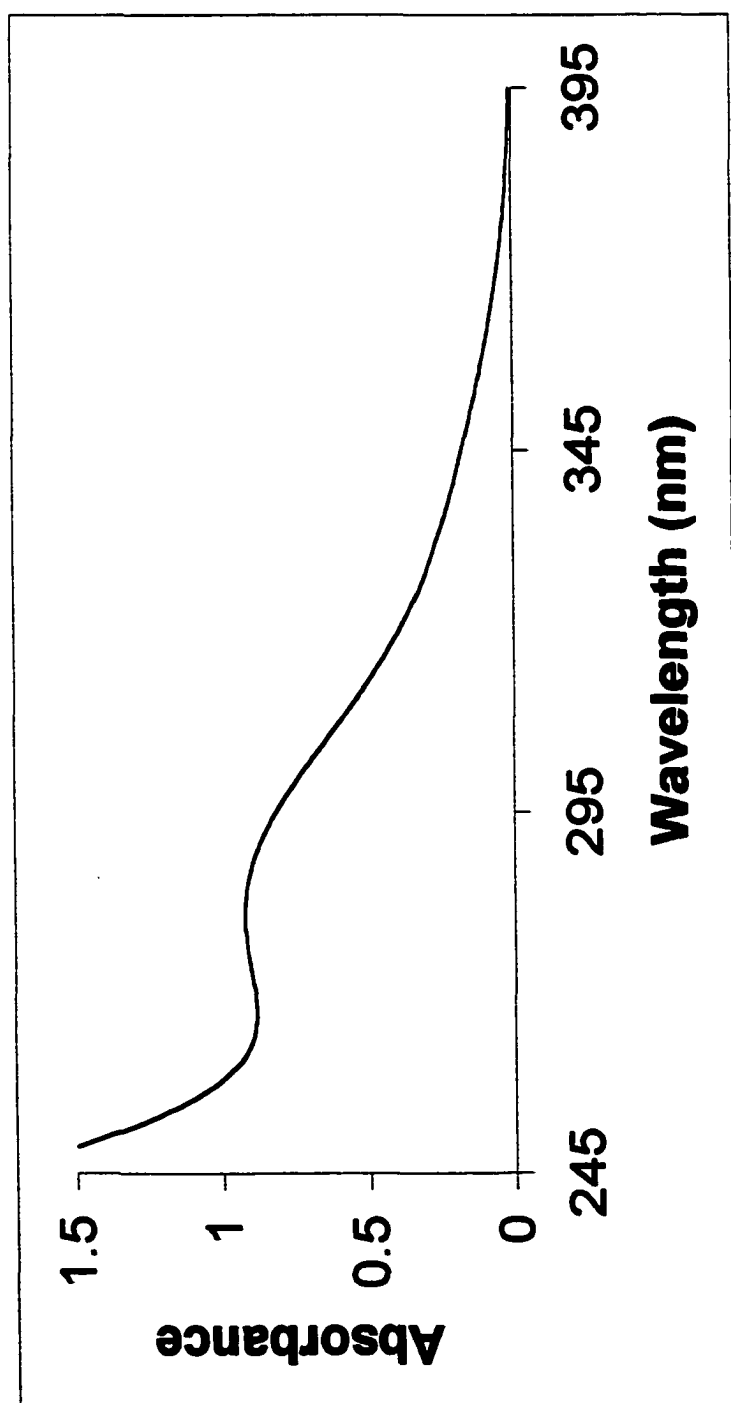


Figure 16. UV-Vis of Compound III-6 (MeOH).

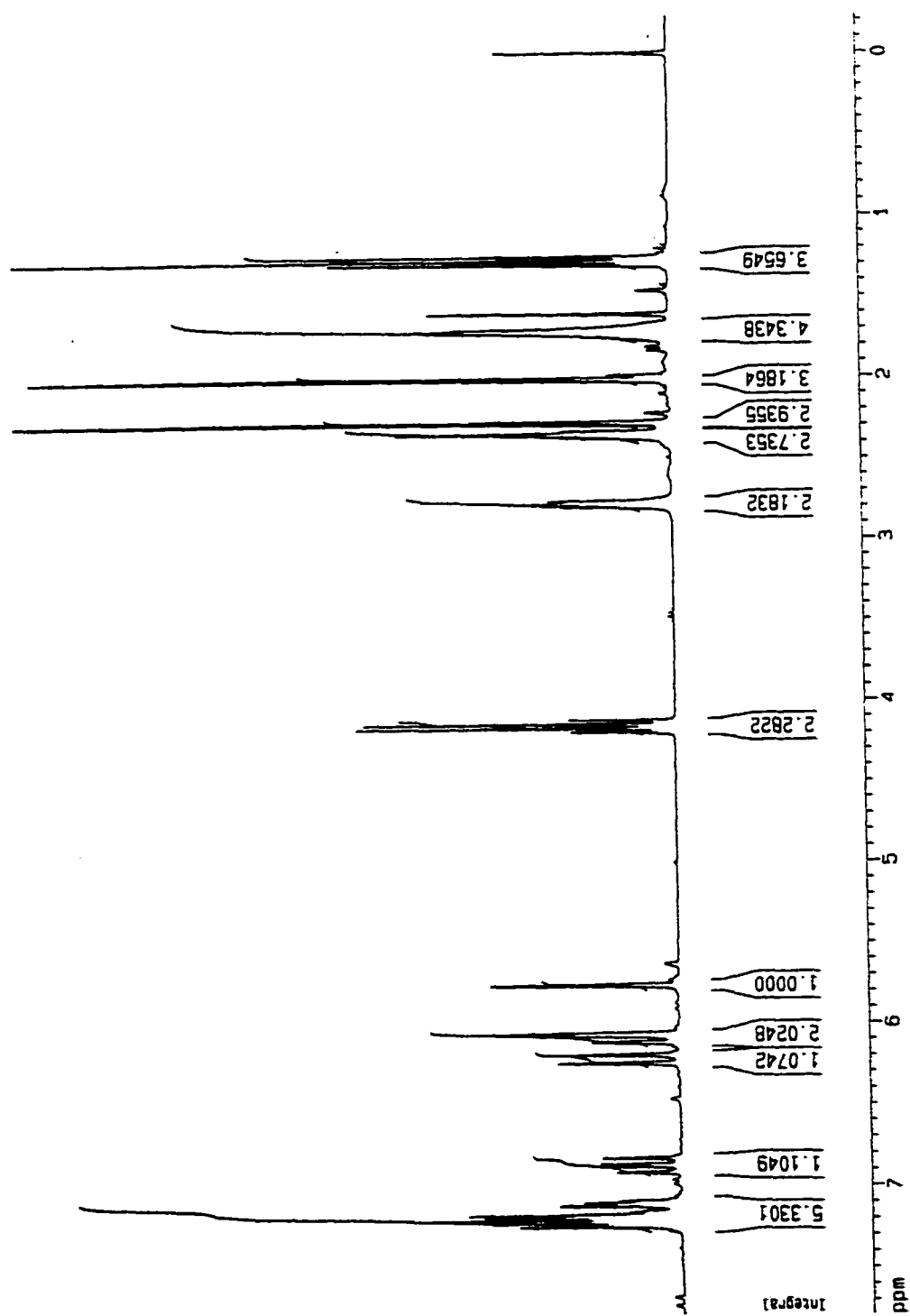


Figure 17. ^1H NMR Spectrum (300 MHz) of Compound III-(9Z,13E)-8 (CDCl_3).

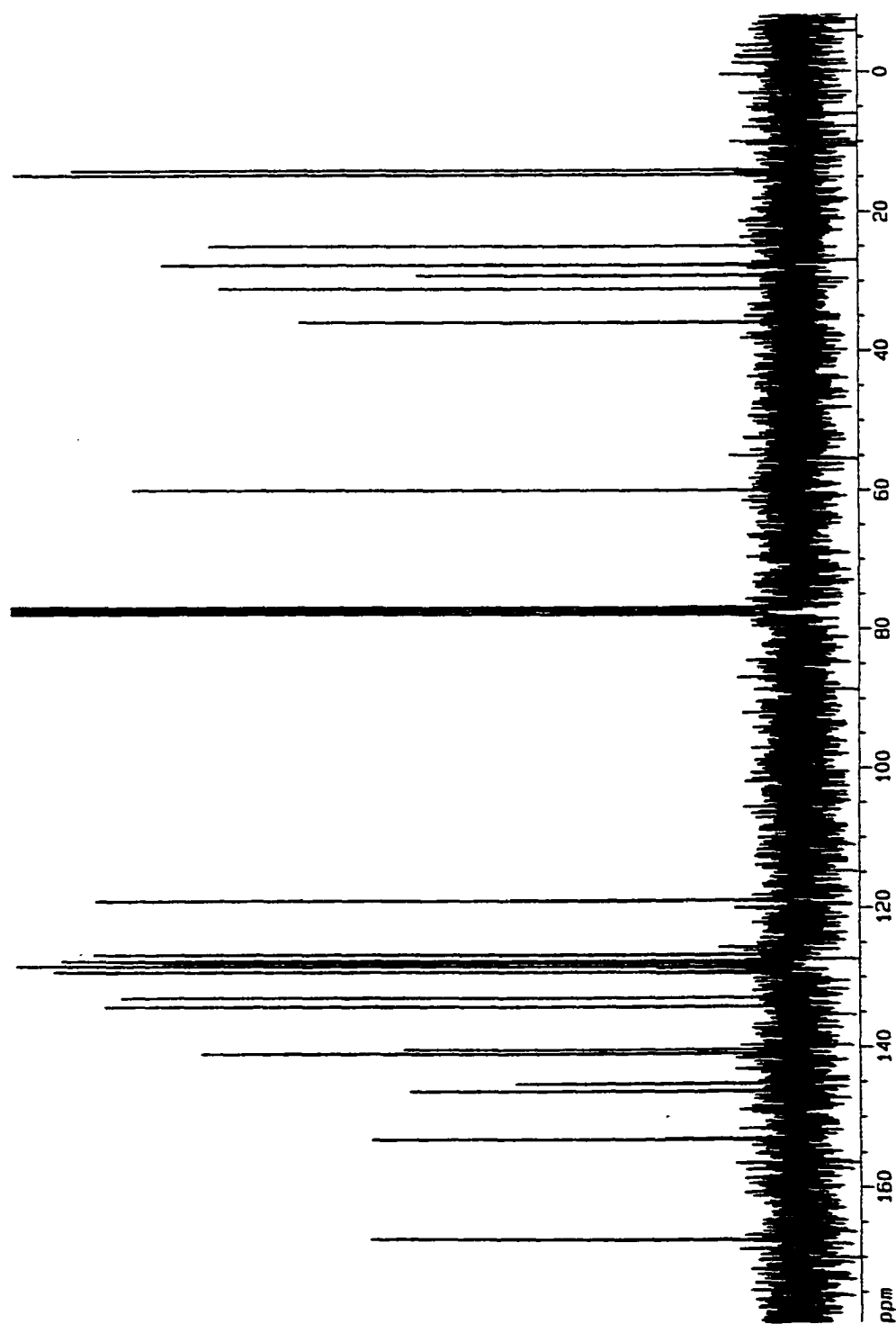


Figure 18. ^{13}C NMR (300 MHz) of Compound III-(9Z,13E)-8 (CDCl_3).

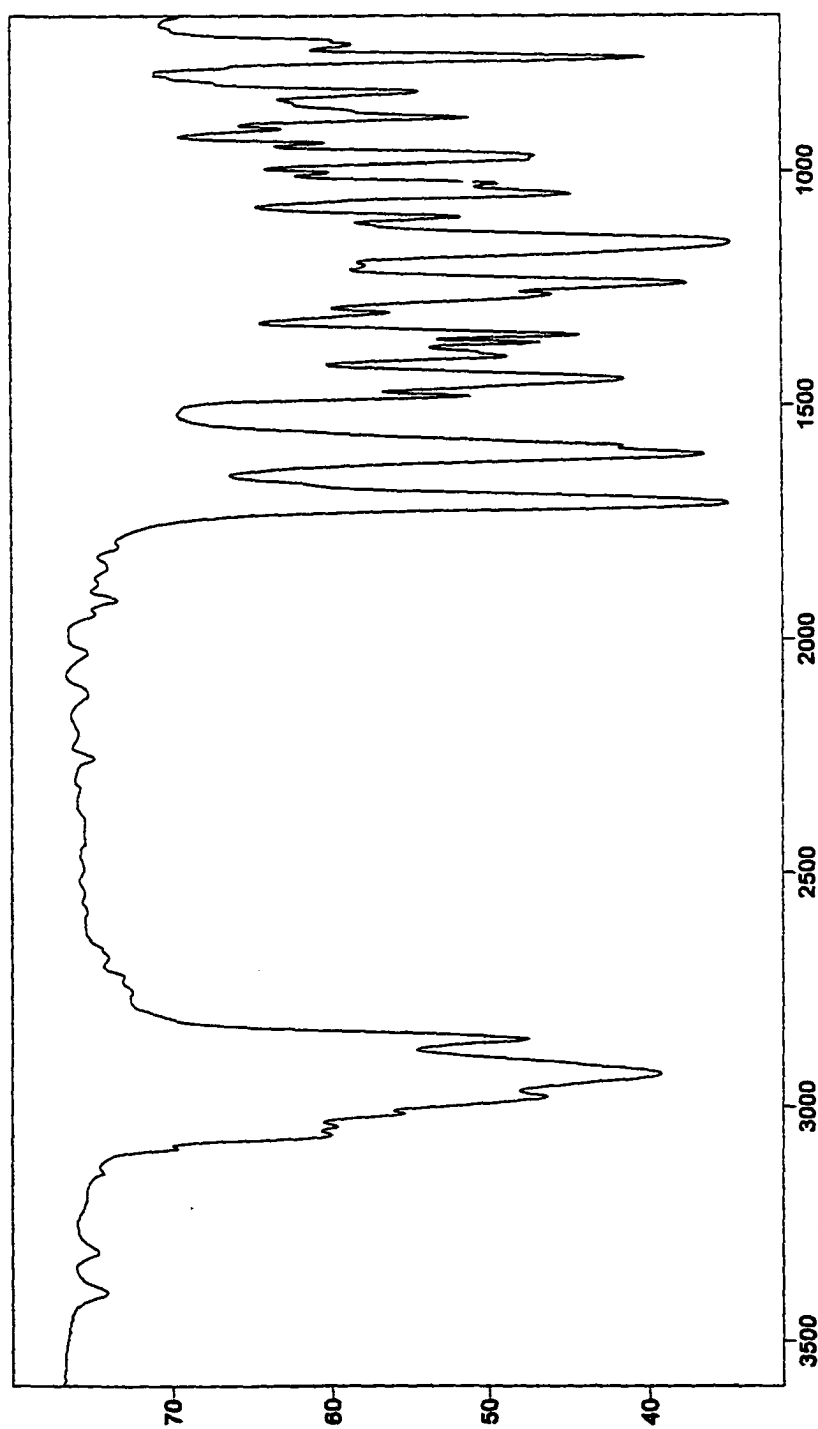


Figure 19. FTIR of Compound **III-(9Z,13E)-8** (neat).

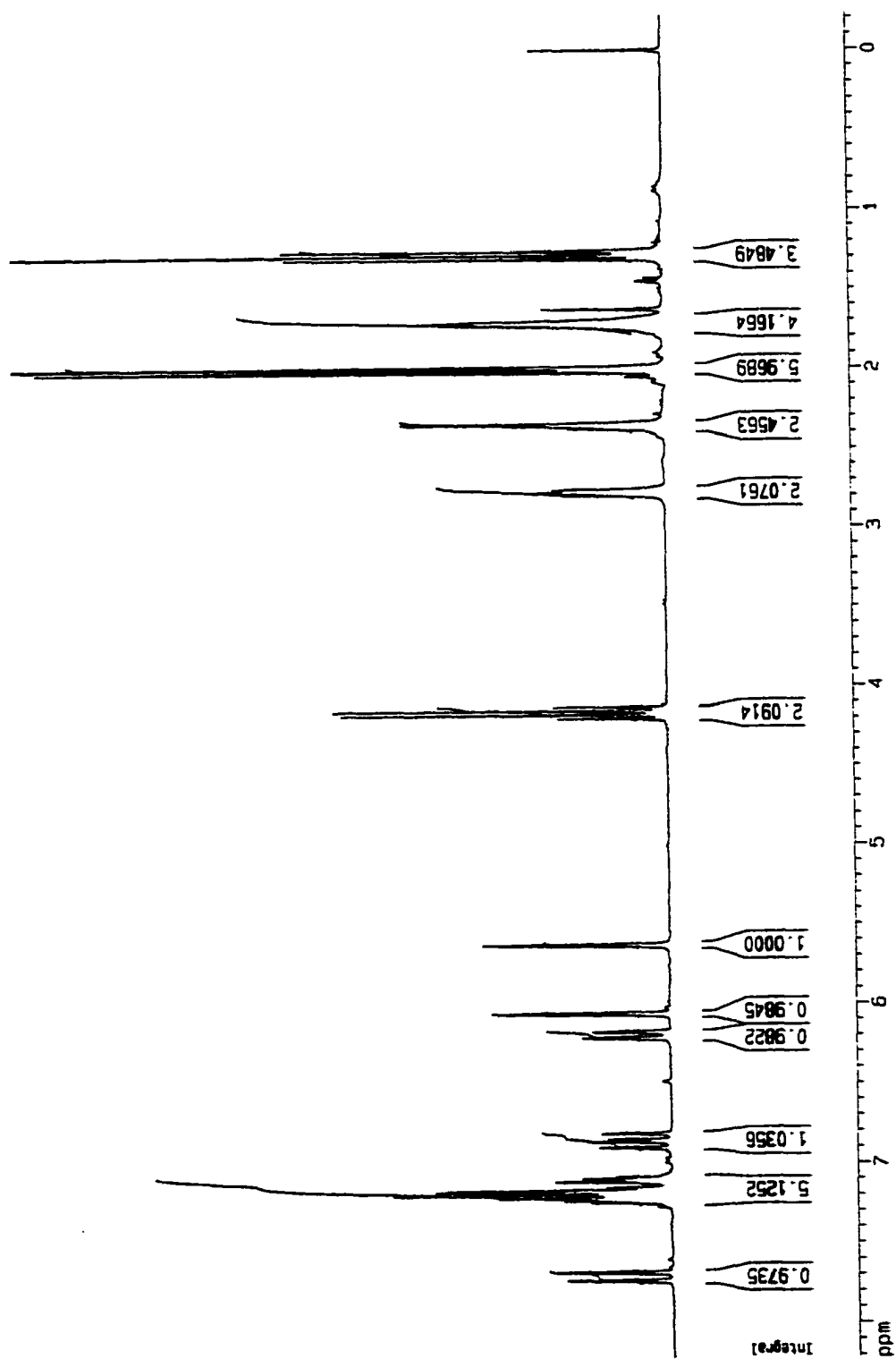


Figure 20. ^1H NMR Spectrum (300 MHz) of Compound III-(9Z,13Z)-8 (CDCl_3).

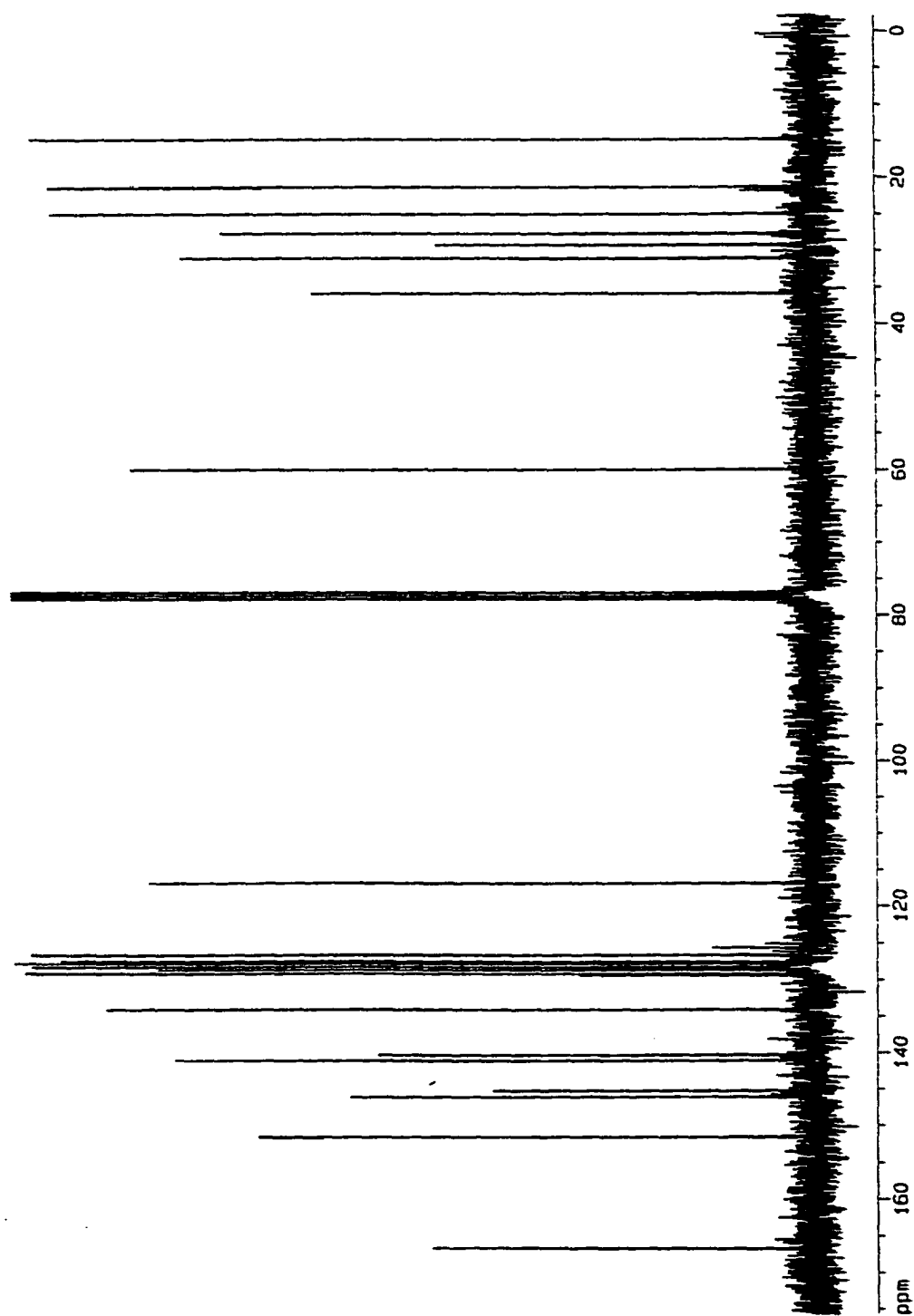


Figure 21. ^{13}C NMR (300 MHz) of Compound III-(9Z,13Z)-8 (CDCl_3).

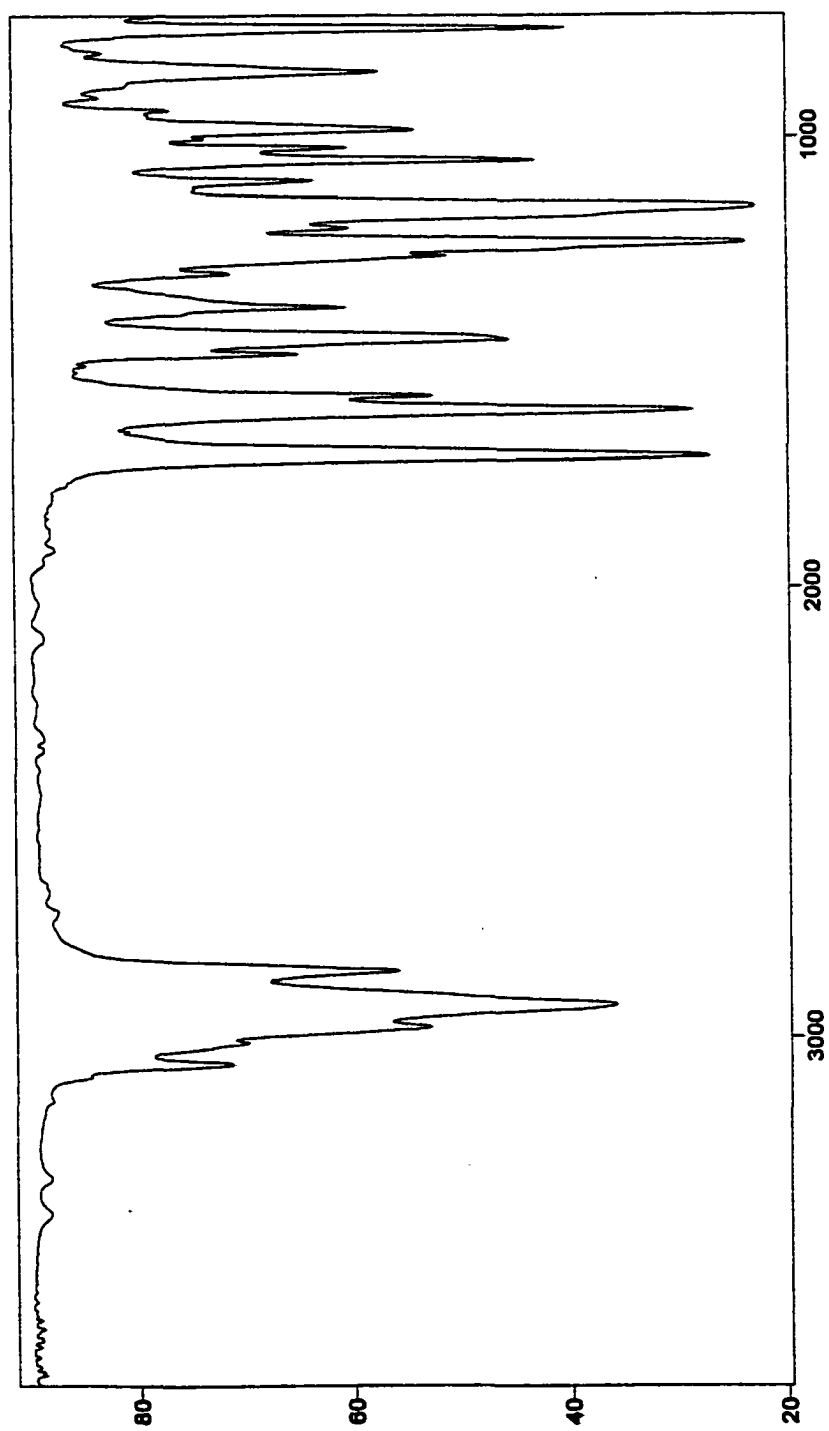


Figure 22. FTIR of Compound **III-(9Z,13Z)-8** (neat).

APPENDIX D

Spectroscopic Data for Compounds in “Conformationally Defined Retinoic Acid Analogues. Synthesis and Nuclear Receptor Transcriptional Activation Activity for Amide Derivatives of (9Z)-UAB30, RAR γ -Selective Ligands”

1

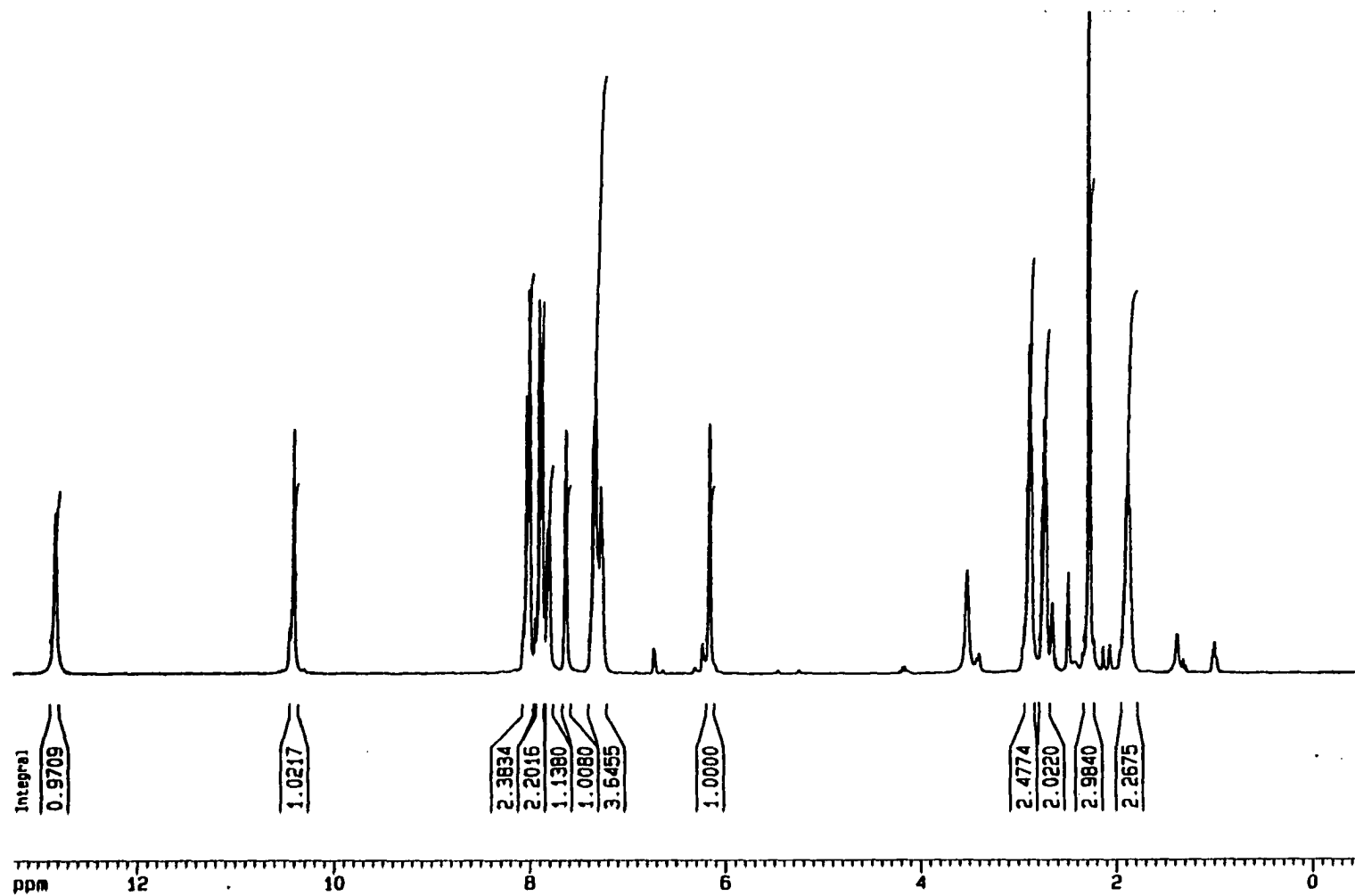


Figure 1. ^1H NMR (300 MHz) of Compound IV-2 (DMSO).

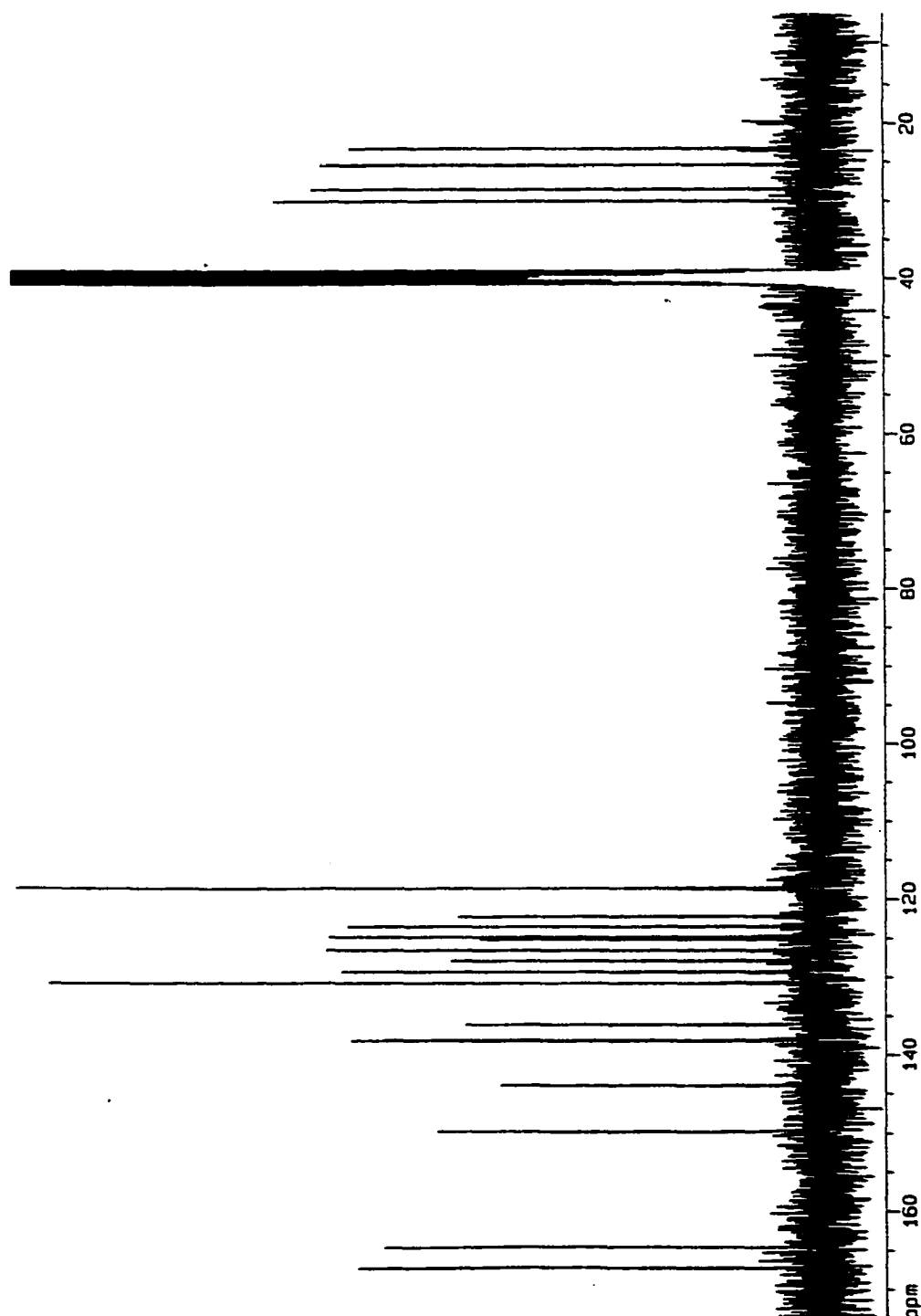


Figure 2. ^{13}C NMR (300 MHz) of Compound IV-2 (DMSO).

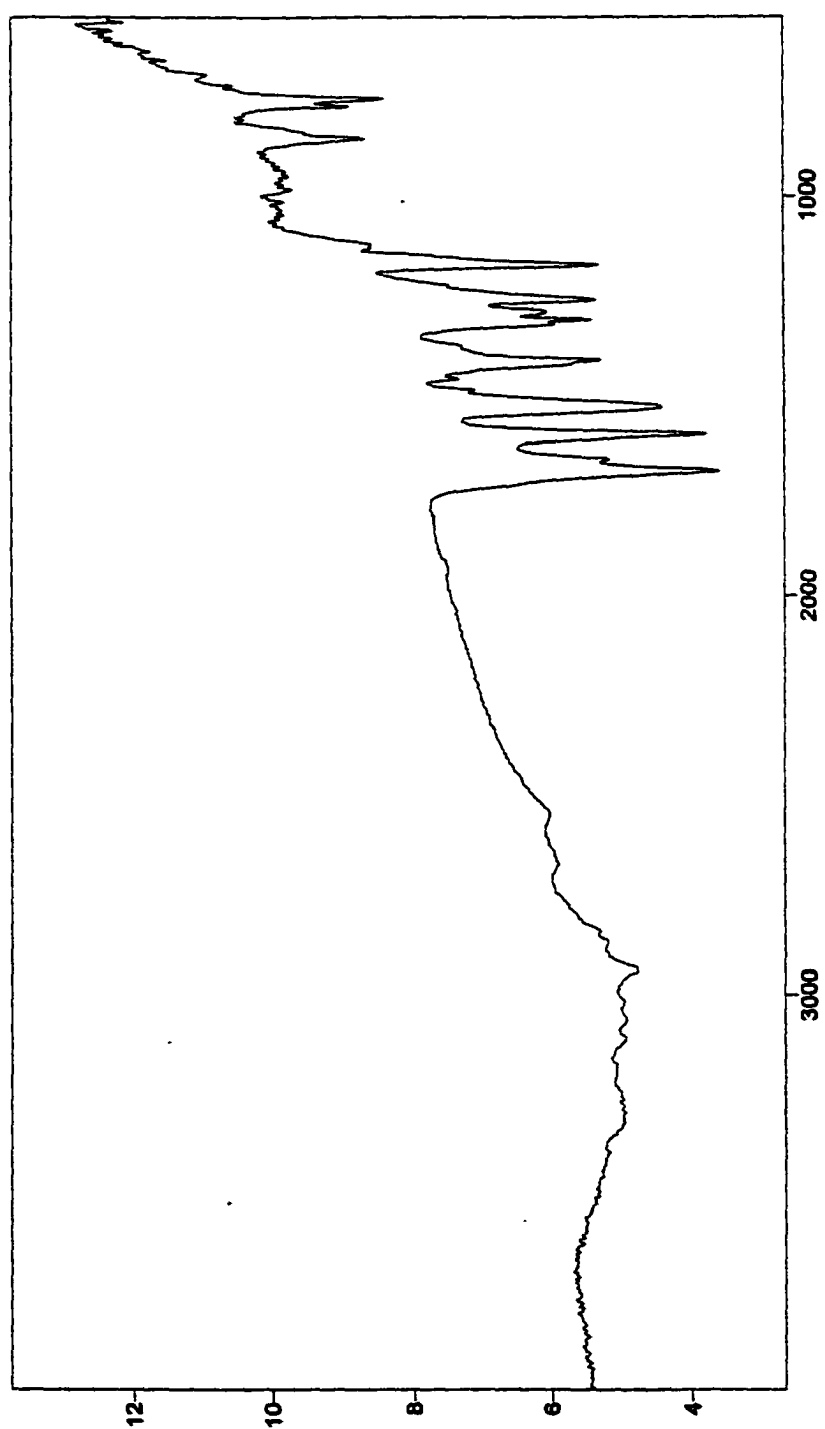


Figure 3. FTIR of Compound IV-2 (KBr).

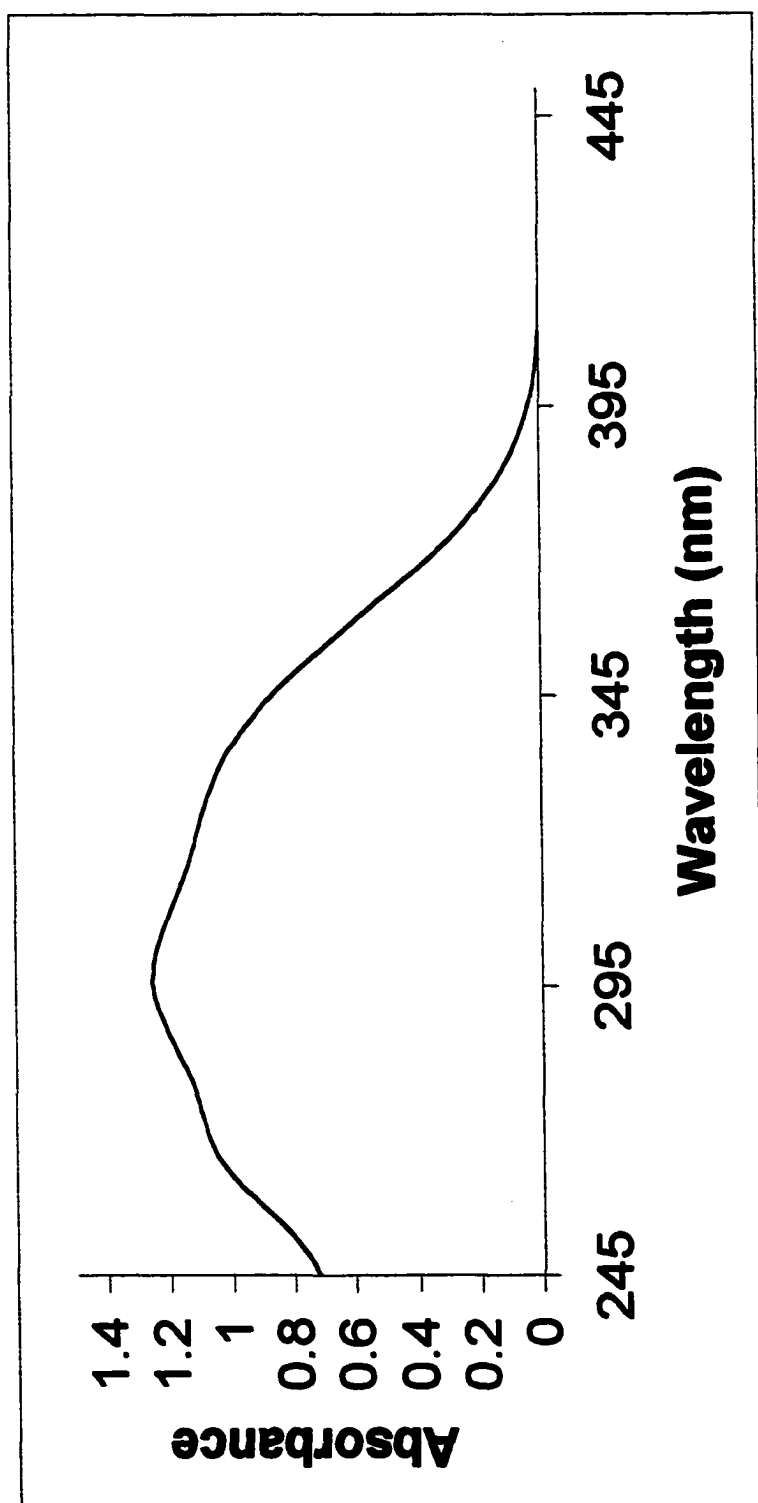


Figure 4. UV-Vis of Compound IV-2 (MeOH).

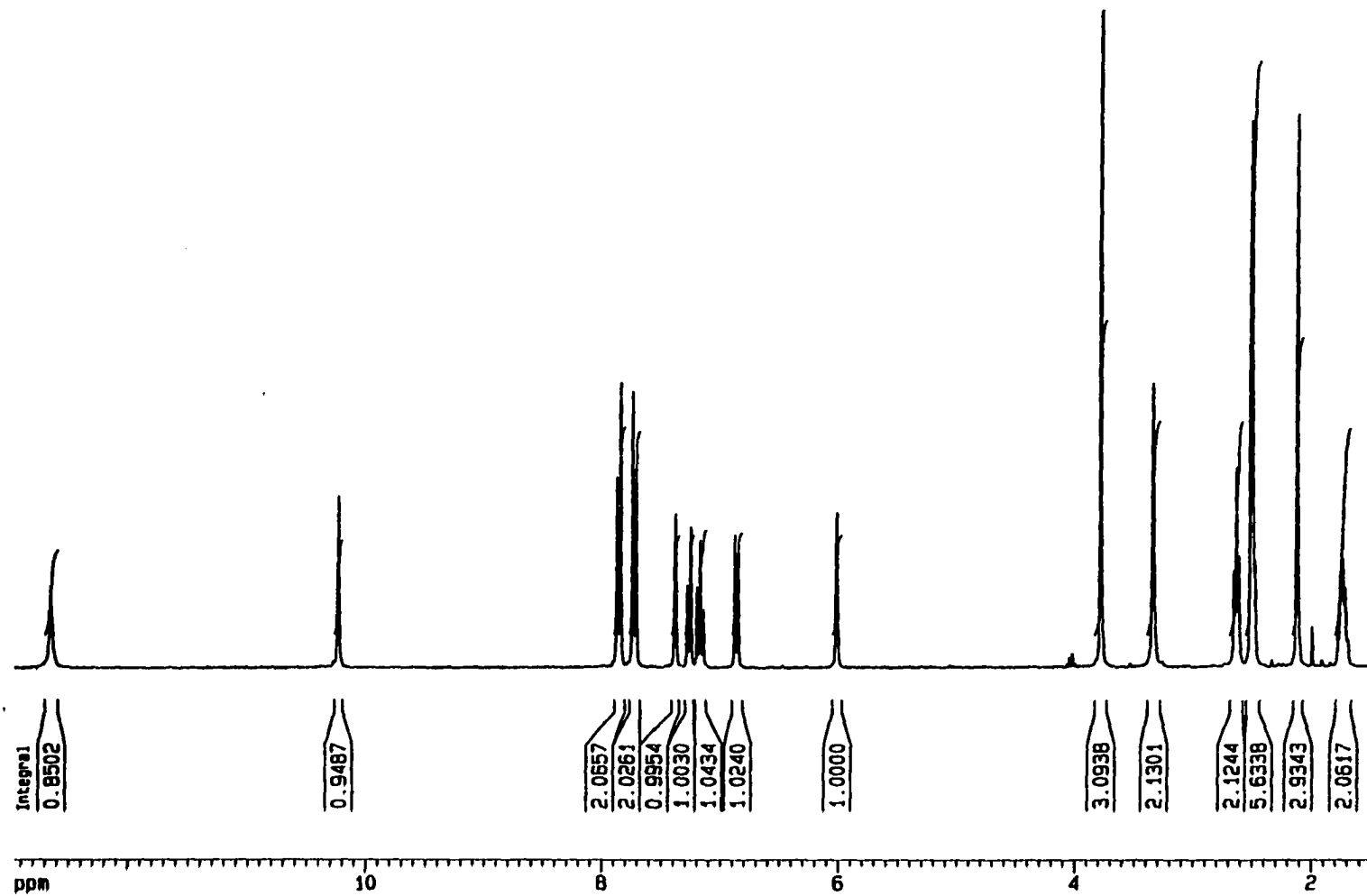


Figure 5. ¹H NMR (300 MHz) of Compound IV-3 (DMSO).

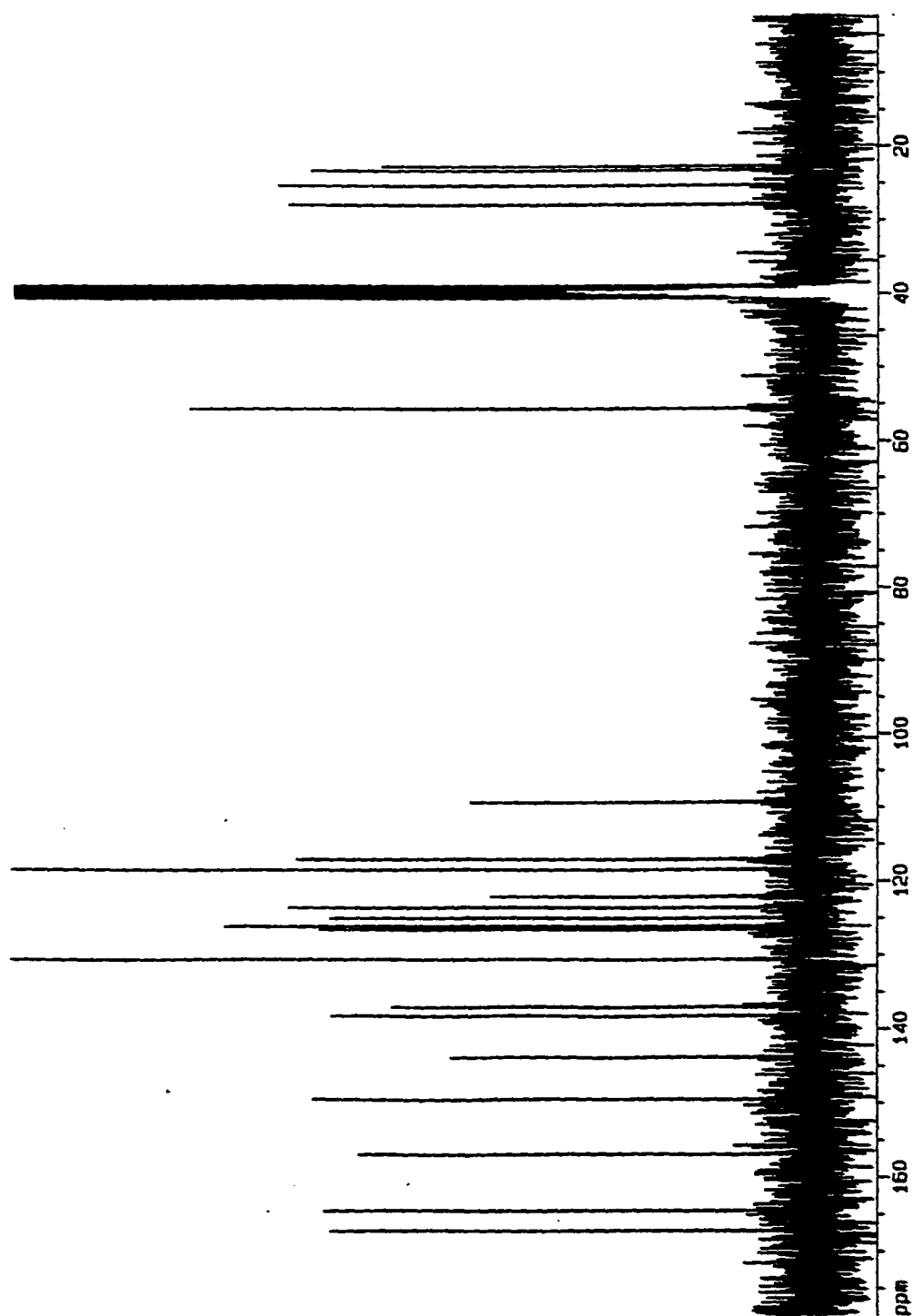


Figure 6. ^{13}C NMR (300 MHz) of Compound IV-3 (DMSO).

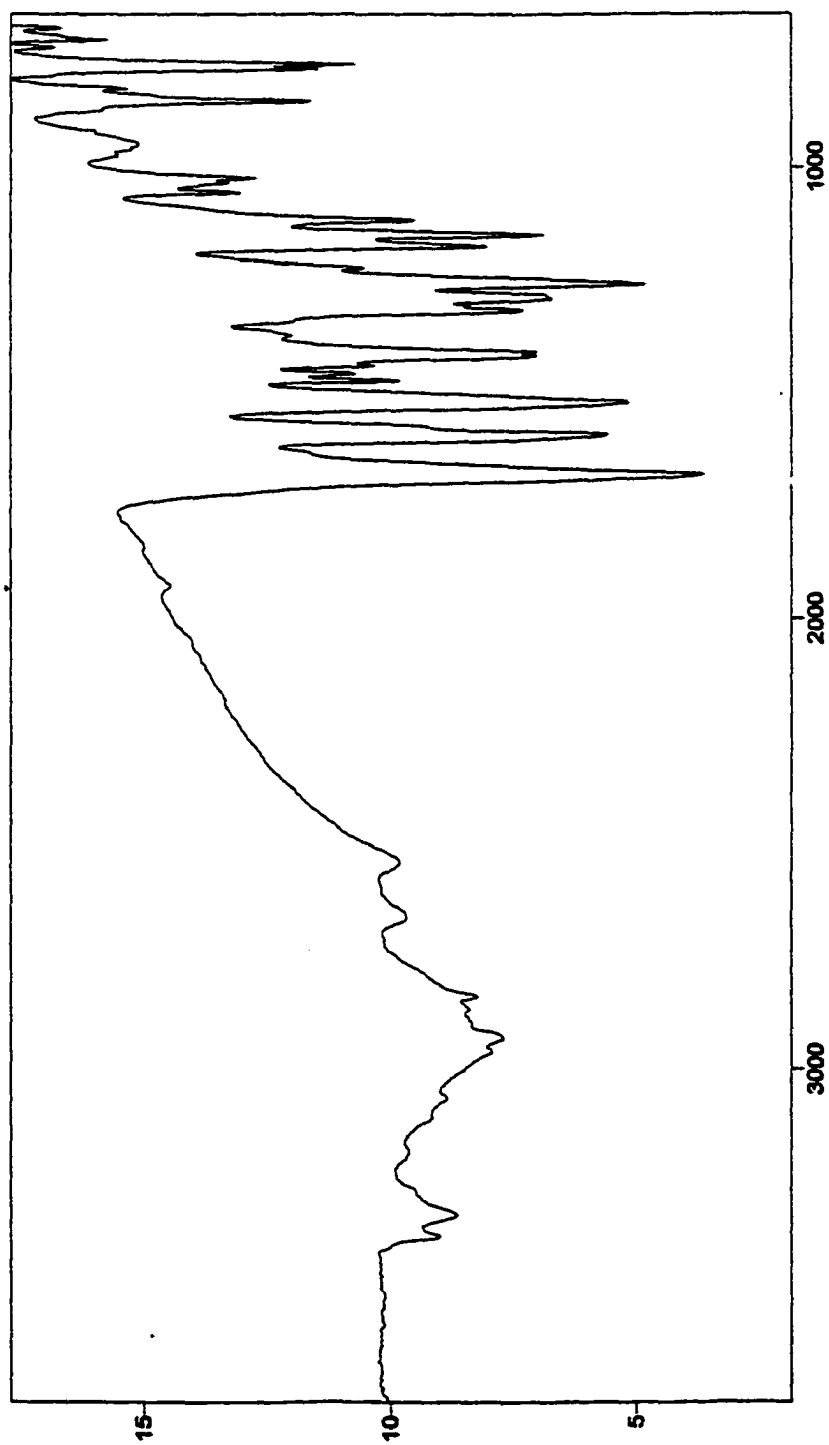


Figure 7. FTIR of Compound IV-3 (KBr).

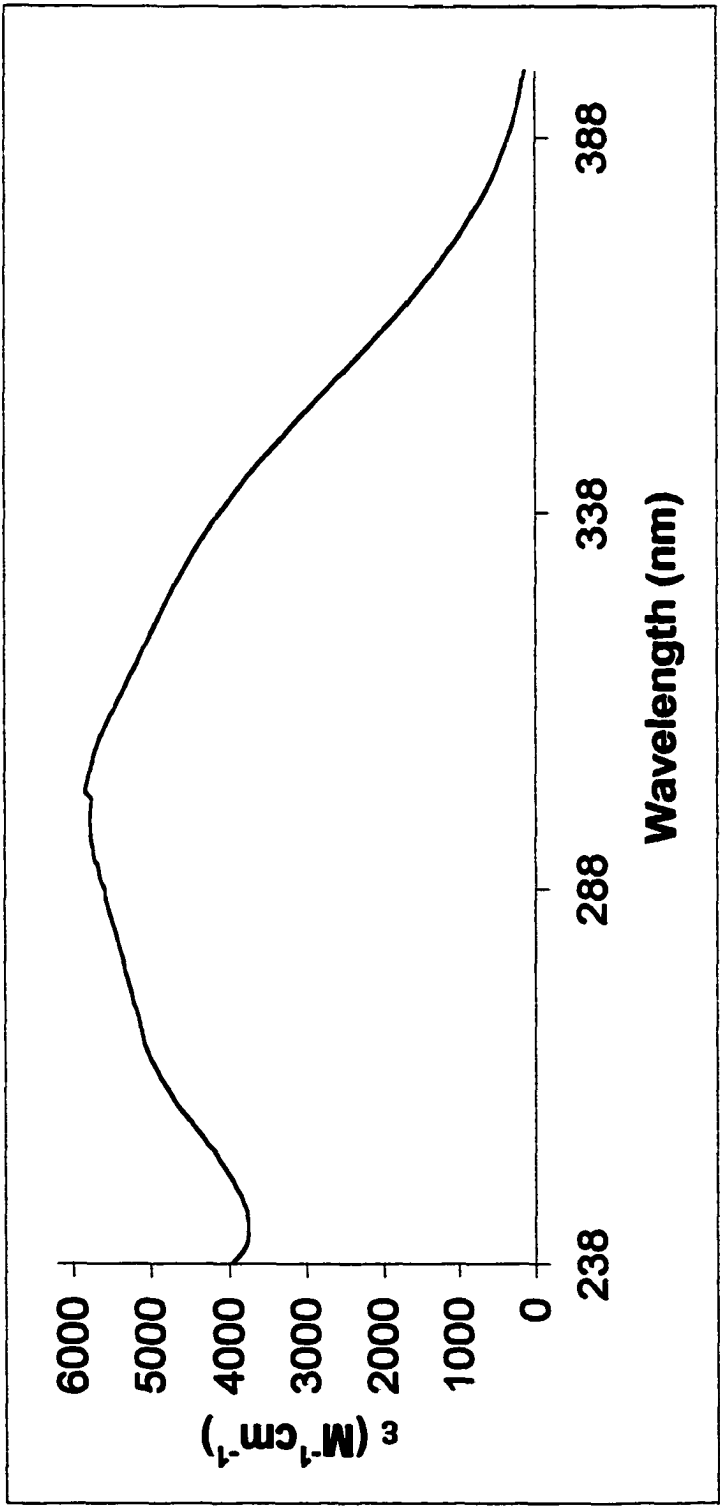


Figure 8. UV-Vis of Compound IV-3 (MeOH).

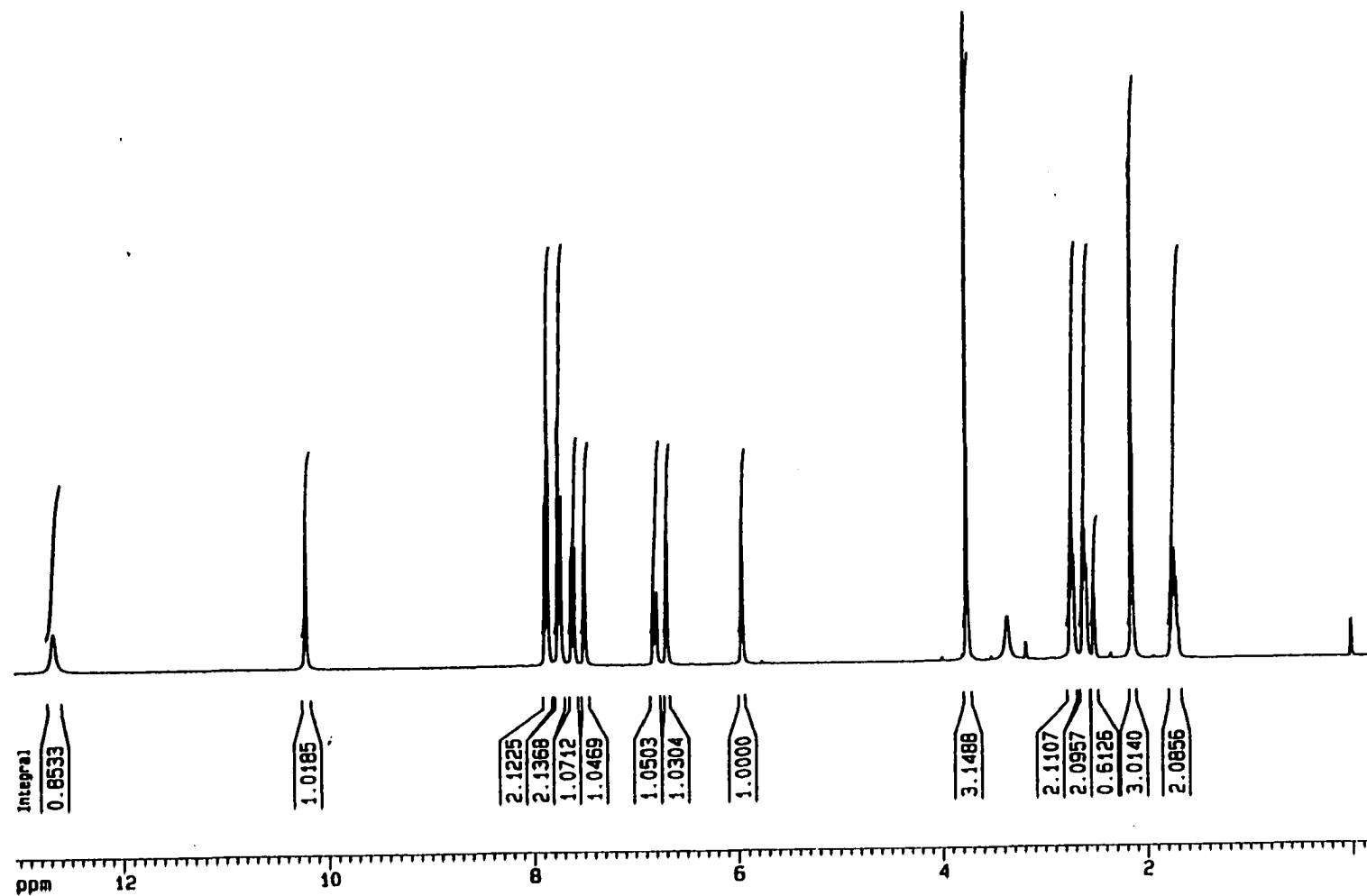


Figure 9. ^1H NMR (300 MHz) of Compound IV-4 (DMSO).

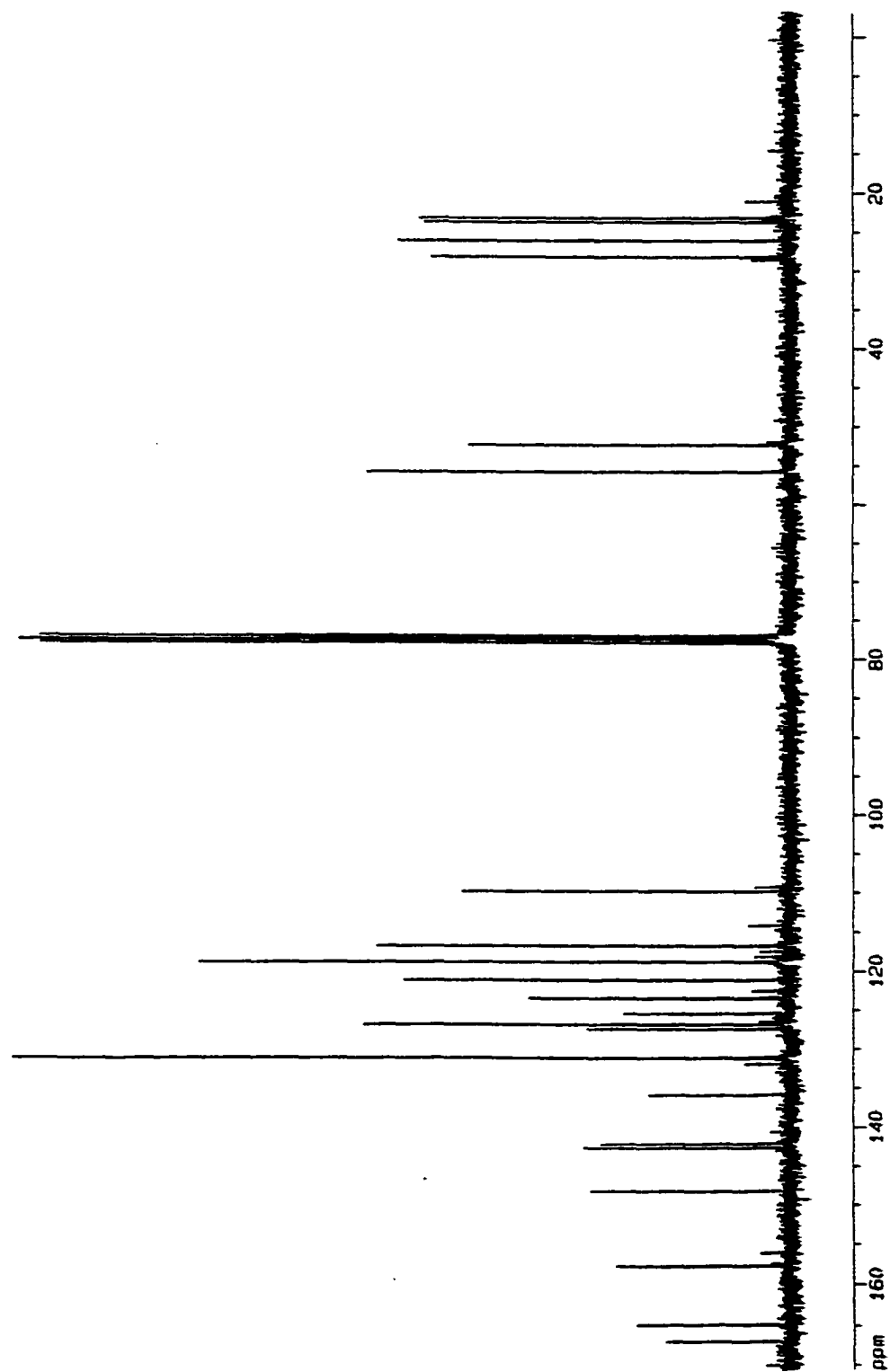


Figure 10. ^{13}C NMR (300 MHz) of Compound IV-4 (DMSO).

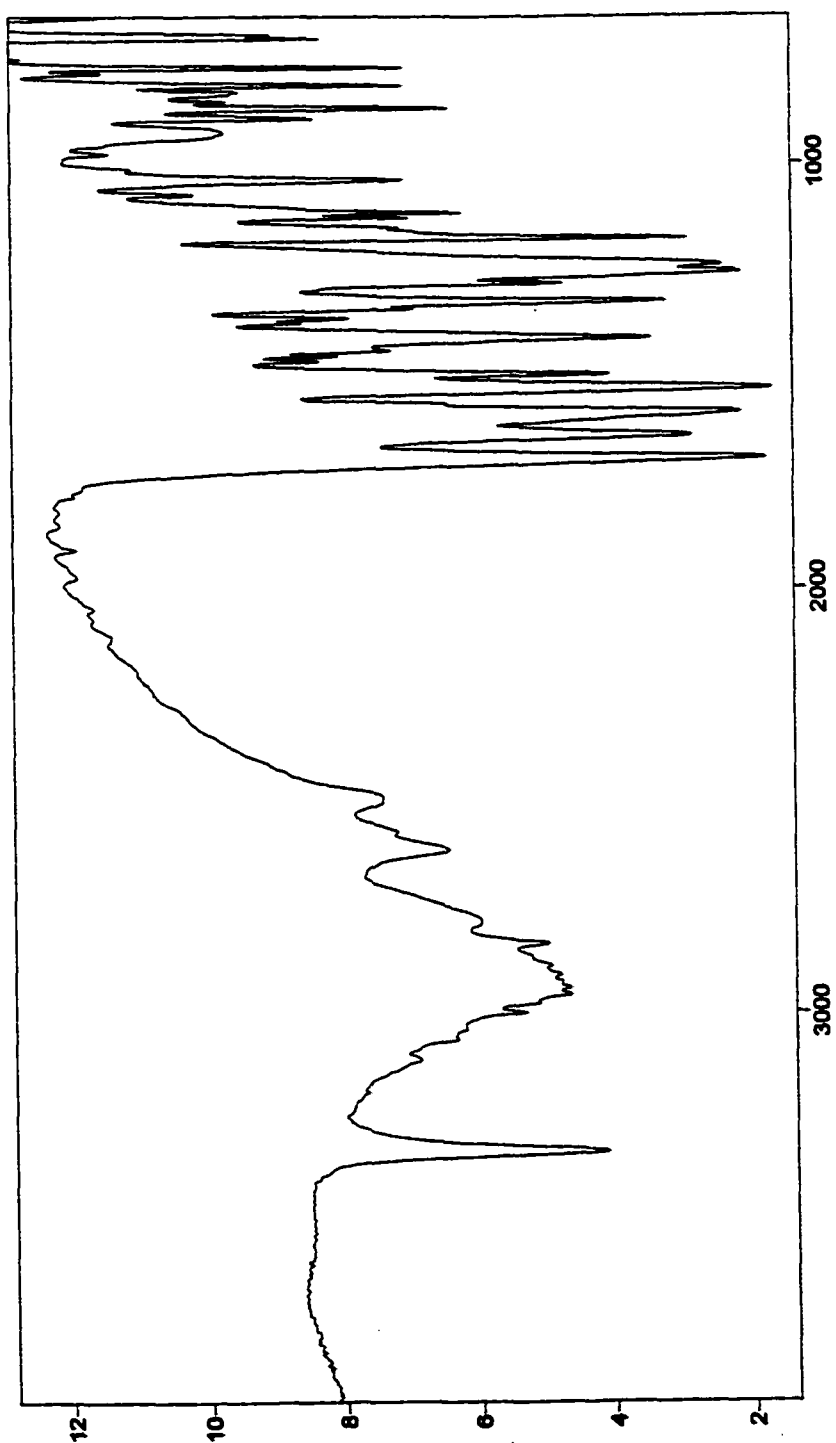


Figure 11. FTIR of Compound IV-4 (KBr).

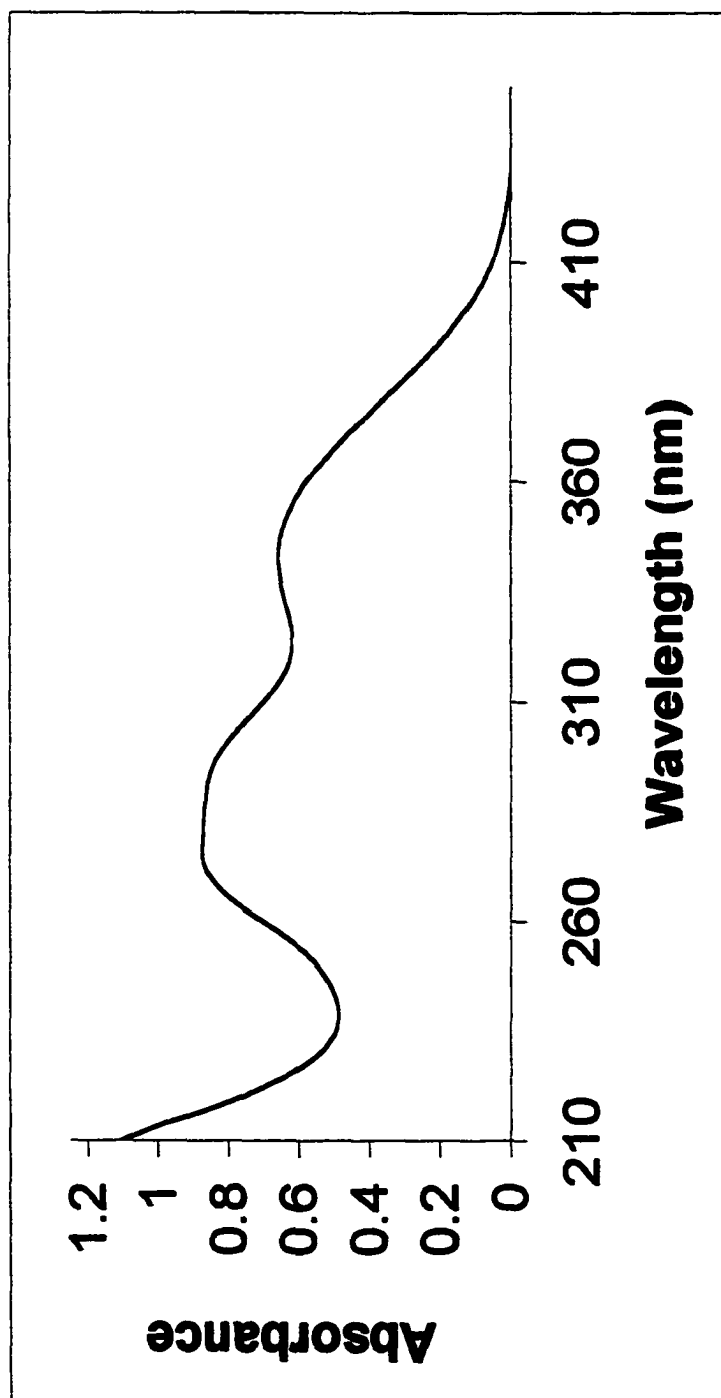


Figure 12. UV-Vis of Compound IV-4 (MeOH).

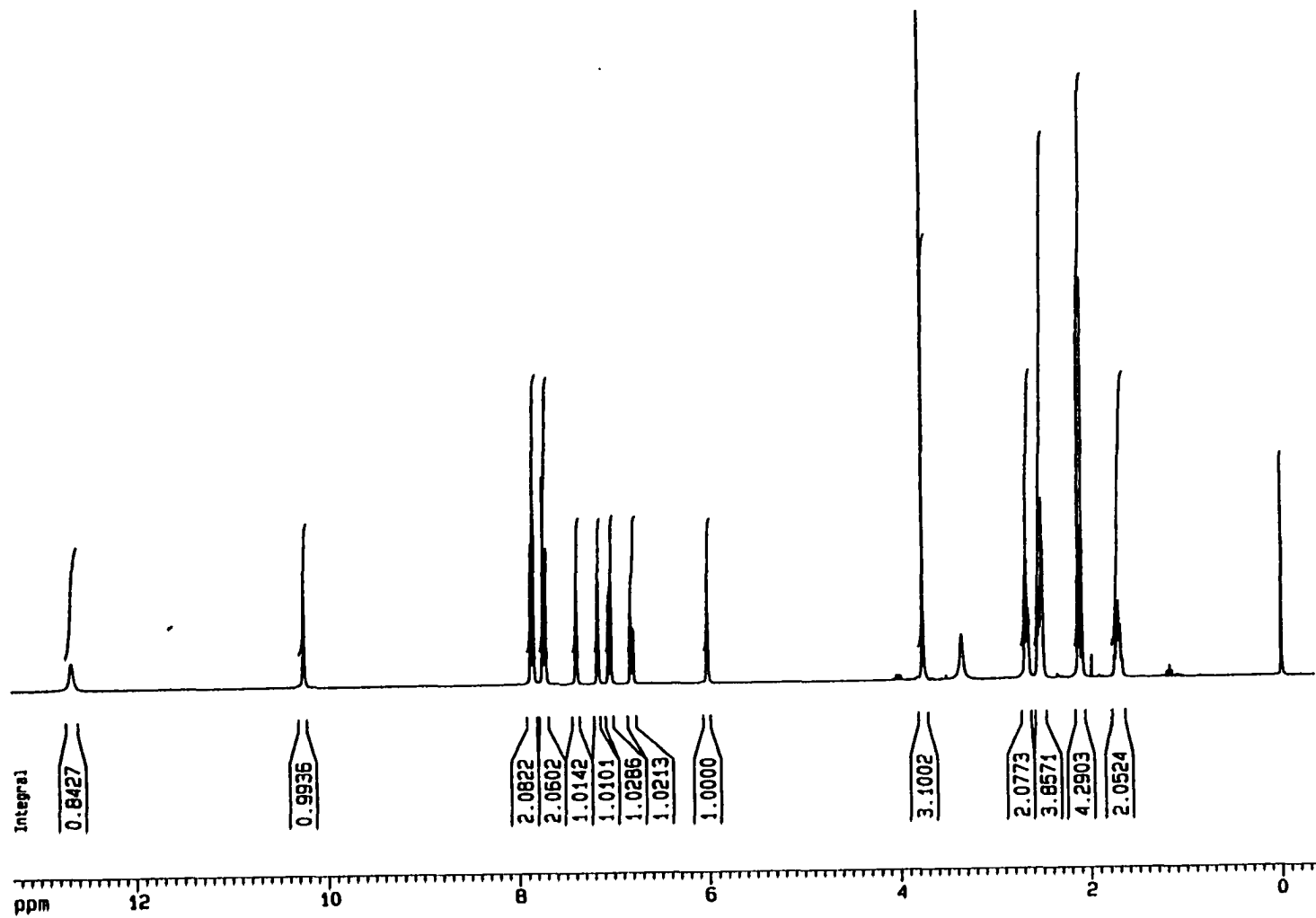


Figure 13. ¹H NMR (300 MHz) of Compound IV-5 (DMSO).

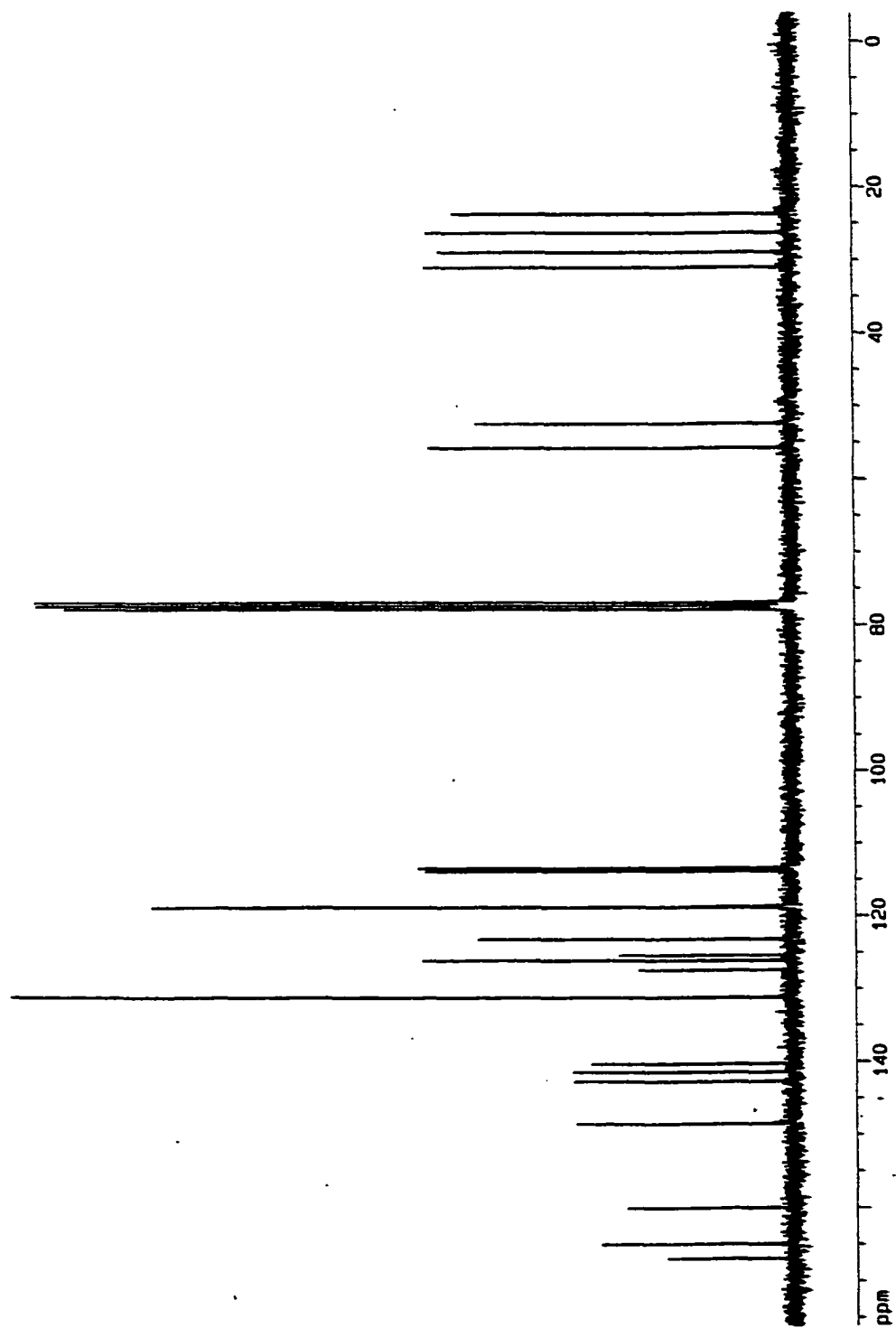


Figure 14. ^{13}C NMR (300 MHz) of Compound IV-5 (DMSO).

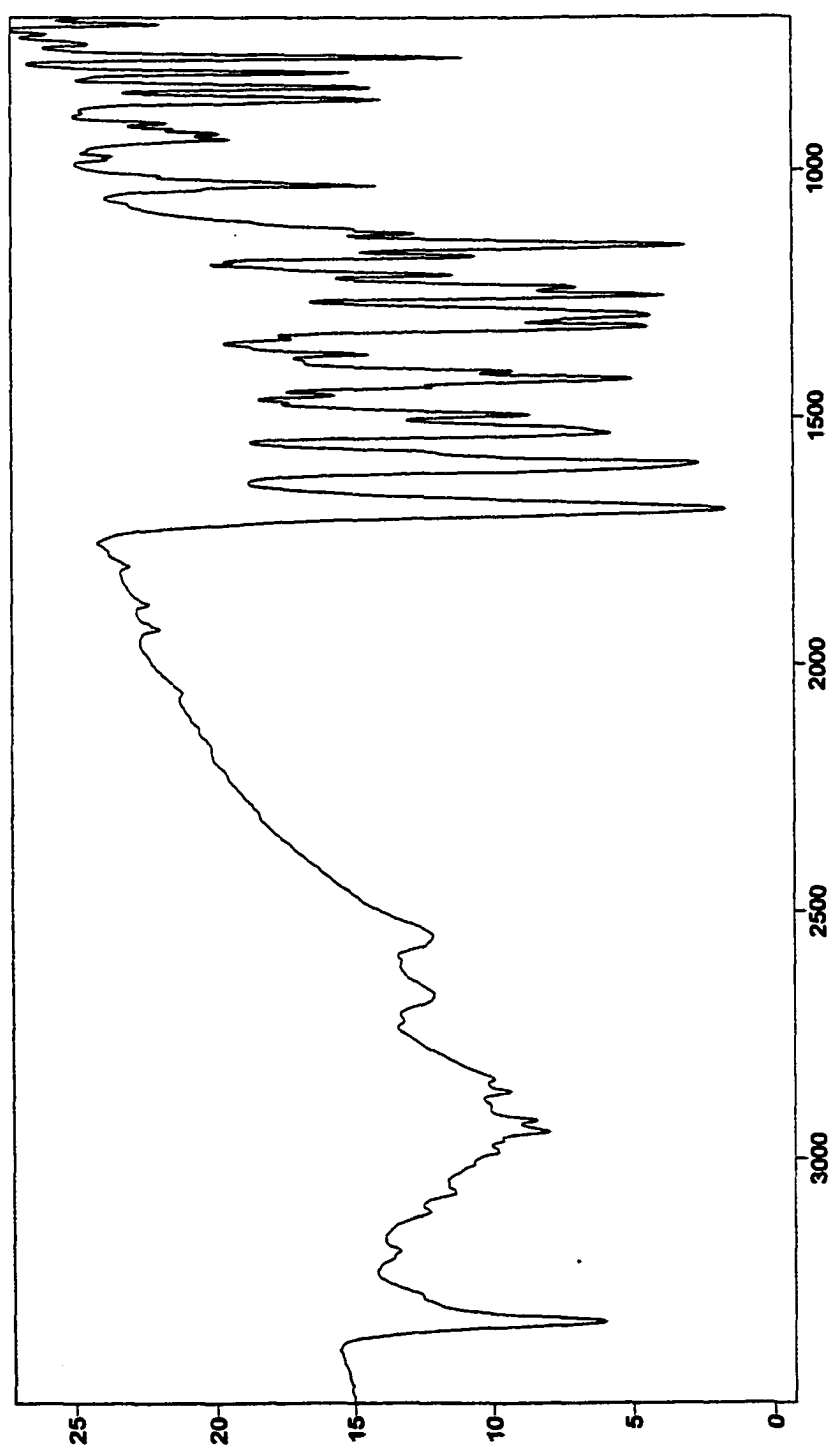


Figure 15. FTIR of Compound IV-5 (KBr).

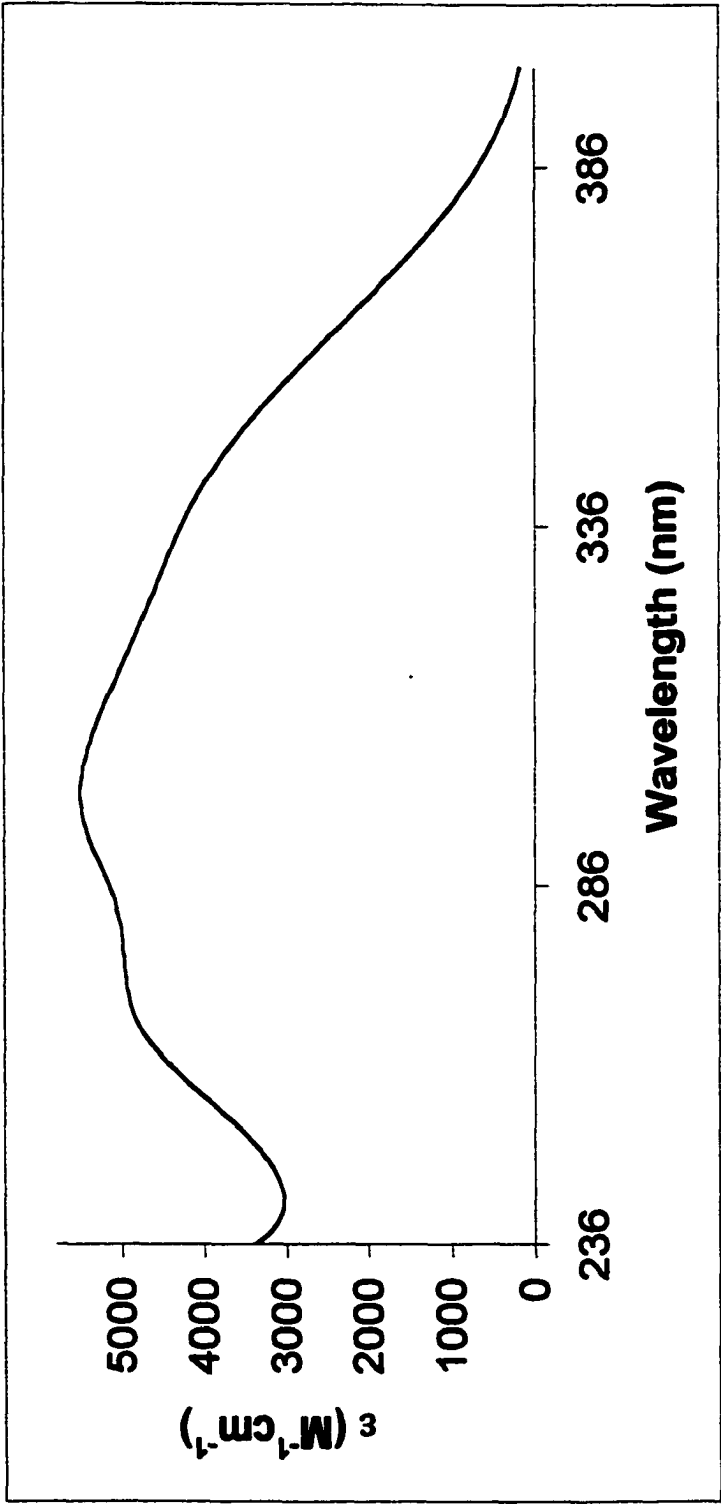


Figure 16. UV-Vis of Compound IV-5 (MeOH).

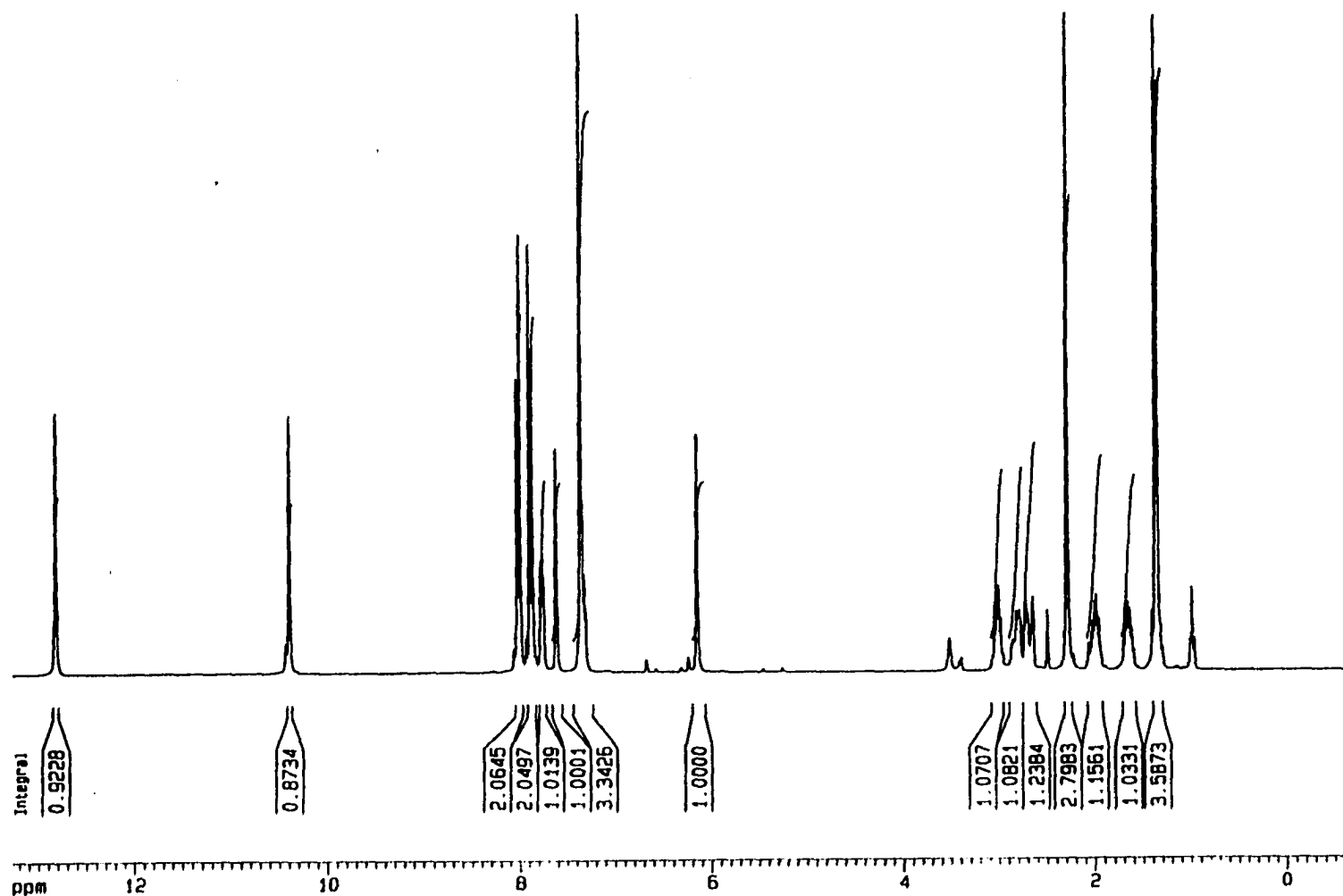


Figure 17. ^1H NMR (300 MHz) of Compound IV-6 (DMSO).

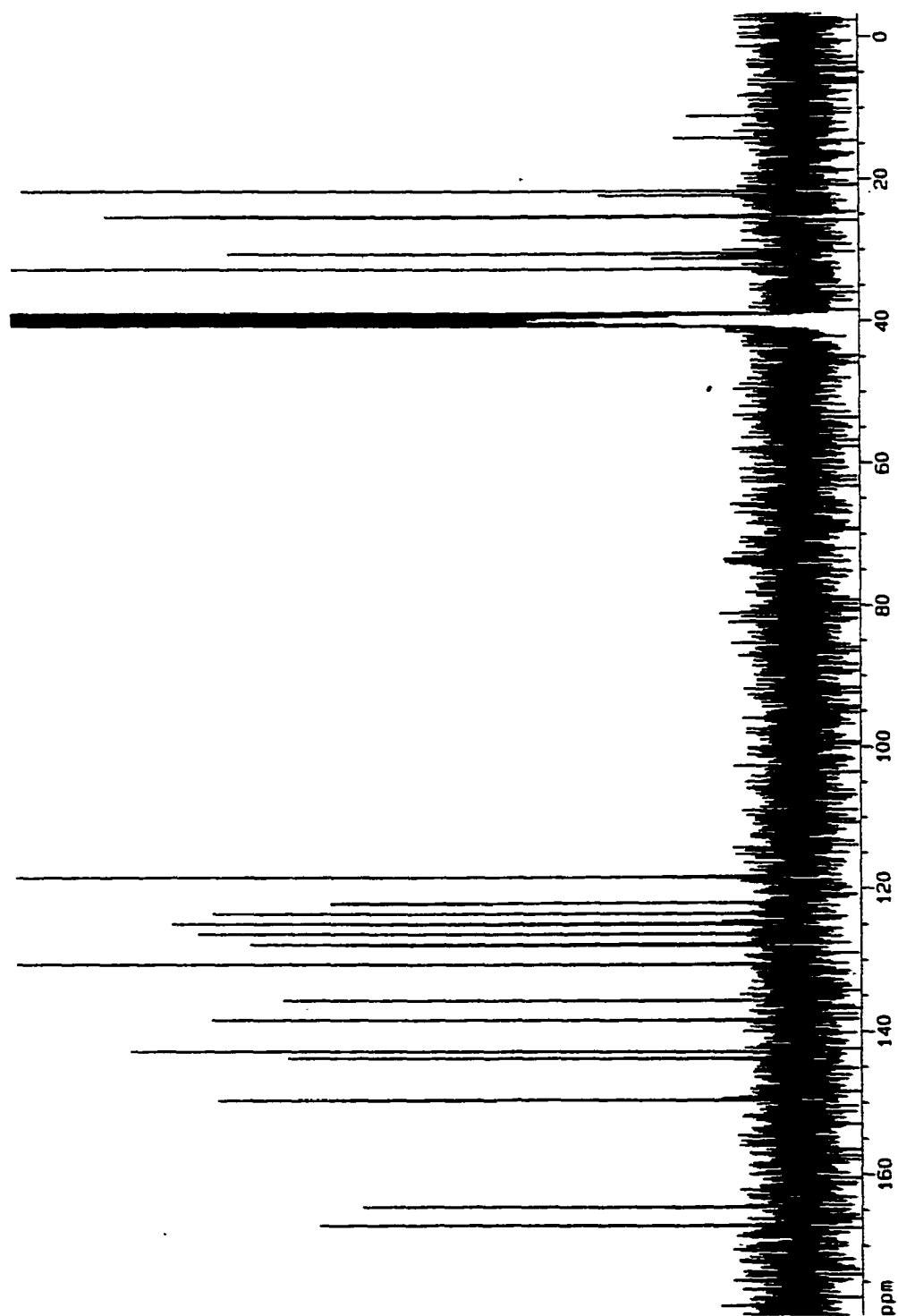


Figure 18. ^{13}C NMR (300 MHz) of Compound IV-6 (DMSO).

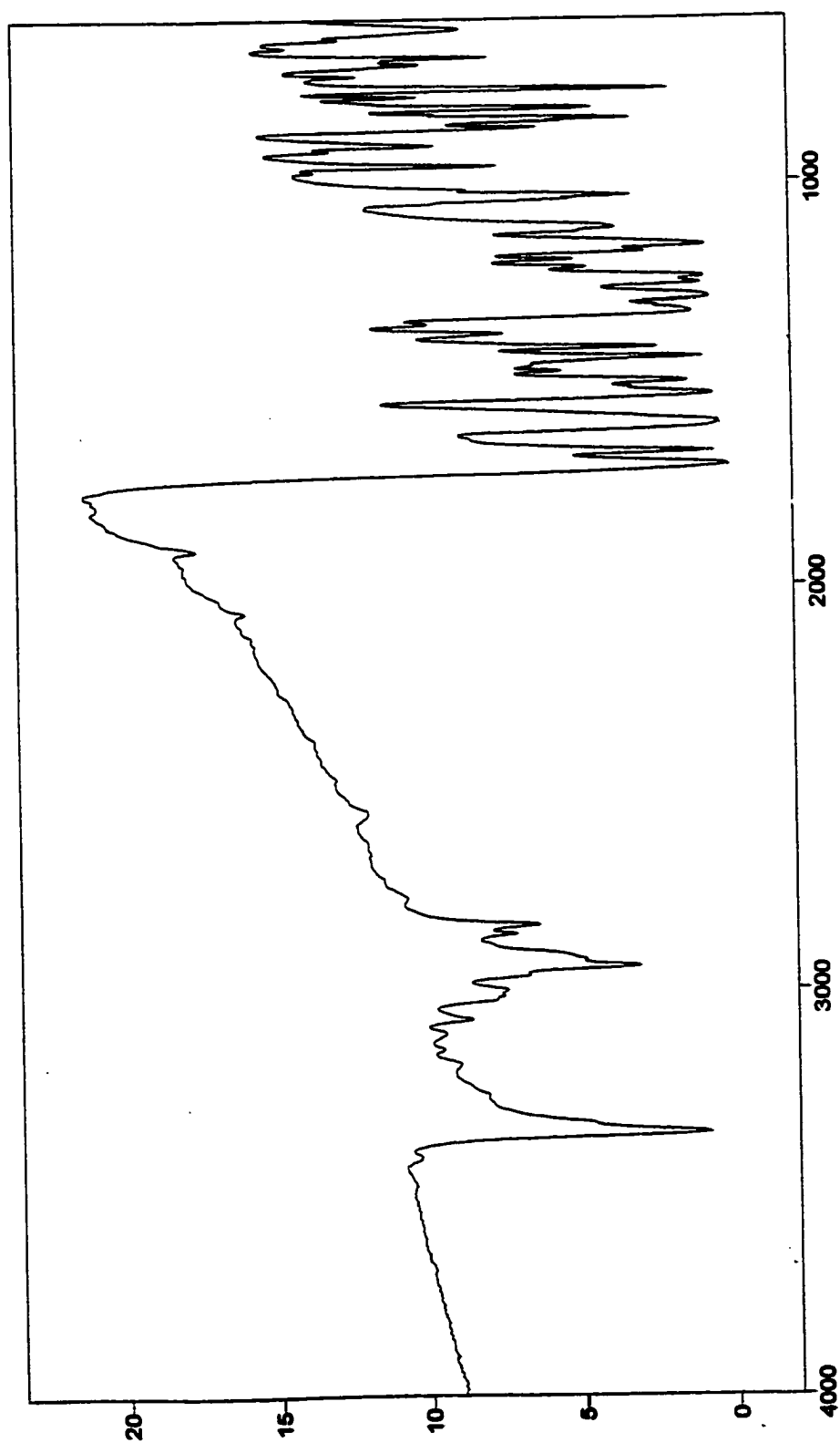


Figure 19. FTIR of Compound IV-6 (KBr).

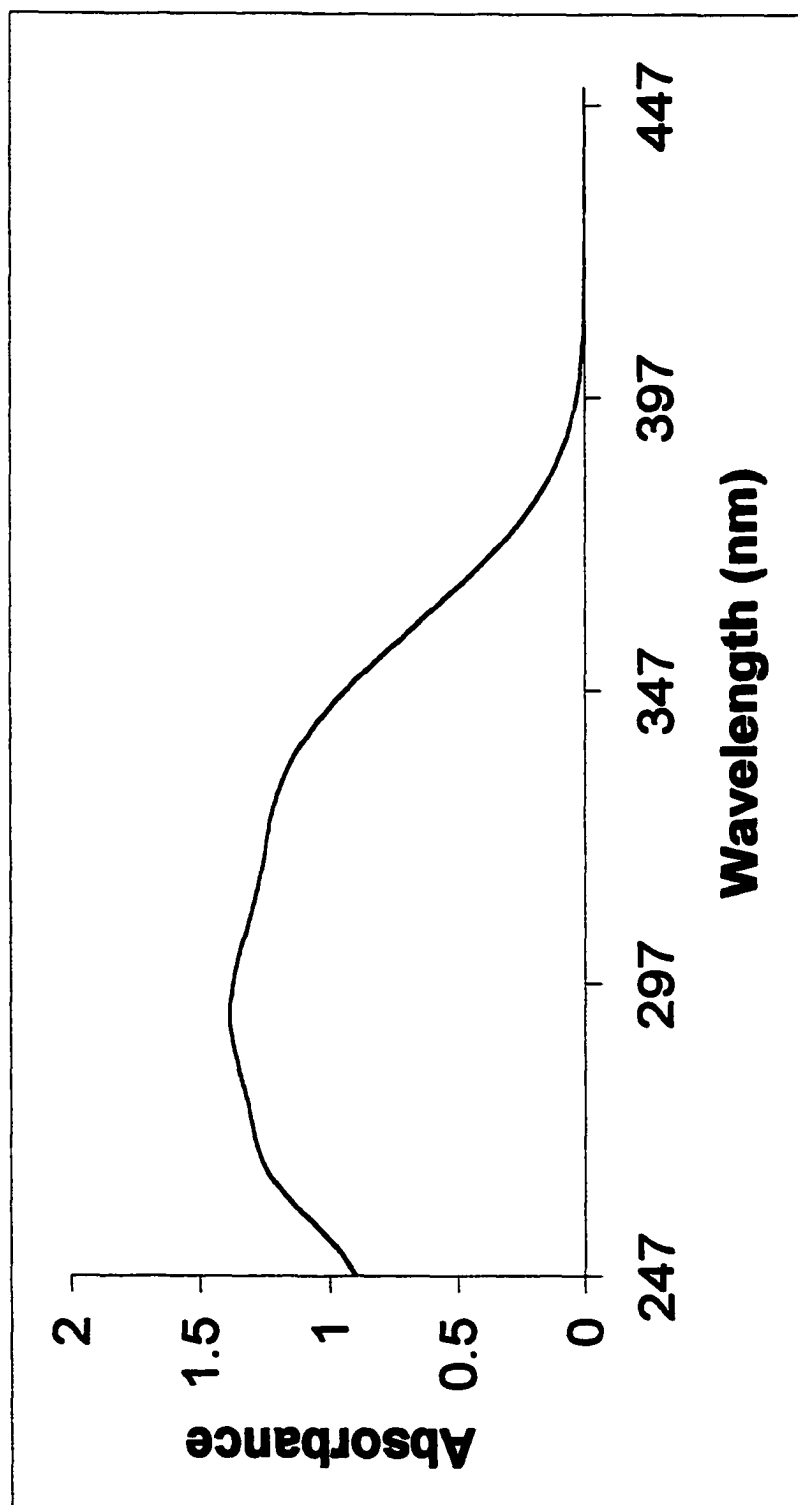


Figure 20. UV-Vis of Compound IV-6 (MeOH).

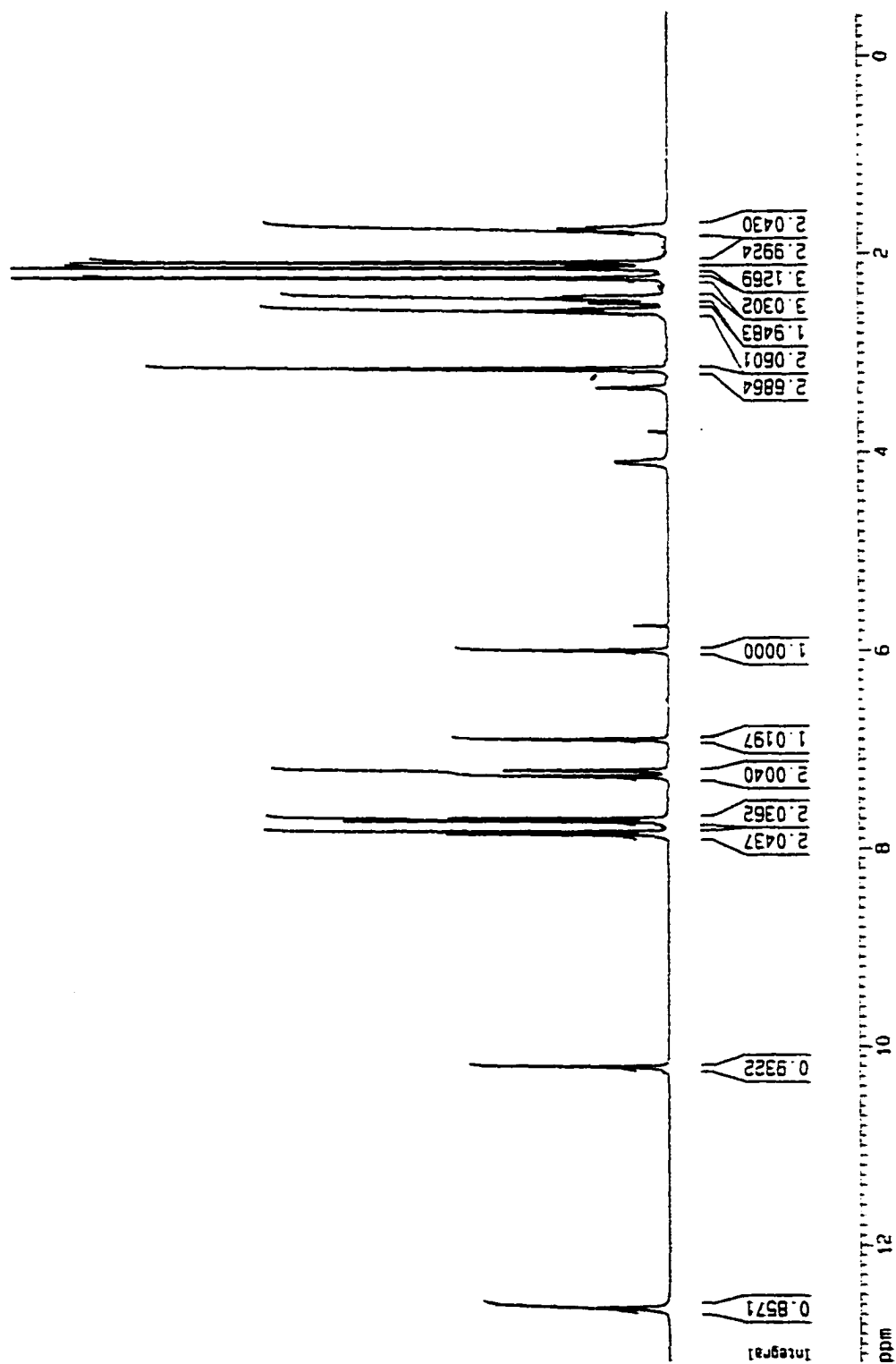


Figure 21. ¹H NMR (300 MHz) of Compound IV-7 (DMSO).

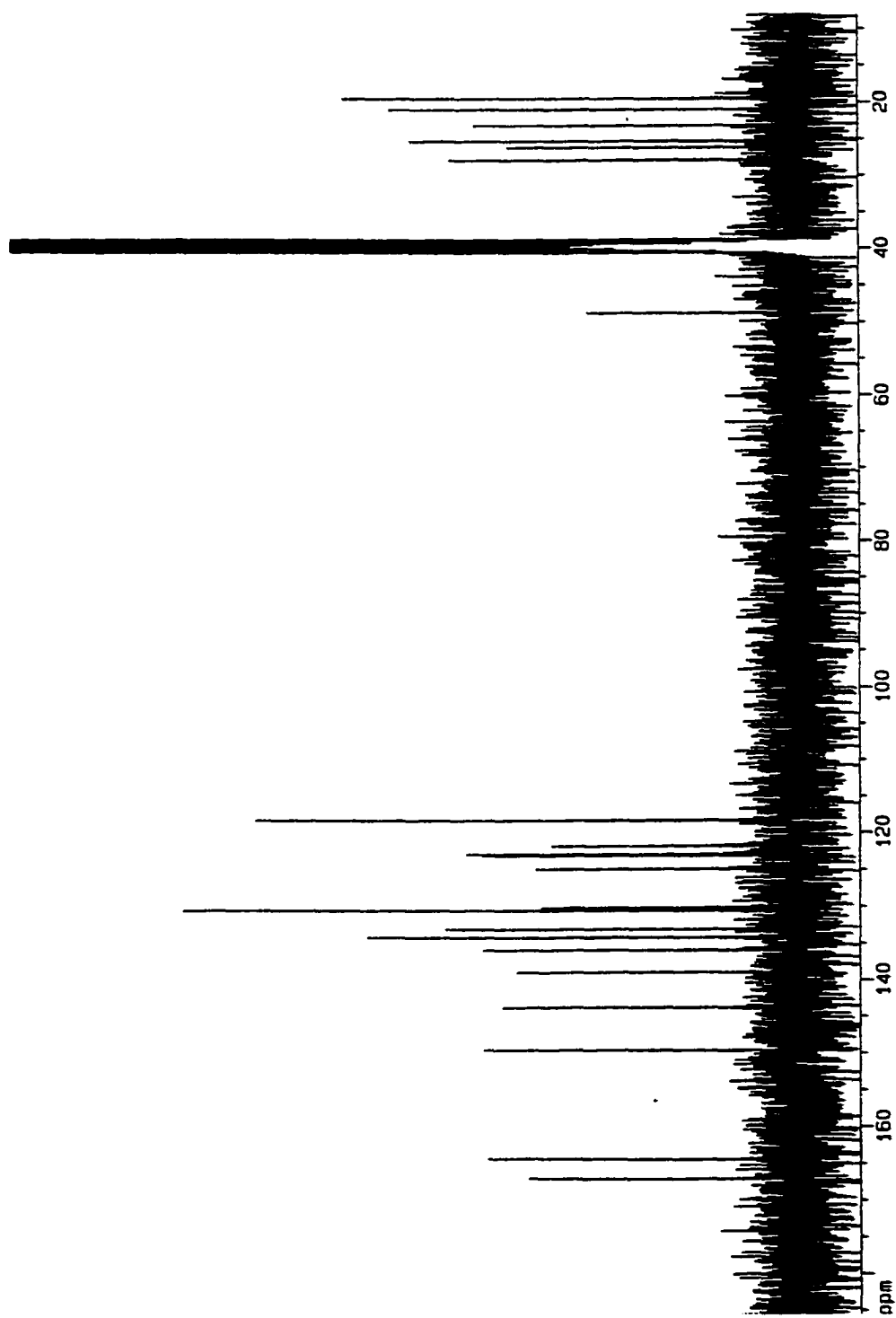


Figure 22. ^{13}C NMR (300 MHz) of Compound IV-7 (DMSO).

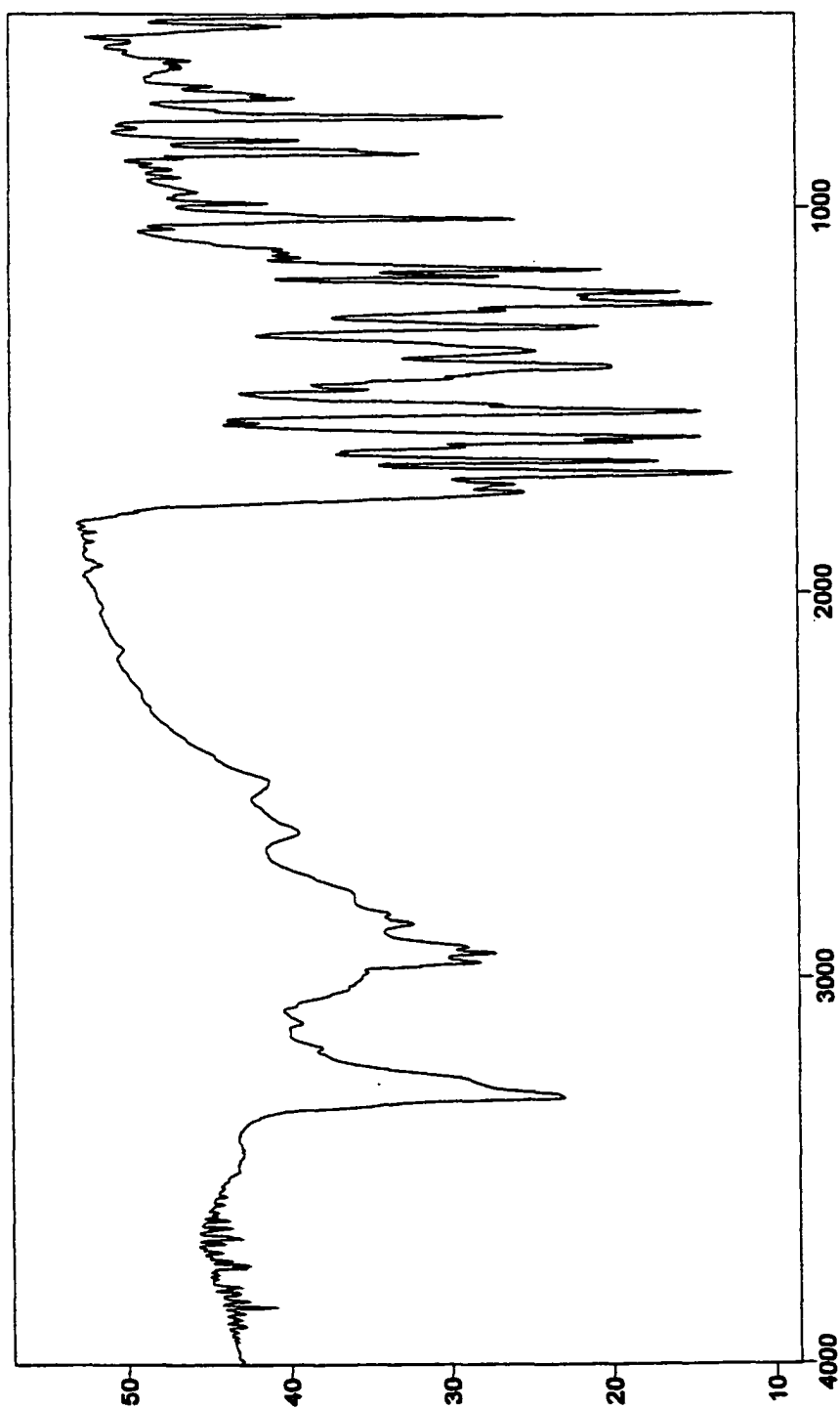


Figure 23. FTIR of Compound IV-7 (KBr).

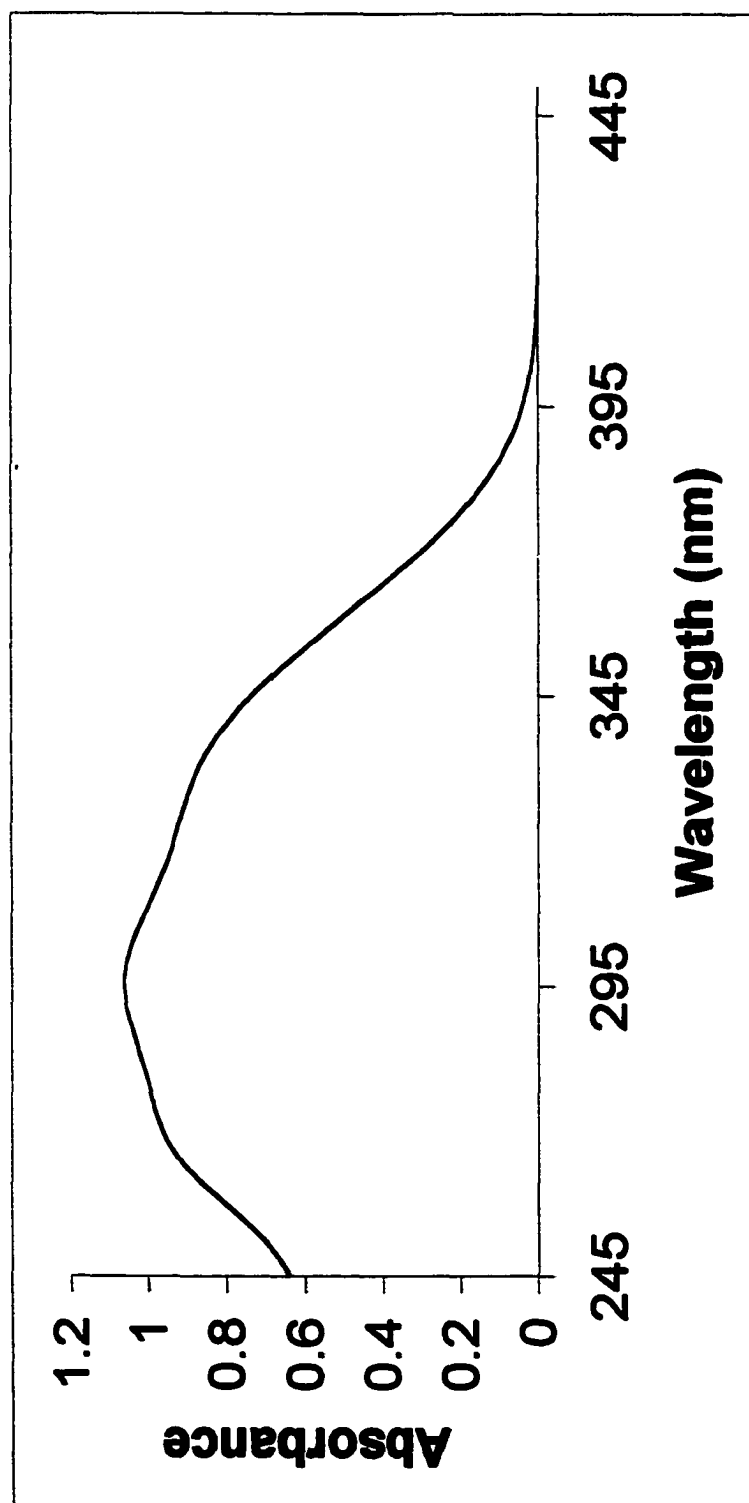


Figure 24. UV-Vis of Compound IV-7 (MeOH).

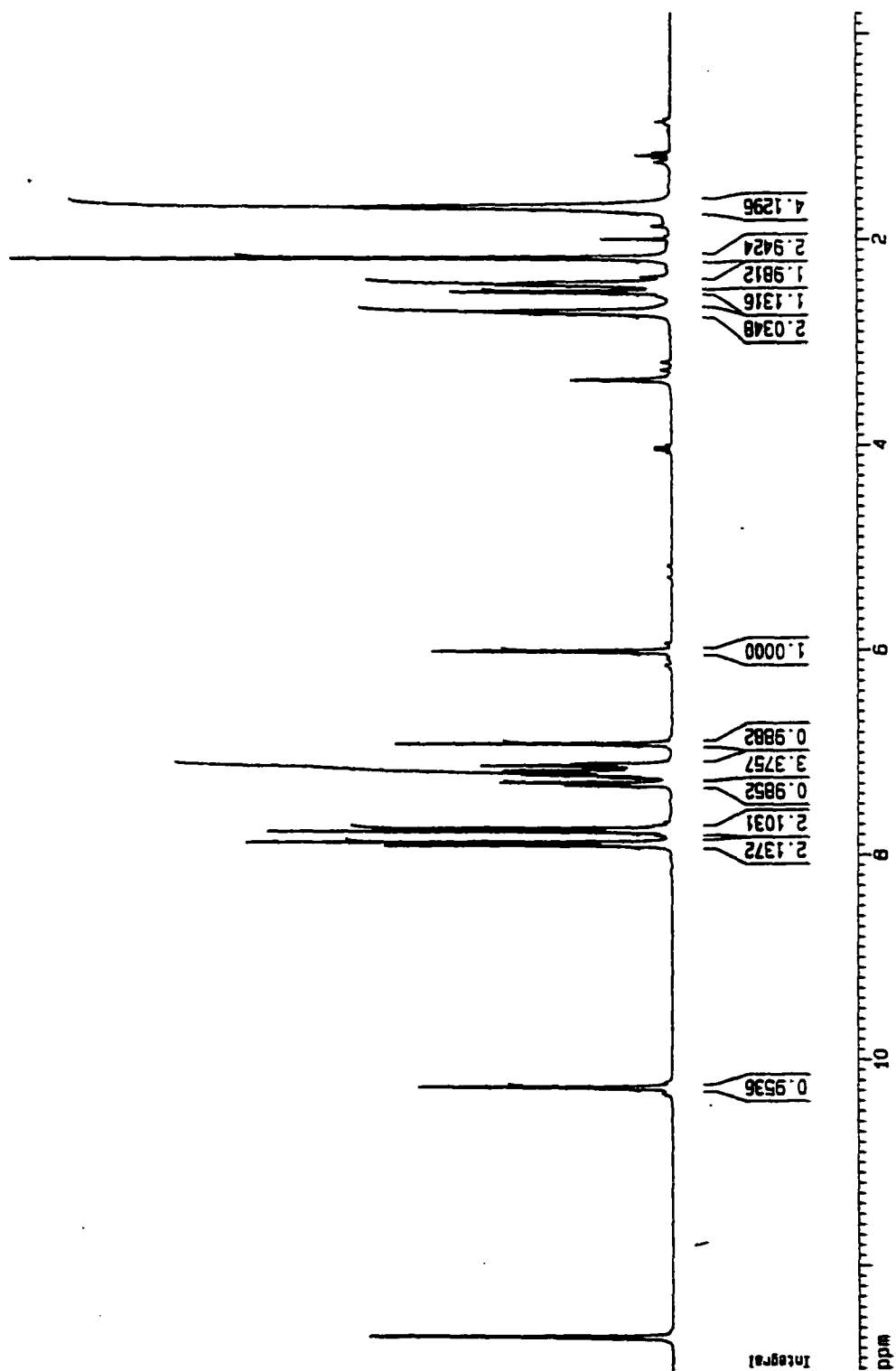


Figure 25. ¹H NMR (300 MHz) of Compound IV-8 (DMSO).

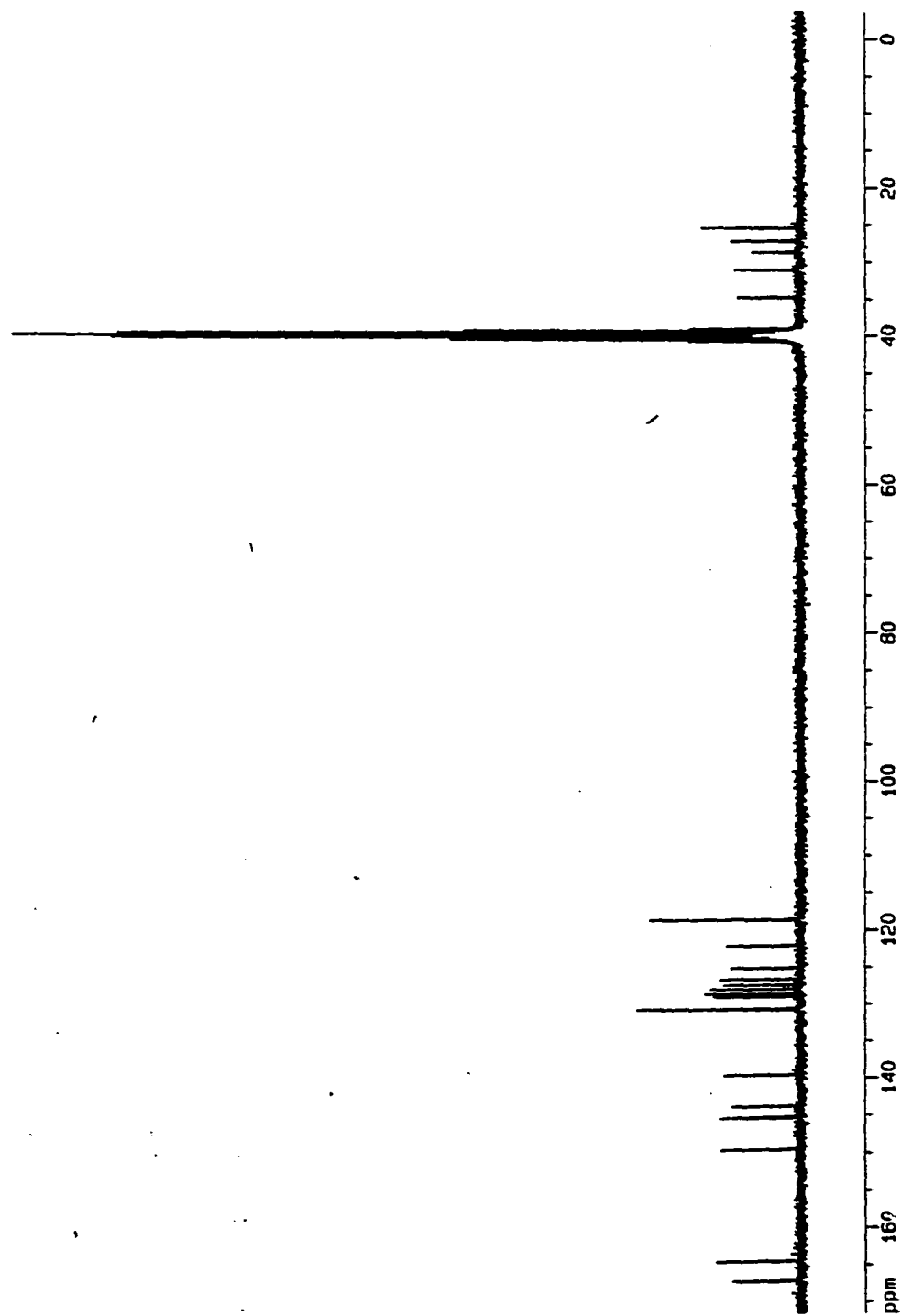


Figure 26. ^{13}C NMR (300 MHz) of Compound IV-8 (DMSO).

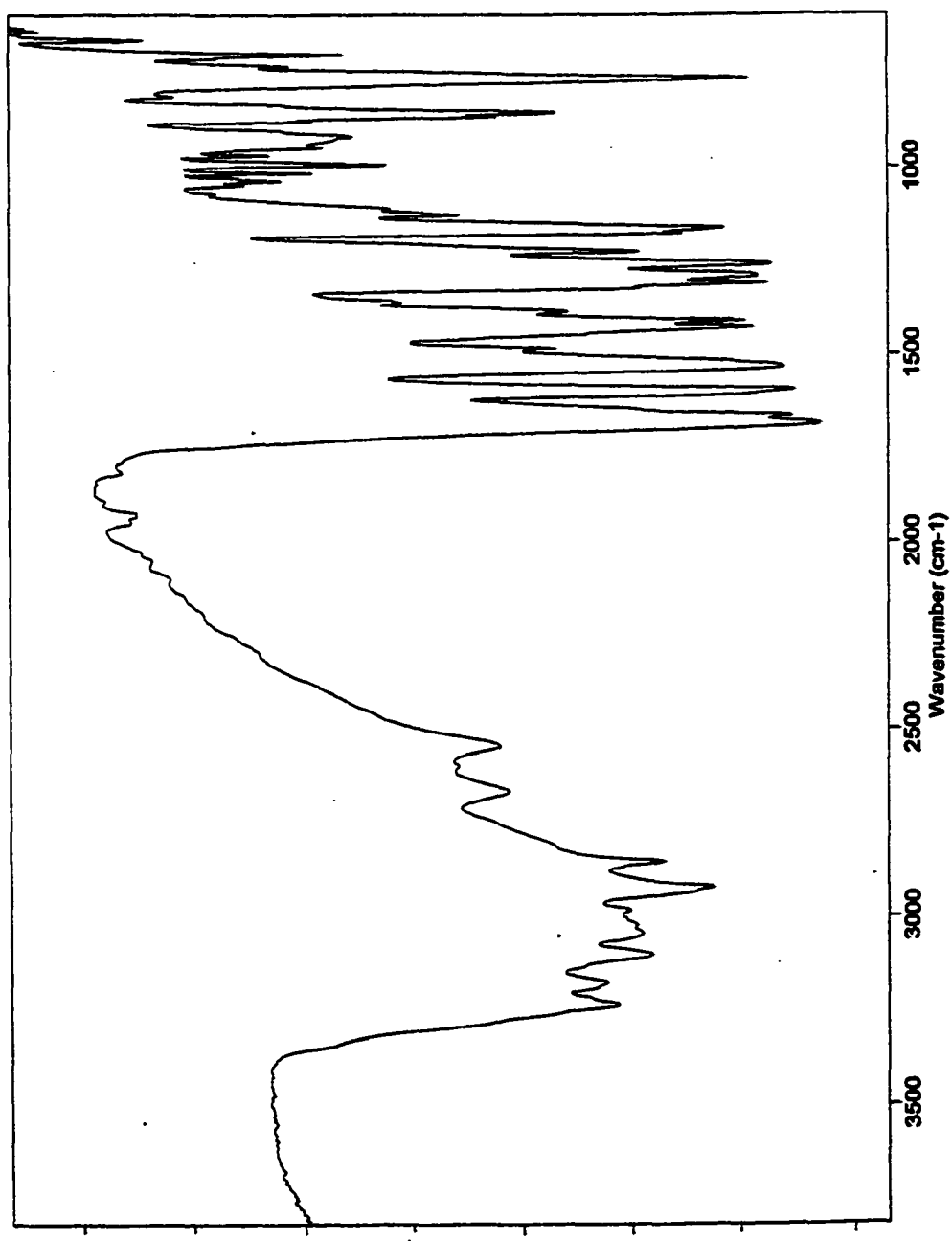


Figure 27. FTIR of Compound IV-8 (KBr).

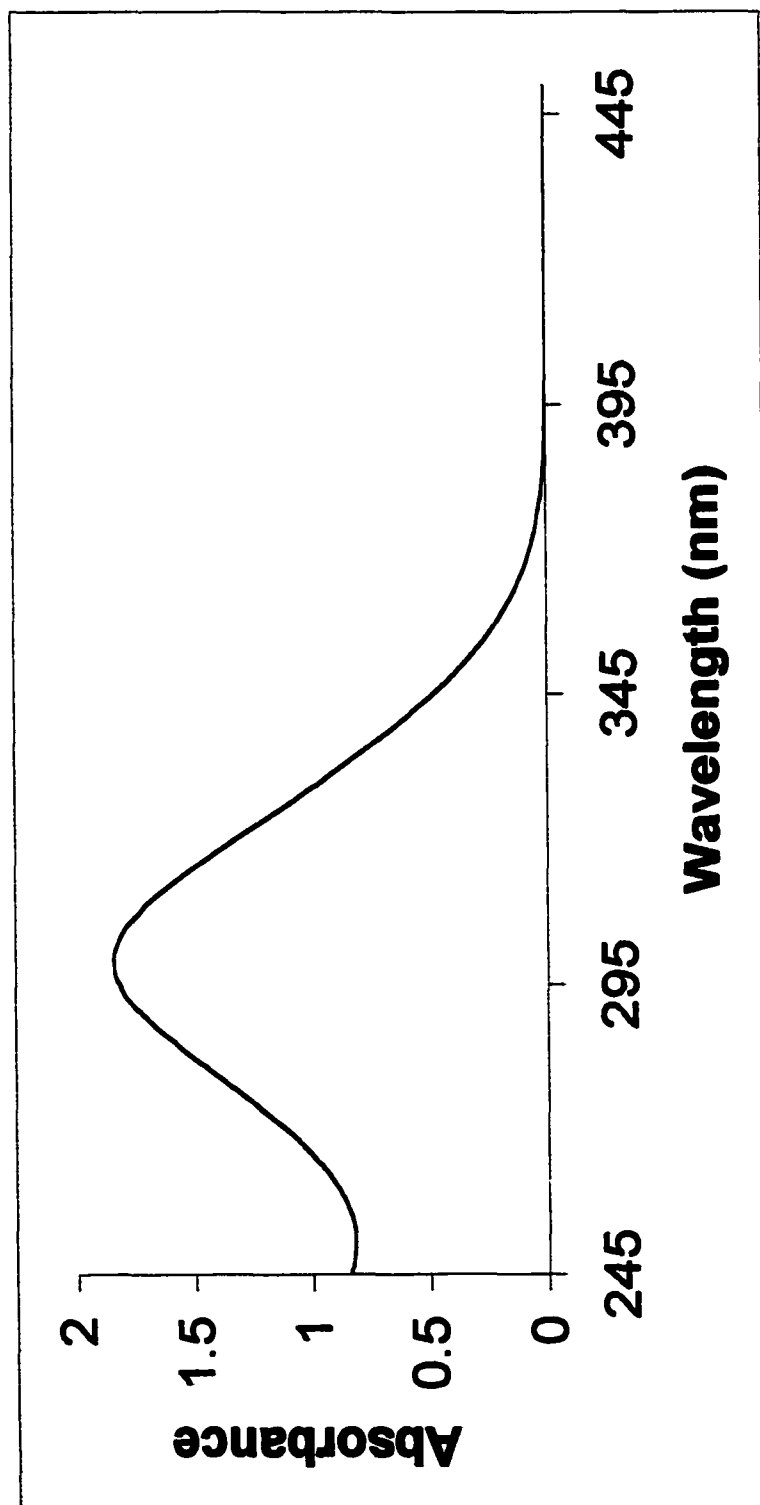


Figure 28. UV-Vis of Compound IV-8 (MeOH).

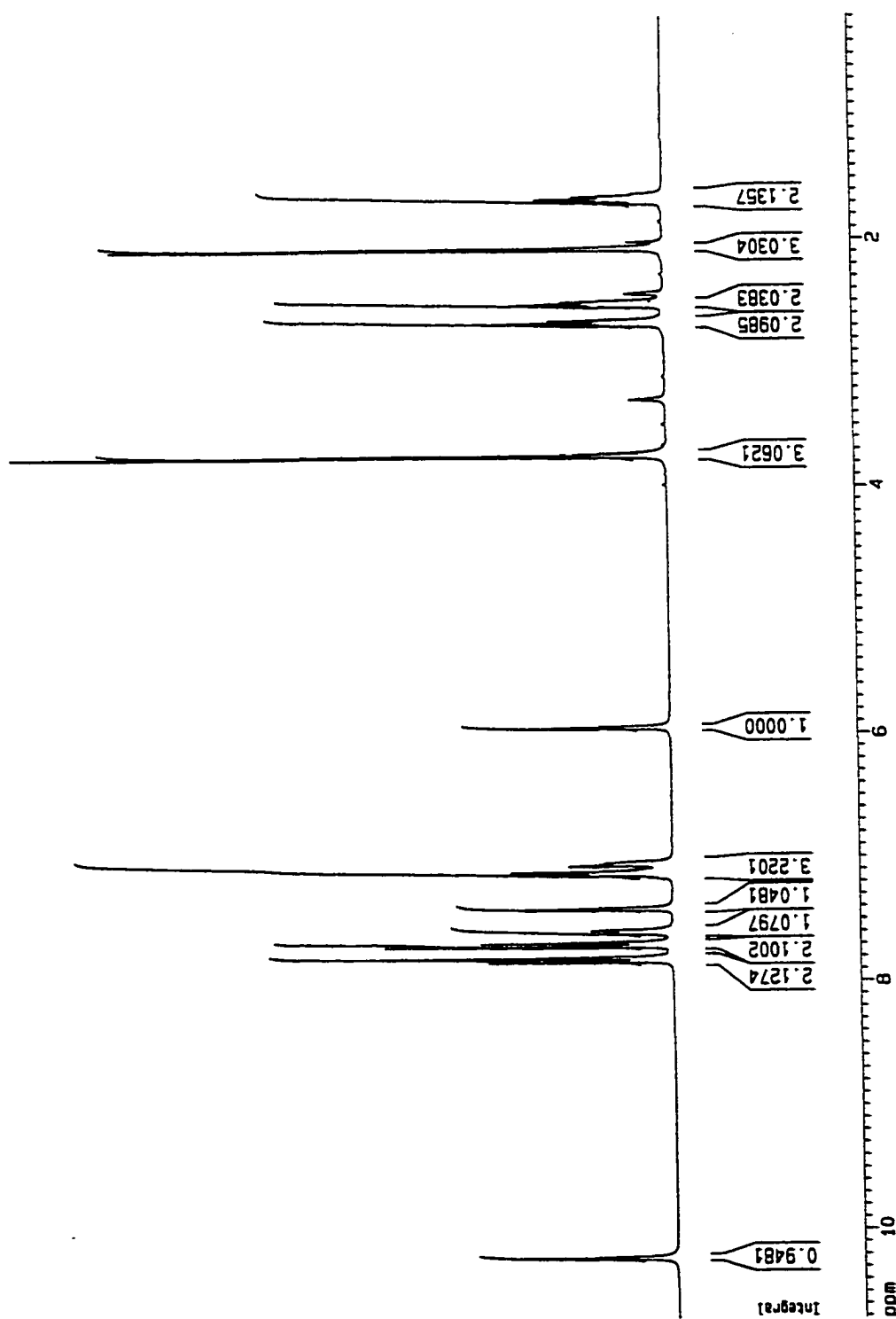


Figure 29. ¹H NMR (300 MHz) of Compound IV-16 (DMSO).

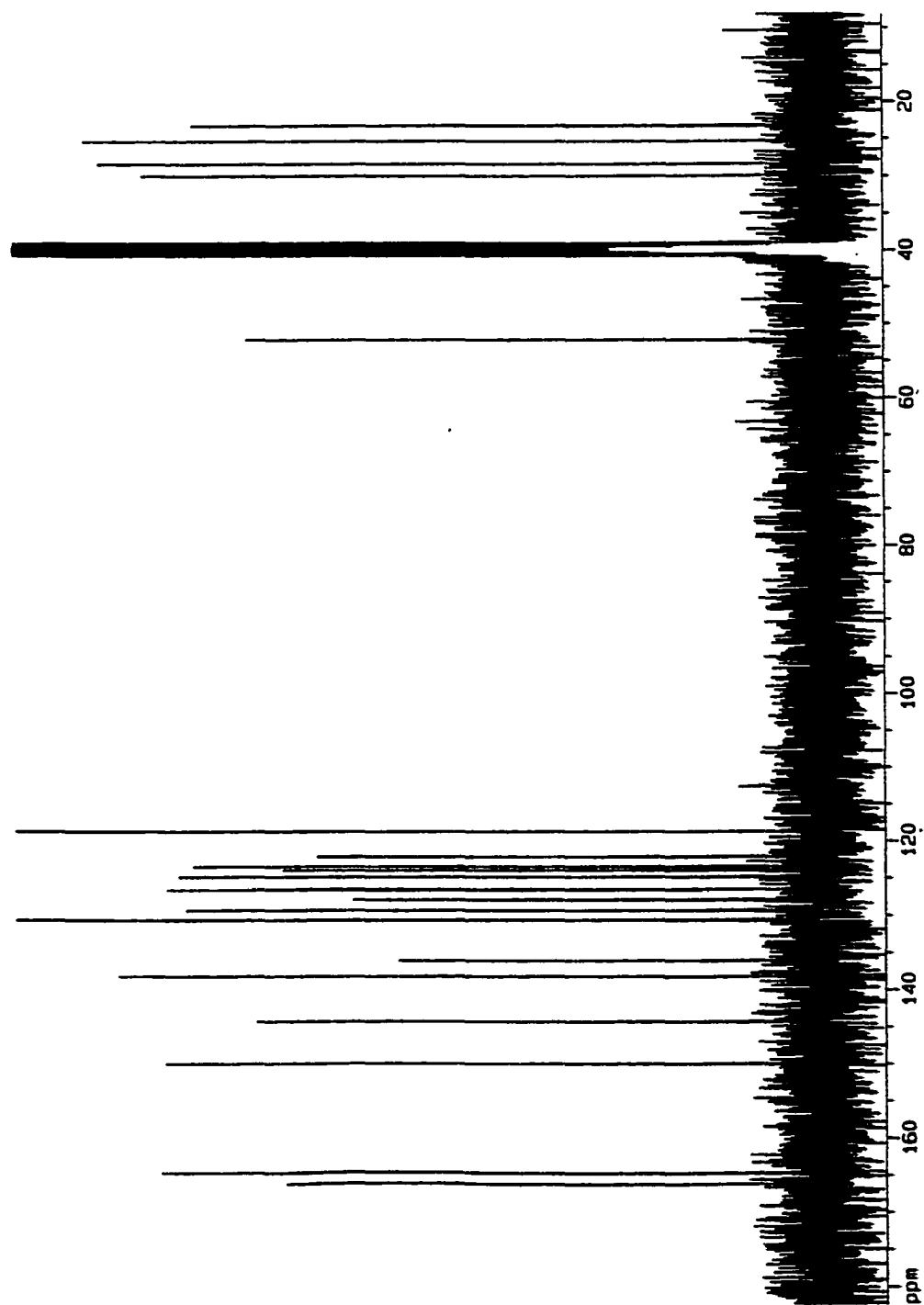


Figure 30. ^{13}C NMR (300 MHz) of Compound IV-16 (DMSO).

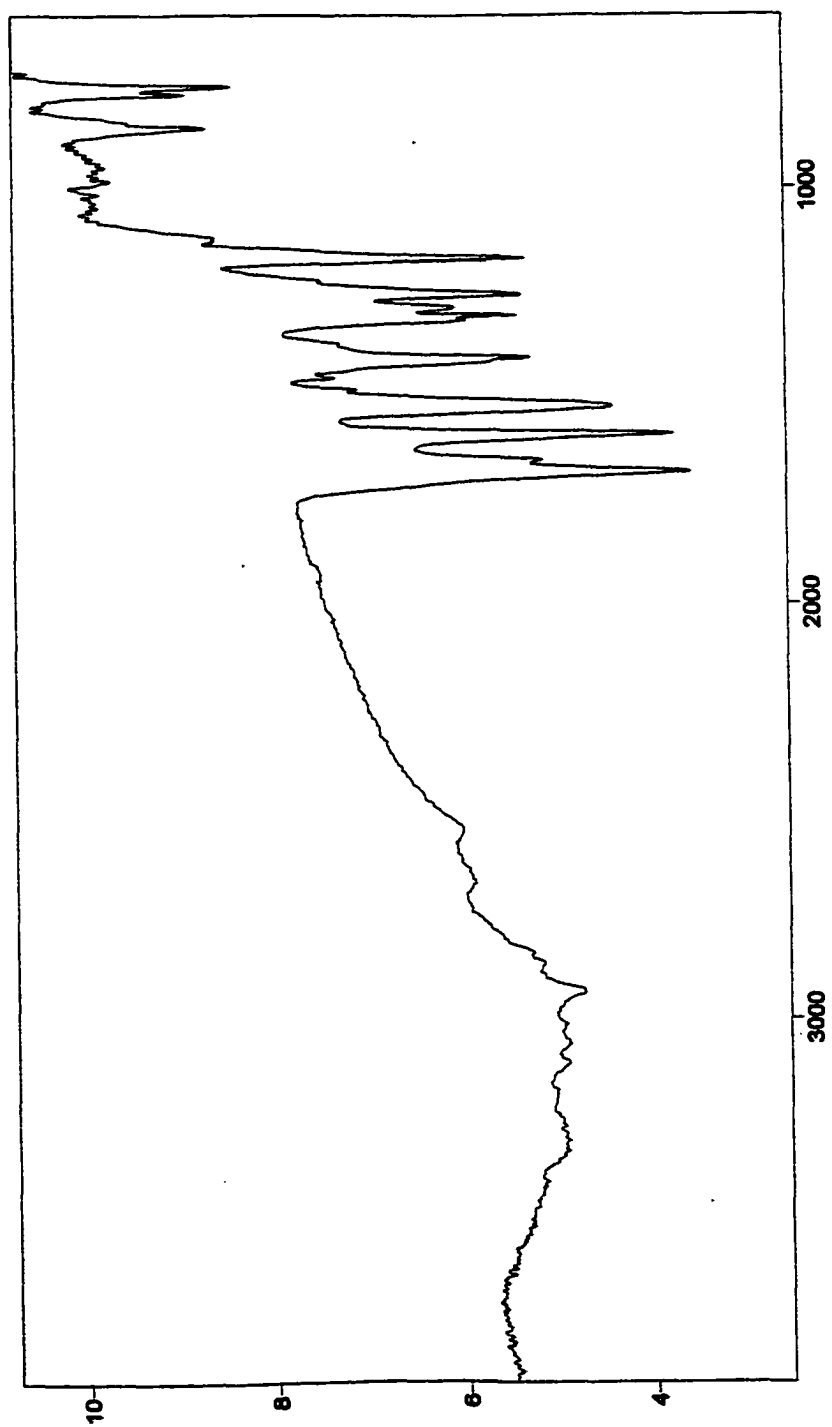


Figure 31. FTIR of Compound IV-16 (KBr).

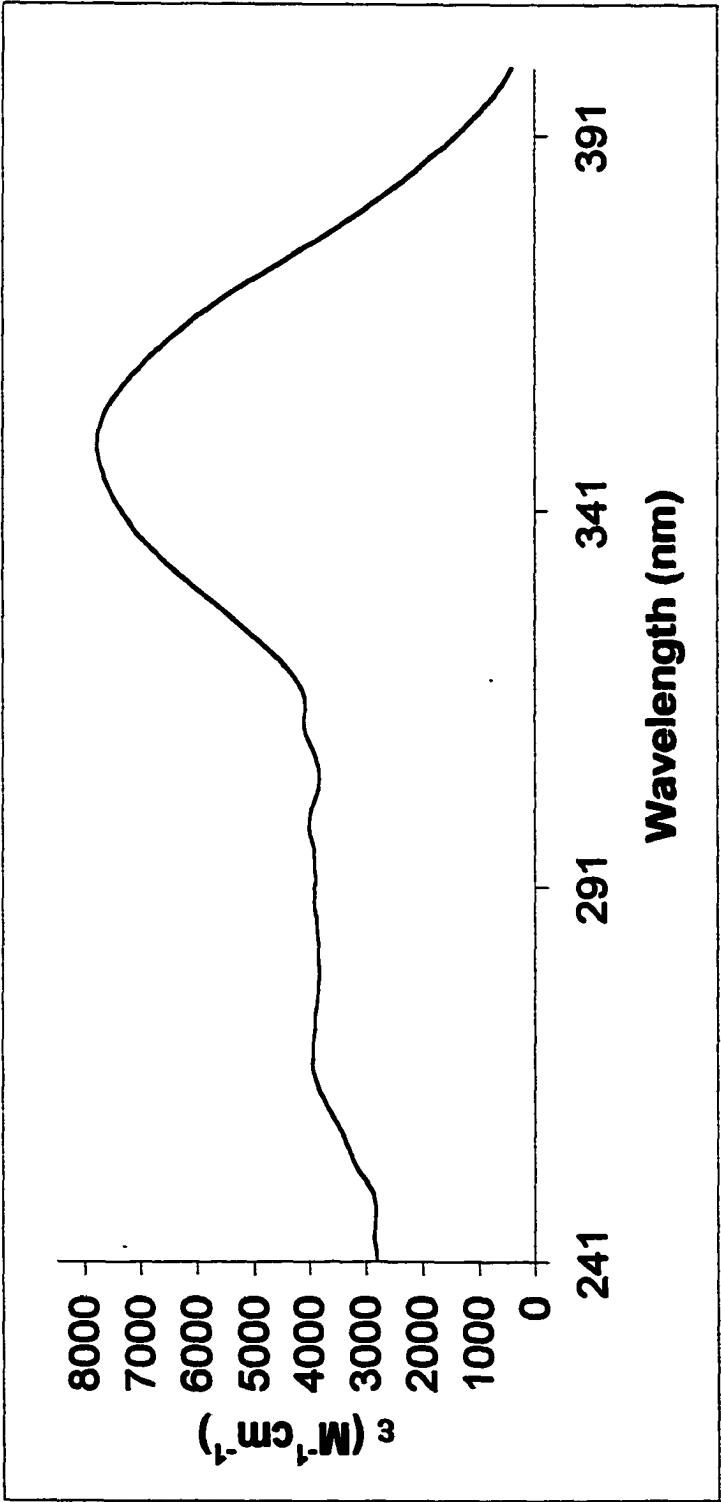


Figure 32. UV-Vis of Compound IV-16 (MeOH).

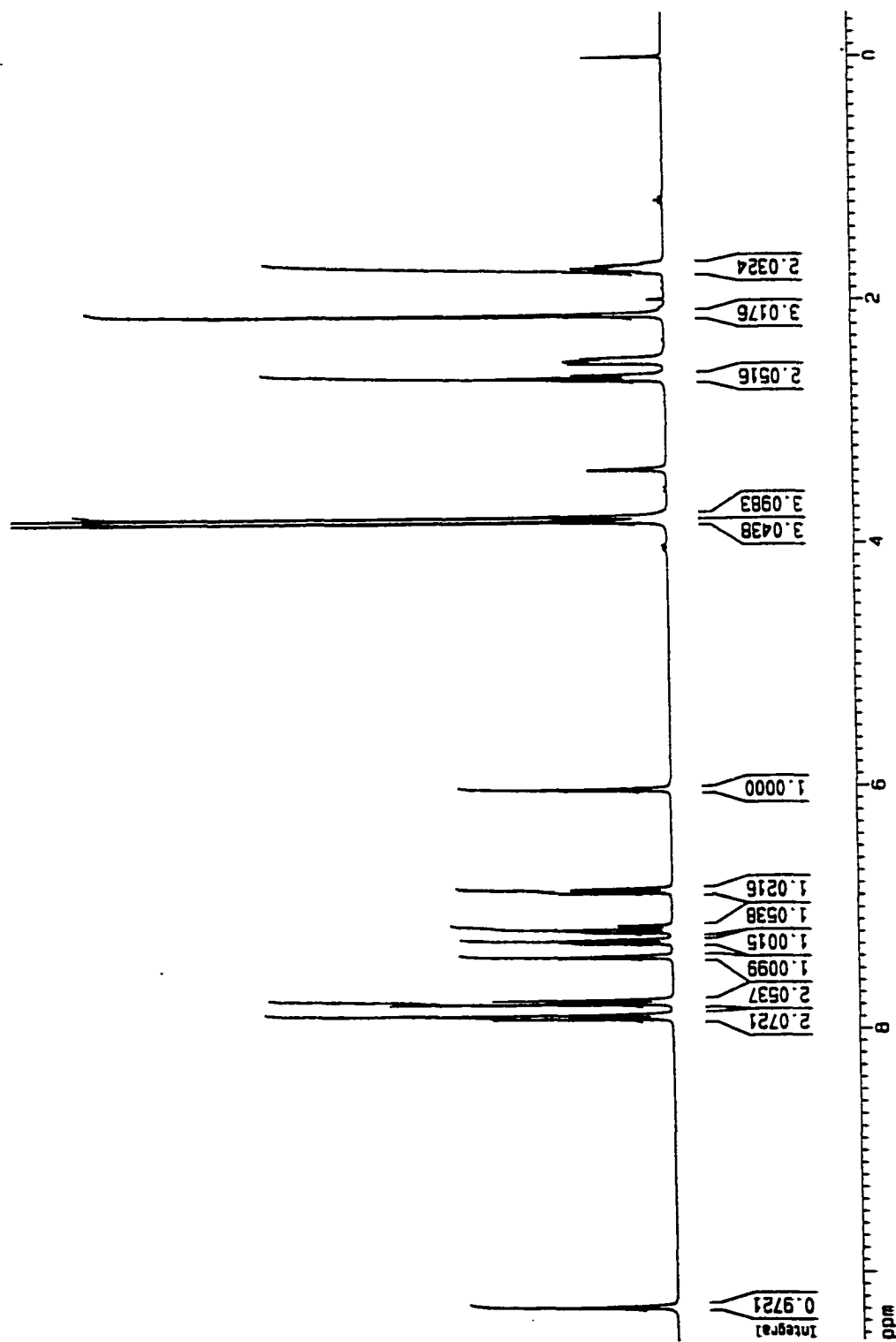


Figure 33. ¹H NMR (300 MHz) of Compound IV-17 (DMSO).

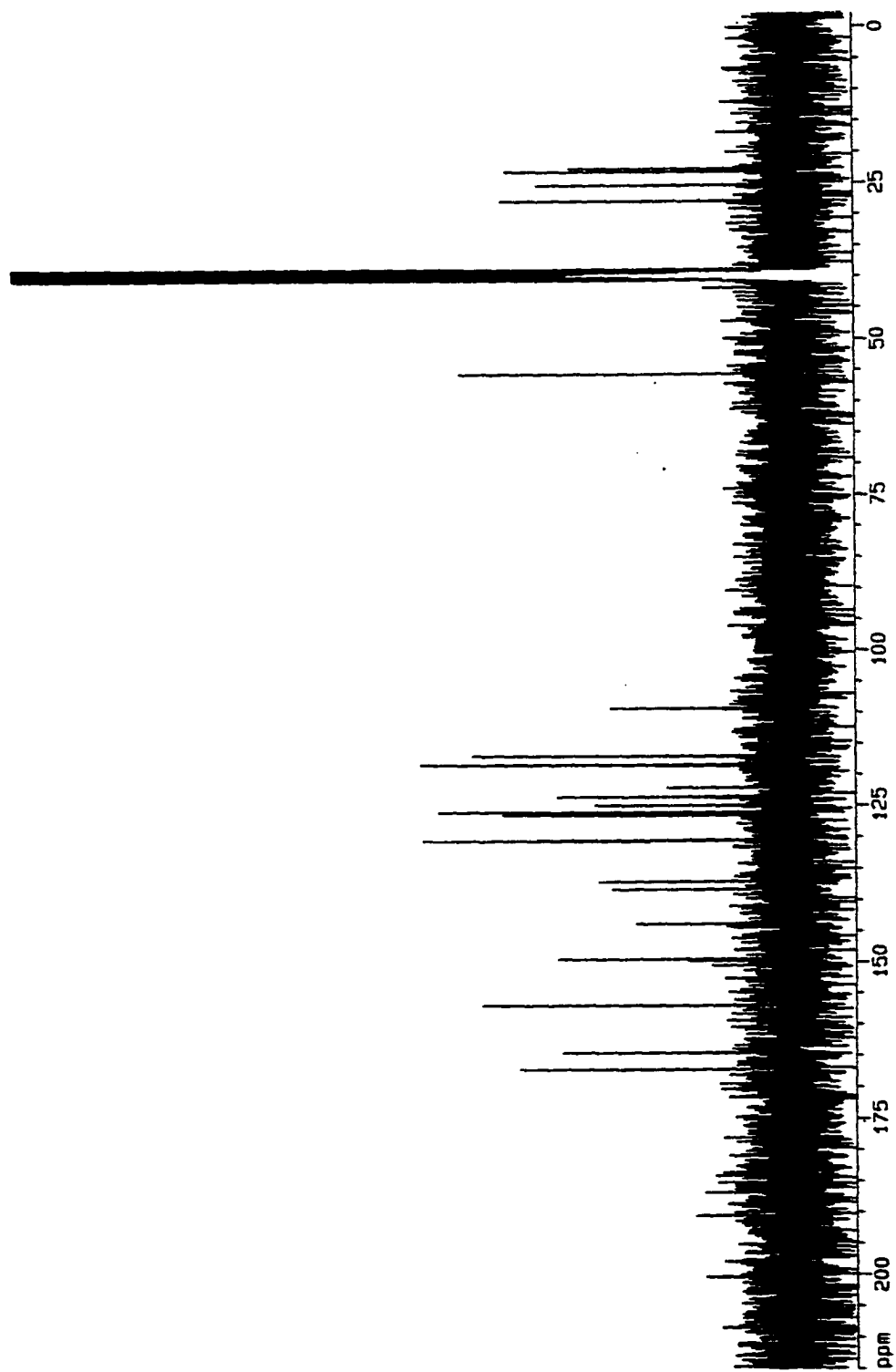


Figure 34. ^{13}C NMR (300 MHz) of Compound IV-17 (DMSO).



Figure 35. FTIR of Compound IV-17 (KBr).

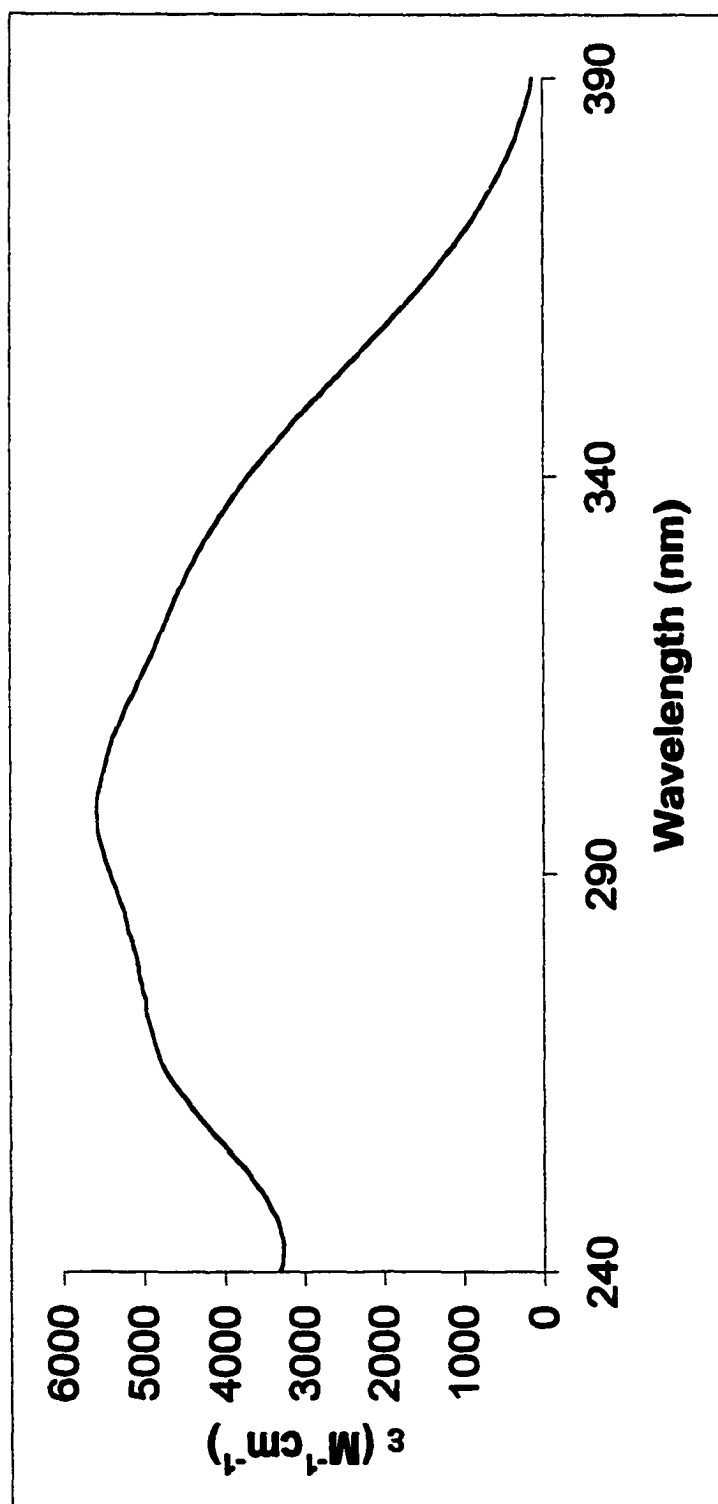


Figure 36. UV-Vis of Compound IV-17 (acetonitrile).

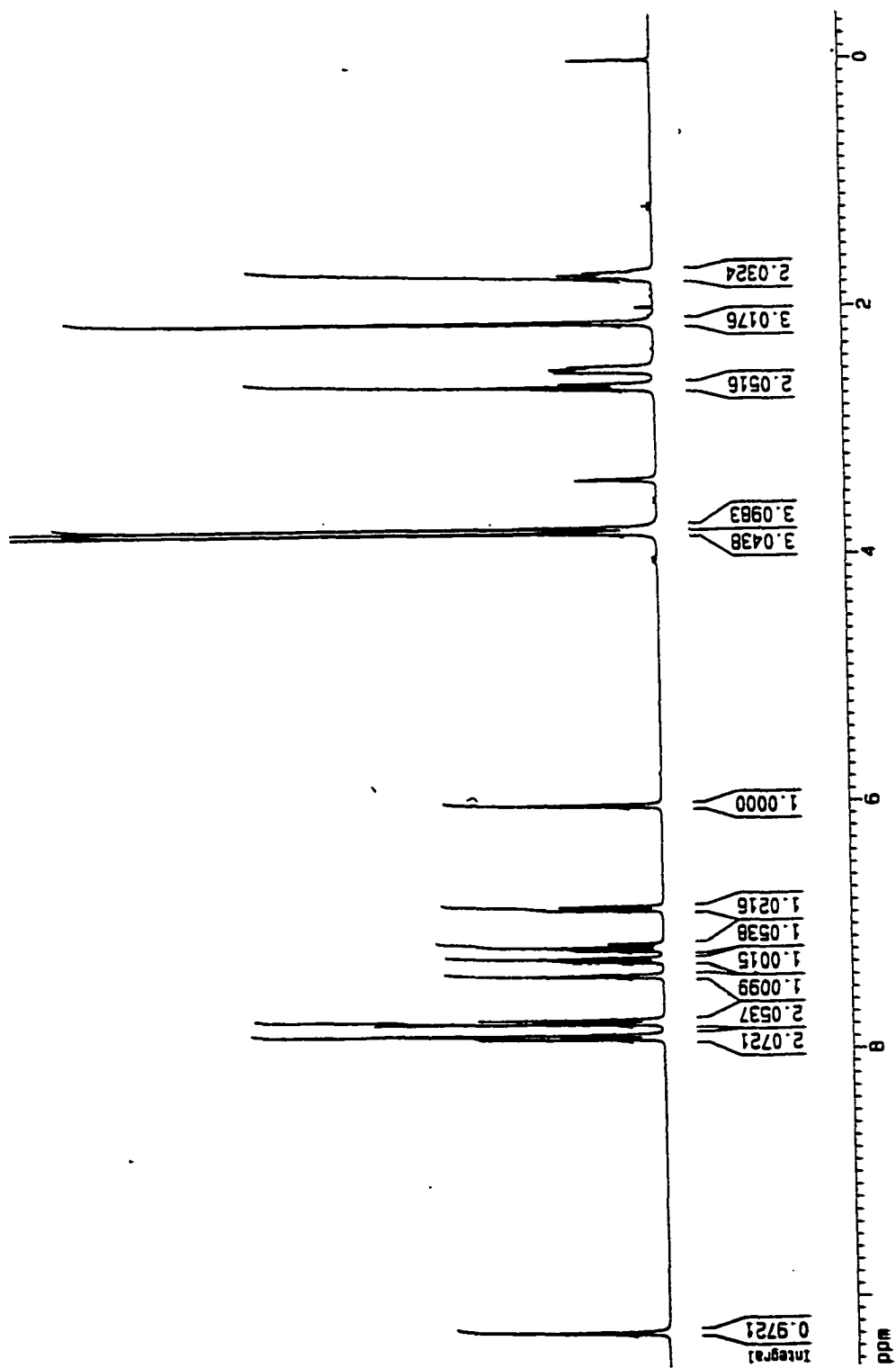


Figure 37. ¹H NMR (300 MHz) of Compound IV-18 (DMSO).

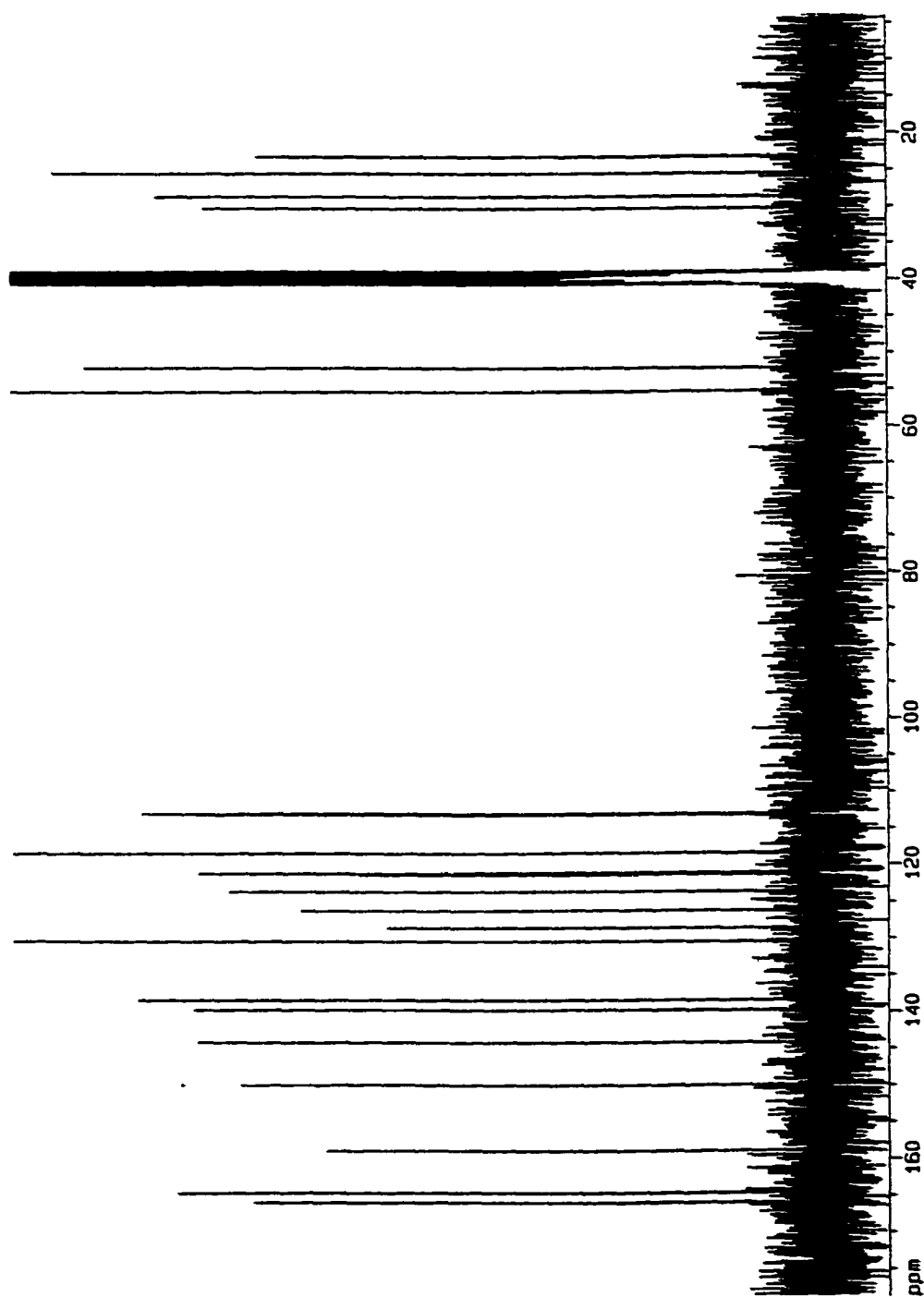


Figure 38. ^{13}C NMR (300 MHz) of Compound IV-18 (DMSO).

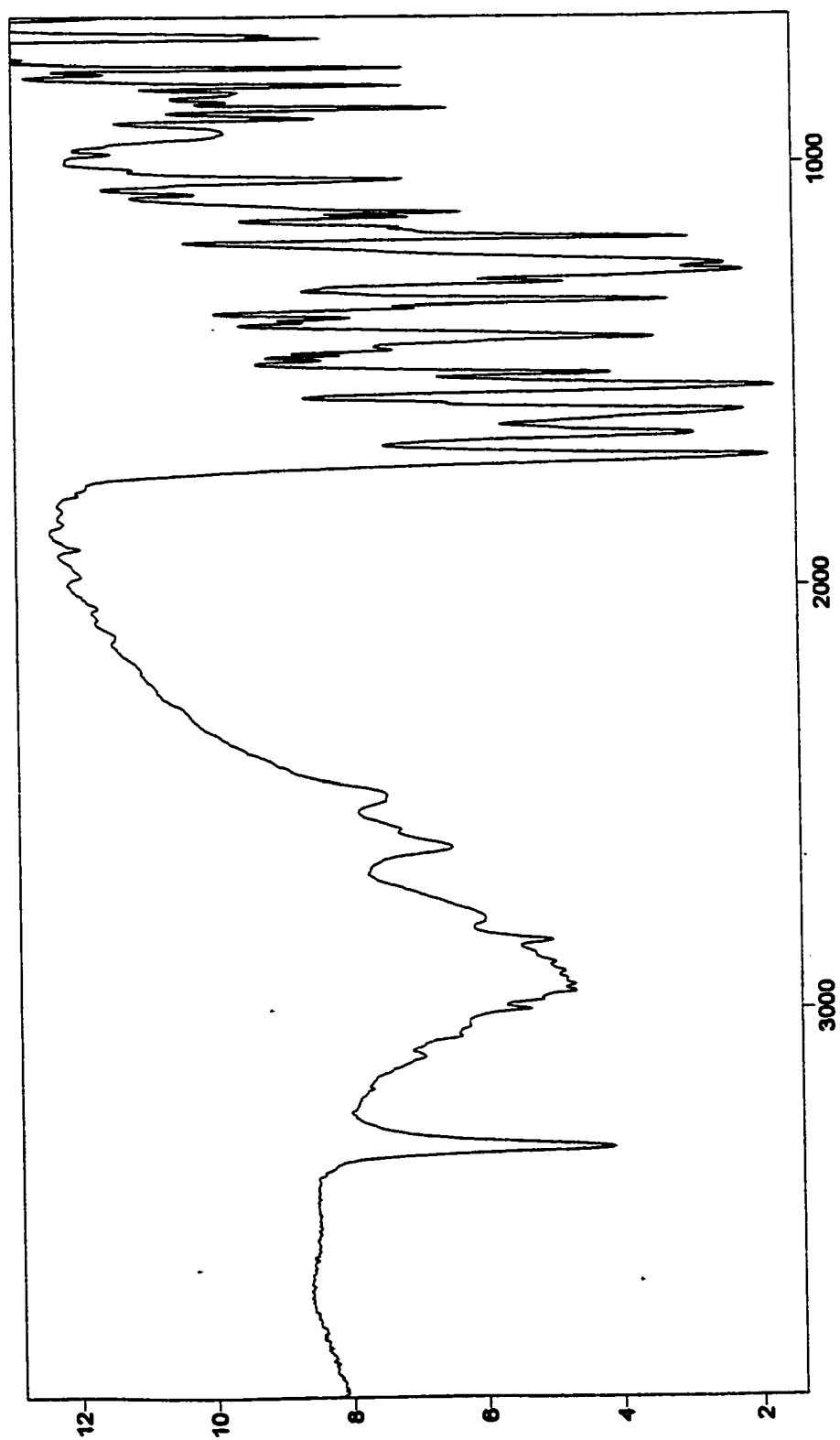


Figure 39. FTIR of Compound IV-18 (KBr).

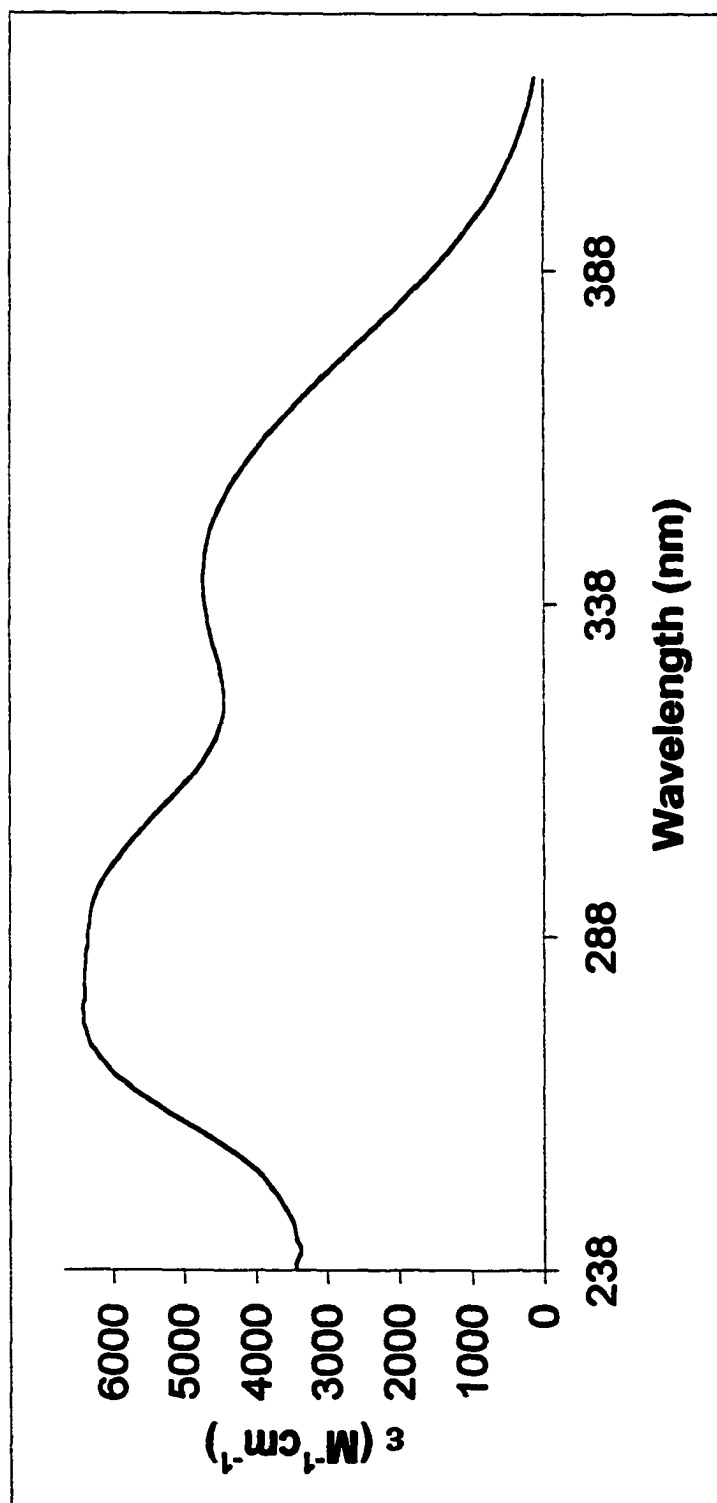


Figure 40. UV-Vis of Compound **IV-18** (acetonitrile).

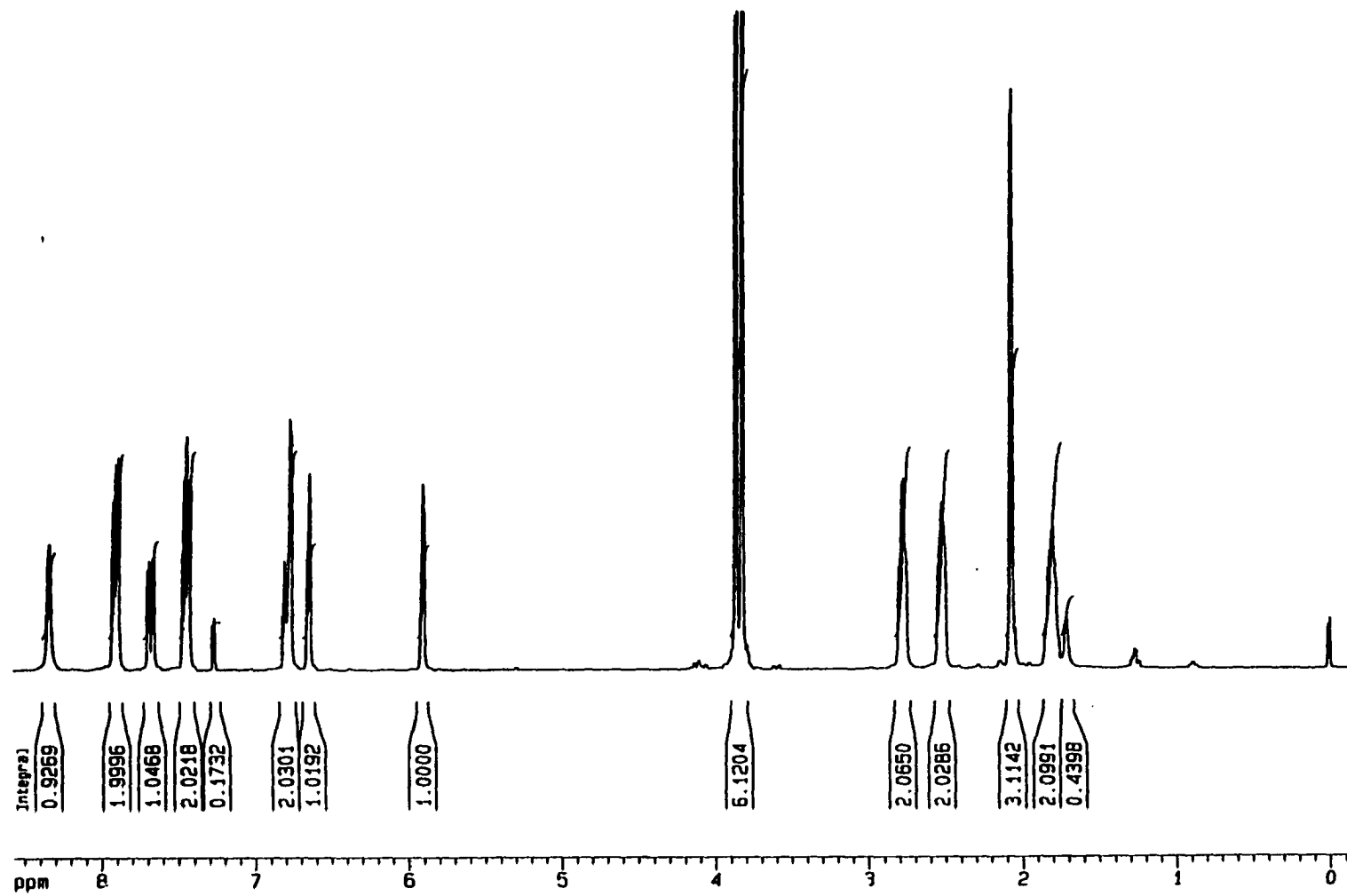


Figure 41. ^1H NMR (300 MHz) of Compound IV-19 (DMSO).

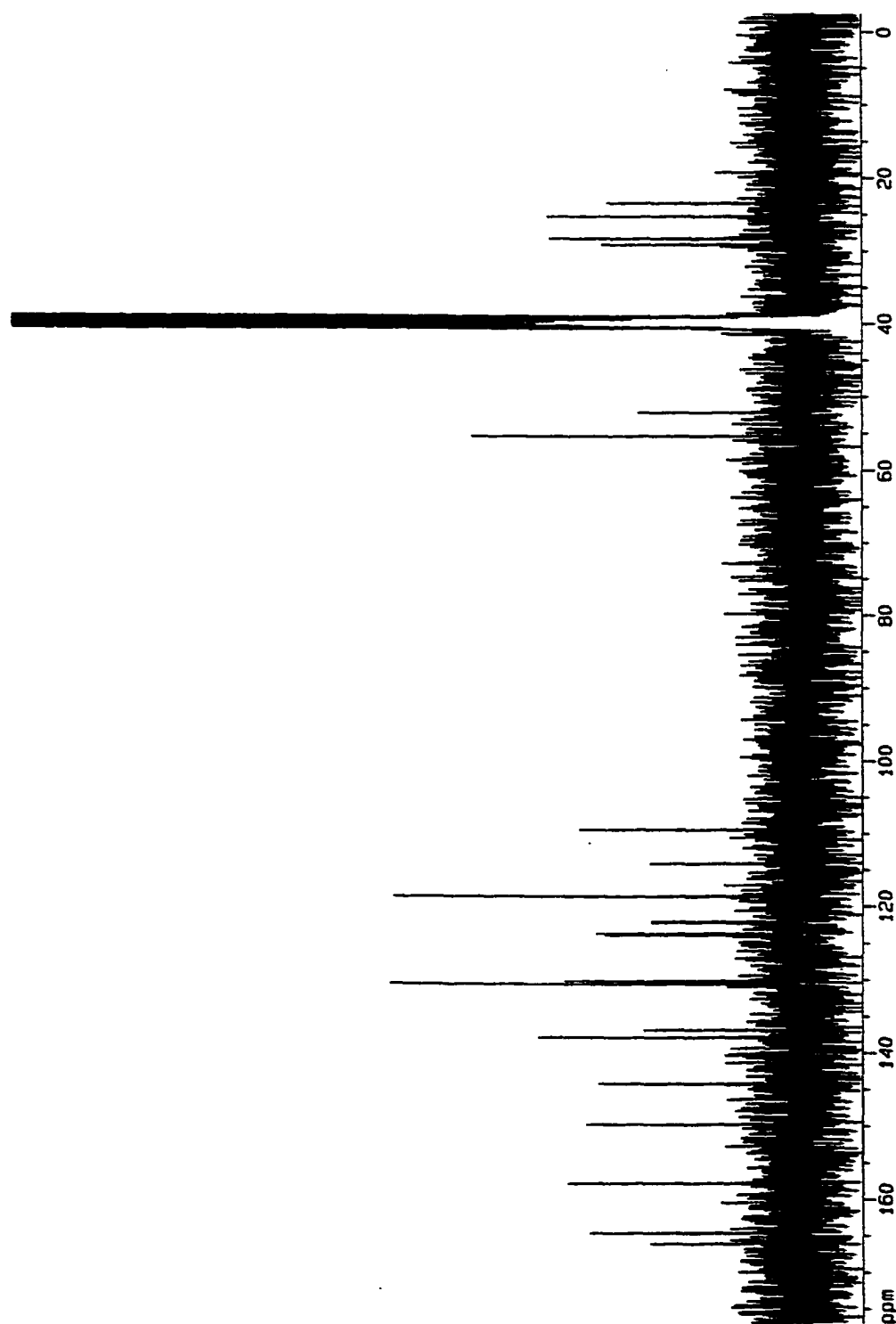


Figure 42. ^{13}C NMR (300 MHz) of Compound IV-19 (DMSO).

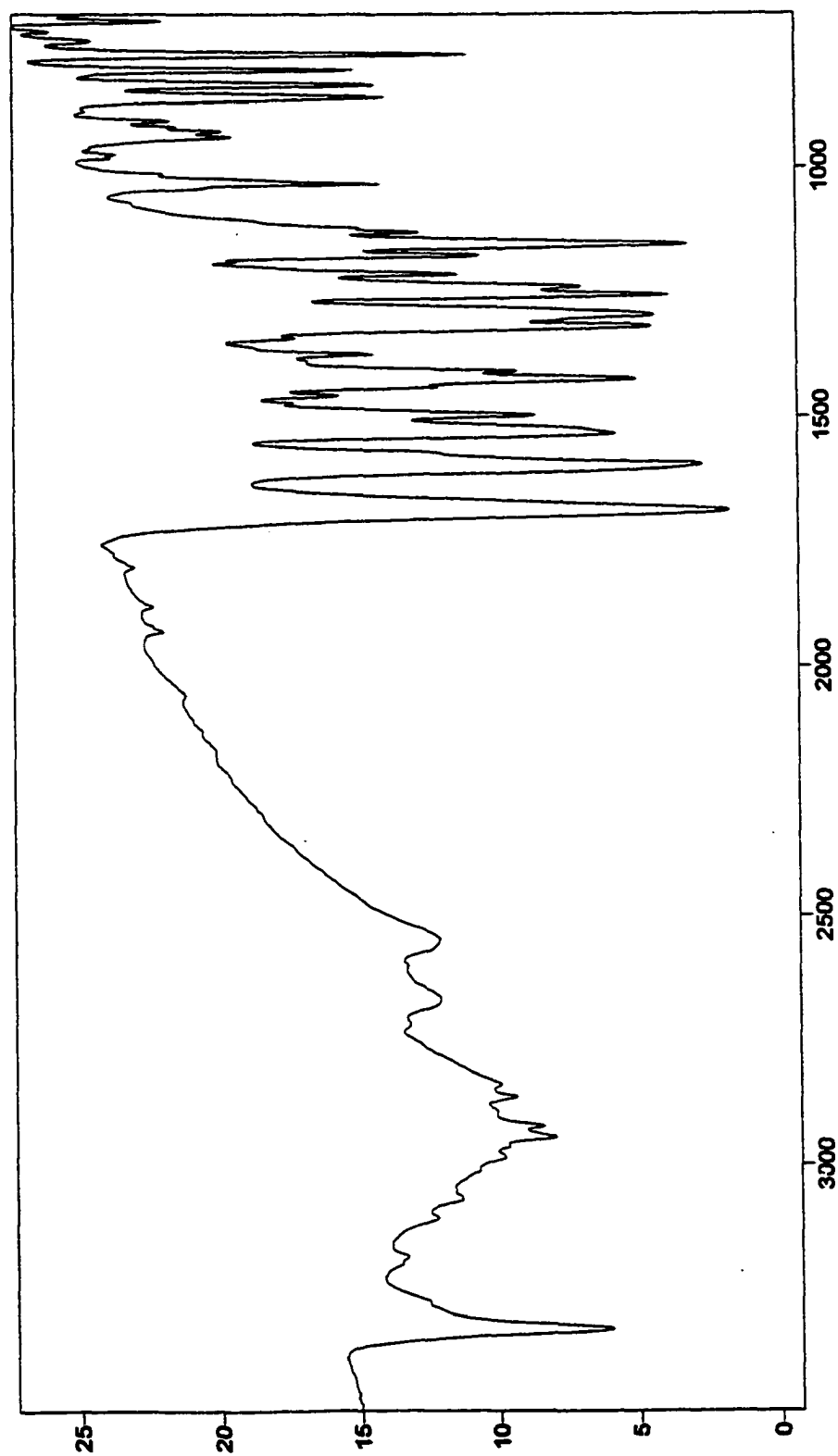


Figure 43. FTIR of Compound IV-19 (KBr).

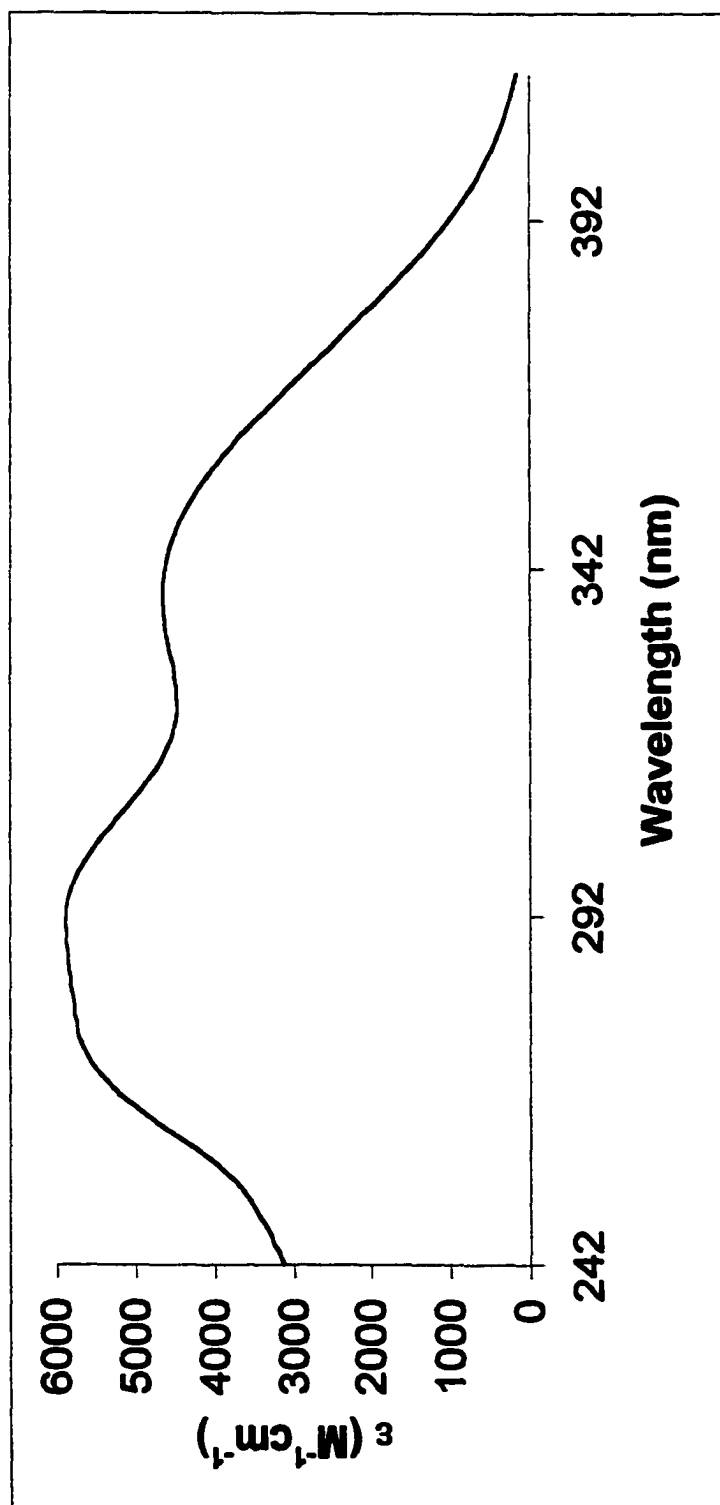


Figure 44. UV-Vis of Compound IV-19 (acetonitrile).

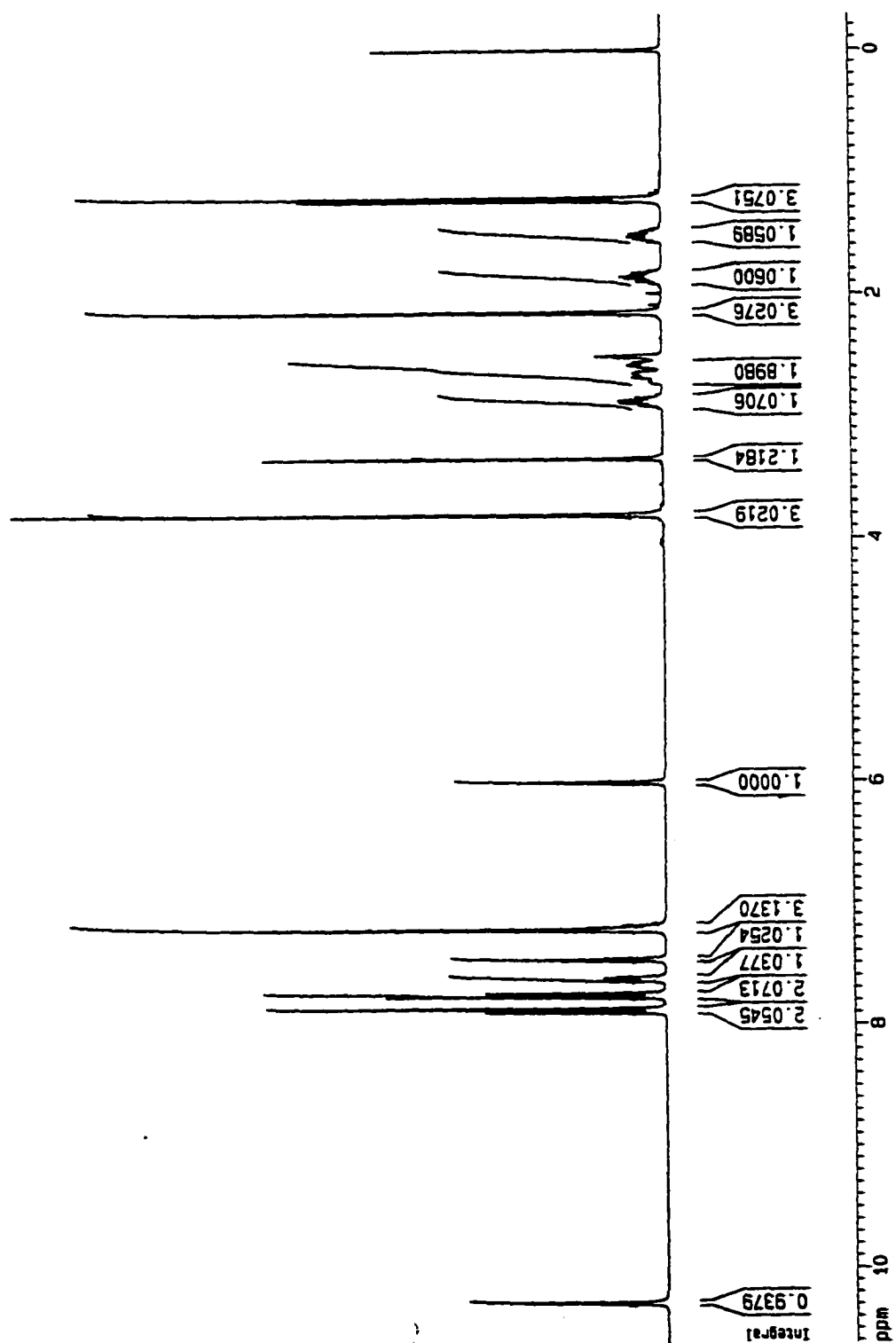


Figure 45. ¹H NMR (300 MHz) of Compound IV-20 (DMSO).

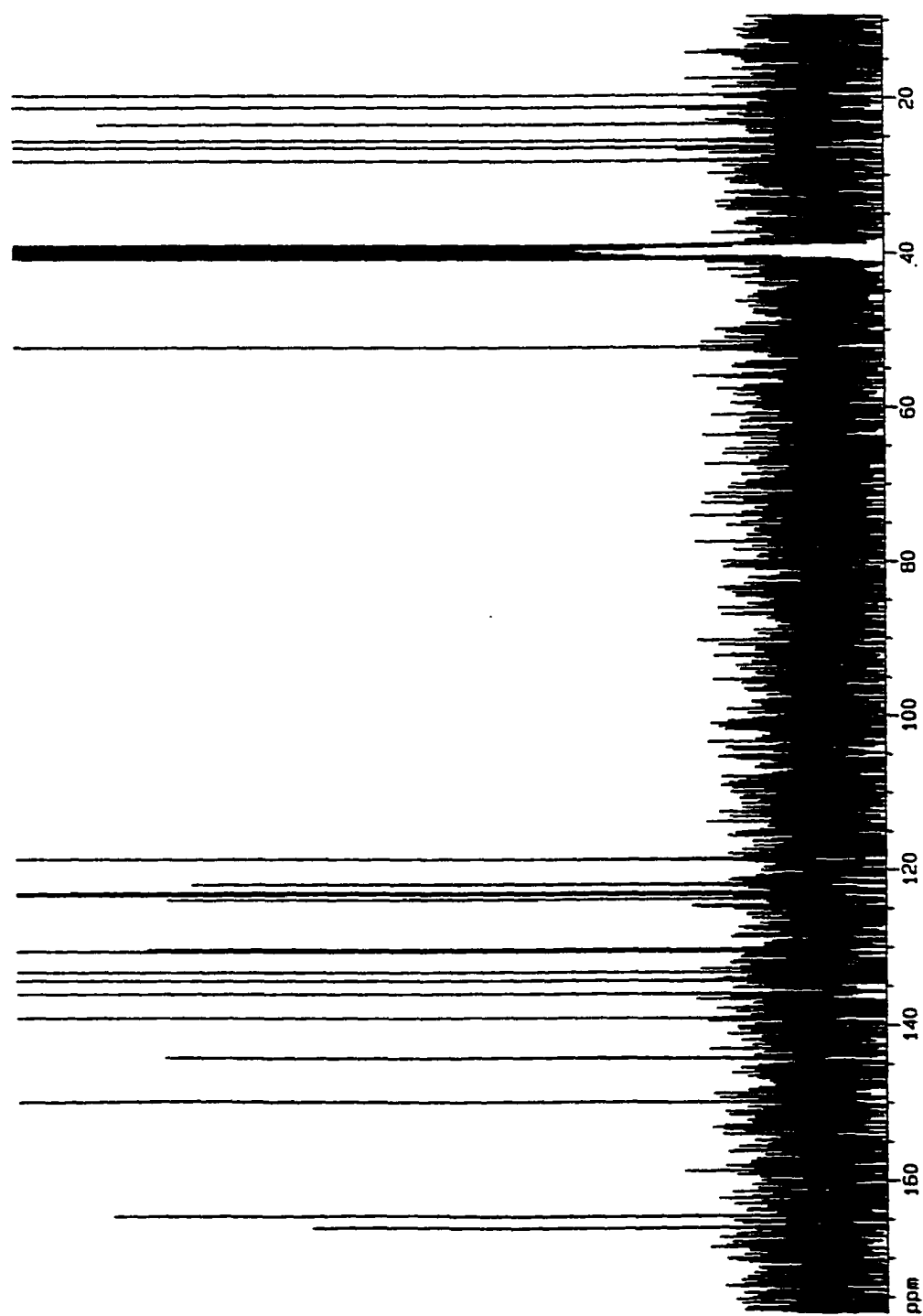


Figure 46. ^{13}C NMR (300 MHz) of Compound IV-20 (DMSO).

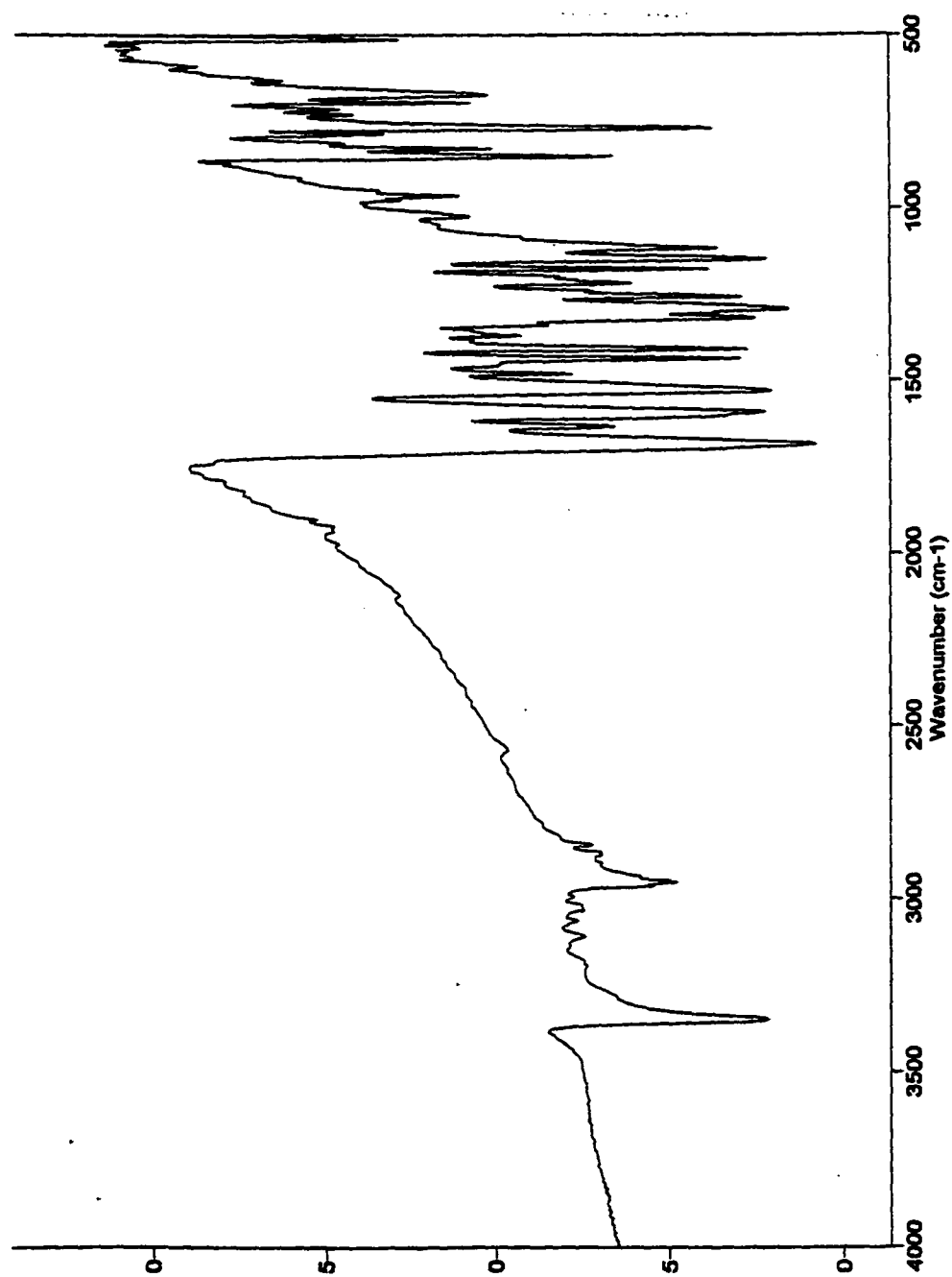


Figure 47. FTIR of Compound IV-20 (KBr).

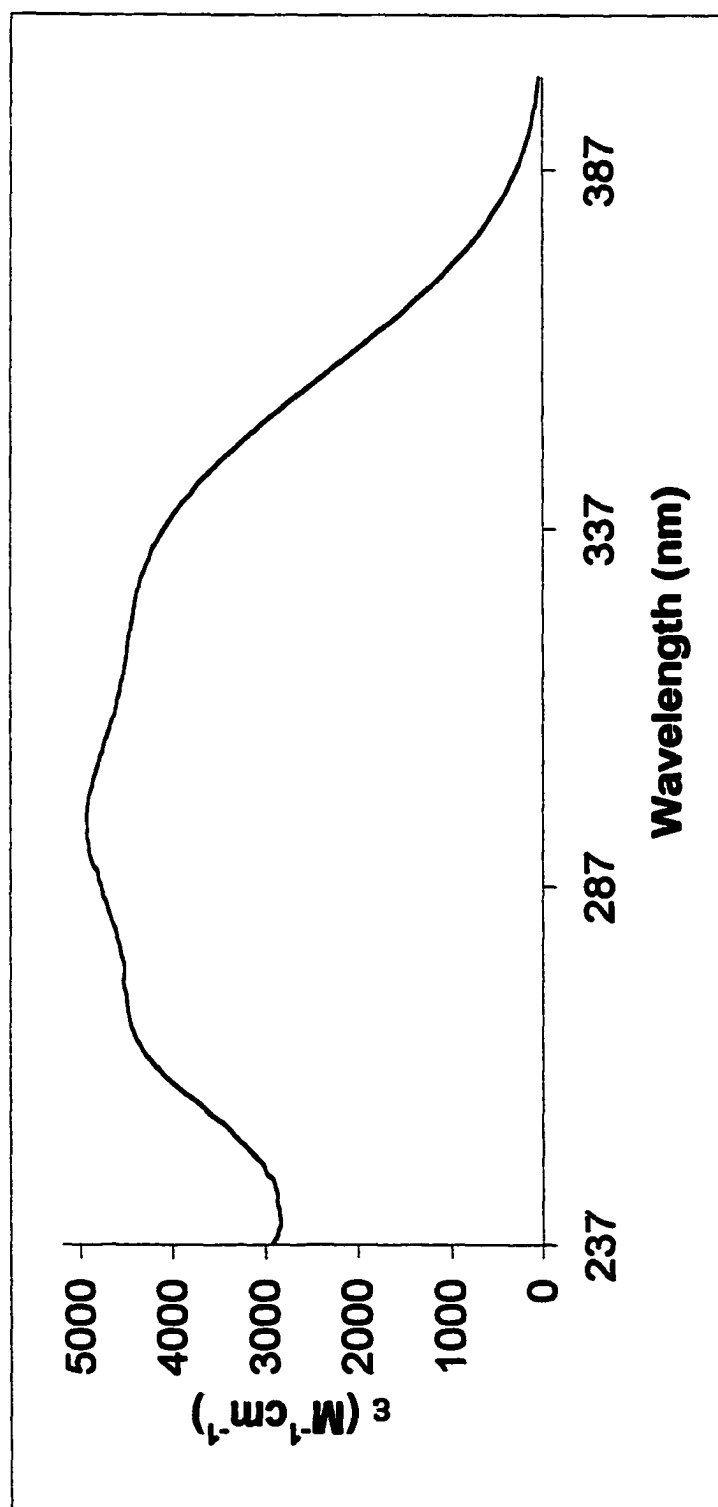
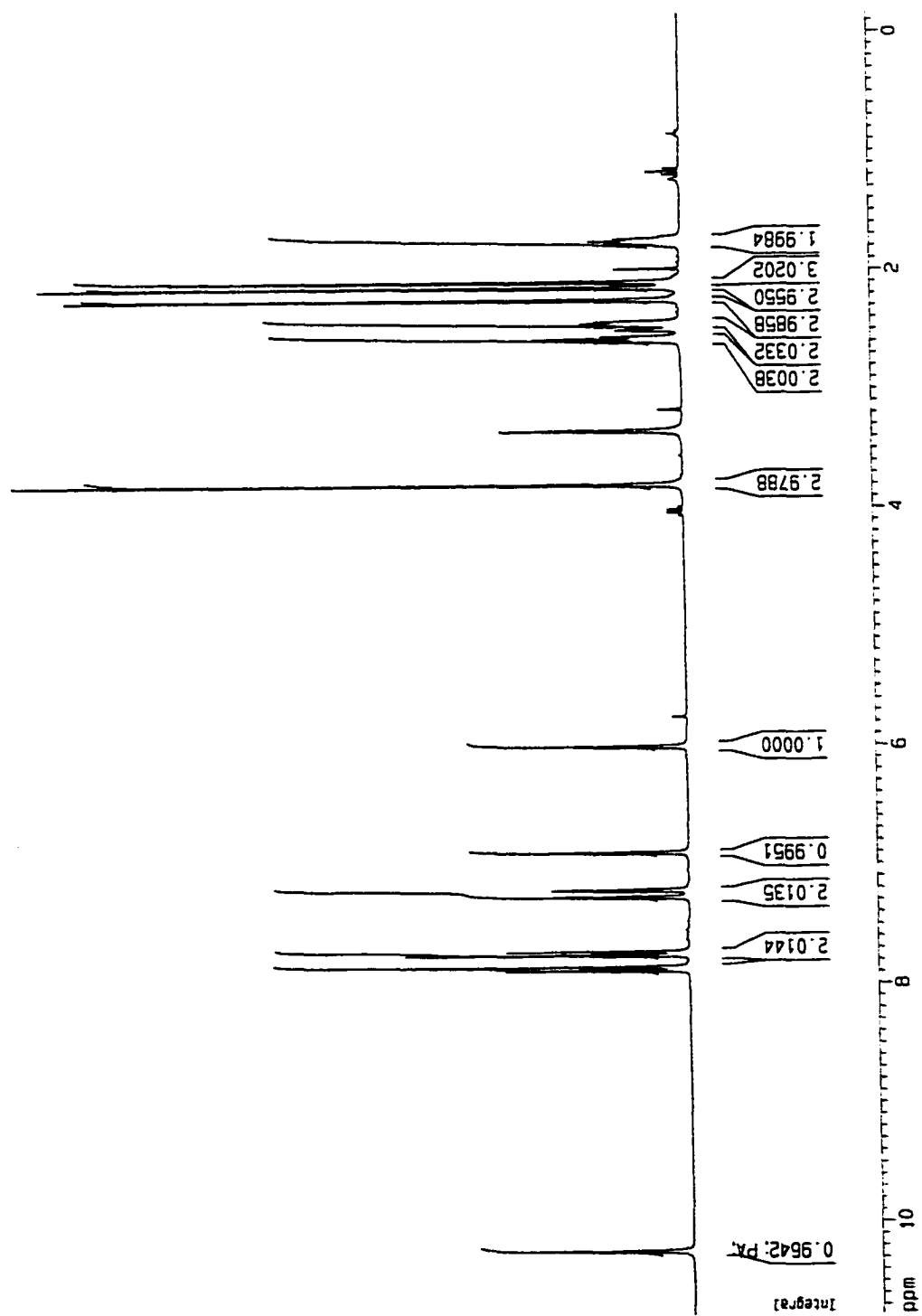


Figure 48. UV-Vis of Compound IV-20 (acetonitrile).



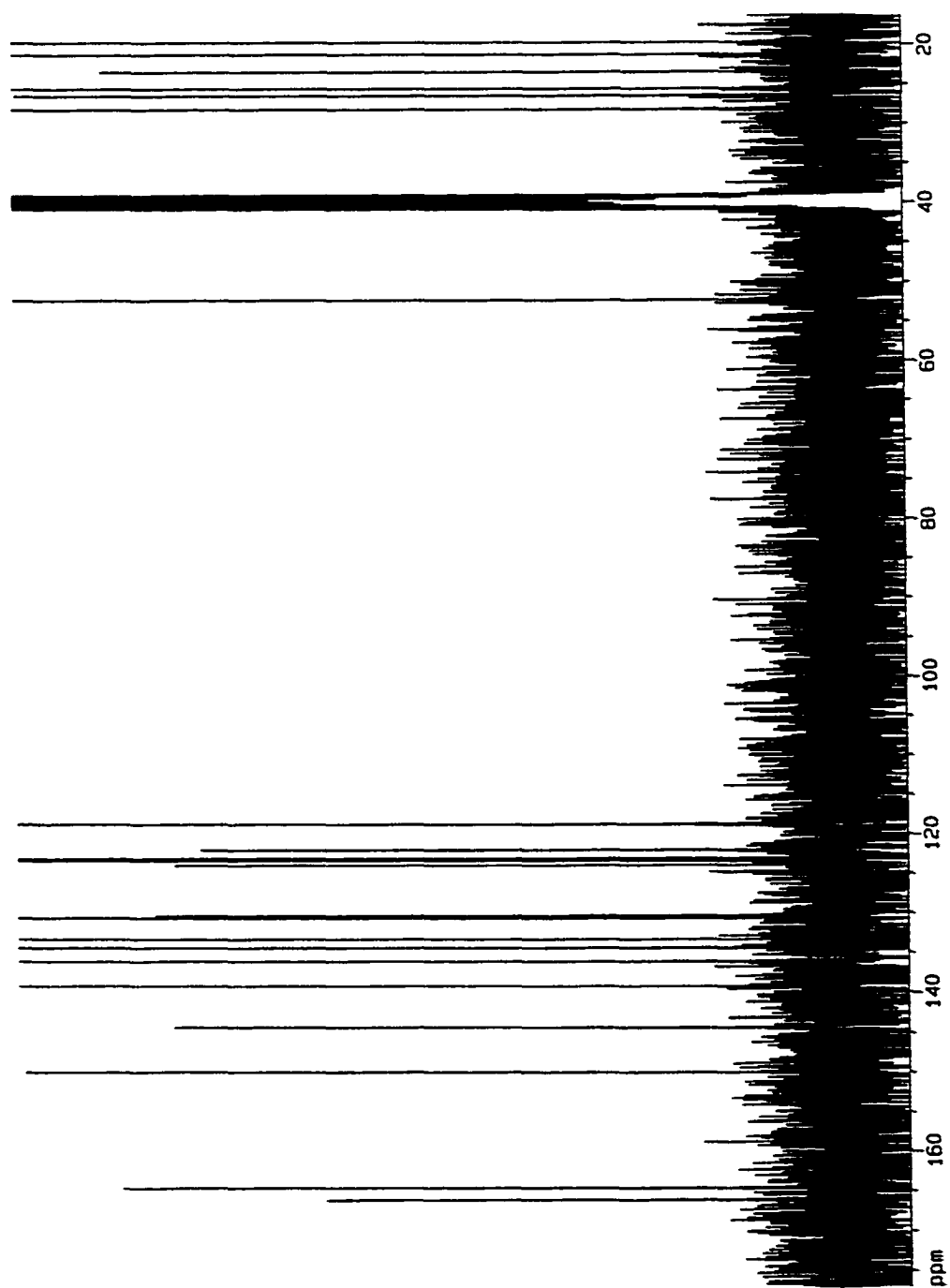


Figure 50. ^{13}C NMR (300 MHz) of Compound IV-21 (DMSO).

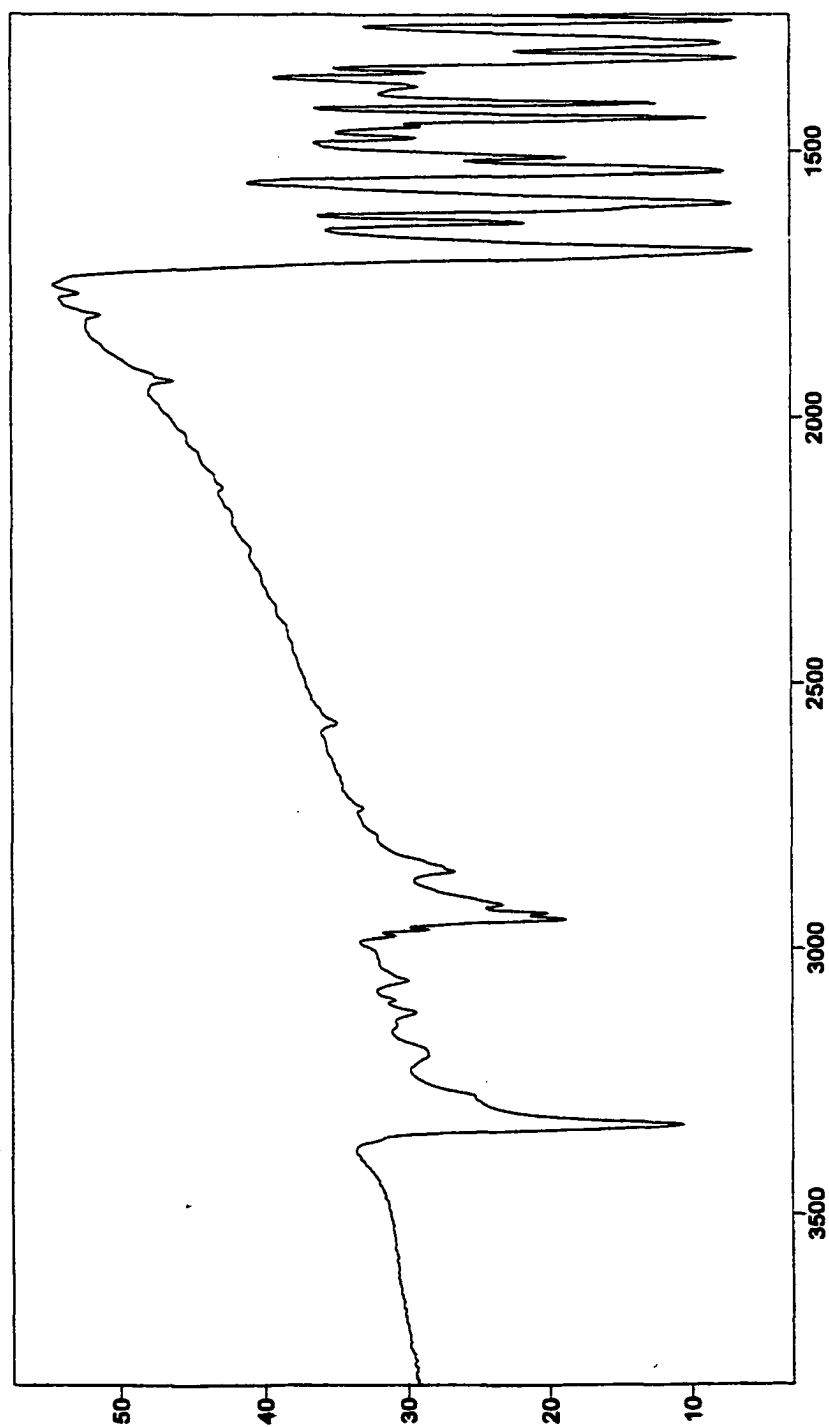


Figure 51. FTIR of Compound IV-21 (KBr).

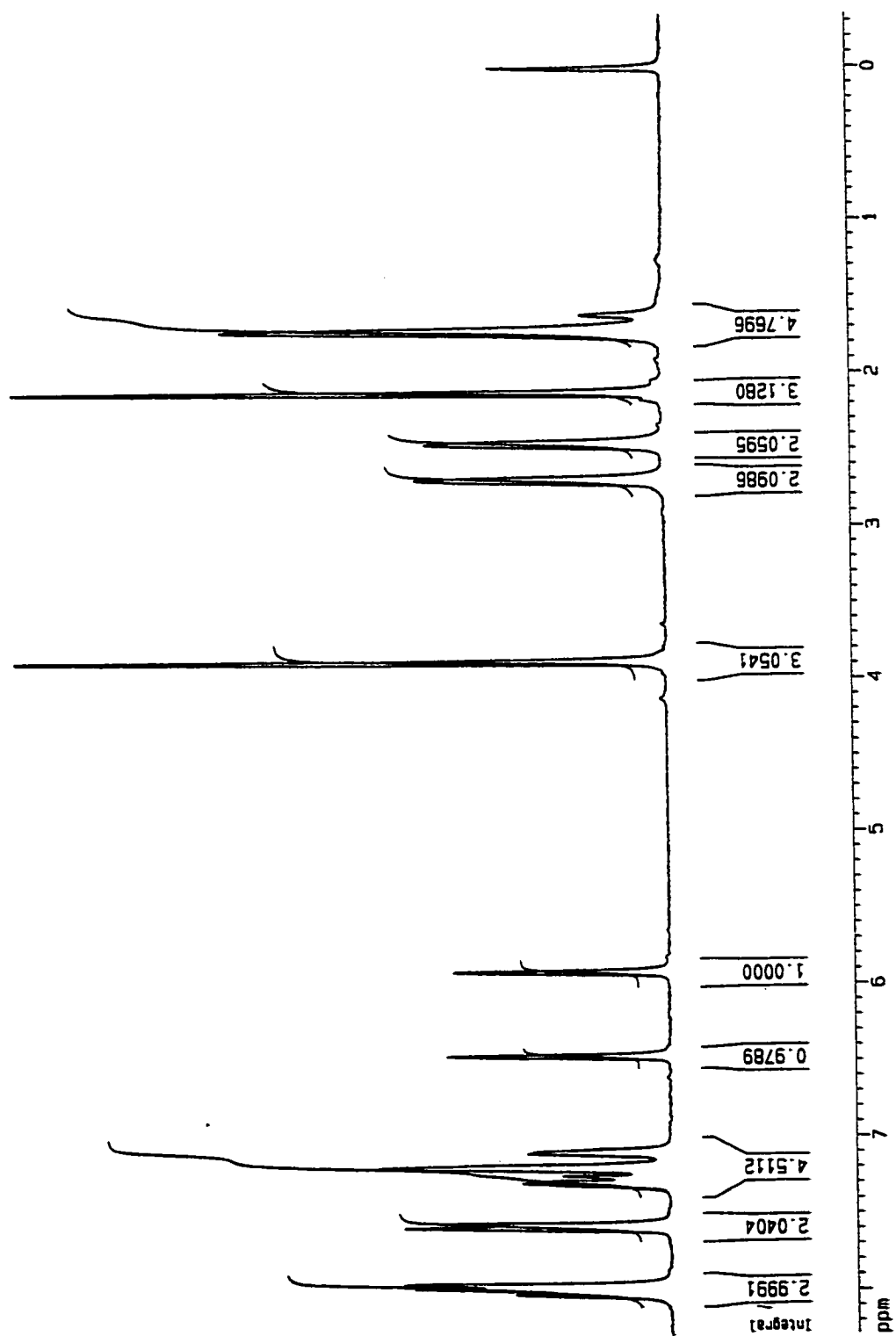


Figure 53. ^1H NMR (300 MHz) of Compound IV-22 (DMSO).

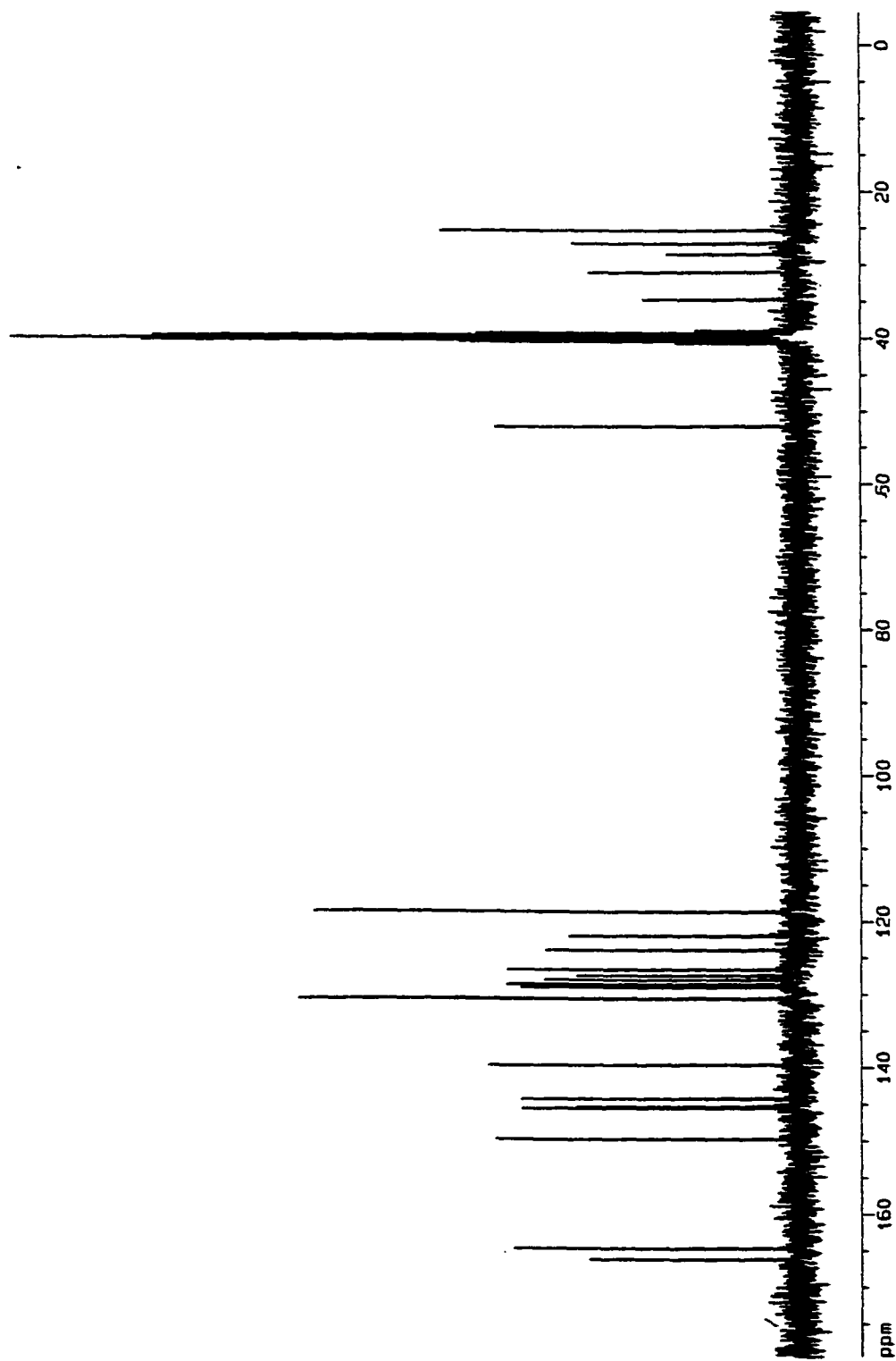


Figure 54. ^{13}C NMR (300 MHz) of Compound IV-22 (DMSO).

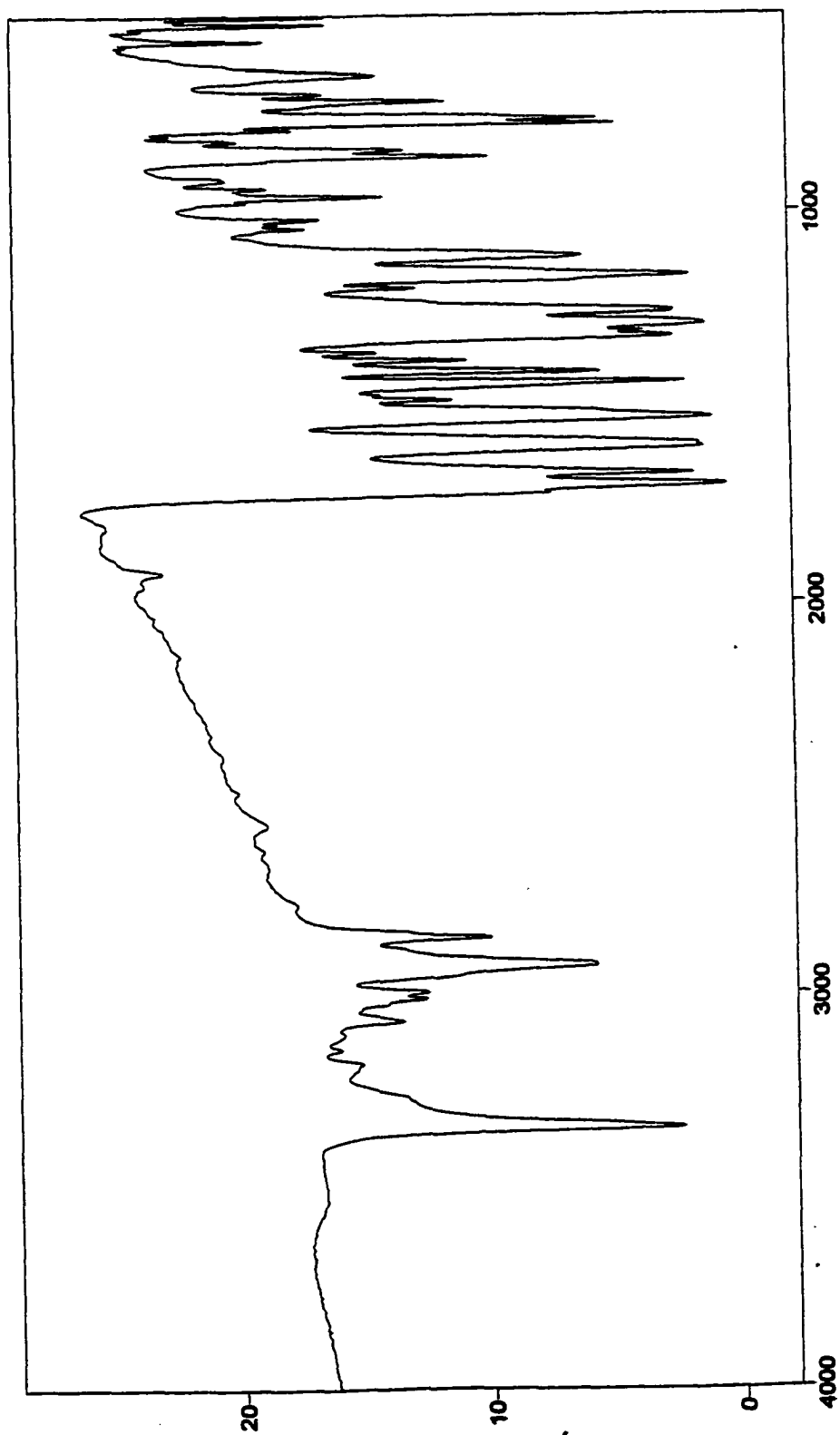


Figure 55. FTIR of Compound IV-22 (KBr).

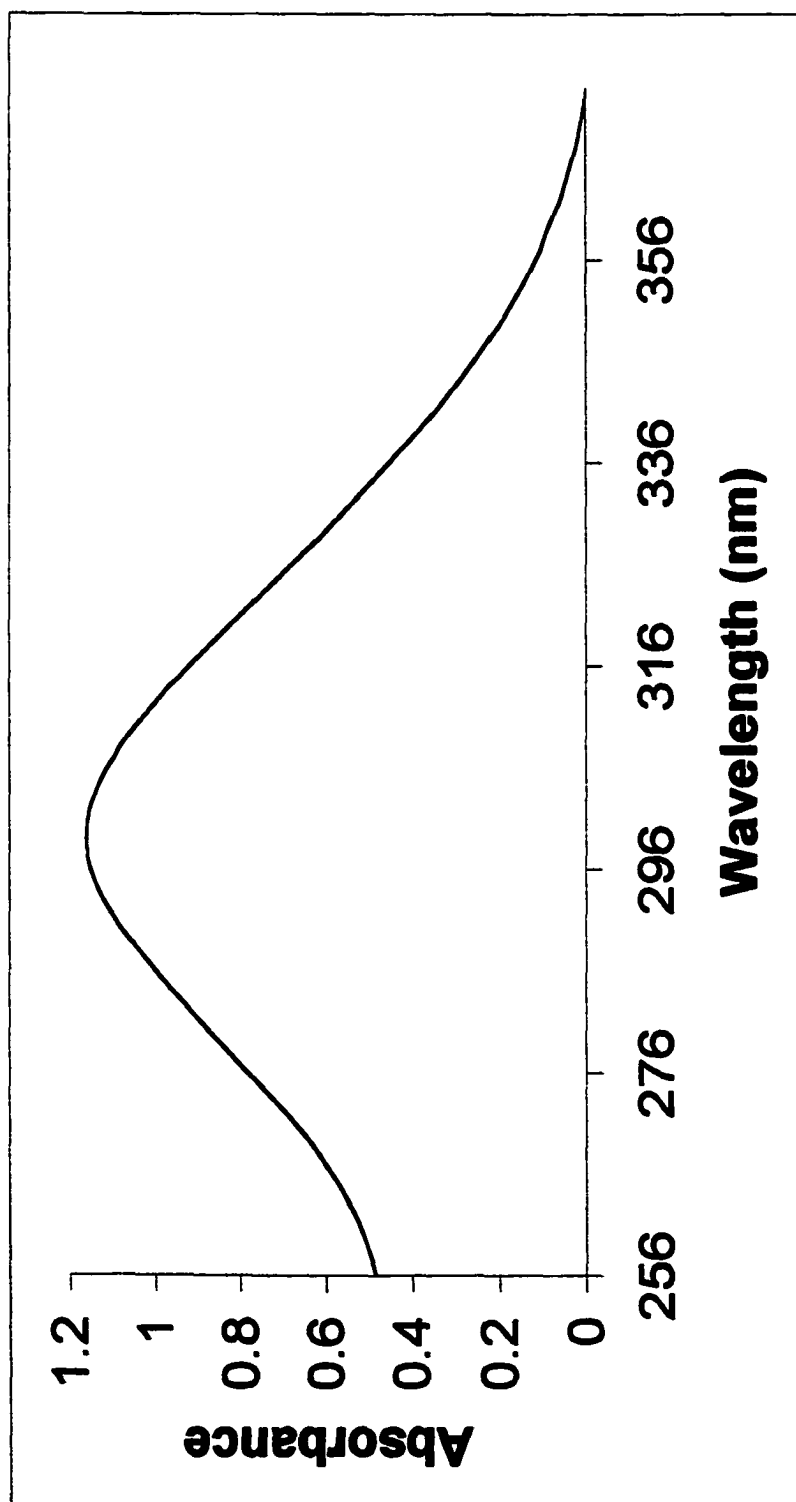


Figure 56. UV-Vis of Compound IV-22 (MeOH).

APPENDIX E

Spectroscopic Data for Compounds in “Unpublished Data”

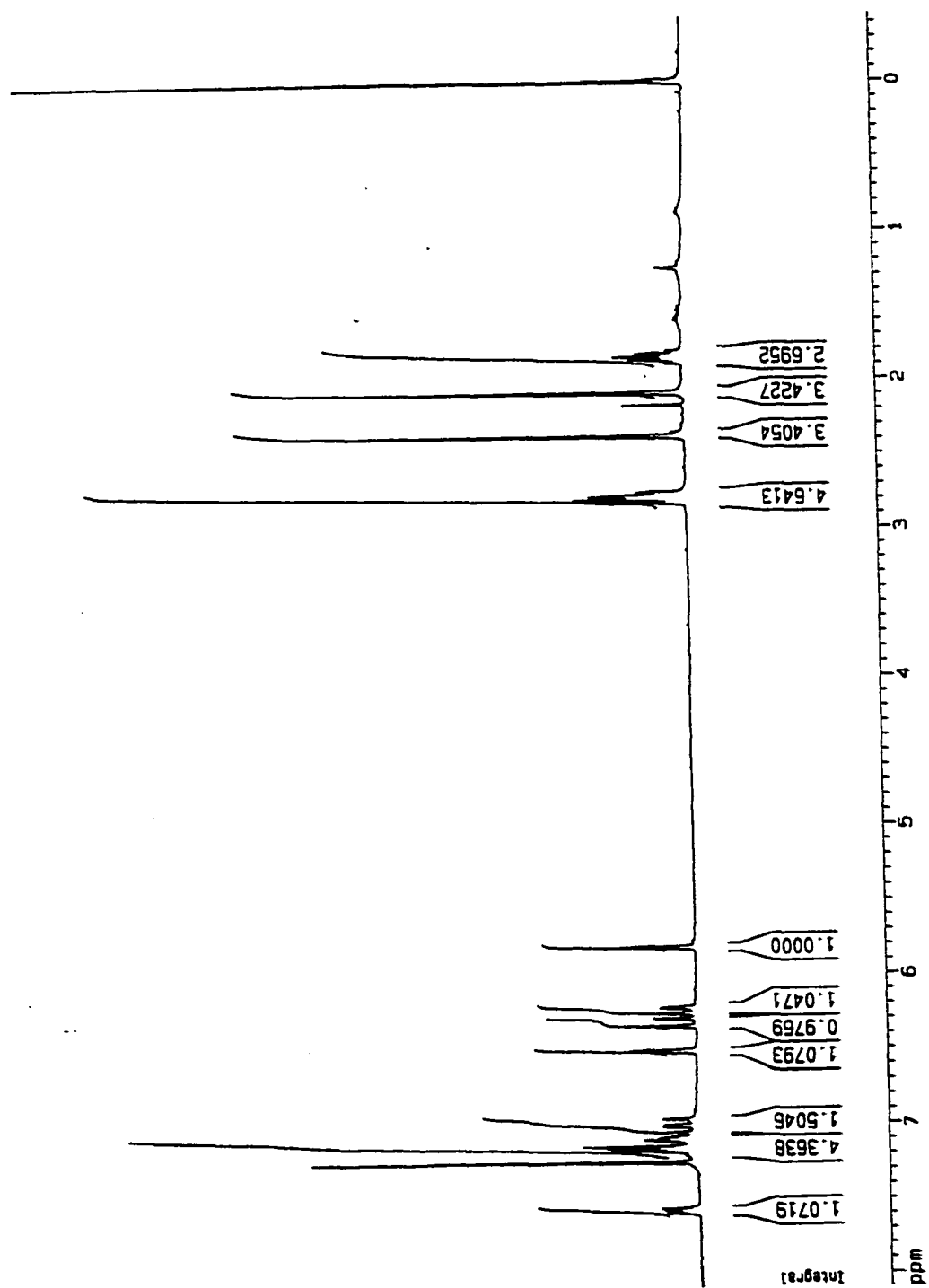


Figure 1. ¹H NMR (300 MHz) of Compound V-5 (CDCl₃).

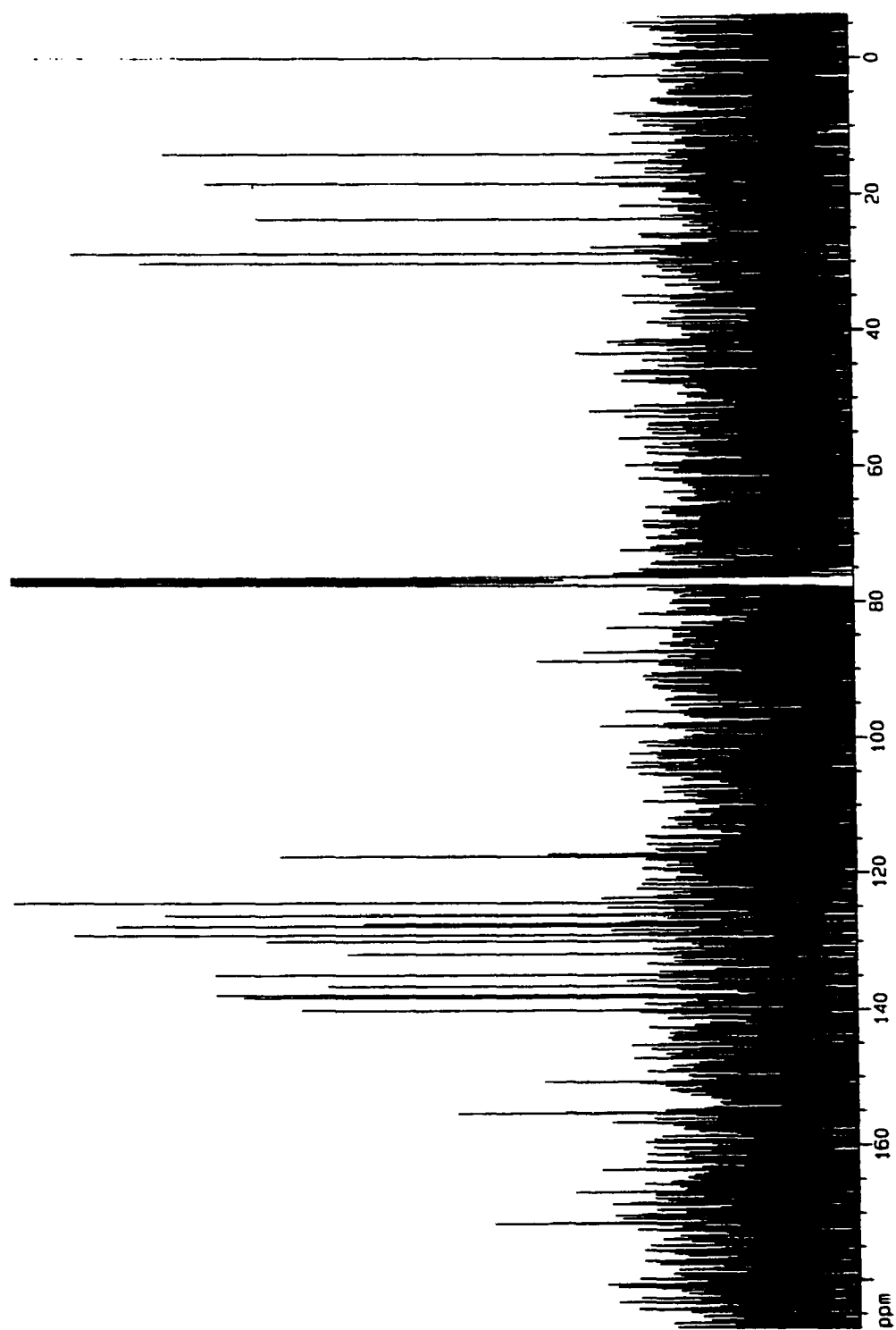


Figure 2. ^{13}C NMR (300 MHz) of Compound V-5 (CDCl_3).

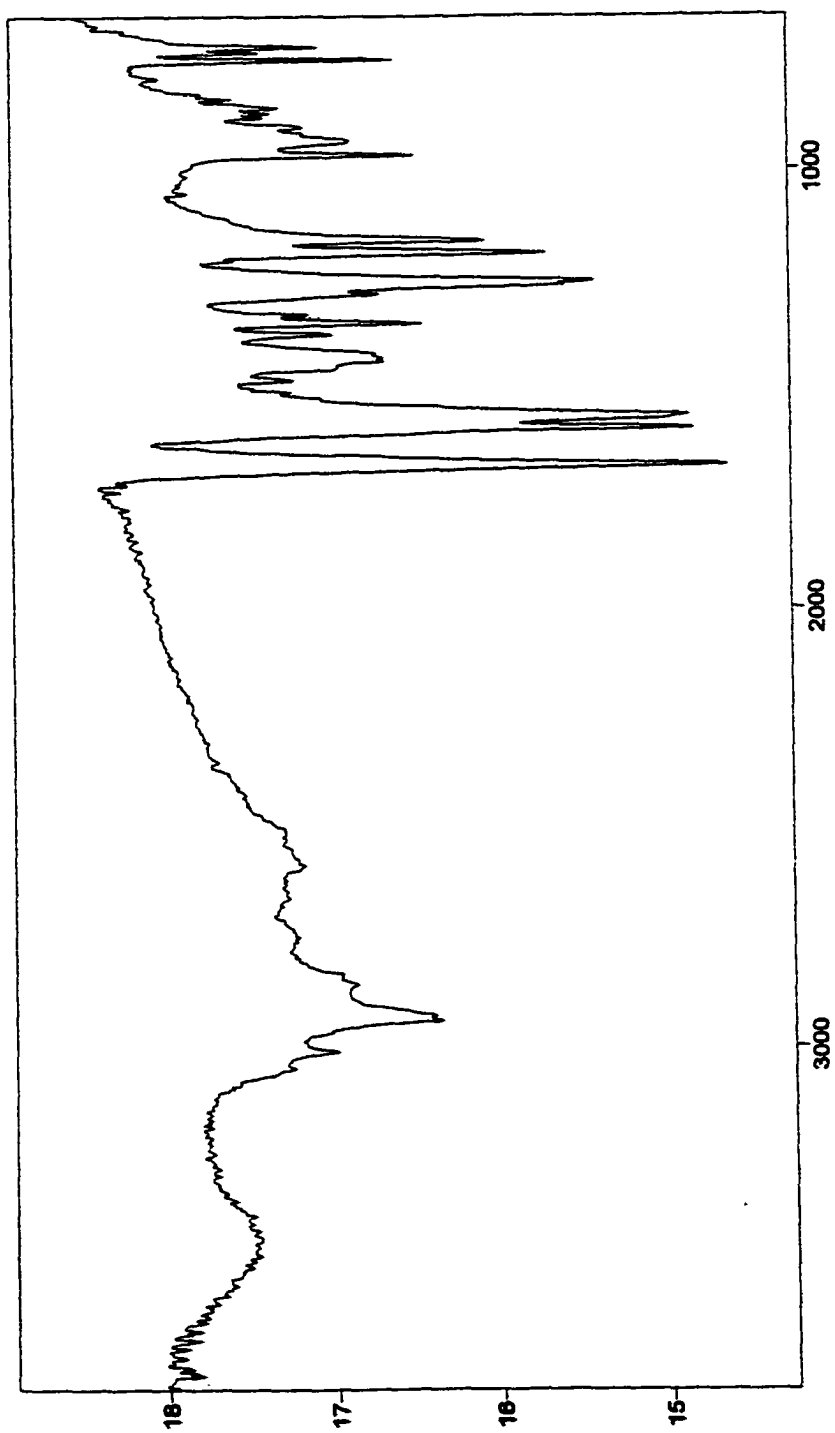


Figure 3. FTIR of Compound V-5 (KBr).

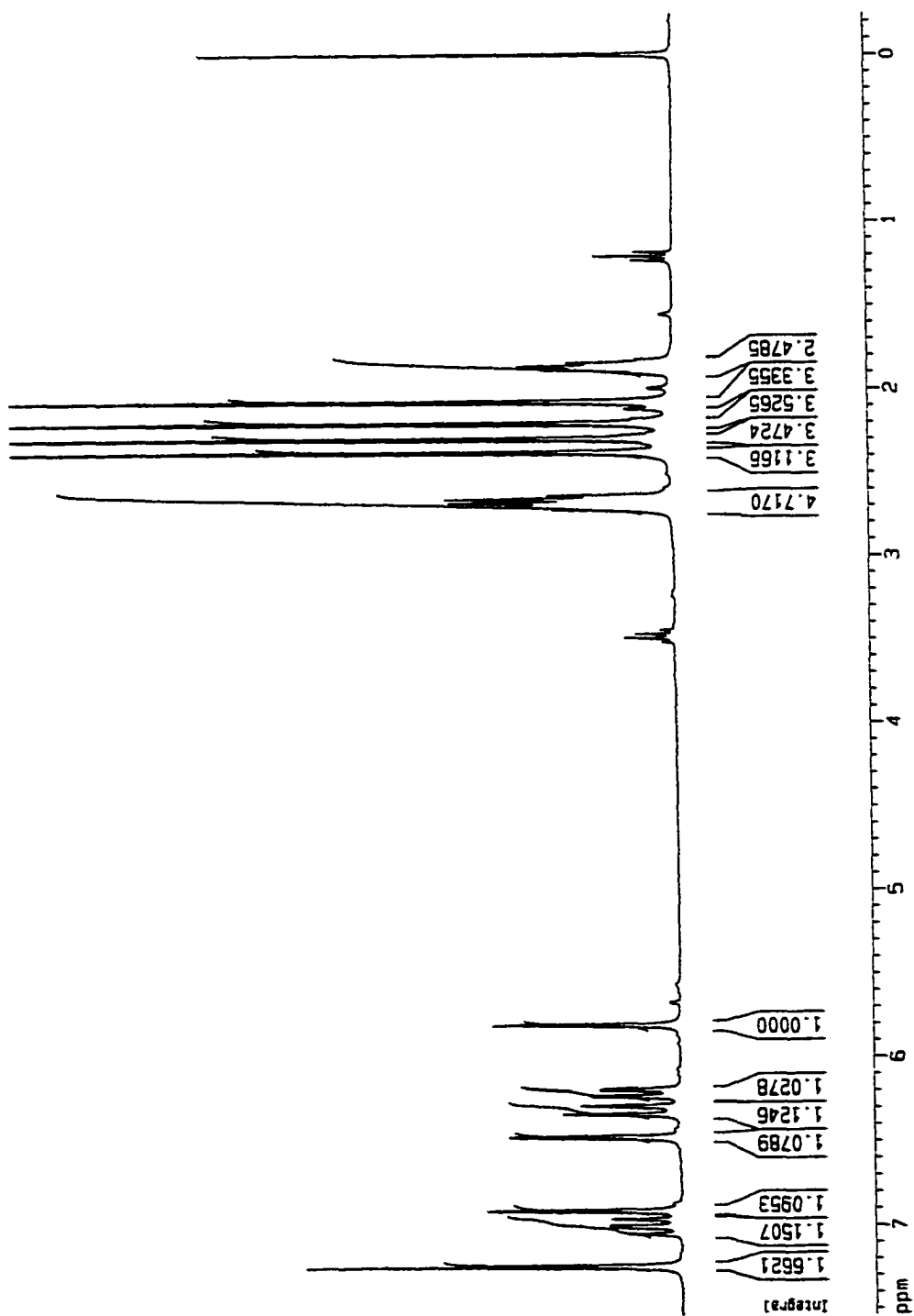


Figure 4. ^1H NMR (300 MHz) of Compound V-7 (CDCl_3).

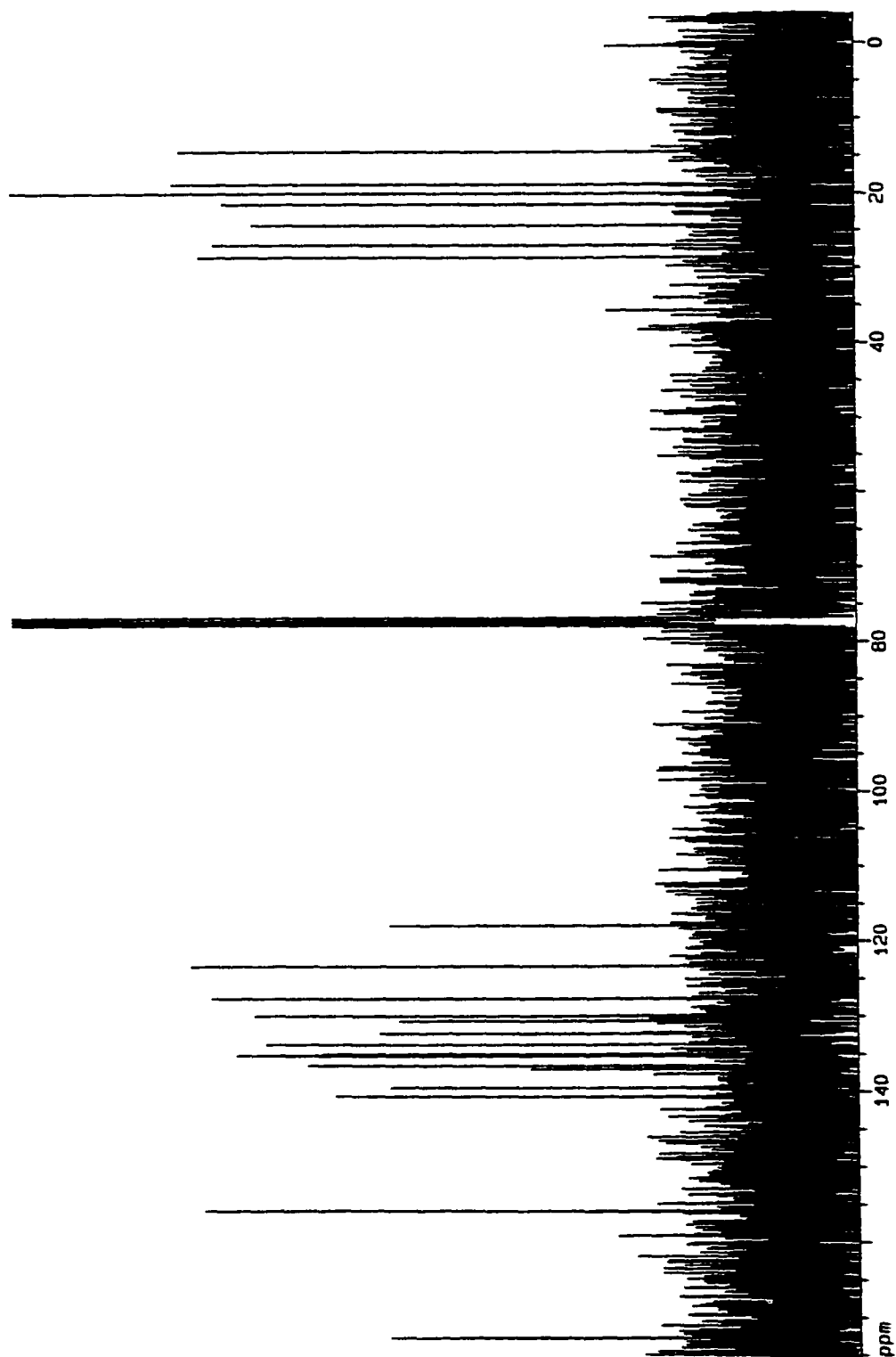


Figure 5. ^{13}C NMR (300 MHz) of Compound V-7 (CDCl_3).

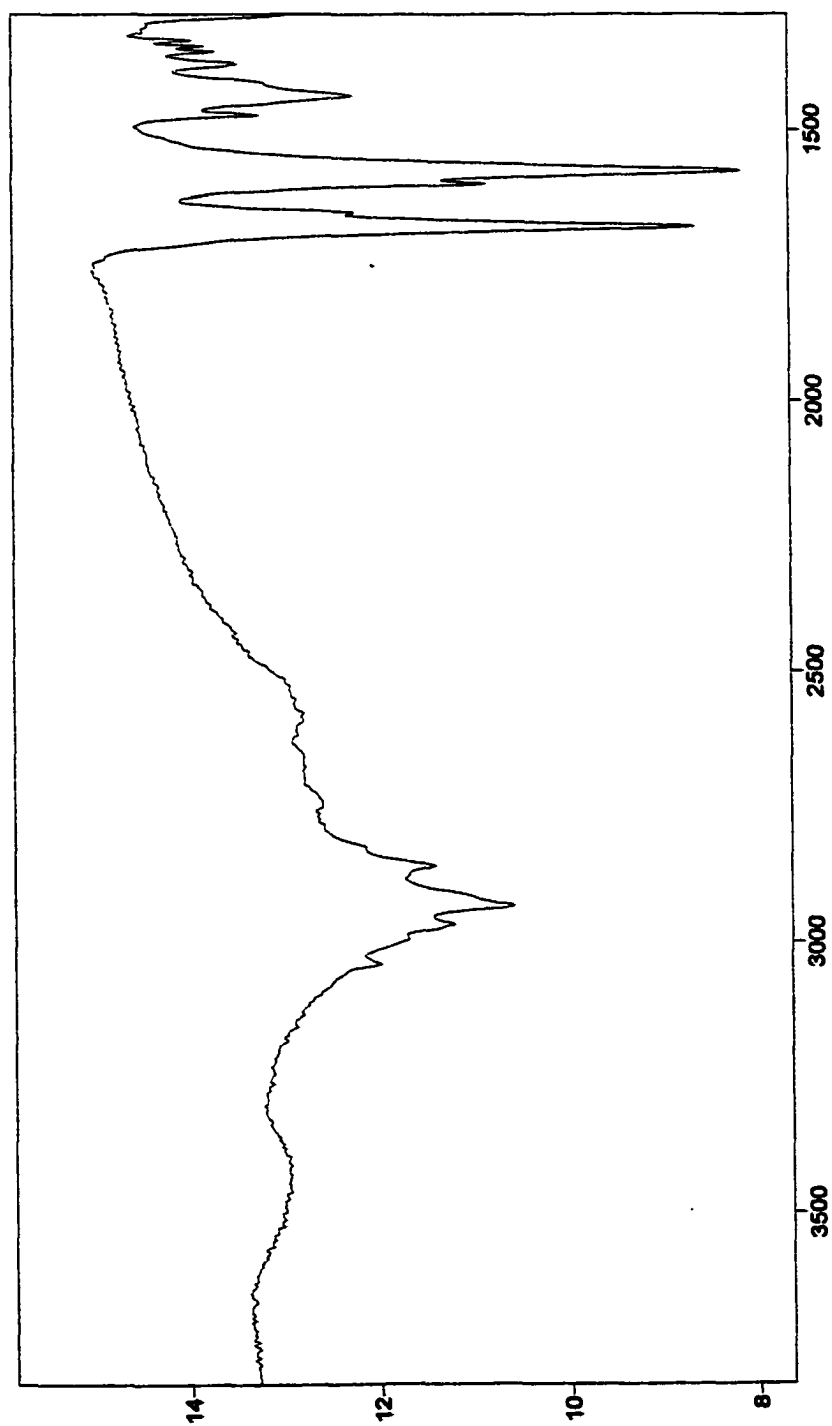


Figure 6. FTIR of Compound V-7 (KBr).

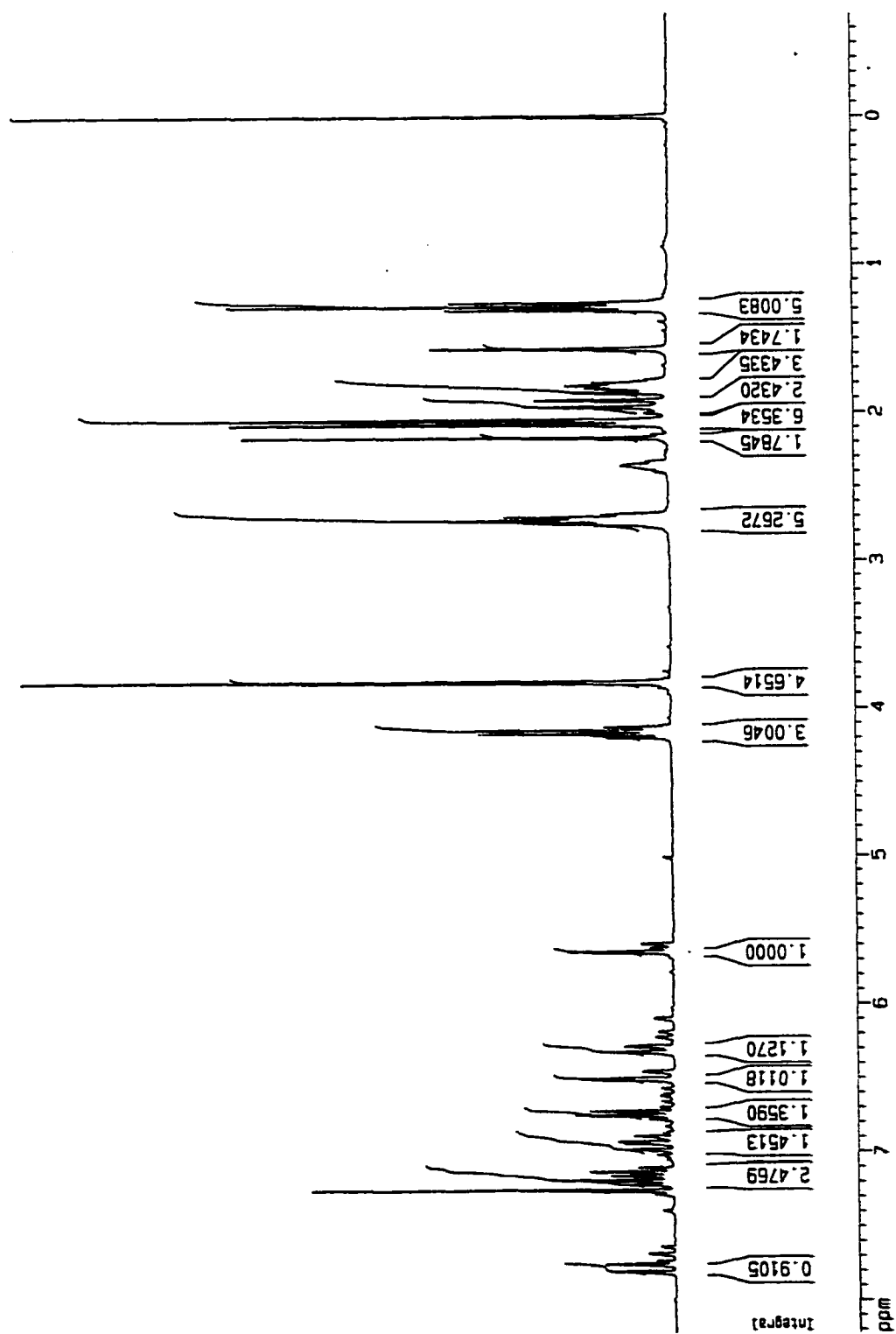


Figure 7. ¹H NMR (300 MHz) of Compound V-14 (CDCl₃).

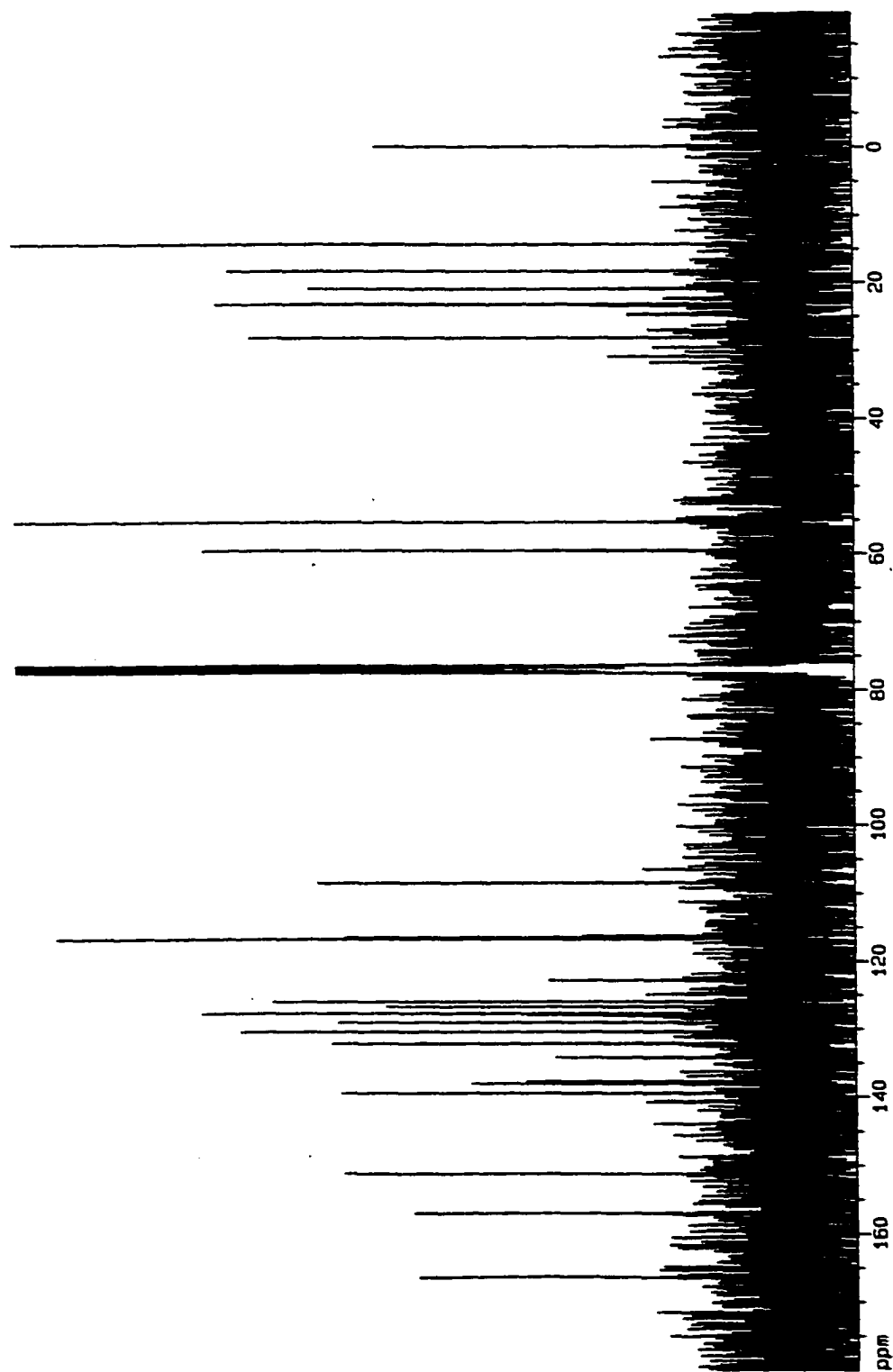


Figure 8. ^{13}C NMR (300 MHz) of Compound V-14 (CDCl_3).

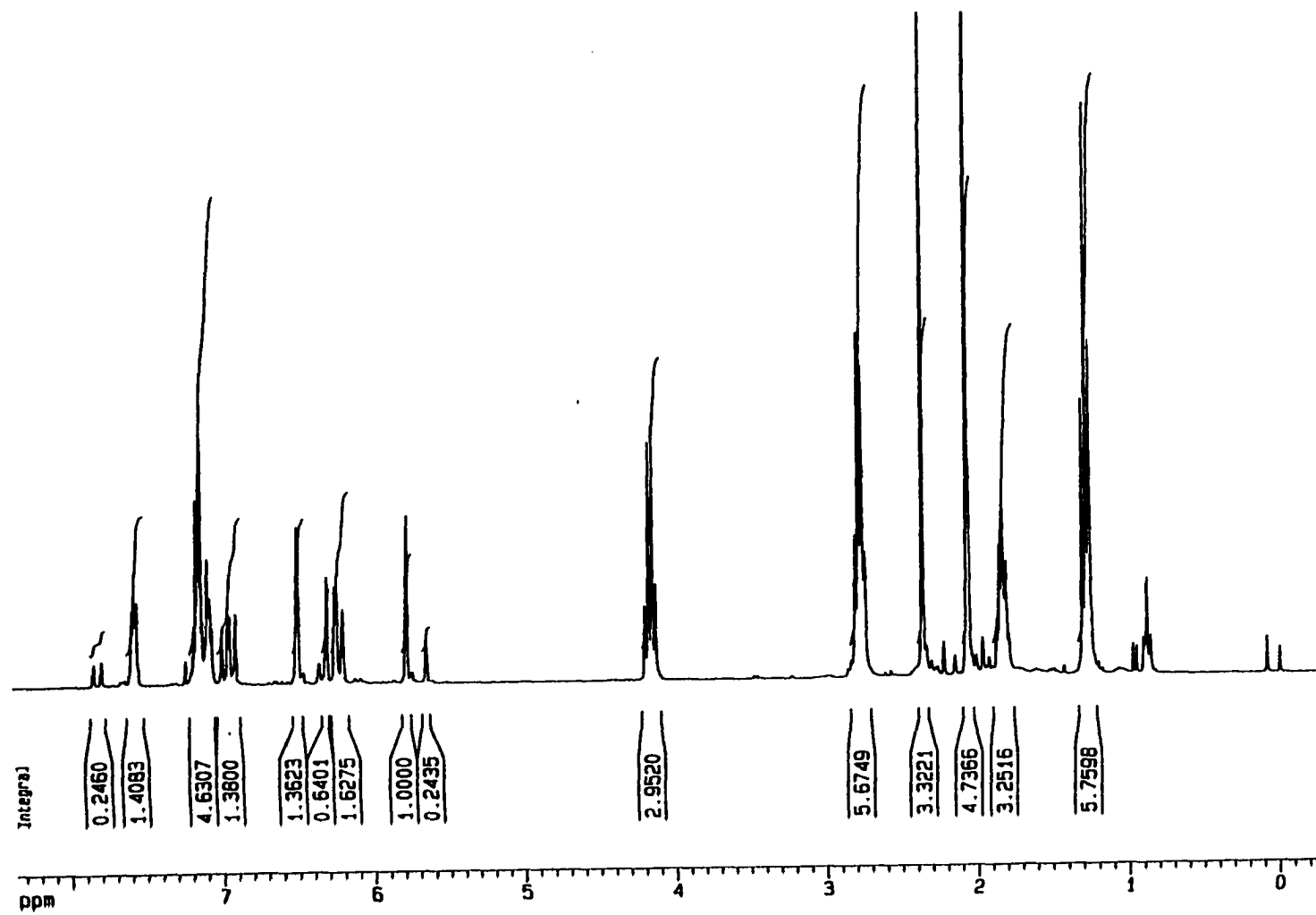


Figure 9. ¹H NMR (300 MHz) of Compound V-16 (CDCl₃).

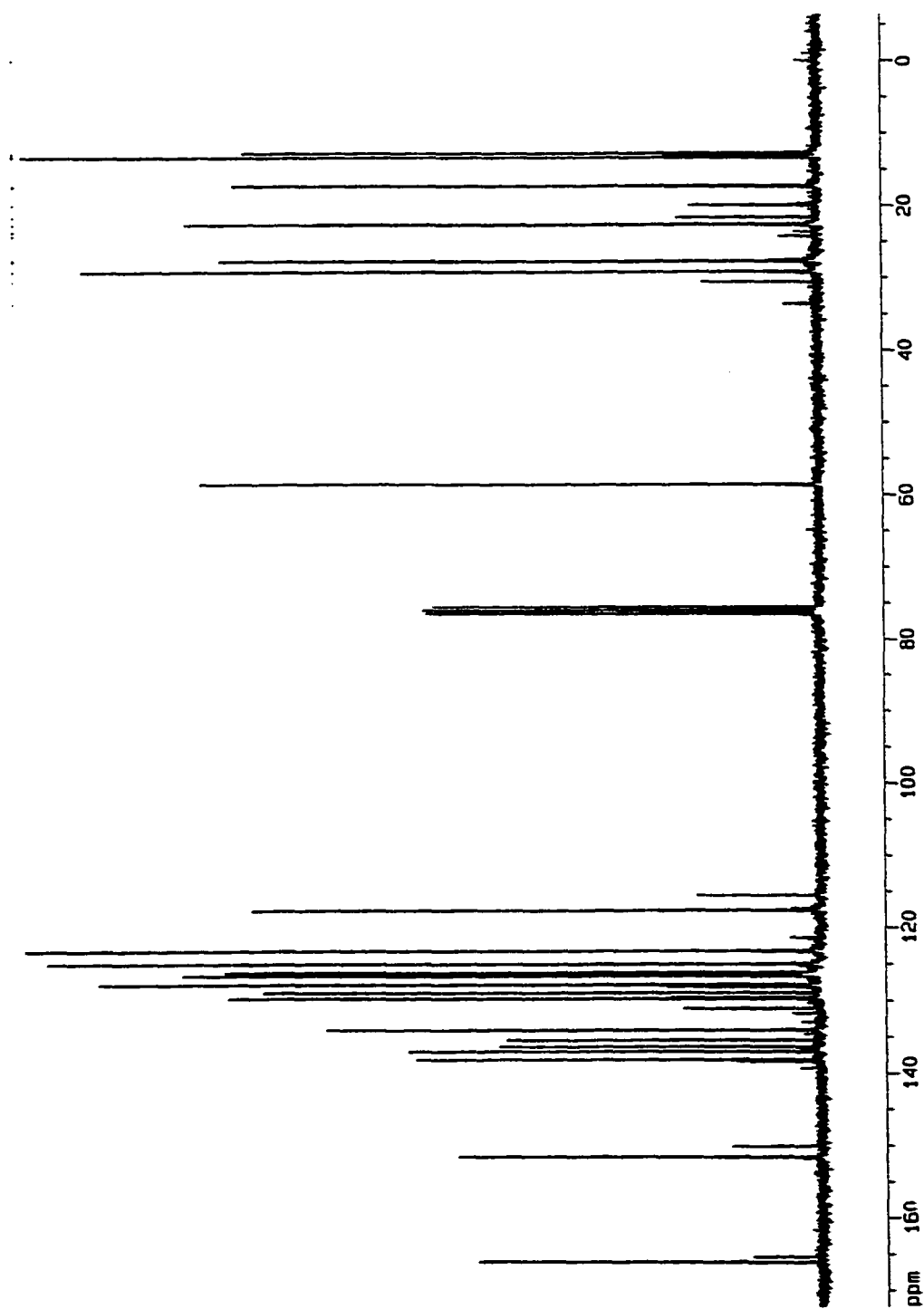


Figure 10. ^{13}C NMR (300 MHz) of Compound V-16 (CDCl_3).

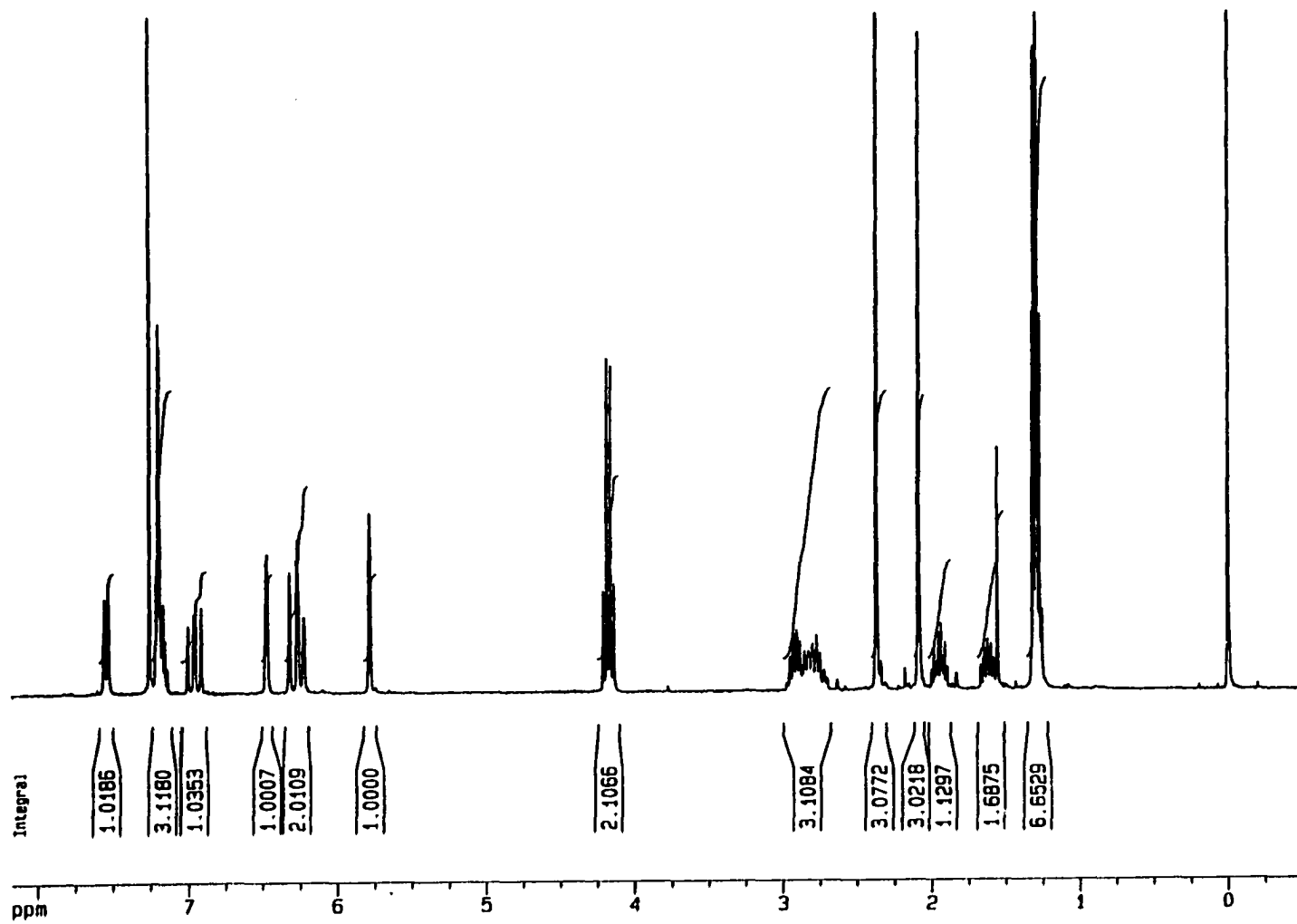


Figure 11. ¹H NMR (300 MHz) of Compound V-17 (CDCl₃).

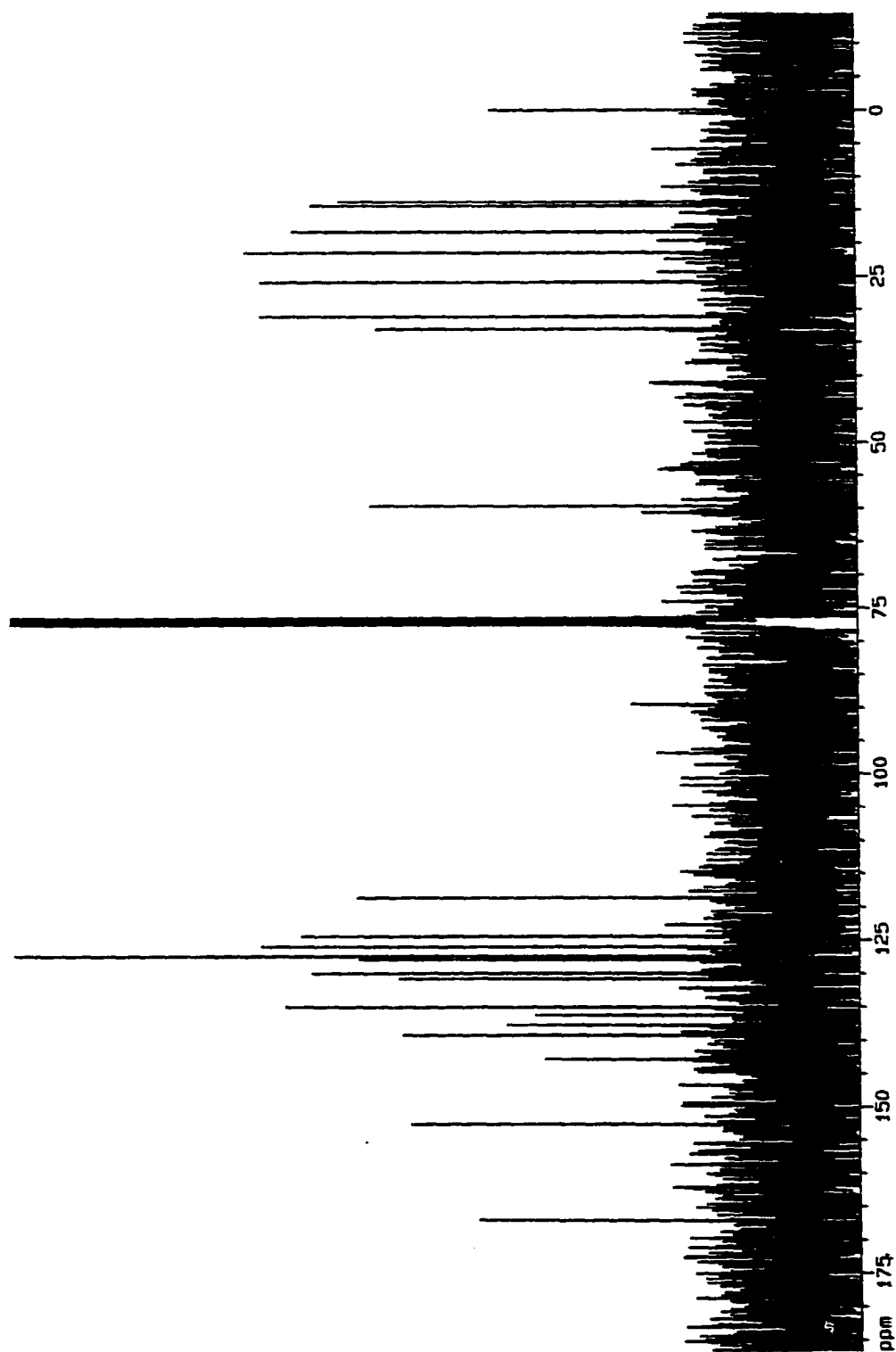


Figure 12. ^{13}C NMR (300 MHz) of Compound V-17 (CDCl_3).

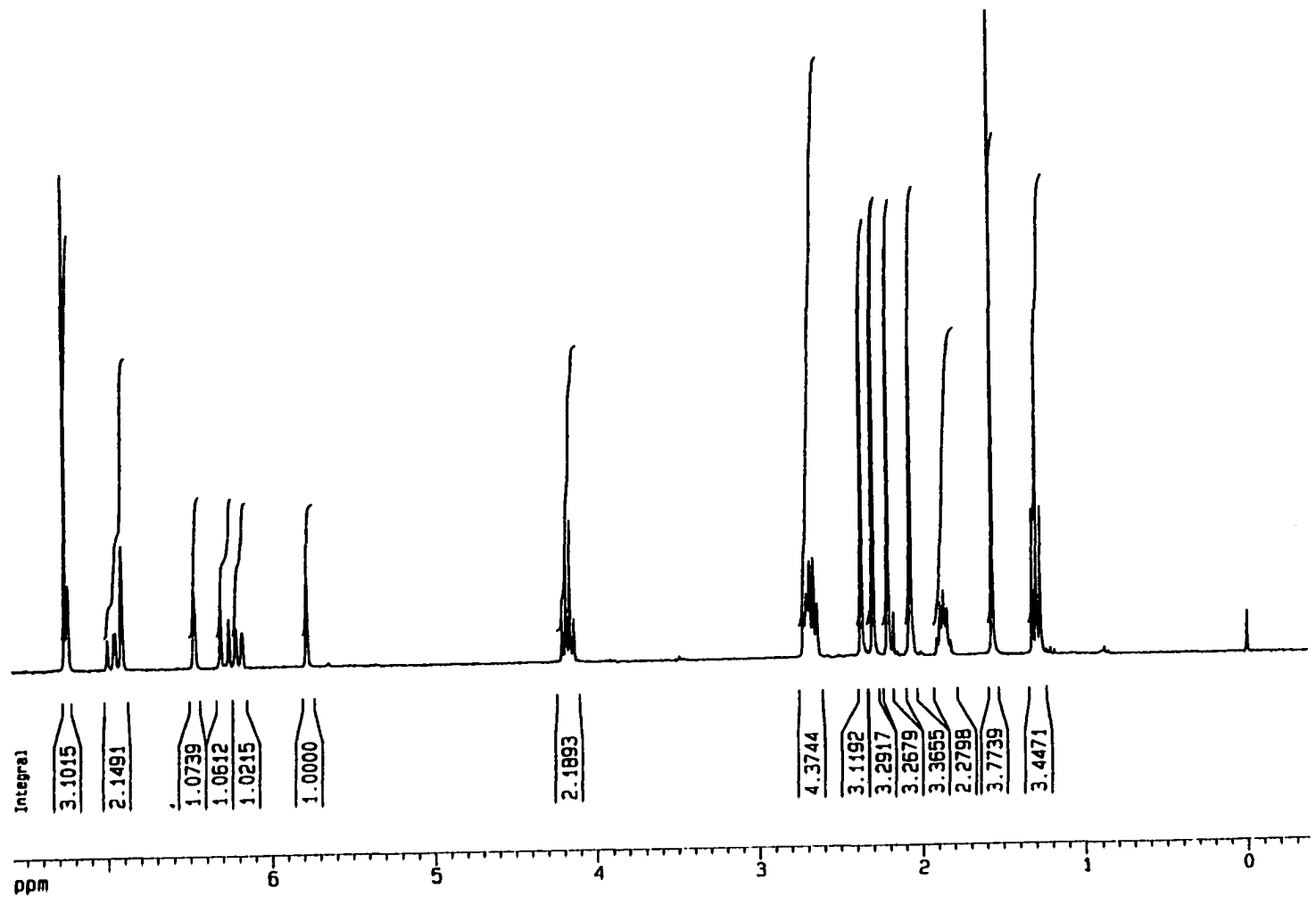


Figure 13. ^1H NMR (300 MHz) of Compound V-18 (CDCl_3).

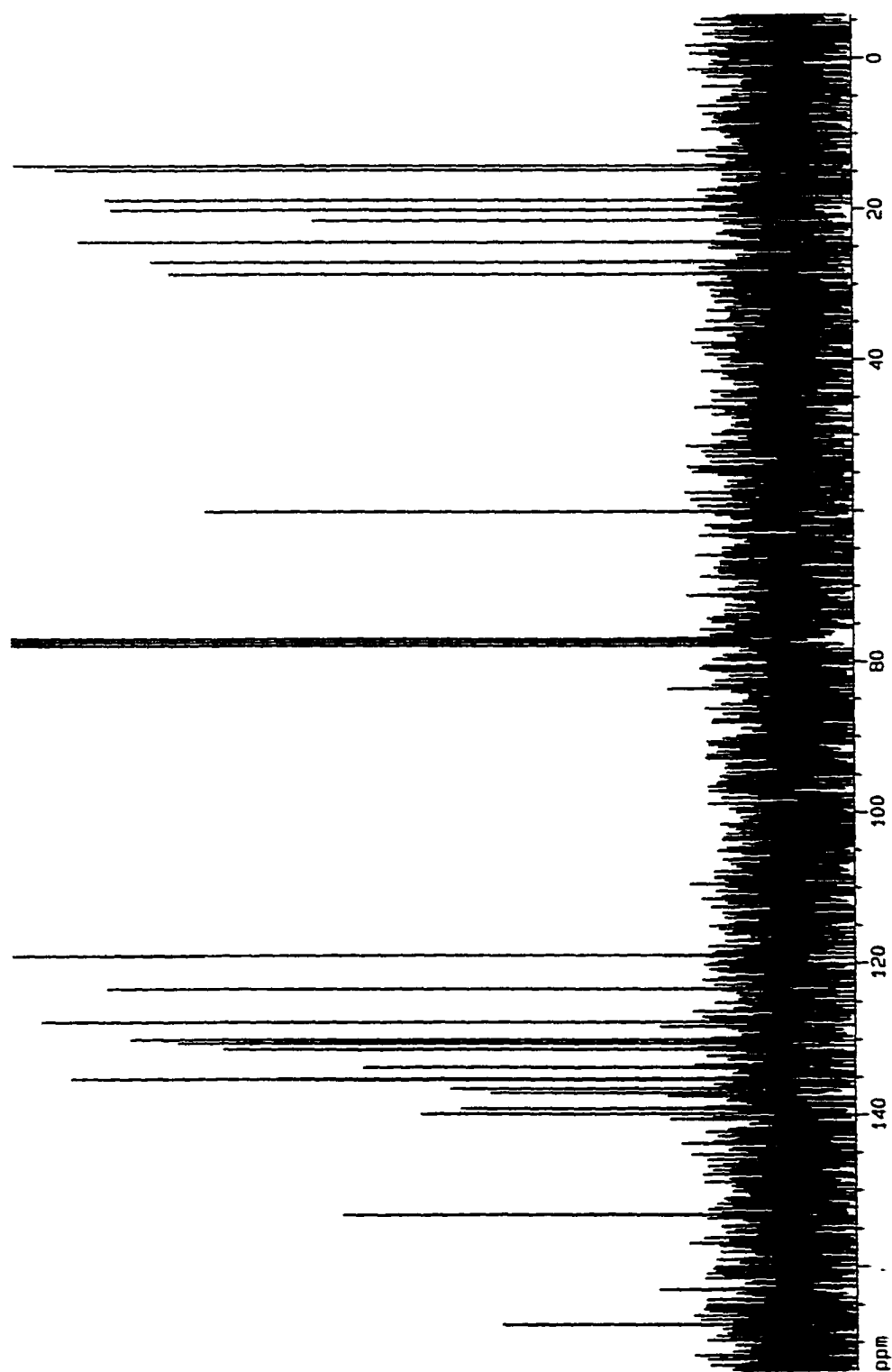


Figure 14. ^{13}C NMR (300 MHz) of Compound V-18 (CDCl_3).

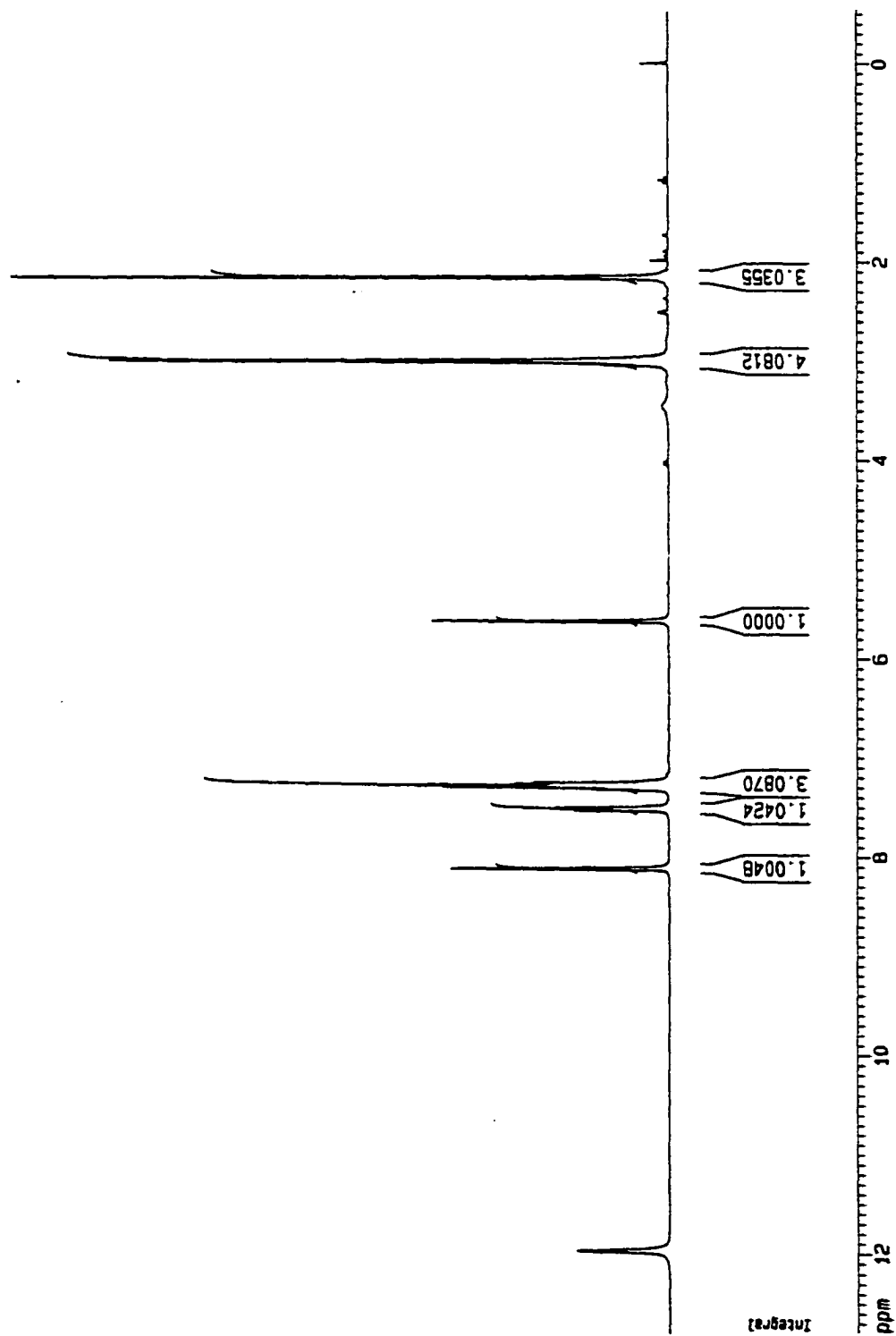


Figure 15. ^1H NMR (300 MHz) of Compound V-22 (CDCl_3).

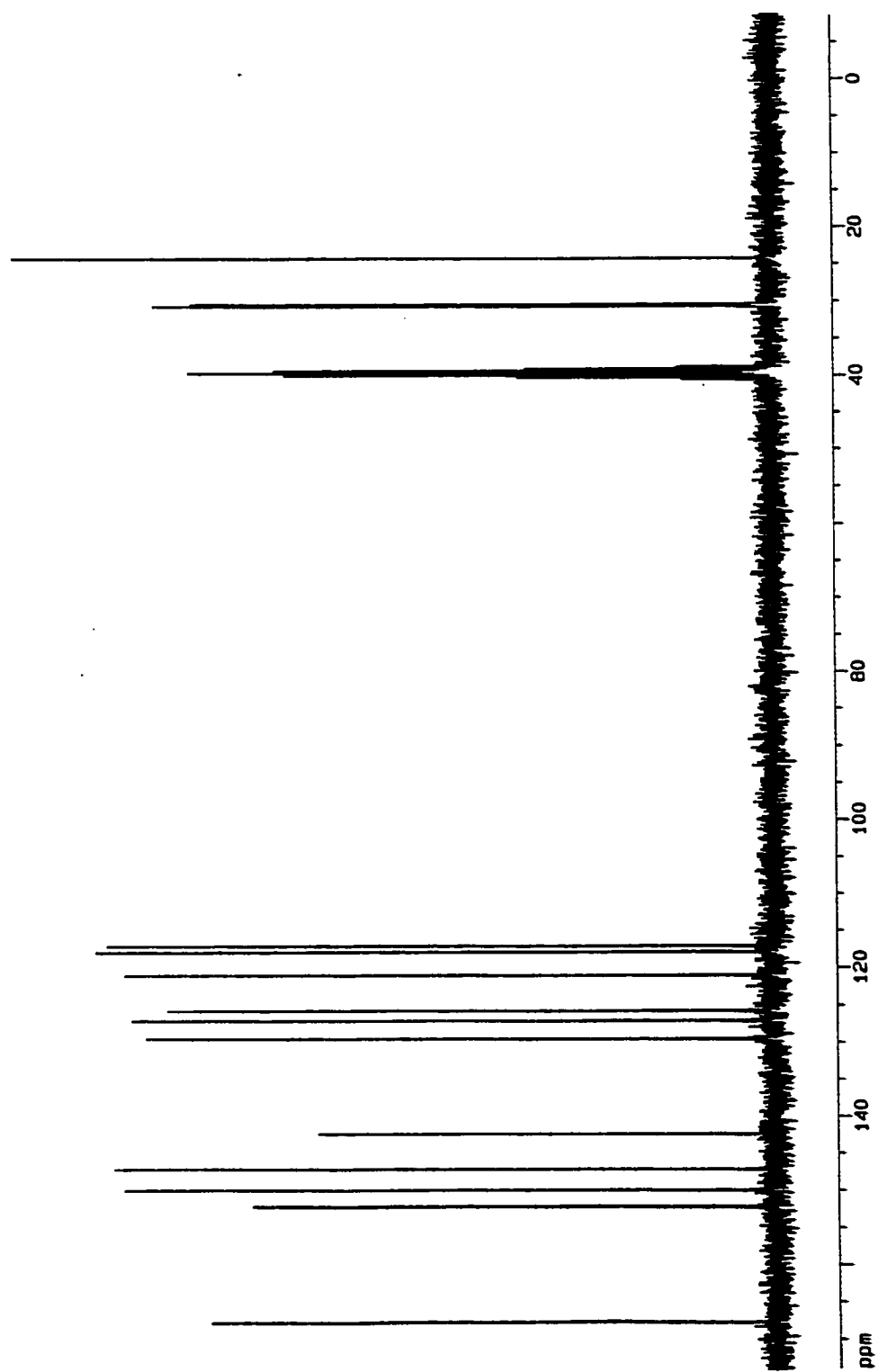


Figure 16. ^{13}C NMR (300 MHz) of Compound V-22 (CDCl_3).

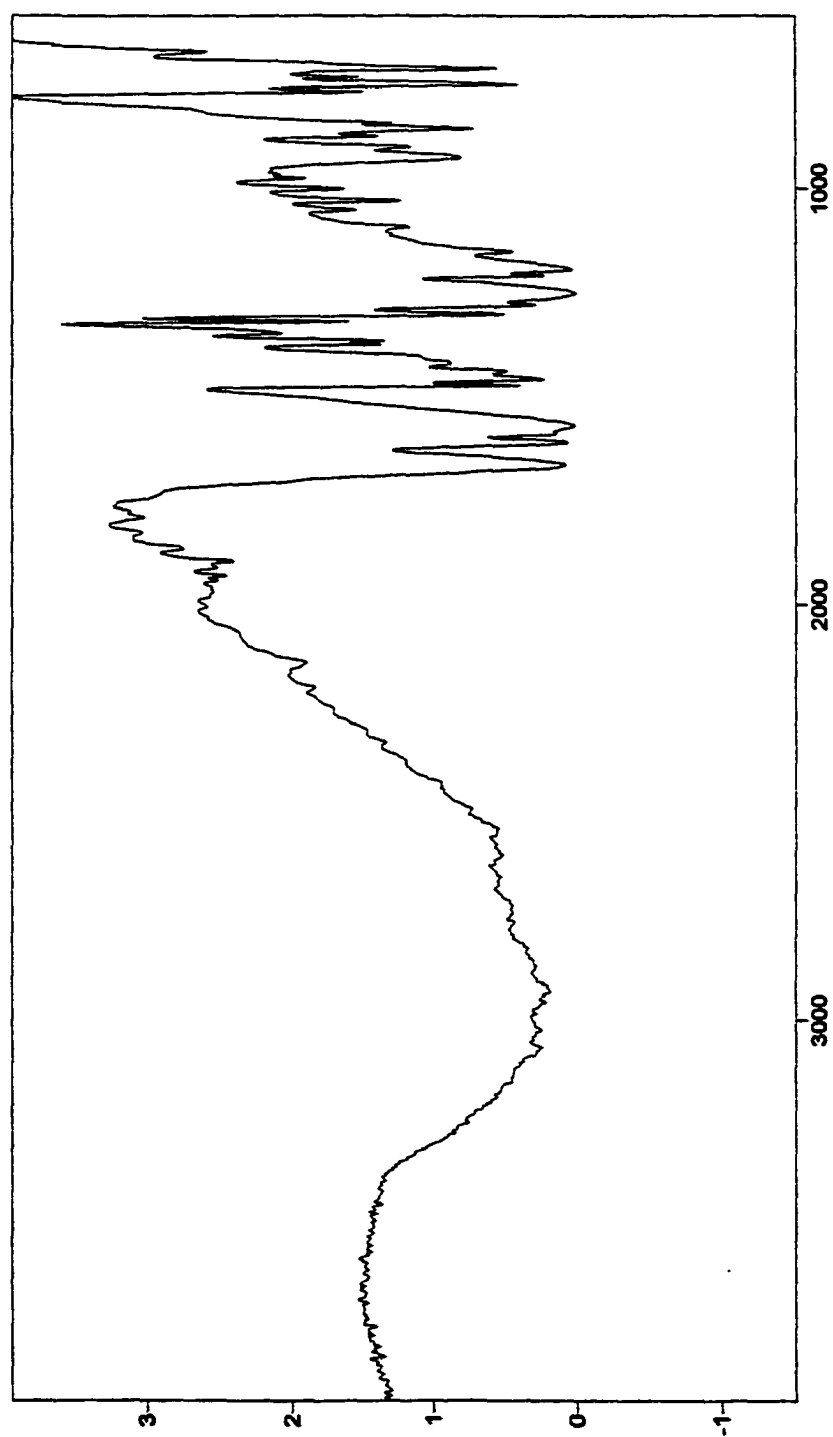


Figure 17. FTIR of Compound V-22 (KBr).

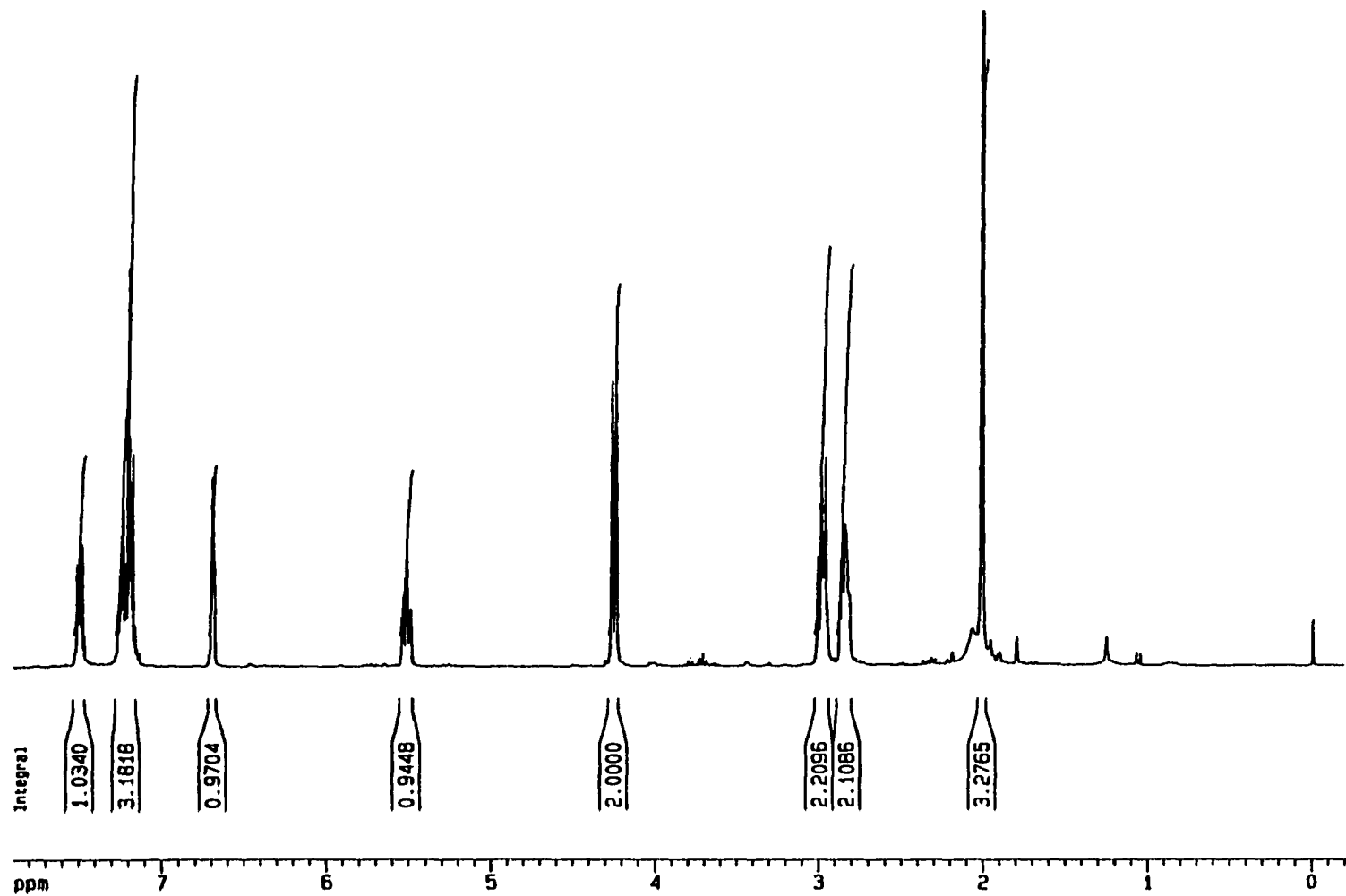


Figure 18. ¹H NMR (300 MHz) of Compound V-23 (CDCl₃).

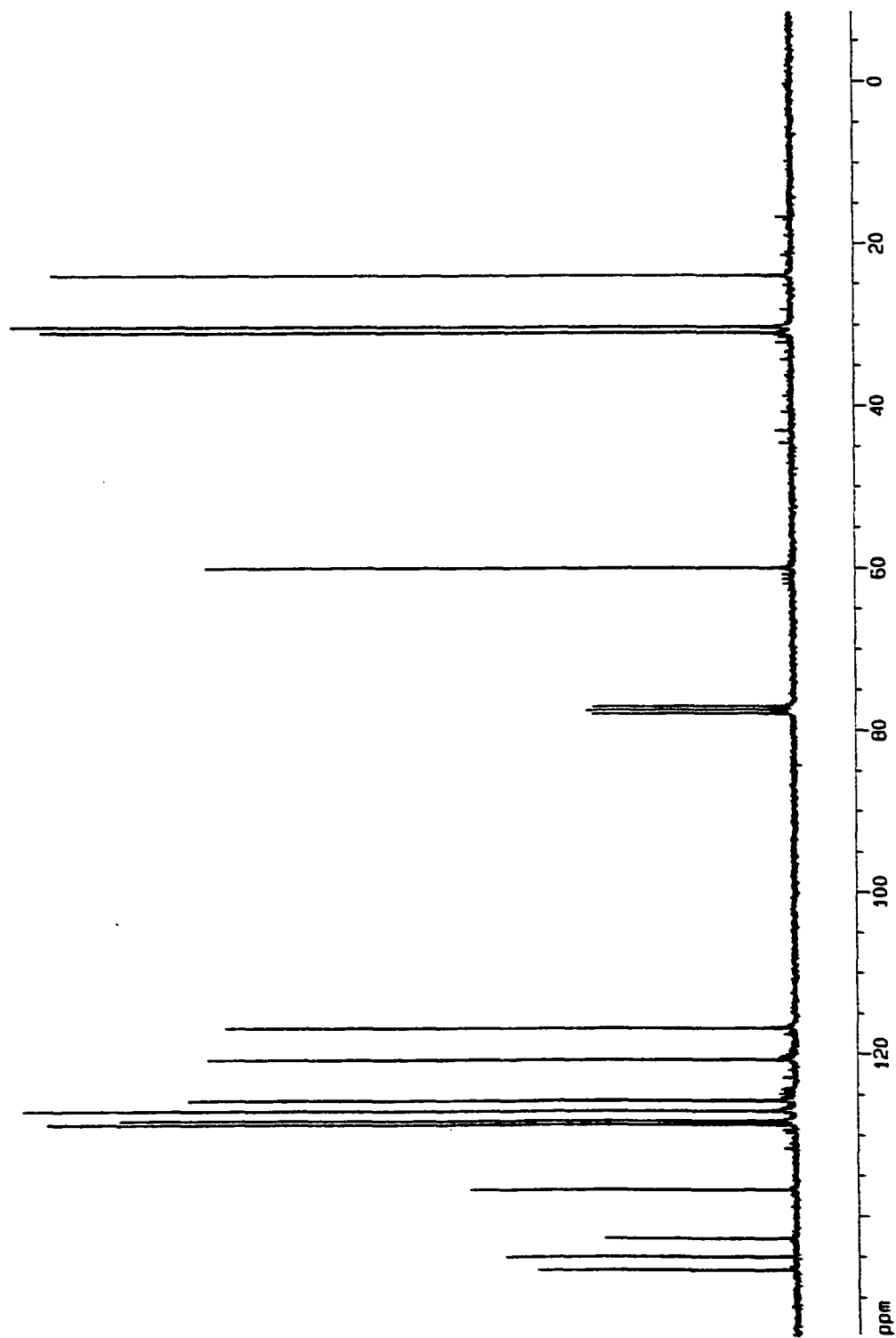


Figure 19. ^{13}C NMR (300 MHz) of Compound V-23 (CDCl_3).

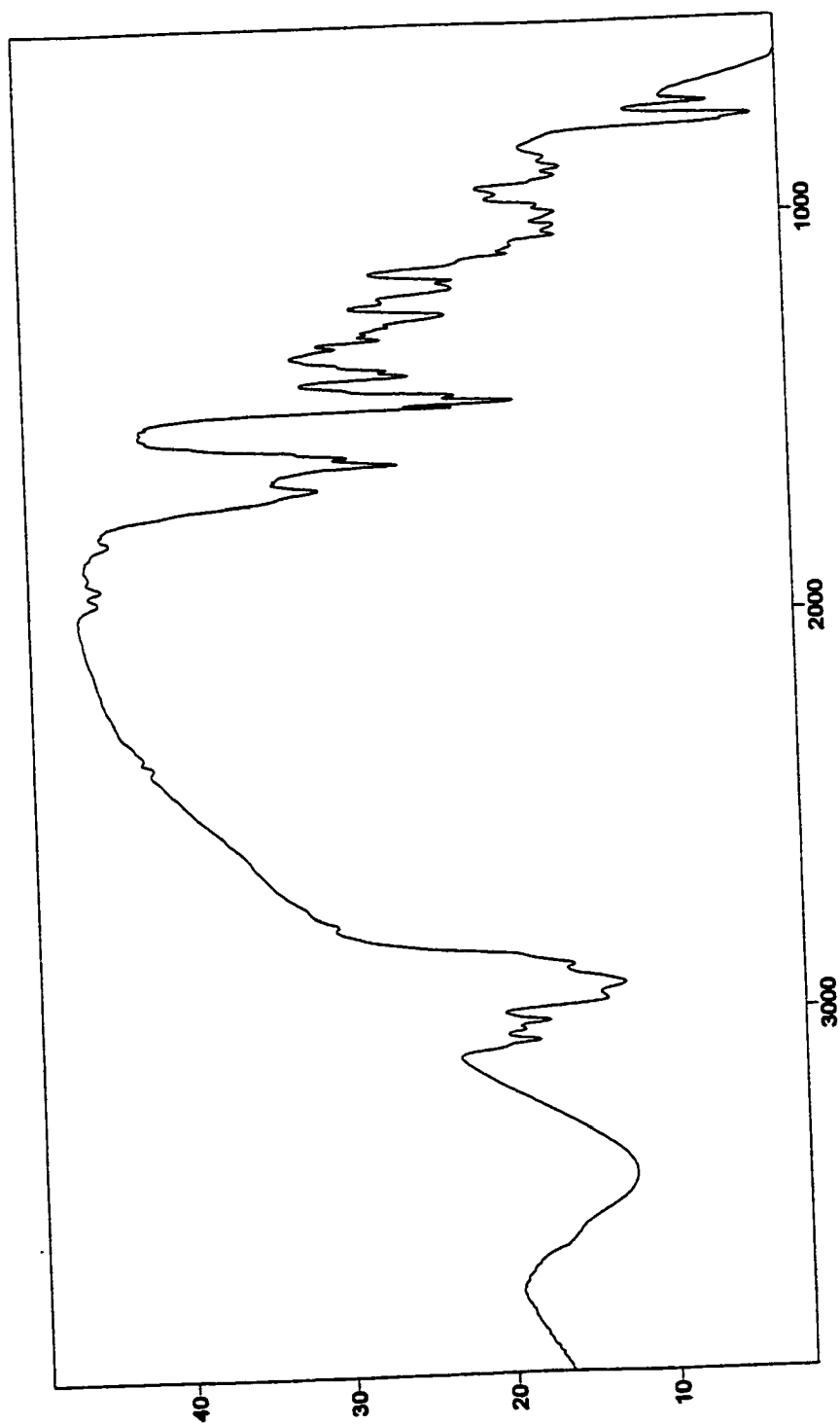


Figure 20. FTIR of Compound V-23 (KBr).

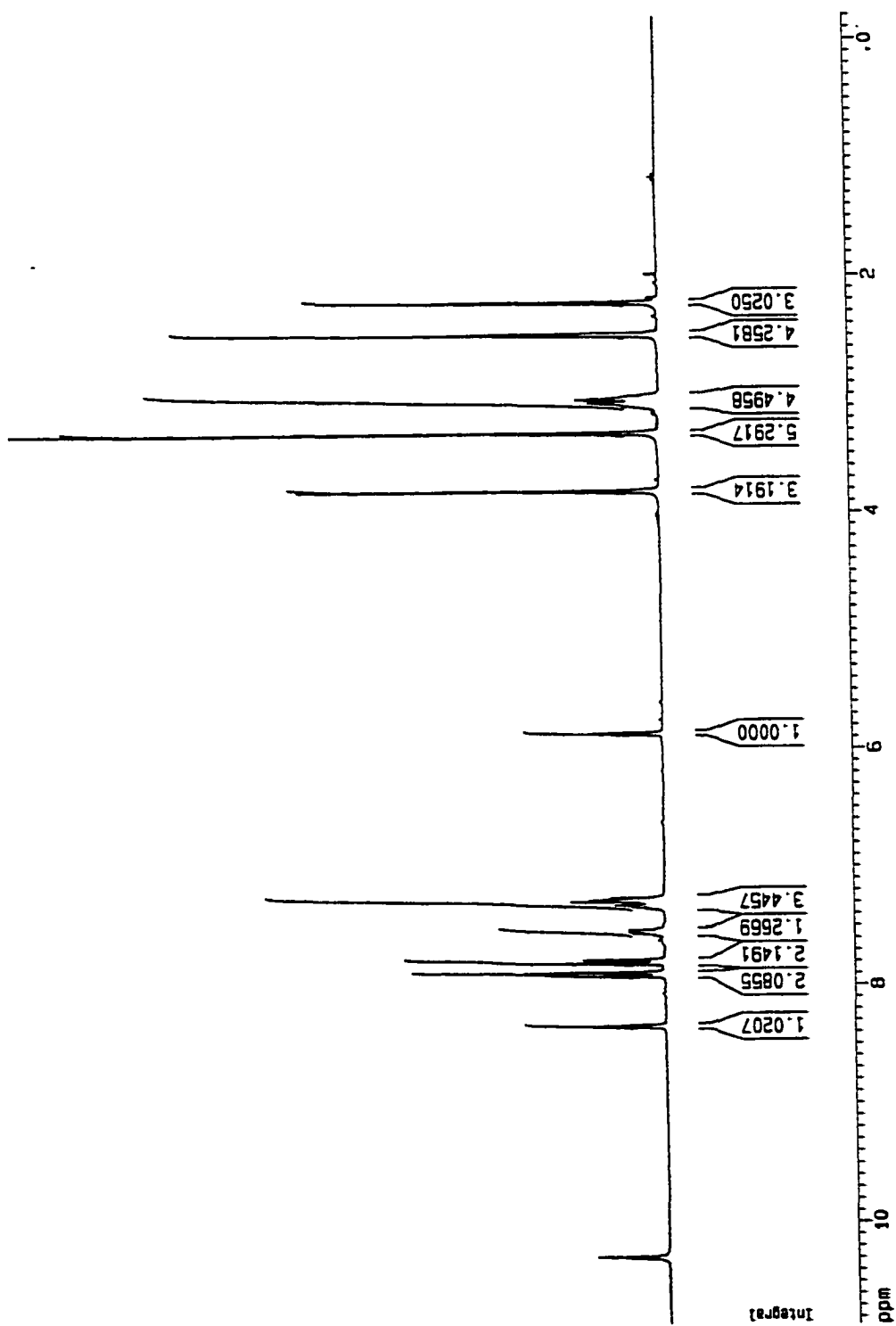


Figure 21. ^1H NMR (300 MHz) of Compound V-34 (DMSO).



Figure 22. ^{13}C NMR (300 MHz) of Compound V-34 (DMSO).

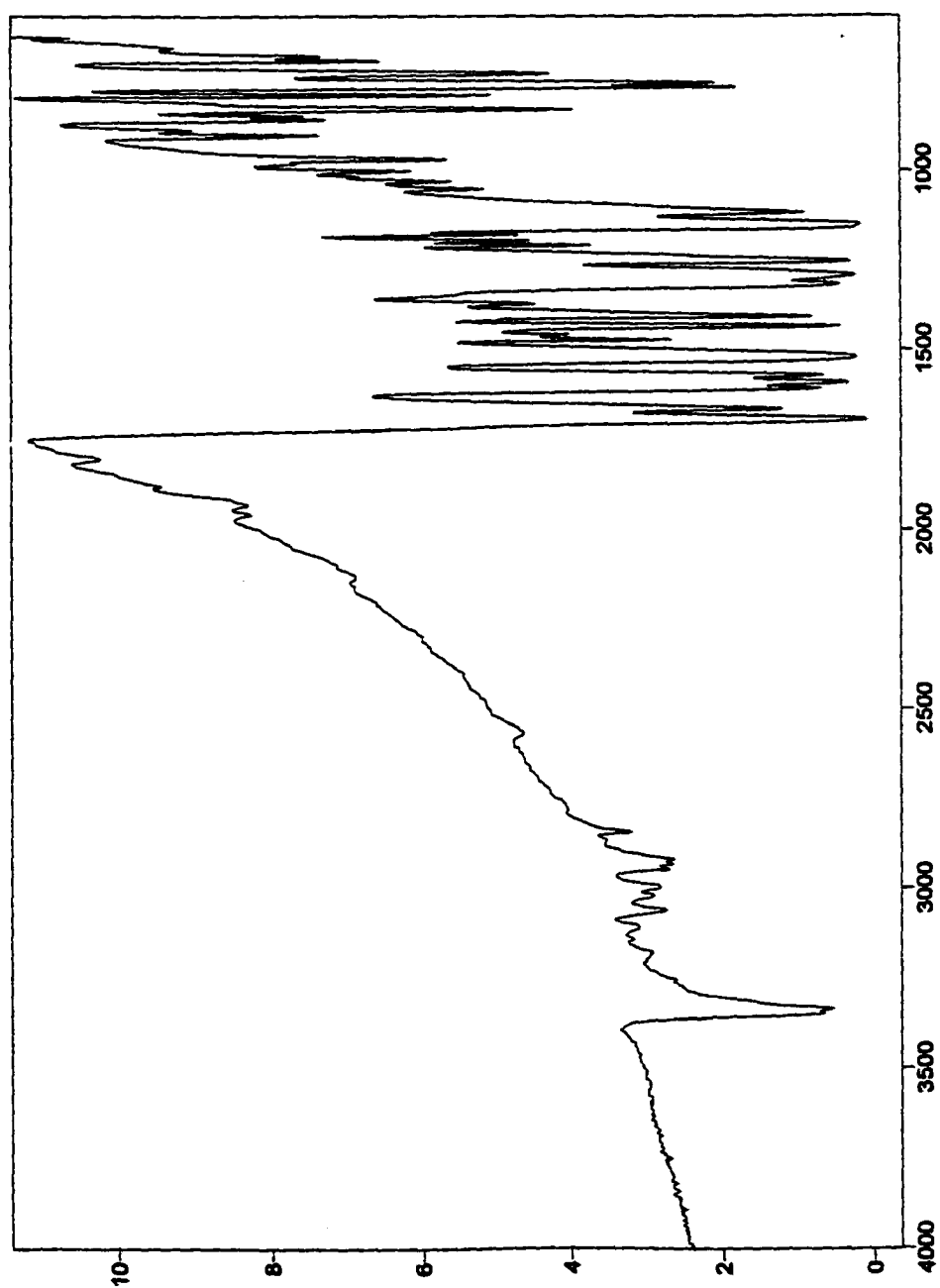


Figure 23. FTIR of Compound V-34 (KBr).

**GRADUATE SCHOOL
UNIVERSITY OF ALABAMA AT BIRMINGHAM
DISSERTATION APPROVAL FORM
DOCTOR OF PHILOSOPHY**

Name of Candidate Kimberly Kay Vines

Graduate Program Chemistry

Title of Dissertation Design of Conformationally Defined Retinoids: Synthesis,

Nuclear Receptor Binding, and Transcriptional Activity of

Derivatives of (9Z)-UAB30

I certify that I have read this document and examined the student regarding its content. In my opinion, this dissertation conforms to acceptable standards of scholarly presentation and is adequate in scope and quality, and the attainments of this student are such that she may be recommended for the degree of Doctor of Philosophy.

Dissertation Committee:

Name		Signature
<u>Wayne J. Brouillette</u>	Co-Chair	<u>Wayne J. Brouillette</u>
<u>Donald Muccio</u>	Co-Chair	<u>Donald Muccio</u>
<u>Peter D. Emanuel</u>		<u>Peter D. Emanuel</u>
<u>Jimmie Mays</u>		<u>Jimmie Mays</u>
<u>Brahma Sani</u>		<u>Brahma P Sani</u>

Director of Graduate Program Ly Q. Qian

Dean, UAB Graduate School Joan L. Rosen

Date 9/26/01